Partnership for AiR Transportation
Noise and Emissions Reduction
An FAA/NASA/Transport Canada-
sponsored Center of Excellence

Passive Sound Insulation

PARTNER Project 1.5 report

prepared by
Daniel H. Robinson, Robert J. Bernhard, Luc G. Mongeau

January 2008

REPORT N0. PARTNER-COE-2008-003

PASSIVE SOUND INSULATION

PARTNER Project 1.5 Report

January 2008

Prepared by:
Daniel Robinson

Robert Bernhard, Luc G. Mongeau
Purdue University

PARTNER Report No.: PARTNER-COE-2008-003

The Partnership for AiR Transportation Noise and Emissions Reduction — PARTNER — is a leading aviation cooperative research organization, and an FAA/NASA/Transport Canada-sponsored Center of Excellence. PARTNER fosters breakthrough technological, operational, policy, and workforce advances for the betterment of mobility, economy, national security, and the environment. The organization's operational headquarters is at the Massachusetts Institute of Technology.

The Partnership for AiR Transportation Noise and Emissions Reduction
Massachusetts Institute of Technology, 77 Massachusetts Avenue, 37-395
Cambridge, MA 02139 USA
http://www.partner.aero
info@partner.aero

PARTNER Project 1.5 Report: Passive Sound Insulation

Daniel H. Robinson

Dr. Robert J. Bernhard and Dr. Luc G. Mongeau
Purdue University

TABLE OF CONTENTS

Page

INTRODUCTION

Passive sound insulation is one of the mitigation strategies that are used to control sound energy transmission into homes. Current sound insulation methods are designed to reduce noise in the frequency range of greatest hearing sensitivity, typically above 250 Hz. In this frequency range, sound insulation is primarily governed by the mass of the structure. Usually, sound transmission is not mass controlled below 250 Hz [1]. In the frequency range below the mass-controlled region, sound transmission is controlled by the resonances and boundary of the structure. Building materials with similar acoustical characteristics above 250 Hz may behave differently below 250 Hz.

Low frequency sound insulation is important in neighborhoods near airports because aviation noise is known to have significant low frequency content. Windows in typical residences have a lower transmission loss than walls, doors, and other façade elements (brick veneer, wood-siding, and stucco) [2]. The poor performance of windows is worse at low frequencies. In this study, the sound reduction potential of window designs and construction types with improved sound transmission loss, such as double and triple pane windows, was investigated to determine the mechanisms of poor low frequency performance. Acoustically-rated windows typical of residential sound insulation projects near airports were measured at NASA Langley's Structural Acoustics Load and Transmission facility. These windows were of different construction types e.g. casement, slider, and picture. The sound transmission loss, vibration response, and mobility of the windows were measured.

PASSIVE LOW FREQUENCY SOUND INSULATION

The objective was to assess the impact of improved acoustic insulation of windows and to evaluate their low frequency sound transmission properties. Five windows were measured in this study, including a horizontal quad-slider, tilt-turn, casement, double-glaze picture, and triple-glaze picture window. The windows in this study are classified into two general groups: high-performance (HP) and ultra-high-performance (UHP). The high-performance windows were selected from the manufacturer specifications based on a mid-thirties STC rating. The ultra-high-performance windows were selected from the manufacturer specifications based on a mid-forties STC rating. The specifications of all of the windows used are shown in Table 0.1.

Table 0.1: Specifications of five windows tested in sound insulation experiment.

Group	Window	Type	Glass Thickness / Air Gap (mm)	Mass per area (kg/m^2)	Frame Thickness (mm)	Manufacturer STC (dB)	Manufacturer OITC (dB)
UHP	A	Quad-Slider	3(**13**)3(**50**)6	35.2	117	45	34
UHP	B	Picture	5(**10**)5(**50**)6	38.6	117	47	35
HP	C	Tilt-Turn	6 Lam.(**16**)5	37.7	89	37	30
HP	D	Casement	6 Lam.(**14**)5	29.3	89	36	28
HP	E	Picture	6 Lam.(**13**)5	26.1	89	36	29

Bold indicates airspace thickness, annealed glass unless noted otherwise; Lam. = laminated glass.

All window units were 1.2 m x 1.2 m (47.5 in. x 47.5 in.) in dimension from outer edge to outer edge and were built by Rehau Inc., The window specification in column three of Table 0.1 designates, in order, the interior glass thickness, the air gap spacing, followed by the second layer glass thickness, and for Windows A and B, a second air gap and the thickness of a third pane on the exterior. The glass thickness and air gap spacing is presented in a format common for the window industry [3]-[4]. The glass is annealed unless otherwise stated. Annealed glass is rolled to thickness during the manufacturing process. Laminated (Lam.) glass is annealed

glass with a thin plastic film applied to one or both sides. The overall window unit frame thickness of 117 mm (4 5/8 in.) is typical of a West Coast 50 mm x 150 mm (2 in. x 6 in.) construction, while 89 mm (3 1/2 in.) is more typical of a Midwest 50 mm x 100 mm (2 in. x 4 in.) construction. The STC and Outdoor-Indoor Transmission Class (OITC) ratings were provided by Architectural Testing Labs, an independent measurement laboratory commissioned by the manufacturer and are representative of the rating for these windows. However, the numerical value may be a measurement for that model with different glass type (annealed or laminated), thickness, and/or geometry. Plots of the transmission losses measured during this investigation and those for comparable windows (same model with possibly different geometries or glass type) as measured by the manufacturer are included in the results section of this chapter.

Photographs (exterior and interior face and corner views) of each window are shown in Figure 0.1 through Figure 0.5. Window A is a quad-slider style window where four window partitions slide independently on four tracks. Two of the partitions are single-pane glass while the other two are double-pane glass with an air gap. In the closed position the unit locks shut so that the double-pane and single-pane partition align together on both halves effectively creating a triple-pane window unit. Windows B and E are picture style windows, which are fixed or non-opening windows. Window B is a triple-pane window unit and Window E is a double-pane window unit.

Window C is a double-pane, tilt-turn style window. The tilt-turn name refers to the two opening orientations. It can swing open like a door (hinging along the vertical axis) or swing down like a hopper-style window (hinging along the bottom horizontal axis). Window D is a double-pane, casement-style window and swings open along the vertical axis by means of a crank mechanism.

(a)

(b)

(c)

Figure 0.1: Photo of window A, triple-pane quad-slider; (a) exterior face, (b) interior face, (c) corner view.

(a)

(b)

(c)

Figure 0.2: Photo of window B, triple-pane picture; (a) exterior face, (b) interior face, (c) corner view.

(a)

(b)

(c)

Figure 0.3: Photo of window C, double-pane tilt-turn; (a) exterior face, (b) interior face, (c) corner view.

(a)

(b)

(c)

Figure 0.4: Photo of window D, double-pane casement; (a) exterior face, (b) interior face, (c) corner view.

(a)

(b)

(c)

Figure 0.5: Photo of window E, double-pane picture; (a) exterior face, (b) interior face, (c) corner view.

TEST METHOD

Transmission Loss Test Facility

To investigate low frequency sound insulation it is desirable to conduct transmission loss measurements in a facility which will allow accurate measurement below 100 Hz. Measurements of sound insulating elements, including windows, are often limited to the frequency range above 100 Hz because of the dimensions of the test facility. The geometry of the source room dictates the acoustic room modes of the test facility and thus the sound field impinging on the test panel. For accurate transmission loss measurement it is required that the sound field impinging on the test panel be diffuse. It is assumed that the sound field at the panel is sufficiently diffuse when three or more room modes exist in each of the one-third octave bands reported. The Structural Acoustic Loads and Transmission (SALT) facility at NASA Langley was designed to make low frequency sound transmission loss measurements down to 56 Hz, which is the lower frequency limit of the 63 Hz one-third octave band. The transmission loss of the windows was measured over the range of 56-4000 Hz.

The schematic of the SALT facility and placement of the reference microphone are shown in Figure 0.1. The SALT reverberation chamber includes non-parallel surfaces. The ceiling is at an angle with the floor and the walls are splayed in order to distribute the frequencies of the low frequency modes. The reverberation and anechoic chambers are vibration isolated from each other and from the building. Both chambers are concrete enclosures resting on independent coil springs and separated by a 735 mm (30 in.) air-space. The SALT facility is instrumented with four B&K 4197 phase-matched microphone pair intensity probes mounted to a computer-controlled positioning device for automated data acquisition. Twenty-four independently driven loudspeaker drivers were used in the reverberation chamber (including four low frequency drivers) to generate a random, diffuse sound field in the source room. Twelve G.R.A.S. Type 26CA stationary reference microphones were located at random locations in the

reverberation chamber to estimate the spatially averaged sound pressure level in the source room. The microphones were hung from the ceiling at random heights along two diagonal lines from the test panel.

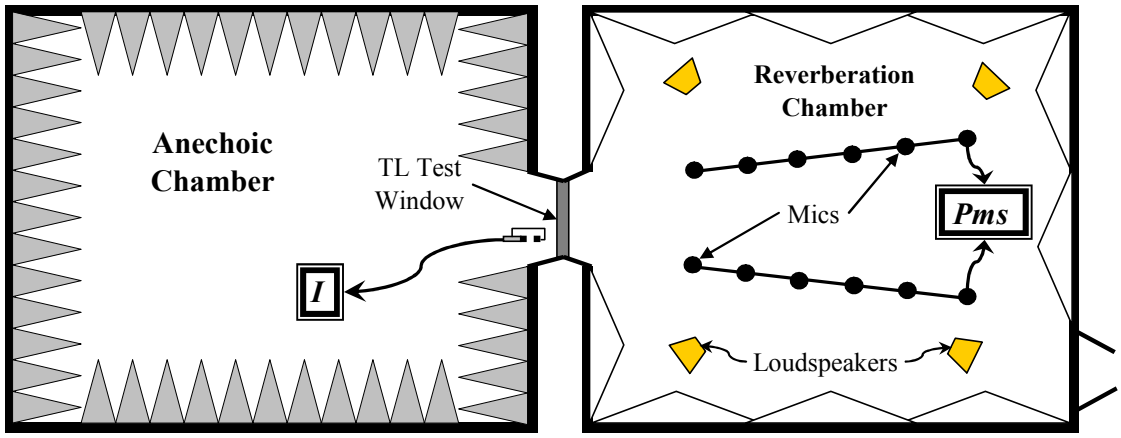

Figure 0.1: Schematic of SALT facility at NASA Langley.

The influence of flanking paths on the accuracy of the SALT facility were determined during a NASA Langley study [5] by inserting medium density fiberboard panels of increasing thicknesses into the transmission loss aperture until no further increase in transmission loss was realized for increased panel thickness as suggested by ISO standard 140 [6]. No evidence of flanking sound transmission paths was observed during the measurement. The background noise floor in both the anechoic and reverberation chambers is shown in Figure 0.2.

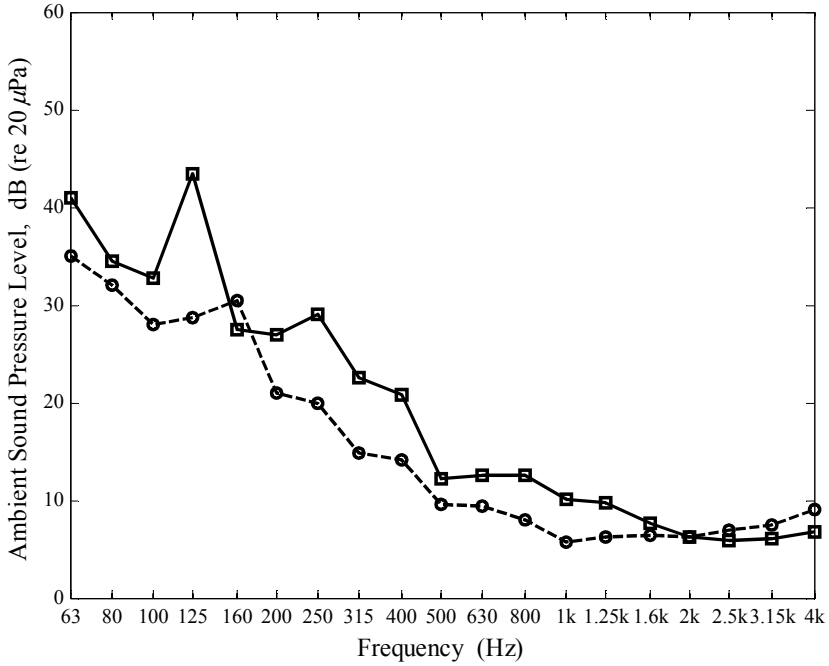

Figure 0.2: Background noise floor for the anechoic chamber (o--o) and reverberation chamber (□—□) at the SALT facility.

Photographs of the reverberation chamber are shown in Figure 0.3 through Figure 0.5. The double-doors at the entrance and transmission loss test aperture on the far wall are shown in Figure 0.3. The interior of the reverberation chamber is shown in Figure 0.4 and Figure 0.5. The wall facing the transmission loss test aperture is shown in Figure 0.4 and a view looking across the reverberation chamber at the side wall is shown in Figure 0.5.

Figure 0.3: Entrance to the reverberation chamber showing the double noise reduction doors [provided by NASA Langley staff].

Figure 0.4: Reverberation chamber showing the transmission loss window with a medium density fiberboard panel installed [provided by NASA Langley staff].

An interior view of the reverberation chamber with measurement equipment in place is shown in Figure 0.5. The mid/high frequency loudspeakers appear as black canisters pointed in random directions along the plane of the wall. The black box in the background is one of the low frequency drivers. The transmission loss aperture is on the left-hand side of the photograph.

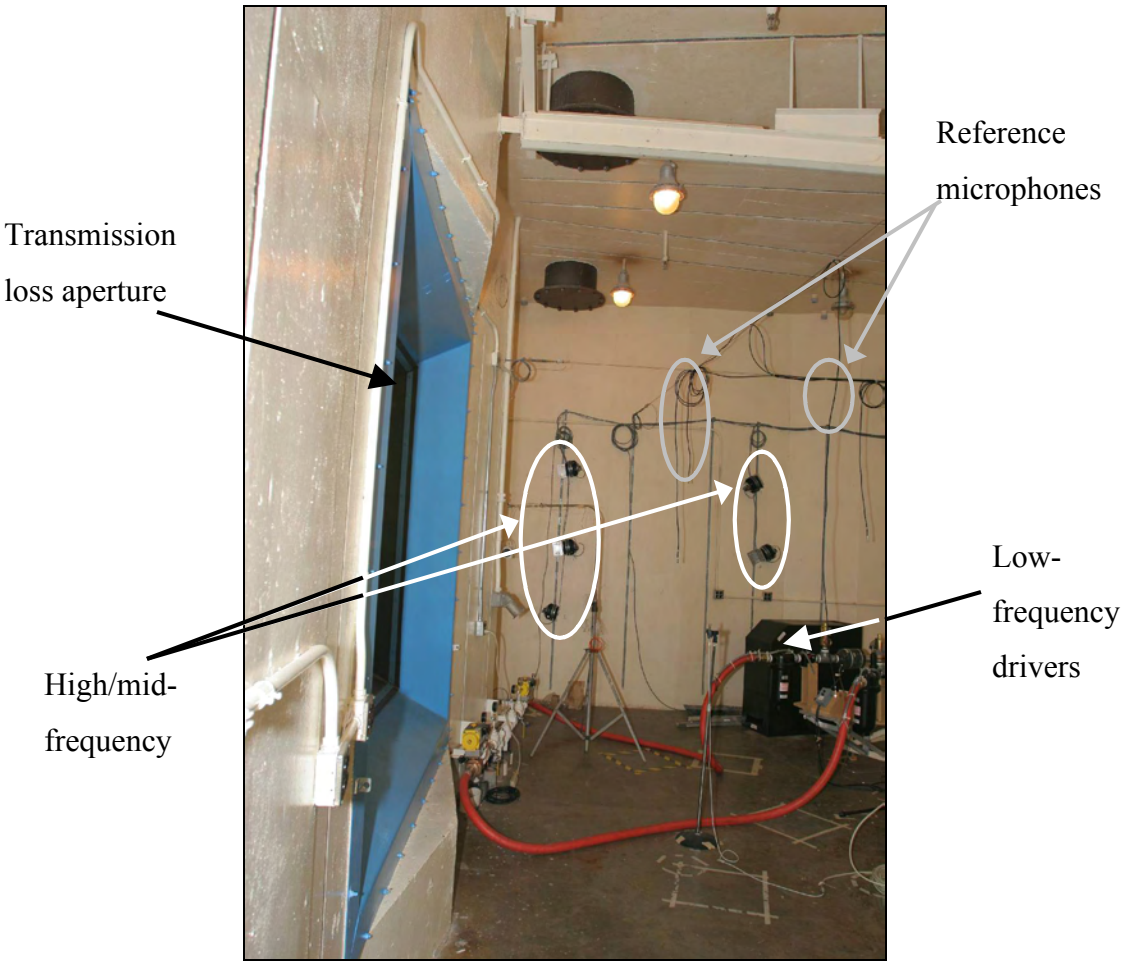

Figure 0.5: Reverberation chamber, side-view of transmission loss aperture.

The transmission loss aperture in the anechoic chamber and the intensity probes are shown in Figure 0.6 and Figure 0.7. The computer-controlled positioning device is the vertical rod with the four intensity probes on rods.

Figure 0.6: Anechoic chamber, view of transmission loss window with Window D installed; computer-controlled intensity probes in foreground.

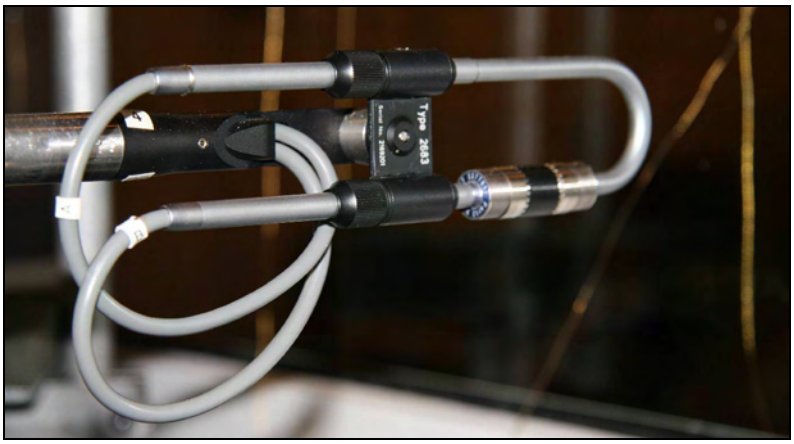

Figure 0.7: Close-up of intensity probe with 12 mm spacer.

The SALT transmission loss aperture measured 1.42 m x 1.42 m (56 in. x 56 in.). In order to test windows that are 1.21 m x 1.21 m (47.5 in. x 47.5 in.) a sub-frame was installed into the SALT transmission loss aperture. The sub-frame was a sand-filled wooden box having a depth of 124 mm (4 7/8 in.) bolted into the SALT transmission loss aperture. The sub-frame was constructed of 20 mm (3/4 in.) plywood. The interior space was filled with sand. The inner dimensions of the sub-frame are 1.21 m x 1.21 m and the outer dimensions are 1.42 m x 1.42 m.

Felt cloth was stapled to the sub-frame before the window was installed in order to seal the interface between the test window and the sub-frame. A picture of Window C installed in sub-frame mounted in the transmission loss aperture is shown in Figure 0.8.

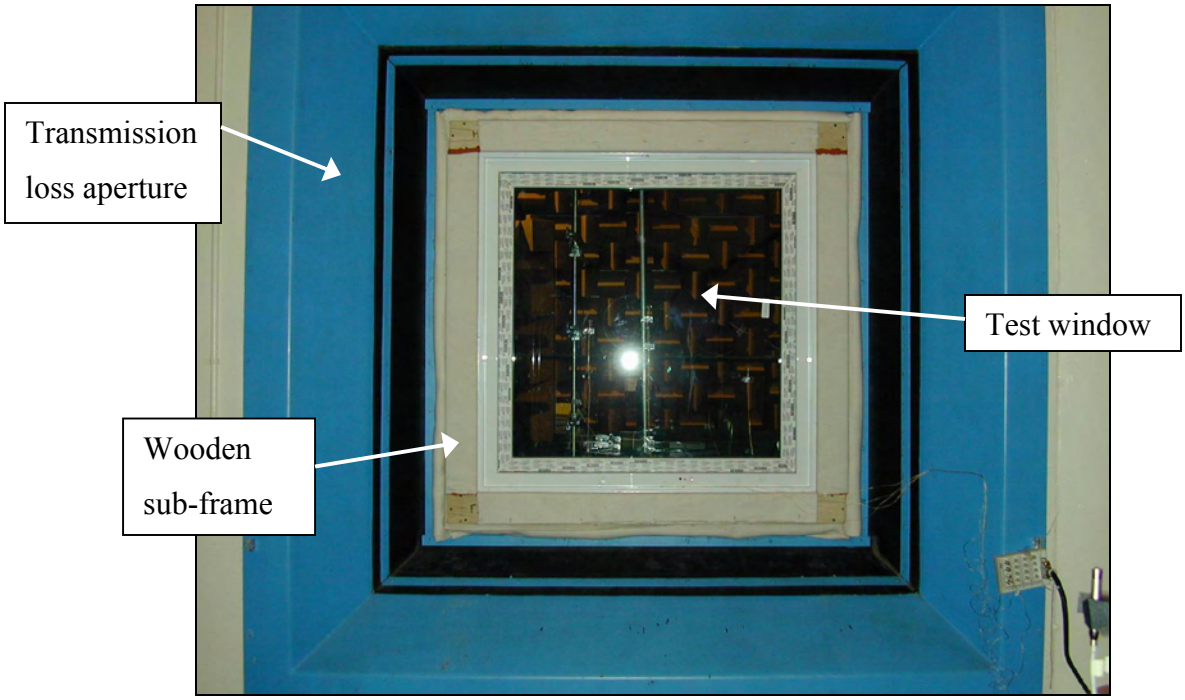

Figure 0.8: Window C installed in the sub-frame mounted in the transmission loss aperture.

The mounting of the test windows in the wooden box sub-frame was as similar as possible to installation of the windows in a typical house as suggested by ASTM E2112 [7] and manufacturer's installation guides [8]-[10]. All five of the windows were pocket (finless) windows, i.e. they had no nailing fin to secure the unit to a wooden frame of a house. The outer edge of the window unit was smooth and provides a flush interface with the sub-frame.

Transmission Loss Test Method

Transmission loss measurements were conducted at NASA Langley's Structural Acoustic Load and Transmission (SALT) facility. The windows were placed in an aperture between a reverberant, source chamber and an anechoic, receiving chamber. The windows were secured by

a wooden sub-frame. The sound intensity method was used to measure the sound transmitted through the windows.

Stationary, random pink noise was generated at 92 dBA overall sound pressure level in the reverberation chamber. The vibration response of the test windows was measured at eight locations with PCB Type 352C22 accelerometers placed away from primary nodal lines, four on each side of the window. An additional accelerometer (9) was placed on the wooden sub-frame on the anechoic chamber side. Accelerometer locations are shown in Figure 0.9 and listed in Table 0.2.

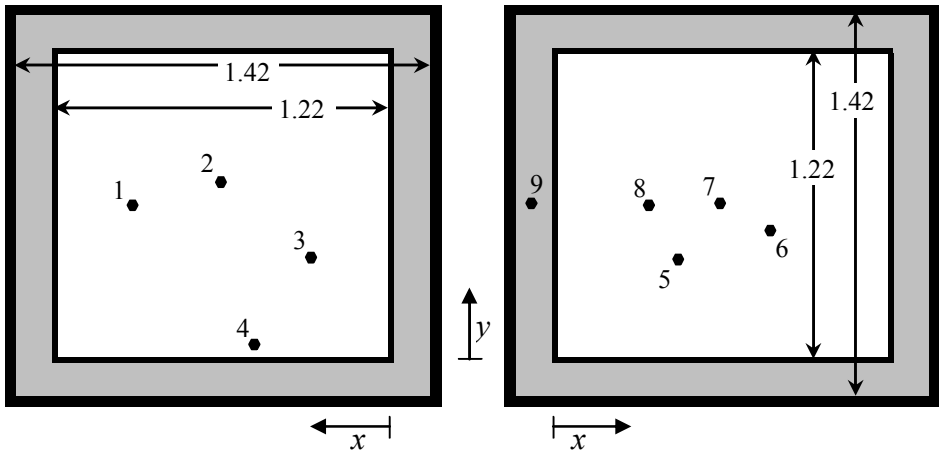

(a) (b)

Figure 0.9: Schematic of accelerometer locations (a) exterior face, (b) interior face. Dimensions in meters.

The white inner box in Figure 0.9 represents the test window while the gray box represents the sub-frame. The exterior face, (a), is viewed by facing the window mounted in the aperture while standing in the reverberation chamber. The interior face, (b), is viewed by facing the window mounted in the aperture while standing in the anechoic chamber. When facing the exterior side of the window, the reference location for the reference position is in the lower right-hand corner. When facing the interior side, the reference position is in the lower left-hand corner.

Table 0.2: Accelerometer locations for transmission loss measurement (steady state excitation).

Accelerometer Locations				
Accl #	*x* (mm)	*y* (mm)	*x* (in)	*y* (in)
1	813	610	32	24
2	603	660	23 3/4	26
3	241	445	9 1/2	17 1/2
4	483	51	19	2
5	381	280	15	11
6	864	368	34	14 1/2
7	603	572	23 3/4	22 1/2
8	305	603	12	23 3/4
9	-51	610	-2	24

A separate mobility test was conducted using an instrumented impact hammer; this was performed to characterize vibration behavior of the windows. The mobility test is discussed in the following section.

The transmission loss measurements were performed using the two-microphone sound intensity method, following standardized procedures ASTM E2249 [11], ISO 15186-1 [12], ISO 15186-3 [13], and ANSI S1.9 [14]. The measurement plane spanned both the surface of the test window and that of the sub-frame. Sound intensity is the time-averaged vector product of the instantaneous pressure and the instantaneous particle velocity at a specific location [15]. Fifty sound intensity averages were done at 551 locations along a grid that included 19 grid-points along the horizontal axis and 29 grid-points along the vertical axis across the surface of the test window. The grid spacing was 75 mm x 50 mm (3 in. x 2 in.) and the stand-off distance was 50 mm (2 in.).

Phase-mismatch and finite-difference error limit the frequency range of applicability of the two-microphone method. Phase-mismatch between the two microphones causes error in the intensity estimation at low frequencies, resulting in a low frequency limit. Phase-mismatch error is minimized by increasing the distance between the intensity probe microphones. The finite-difference error is an artifact resulting from estimating the pressure gradient from a two-point finite-difference scheme. This error becomes large at high frequencies, thus providing a high

frequency measurement limit. The finite-difference error is minimized by decreasing the distance between the intensity probe microphones. Phase-mismatch and finite-difference errors are at odds with each other and a compromise must be made. The low frequency limit when a 12 mm spacer is placed between the two intensity probe microphones is approximately 125 Hz. Since frequencies below 125 Hz are of interest for this investigation, a larger spacing must be used. The 50 mm spacer provides minimum phase mismatch error for frequencies less than 50 Hz (the lower frequency limit of the SALT source room). However, the 50 mm spacer does not provide accurate transmission loss measurements above 1000 Hz. Thus the sound intensity measurements were repeated using both the 12 mm and 50 mm spacers. The results from the 50 mm spacer measurements were used for the 56-1000 Hz range and the results from the 12 mm spacer measurements were used for the range 1-4 kHz. The 12mm and 50 mm spacer measurements were recorded at a sampling rate of 10 kHz and 2554 Hz, respectively.

Mobility Test Method

Mobility measurements were made at Purdue University's Ray W. Herrick Laboratories. Mobility is the complex ratio of velocity and force for a particular structure [16]-[17]. Similarly, accelerance is the complex ratio of acceleration and force. The accelerance of each test window was measured using the impact method, using an instrumented hammer and measuring the vibration response with an accelerometer. A force window with 10% trigger was applied to the input channel (PCB Type 086C03 medium impact hammer) and an exponential window with time constant, $\tau = 0.6948$ seconds, was applied to the output channels (PCB Type 333B32 accelerometers) in order to minimize background noise. Six accelerometers were placed at locations away from nodal lines, three on each side of the window. The locations of the accelerometers are shown in Figure 0.10 and are tabulated in Table 0.3.

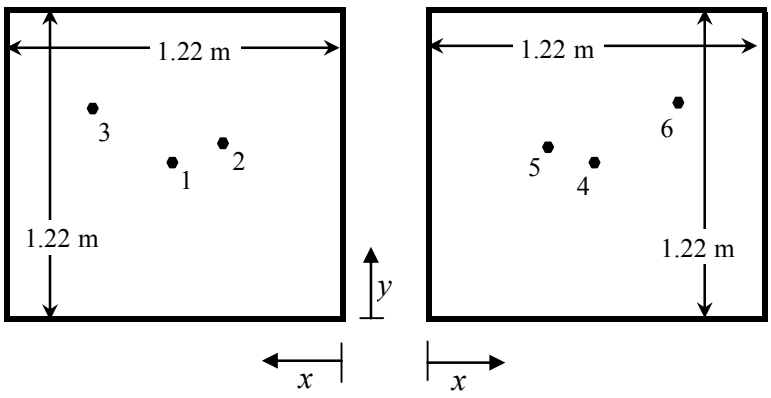

(a) (b)

Figure 0.10: Schematic of mobility test accelerometer locations (a) exterior face, (b) interior face. Dimensions in meters.

Table 0.3: Accelerometer locations for mobility test measurement.

Mobility Accelerometer Locations				
Accl #	*x* (mm)	*y* (mm)	*x* (in)	*y* (in)
1	603	603	23 3/4	23 3/4
2	475	704	18 2/3	27.7
3	927	853	36 1/2	33 3/5
4	603	603	23 3/4	23 3/4
5	475	704	18 2/3	27.7
6	927	853	36 1/2	33 3/5

The accelerance of each window was measured by successively striking the window as near to each accelerometer location as possible and simultaneously measuring the vibration response at all six accelerometer locations. The result was six hit locations with corresponding measurements at all six accelerometer locations. Thus 36 accelerance measurements were taken on each window. The window was struck three times at each hit location and the measured response averaged. A measurement at a corresponding hit location is called drive-point mobility while a measurement at a location not corresponding to a hit location is called cross-mobility.

EXPERIMENTAL RESULTS

The results of the low frequency sound insulation experiment include the transmission loss tests conducted at NASA Langley's SALT facility and a separate mobility test conducted at Purdue University's Ray W. Herrick Laboratories. The measured transmission loss of the five high-performance windows is presented in both one-third octave data and narrow-band forms. A comparison is also made with the mass-law transmission loss prediction based on mass-law theory [17]:

$$TL_{mass\ law} = 10\log_{10}\left[1+\frac{1}{2}\left(\frac{\pi f m''}{\rho_0 c_0}\right)^2\right]; \quad f \square\ f_c \tag{2.1}$$

where m'' is the mass per unit area of a single panel, f_c is the coincidence frequency and ρ_0 and c_0 are the density and speed of sound in a fluid, respectively. In equation (2.1) it is assumed that angles of incident sound are oblique and uniformly distributed for all angles.

STC and OITC Results

In this section the transmission loss measurement results with corresponding STC curve-fits are presented. Plots of the transmission loss test results of the five high-performance windows tested at the SALT facility and the corresponding Sound Transmission Class (STC) and Outdoor-Indoor Transmission Class (OITC) calculations are shown in Figure 0.1 through Figure 0.5. The combined transmission loss results for the intensity scans using both the 12 mm and 50 mm spacer are shown. A synthesis of the 50 mm spacer results in the frequency range 56-1000 Hz and 12 mm spacer results in the frequency range 1000-4000 Hz was used. Deficiencies between the measured transmission loss values and the idealized STC curve were summed for the STC determination. Only positive value deficiencies are considered and shown as black square markers in each one-third octave band. Deficiencies are used as part of the curve-fitting

with no deficiency to exceed 8 dB for any one-third octave band and the sum of the positive deficiencies to total no more that 32 dB as per ASTM E413 [18]. The OITC was calculated as per ASTM E1332 [19].

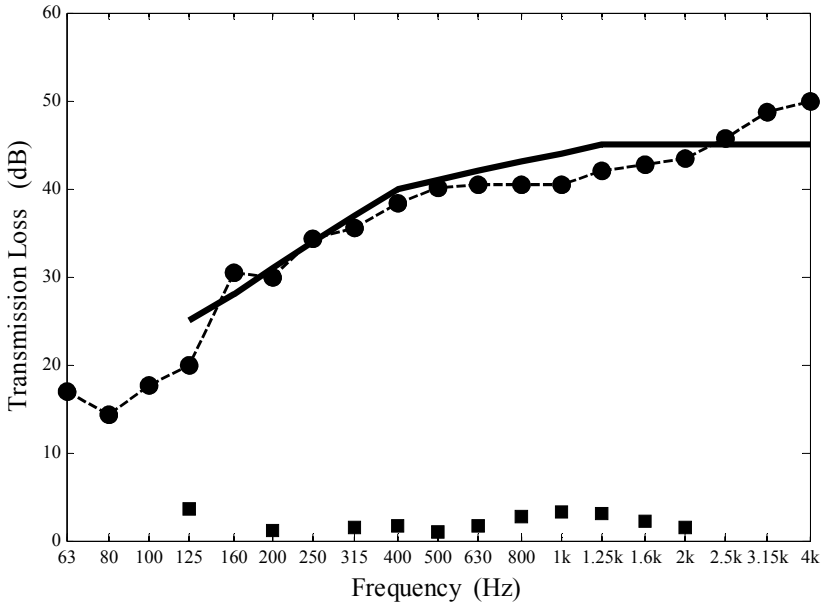

Figure 0.1: Sound transmission loss vs. frequency, Window A.
Transmission loss (●--); STC = 41 dB curve (—); STC deficiency (■); OITC = 30 dB.

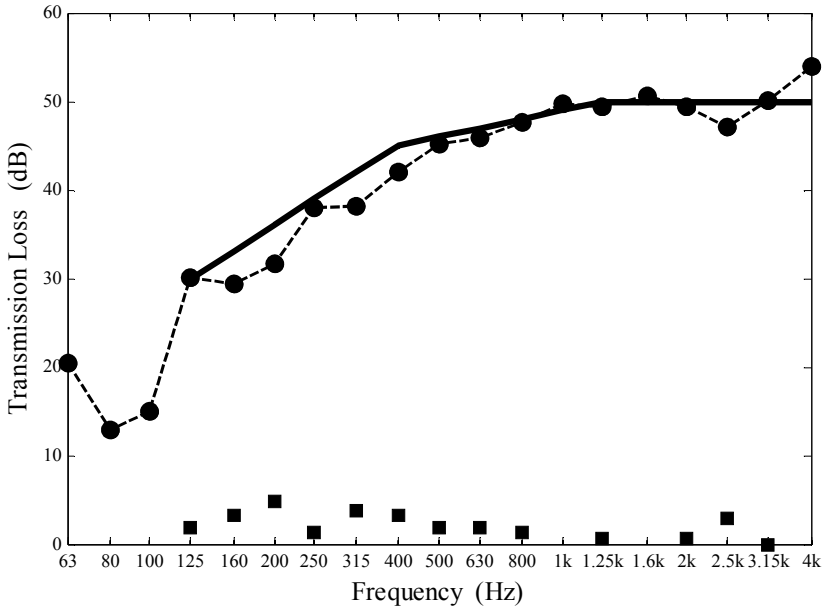

Figure 0.2: Sound transmission loss vs. frequency, Window B.
Transmission loss (●--); STC = 46 dB curve (—); STC deficiency (■); OITC = 29 dB.

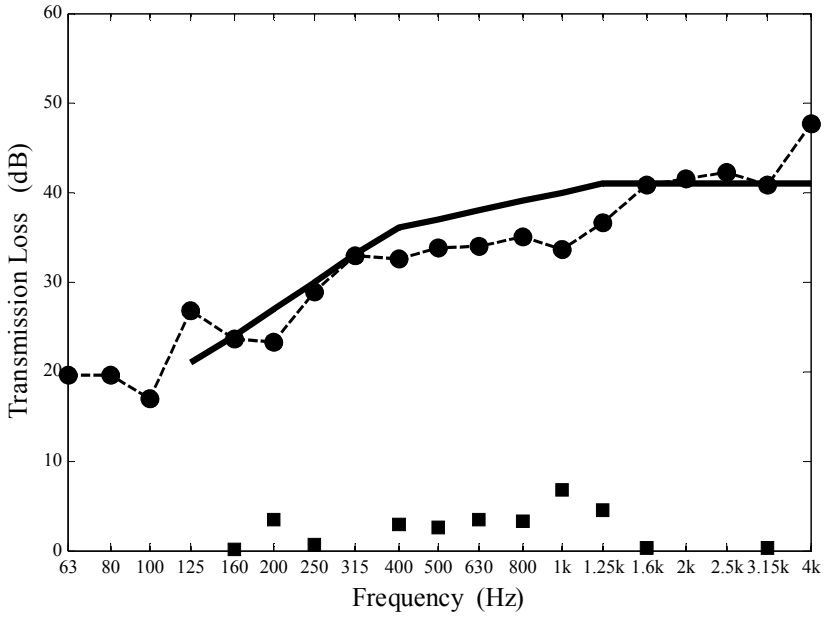

Figure 0.3: Sound transmission loss vs. frequency, Window C.
Transmission loss (●--); STC = 37 dB curve (—); STC deficiency (■); OITC = 29 dB.

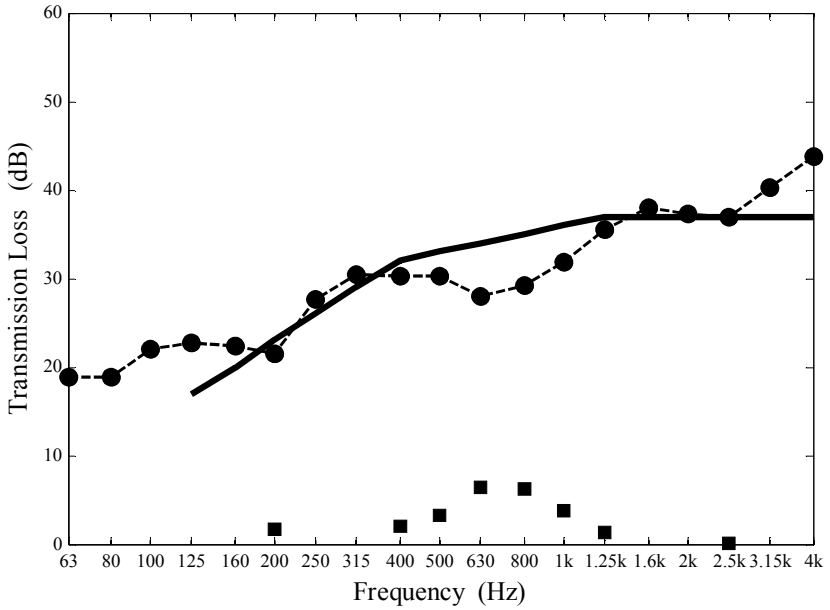

Figure 0.4: Sound transmission loss vs. frequency, Window D.
Transmission loss (●--); STC = 33 dB curve (—); STC deficiency (■); OITC = 28 dB.

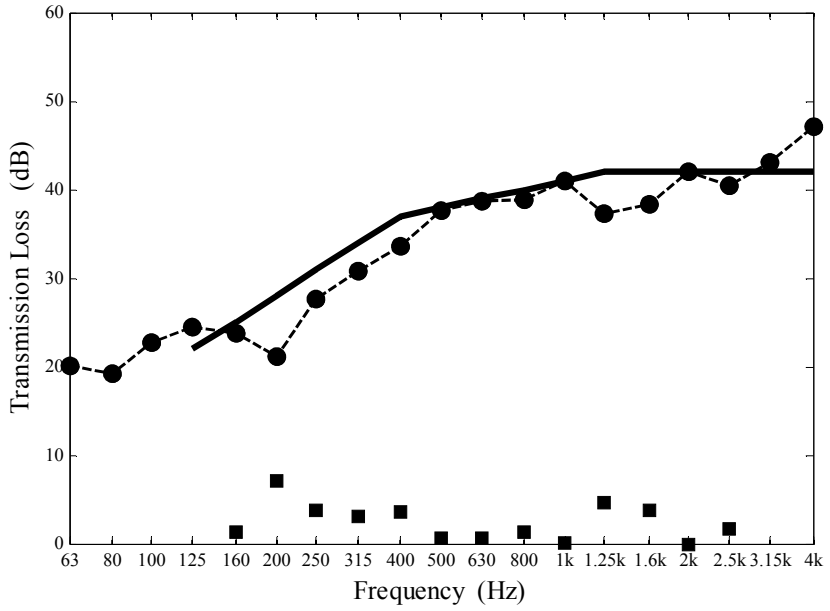

Figure 0.5: Sound transmission loss vs. frequency, Window E.
Transmission loss (●--); STC = 38 dB curve (—); STC deficiency (■); OITC = 30 dB.

By comparing low frequency sound transmission loss within groups and across groups it can be seen that a high STC rating does not ensure good low frequency performance or good OITC rating. All five windows had similar OITC ratings despite significantly better transmission loss for windows A and B above 160 Hz. The one-third octave band transmission loss values for all five high-performance windows are shown in Figure 0.6.

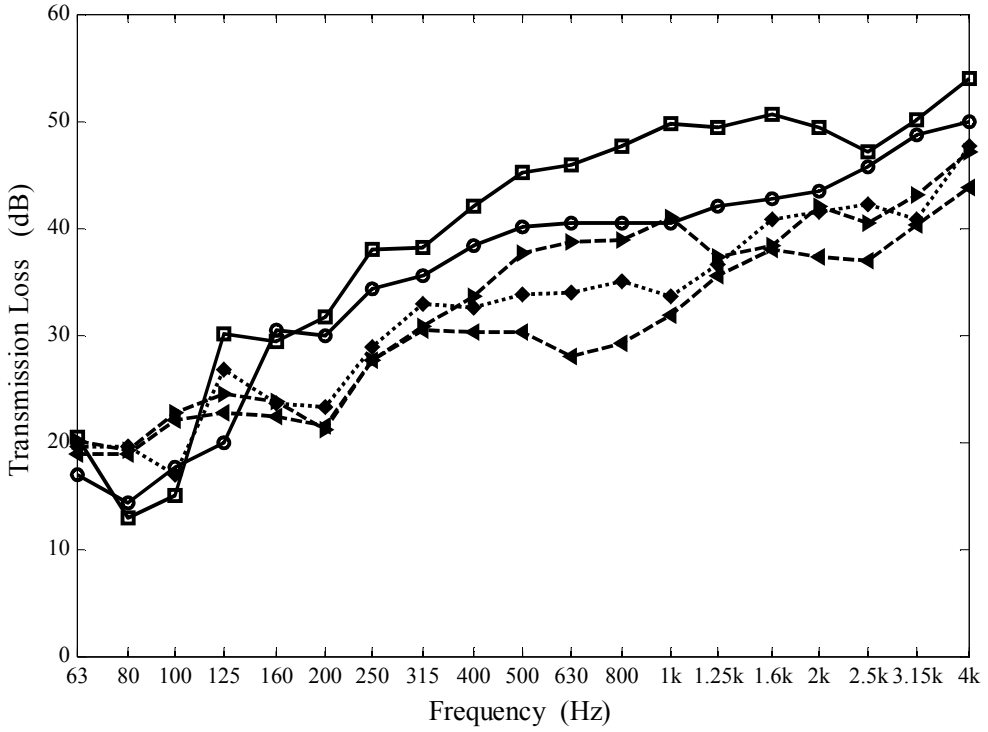

Figure 0.6: Transmission loss of five high-performance windows. Window A (o-), Window B (□-), Window C (♦..), Window D (◄--), Window E (►--).

The transmission loss of the ultra-high-performance group (Windows A and B) is consistently higher than the high-performance group (Windows C, D, and E) at frequencies above 125 Hz. It is understandable that Windows A and B have higher STC rating because the STC calculation includes transmission loss data in the frequency range 125-4000 Hz. However, below 125 Hz the transmission loss of the ultra-high-performance group was as much as 7 dB less than the transmission loss of the high-performance group. For the five windows tested in

this investigation, the ultra-high-performance windows were consistently poorer than the high-performance windows in the 80 and 100 Hz bands.

Resonant Transmission Loss

It is useful to identify the natural frequencies of the test windows in this investigation. The natural frequencies can be estimated from theoretical calculations of a thin, uniform panel. The low-order natural frequencies for a simply-supported, thin plate is [16],

$$f_{m,n} = \sqrt{\frac{\pi^2 D}{4m''}}\left[\left(m/L_x\right)^2 + \left(n/L_y\right)^2\right], \qquad (2.2)$$

where $D = Eh^3/12\left(1-\upsilon^2\right)$ is the bending stiffness and *m"* is the mass per unit area.

The natural frequencies of several low-order modes are shown in Table 0.5 for free-free, simply-supported and clamped-clamped boundary conditions. The free-free and clamped-clamped boundary conditions are determined from Leissa [20]. The window properties used to calculate the theoretical natural frequencies are given in Table 0.4.

Table 0.4: Window properties for calculating theoretical natural frequencies of a solid, thin glass plate.

Window Properties			
Variable	*Value*	*Unit*	*Description*
L_x	1.22	m	x-dimension
L_y	1.22	m	y-dimension
h	7	mm	Thickness
ρ	25	kg/m^3	Density
E	6.77 x 10^{10}	N/m^2	Young's Modulus
ν	0.24	--	Poisson's Ratio

Table 0.5: Theoretical natural frequencies (Hz) of a solid, thin glass plate of size 1.22 m x 1.22 m (48 in x 48 in) for low order modes below 300 Hz.

Free-Free		*Simply Supported*		*Clamped-Clamped*	
Mode	Hz	Mode	Hz	Mode	Hz
(0,0)	0	(1,1)	7	(1,1)	13
(0,1)	0	(1,2)	18	(1,2)	26
(1,1)	5	(2,2)	28	(2,2)	39
(0,2)	8	(1,3)	35	(1,3)	47
(1,2)	14	(2,3)	45	(2,3)	59
(0,3)	22	(1,4)	60	(1,4)	75
(2,2)	25	(3,3)	63	(3,3)	79
(1,3)	27	(2,4)	70	(2,4)	87
(2,3)	41	(3,4)	88	(3,4)	106
(0,4)	43	(1,5)	91	(1,5)	111
(1,4)	48	(2,5)	102	(2,5)	122
(3,3)	59	(4,4)	112	(4,4)	132
(2,4)	62	(3,5)	120	(3,5)	141
(0,5)	71	(1,6)	130	(1,6)	153
(1,5)	76	(2,6)	141	(2,6)	164
(3,4)	81	(4,5)	144	(4,5)	167
(2,5)	90	(3,6)	158	(3,6)	183
(4,4)	106	(5,5),(1,7)	176	(5,5)	201
(0,6)	107	(4,6)	183	(1,7)	202
(3,5)	110	(2,7)	187	(4,6)	209
(1,6)	111	(3,7)	204	(2,7)	213
(2,6)	125	(5,6)	214	(3,7)	232
(3,6)	146	(1,8),(4,7)	229	(5,6)	242
(0,7)	148	(2,8)	240	(4,7)	258
(1,7)	153	(6,6)	254	(1,8)	259
(2,7)	167	(3,8)	257	(2,8)	270
(3,7)	188	(5,7)	261	(6,6)	283
(0,8)	198	(4,8)	281	(3,8)	288
(1,8)	202	(1,9)	289	(5,7)	291
(5,6)	205	(2,9)	299		
(4,7)	215				
(2,8)	216				
(3,8)	237				
(5,7)	248				
(0,9)	254				
(1,9)	258				
(2,9)	272				
(6,7)	287				
(3,9)	294				
(5,8)	299				

From the theoretical natural frequencies it is reasonable to assume that the resonant region of the windows is between 15 and 200 Hz.

The measured transmission loss and vibration response for each window for both the SALT facility test and mobility test are shown in Figure 0.7 through Figure 0.11. The acceleration level, narrow band and one-third octave band transmission loss were measured at the SALT facility. The average acceleration level, L_{accl}, is the average level of all eight accelerometers measured at the SALT facility.

$$L_{accl} = 10\log_{10} \sum_{q} G_{aa,q} \Big/ N_q \,, \tag{2.3}$$

where G_{aa} is the power spectral density (auto-spectra) for the accelerometer and q is the accelerometer indices. There was eight accelerometers on the window for the SALT facility measurements (refer to Figure 0.9), thus $N_q = 8$.

The accelerance level was measured at Herrick Labs during the mobility test. The average accelerance level, L_a, is the average of the magnitude of the cross-mobilities, a_{ij}, $i \neq j$ from the mobility tests and excludes the drive-point accelerance, a_{ij}, $i = j$.

$$L_a = 20\log_{10} \frac{\sum_{i}\sum_{j} \left| a_{ij} \right|}{(ij - i)}, \quad i \neq j \,, \tag{2.4}$$

where i is the accelerance index for hit location and j is the index for measurement location. There was six accelerometers on the windows for the mobility measurement (refer to Figure 0.10), thus $i = j = 6$. The mass-law transmission loss curve was calculated from equation (2.1). It is important to note that the accelerometer locations were different for the SALT facility measurements and the mobility test (refer to Figure 0.9 and Figure 0.10). Because a relatively small number of accelerometers were used (eight accelerometers for the SALT facility test and six for the mobility test) the measured acceleration response was "blind" to some modes. The accelerometers were placed away from nodal lines of the lowest order modes to minimize this effect. Also, because the accelerometers were placed at different locations for the two tests the average acceleration level and average accelerance level were each "blind" to different modes. This phenomenon occurs for Window B between 80 and 100 Hz. The average acceleration level and the accelerance level are representative of different excitation mechanisms. The windows were acoustically loaded for the SALT facility measurements, while the windows were forced, impact excitation for the mobility test. Because Window A had four independent sliding glass

panels a mobility measurement was difficult and thus it was not measured during the mobility test.

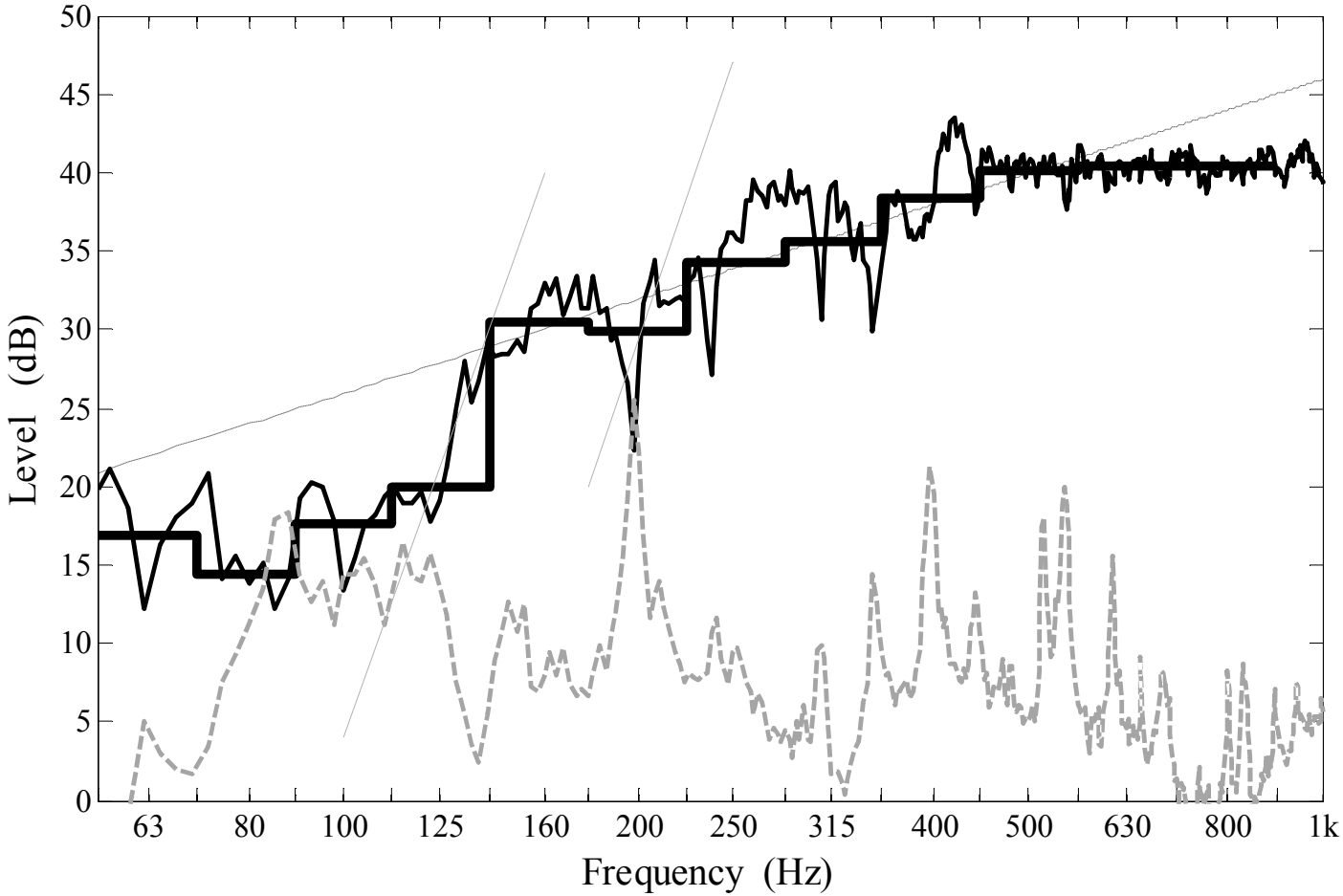

Figure 0.7: Window A sound transmission loss (TL) and acceleration level vs. frequency; narrow-band TL (—), one-third octave band TL (**—**), and mass-law TL (..), average acceleration level (--), 18 dB/octave trend-line (—).

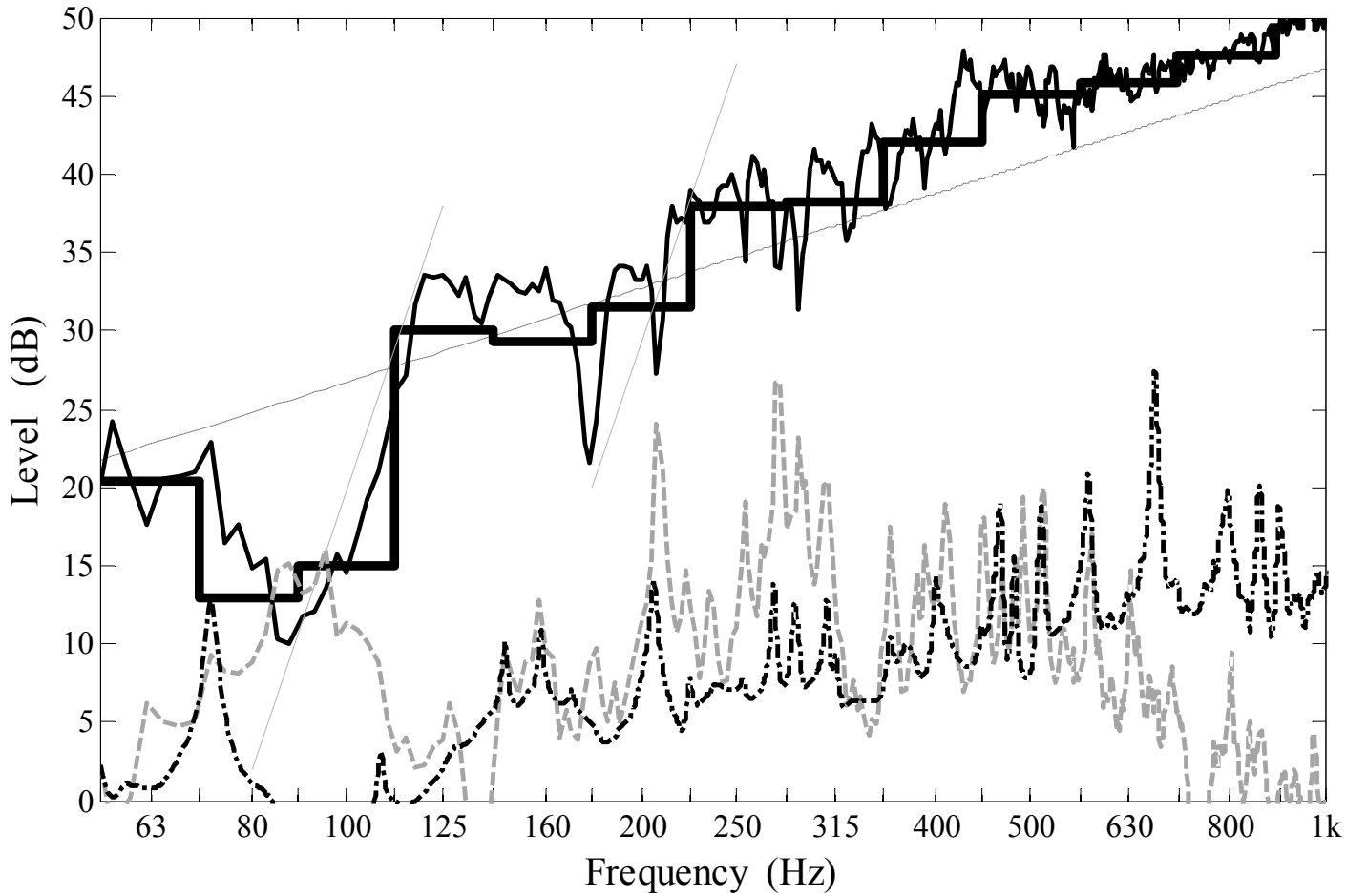

Figure 0.8: Window B sound transmission loss (TL) and acceleration level vs. frequency; narrow-band TL (—), one-third octave band TL (**—**), mass-law TL (..), average acceleration level (--), average accelerance level (-.-), 18 dB/octave trend-line (—).

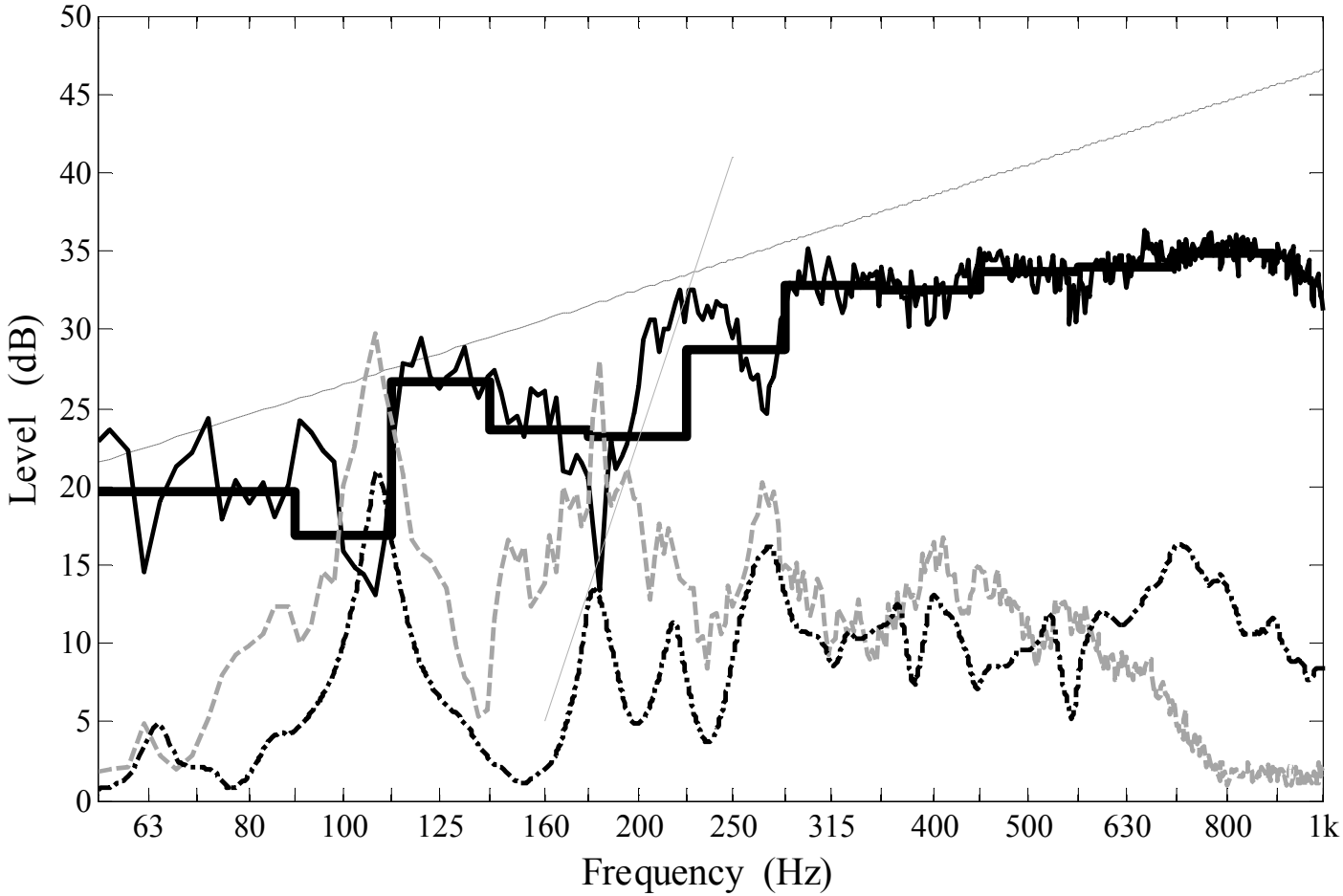

Figure 0.9: Window C sound transmission loss (TL) and acceleration level vs. frequency; narrow-band TL (—), one-third octave band TL (**—**), mass-law TL (..), average acceleration level (--), average accelerance level (-.-), 18 dB/octave trend-line (—).

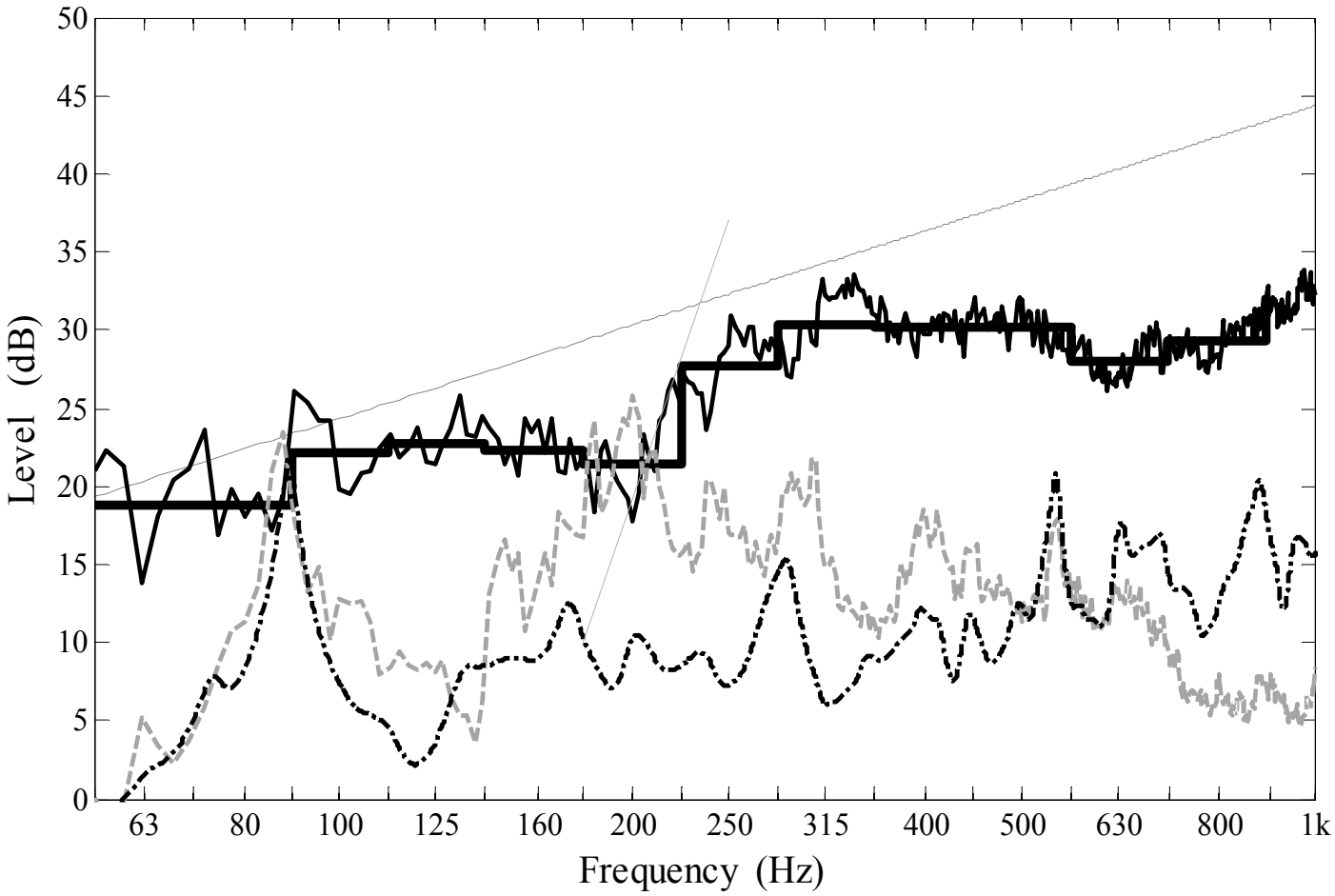

Figure 0.10: Window D sound transmission loss (TL) and acceleration level vs. frequency; narrow-band TL (—), one-third octave band TL (**—**), mass-law TL (..), average acceleration level (--), average accelerance level (-.-), 18 dB/octave trend-line (—).

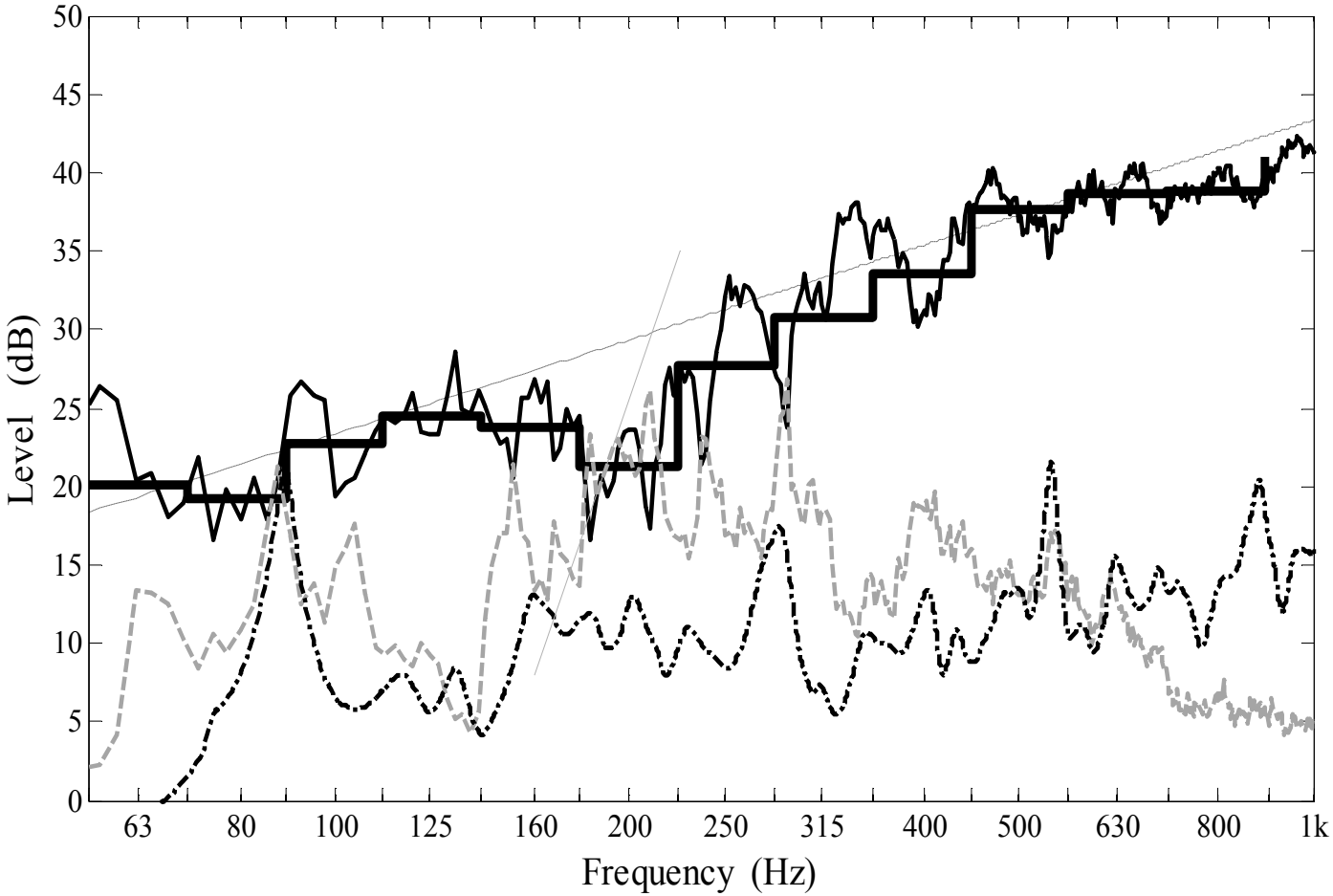

Figure 0.11: Window E sound transmission loss (TL) and acceleration level vs. frequency; narrow-band TL (—), one-third octave band TL (**—**), mass-law TL (..), average acceleration level (--), average accelerance level (-.-), 18 dB/octave trend-line (—).

In Figure 0.7 through Figure 0.11 the average acceleration level and the accelerance level are consistent, as expected. Also, regions of increased acceleration and accelerance response ("peaks") correspond to a decrease in transmission loss ("dips"). For example, this phenomenon occurs for Window C in Figure 0.9 at 63, 85, 107, 180, and 270 Hz. The resonant response of the window corresponds to decreased transmission loss at the resonance frequencies.

The mass-air-mass resonance is a well-known phenomenon in multi-panel structures, where the air space acts as compliance between the masses of two of the glass panels. The mass-air-mass resonant frequency, f_m, is approximately determined by [21]:

$$f_m = \left[\frac{\rho_0 c_0^2}{4\pi^2 d} \left(\frac{m_1 + m_2}{m_1 m_2} \right) \right]^{1/2} \tag{2.5}$$

where m_1 and m_2 are the masses of two of the glass panels, d is the depth of the air space between the glass panels, and ρ_0 and c_0 are the density and speed of sound, respectively.

The double pane windows (C, D, and E) will have one mass-air-mass resonance. The triple pane windows (A and B) could have three distinct mass-air-mass resonances. A crude estimate of these resonances can be made by assuming only two of the panels interact with each other simultaneously. This assumes the third panel is passive. If the individual panes of glass in the triple pane windows were labeled (1), (2), and (3) then mass-air-mass resonances could exist between (1)-(2), (2)-(3), and (1)-(3). The mass of each window was measured and is tabulated in Table 0.1. The mass of each individual glass pane could not be determined because the windows were manufactured as a single-piece unit. Thus, the mass of the individual panes was estimated as a fraction of the total window unit mass and the glass thickness. The estimated mass-air-mass resonances for each test window, as calculated by equation (2.5), are tabulated in Table 0.6.

Table 0.6: Estimated mass-air-mass resonances for five test windows.

Mass-Air-Mass Resonant Frequencies	
Window	*Frequency* (Hz)
A	115, 125, 200
B	85, 95, 208
C	180
D	200
E	183

Theory predicts that for the frequencies immediately following the mass-air-mass resonance the transmission loss increases at 18 dB/octave [21]. Trend-lines following this 18 dB/octave increase have been plotted in Figure 0.7 through Figure 0.11 to highlight the mass-air-mass resonances. Only two trend-lines have been plotted for the triple pane windows (A and B). The trend-line following the lowest mass-air-mass resonance has been omitted. The effect of the lowest two mass-air-mass resonances is noticed by a wider "dip" in transmission loss between the two resonances. It is evident that both flexural resonances and mass-air-mass resonances contribute to the decrease of transmission loss at low frequencies.

To further demonstrate the resonant behavior of the windows at low frequencies, the particle velocity magnitude level, L_u, normal signed sound intensity level, L_{In}, sound pressure level, L_p, and pressure-residual intensity index, δ_{pIo}, are plotted for window C. The particle velocity magnitude is given by the spectral formulation [22]:

$$|u|^2 = G_{uu} = \left(G_{11} + G_{22} - 2\,\mathrm{Re}\,G_{12}\right) \Big/ \left(\rho_0 \omega \Delta\right)^2 , \tag{2.6}$$

where G_{11} and G_{22} are the power spectral density (auto-spectra) of the probe microphones, G_{12} is the cross spectral density (cross-spectra) between the probe microphones, ρ_0 is the density of the fluid (air), ω is the circular frequency, and Δ is the spacer width between the intensity probe microphones. The particle velocity level is given by:

$$L_u = 10 \log_{10} \left(G_{uu} \big/ u_{ref}^2 \right), \tag{2.7}$$

where u_{ref} = 1 mm/s. The sound intensity is given by [11],

$$I_n = -\,\mathrm{Im}\left\{G_{12}\right\} \big/ \rho_0 \omega \Delta , \tag{2.8}$$

and the normal signed sound intensity level is given by [11],

$$L_{In} = \mathrm{sgn}\left(I_n\right) 10 \log_{10}\left(\left|I_n\right| / I_{ref}\right), \tag{2.9}$$

where I_{ref} = 1 pW/m^2. From the normal signed sound intensity level the direction and magnitude of sound energy flow can be determined. The normal unsigned sound intensity level is given by,

$$L_{|In|} = 10 \log_{10}\left(\left|I_n\right| / I_{ref}\right). \tag{2.10}$$

The sound pressure level is given by,

$$L_p = 10 \log_{10}\left(\overline{p}^2 / p_{ref}^2\right), \tag{2.11}$$

where $\overline{p} = \left(\sqrt{G_{11}} + \sqrt{G_{22}}\right)/2$ and p_{ref} = 20 μPa. The press-residual intensity index, δ_{pIo}, is a quality measure of the sound intensity measurement. It is the difference between the sound pressure level at the intensity probe and the normal unsigned intensity level:

$$\delta_{pI_0} = L_p - L_{|I_n|}. \tag{2.12}$$

Large pressure-residual intensity index values indicate a reactive sound field where sound energy is not radiating away from the window but rather is flowing in the plane of the window.

These four metrics are plotted at select resonant frequencies (including the mass-air-mass resonance) and non-resonant frequencies in Figure 0.12 through Figure 0.18. From the transmission loss plot of window C in Figure 0.9 five resonant frequencies were selected (62.5, 107.5, 180, 270, and 400 Hz) and two non-resonant frequencies (72.5 and 140 Hz). The mass-air-mass resonance for window C is at 180 Hz. For similar plots of all five windows at more frequencies refer to Appendices A through E. In Figure 0.12 through Figure 0.18 each shaded rectangular area is representative of an intensity measurement grid-point. The black square line represents the perimeter of the test window, while the region outside the black line represents the sub-frame. An air leak was noticed in the closure mechanism for window C on the left-center side during testing. The effect of the air leak resulted in higher measured values near the source. This is most apparent in the particle velocity measurement.

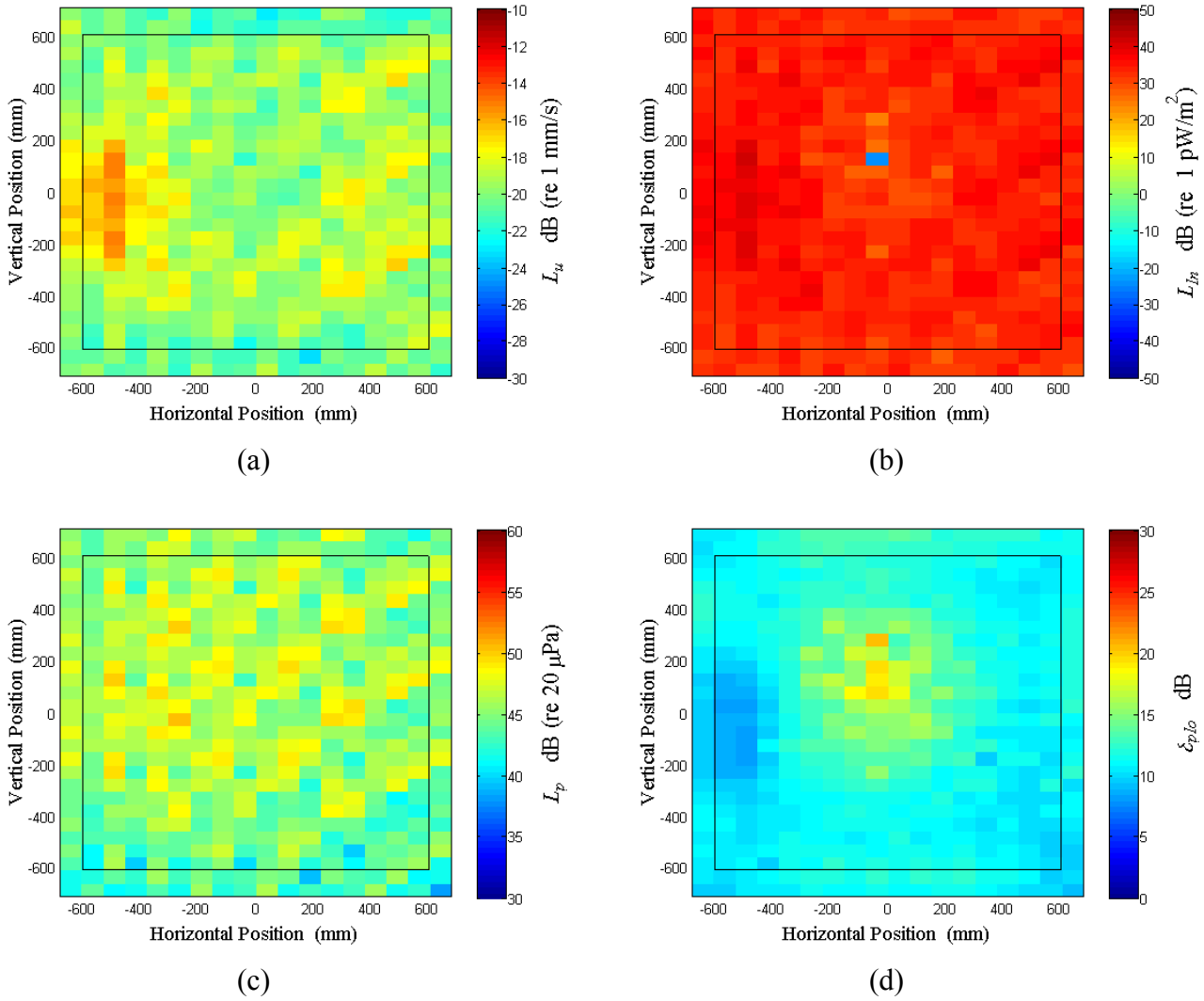

Figure 0.12: Surface scan of Window C at 62.5 Hz (a) particle velocity level, L_u (b) normal signed sound intensity level, L_{In} (c) sound pressure level, L_p (d) pressure-residual intensity index, δ_{pIo}.

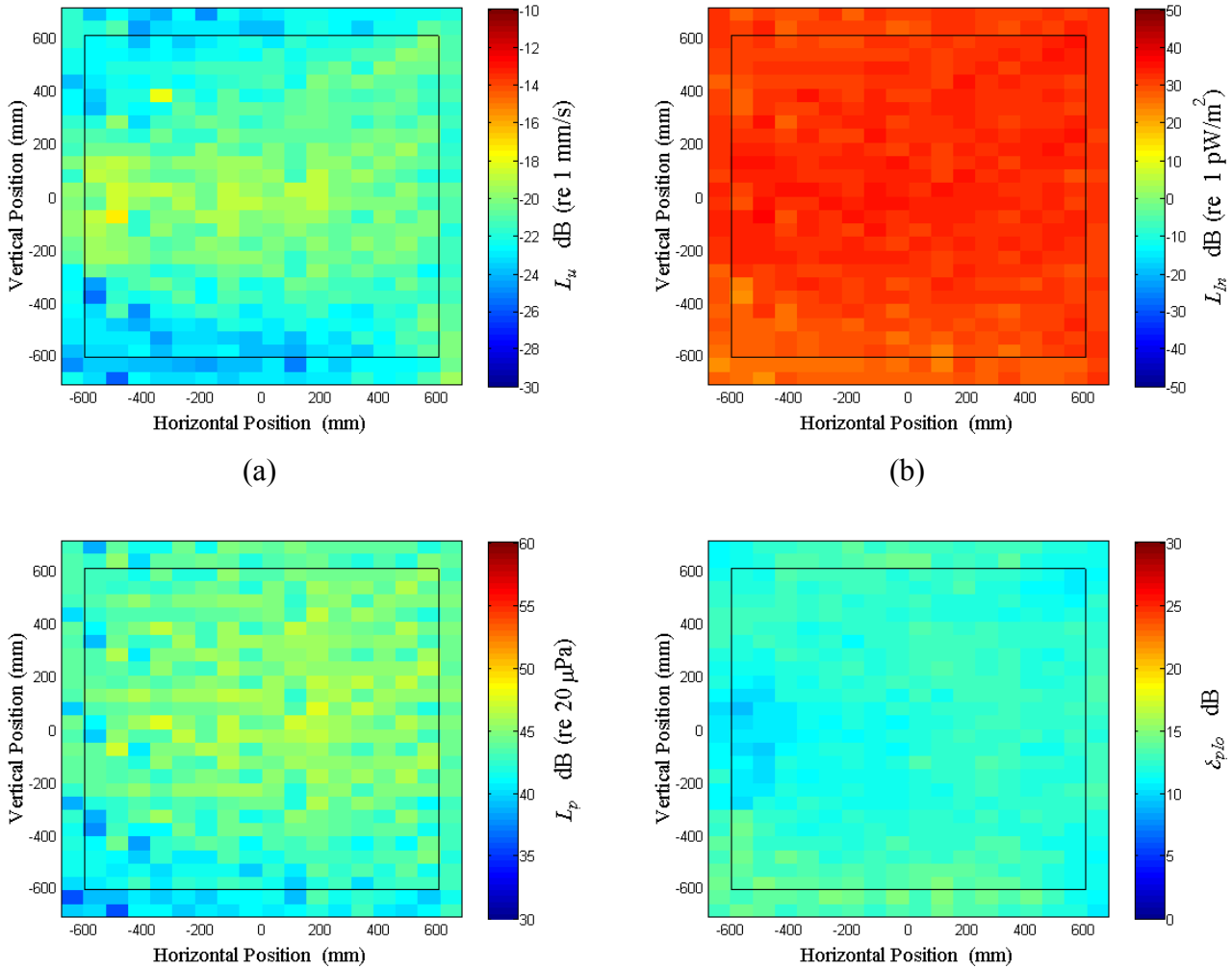

Figure 0.13: Surface scan of Window C at 72.5 Hz (a) particle velocity level, L_u (b) normal signed sound intensity level, L_{In} (c) sound pressure level, L_p (d) pressure-residual intensity index, δ_{pIo}.

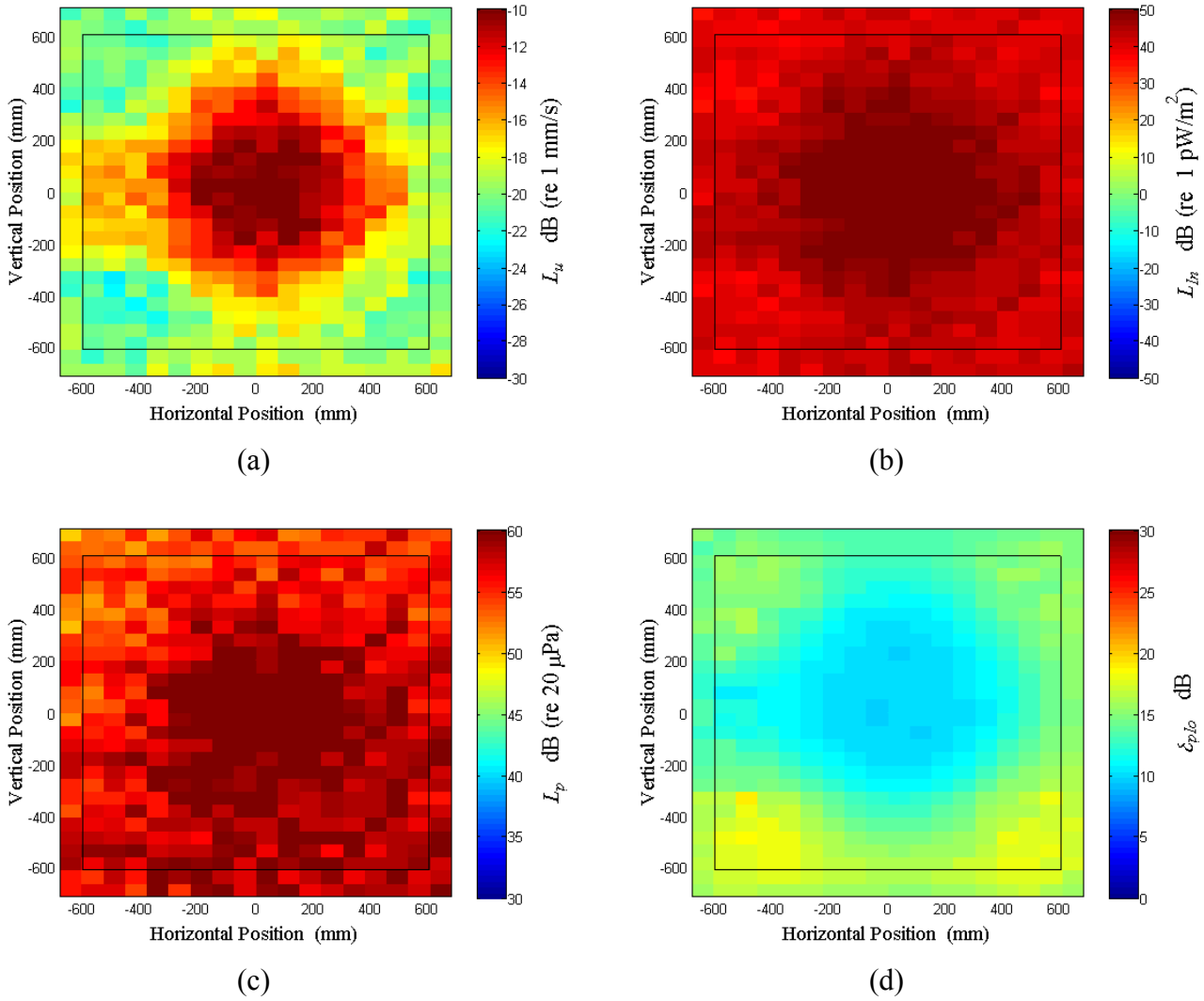

Figure 0.14: Surface scan of Window C at 107.5 Hz (a) particle velocity level, L_u (b) normal signed sound intensity level, L_{In} (c) sound pressure level, L_p (d) pressure-residual intensity index, δ_{pIo}.

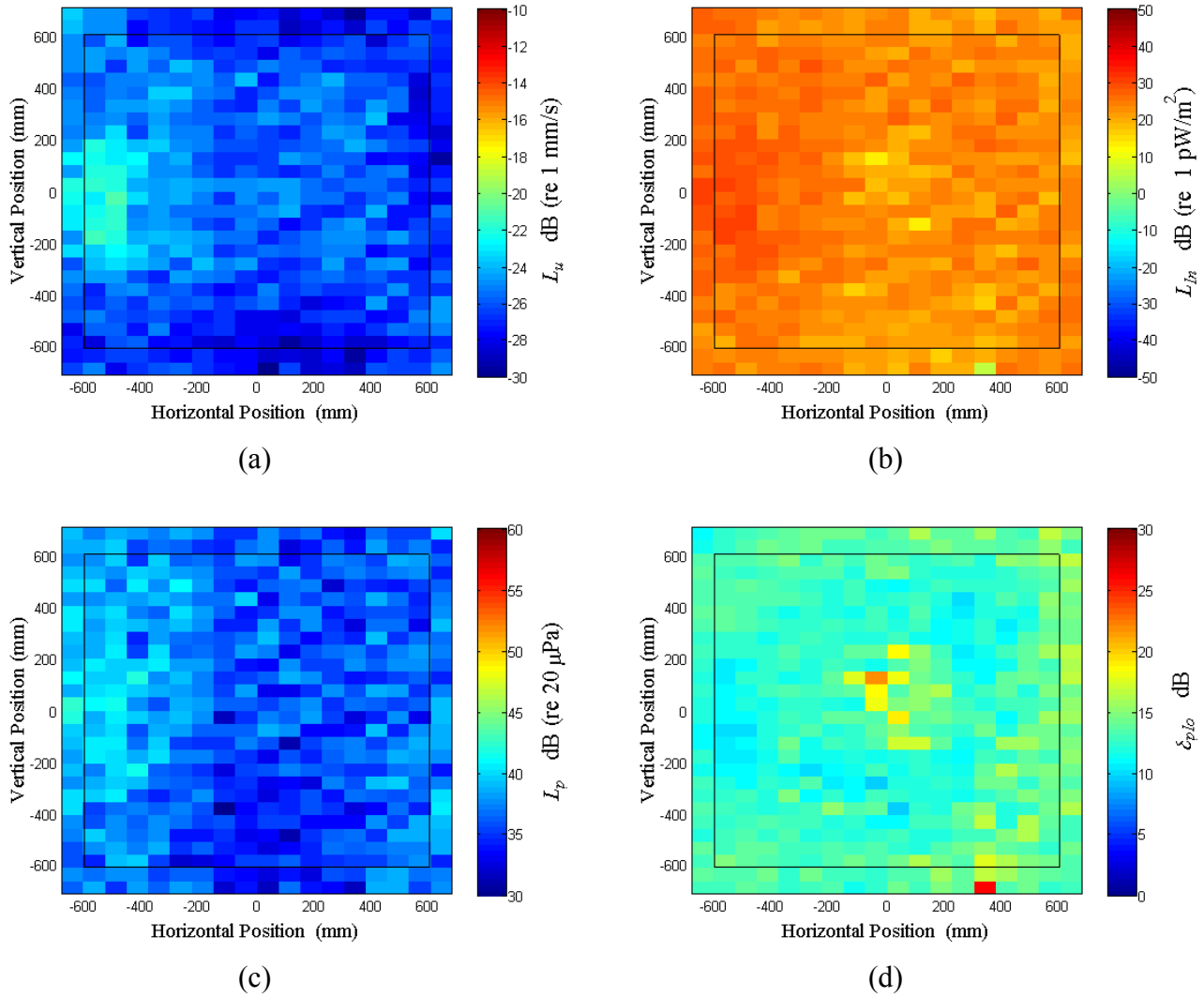

Figure 0.15: Surface scan of Window C at 140 Hz (a) particle velocity level, L_u (b) normal signed sound intensity level, L_{In} (c) sound pressure level, L_p (d) pressure-residual intensity index, δ_{pIo}.

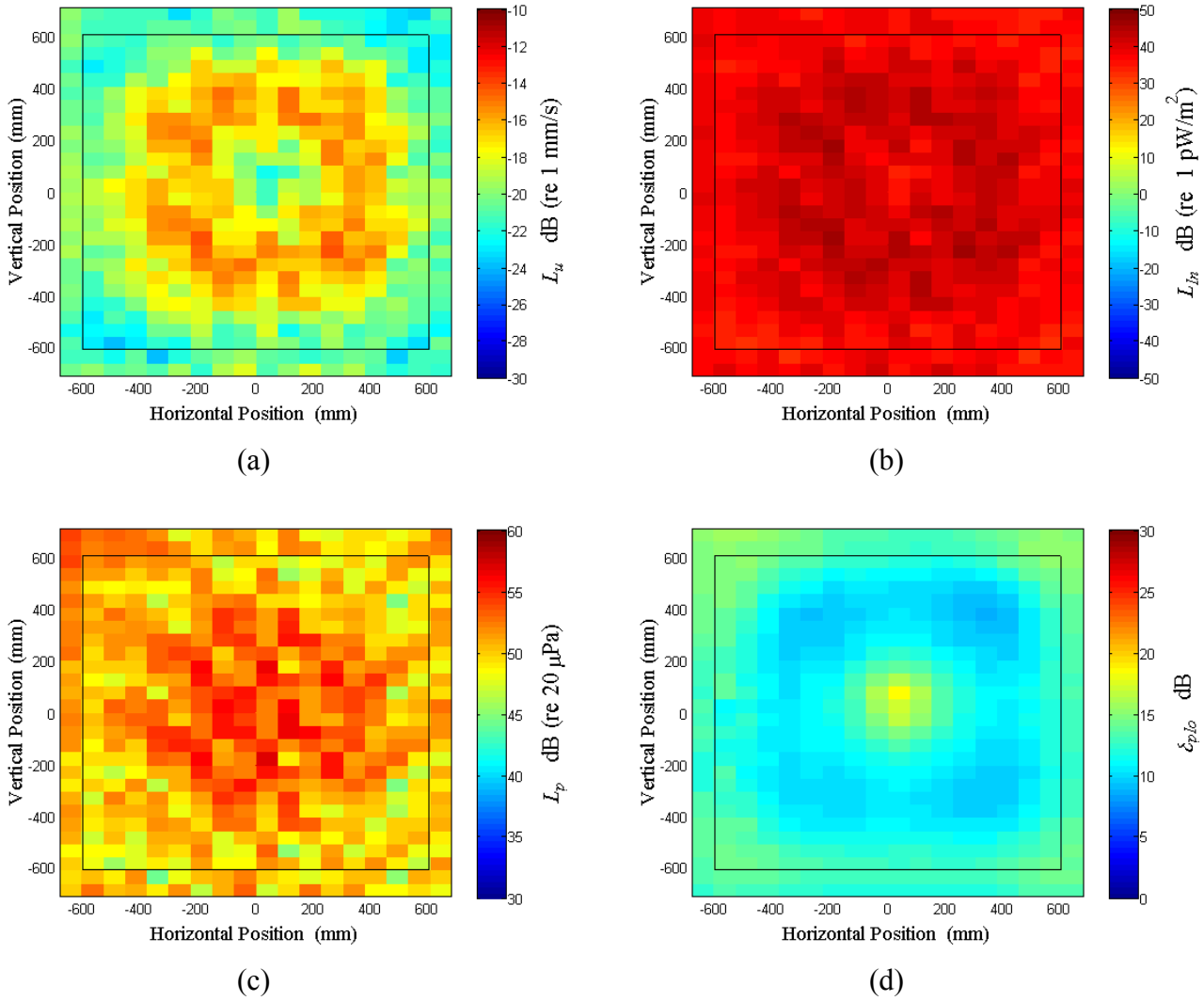

Figure 0.16: Surface scan of Window C at 180 Hz (a) particle velocity level, L_u (b) normal signed sound intensity level, L_{In} (c) sound pressure level, L_p (d) pressure-residual intensity index, δ_{pIo}.

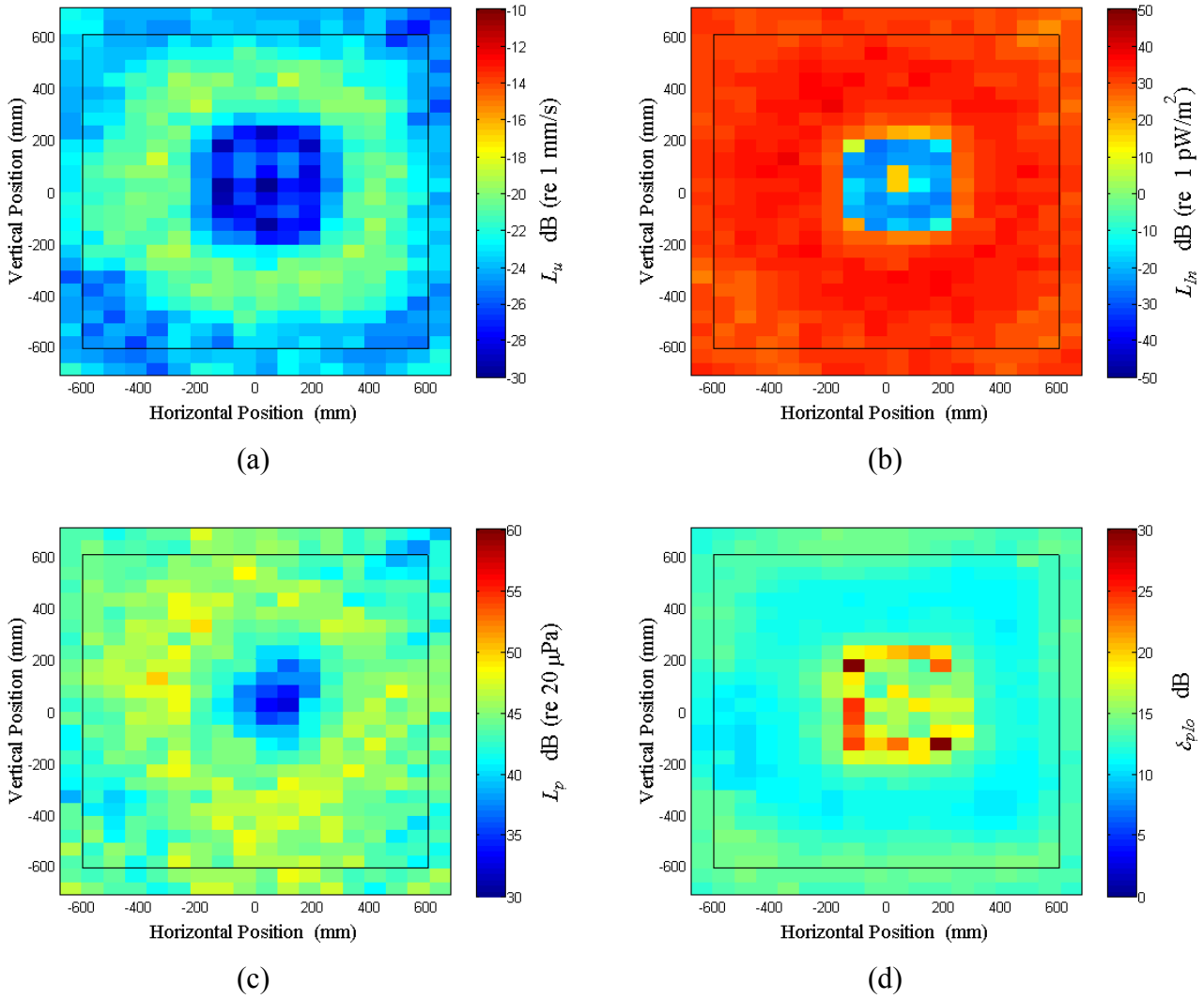

Figure 0.17: Surface scan of Window C at 270 Hz (a) particle velocity level, L_u (b) normal signed sound intensity level, L_{In} (c) sound pressure level, L_p (d) pressure-residual intensity index, δ_{pIo}.

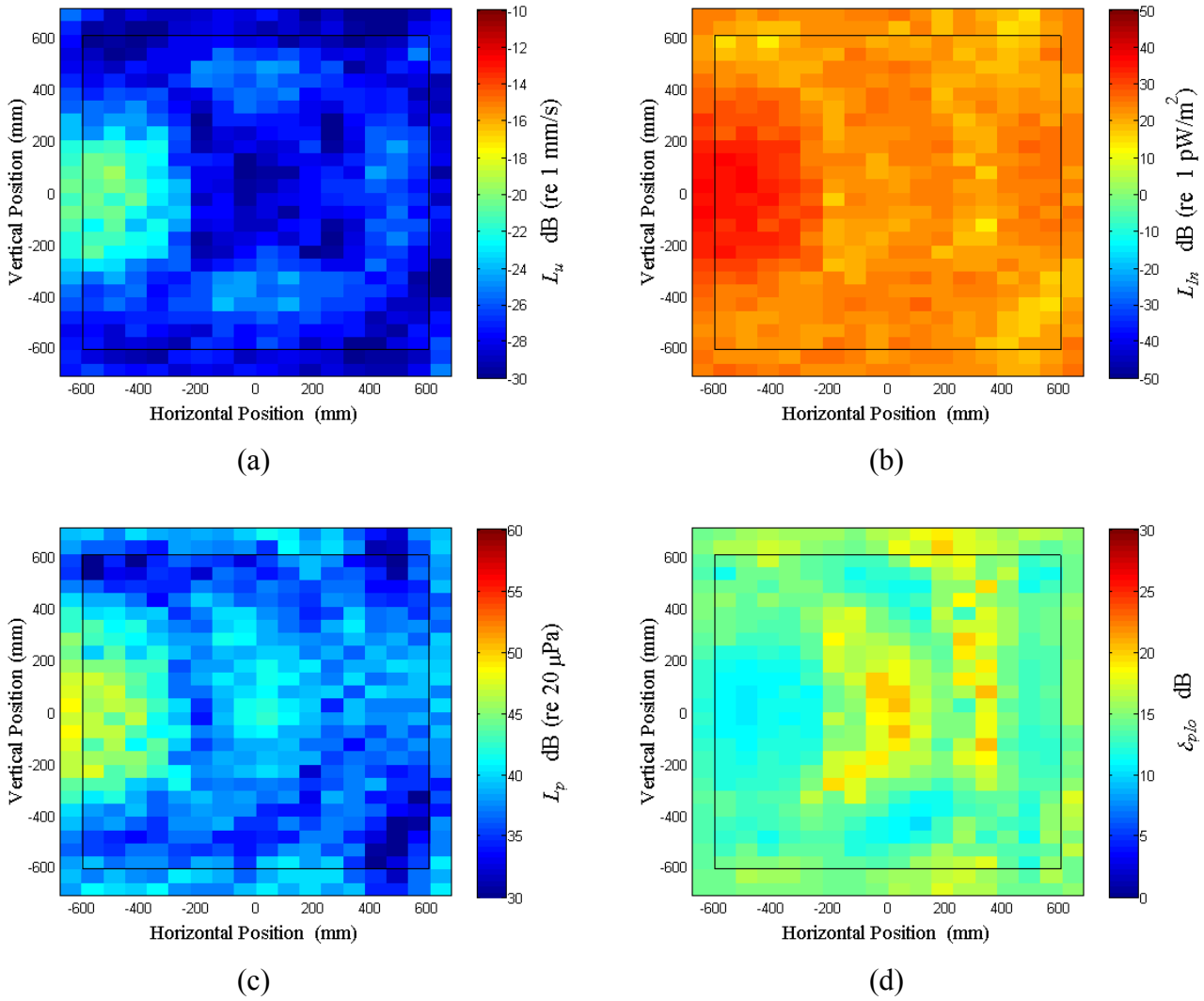

Figure 0.18: Surface scan of Window C at 400 Hz (a) particle velocity level, L_u (b) normal signed sound intensity level, L_{In} (c) sound pressure level, L_p (d) pressure-residual intensity index, δ_{pIo}.

From the particle velocity level plots in Figure 0.12, Figure 0.14, Figure 0.16, Figure 0.17, and Figure 0.18 (62.5, 107.5, 180, 270, and 400 Hz, respectively) distinct standing wave patterns are apparent in the plate. At low modal density, this is generally indicative of a dominant modal response. At the non-resonant frequencies, the vibration pattern has no distinctive standing wave pattern indicating low response and superposition of multiple modes. In each of these five figures the sound intensity level is large indicating large amounts of sound energy radiating from the window, and consequently, low transmission loss at that particular frequency as observed in Figure 0.9. From the particle velocity level plots in Figure 0.13 and Figure 0.15 (72.5 and 140 Hz) no standing wave pattern was observed indicating superposition of multiple modes, e.g. non-resonant behavior. In both of these figures the sound intensity level is relatively small indicating that smaller amounts of sound energy were radiating from the window and consequently higher transmission loss at that particular frequency as observed in Figure 0.9.

These results support the notion that resonant response, for both flexural modes and mass-air-mass resonances, is the cause for decrease in transmission loss in high-performance windows at low frequencies. Both flexural and mass-air-mass resonances caused a decrease in transmission loss and may occur within the same range of frequencies. The mass-air-mass resonance of the triple pane windows appear to have been designed to be below 125 Hz on order to optimize STC ratings but cause reduced performance in the 80 and 100 Hz one-third octave bands and decreased the OITC rating as a result.

SUMMARY AND CONCLUSIONS

The low frequency sound reducing potential of window designs and construction methods with improved low frequency sound transmission loss, such as double and triple pane windows, was assessed. The transmission loss, vibration response, and mobility of five acoustically-rated windows were measured.

It was found that resonant response, including flexural and mass-air-mass resonances of the windows is most likely the cause for decreased transmission loss at low frequencies. Flexural resonant response is damping-controlled and thus minimized by increasing damping of the glass panel in the window. This could be accomplished by constructing the window with laminated glass and/or increasing the effective damping of the seals between the glass panel and the window unit frame. The mass-air-mass resonance is primarily controlled by the mass of the individual glass panels and the distance between them. If possible, these resonances should be shifted by adjusting mass or the depth of the air gaps to optimize window performance.

For the five windows tested in this investigation the HP windows performed better in the 80 and 100 Hz one-third octave bands than the two UHP windows. This is because two mass-air-mass resonances were in the 80 and 100 Hz one-third octave band for both UHP windows. This is a small sample and cannot be generalized to all such windows, but it does illustrate that high Sound Transmission Class (STC) rating does not ensure good low frequency transmission loss performance.

The measured OITC values for all five windows were approximately equivalent. This was because the relatively poor low frequency performance of the UHP windows in the 80 and 100 Hz one-third octave bands was included in the calculation of the OITC rating. Frequency content in the 80 to the 4000 Hz one-third octave bands are included in the calculation of the OITC rating, whereas only frequency content in the 125 to the 4000 Hz one-third octave bands are included in the STC rating. In practice, architects and

contractors often select windows and other exterior elements by STC rating despite the fact that STC is intended to be applied to interior partitions. Had the five windows in this study been selected based on their OITC value, rather than STC, it would have been apparent that their low frequency performance was not exceptional. Thus potential poor low frequency performance is neglected when selection is based on the STC rating rather than the OITC rating. The OITC rating is recommended when selecting exterior elements, such as doors and windows, where low frequency performance is important.

LIST OF REFERENCES

[1] L.L. Beranek (Ed.), *Noise Reduction*, New York, McGraw-Hill, (1947).

[2] L.C. Sutherland, S. Fidell, and A. Harris, Findings of the Low-Frequency Noise Expert Panel of the Rickfield-MAC Mitigation Agreement of 17 December 1998, Volumes I, II, and III, 30 September (2000).

[3] J.D. Quirt, Sound Transmission through Window I. Single and Double Glazing, *Journal of the Acoustical Society of America*, v. 73, n. 3, pp. 834-844, (1982).

[4] J.D. Quirt, Sound Transmission through Windows II. Double and Triple Glazing, *Journal of the Acoustical Society of America*, v. 74, n. 2, pp.534-542, (1983).

[5] F.W. Grosveld, Design and Calibration of the Structural Acoustics Loads and Transmission (SALT) Facility at NASA Langley Research Center, *Unpublished NASA/CR Report*, (2004).

[6] Y.T. Kim, H.C. Kim, S.S. Jung, M.J. Jho, and S.J. Suh, Dependence of Coincidence Frequency in Double-glazed Window on Glass Thickness and Inter-pane Cavity, *Applied Acoustics*, v. 63, pp.927-936, (2002).

[7] ASTM E2112, Standard Practice for Installation of Exterior Windows, Doors and Skylights, American Society for Testing and Materials (ASTM), West Conshohocken, PA, (2001).

[8] Manufacturer Installation Guide, Installation for Finless (Pocket) Vinyl Windows, Jeld-Wen Inc., *JII011*, (2003).

[9] Manufacturer Installation Guide, How to Inspect a Window Installation, Jeld-Wen Inc., *JGI022*, (2004).

[10] Manufacturer Installation Guide, Troubleshooting Operational Problems, Jeld-Wen Inc., *JGI029*, (2005).

[11] ASTM E2249, Standard Test Method for Laboratory Measurement of Airborne Transmission Loss of Building Partitions and Elements Using Sound Intensity, American Society for Testing and Materials (ASTM), West Conshohocken, PA, (2002).

[12] ISO 15186-1, Acoustics—Measurement of Sound Insulation in Buildings and of Building Elements Using Sound Intensity—Part 1: Laboratory Measurements, International Organization for Standardization (ISO), Geneva, (2000).

[13] ISO 15186-3, Acoustics—Measurement of Sound Insulation in Buildings and of Building Elements Using Sound Intensity—Part 3: Laboratory Measurements at

Low Frequencies, International Organization for Standardization (ISO), Geneva, (2002).

[14] ANSI S1.9, Instruments for the Measurement of Sound Intensity, American National Standards Institute (ANSI), New York, NY, (1996).

[15] F.J. Fahy, *Sound Intensity*, Elsevier Applied Science, New York, (1989).

[16] F.J. Fahy, *Sound and Structural Vibration*, Academic Press, New York, (1985).

[17] L. Cremer, M. Heckl, and B.A.T. Petersson, *Structure-Borne Sound*, 3rd Ed., Springer, Berlin, (2005).

[18] ASTM E413, Classification for Rating Sound Insulation, American Society for Testing and Materials (ASTM), West Conshohocken, PA, (2004).

[19] ASTM E1332, Standard Classification for Determination of Outdoor-Indoor Transmission Class, American Society for Testing and Materials (ASTM), West Conshohocken, PA, (2003).

[20] A.W. Leissa, *Vibration of Plates*, 2nd Ed., Acoustical Society of America, (1993).

[21] J.M. Mason and F.J. Fahy, The Use of Acoustically Tuned Resonators to Improve the Sound Transmission Loss of Double-Panel Partitions, *Journal of Sound and Vibration*, v. 124, n. 2, pp. 367-379, (1988).

[22] G.C. Steyer, R. Singh, and D.R. Houser, Alternative Spectral Formulations for Acoustic Velocity Measurement, *Journal of the Acoustical Society of America*, v. 81, n. 6, pp. 1955-1961.

[23] ASTM E966, Standard Guide for Field Measurements of Airborne Sound Insulation of Building Façade Elements, American Society for Testing and Materials (ASTM), West Conshohocken, PA, (2002).

[24] H. Kess, MRIT and X-Modal Users Manual, Purdue University, December, (2004).

[25] V. Hongsito, J. Keränen, and M. Lindgren, Sound Insulation of Doors—Part 2: Comparison Between Measurement Results and Predictions, *Journal of Sound and Vibration*, v. 230, n. 1, pp. 149-170, (2000).

[26] A.J.B. Tadeu and D.M.R. Mateus, Sound Transmission through Single, Double and Triple Glazing. Experimental Evaluation, *Applied Acoustics*, v. 62, pp. 307-325, (2001).

APPENDICES

APPENDIX A. WINDOW A

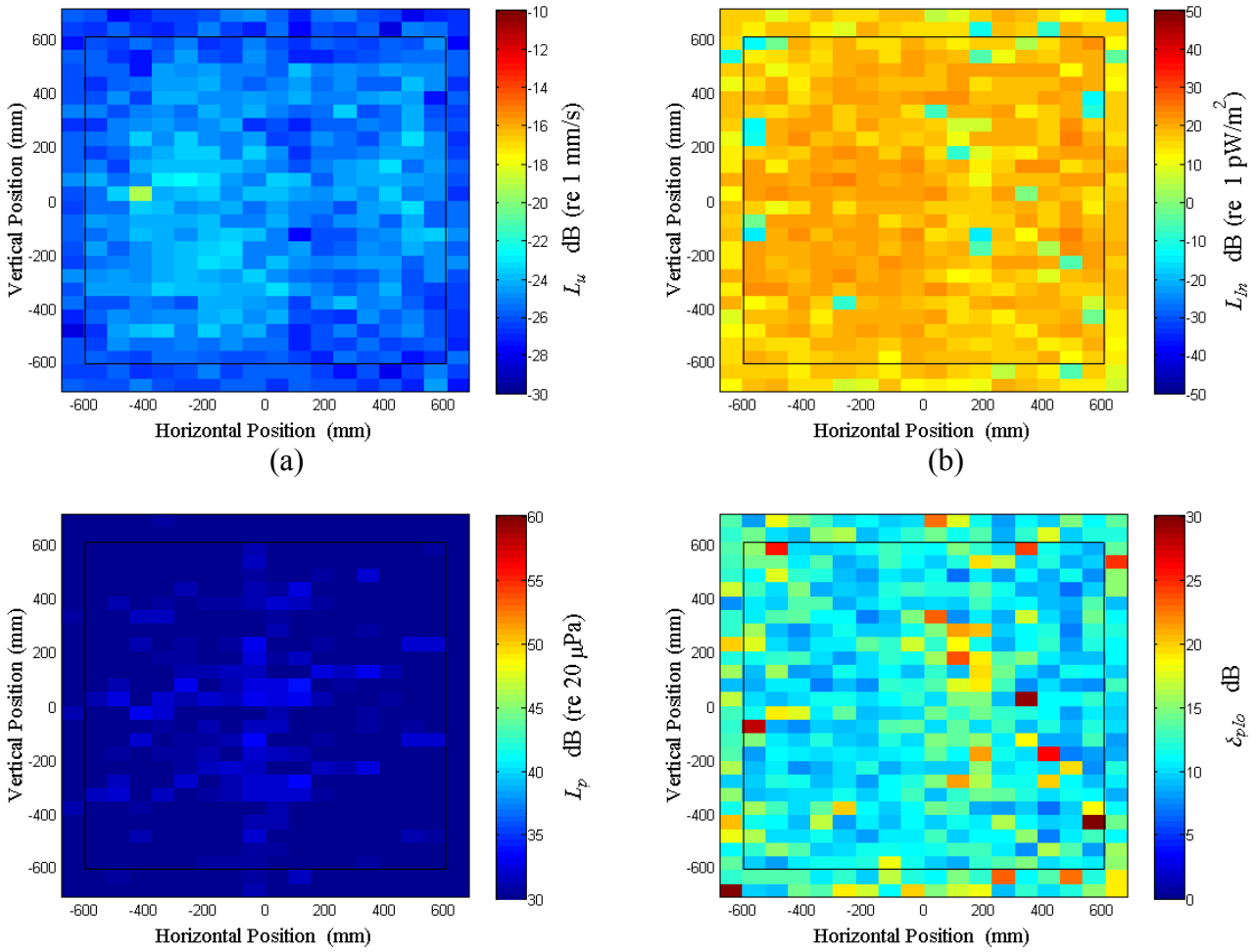

Figure A.1: Surface scan of Window A at 50 Hz (a) particle velocity level, L_u (b) normal signed sound intensity level, L_{In} (c) sound pressure level, L_p (d) pressure-residual intensity index, δ_{pIo}.

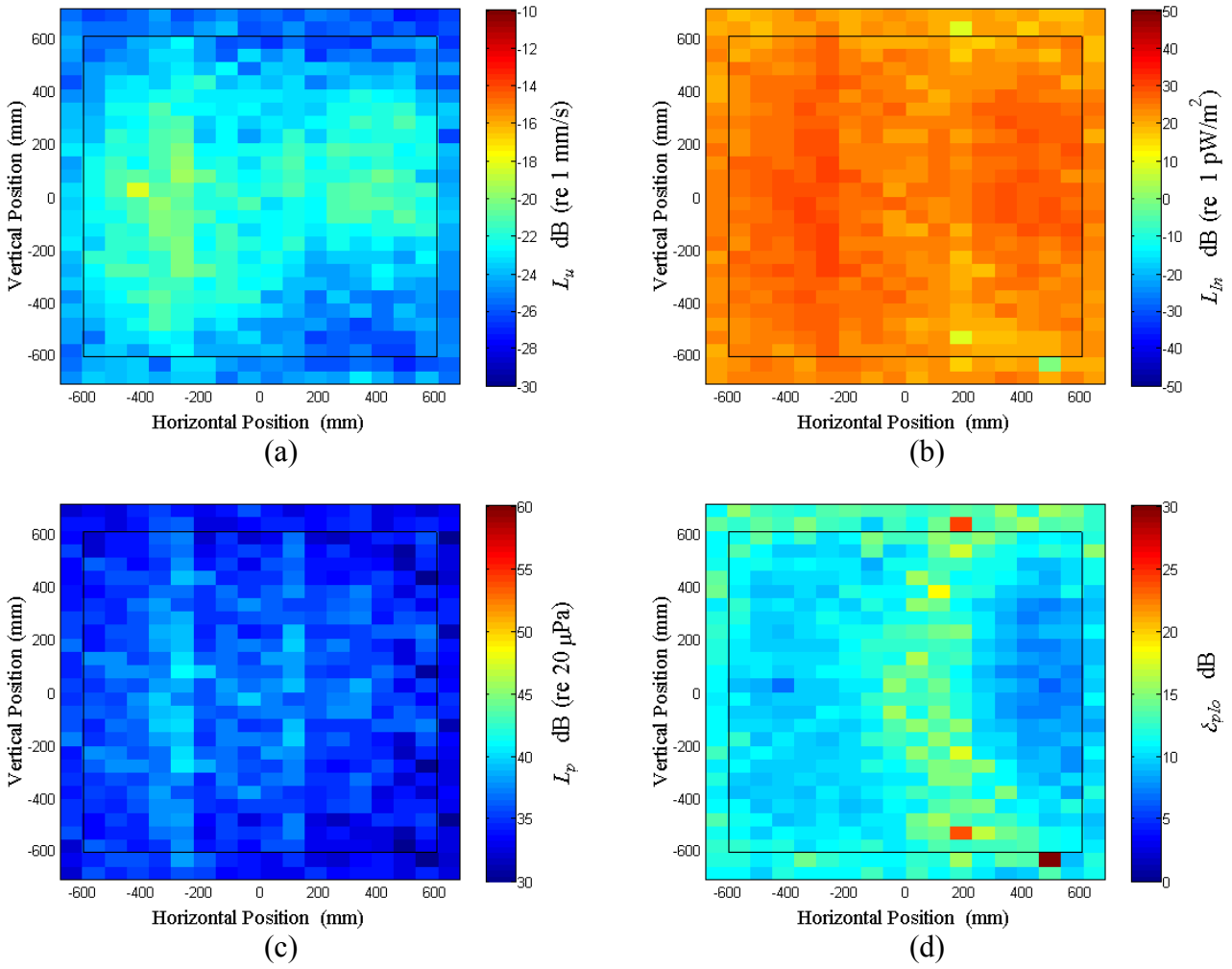

Figure A.2: Surface scan of Window A at 52.5 Hz (a) particle velocity level, L_u (b) normal signed sound intensity level, L_{In} (c) sound pressure level, L_p (d) pressure-residual intensity index, δ_{pIo}.

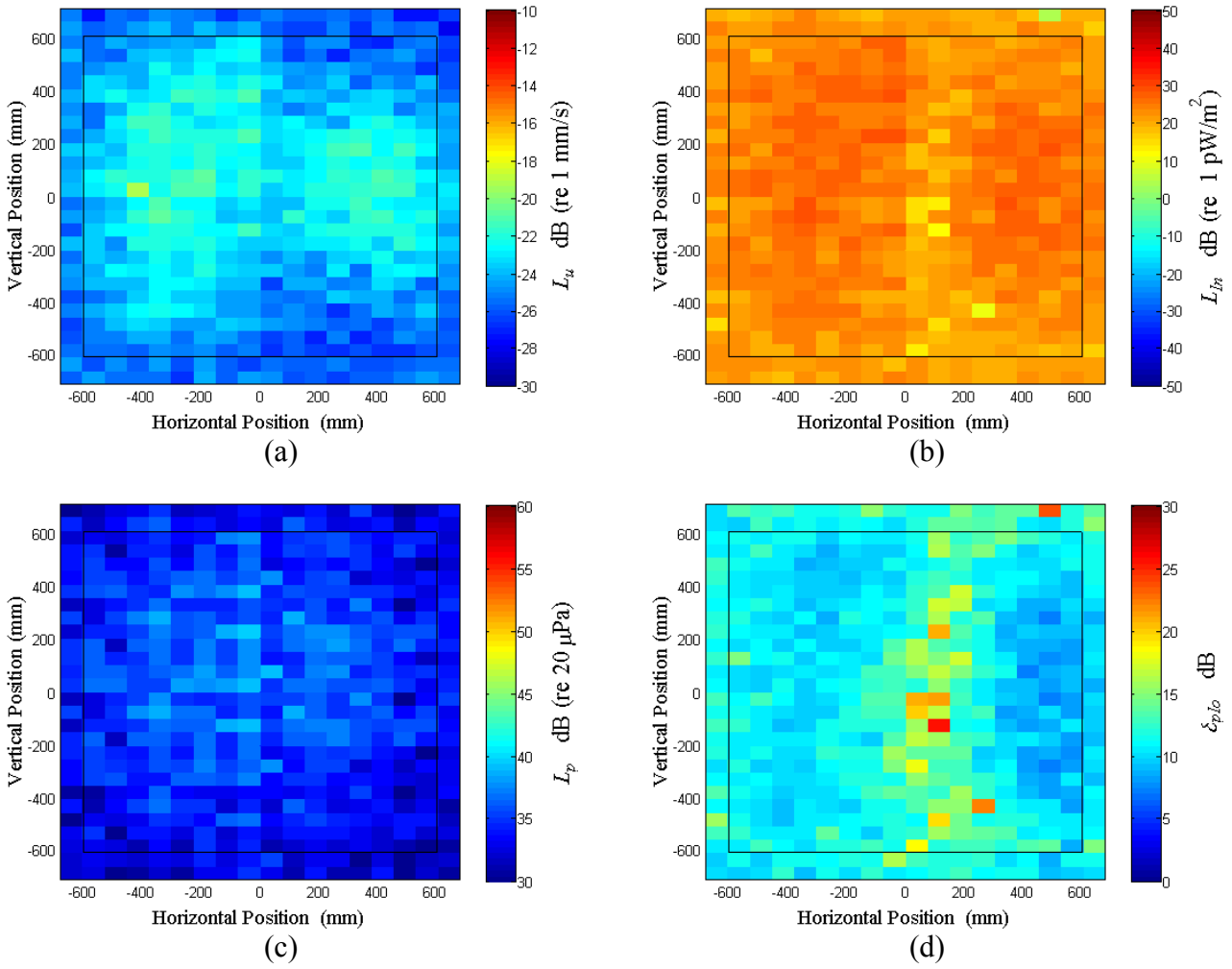

Figure A.3: Surface scan of Window A at 55 Hz (a) particle velocity level, L_u (b) normal signed sound intensity level, L_{In} (c) sound pressure level, L_p (d) pressure-residual intensity index, δ_{pIo}.

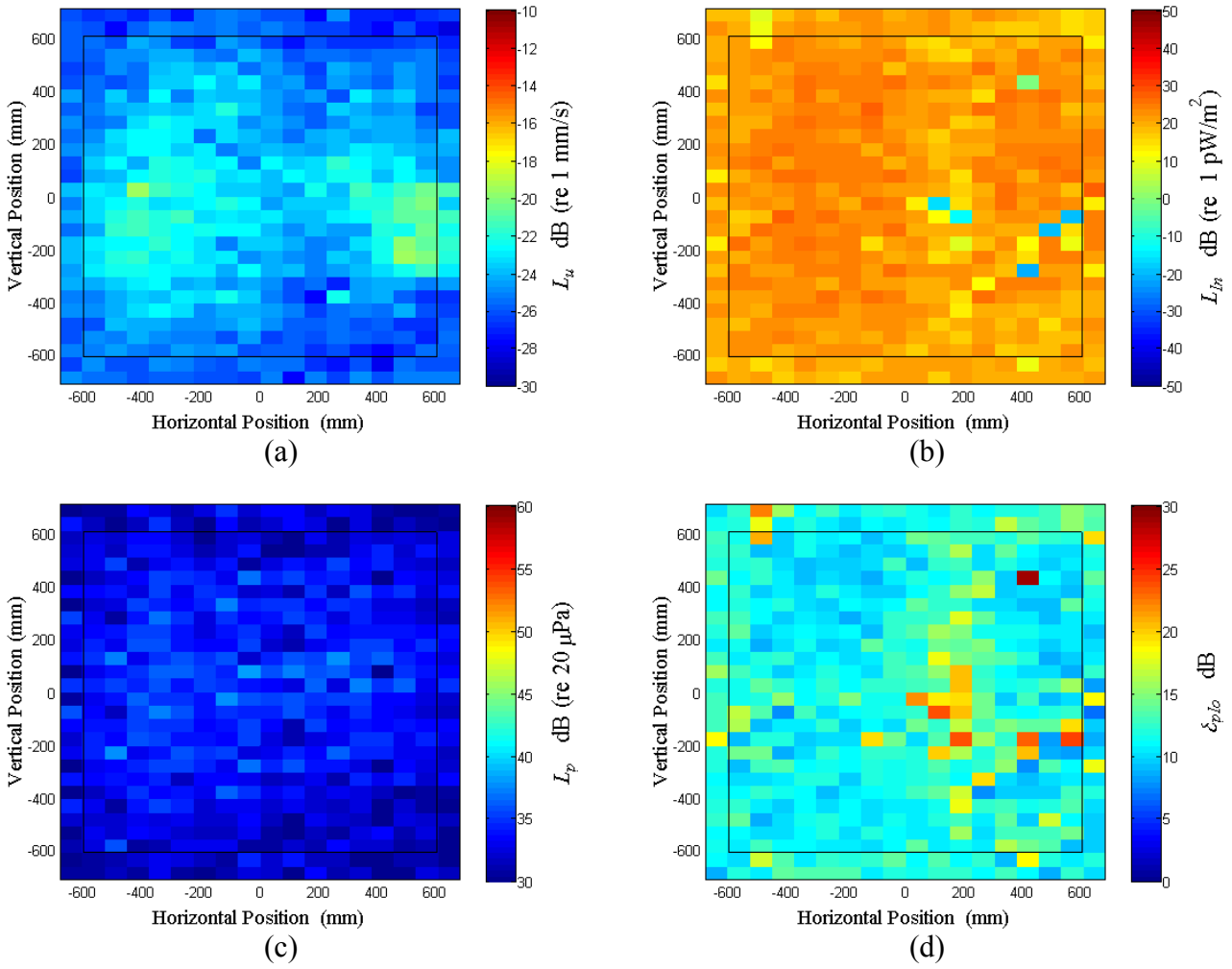

Figure A.4: Surface scan of Window A at 57.5 Hz (a) particle velocity level, L_u (b) normal signed sound intensity level, L_{In} (c) sound pressure level, L_p (d) pressure-residual intensity index, δ_{pIo}.

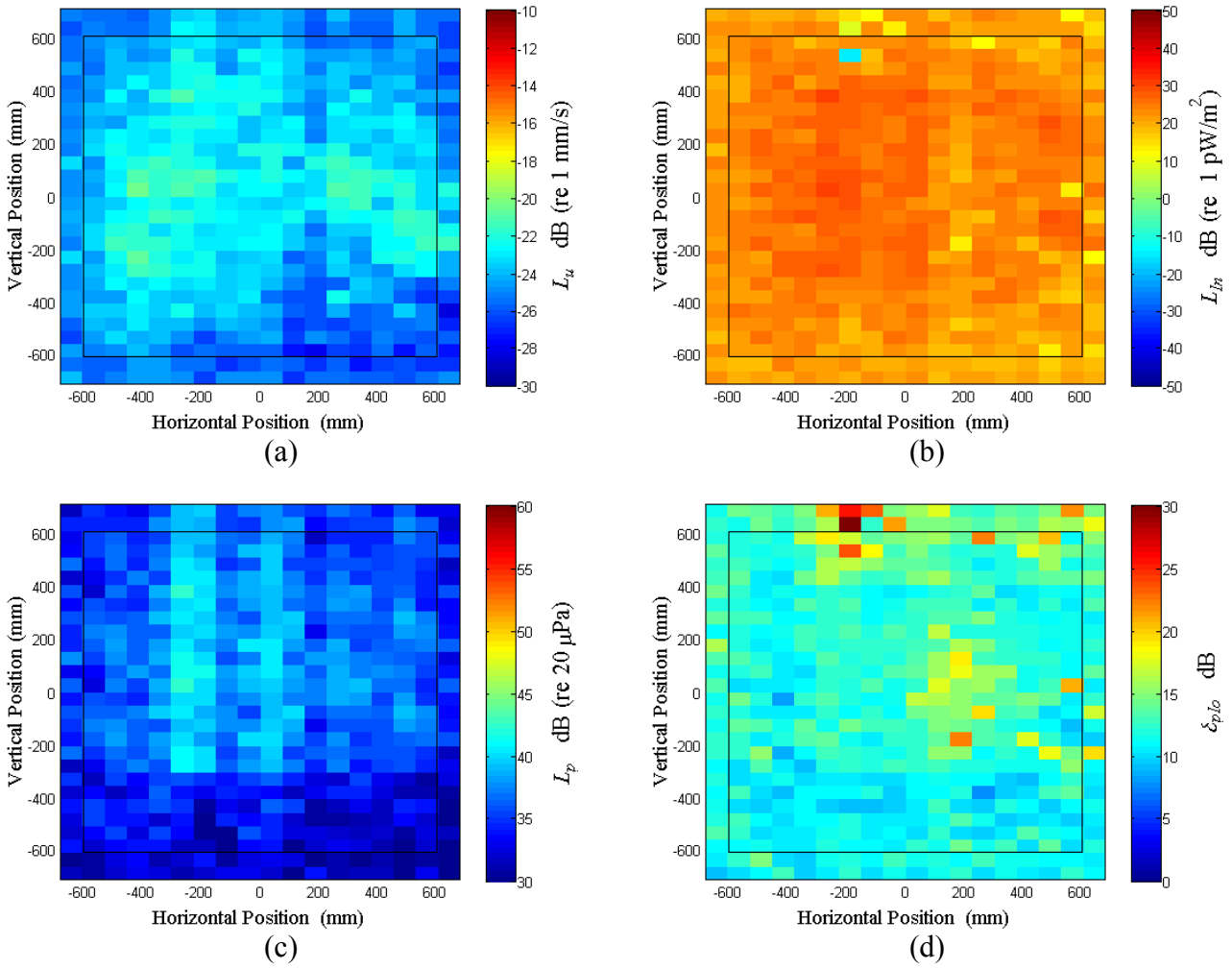

Figure A.5: Surface scan of Window A at 60 Hz (a) particle velocity level, L_u (b) normal signed sound intensity level, L_{In} (c) sound pressure level, L_p (d) pressure-residual intensity index, δ_{pIo}.

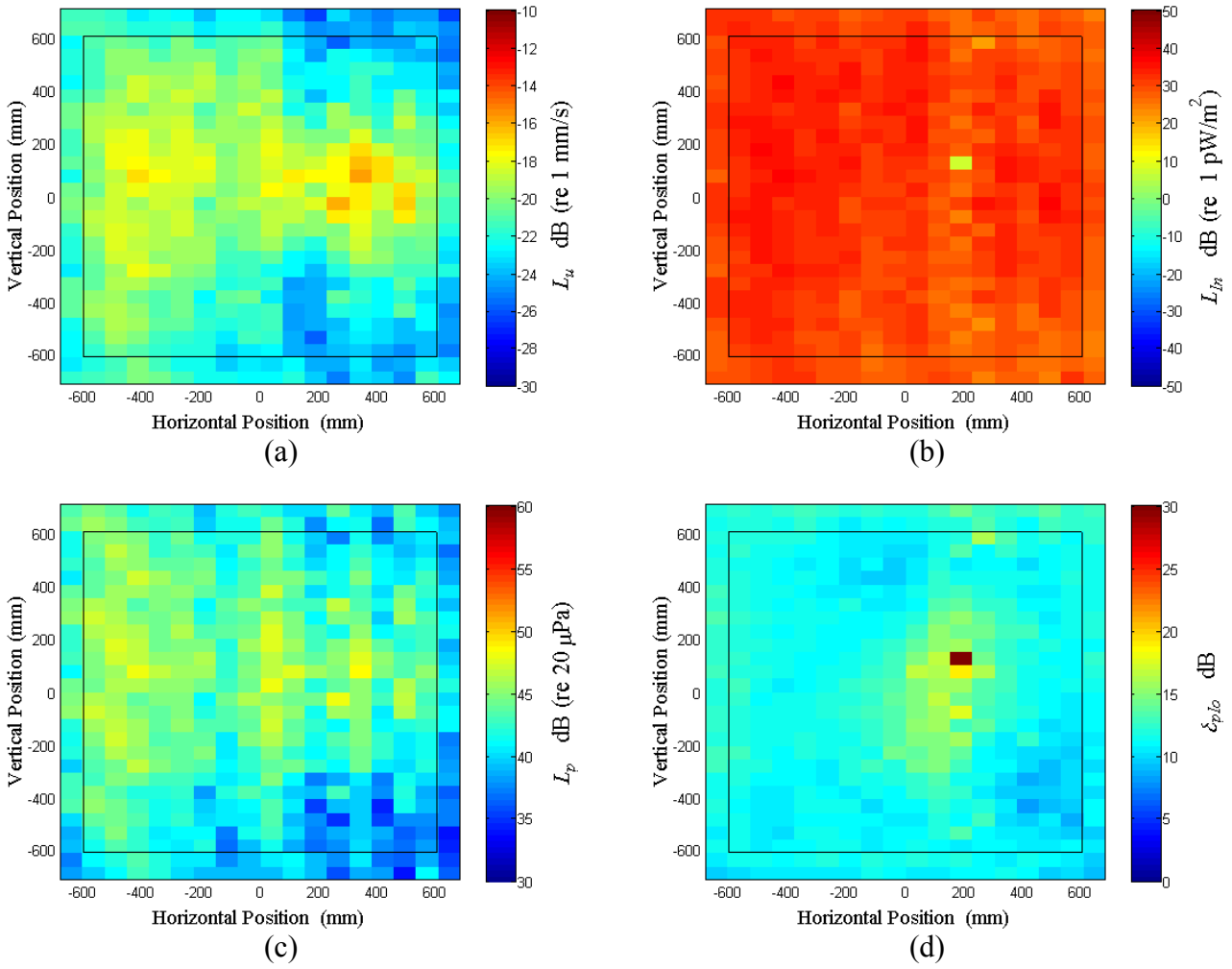

Figure A.6: Surface scan of Window A at 62.5 Hz (a) particle velocity level, L_u (b) normal signed sound intensity level, L_{In} (c) sound pressure level, L_p (d) pressure-residual intensity index, δ_{pIo}.

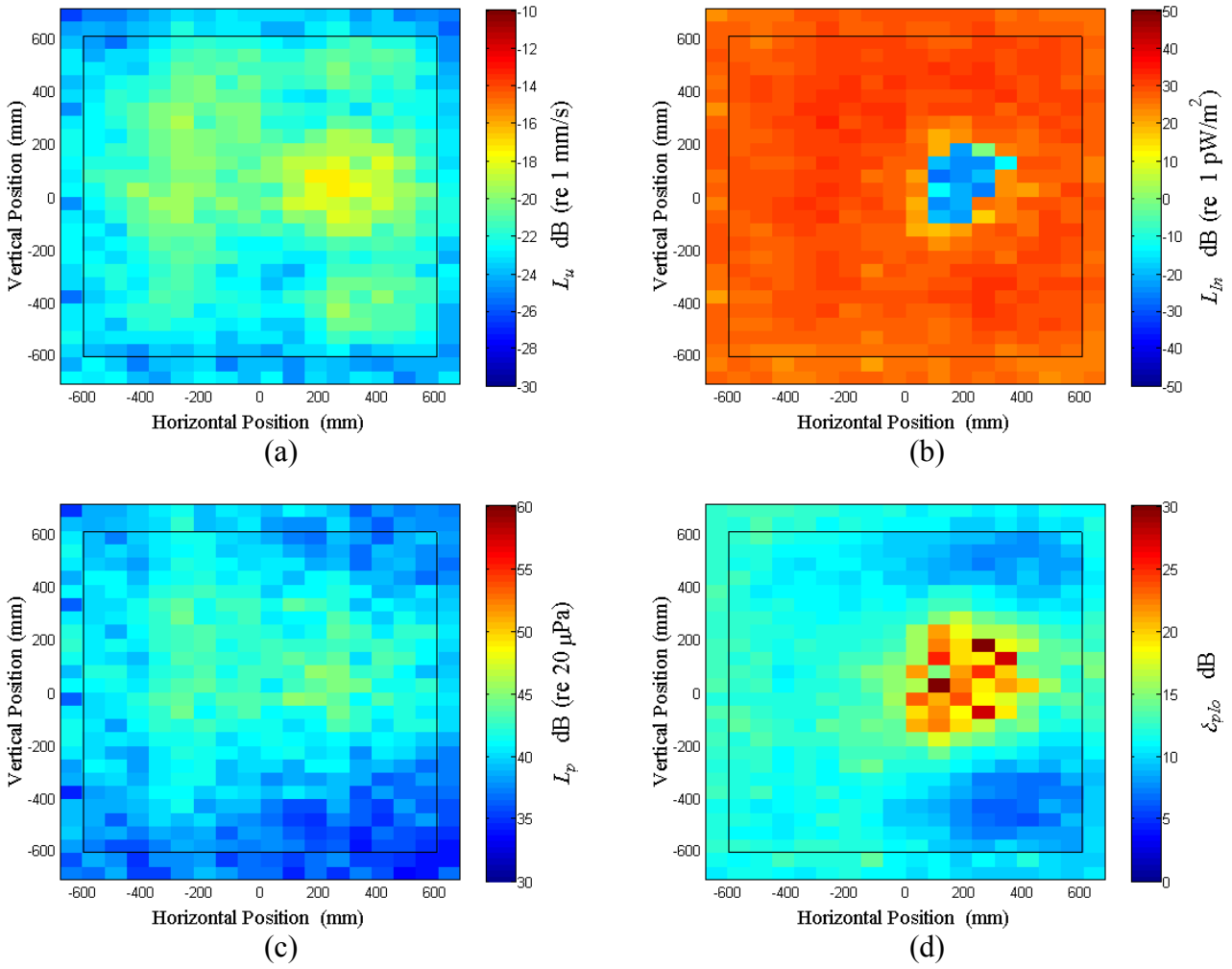

Figure A.7: Surface scan of Window A at 65 Hz (a) particle velocity level, L_u (b) normal signed sound intensity level, L_{In} (c) sound pressure level, L_p (d) pressure-residual intensity index, δ_{pIo}.

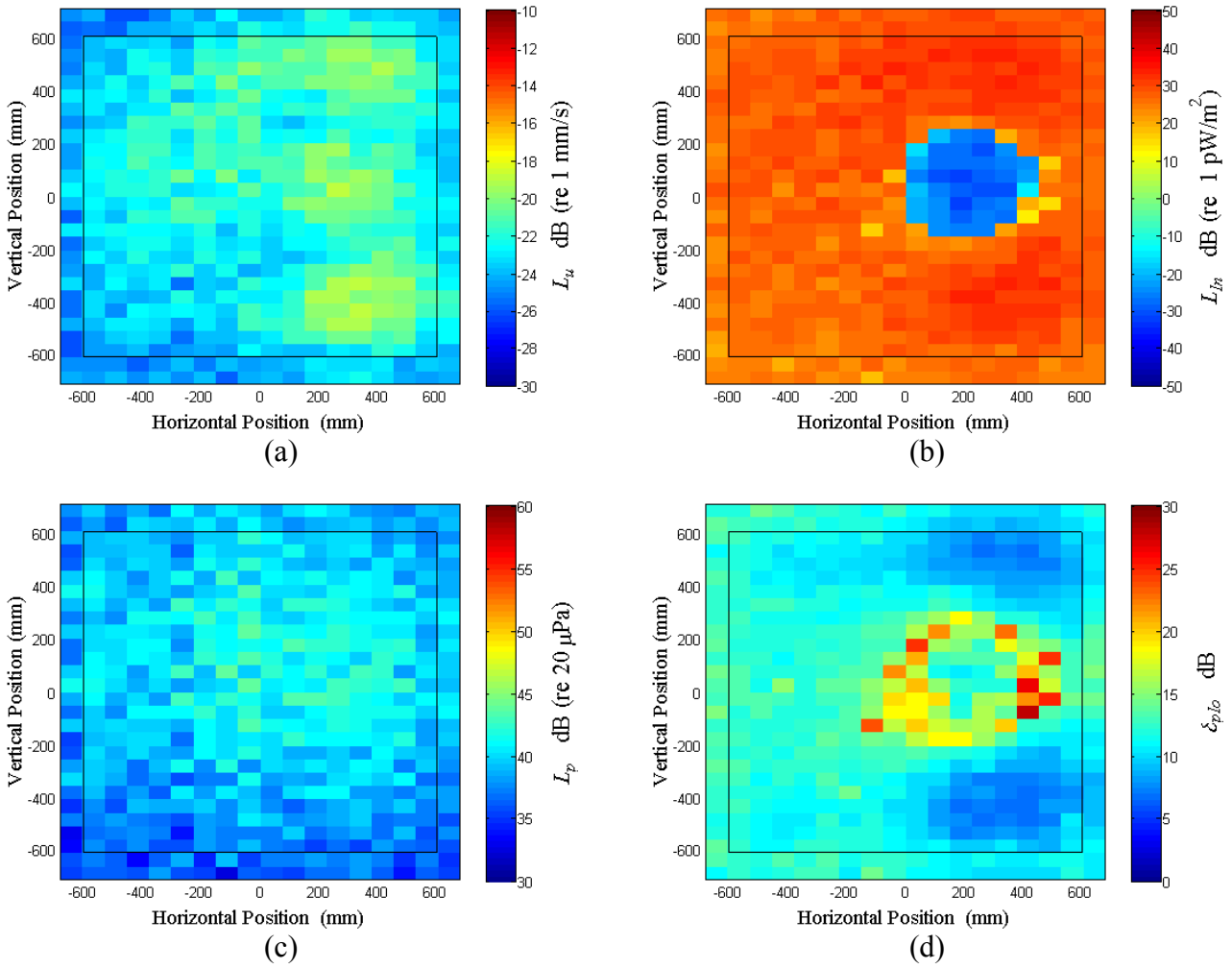

Figure A.8: Surface scan of Window A at 67.5 Hz (a) particle velocity level, L_u (b) normal signed sound intensity level, L_{In} (c) sound pressure level, L_p (d) pressure-residual intensity index, δ_{pIo}.

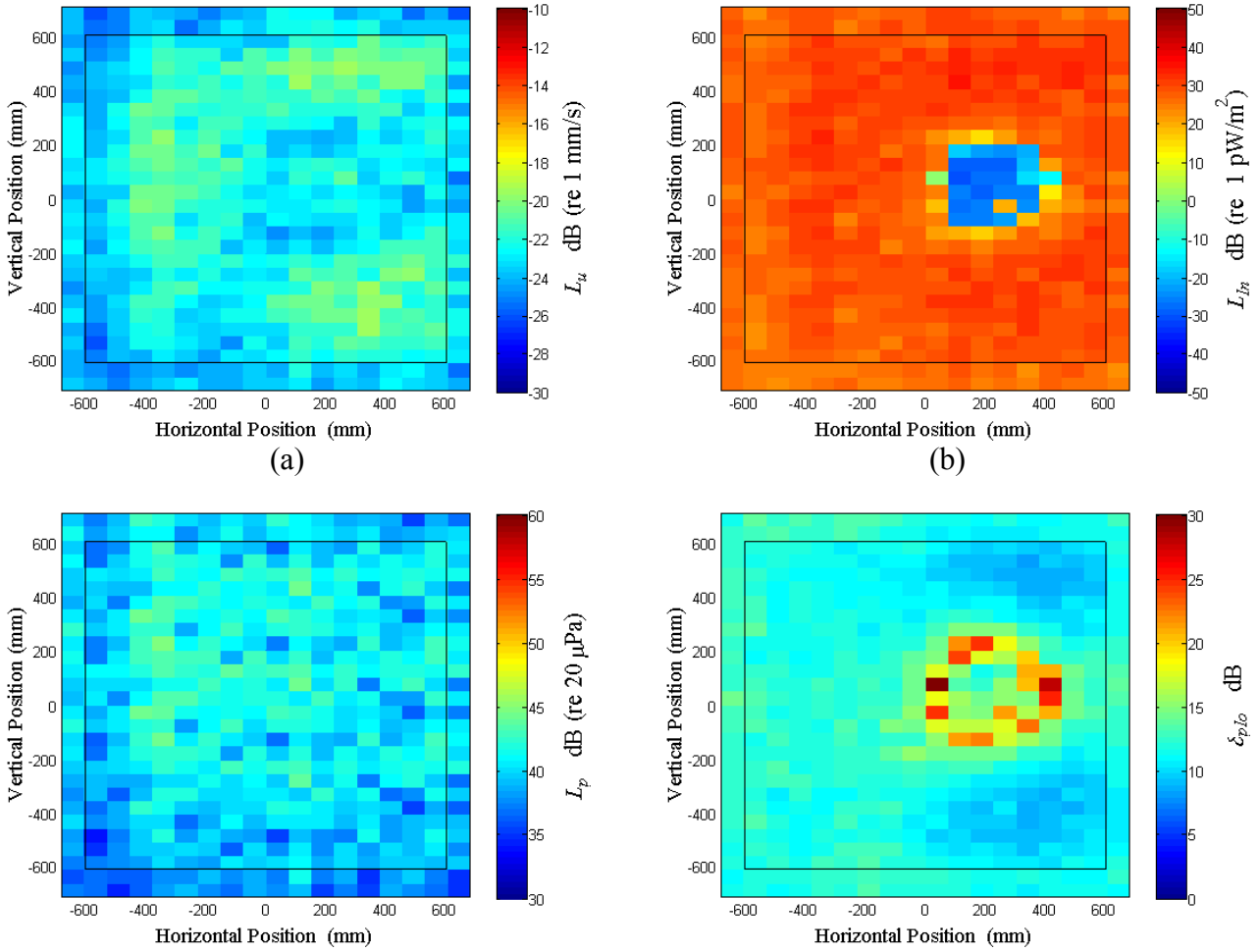

Figure A.9: Surface scan of Window A at 70 Hz (a) particle velocity level, L_u (b) normal signed sound intensity level, L_{In} (c) sound pressure level, L_p (d) pressure-residual intensity index, δ_{pIo}.

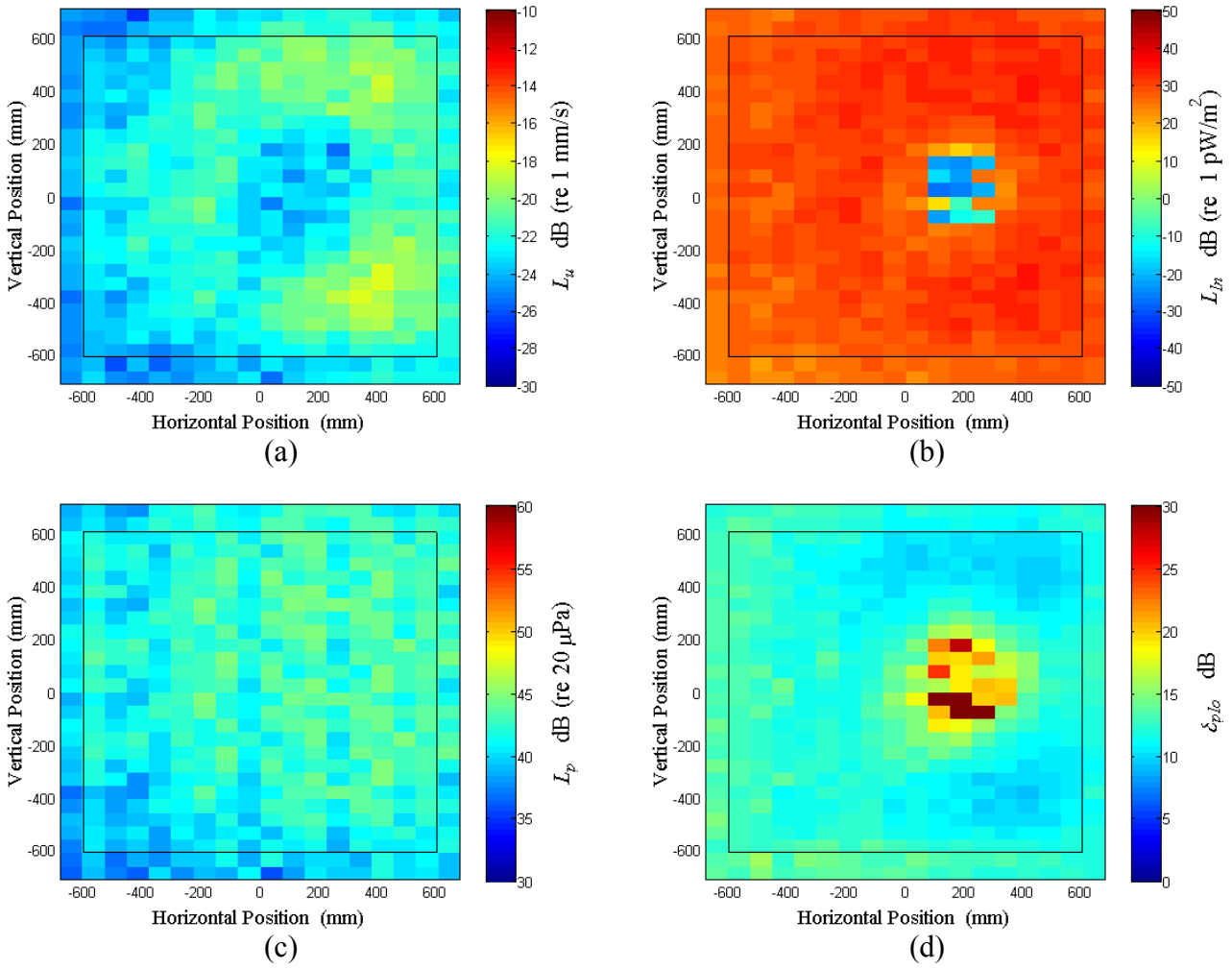

Figure A.10: Surface scan of Window A at 72.5 Hz (a) particle velocity level, L_u (b) normal signed sound intensity level, L_{In} (c) sound pressure level, L_p (d) pressure-residual intensity index, δ_{pIo}.

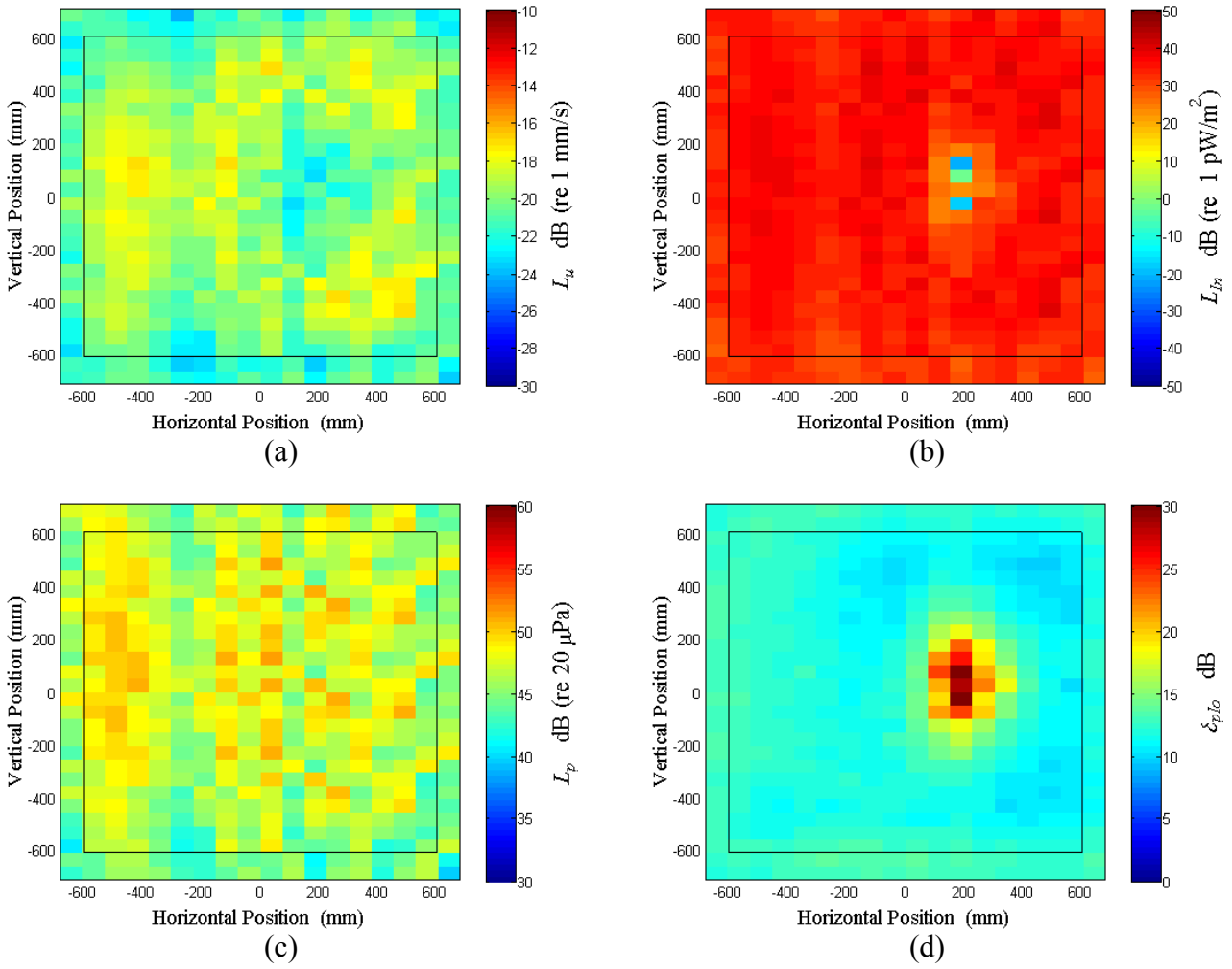

Figure A.11: Surface scan of Window A at 75 Hz (a) particle velocity level, L_u (b) normal signed sound intensity level, L_{In} (c) sound pressure level, L_p (d) pressure-residual intensity index, δ_{pIo}.

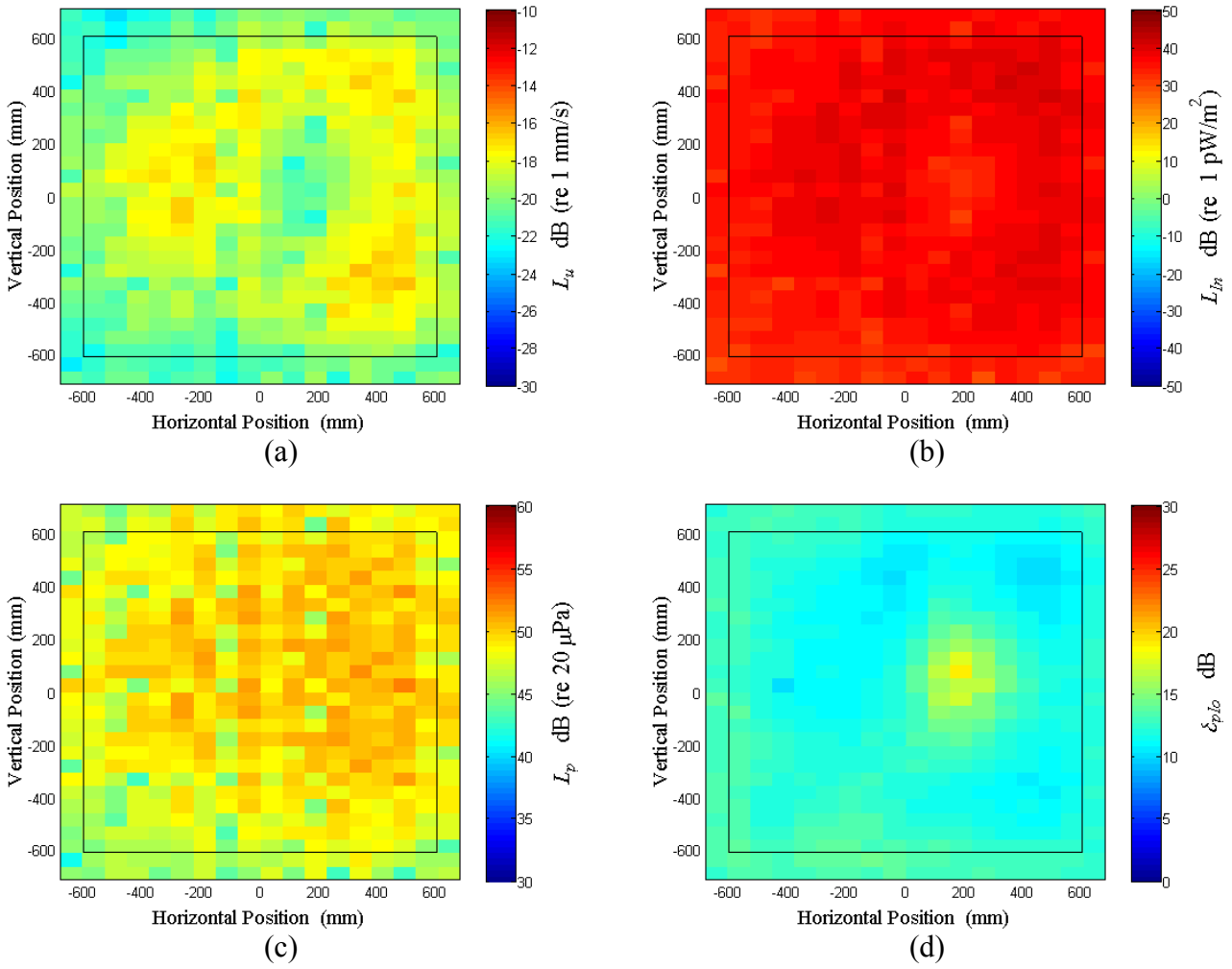

Figure A.12: Surface scan of Window A at 77.5 Hz (a) particle velocity level, L_u (b) normal signed sound intensity level, L_{In} (c) sound pressure level, L_p (d) pressure-residual intensity index, δ_{pIo}.

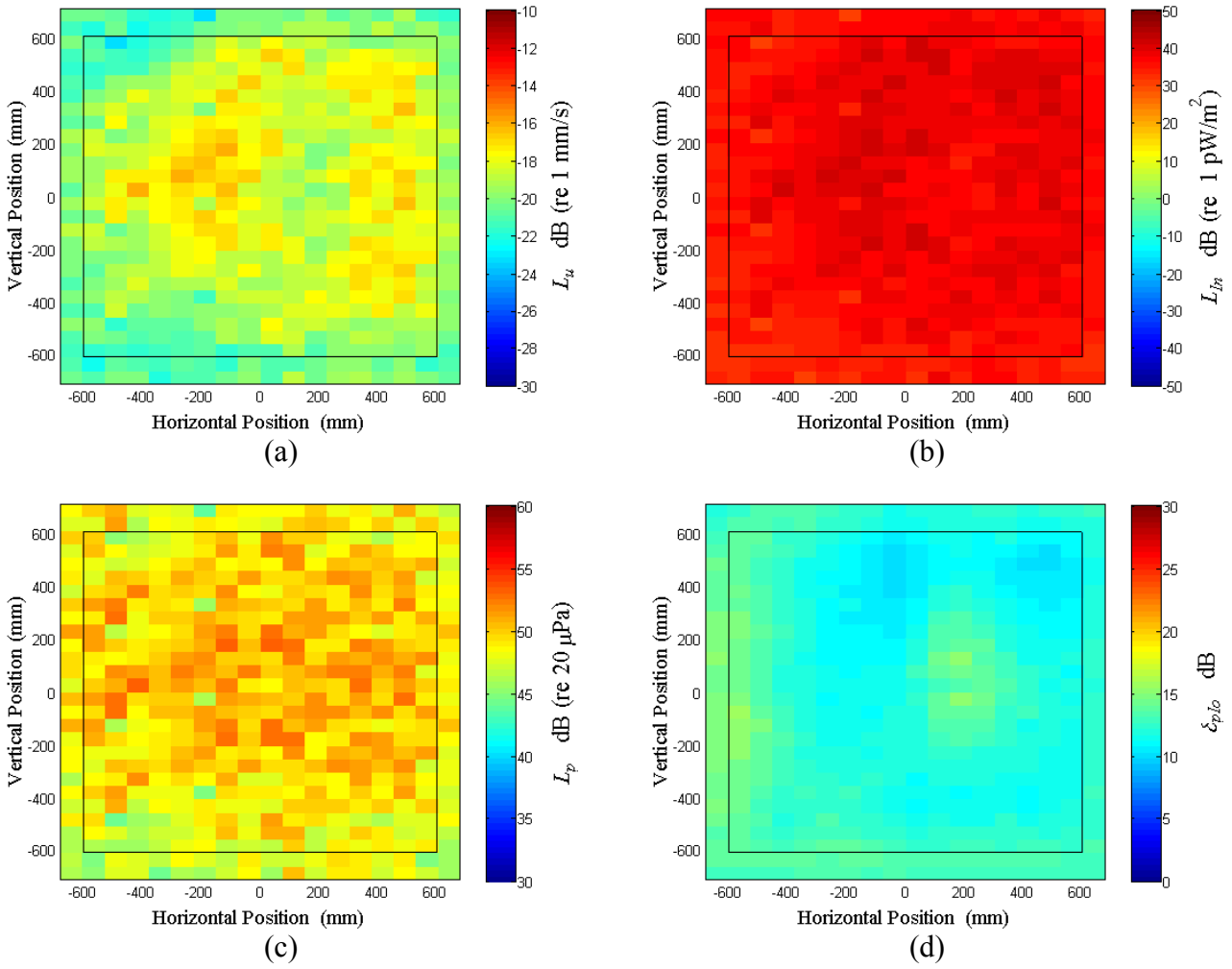

Figure A.13: Surface scan of Window A at 80 Hz (a) particle velocity level, L_u (b) normal signed sound intensity level, L_{In} (c) sound pressure level, L_p (d) pressure-residual intensity index, δ_{pIo}.

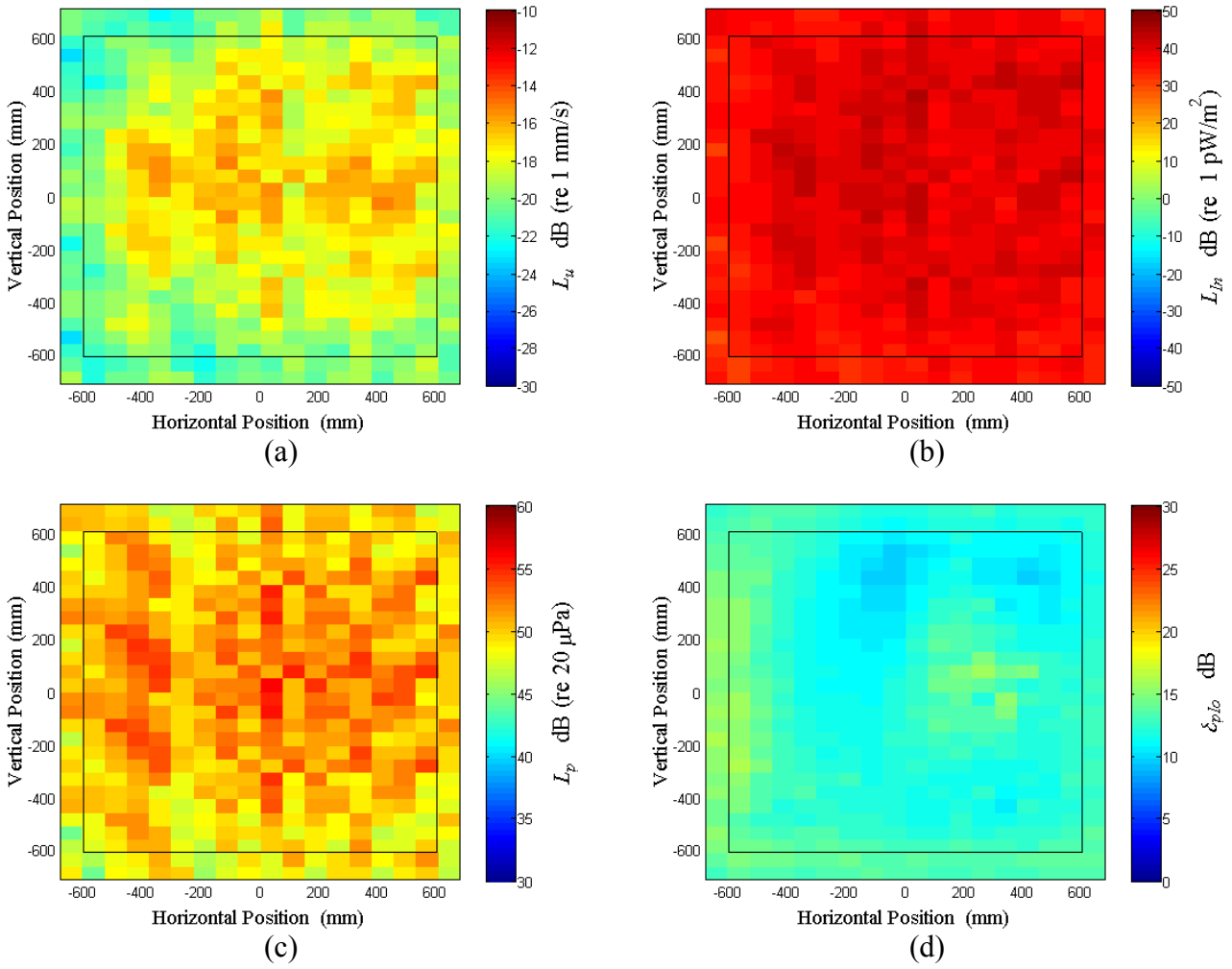

Figure A.14: Surface scan of Window A at 82.5 Hz (a) particle velocity level, L_u (b) normal signed sound intensity level, L_{In} (c) sound pressure level, L_p (d) pressure-residual intensity index, δ_{pIo}.

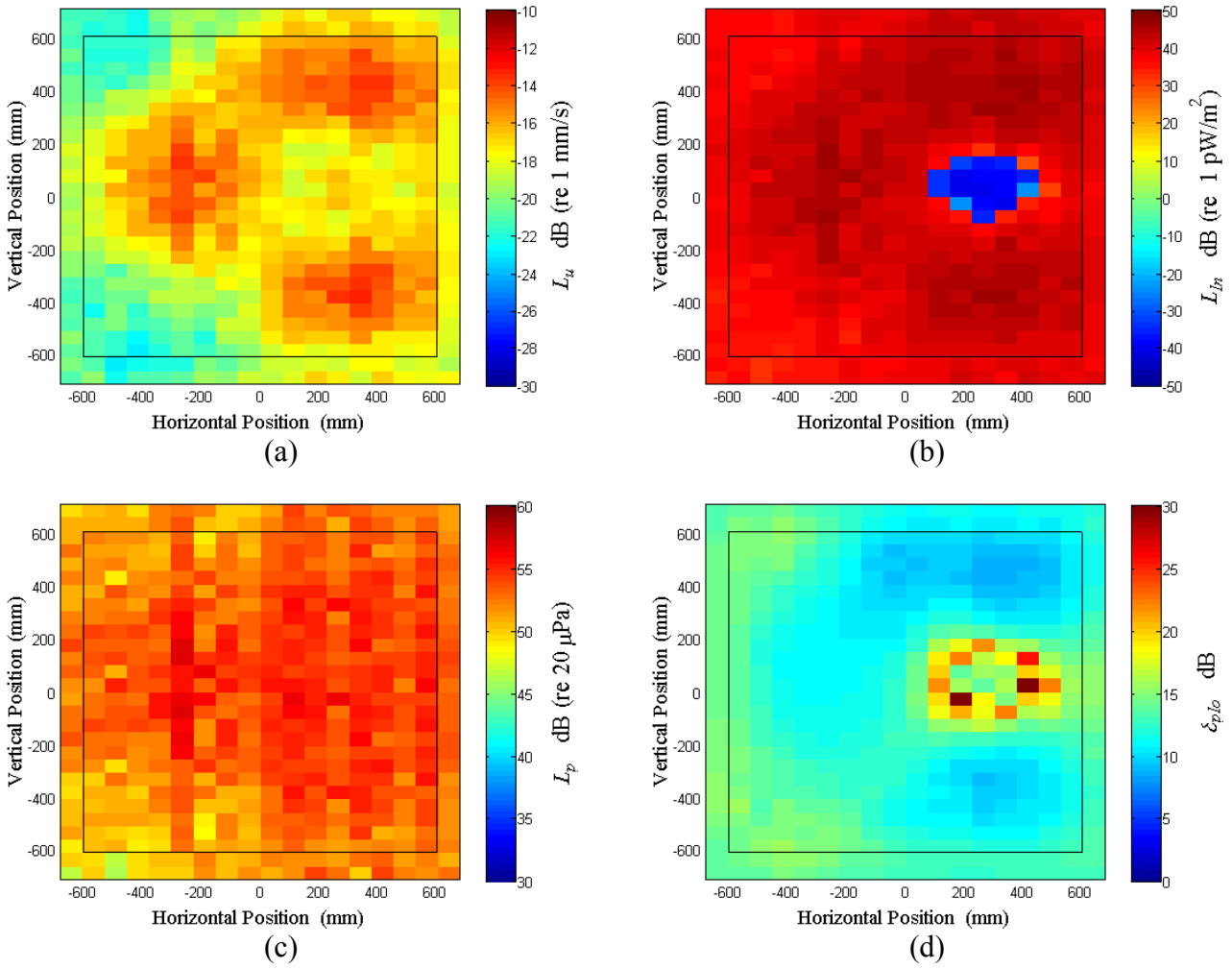

Figure A.15: Surface scan of Window A at 85 Hz (a) particle velocity level, L_u (b) normal signed sound intensity level, L_{In} (c) sound pressure level, L_p (d) pressure-residual intensity index, δ_{pIo}.

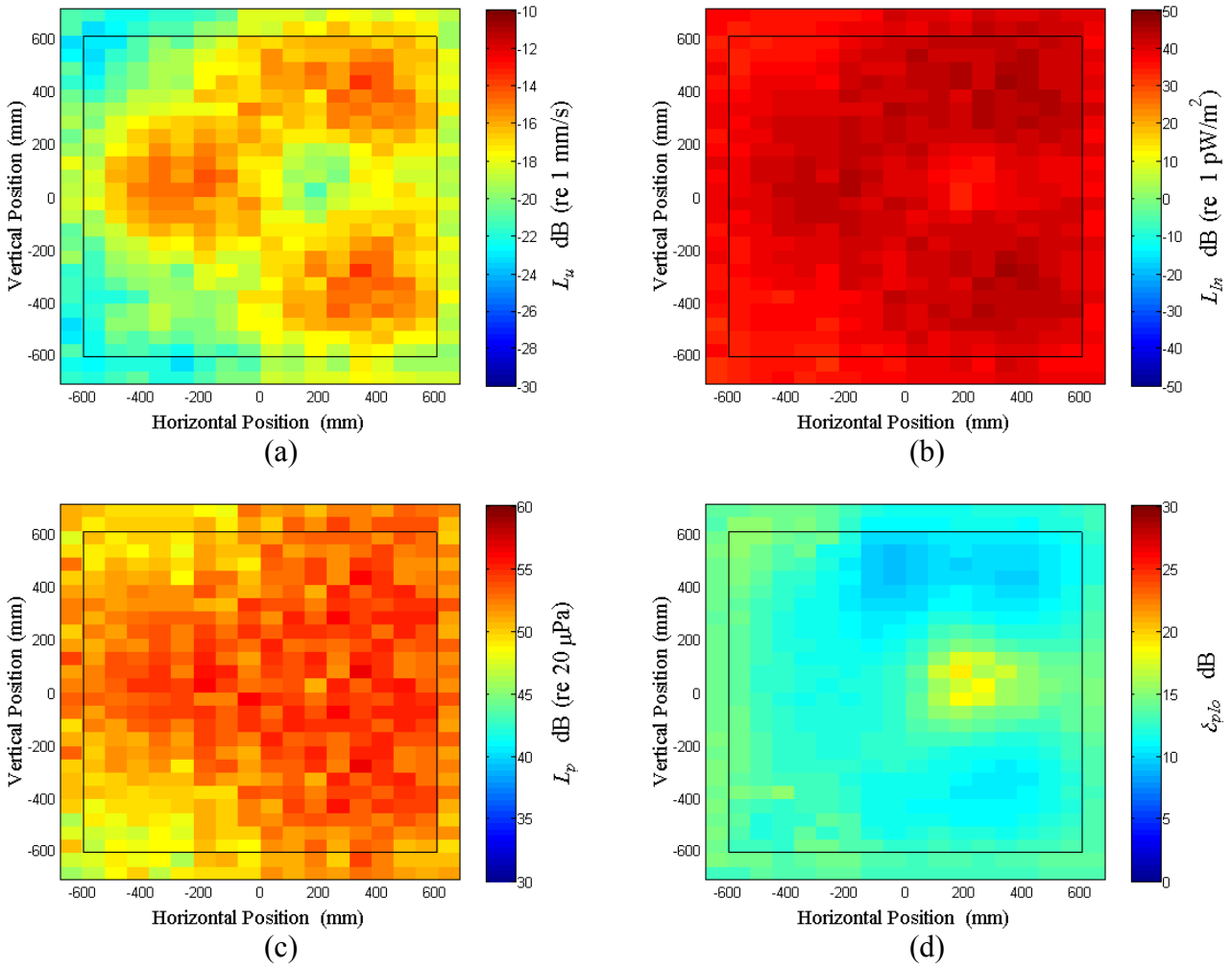

Figure A.16: Surface scan of Window A at 87.5 Hz (a) particle velocity level, L_u (b) normal signed sound intensity level, L_{In} (c) sound pressure level, L_p (d) pressure-residual intensity index, δ_{pIo}.

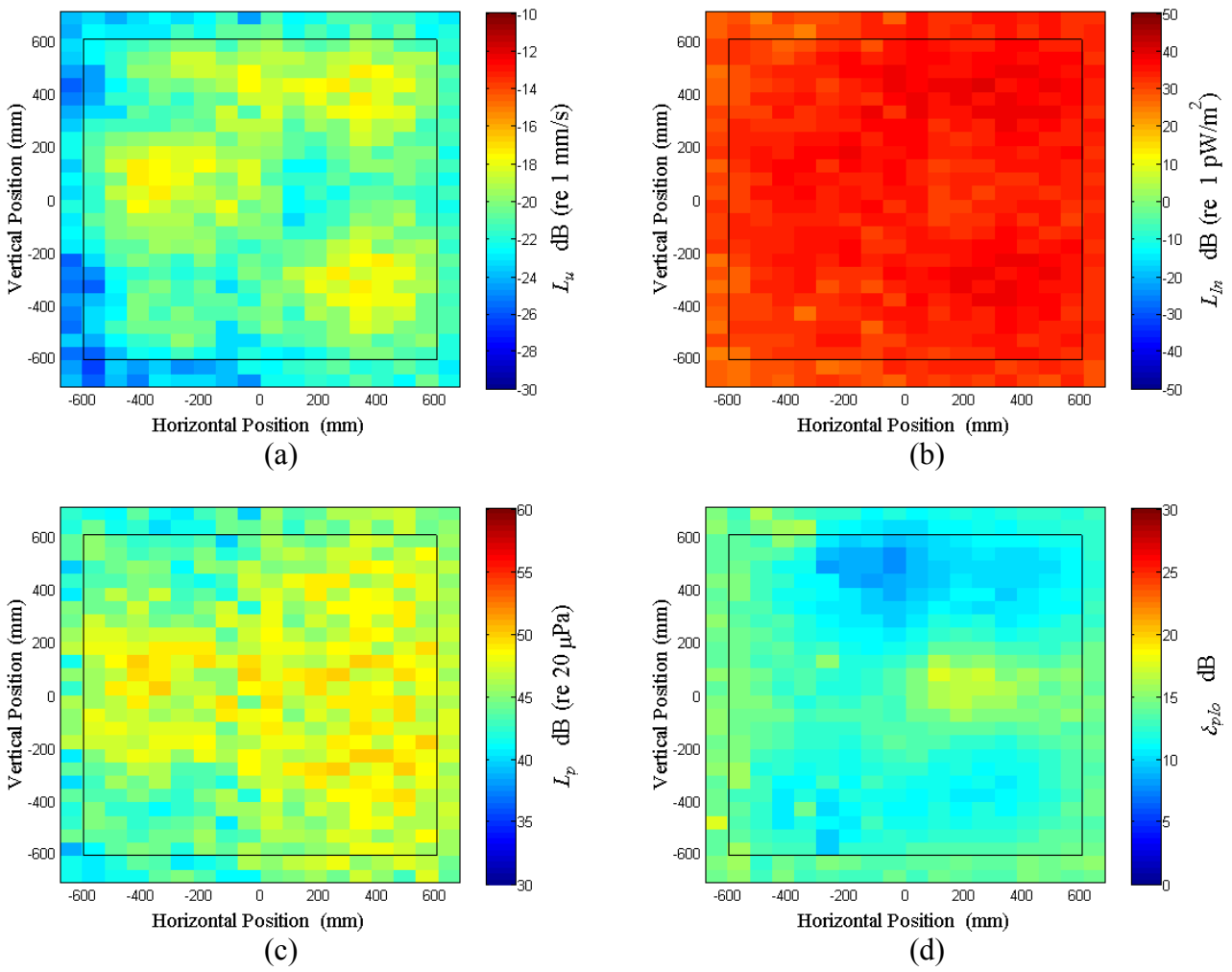

Figure A.17: Surface scan of Window A at 90 Hz (a) particle velocity level, L_u (b) normal signed sound intensity level, L_{In} (c) sound pressure level, L_p (d) pressure-residual intensity index, δ_{pIo}.

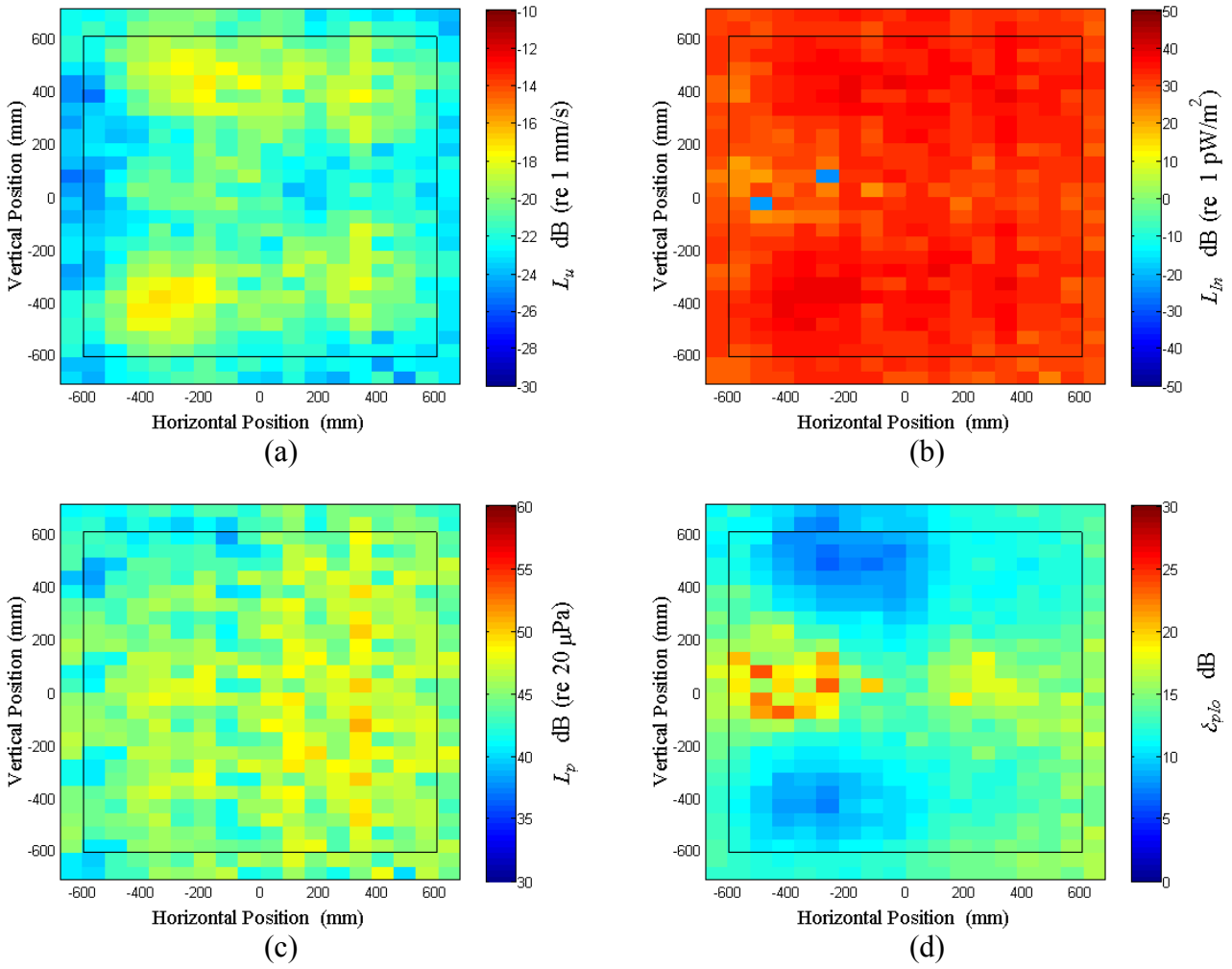

Figure A.18: Surface scan of Window A at 92.5 Hz (a) particle velocity level, L_u (b) normal signed sound intensity level, L_{In} (c) sound pressure level, L_p (d) pressure-residual intensity index, δ_{pIo}.

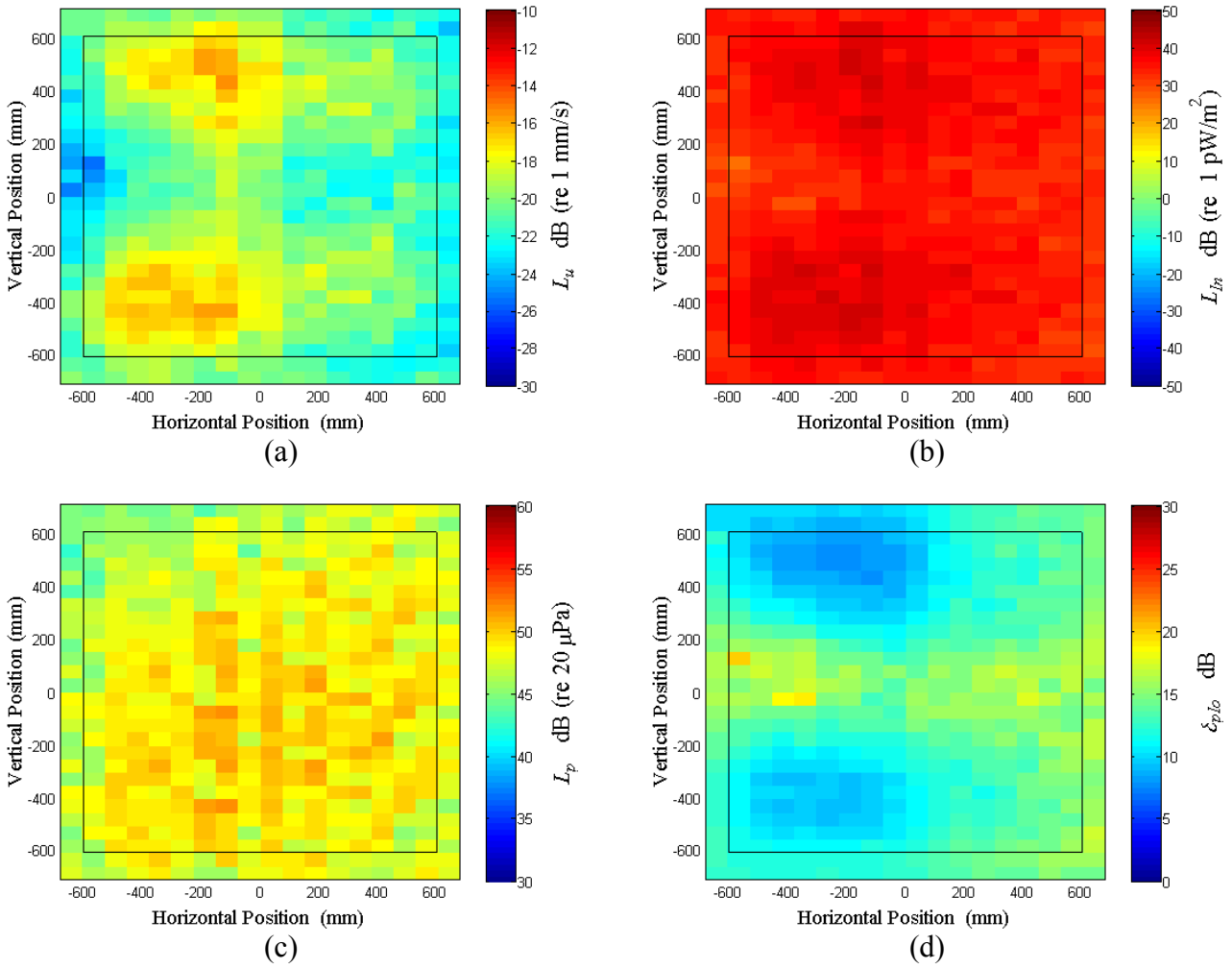

Figure A.19: Surface scan of Window A at 95 Hz (a) particle velocity level, L_u (b) normal signed sound intensity level, L_{In} (c) sound pressure level, L_p (d) pressure-residual intensity index, δ_{pIo}.

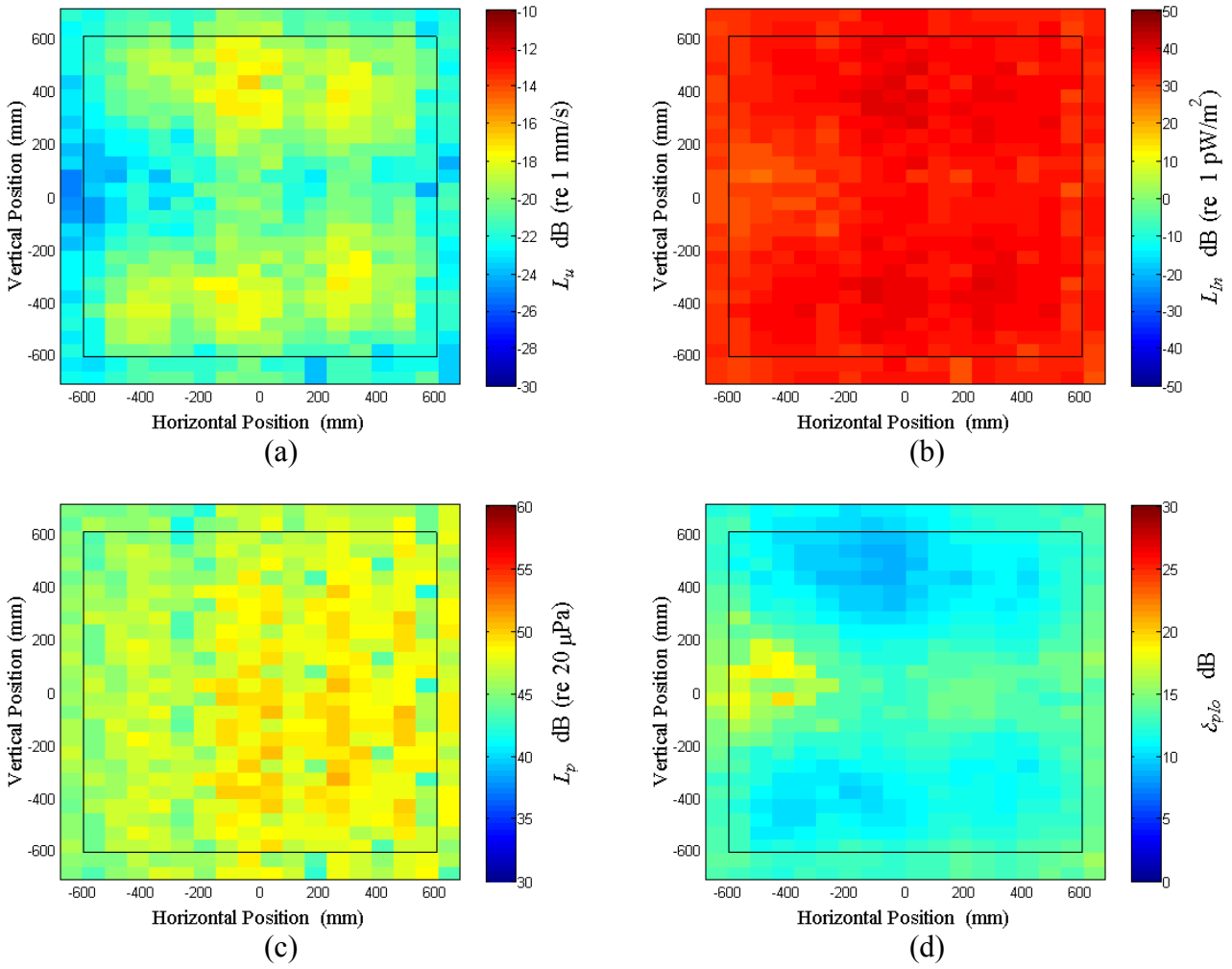

Figure A.20: Surface scan of Window A at 97.5 Hz (a) particle velocity level, L_u (b) normal signed sound intensity level, L_{In} (c) sound pressure level, L_p (d) pressure-residual intensity index, δ_{pIo}.

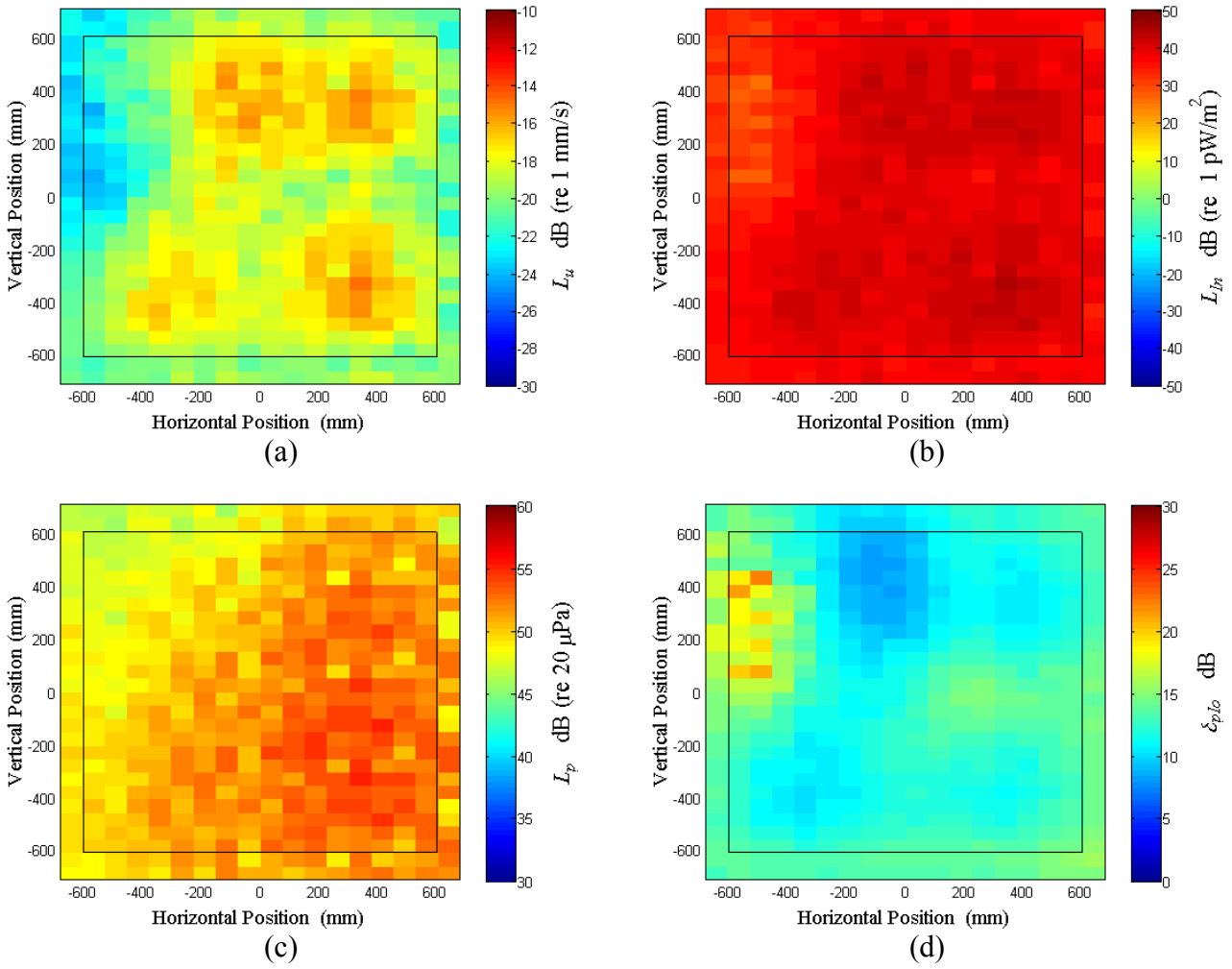

Figure A.21: Surface scan of Window A at 100 Hz (a) particle velocity level, L_u (b) normal signed sound intensity level, L_{In} (c) sound pressure level, L_p (d) pressure-residual intensity index, δ_{pIo}.

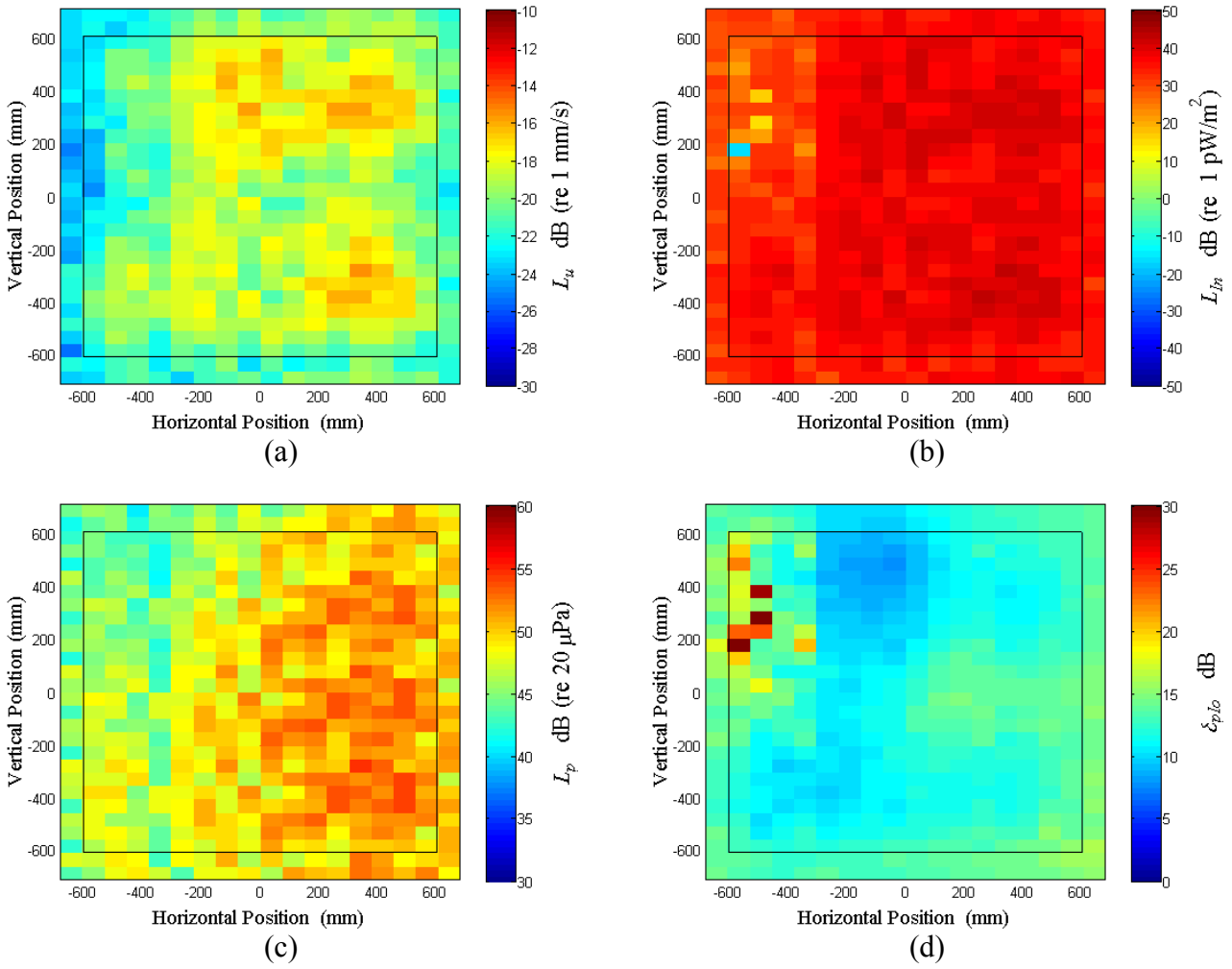

Figure A.22: Surface scan of Window A at 102.5 Hz (a) particle velocity level, L_u (b) normal signed sound intensity level, L_{In} (c) sound pressure level, L_p (d) pressure-residual intensity index, δ_{pIo}.

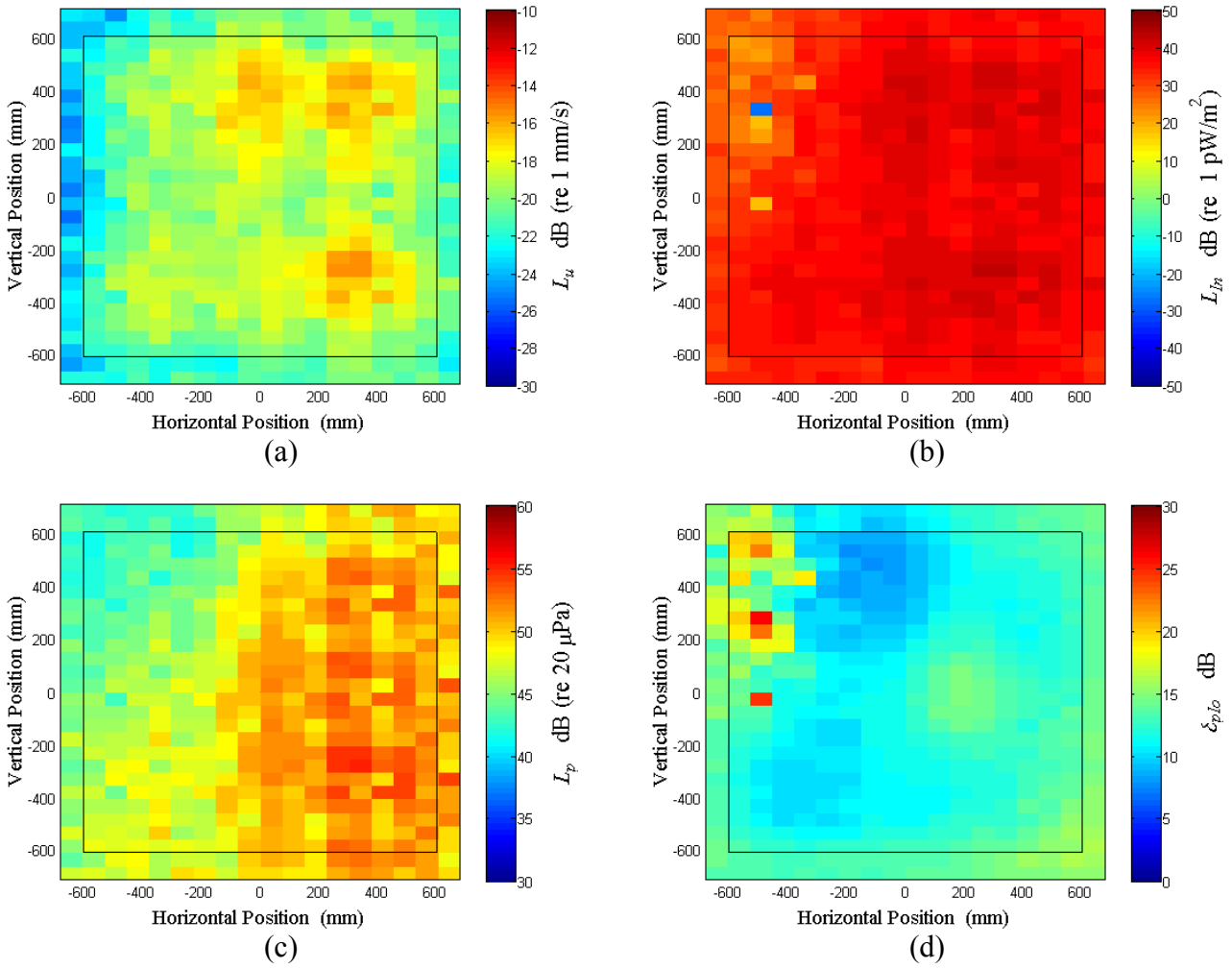

Figure A.23: Surface scan of Window A at 105 Hz (a) particle velocity level, L_u (b) normal signed sound intensity level, L_{In} (c) sound pressure level, L_p (d) pressure-residual intensity index, δ_{pIo}.

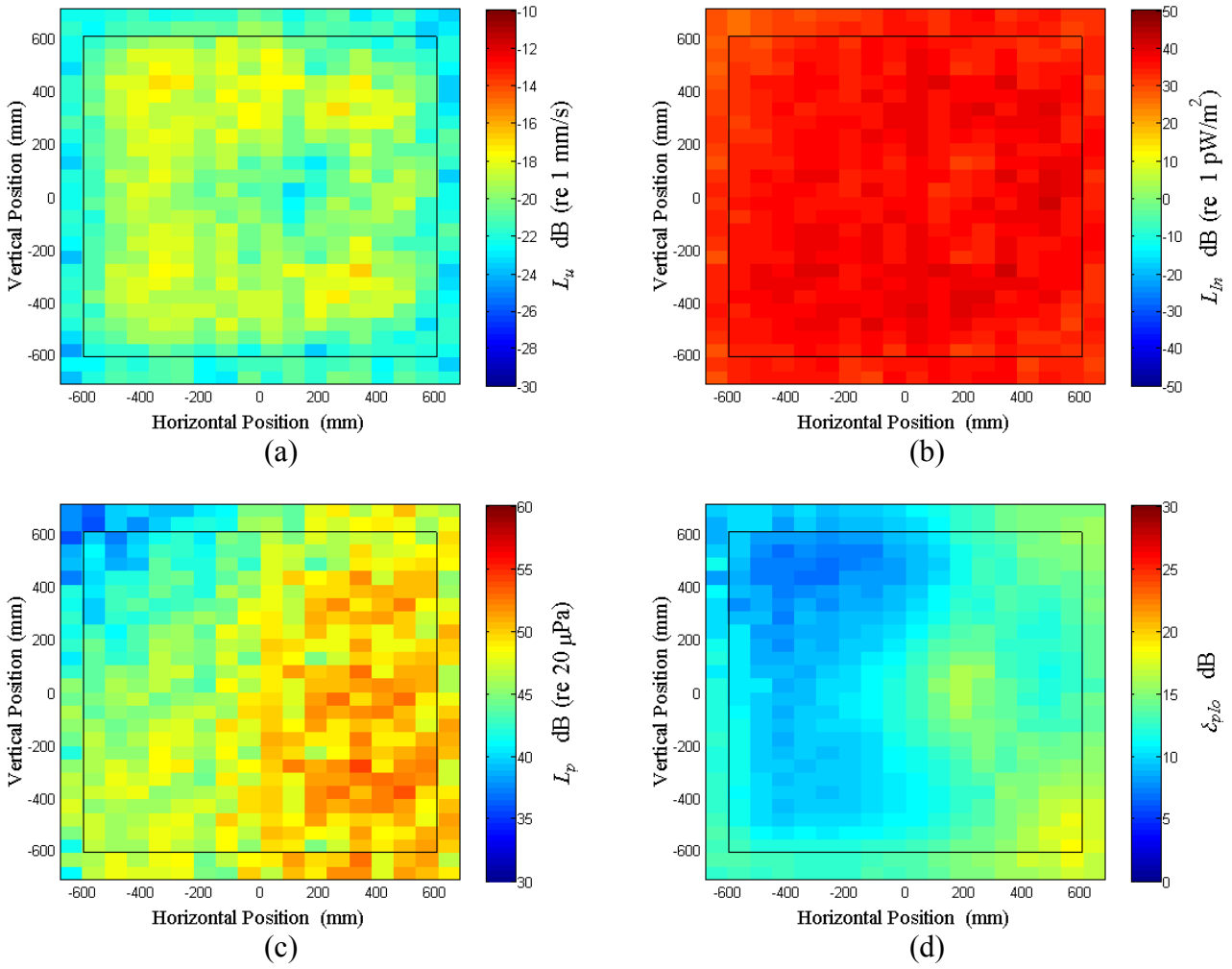

Figure A.24: Surface scan of Window A at 107.5 Hz (a) particle velocity level, L_u (b) normal signed sound intensity level, L_{In} (c) sound pressure level, L_p (d) pressure-residual intensity index, δ_{pIo}.

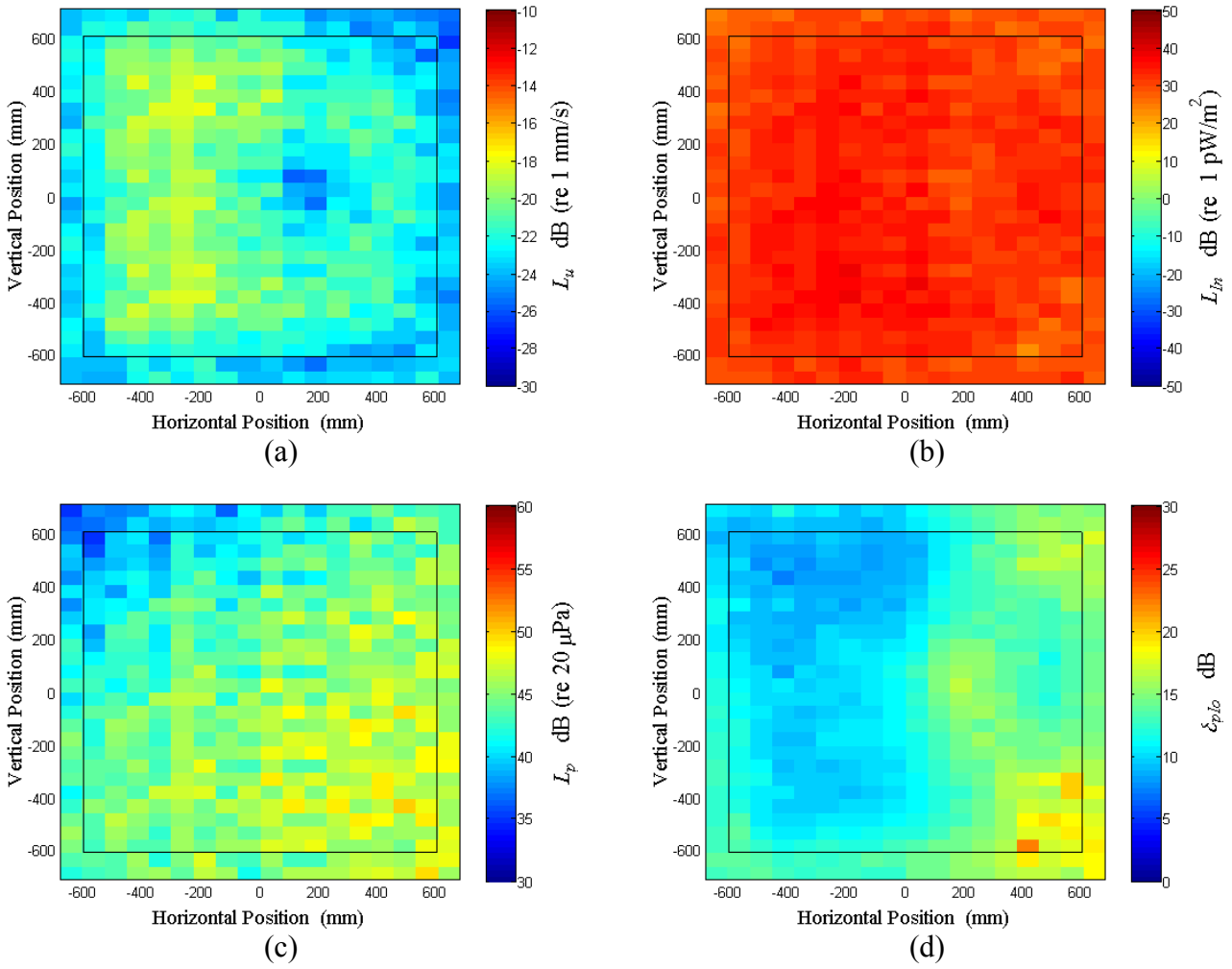

Figure A.25: Surface scan of Window A at 110 Hz (a) particle velocity level, L_u (b) normal signed sound intensity level, L_{In} (c) sound pressure level, L_p (d) pressure-residual intensity index, δ_{pIo}.

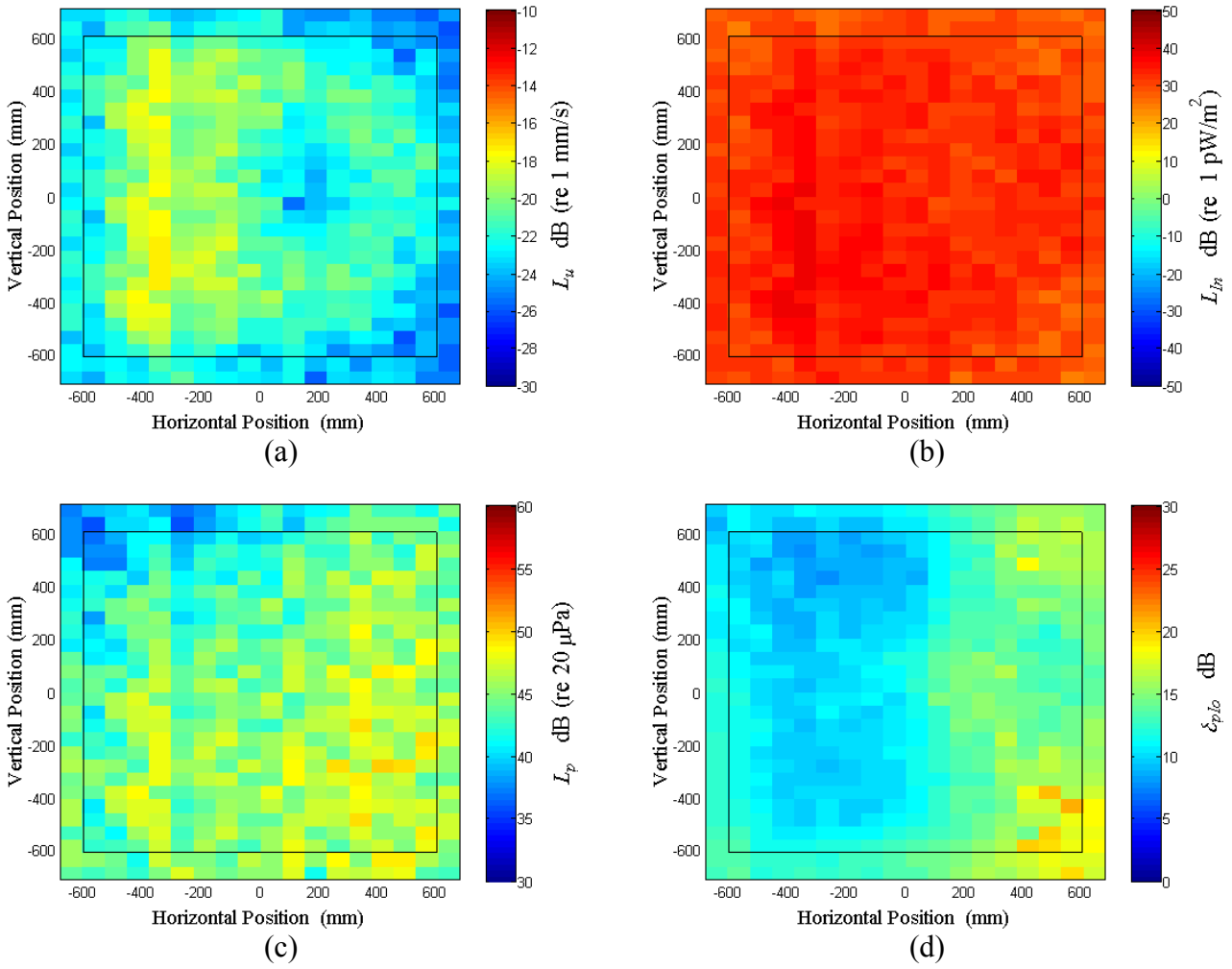

Figure A.26: Surface scan of Window A at 112.5 Hz (a) particle velocity level, L_u (b) normal signed sound intensity level, L_{In} (c) sound pressure level, L_p (d) pressure-residual intensity index, δ_{pIo}.

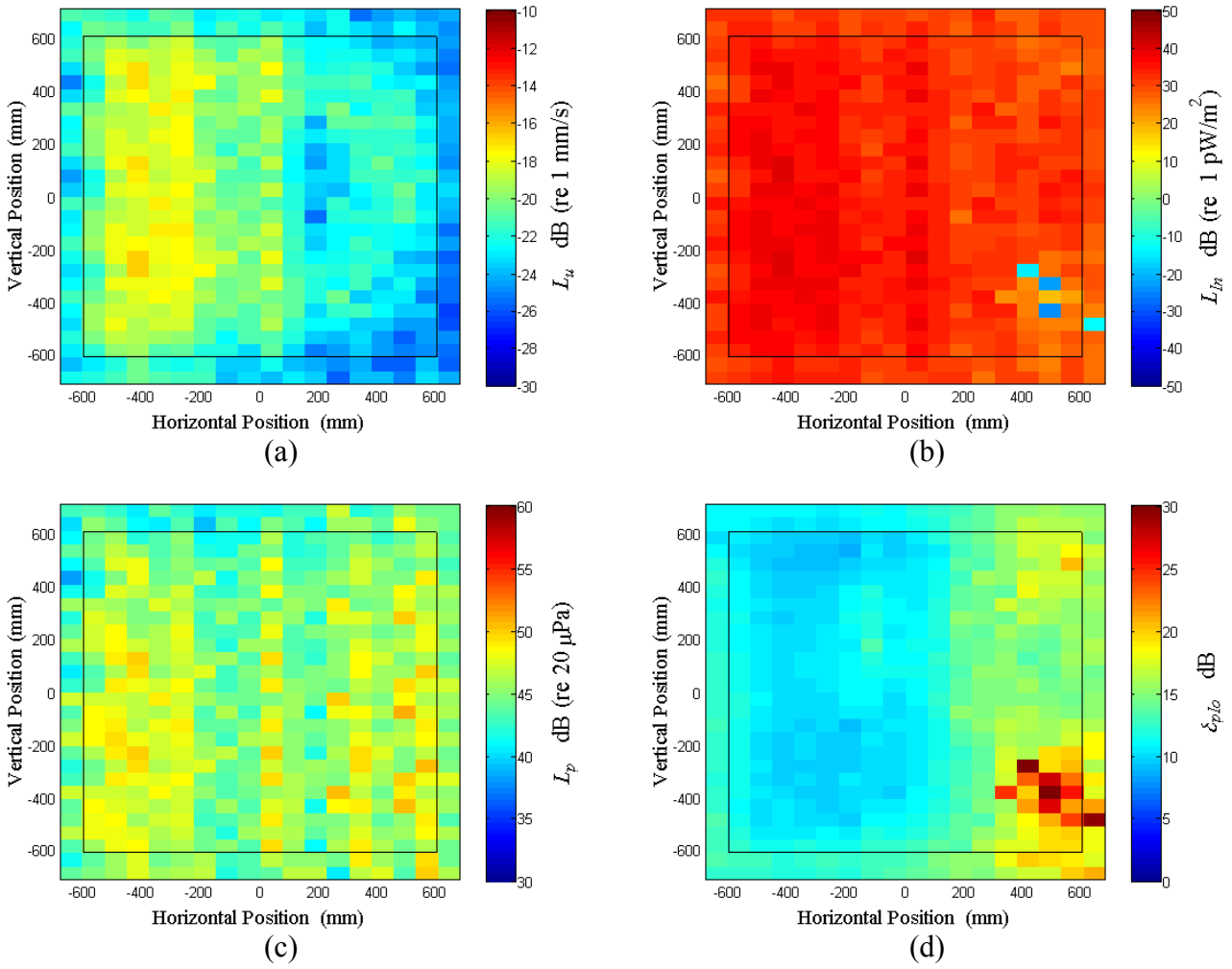

Figure A.27: Surface scan of Window A at 115 Hz (a) particle velocity level, L_u (b) normal signed sound intensity level, L_{In} (c) sound pressure level, L_p (d) pressure-residual intensity index, δ_{pIo}.

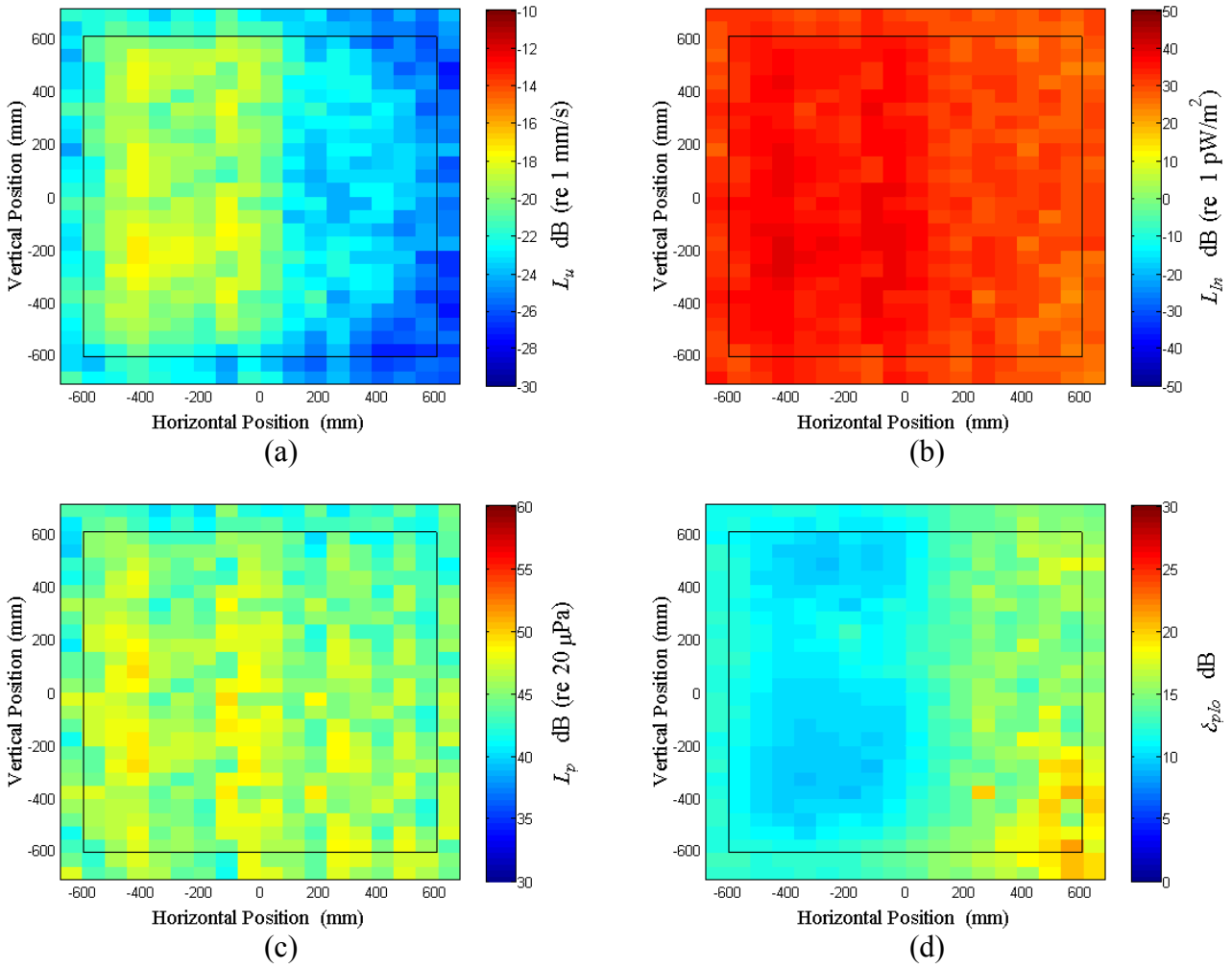

Figure A.28: Surface scan of Window A at 117.5 Hz (a) particle velocity level, L_u (b) normal signed sound intensity level, L_{In} (c) sound pressure level, L_p (d) pressure-residual intensity index, δ_{pIo}.

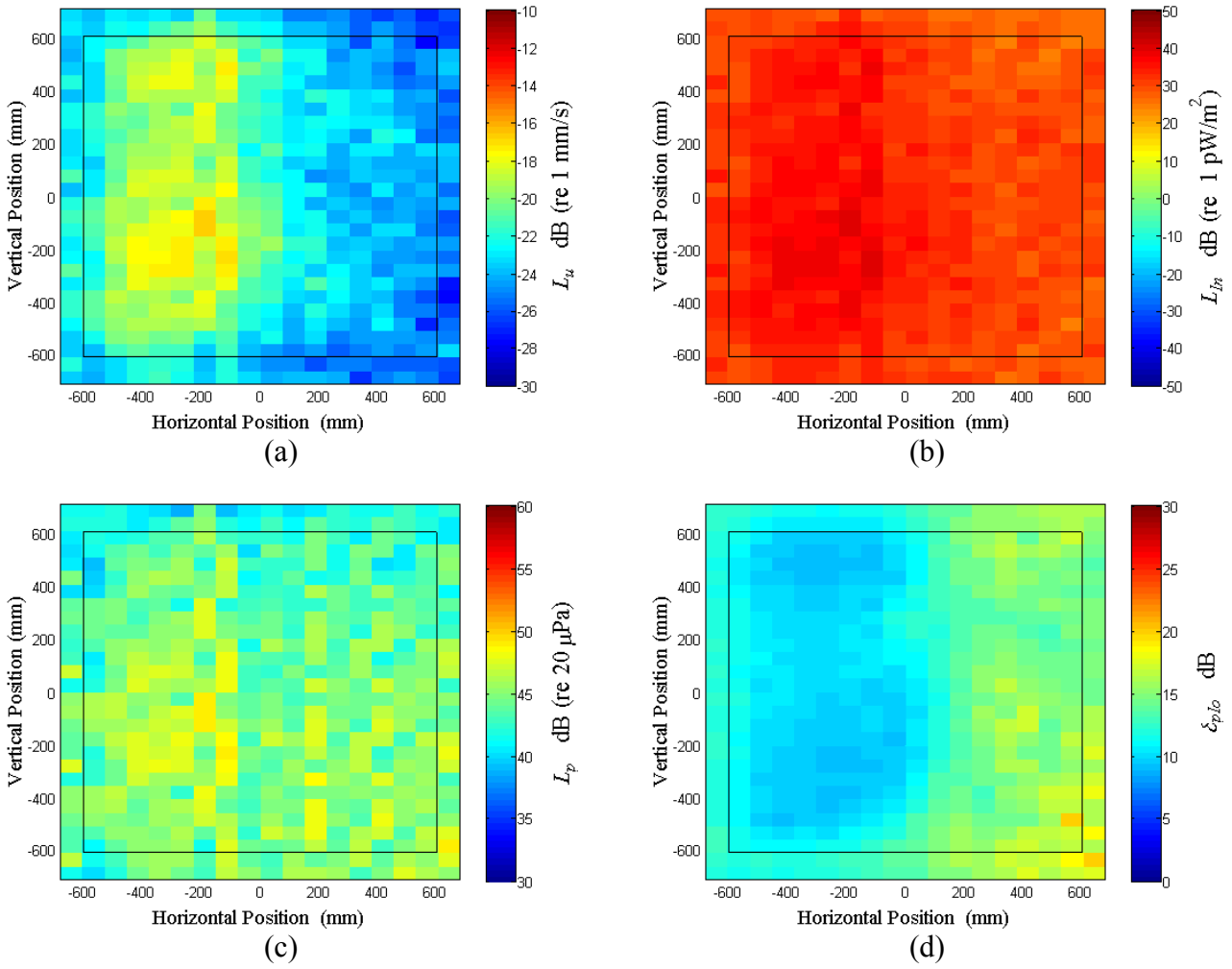

Figure A.29: Surface scan of Window A at 120 Hz (a) particle velocity level, L_u (b) normal signed sound intensity level, L_{In} (c) sound pressure level, L_p (d) pressure-residual intensity index, δ_{pIo}.

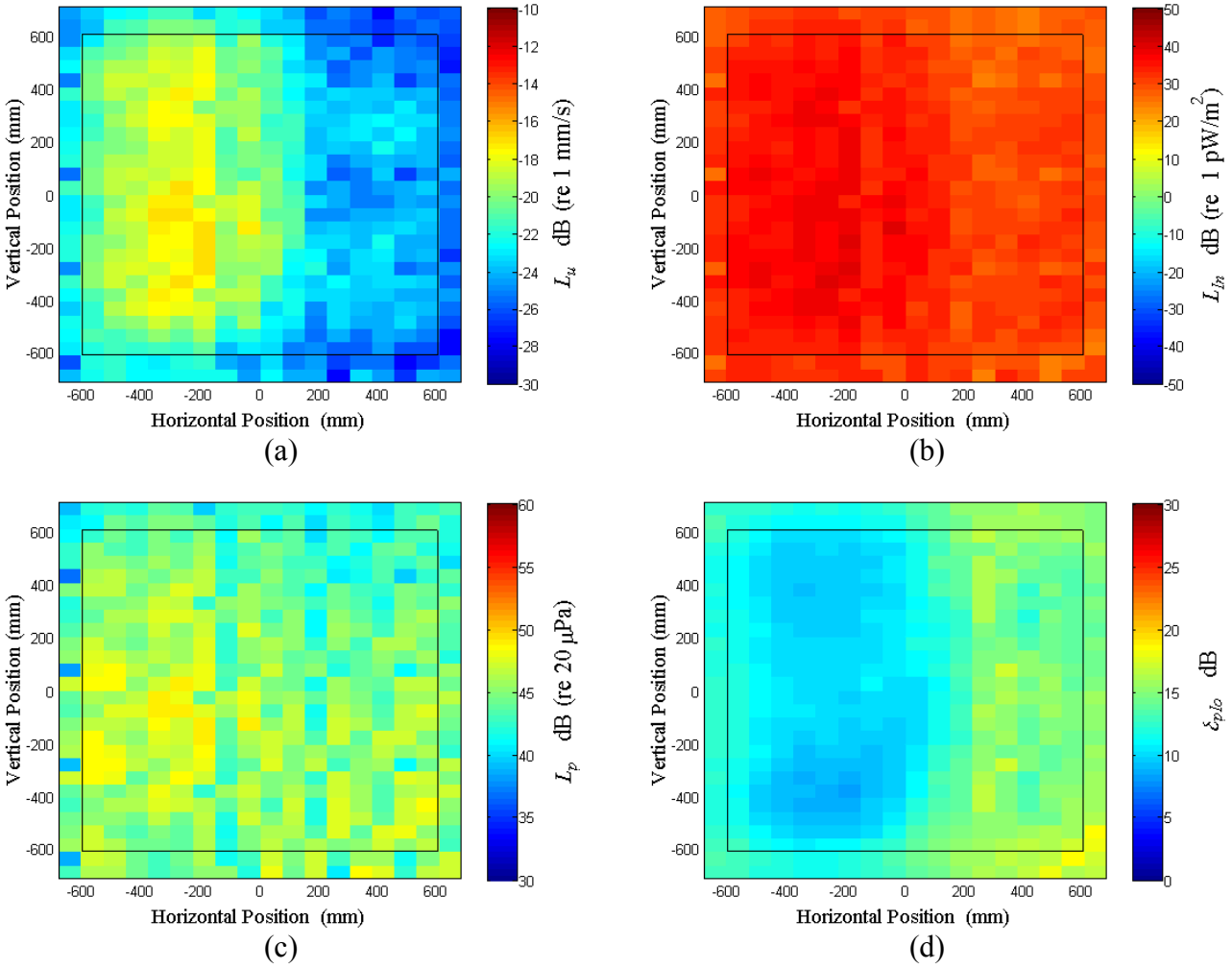

Figure A.30: Surface scan of Window A at 122.5 Hz (a) particle velocity level, L_u (b) normal signed sound intensity level, L_{In} (c) sound pressure level, L_p (d) pressure-residual intensity index, δ_{pIo}.

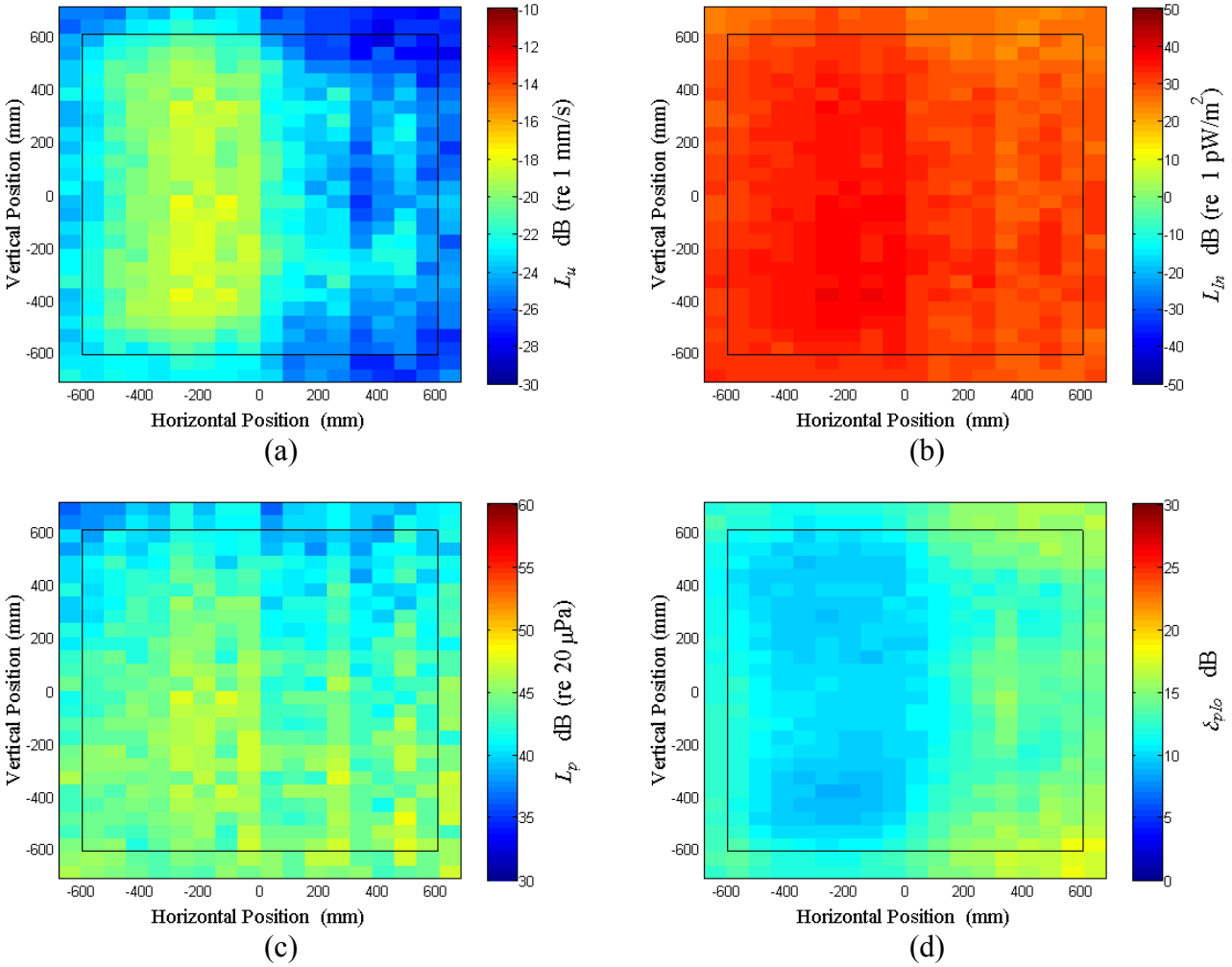

Figure A.31: Surface scan of Window A at 125 Hz (a) particle velocity level, L_u (b) normal signed sound intensity level, L_{In} (c) sound pressure level, L_p (d) pressure-residual intensity index, δ_{pIo}.

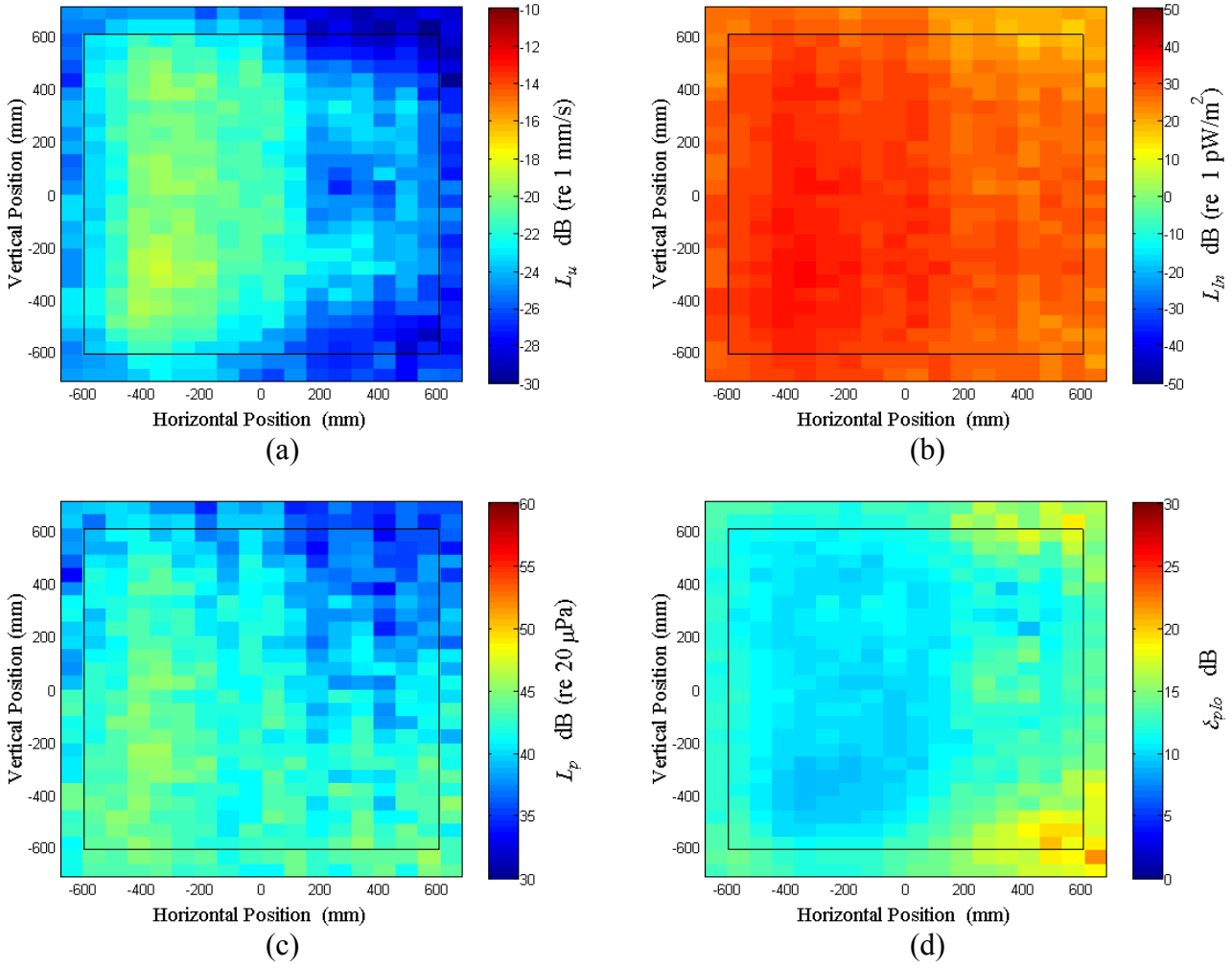

Figure A.32: Surface scan of Window A at 127.5 Hz (a) particle velocity level, L_u (b) normal signed sound intensity level, L_{In} (c) sound pressure level, L_p (d) pressure-residual intensity index, δ_{pIo}.

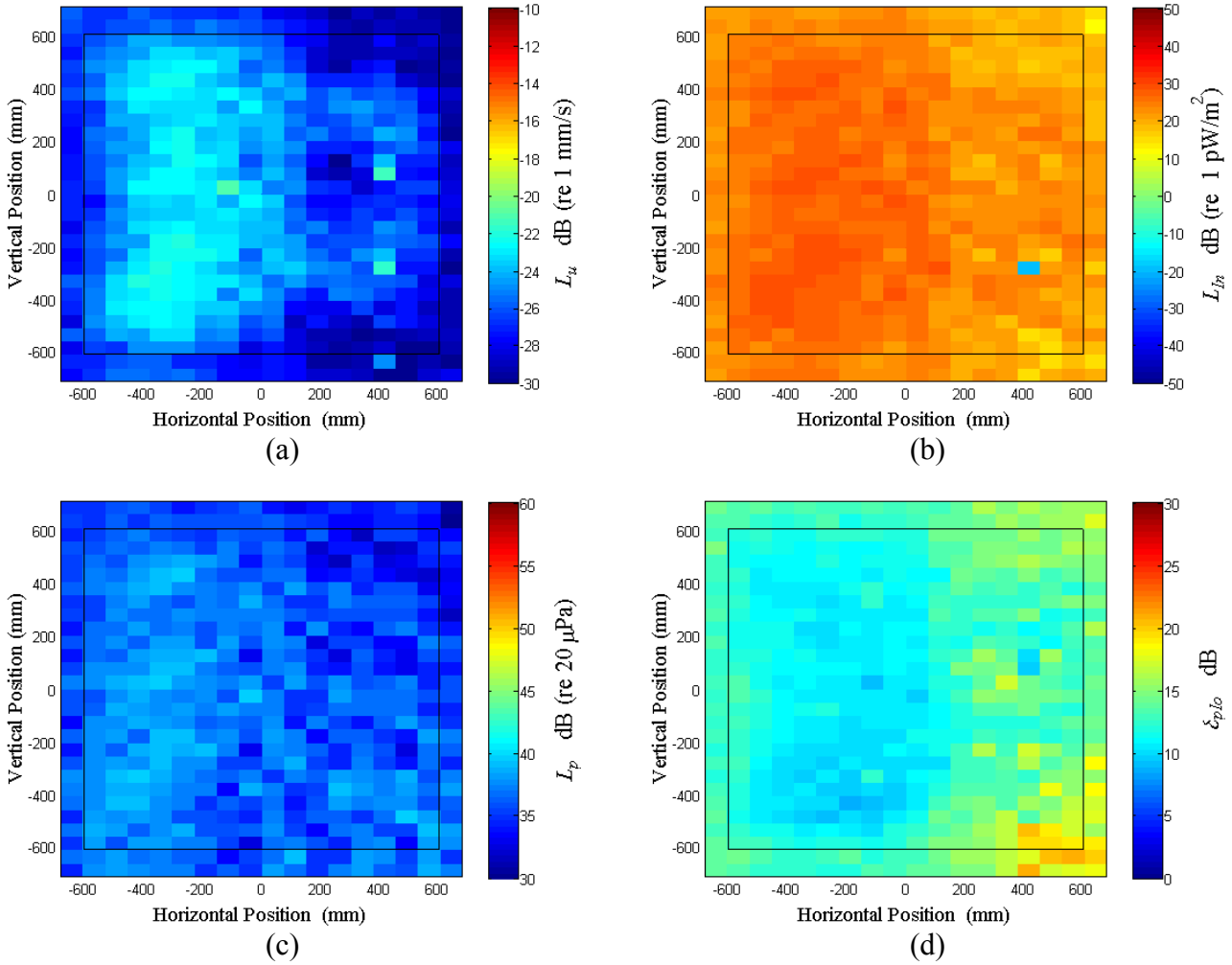

Figure A.33: Surface scan of Window A at 130 Hz (a) particle velocity level, L_u (b) normal signed sound intensity level, L_{In} (c) sound pressure level, L_p (d) pressure-residual intensity index, δ_{pIo}.

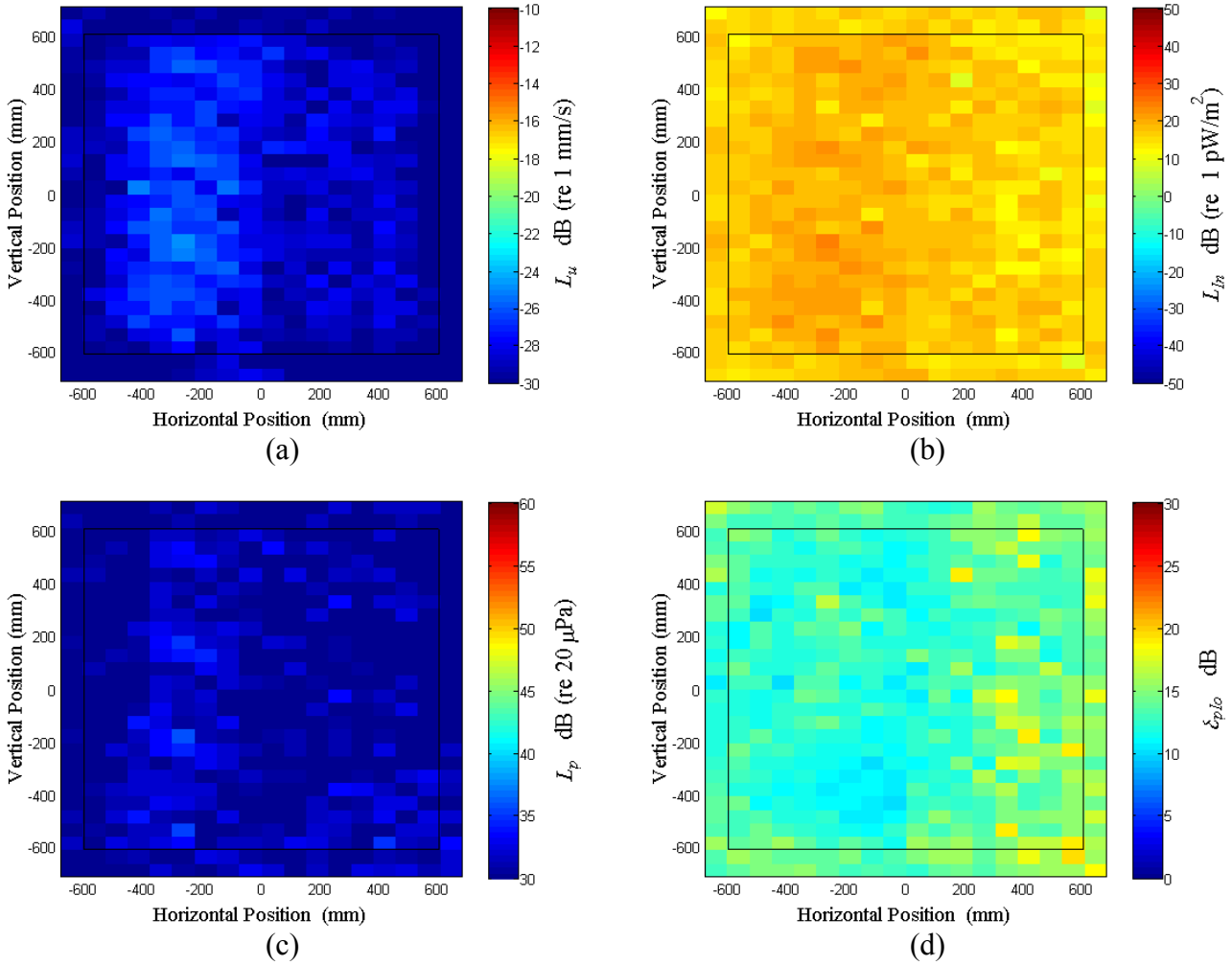

Figure A.34: Surface scan of Window A at 140 Hz (a) particle velocity level, L_u (b) normal signed sound intensity level, L_{In} (c) sound pressure level, L_p (d) pressure-residual intensity index, δ_{pIo}.

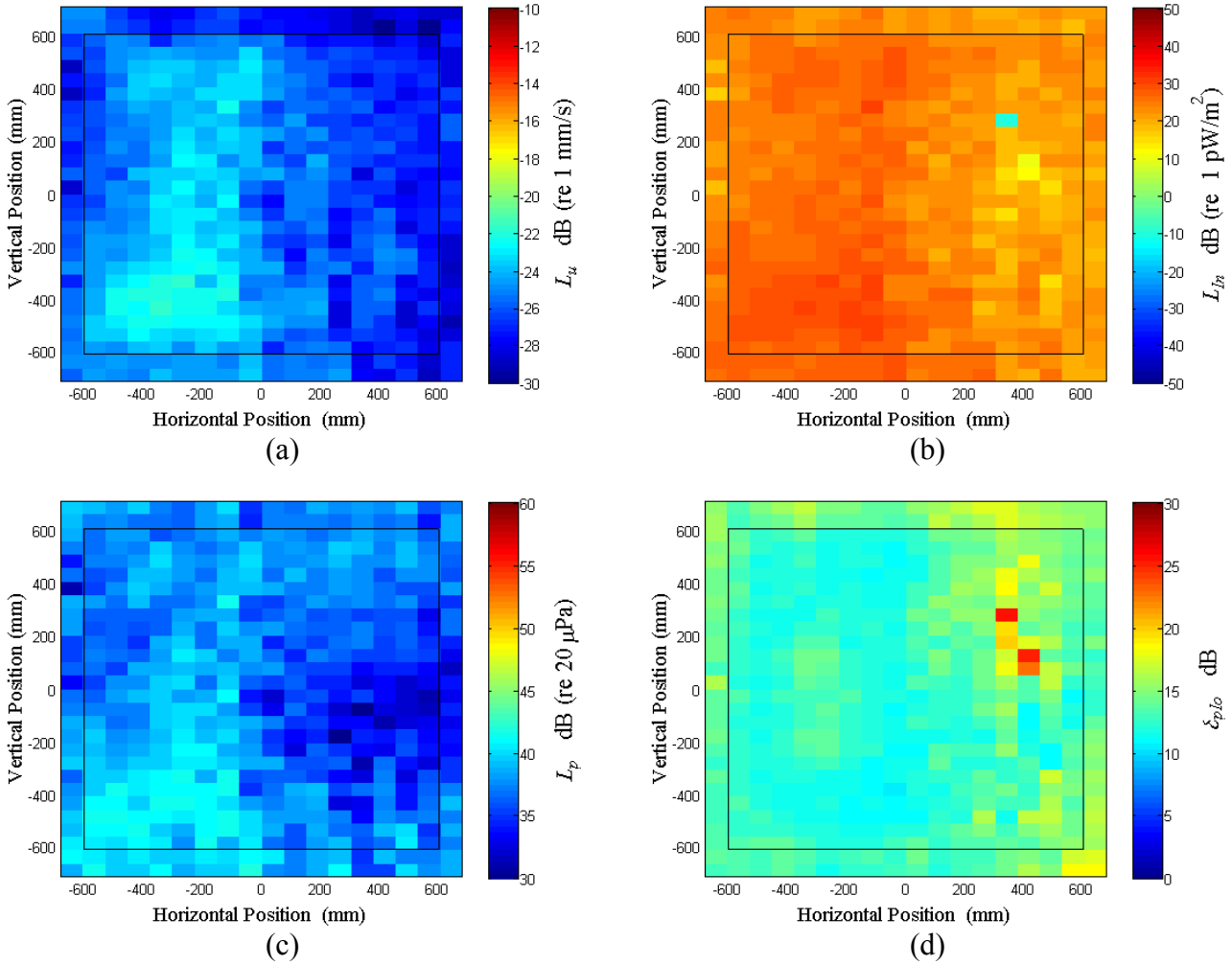

Figure A.35: Surface scan of Window A at 150 Hz (a) particle velocity level, L_u (b) normal signed sound intensity level, L_{In} (c) sound pressure level, L_p (d) pressure-residual intensity index, δ_{pIo}.

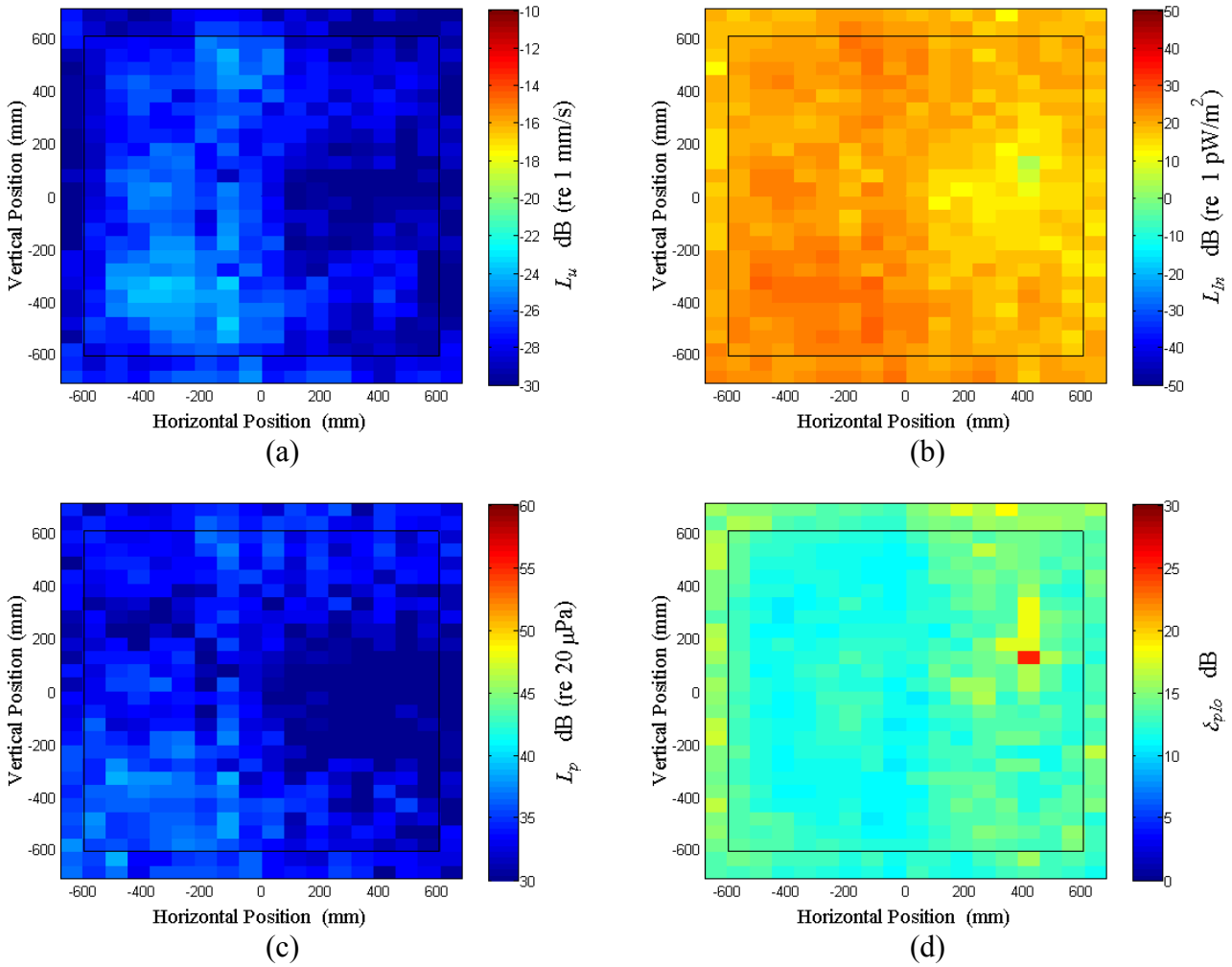

Figure A.36: Surface scan of Window A at 160 Hz (a) particle velocity level, L_u (b) normal signed sound intensity level, L_{In} (c) sound pressure level, L_p (d) pressure-residual intensity index, δ_{pIo}.

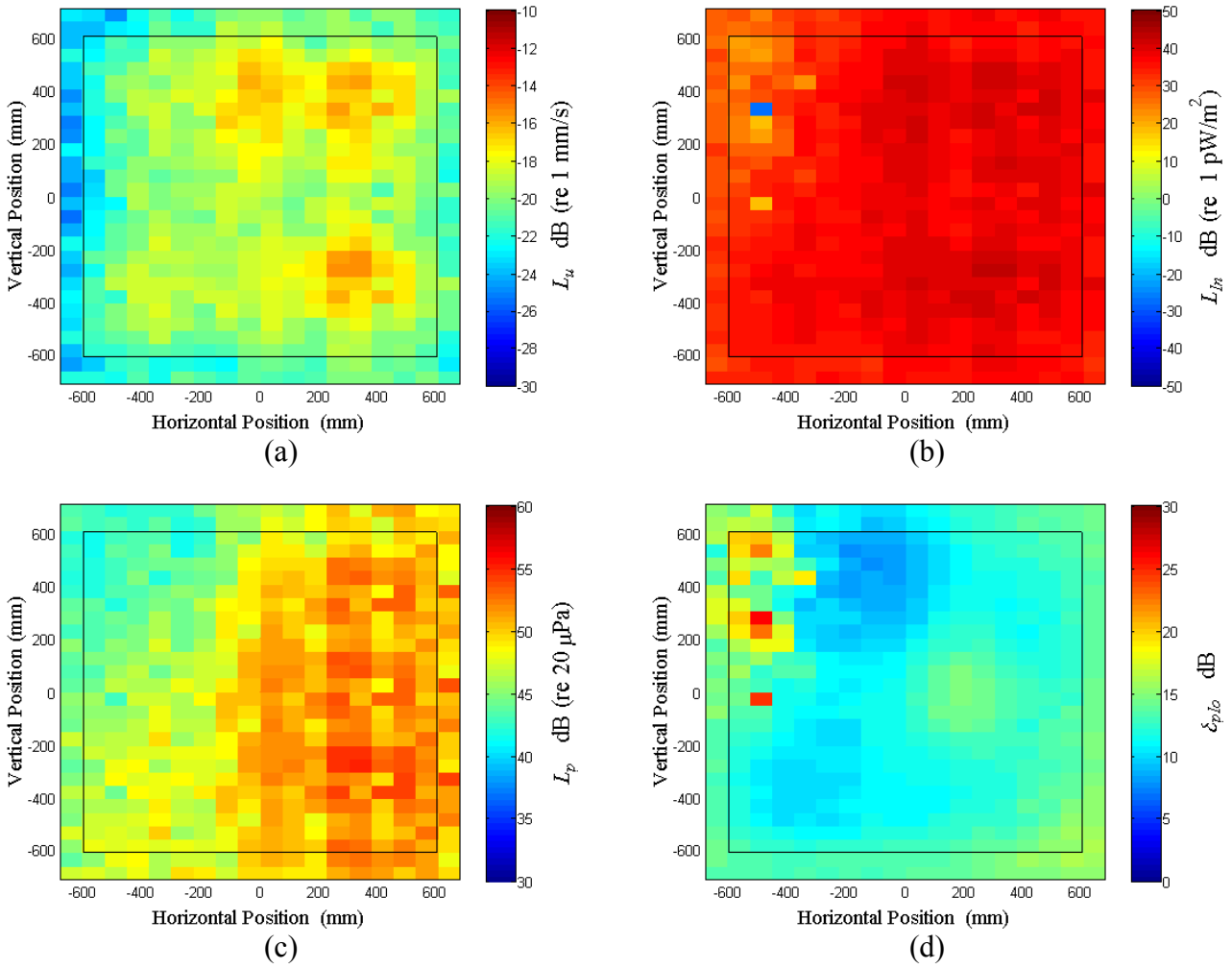

Figure A.37: Surface scan of Window A at 170 Hz (a) particle velocity level, L_u (b) normal signed sound intensity level, L_{In} (c) sound pressure level, L_p (d) pressure-residual intensity index, δ_{pIo}.

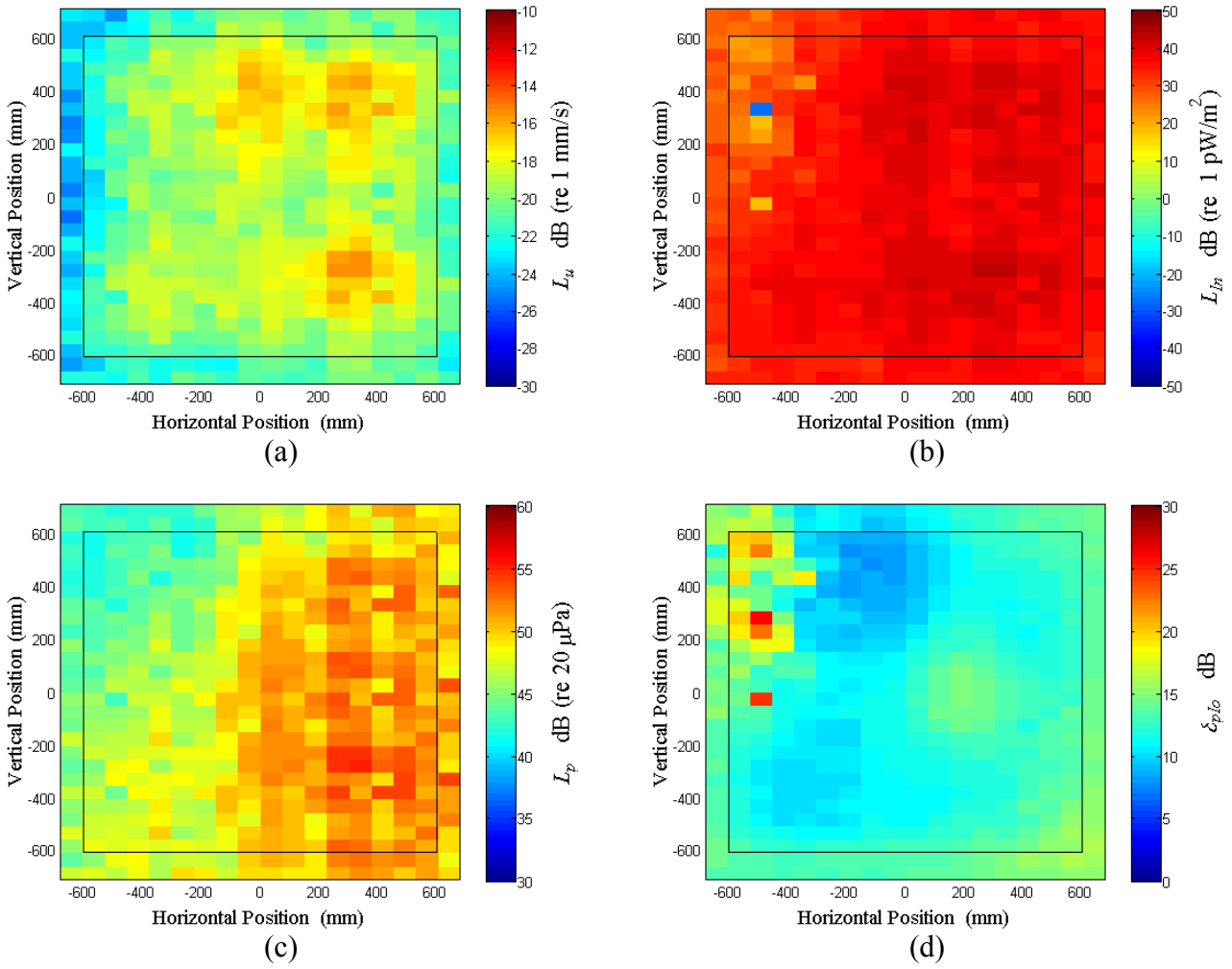

Figure A.38: Surface scan of Window A at 180 Hz (a) particle velocity level, L_u (b) normal signed sound intensity level, L_{In} (c) sound pressure level, L_p (d) pressure-residual intensity index, δ_{pIo}.

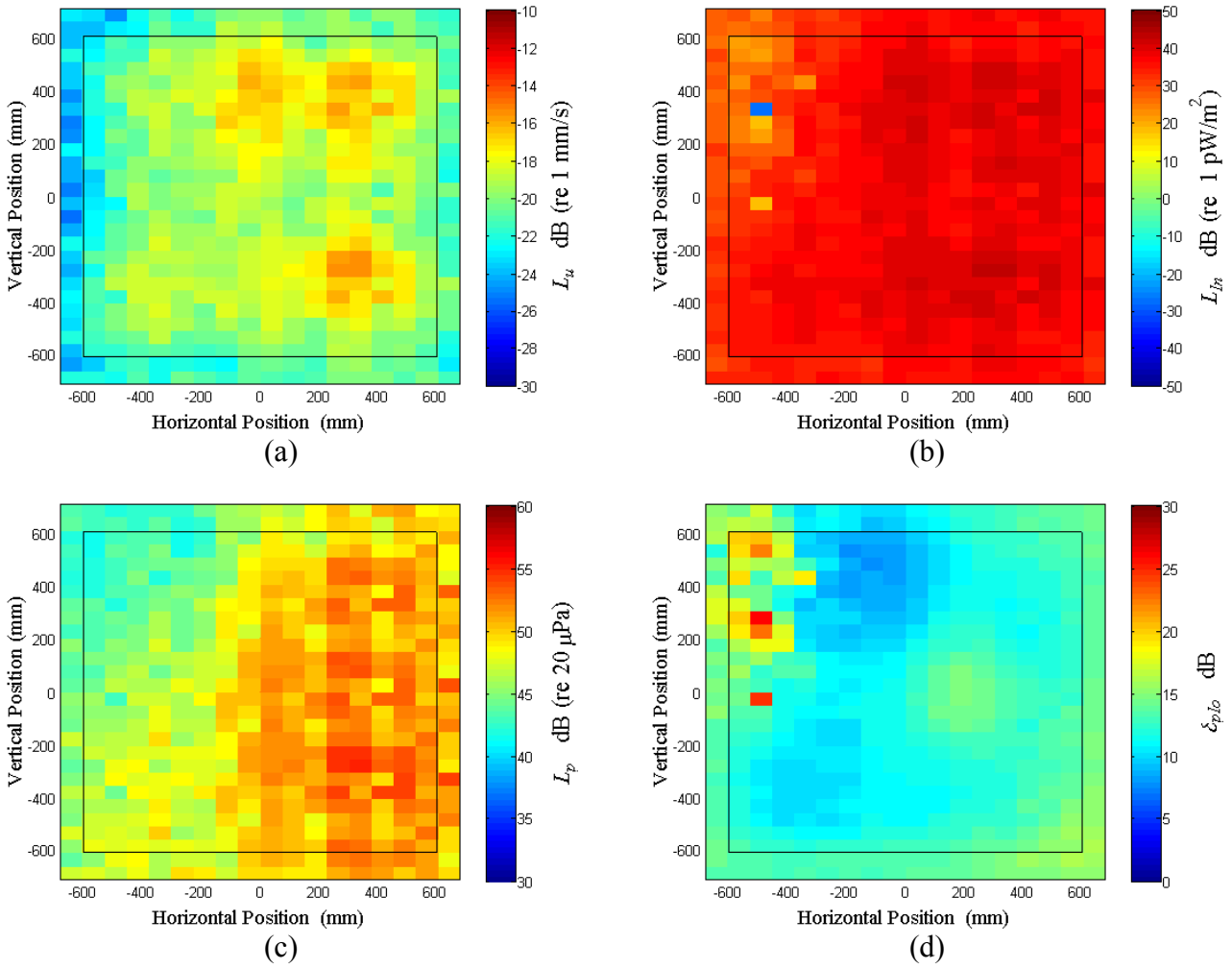

Figure A.39: Surface scan of Window A at 190 Hz (a) particle velocity level, L_u (b) normal signed sound intensity level, L_{In} (c) sound pressure level, L_p (d) pressure-residual intensity index, δ_{pIo}.

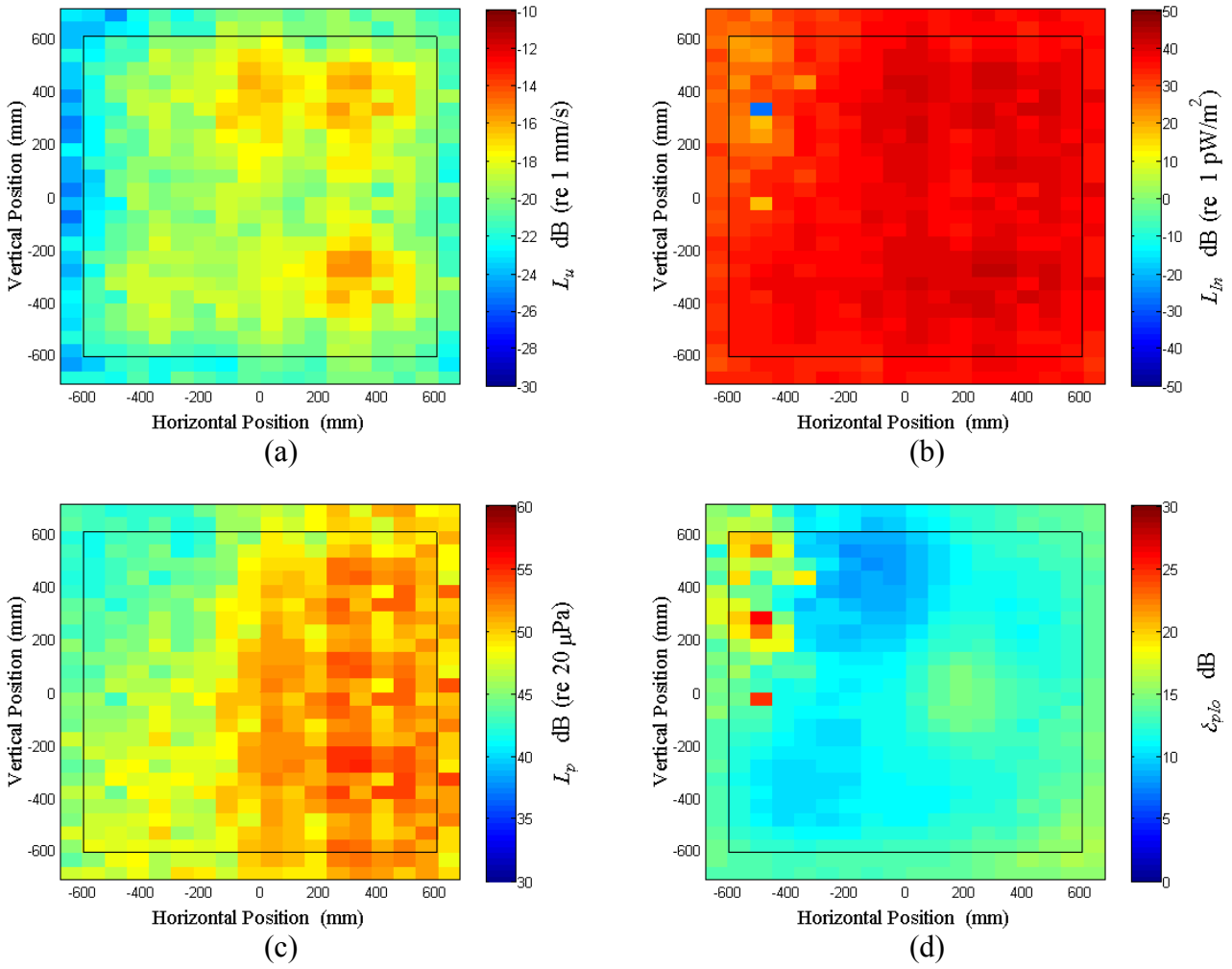

Figure A.40: Surface scan of Window A at 200 Hz (a) particle velocity level, L_u (b) normal signed sound intensity level, L_{In} (c) sound pressure level, L_p (d) pressure-residual intensity index, δ_{pIo}.

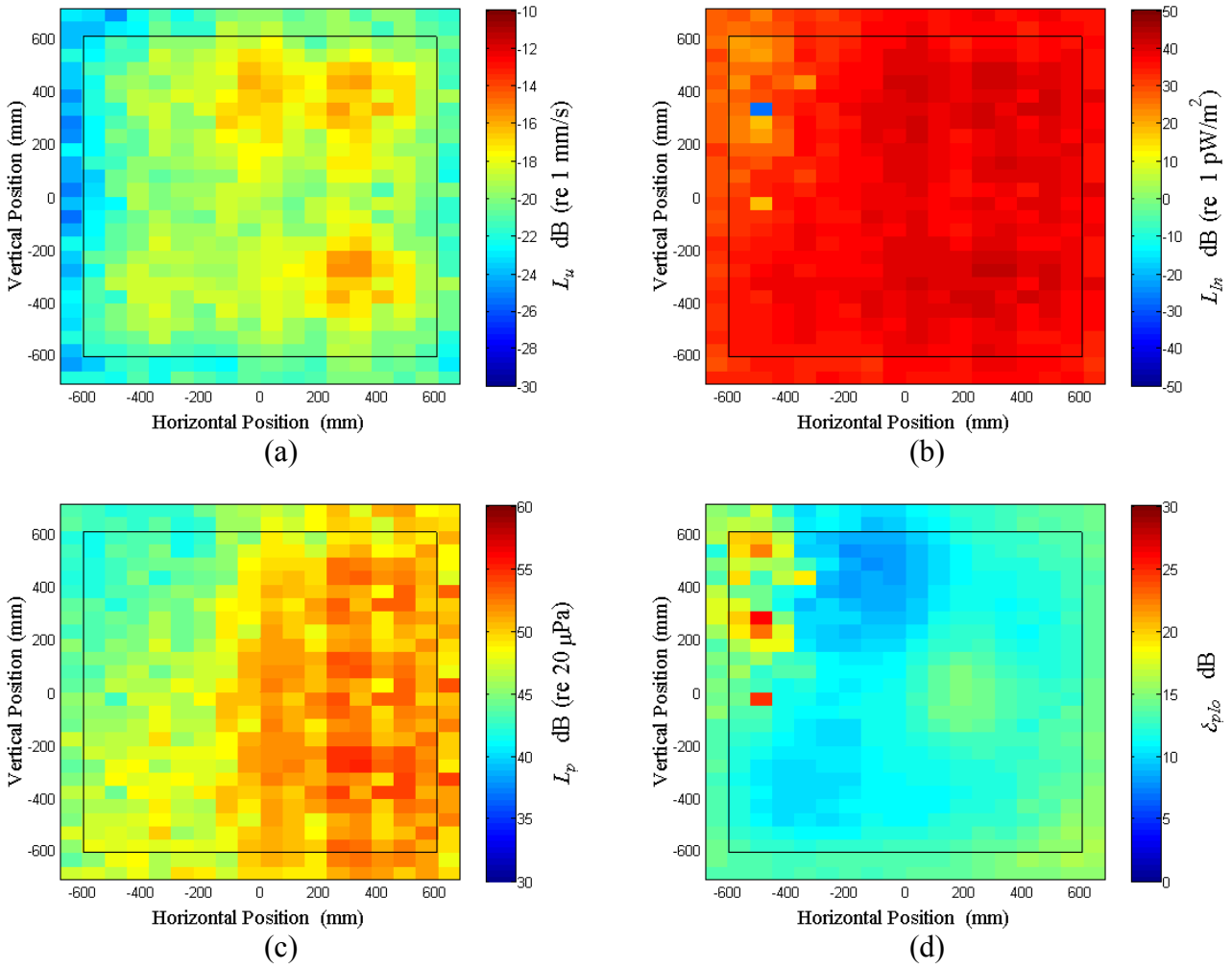

Figure A.41: Surface scan of Window A at 210 Hz (a) particle velocity level, L_u (b) normal signed sound intensity level, L_{In} (c) sound pressure level, L_p (d) pressure-residual intensity index, δ_{pIo}.

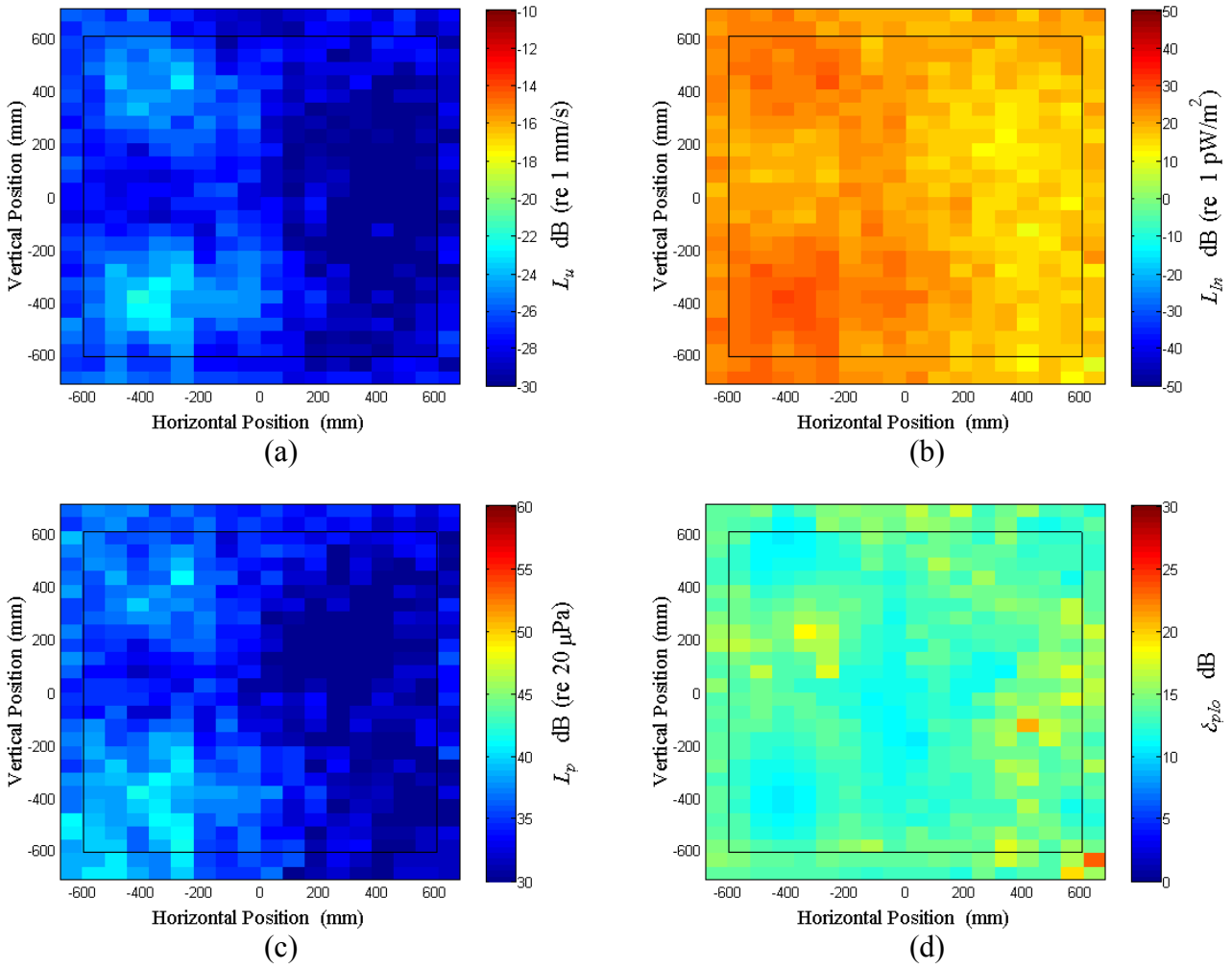

Figure A.42: Surface scan of Window A at 220 Hz (a) particle velocity level, L_u (b) normal signed sound intensity level, L_{In} (c) sound pressure level, L_p (d) pressure-residual intensity index, δ_{pIo}.

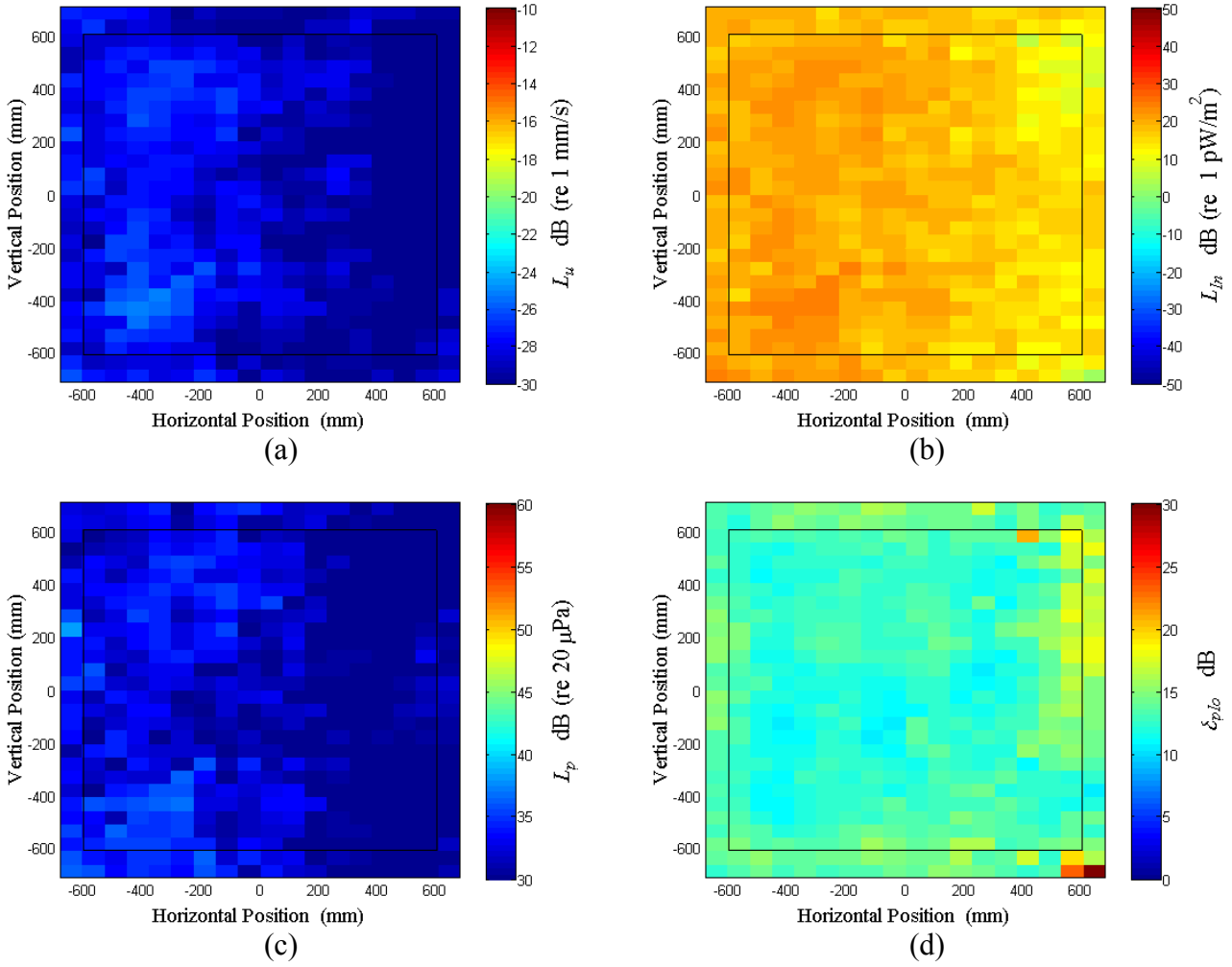

Figure A.43: Surface scan of Window A at 230 Hz (a) particle velocity level, L_u (b) normal signed sound intensity level, L_{In} (c) sound pressure level, L_p (d) pressure-residual intensity index, δ_{pIo}.

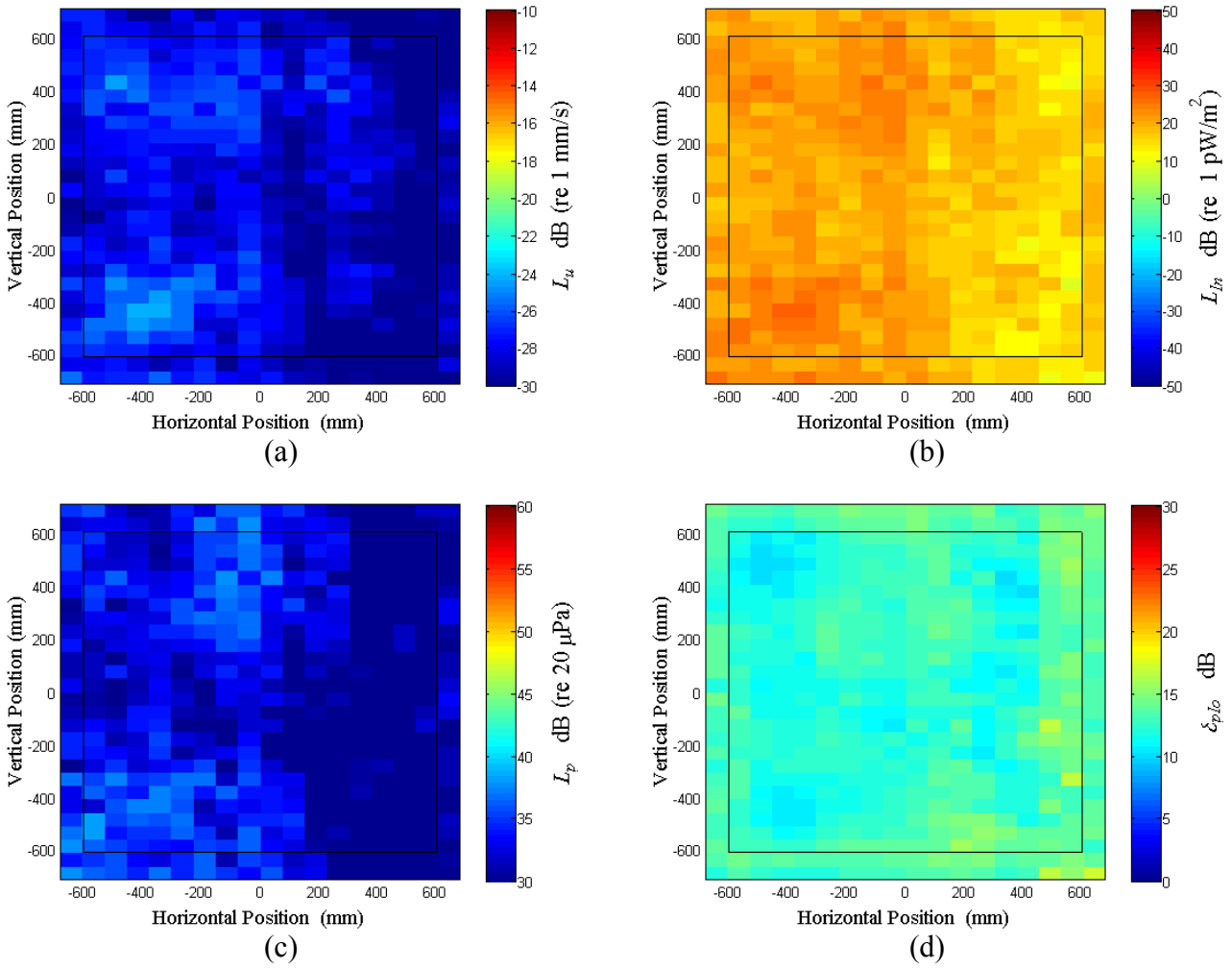

Figure A.44: Surface scan of Window A at 240 Hz (a) particle velocity level, L_u (b) normal signed sound intensity level, L_{In} (c) sound pressure level, L_p (d) pressure-residual intensity index, δ_{pIo}.

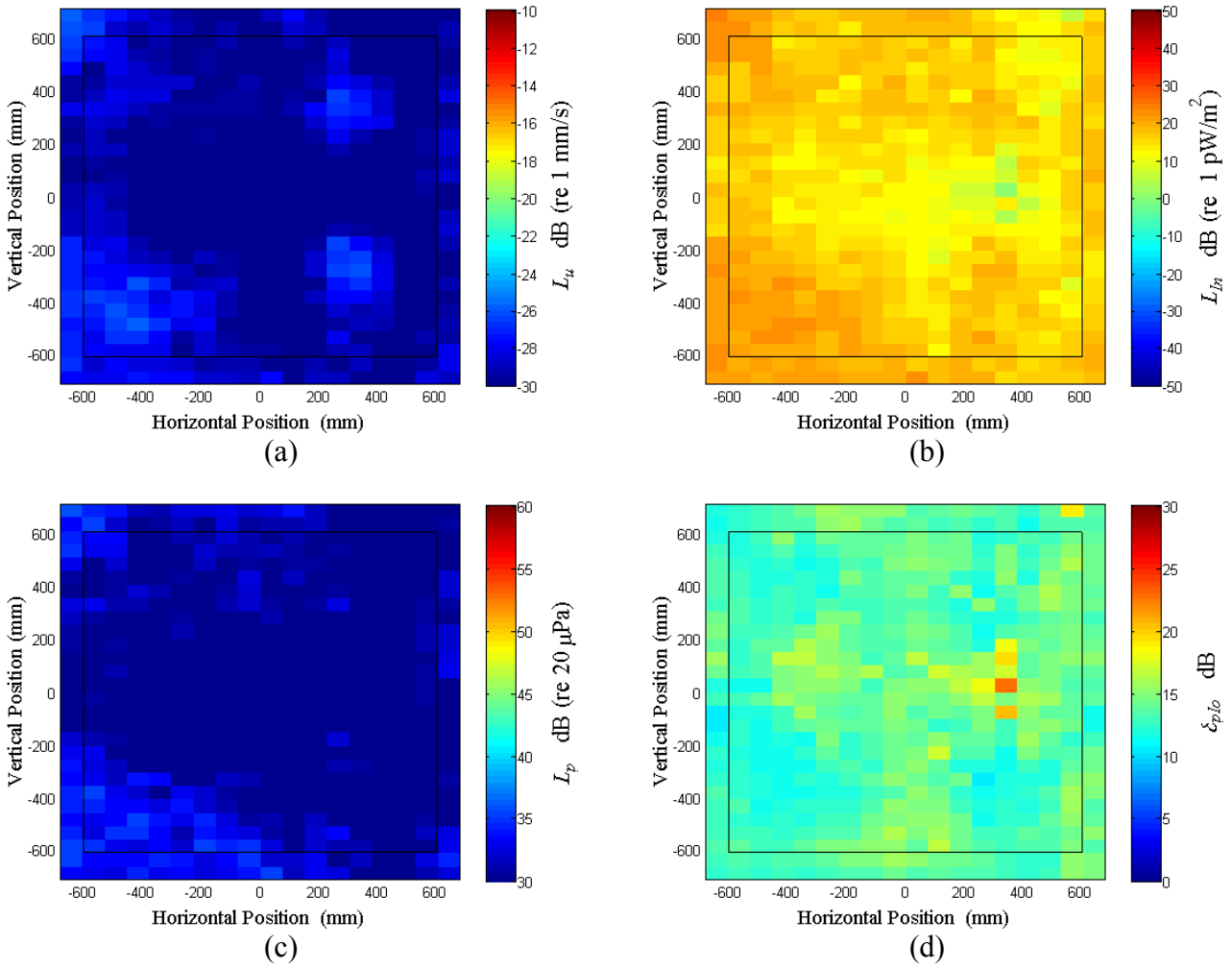

Figure A.45: Surface scan of Window A at 250 Hz (a) particle velocity level, L_u (b) normal signed sound intensity level, L_{In} (c) sound pressure level, L_p (d) pressure-residual intensity index, δ_{pIo}.

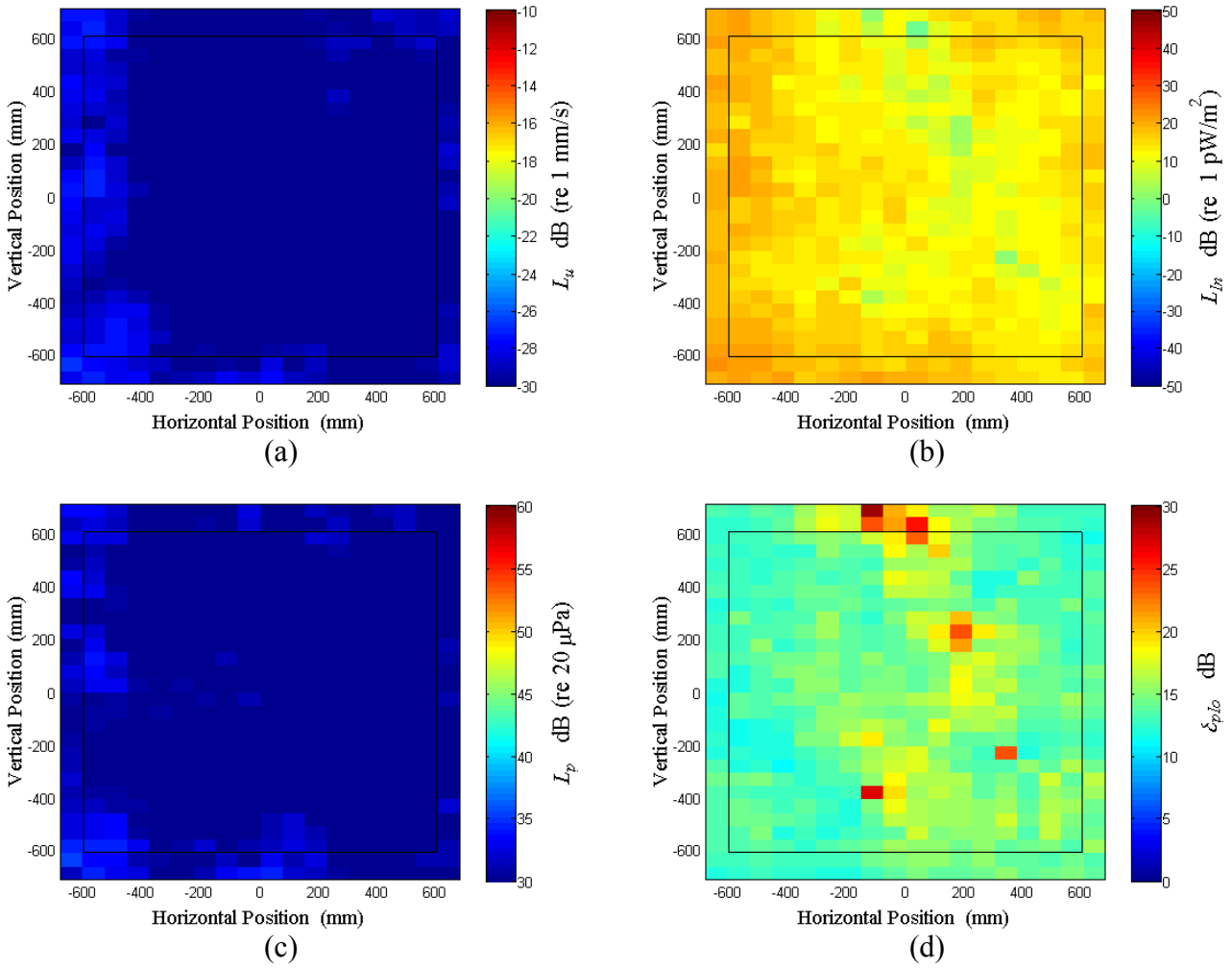

Figure A.46: Surface scan of Window A at 260 Hz (a) particle velocity level, L_u (b) normal signed sound intensity level, L_{In} (c) sound pressure level, L_p (d) pressure-residual intensity index, δ_{pIo}.

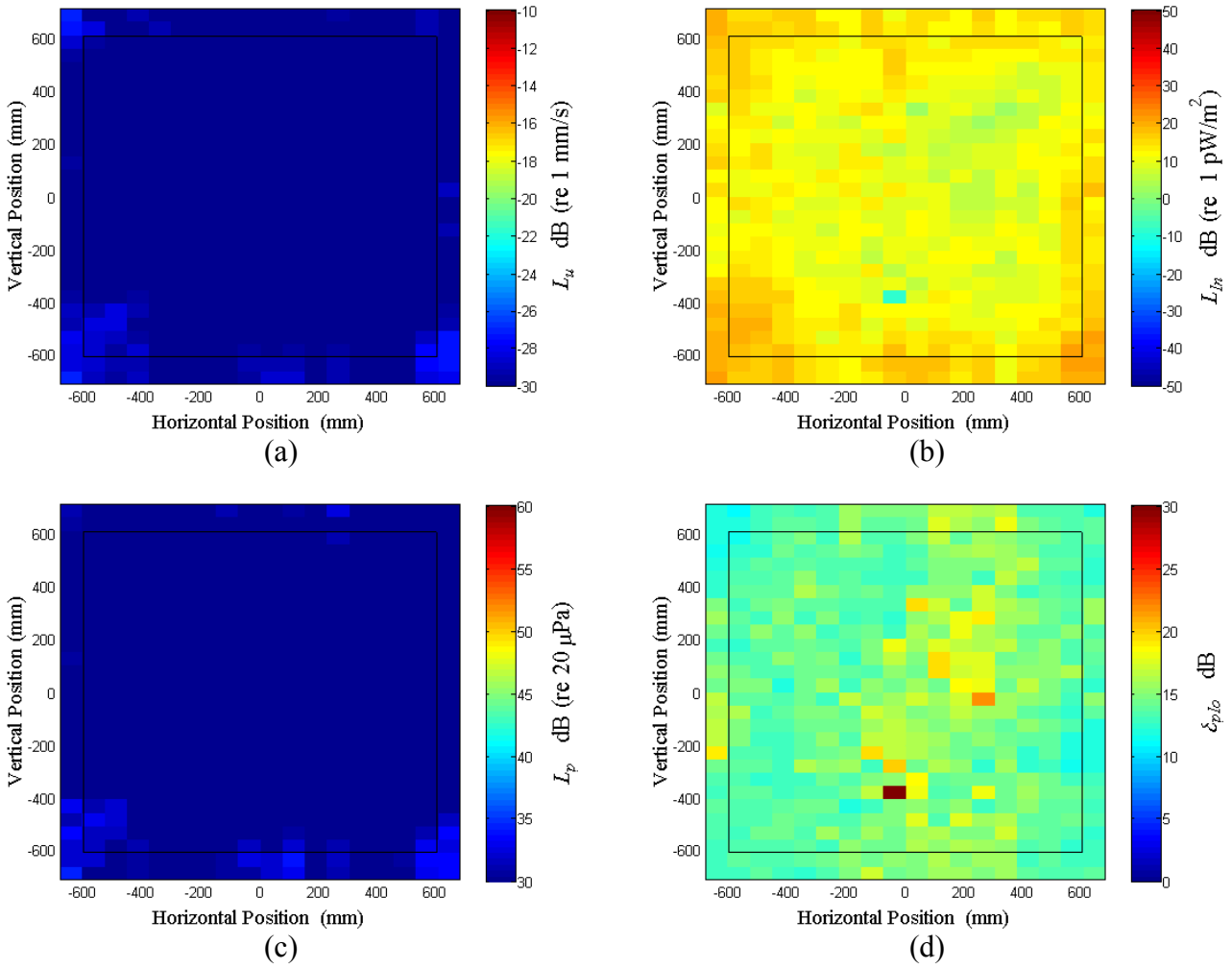

Figure A.47: Surface scan of Window A at 270 Hz (a) particle velocity level, L_u (b) normal signed sound intensity level, L_{In} (c) sound pressure level, L_p (d) pressure-residual intensity index, δ_{pIo}.

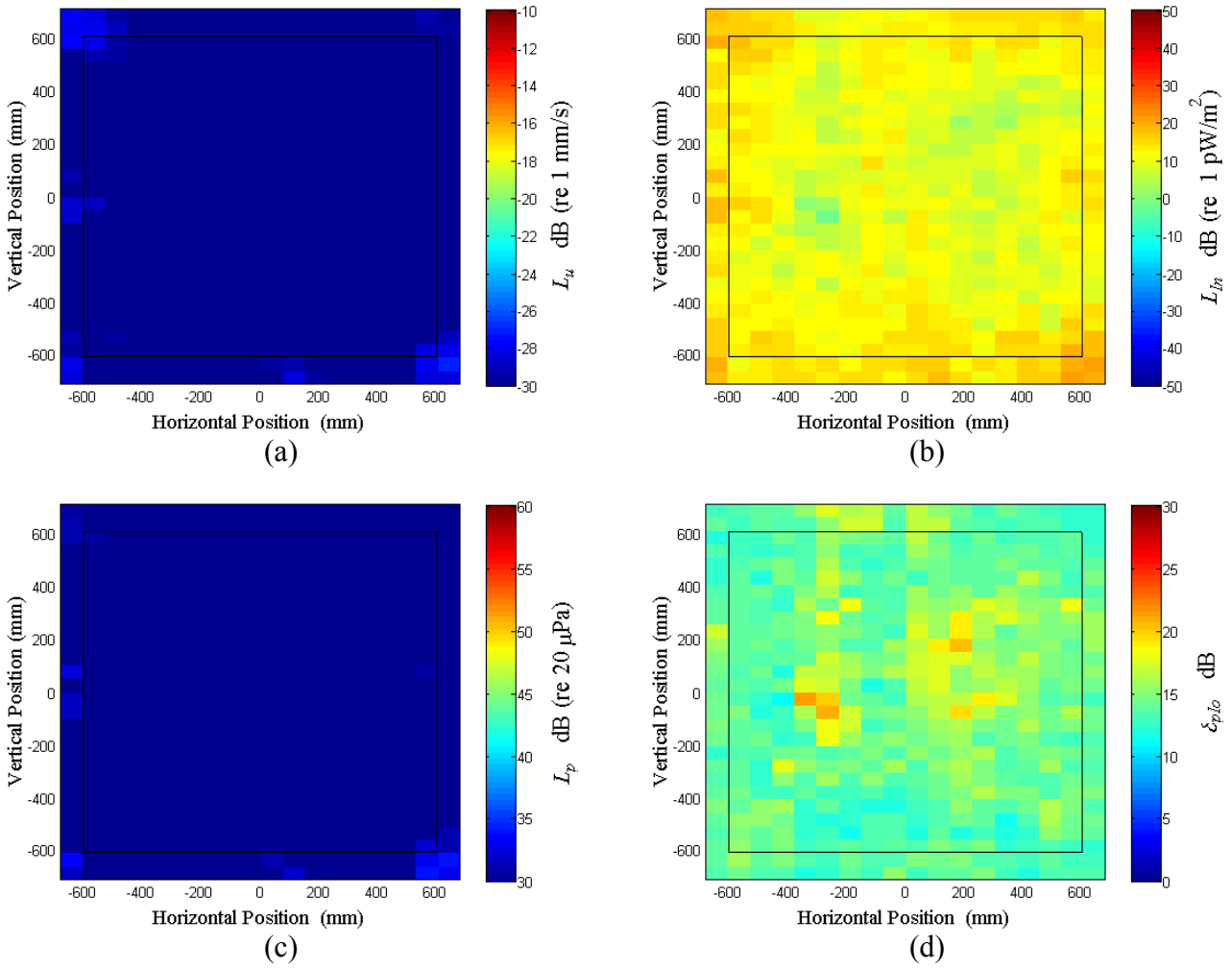

Figure A.48: Surface scan of Window A at 280 Hz (a) particle velocity level, L_u (b) normal signed sound intensity level, L_{In} (c) sound pressure level, L_p (d) pressure-residual intensity index, δ_{pIo}.

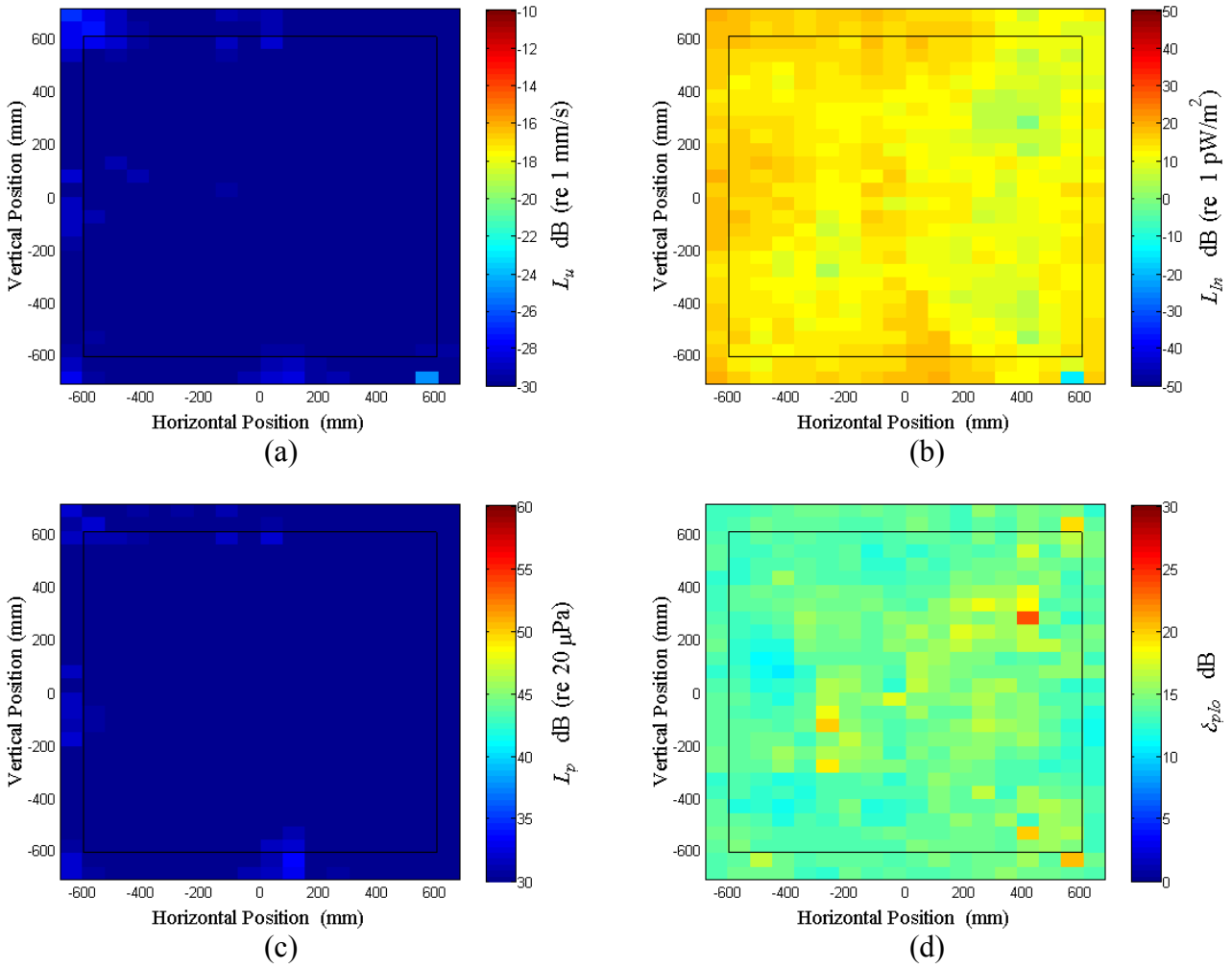

Figure A.49: Surface scan of Window A at 290 Hz (a) particle velocity level, L_u (b) normal signed sound intensity level, L_{In} (c) sound pressure level, L_p (d) pressure-residual intensity index, δ_{pIo}.

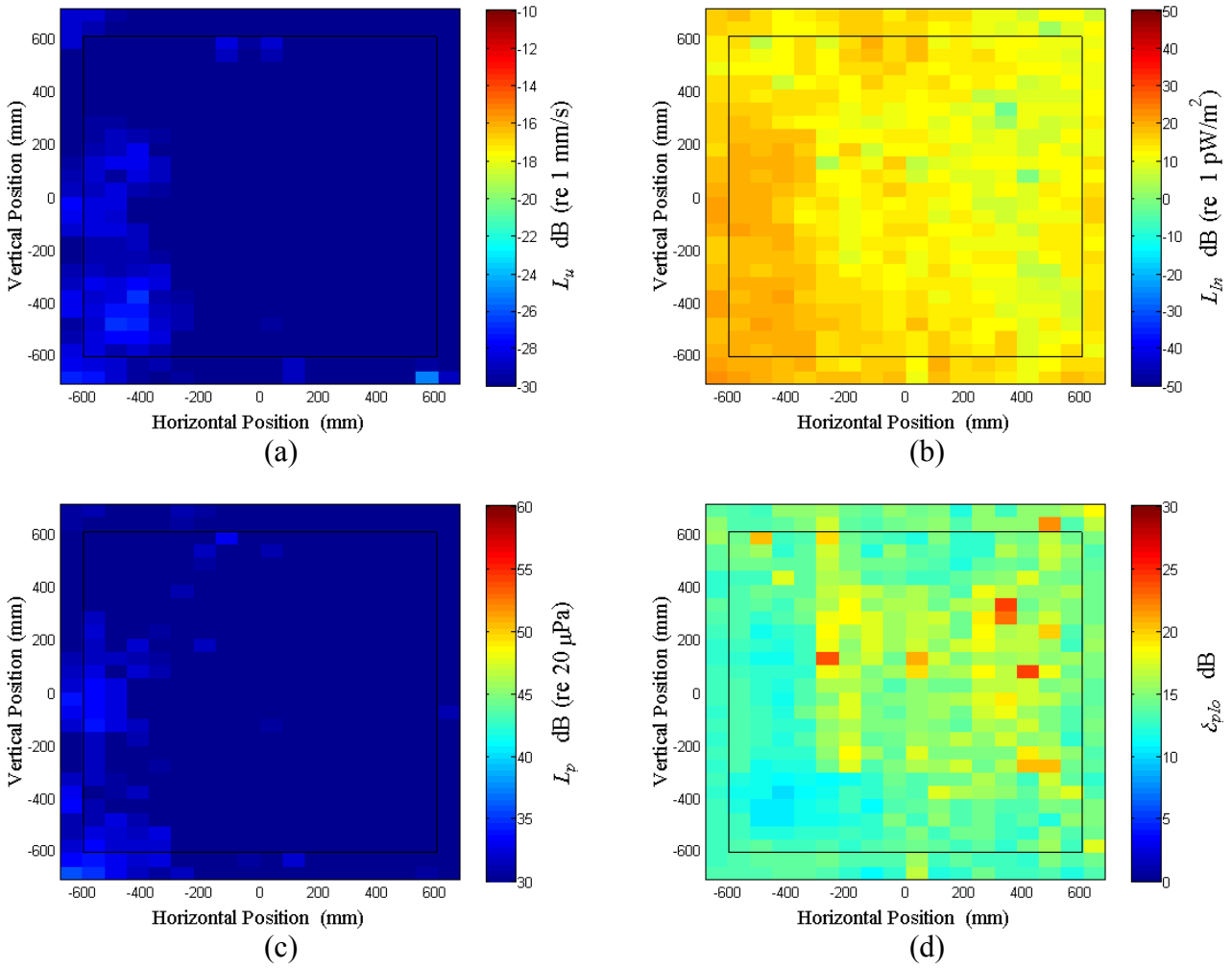

Figure A.50: Surface scan of Window A at 300 Hz (a) particle velocity level, L_u (b) normal signed sound intensity level, L_{In} (c) sound pressure level, L_p (d) pressure-residual intensity index, δ_{pIo}.

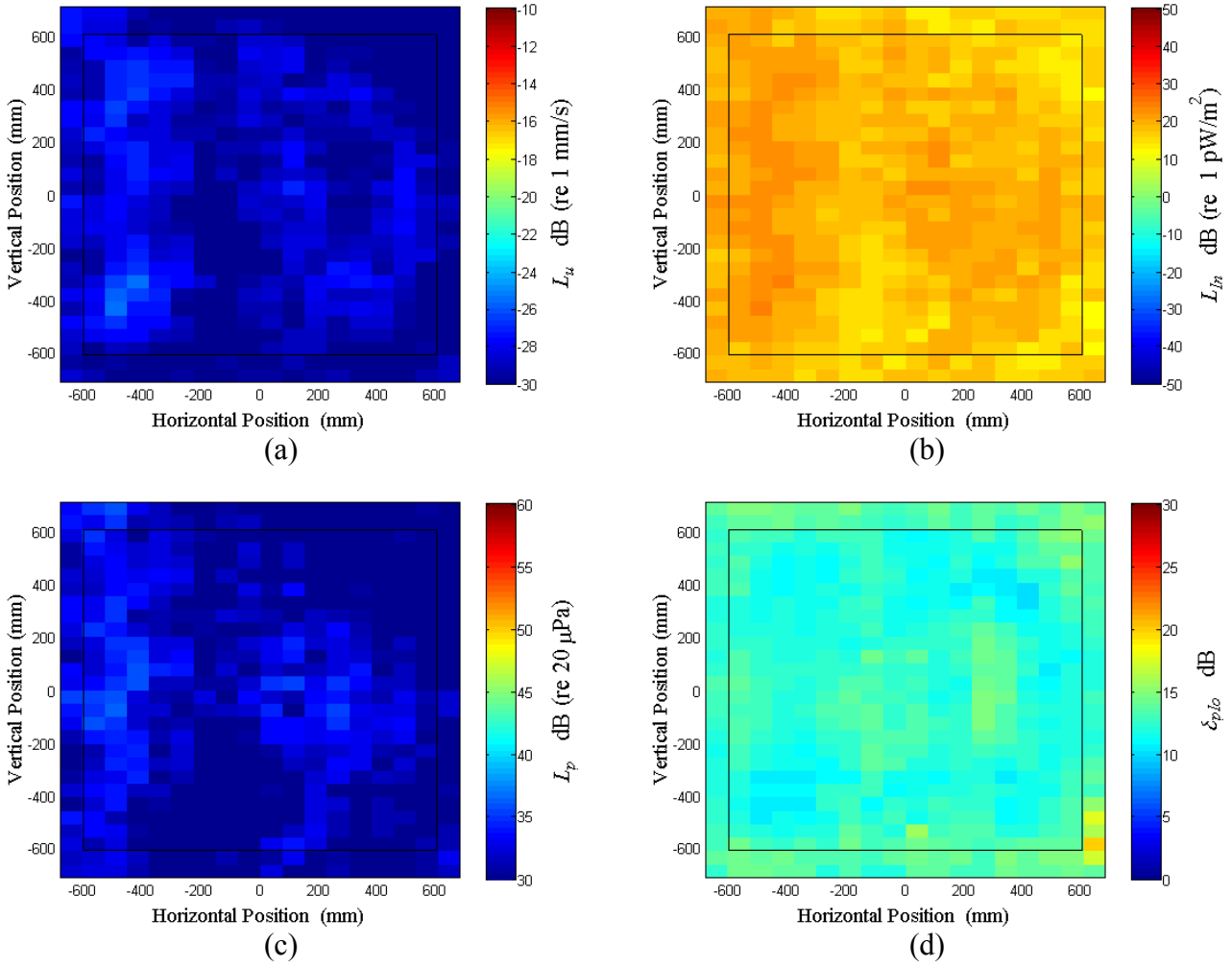

Figure A.51: Surface scan of Window A at 310 Hz (a) particle velocity level, L_u (b) normal signed sound intensity level, L_{In} (c) sound pressure level, L_p (d) pressure-residual intensity index, δ_{pIo}.

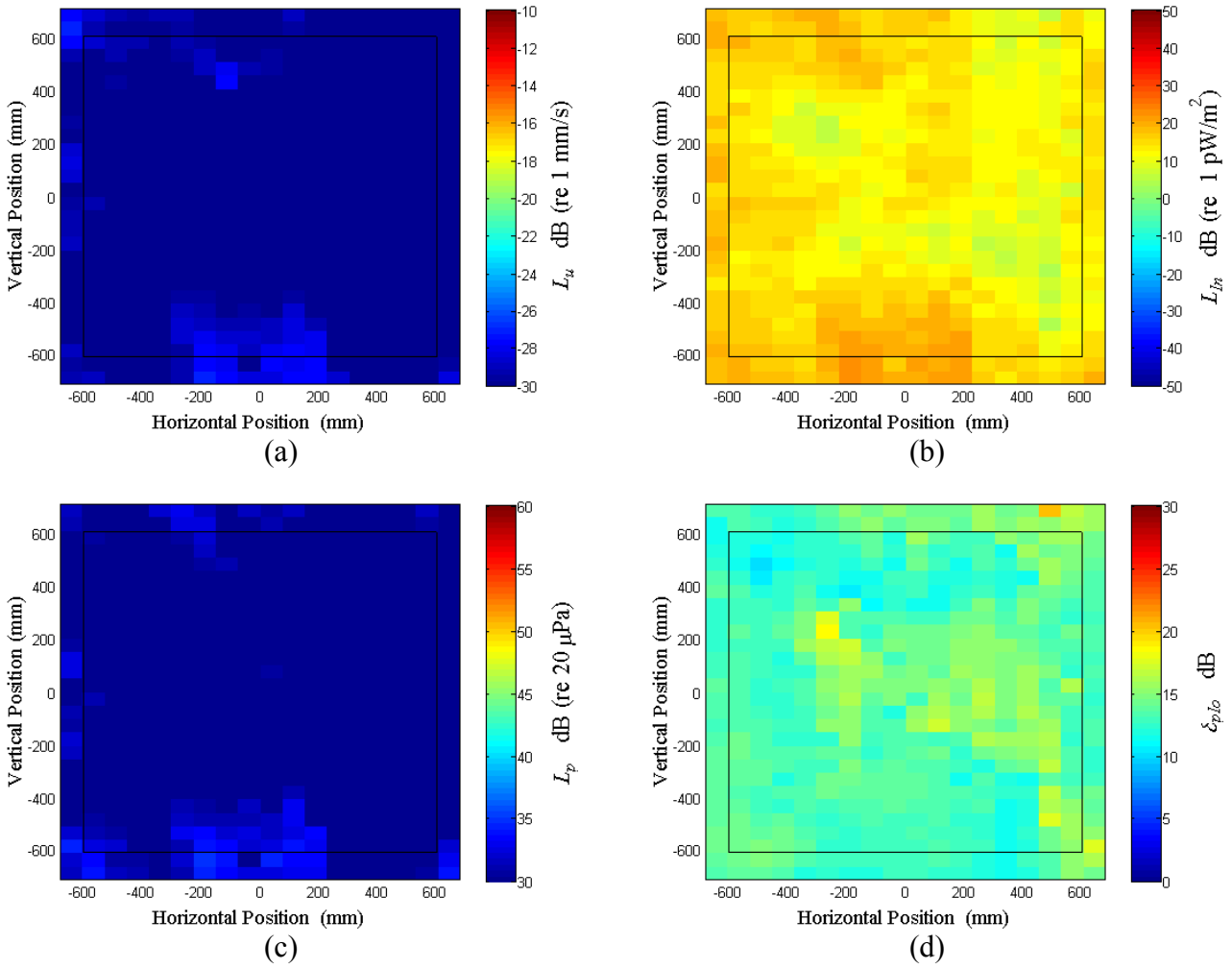

Figure A.52: Surface scan of Window A at 320 Hz (a) particle velocity level, L_u (b) normal signed sound intensity level, L_{In} (c) sound pressure level, L_p (d) pressure-residual intensity index, δ_{pIo}.

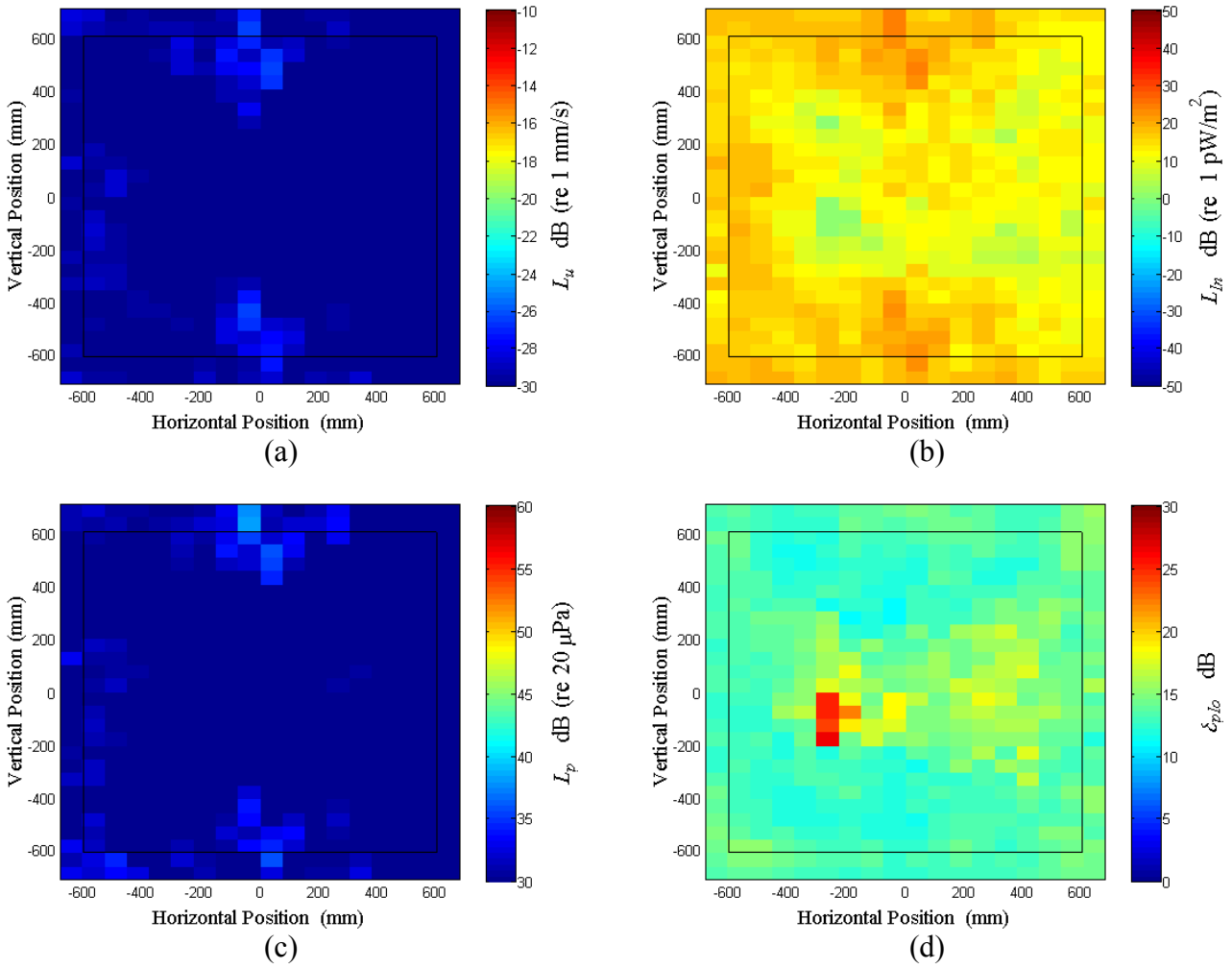

Figure A.53: Surface scan of Window A at 330 Hz (a) particle velocity level, L_u (b) normal signed sound intensity level, L_{In} (c) sound pressure level, L_p (d) pressure-residual intensity index, δ_{pIo}.

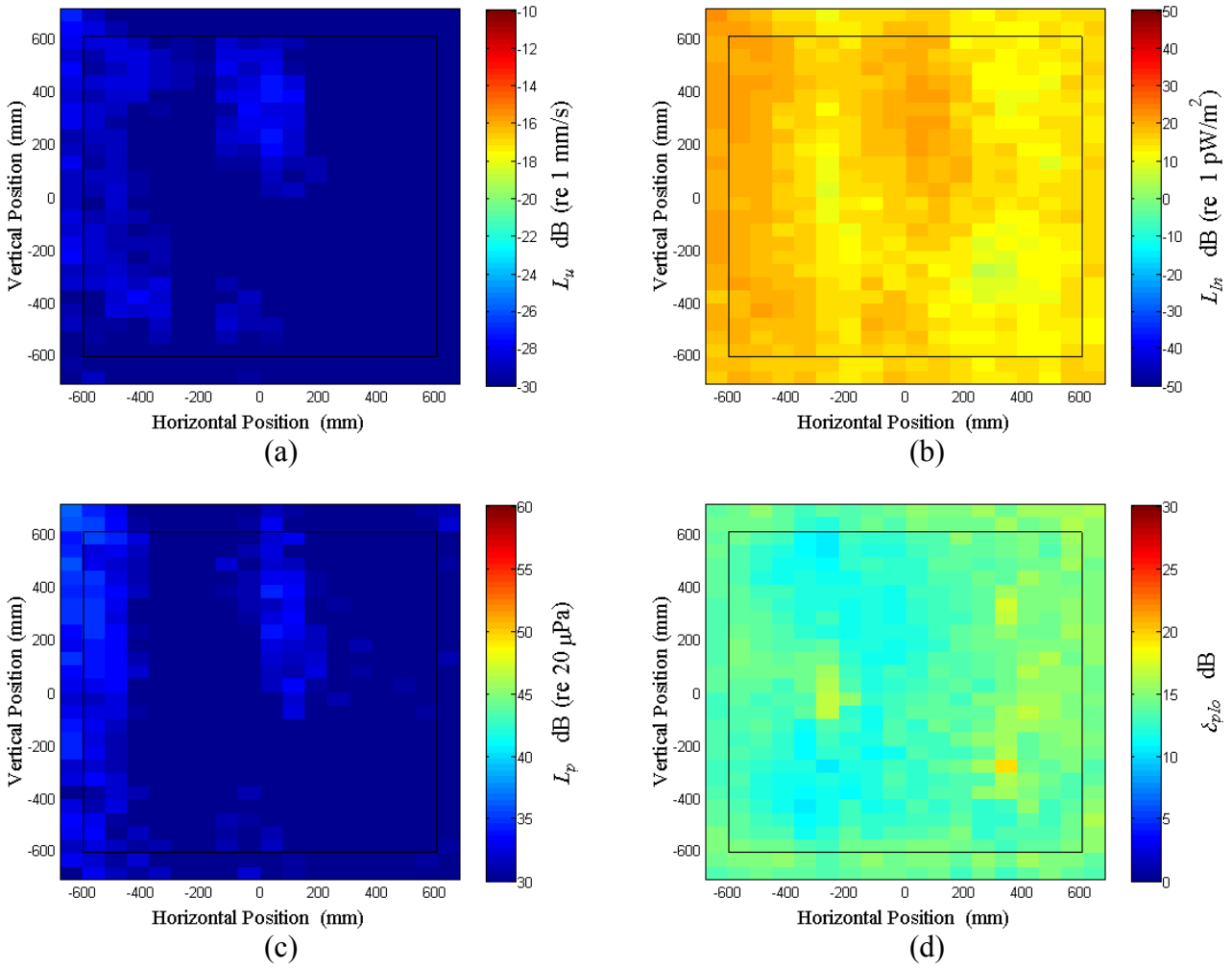

Figure A.54: Surface scan of Window A at 340 Hz (a) particle velocity level, L_u (b) normal signed sound intensity level, L_{In} (c) sound pressure level, L_p (d) pressure-residual intensity index, δ_{pIo}.

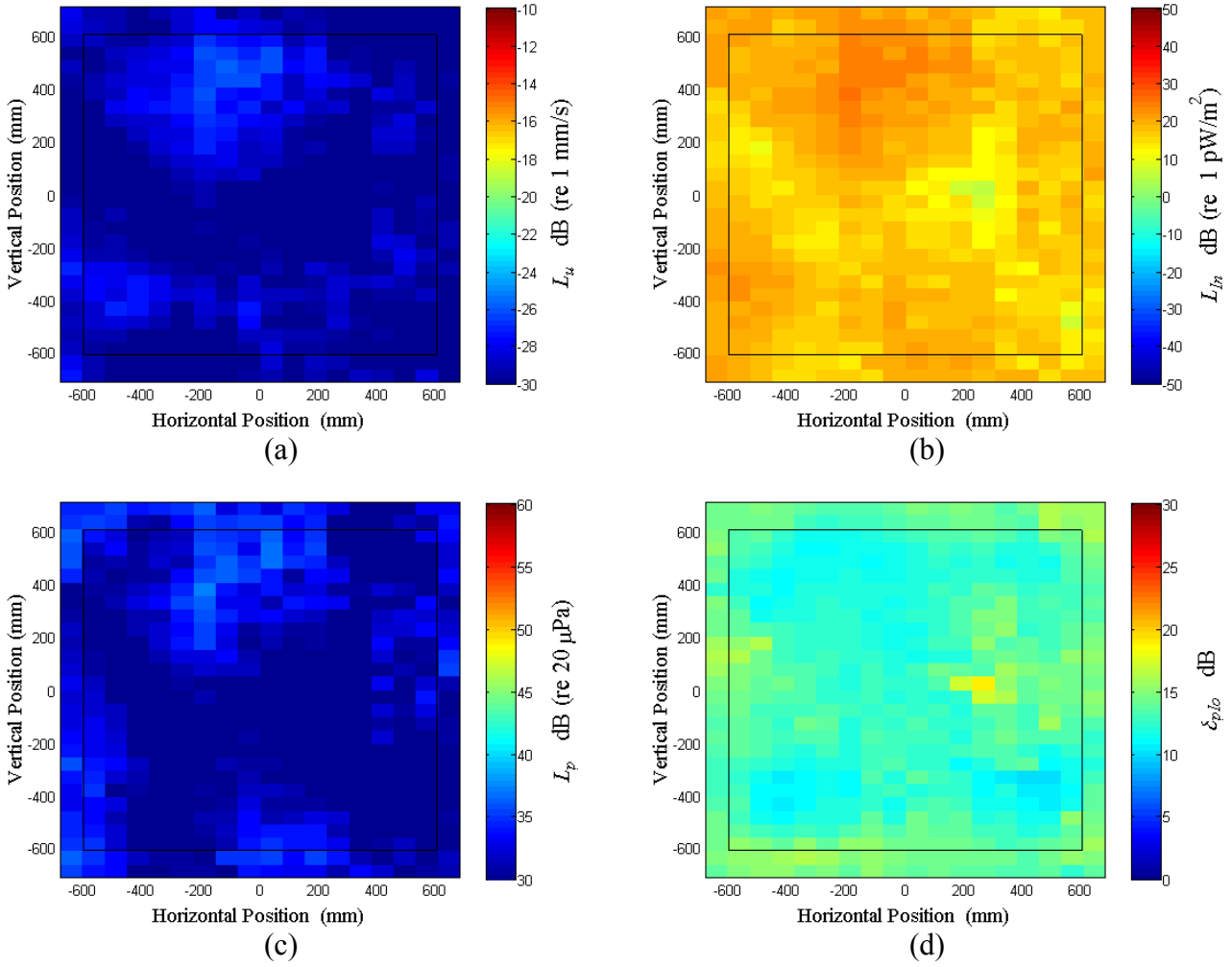

Figure A.55: Surface scan of Window A at 350 Hz (a) particle velocity level, L_u (b) normal signed sound intensity level, L_{In} (c) sound pressure level, L_p (d) pressure-residual intensity index, δ_{pIo}.

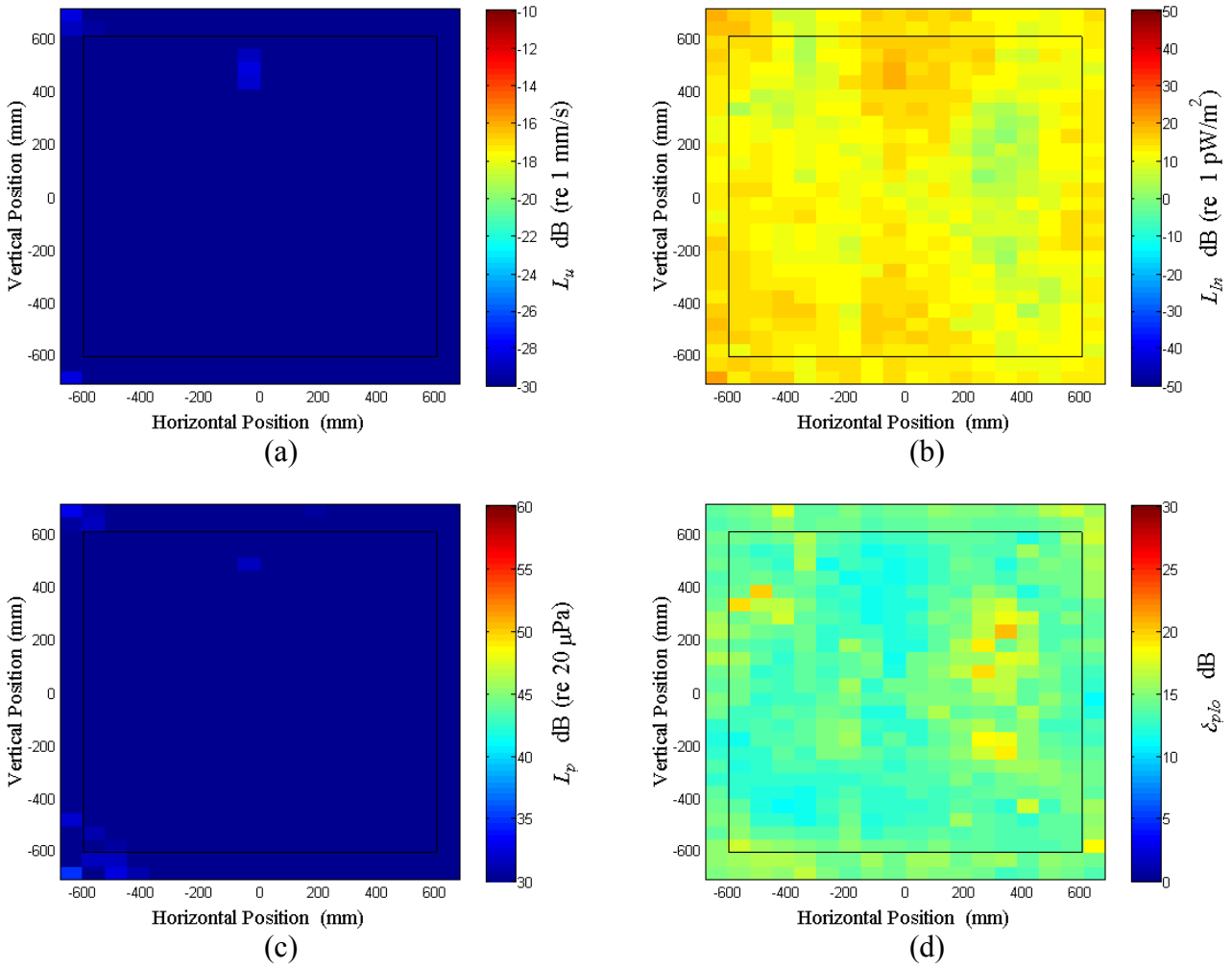

Figure A.56: Surface scan of Window A at 360 Hz (a) particle velocity level, L_u (b) normal signed sound intensity level, L_{In} (c) sound pressure level, L_p (d) pressure-residual intensity index, δ_{pIo}.

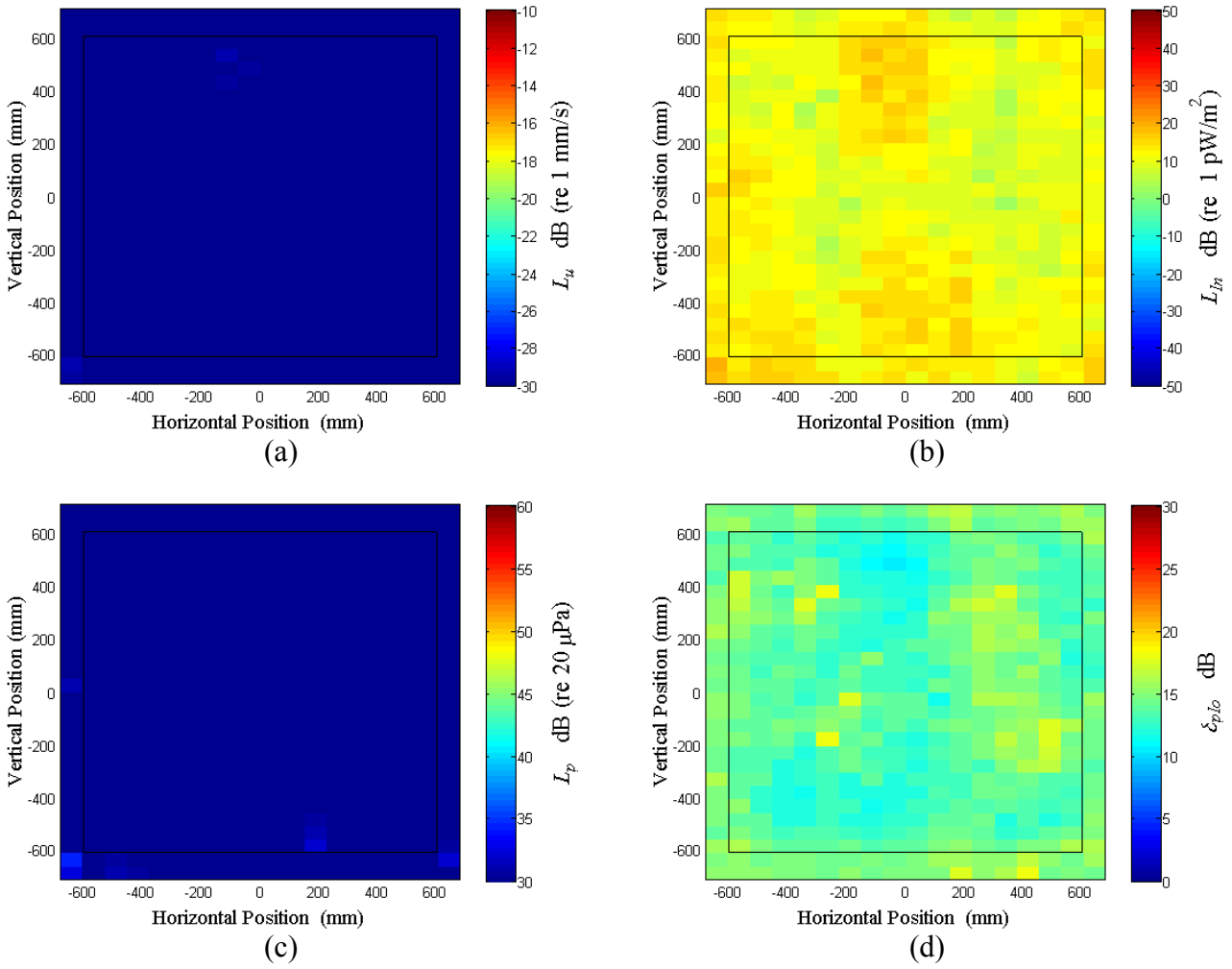

Figure A.57: Surface scan of Window A at 370 Hz (a) particle velocity level, L_u (b) normal signed sound intensity level, L_{In} (c) sound pressure level, L_p (d) pressure-residual intensity index, δ_{pIo}.

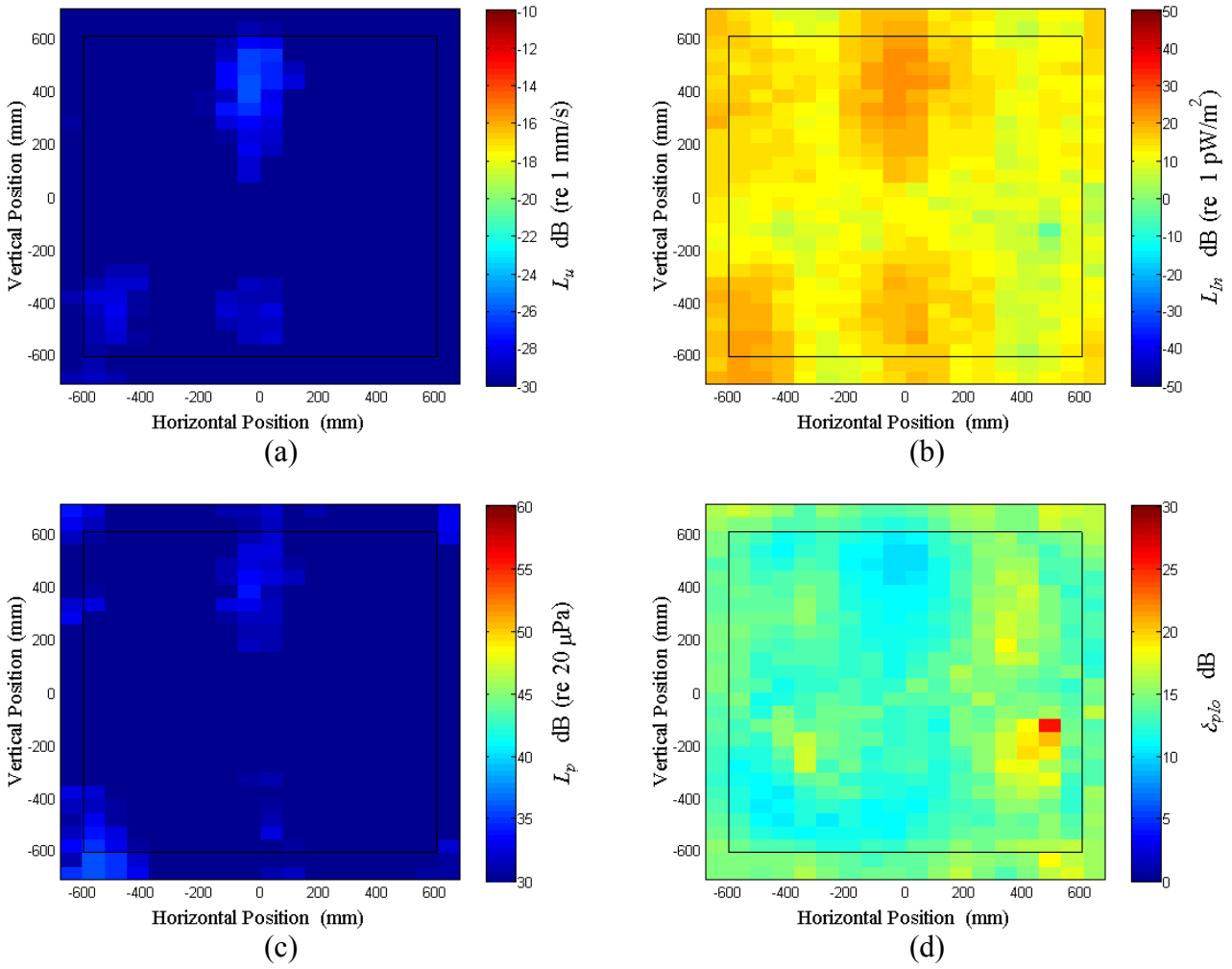

Figure A.58: Surface scan of Window A at 380 Hz (a) particle velocity level, L_u (b) normal signed sound intensity level, L_{In} (c) sound pressure level, L_p (d) pressure-residual intensity index, δ_{pIo}.

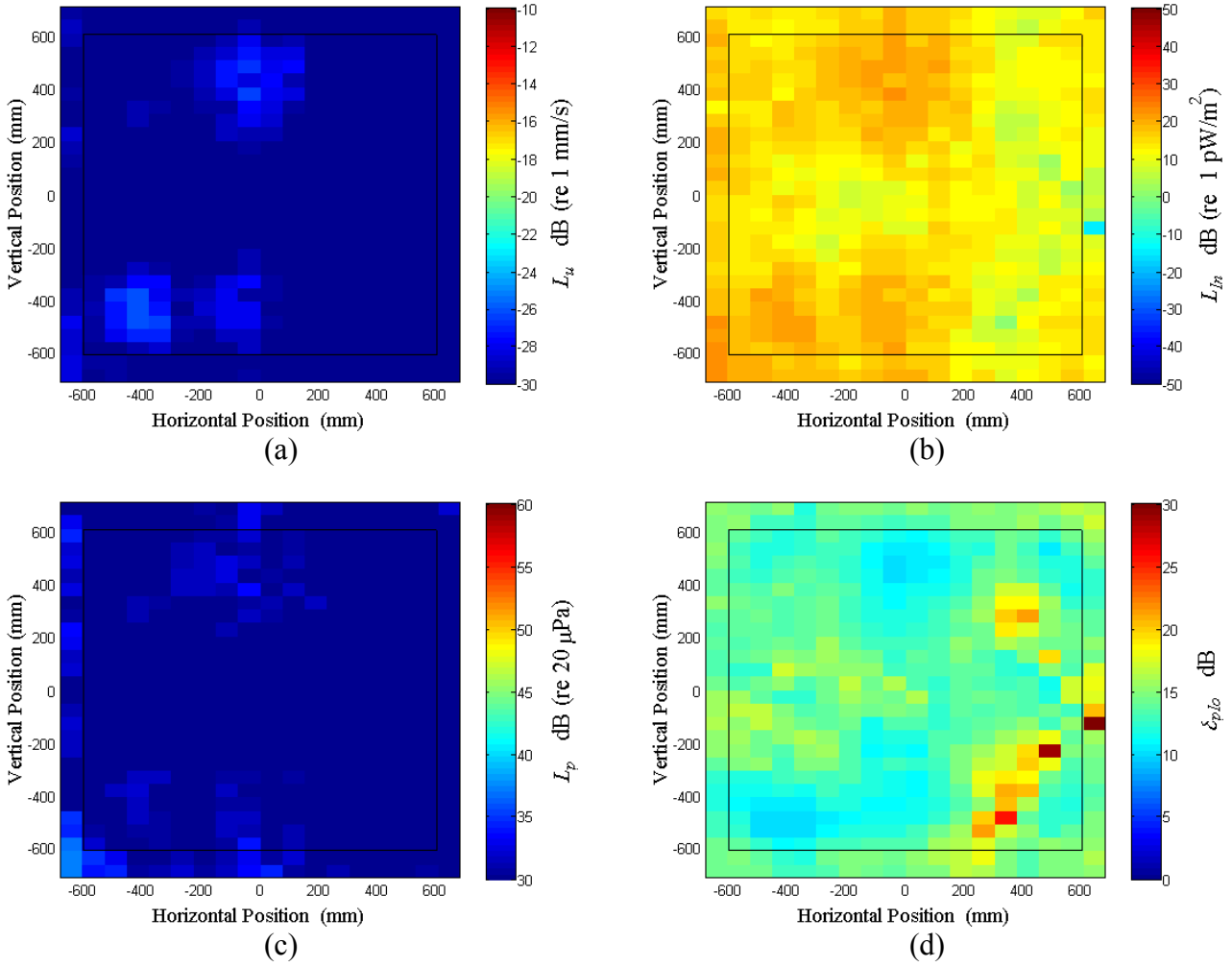

Figure A.59: Surface scan of Window A at 390 Hz (a) particle velocity level, L_u (b) normal signed sound intensity level, L_{In} (c) sound pressure level, L_p (d) pressure-residual intensity index, δ_{pIo}.

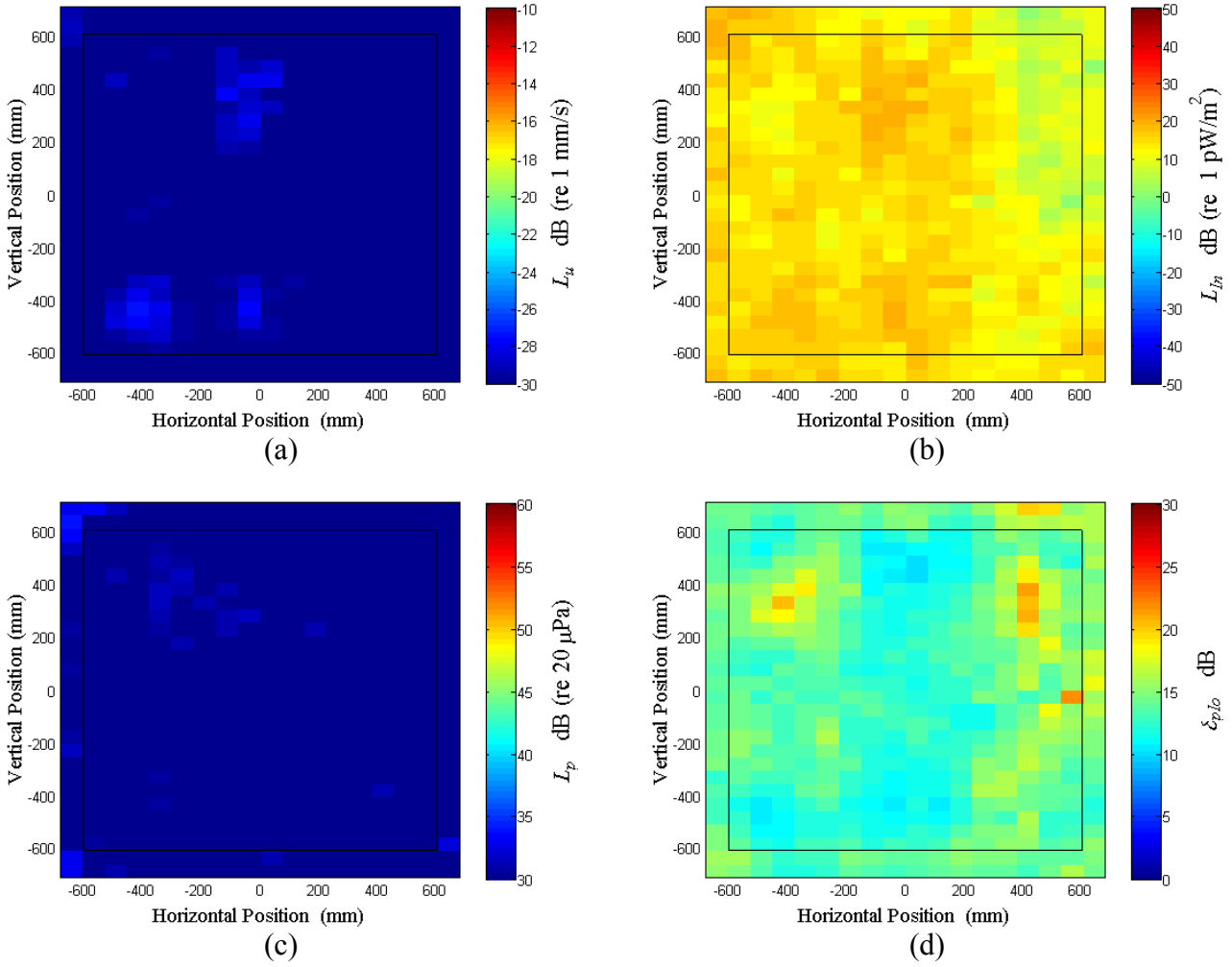

Figure A.60: Surface scan of Window A at 400 Hz (a) particle velocity level, L_u (b) normal signed sound intensity level, L_{In} (c) sound pressure level, L_p (d) pressure-residual intensity index, δ_{pIo}.

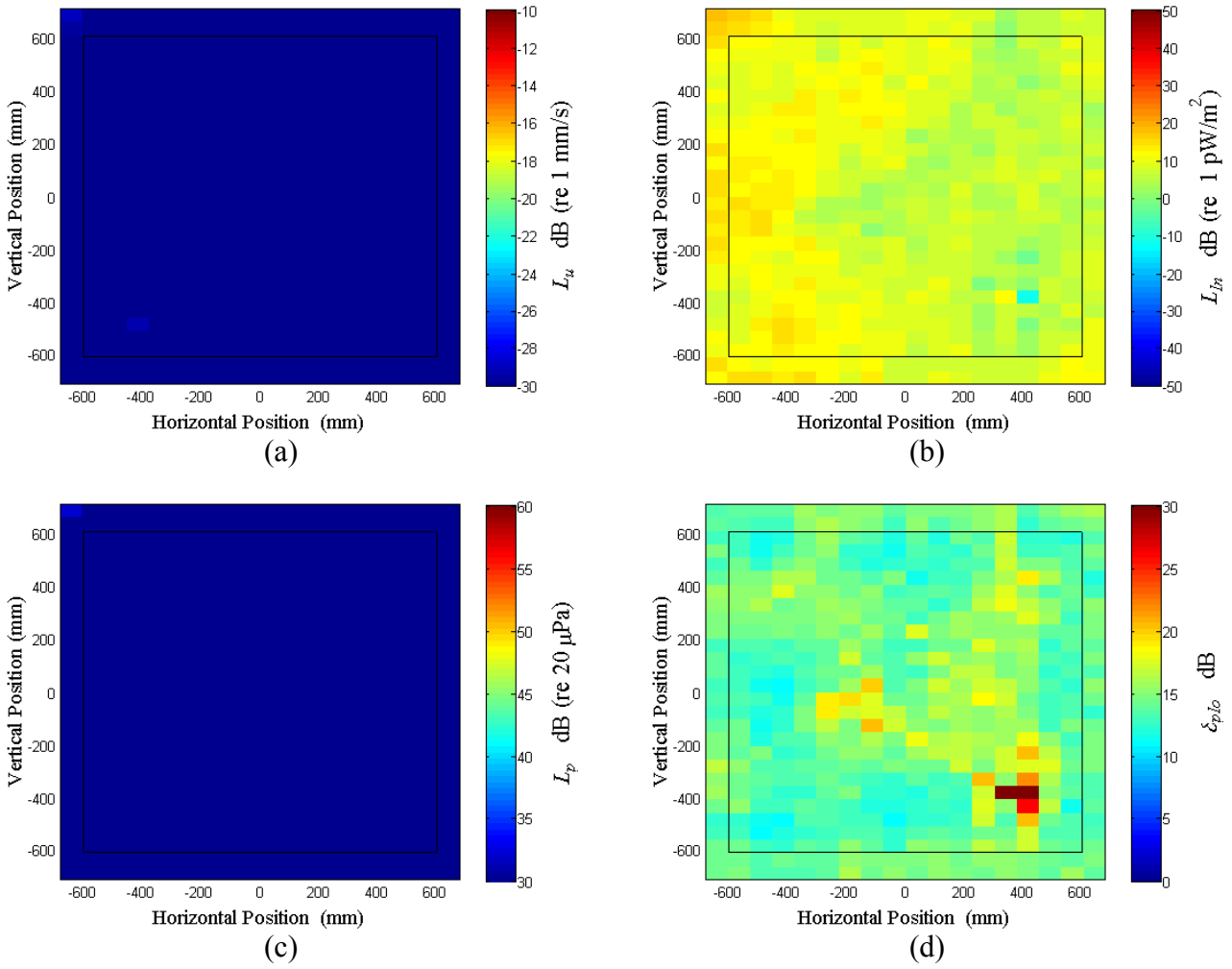

Figure A.61: Surface scan of Window A at 410 Hz (a) particle velocity level, L_u (b) normal signed sound intensity level, L_{In} (c) sound pressure level, L_p (d) pressure-residual intensity index, δ_{pIo}.

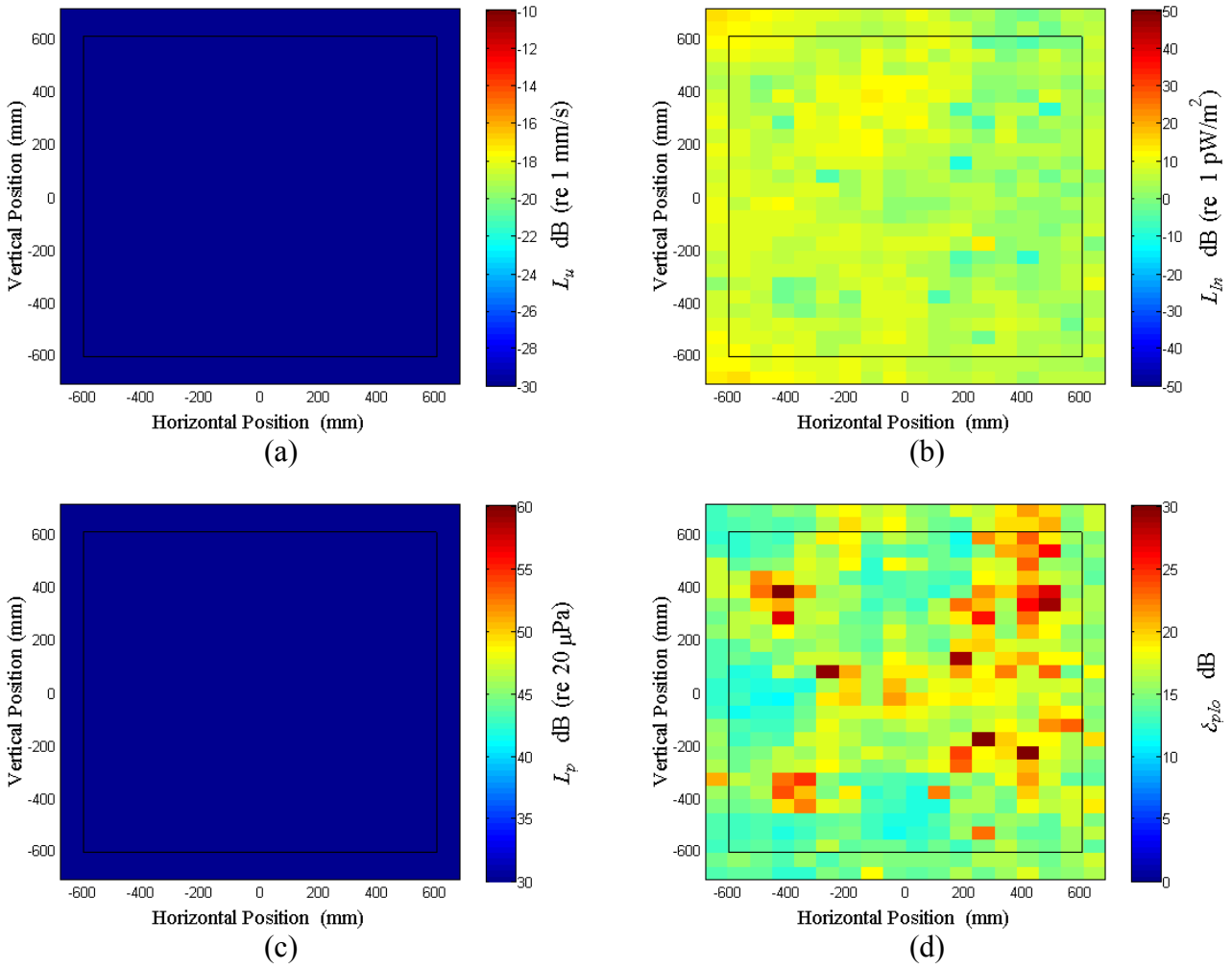

Figure A.62: Surface scan of Window A at 420 Hz (a) particle velocity level, L_u (b) normal signed sound intensity level, L_{In} (c) sound pressure level, L_p (d) pressure-residual intensity index, δ_{pIo}.

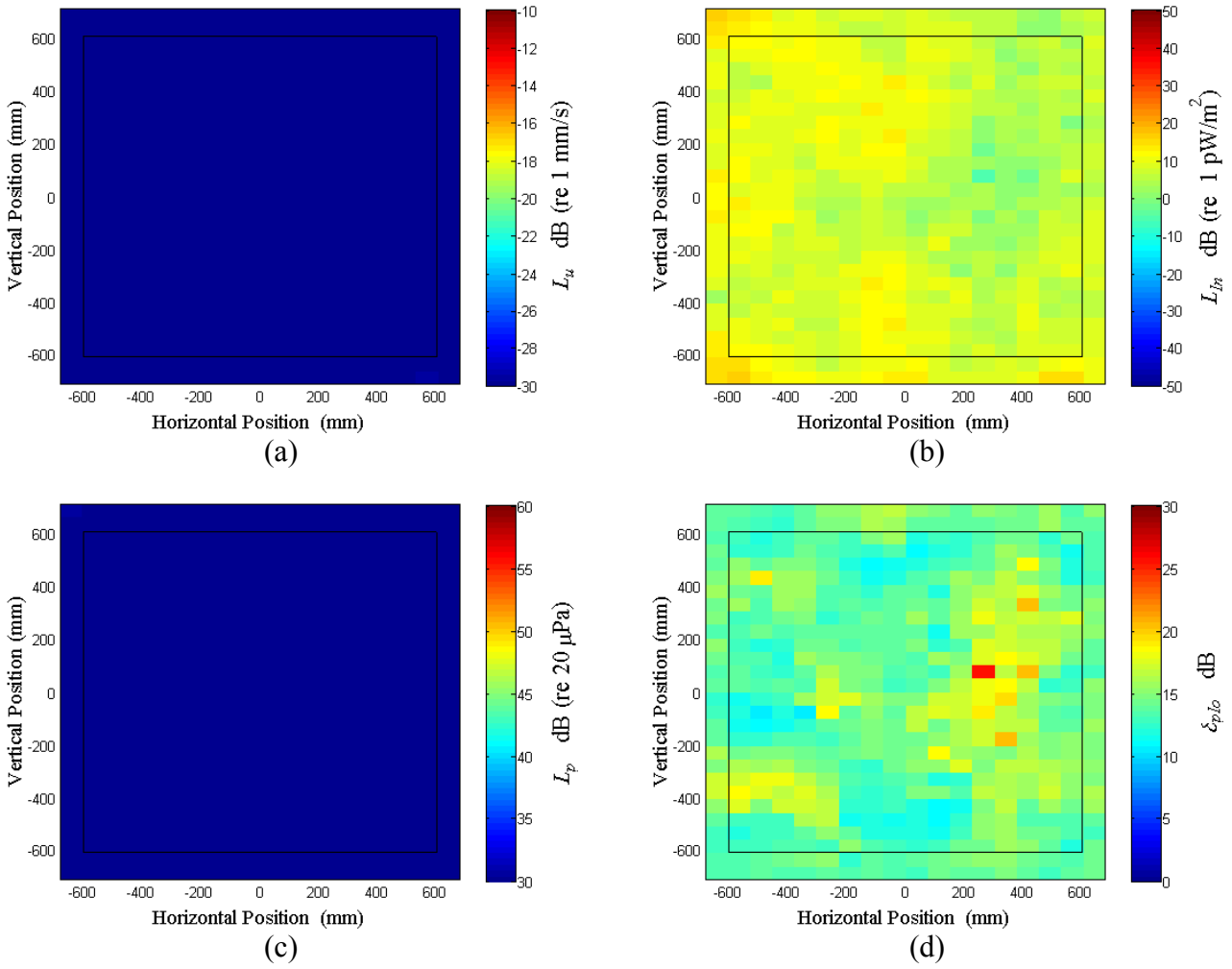

Figure A.63: Surface scan of Window A at 430 Hz (a) particle velocity level, L_u (b) normal signed sound intensity level, L_{In} (c) sound pressure level, L_p (d) pressure-residual intensity index, δ_{pIo}.

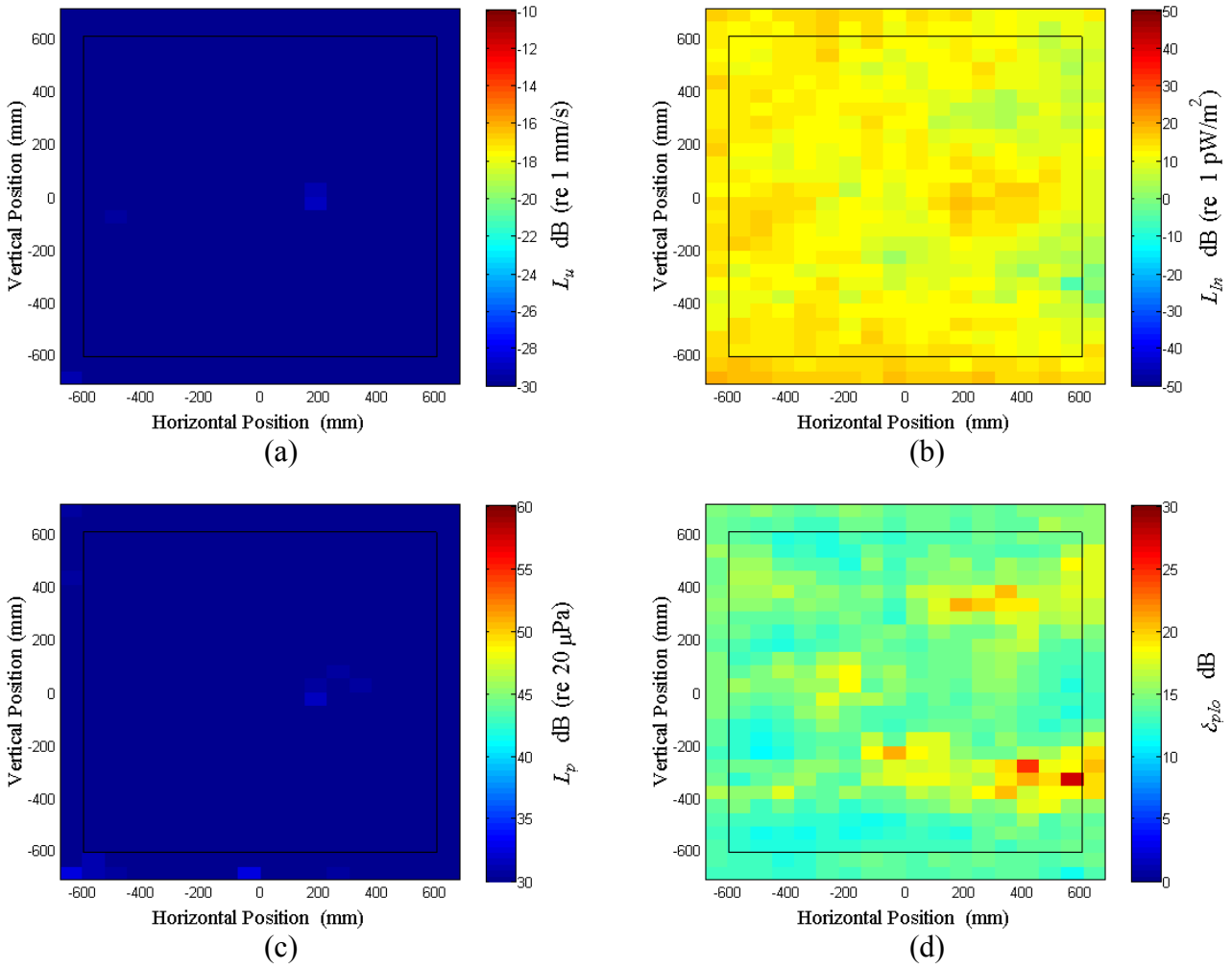

Figure A.64: Surface scan of Window A at 440 Hz (a) particle velocity level, L_u (b) normal signed sound intensity level, L_{In} (c) sound pressure level, L_p (d) pressure-residual intensity index, δ_{pIo}.

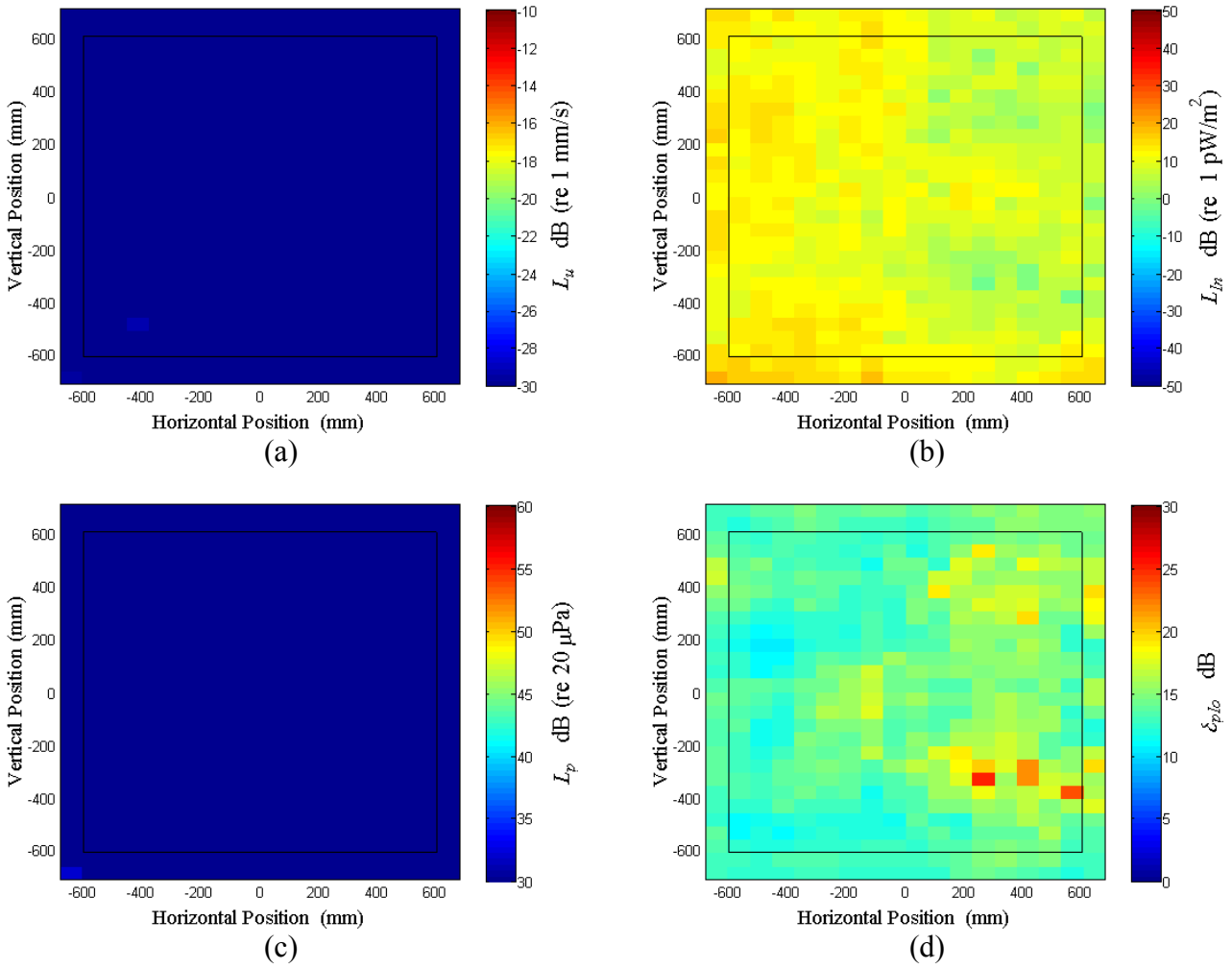

Figure A.65: Surface scan of Window A at 450 Hz (a) particle velocity level, L_u (b) normal signed sound intensity level, L_{In} (c) sound pressure level, L_p (d) pressure-residual intensity index, δ_{pIo}.

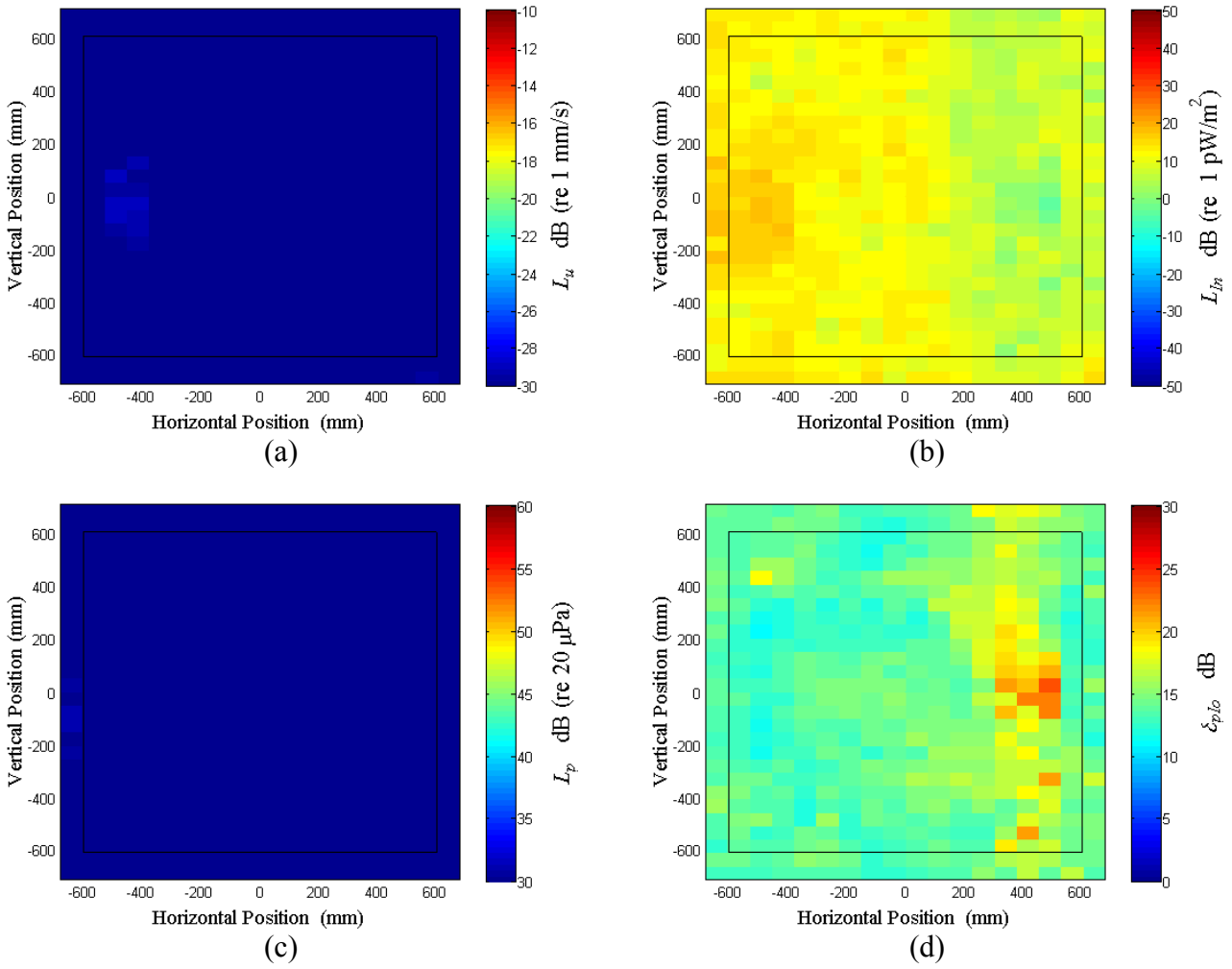

Figure A.66: Surface scan of Window A at 460 Hz (a) particle velocity level, L_u (b) normal signed sound intensity level, L_{In} (c) sound pressure level, L_p (d) pressure-residual intensity index, δ_{pIo}.

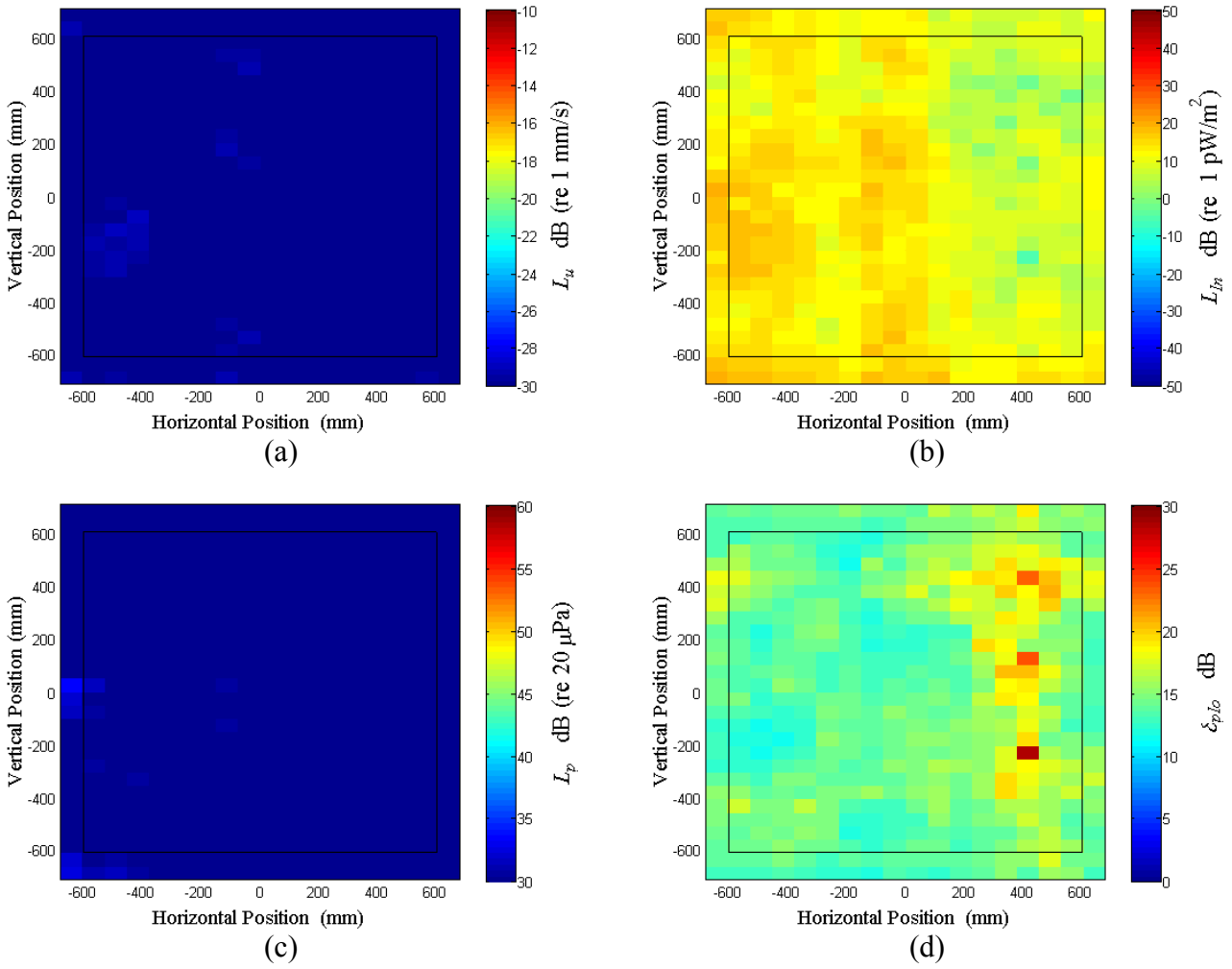

Figure A.67: Surface scan of Window A at 470 Hz (a) particle velocity level, L_u (b) normal signed sound intensity level, L_{In} (c) sound pressure level, L_p (d) pressure-residual intensity index, δ_{pIo}.

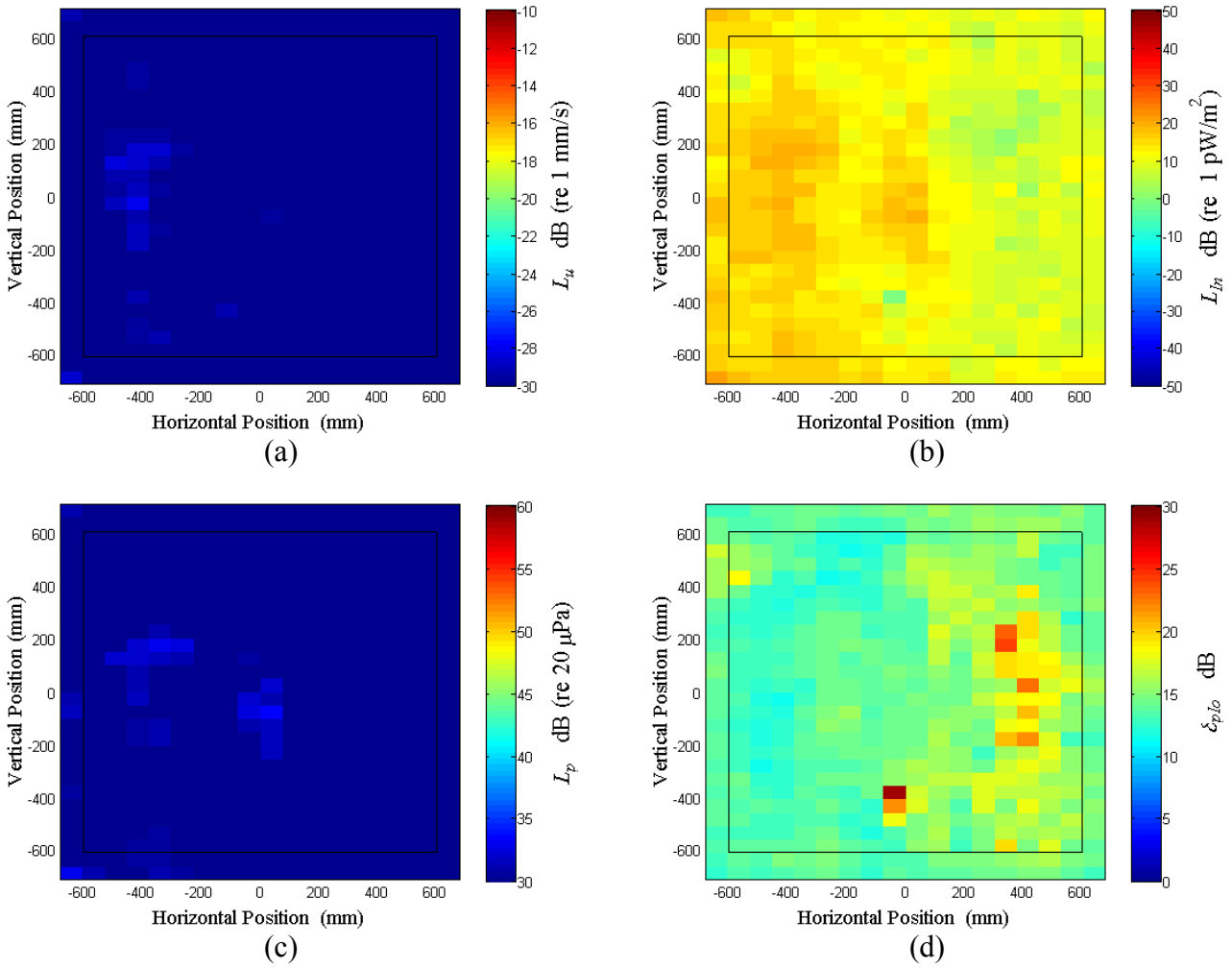

Figure A.68: Surface scan of Window A at 480 Hz (a) particle velocity level, L_u (b) normal signed sound intensity level, L_{In} (c) sound pressure level, L_p (d) pressure-residual intensity index, δ_{pIo}.

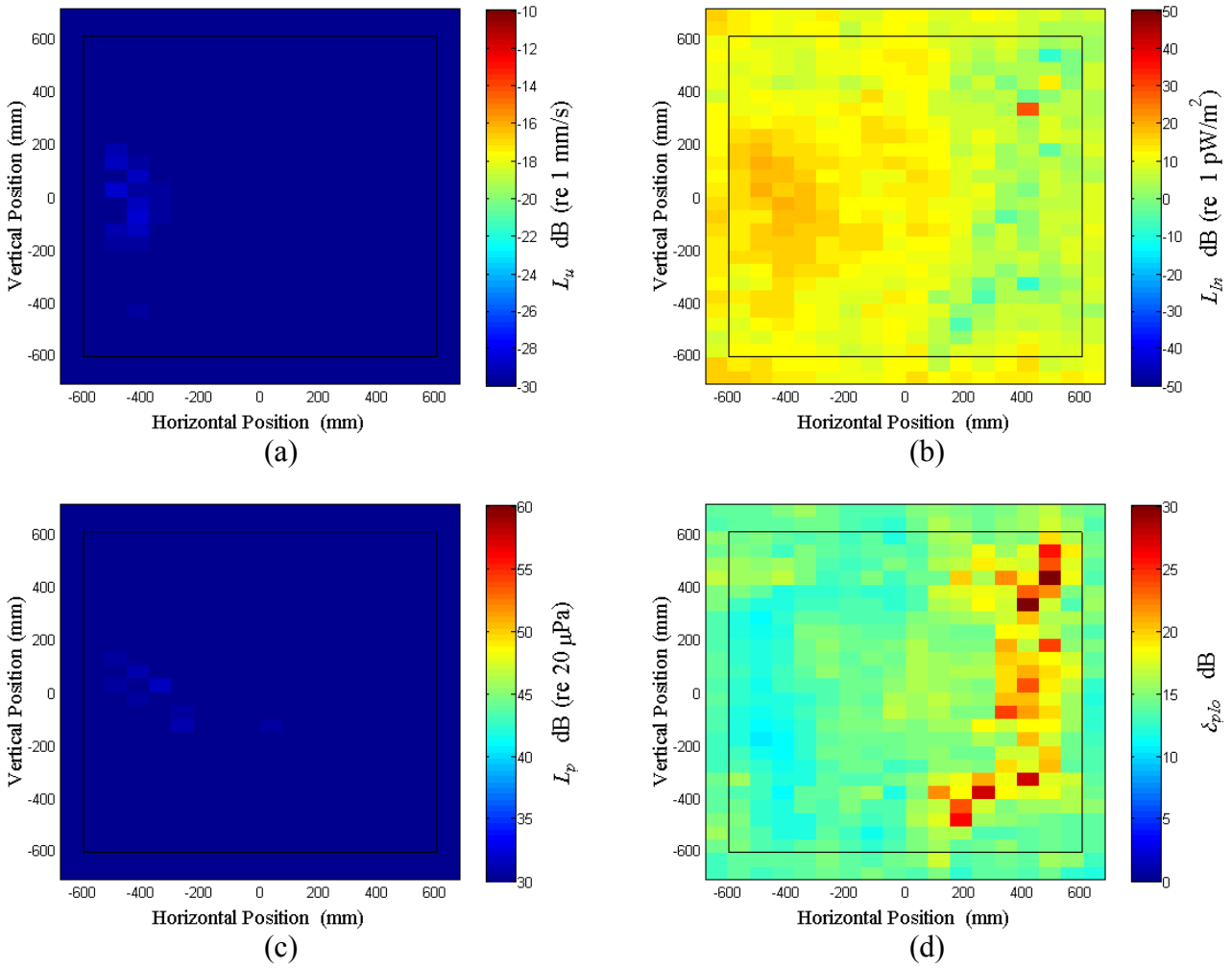

Figure A.69: Surface scan of Window A at 490 Hz (a) particle velocity level, L_u (b) normal signed sound intensity level, L_{In} (c) sound pressure level, L_p (d) pressure-residual intensity index, δ_{pIo}.

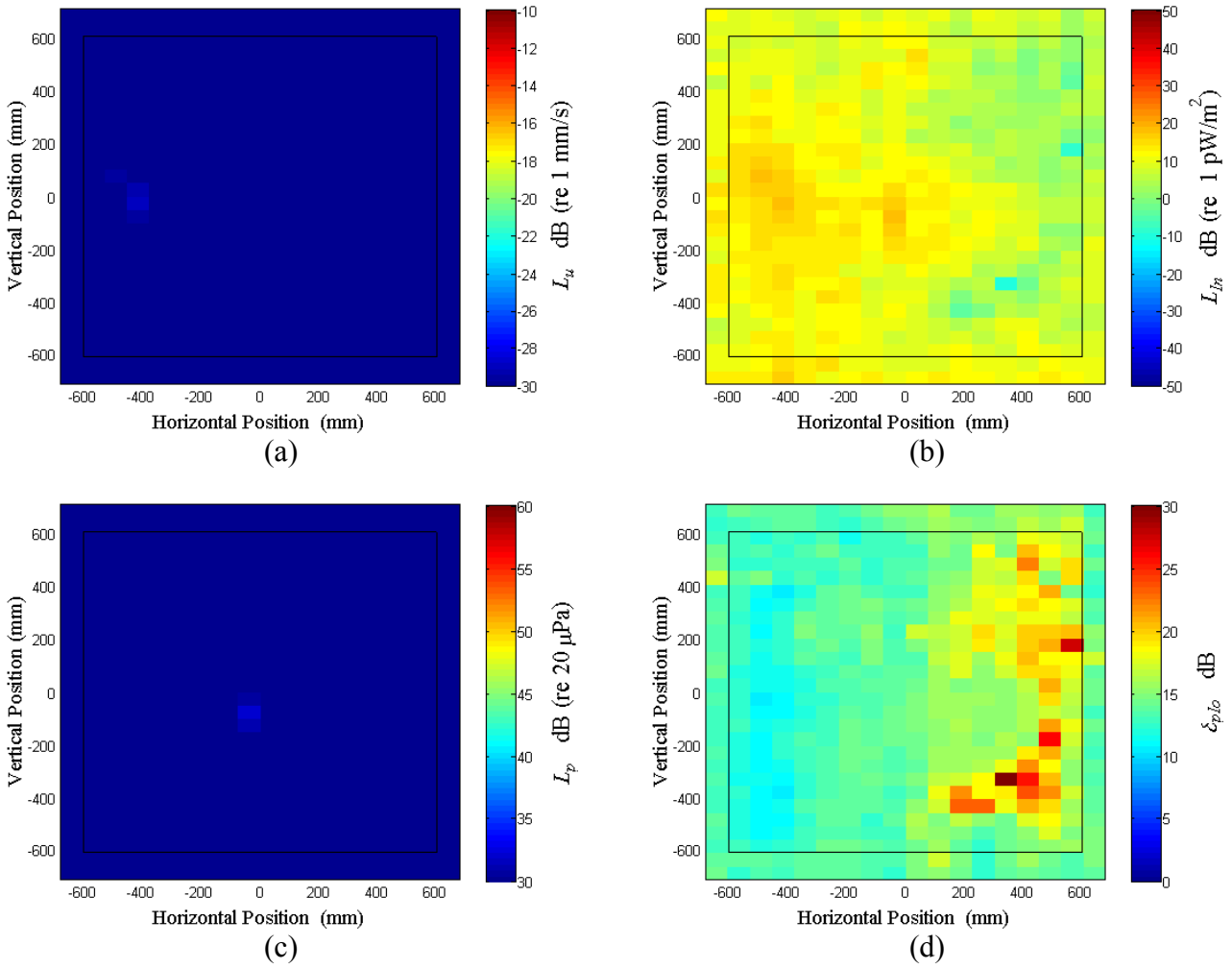

Figure A.70: Surface scan of Window A at 500 Hz (a) particle velocity level, L_u (b) normal signed sound intensity level, L_{In} (c) sound pressure level, L_p (d) pressure-residual intensity index, δ_{pIo}.

APPENDIX B. WINDOW B

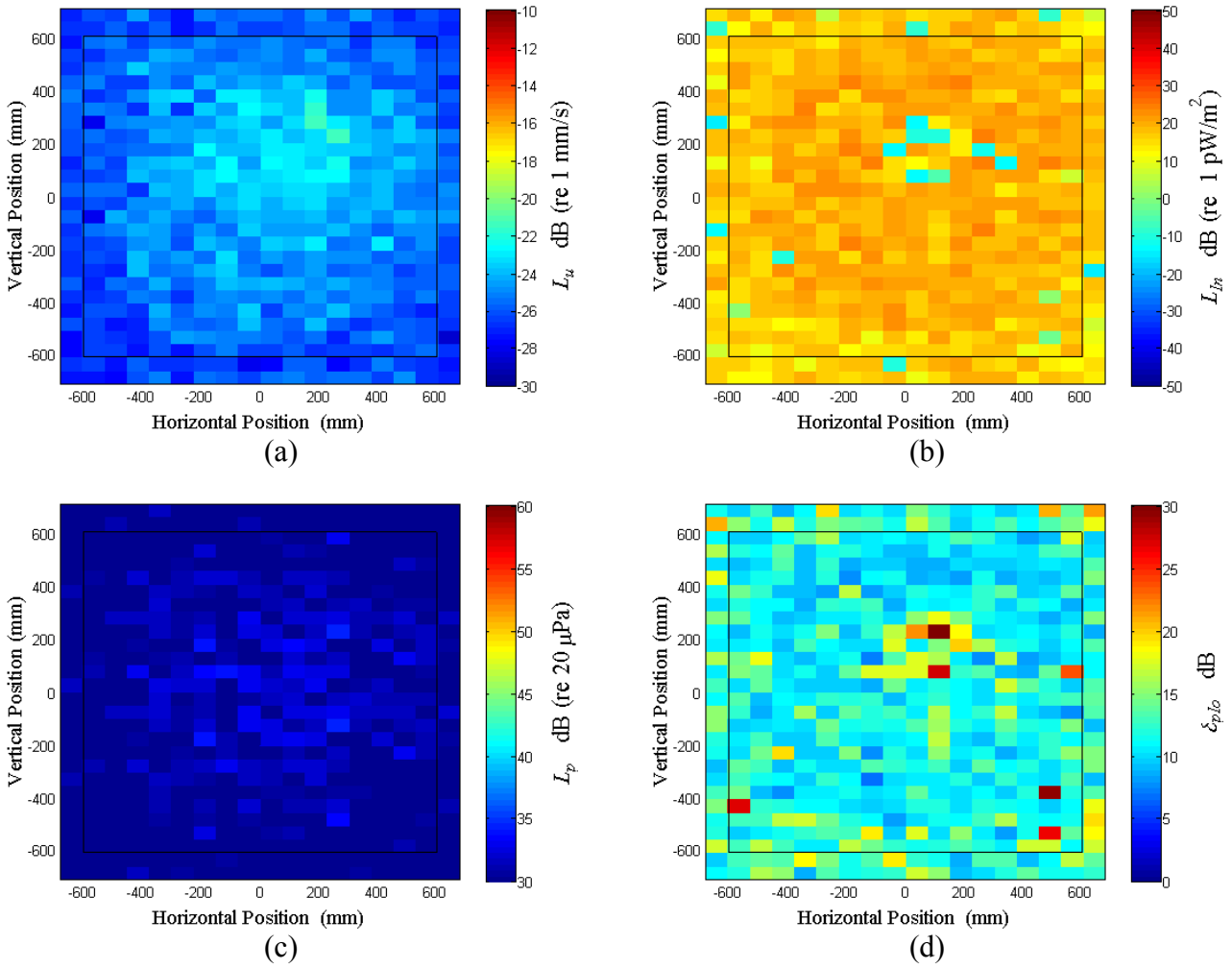

Figure B.1: Surface scan of Window B at 50 Hz (a) particle velocity level, L_u (b) normal signed sound intensity level, L_{In} (c) sound pressure level, L_p (d) pressure-residual intensity index, δ_{pIo}.

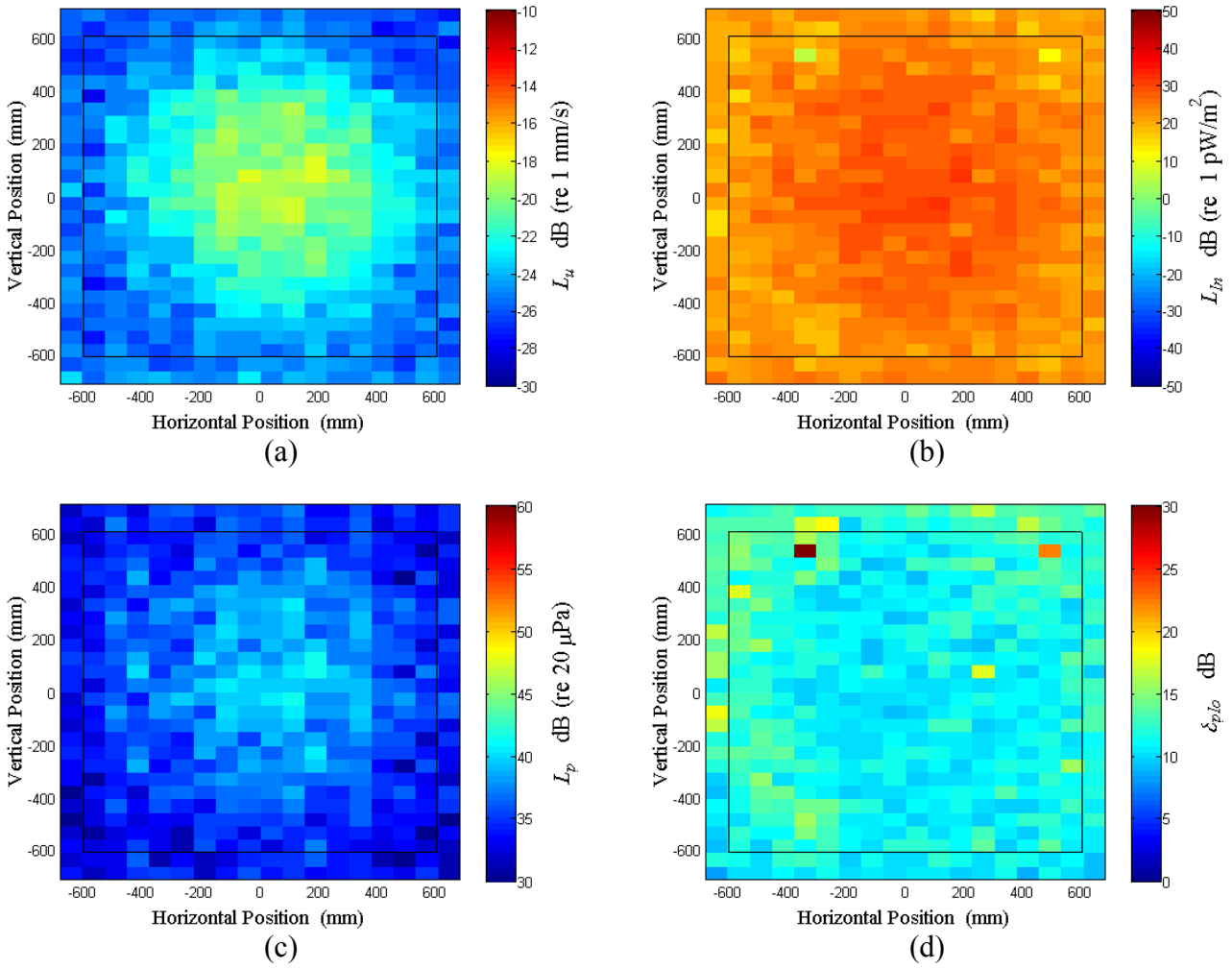

Figure B.2: Surface scan of Window B at 52.5 Hz (a) particle velocity level, L_u (b) normal signed sound intensity level, L_{In} (c) sound pressure level, L_p (d) pressure-residual intensity index, δ_{pIo}.

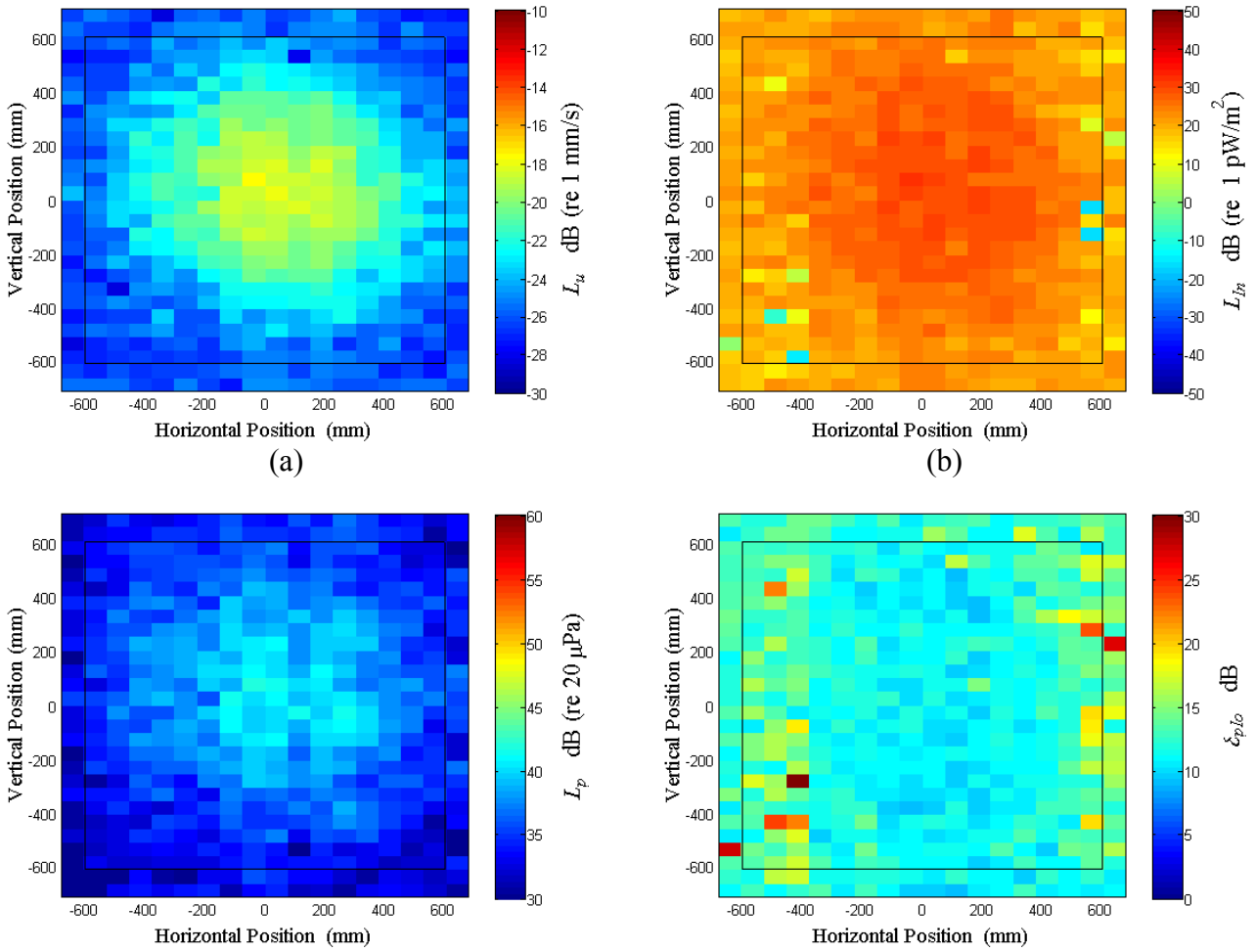

Figure B.3: Surface scan of Window B at 55 Hz (a) particle velocity level, L_u (b) normal signed sound intensity level, L_{In} (c) sound pressure level, L_p (d) pressure-residual intensity index, δ_{pIo}.

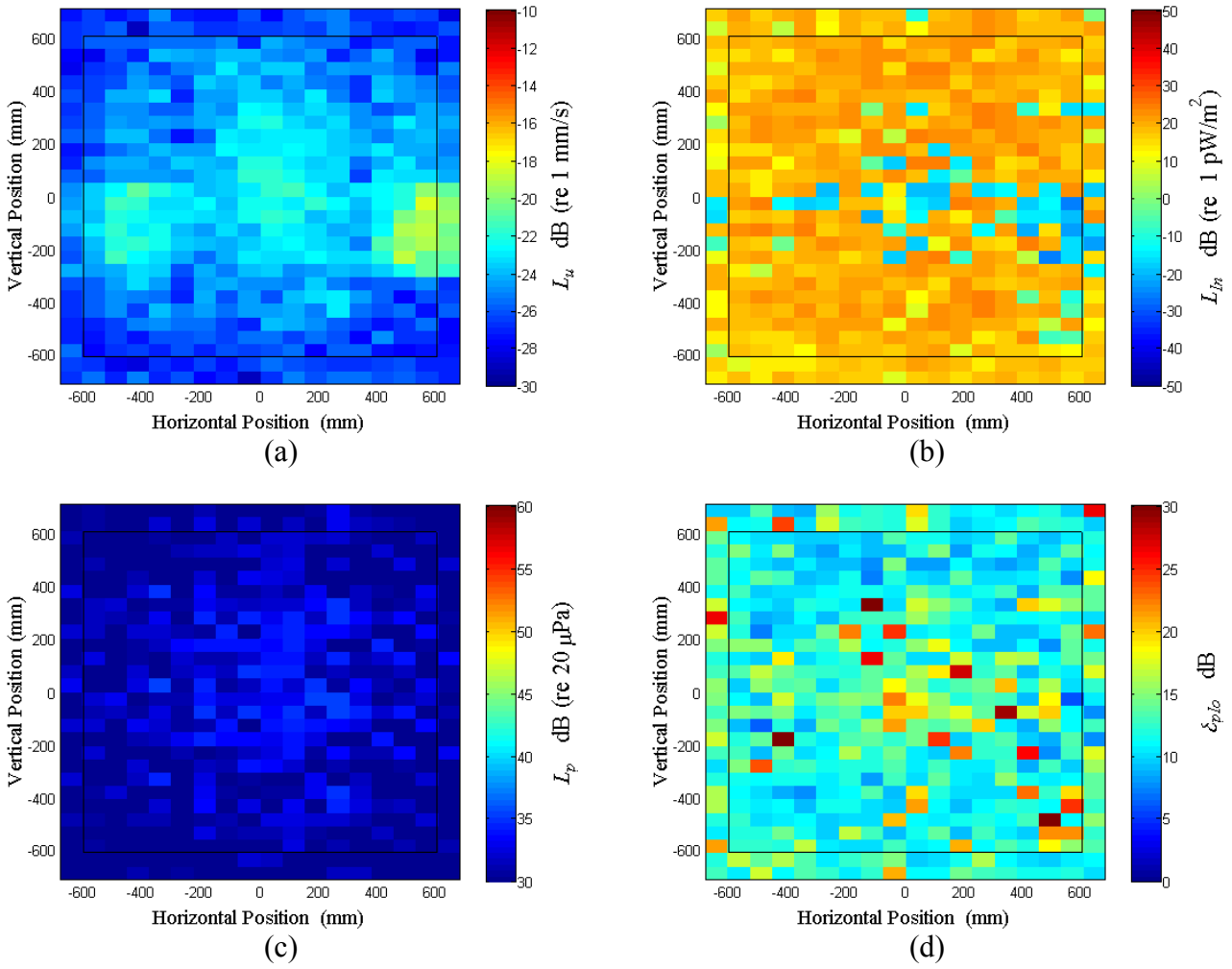

Figure B.4: Surface scan of Window B at 57.5 Hz (a) particle velocity level, L_u (b) normal signed sound intensity level, L_{In} (c) sound pressure level, L_p (d) pressure-residual intensity index, δ_{pIo}.

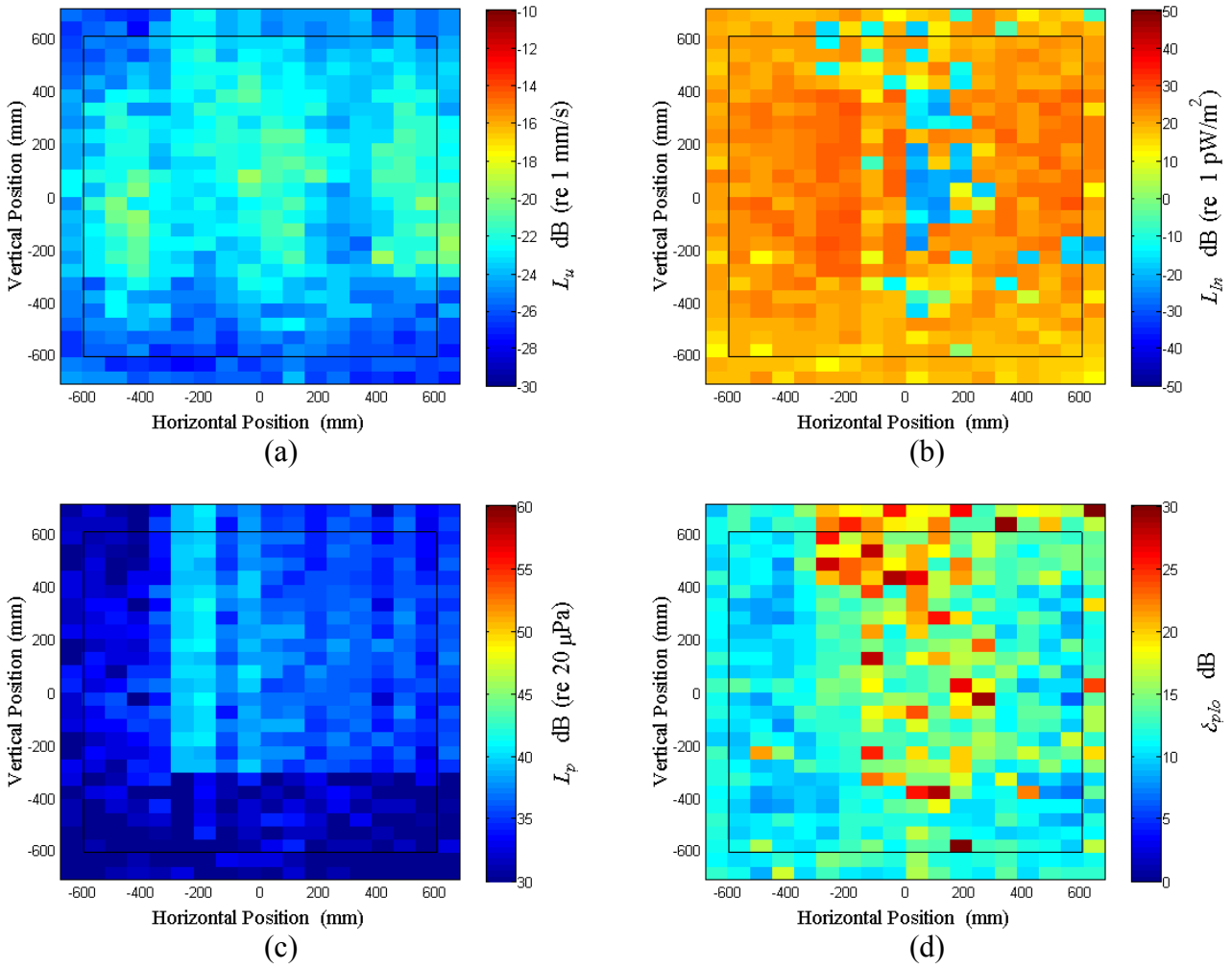

Figure B.5: Surface scan of Window B at 60 Hz (a) particle velocity level, L_u (b) normal signed sound intensity level, L_{In} (c) sound pressure level, L_p (d) pressure-residual intensity index, δ_{pIo}.

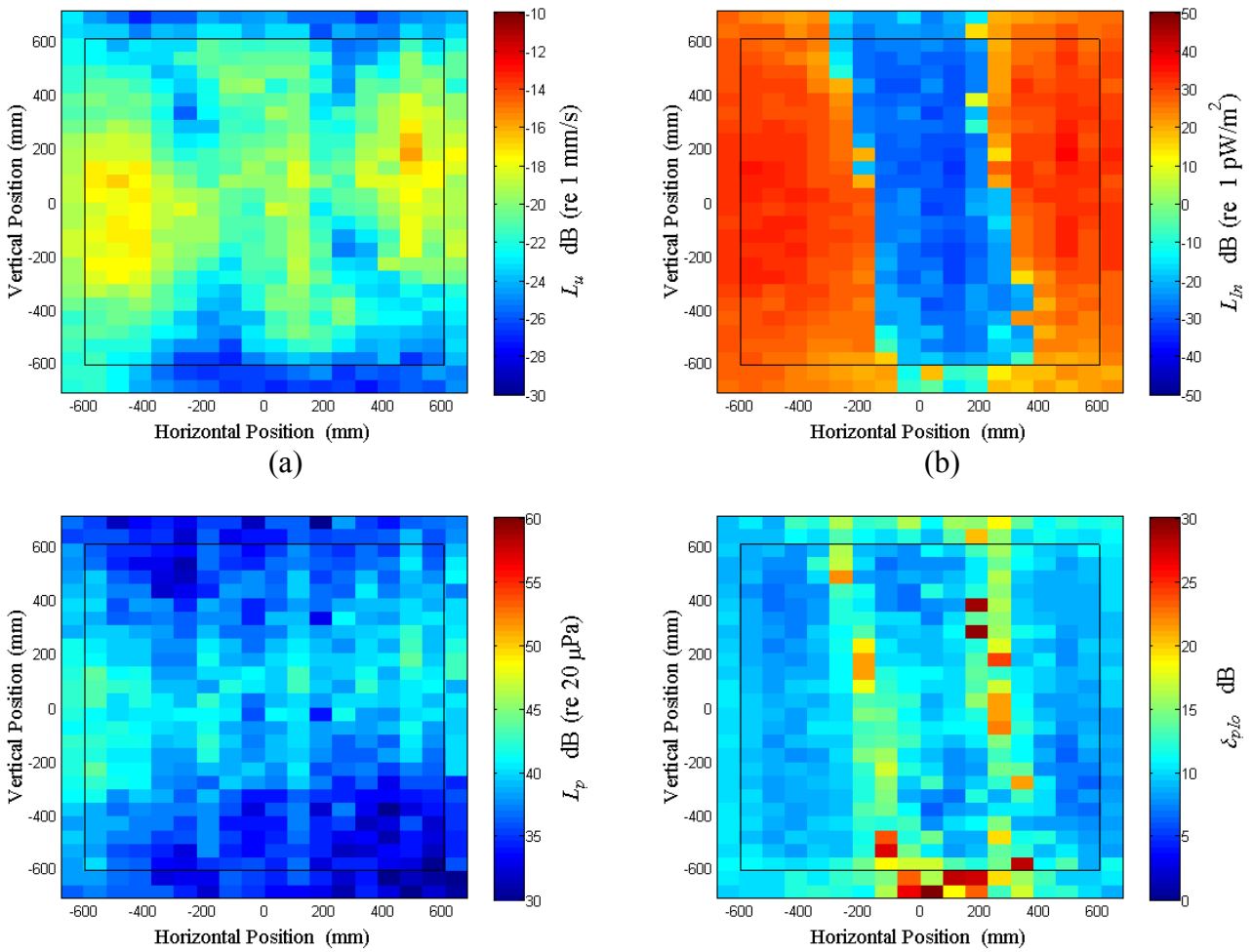

Figure B.6: Surface scan of Window B at 62.5 Hz (a) particle velocity level, L_u (b) normal signed sound intensity level, L_{In} (c) sound pressure level, L_p (d) pressure-residual intensity index, δ_{pIo}.

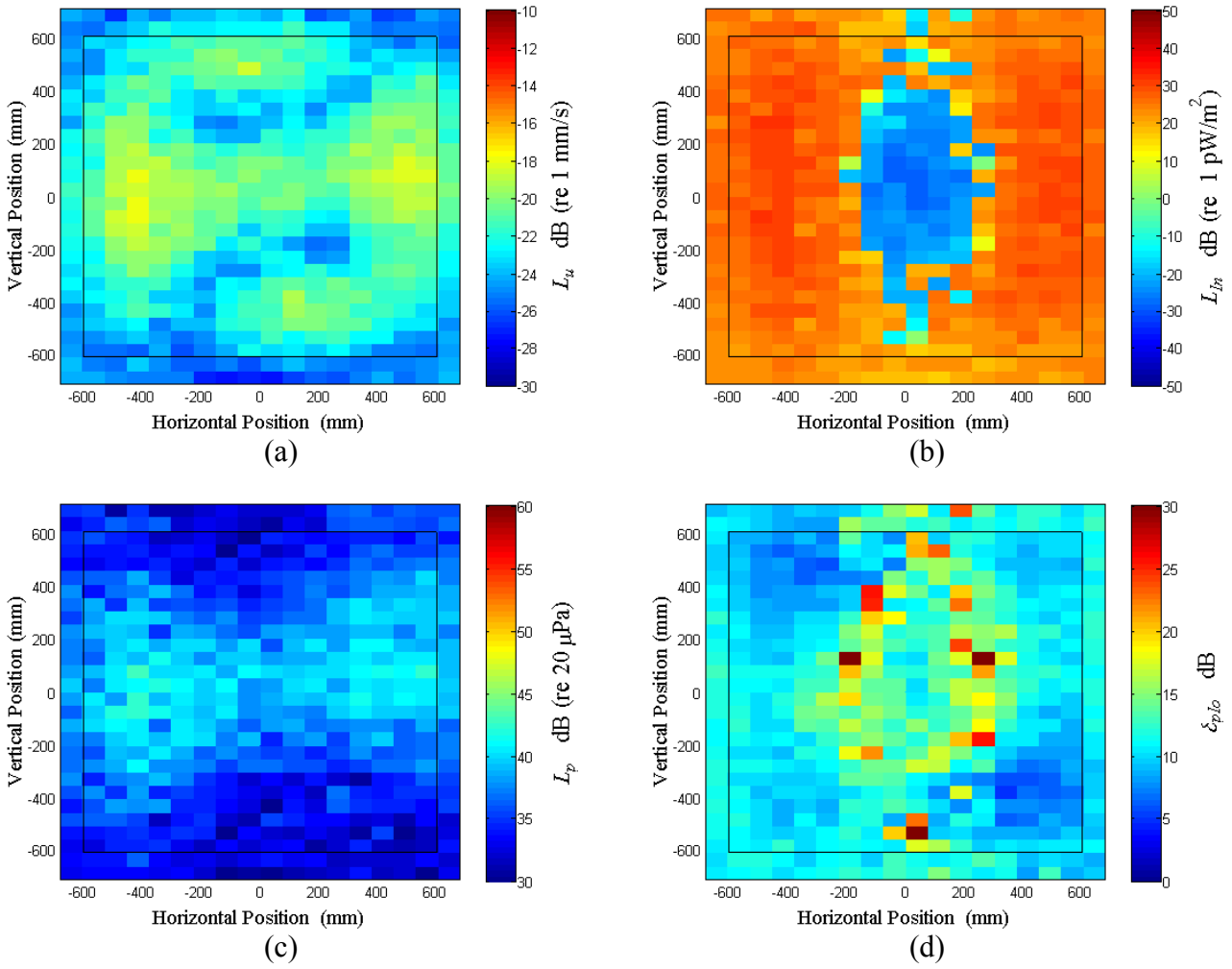

Figure B.7: Surface scan of Window B at 65 Hz (a) particle velocity level, L_u (b) normal signed sound intensity level, L_{In} (c) sound pressure level, L_p (d) pressure-residual intensity index, δ_{pIo}.

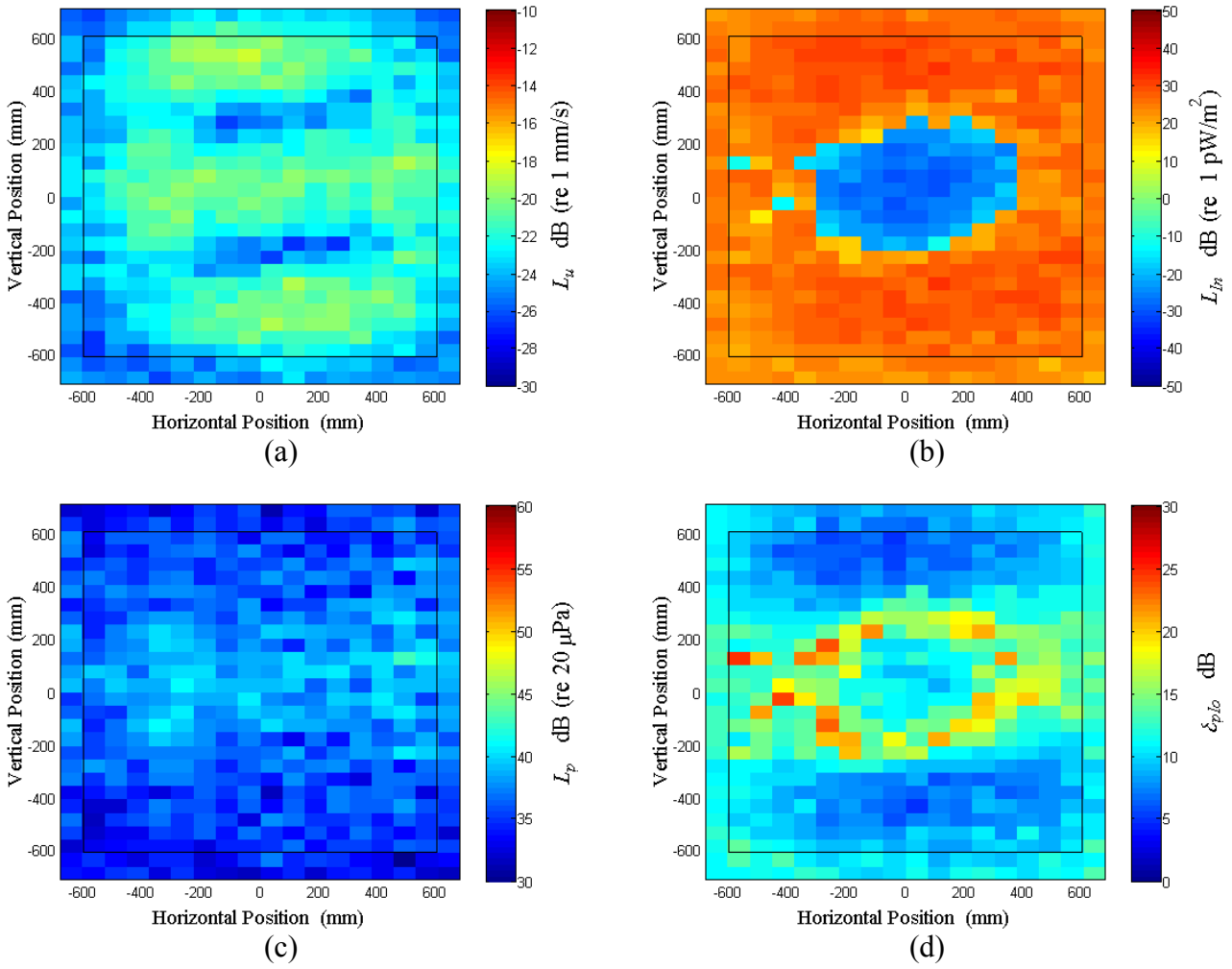

Figure B.8: Surface scan of Window B at 67.5 Hz (a) particle velocity level, L_u (b) normal signed sound intensity level, L_{In} (c) sound pressure level, L_p (d) pressure-residual intensity index, δ_{pIo}.

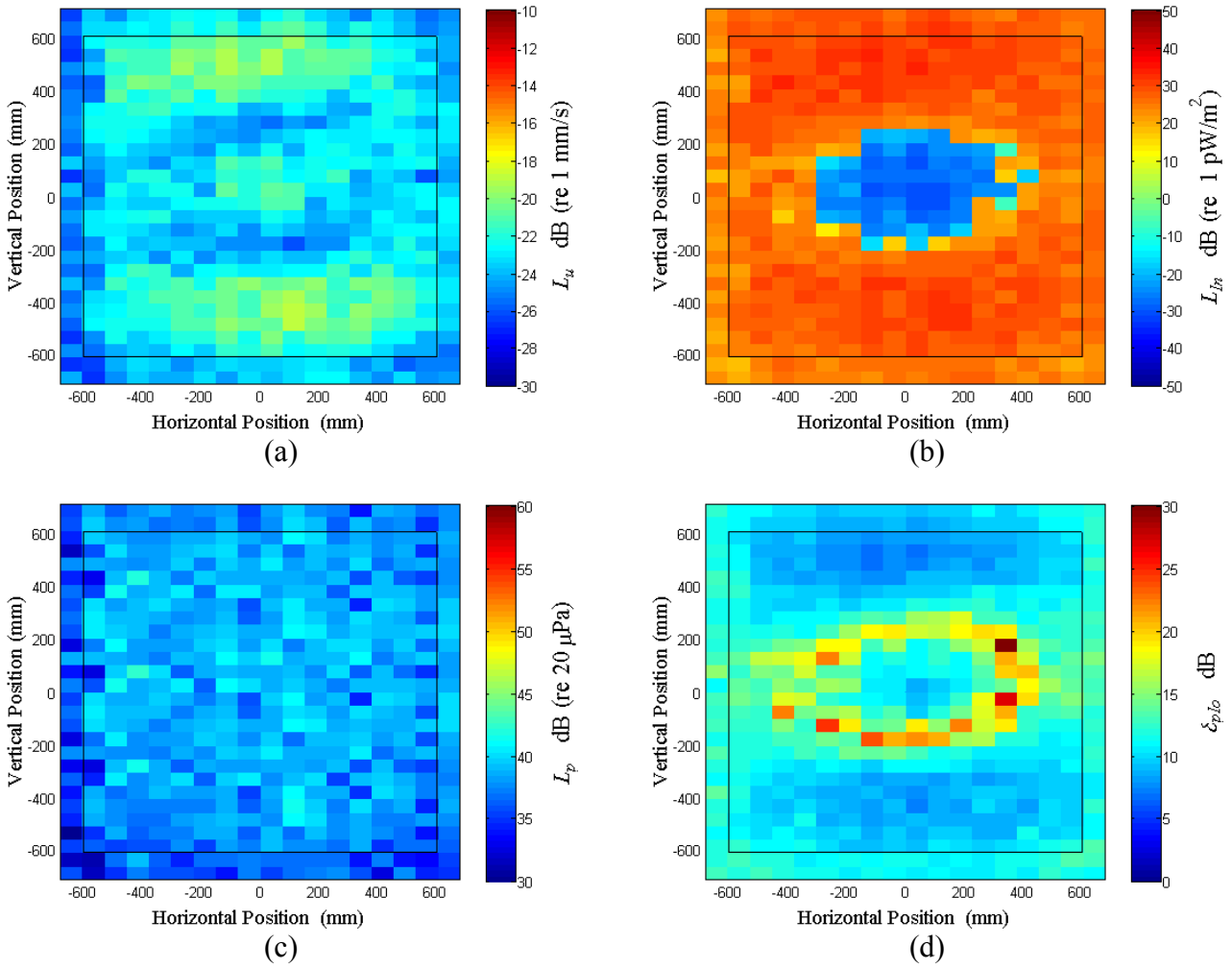

Figure B.9: Surface scan of Window B at 70 Hz (a) particle velocity level, L_u (b) normal signed sound intensity level, L_{In} (c) sound pressure level, L_p (d) pressure-residual intensity index, δ_{pIo}.

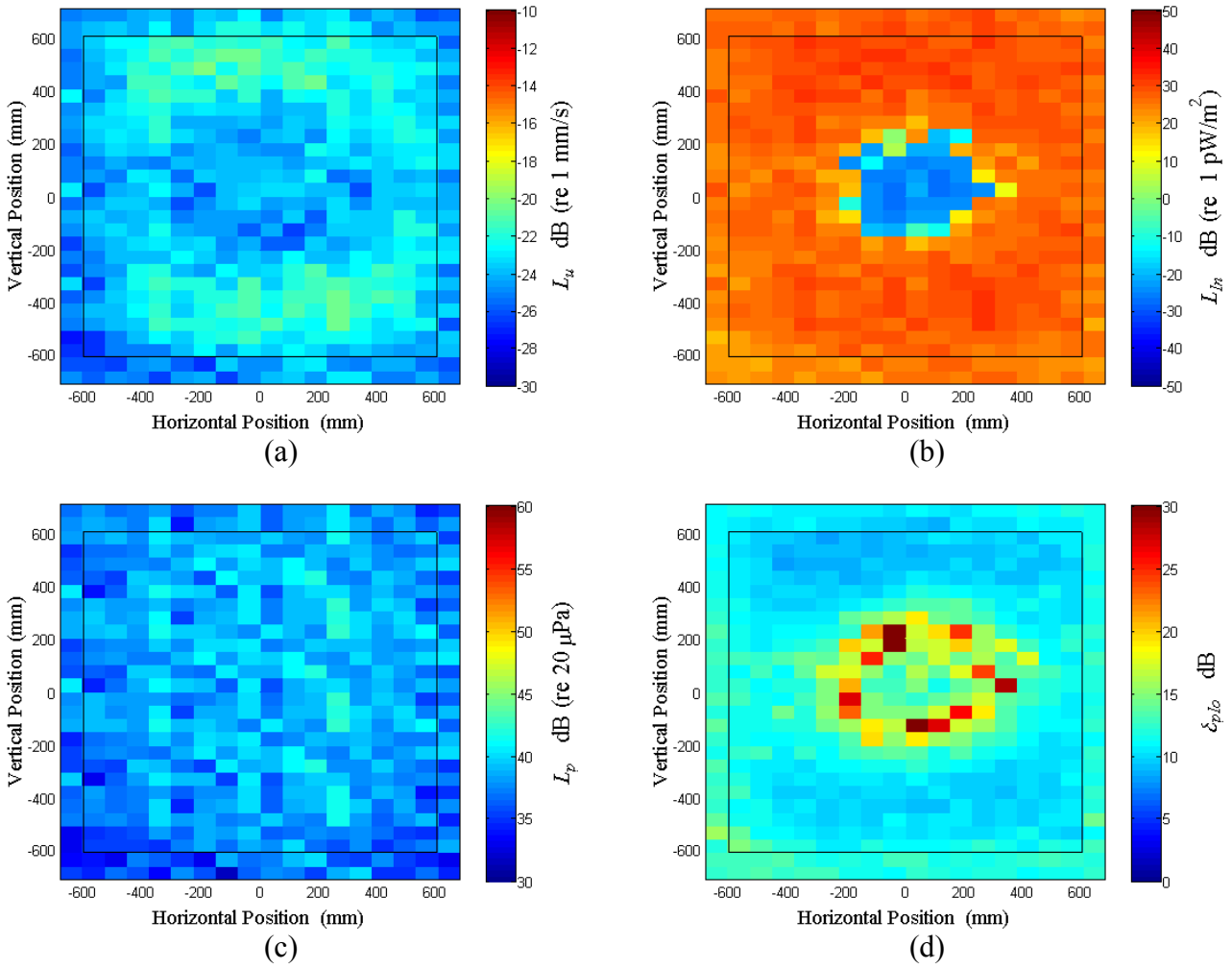

Figure B.10: Surface scan of Window B at 72.5 Hz (a) particle velocity level, L_u (b) normal signed sound intensity level, L_{In} (c) sound pressure level, L_p (d) pressure-residual intensity index, δ_{pIo}.

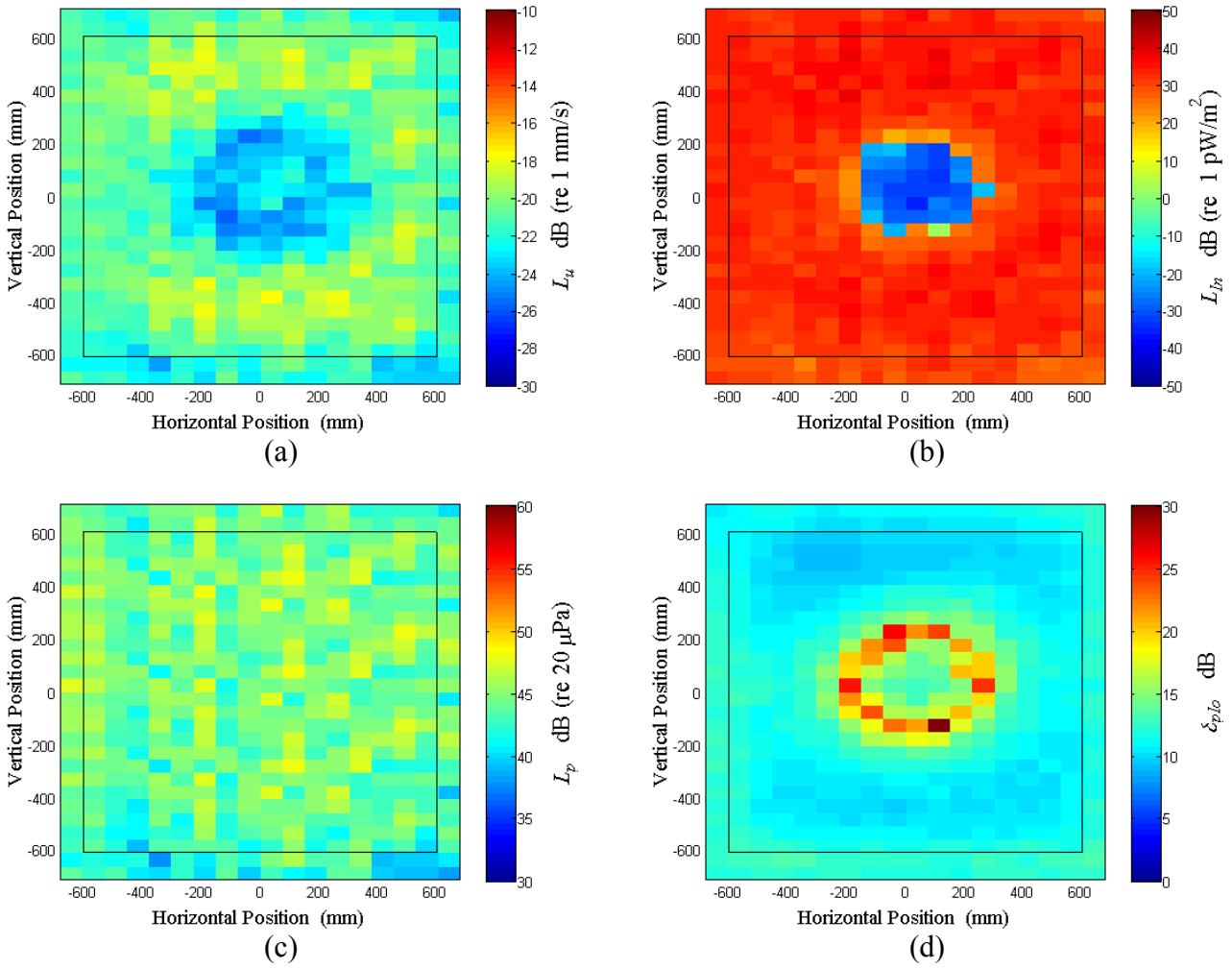

Figure B.11: Surface scan of Window B at 75 Hz (a) particle velocity level, L_u (b) normal signed sound intensity level, L_{In} (c) sound pressure level, L_p (d) pressure-residual intensity index, δ_{pIo}.

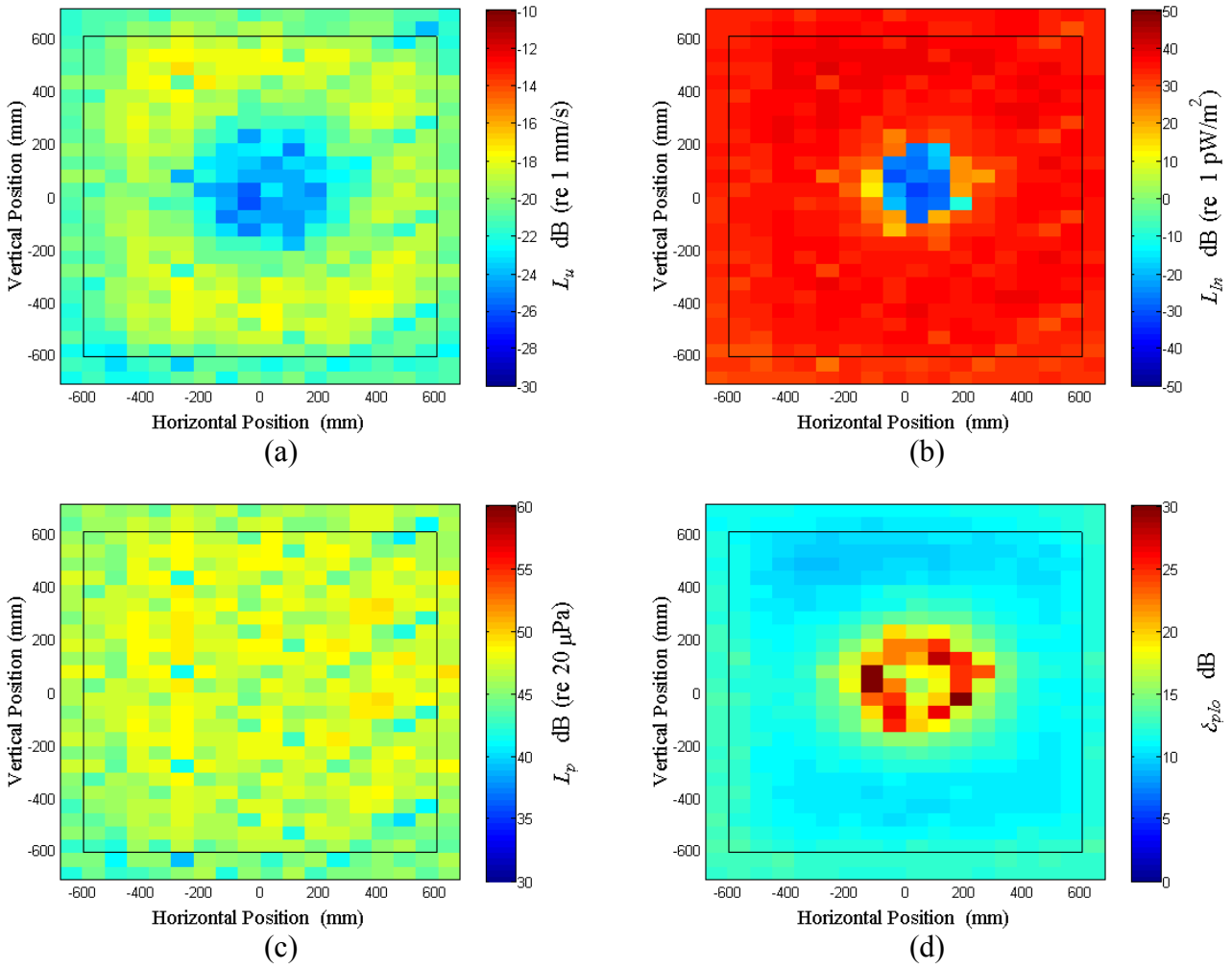

Figure B.12: Surface scan of Window B at 77.5 Hz (a) particle velocity level, L_u (b) normal signed sound intensity level, L_{In} (c) sound pressure level, L_p (d) pressure-residual intensity index, δ_{pIo}.

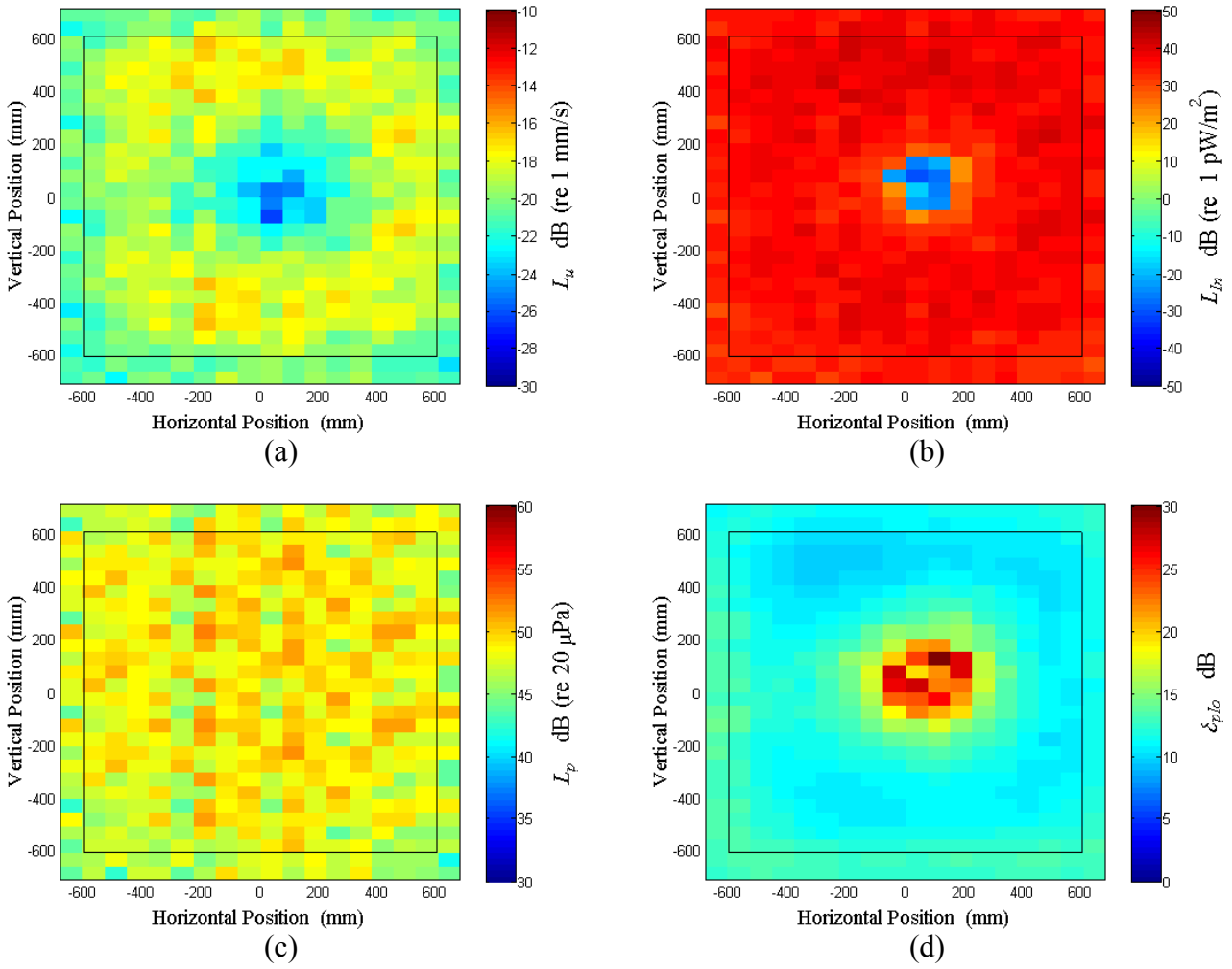

Figure B.13: Surface scan of Window B at 80 Hz (a) particle velocity level, L_u (b) normal signed sound intensity level, L_{In} (c) sound pressure level, L_p (d) pressure-residual intensity index, δ_{pIo}.

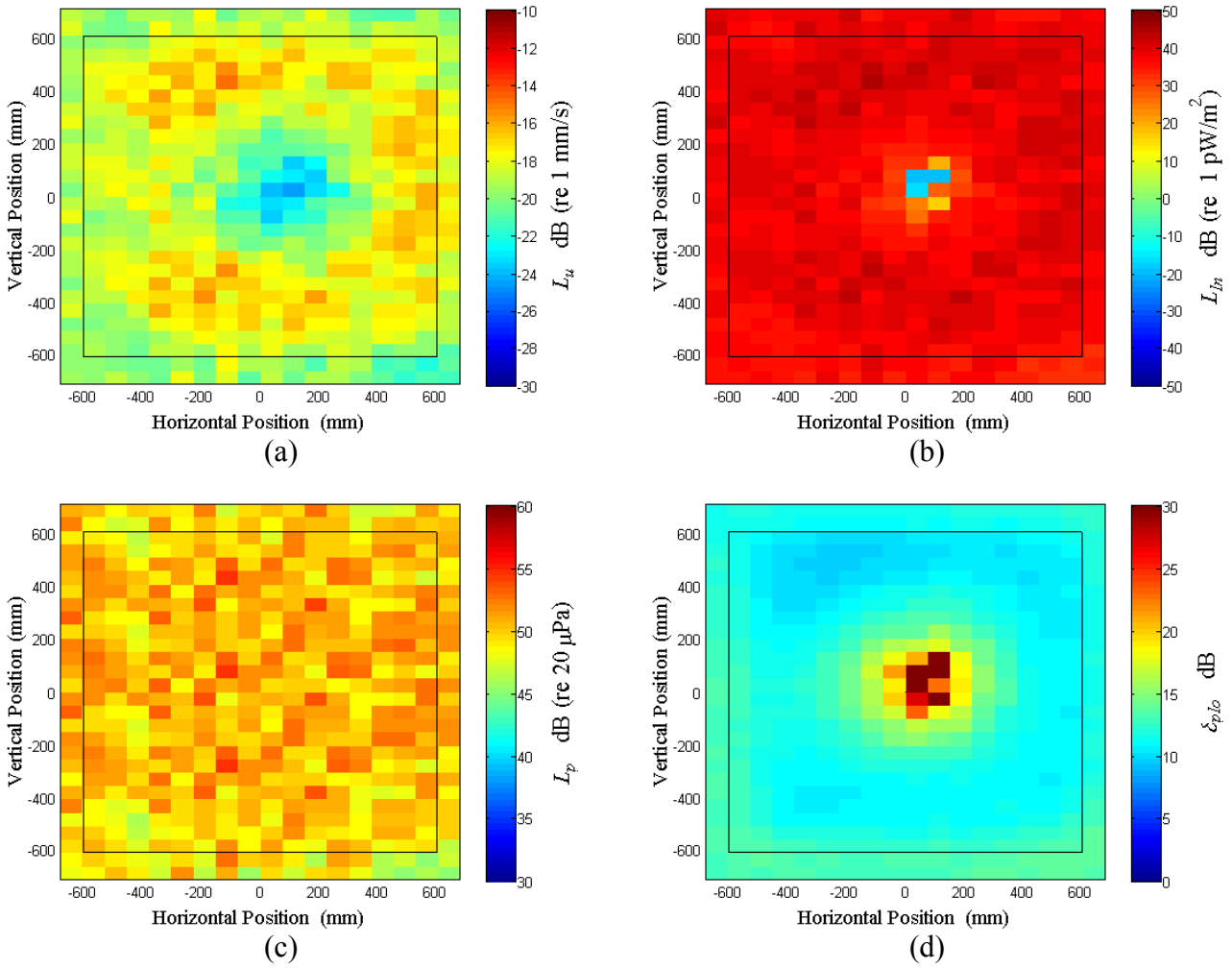

Figure B.14: Surface scan of Window B at 82.5 Hz (a) particle velocity level, L_u (b) normal signed sound intensity level, L_{In} (c) sound pressure level, L_p (d) pressure-residual intensity index, δ_{pIo}.

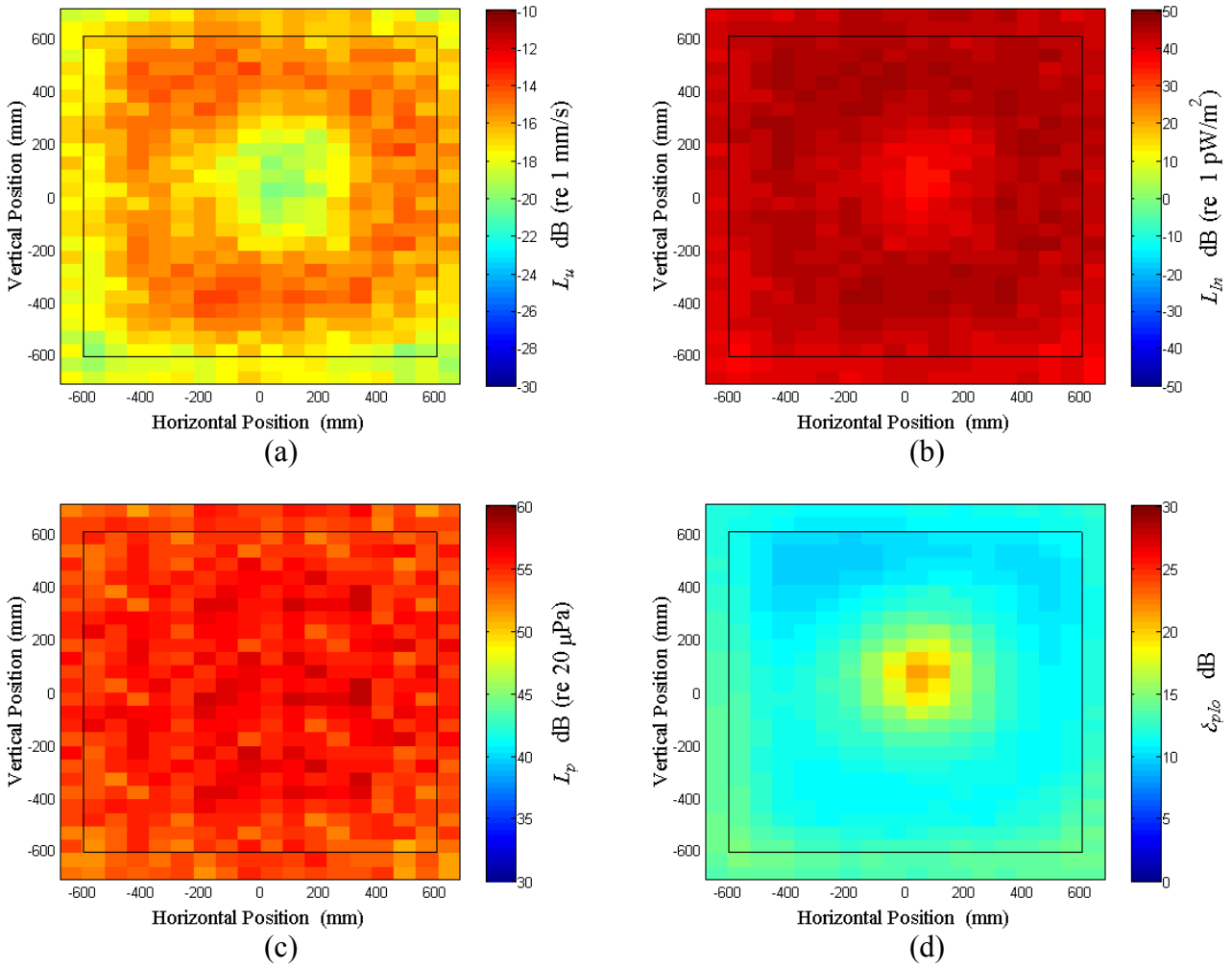

Figure B.15: Surface scan of Window B at 85 Hz (a) particle velocity level, L_u (b) normal signed sound intensity level, L_{In} (c) sound pressure level, L_p (d) pressure-residual intensity index, δ_{pIo}.

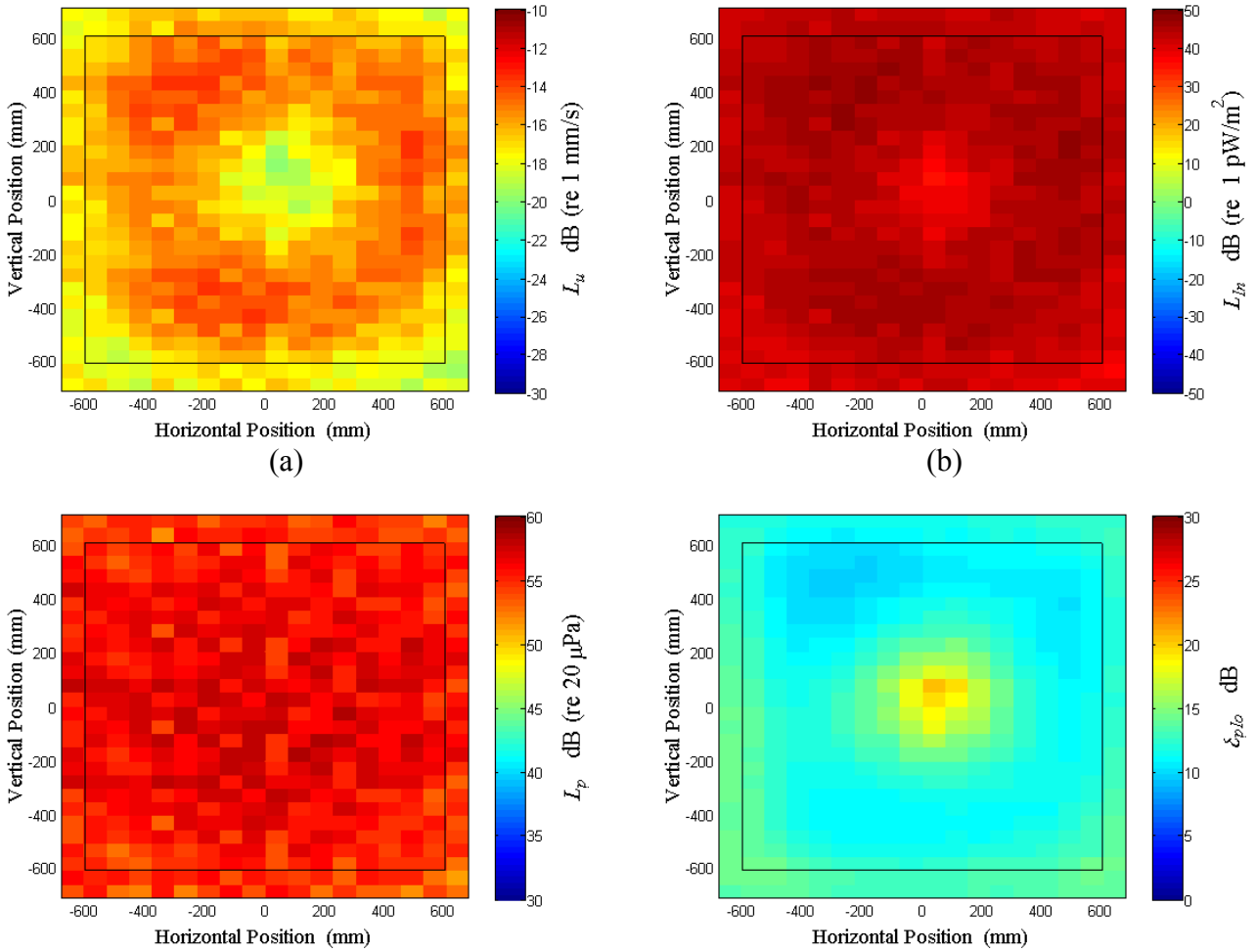

Figure B.16: Surface scan of Window B at 87.5 Hz (a) particle velocity level, L_u (b) normal signed sound intensity level, L_{In} (c) sound pressure level, L_p (d) pressure-residual intensity index, δ_{pIo}.

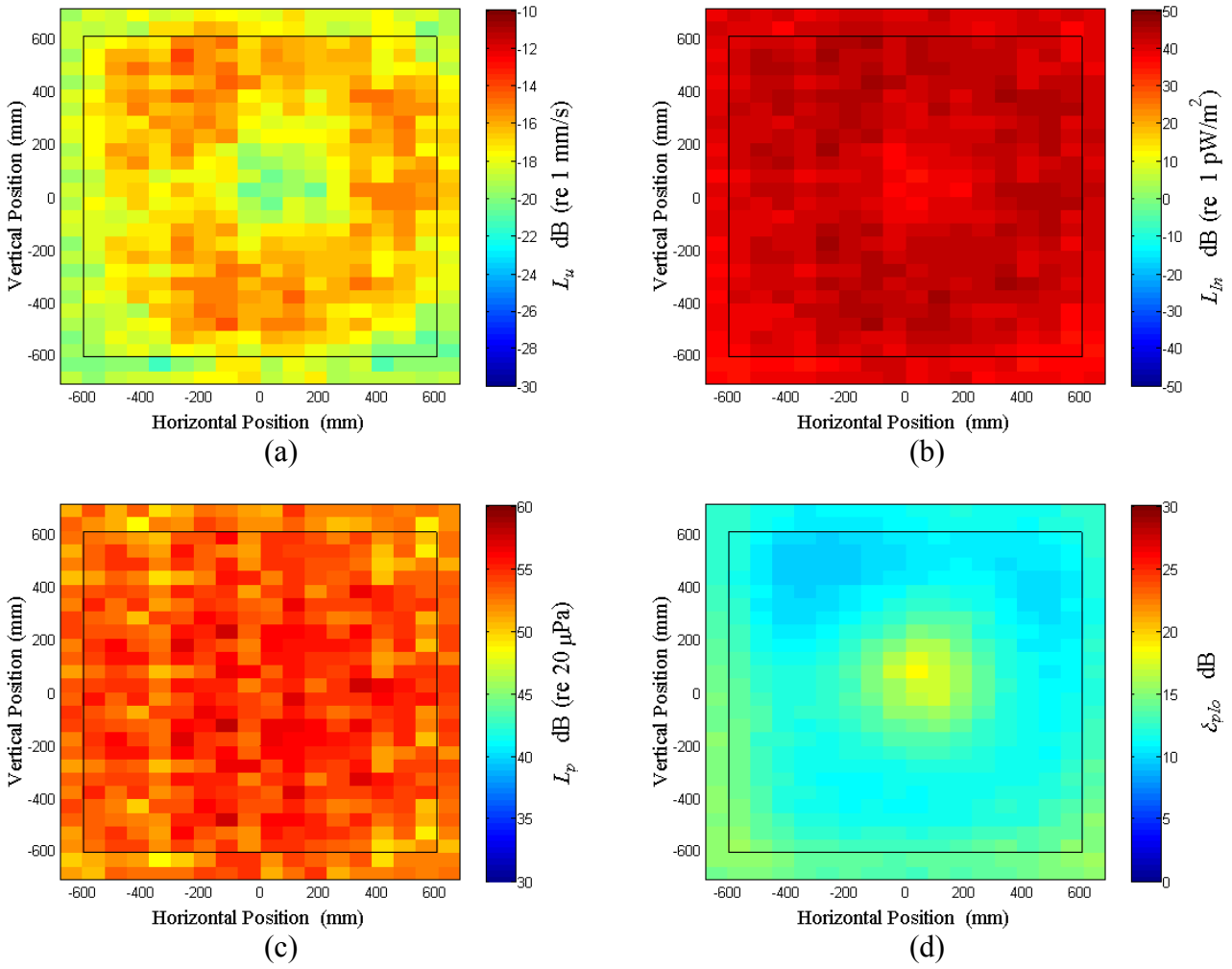

Figure B.17: Surface scan of Window B at 90 Hz (a) particle velocity level, L_u (b) normal signed sound intensity level, L_{In} (c) sound pressure level, L_p (d) pressure-residual intensity index, δ_{pIo}.

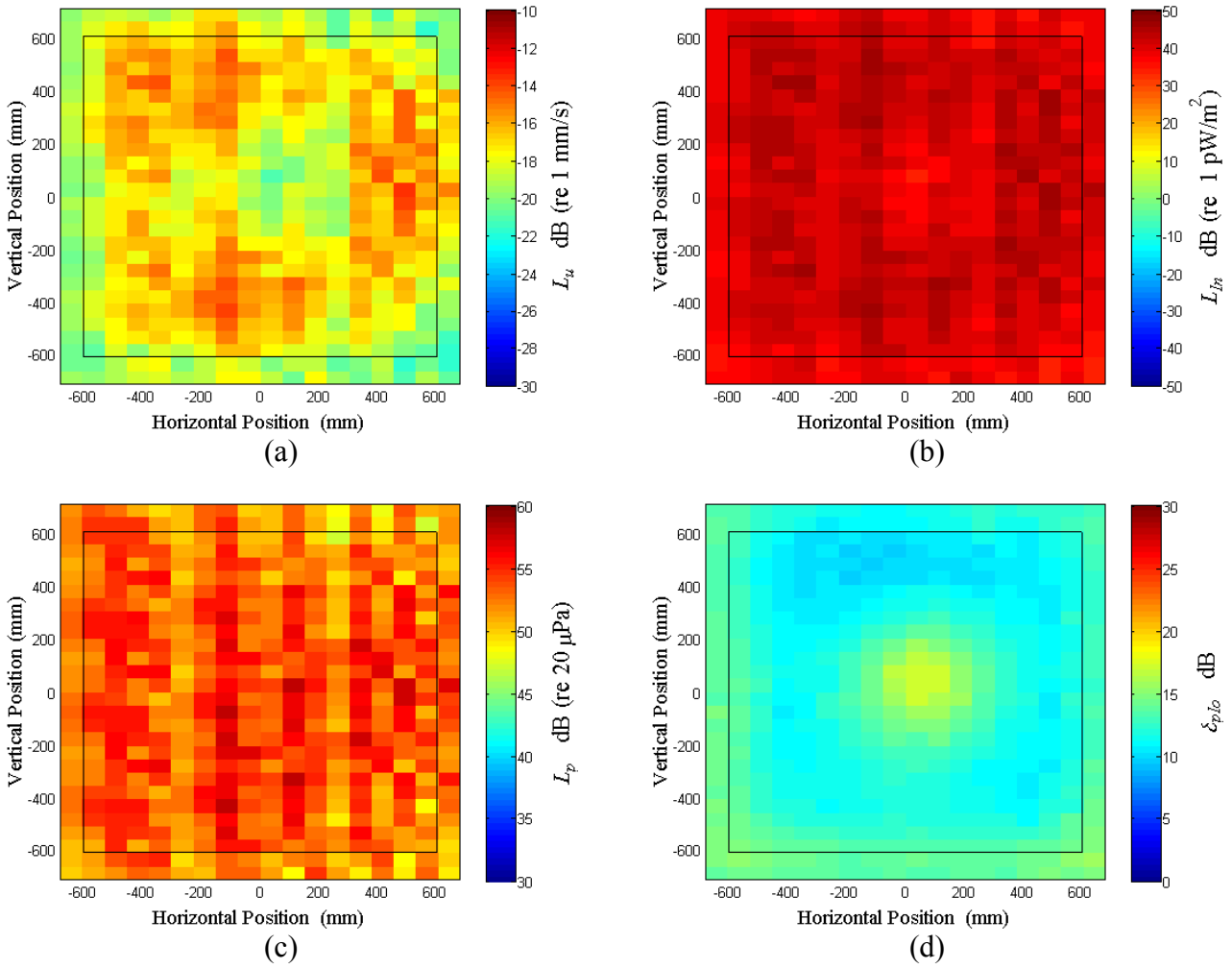

Figure B.18: Surface scan of Window B at 92.5 Hz (a) particle velocity level, L_u (b) normal signed sound intensity level, L_{In} (c) sound pressure level, L_p (d) pressure-residual intensity index, δ_{pIo}.

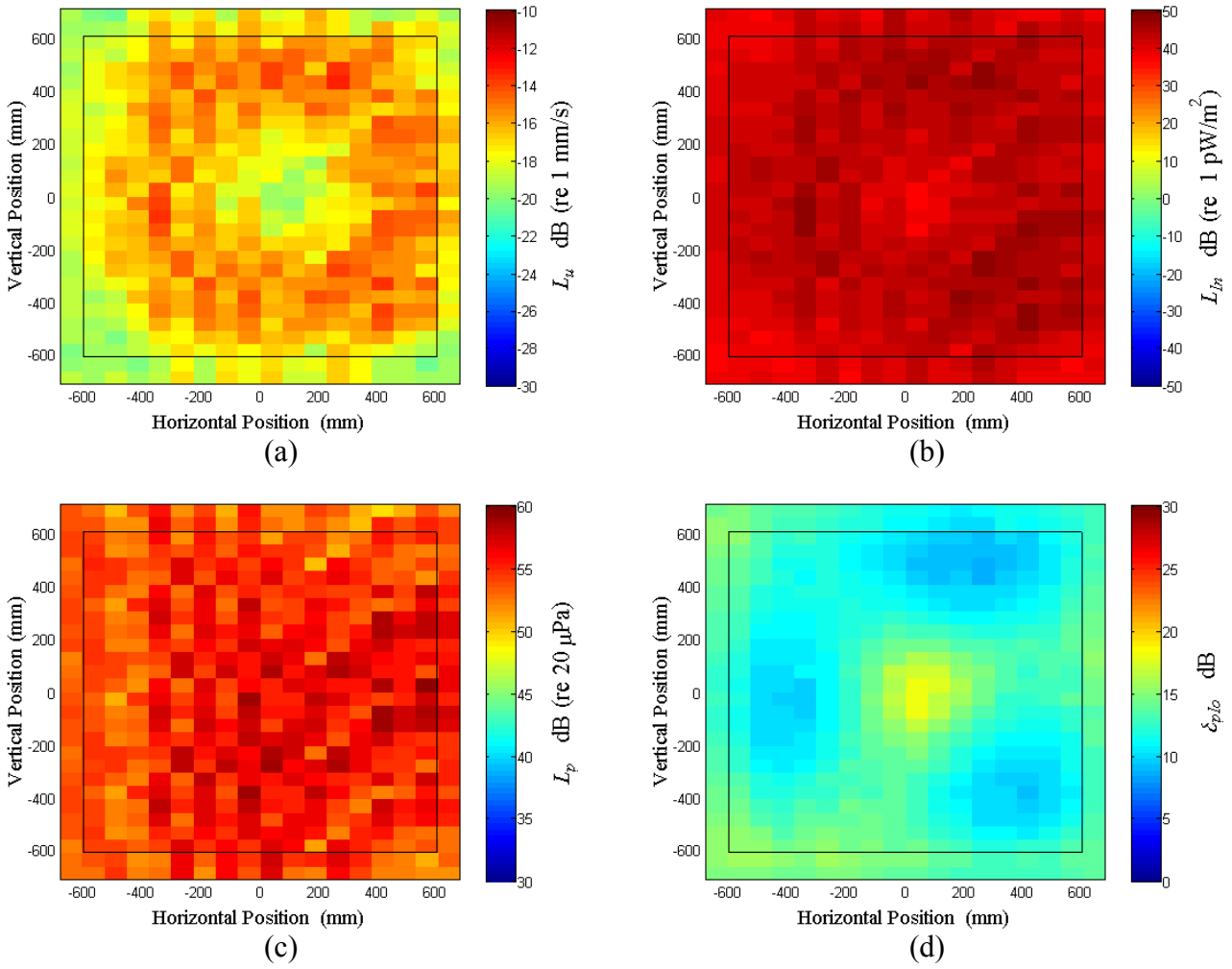

Figure B.19: Surface scan of Window B at 95 Hz (a) particle velocity level, L_u (b) normal signed sound intensity level, L_{In} (c) sound pressure level, L_p (d) pressure-residual intensity index, δ_{pIo}.

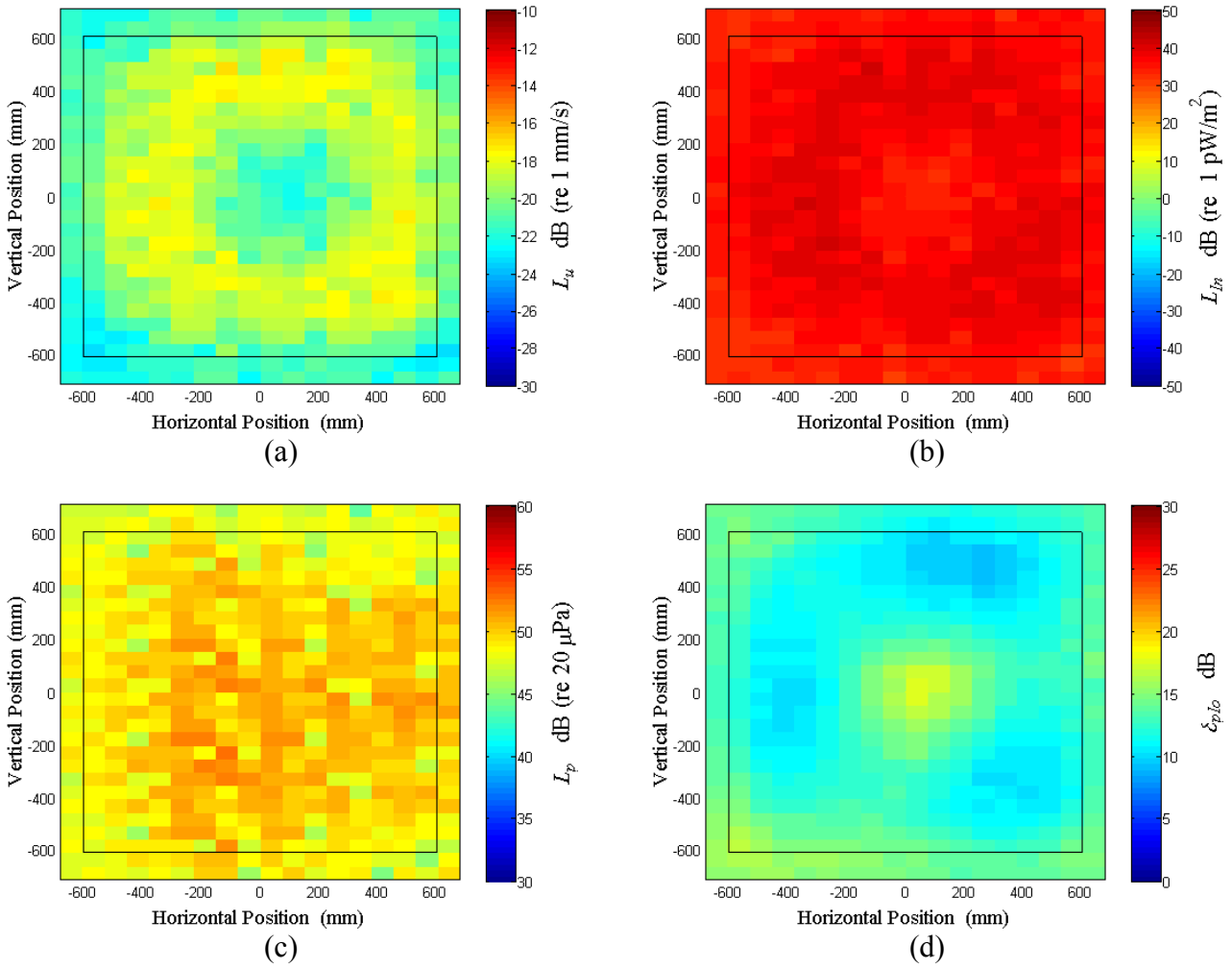

Figure B.20: Surface scan of Window B at 97.5 Hz (a) particle velocity level, L_u (b) normal signed sound intensity level, L_{In} (c) sound pressure level, L_p (d) pressure-residual intensity index, δ_{pIo}.

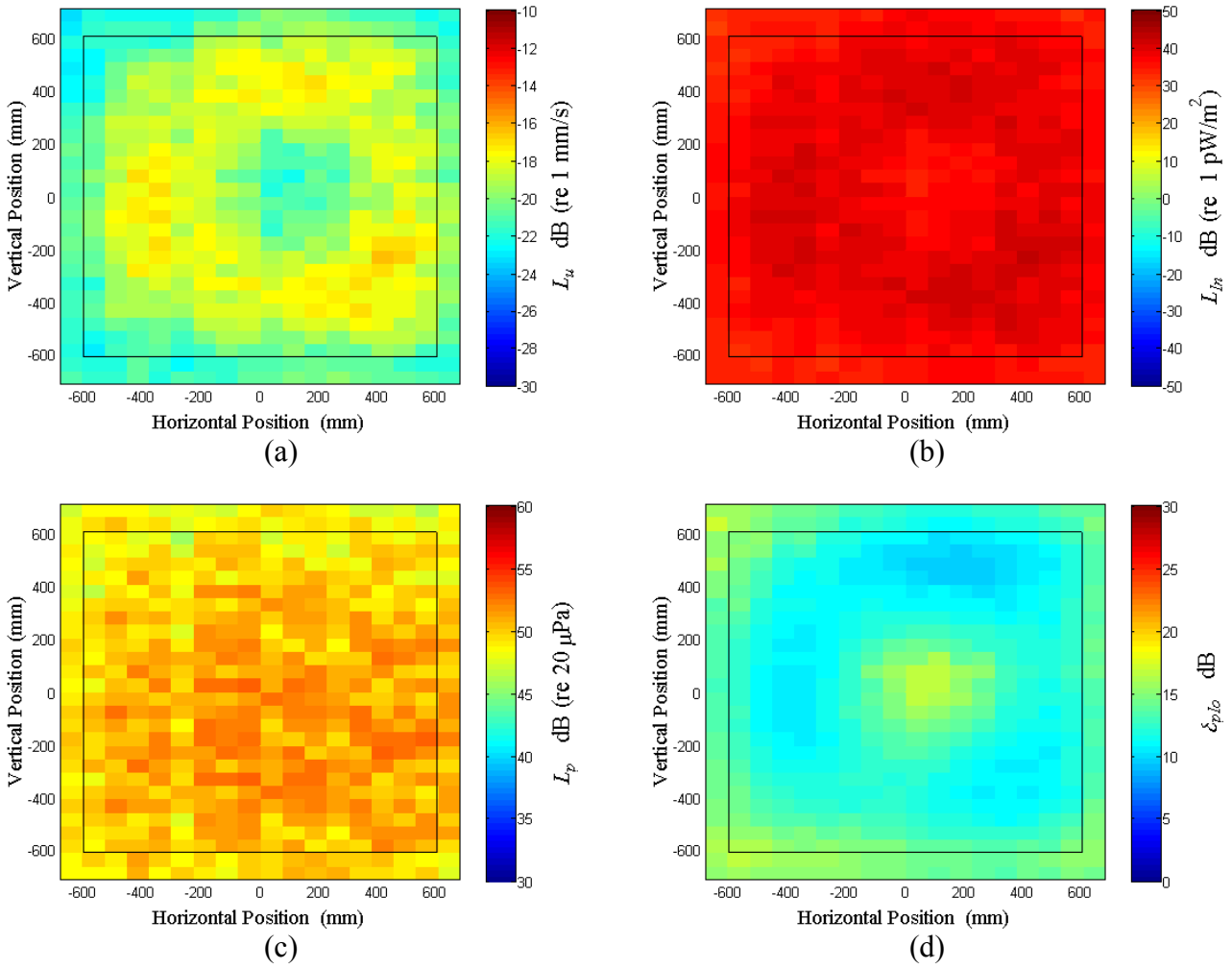

Figure B.21: Surface scan of Window B at 100 Hz (a) particle velocity level, L_u (b) normal signed sound intensity level, L_{In} (c) sound pressure level, L_p (d) pressure-residual intensity index, δ_{pIo}.

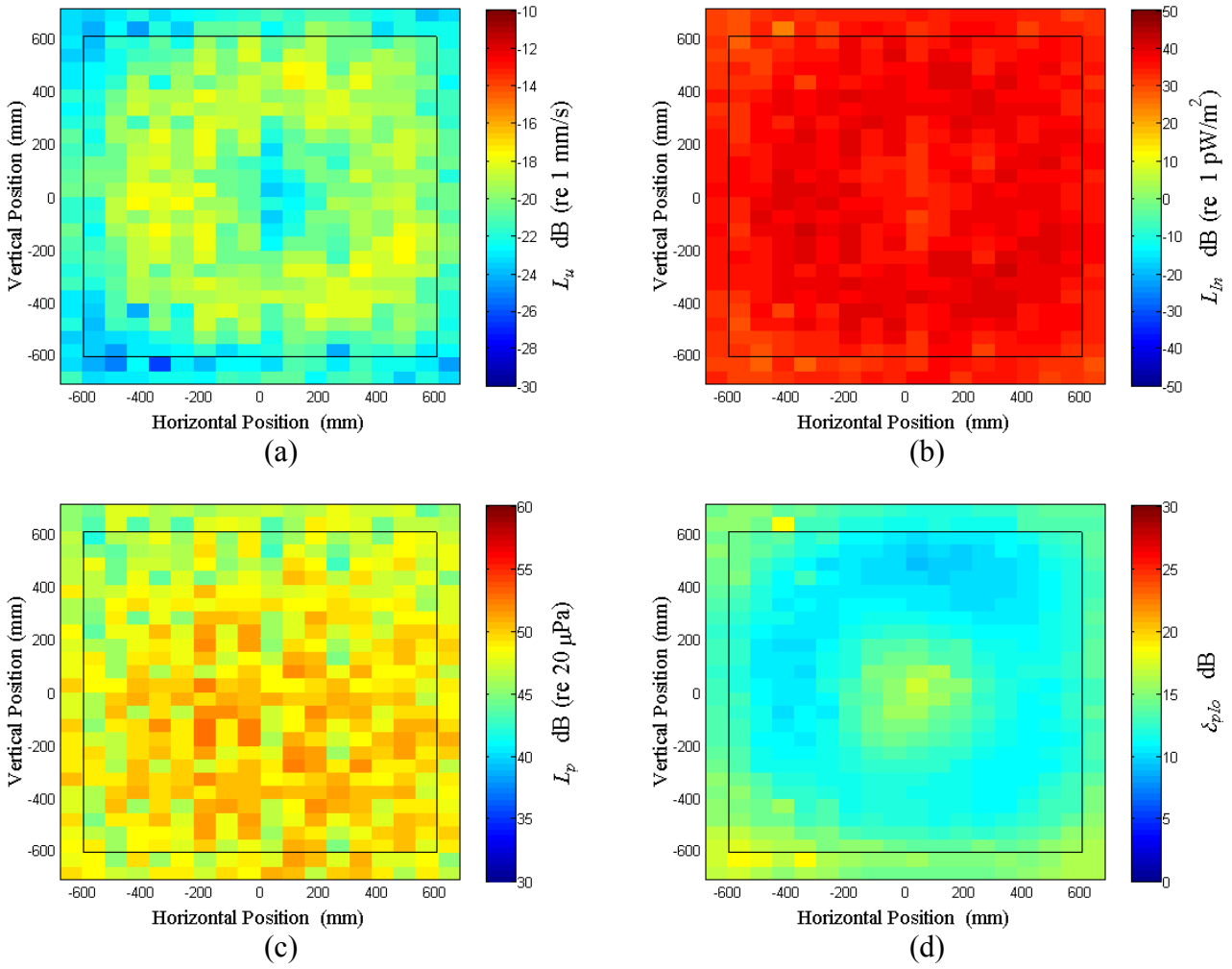

Figure B.22: Surface scan of Window B at 102.5 Hz (a) particle velocity level, L_u (b) normal signed sound intensity level, L_{In} (c) sound pressure level, L_p (d) pressure-residual intensity index, δ_{pIo}.

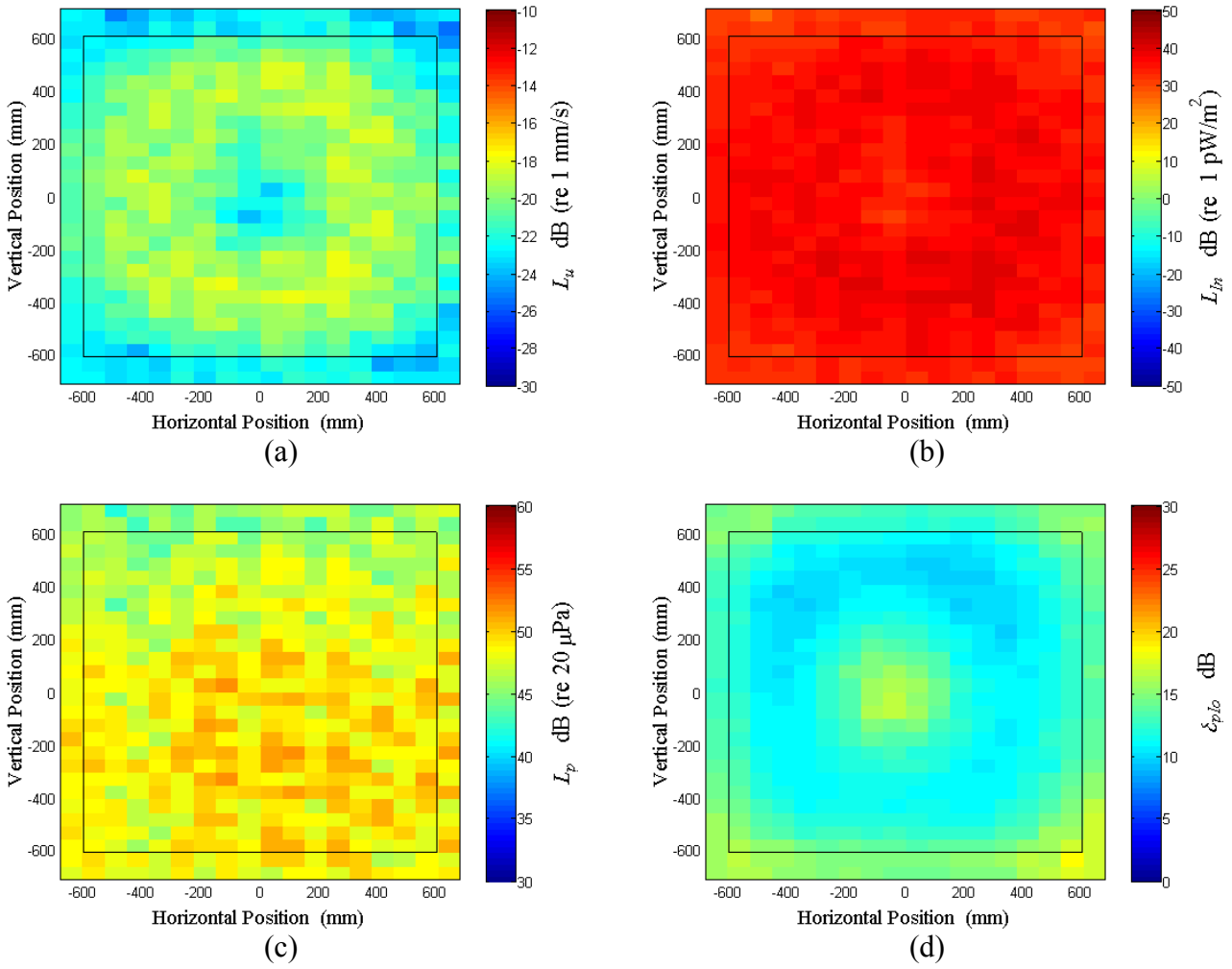

Figure B.23: Surface scan of Window B at 105 Hz (a) particle velocity level, L_u (b) normal signed sound intensity level, L_{In} (c) sound pressure level, L_p (d) pressure-residual intensity index, δ_{pIo}.

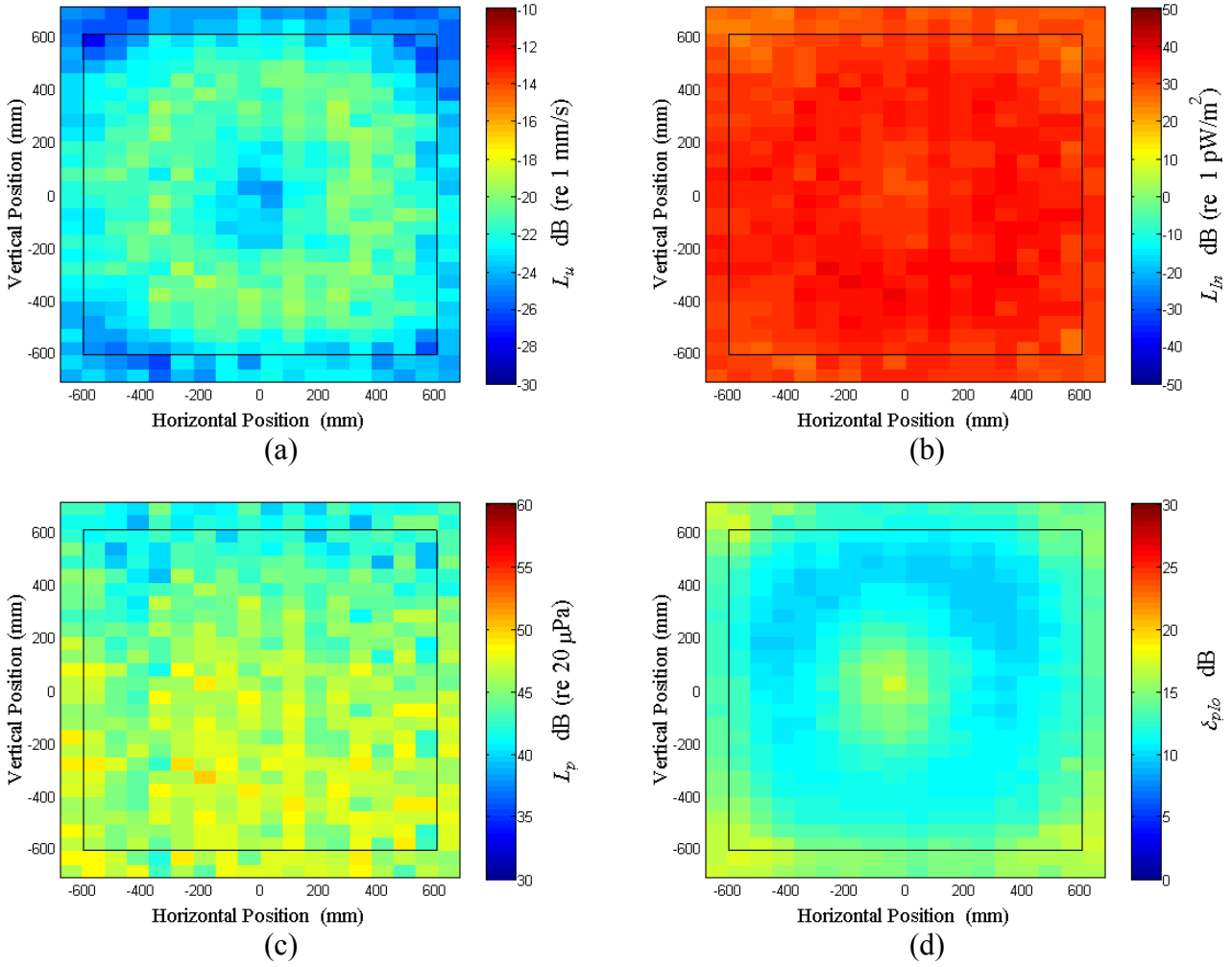

Figure B.24: Surface scan of Window B at 107.5 Hz (a) particle velocity level, L_u (b) normal signed sound intensity level, L_{In} (c) sound pressure level, L_p (d) pressure-residual intensity index, δ_{pIo}.

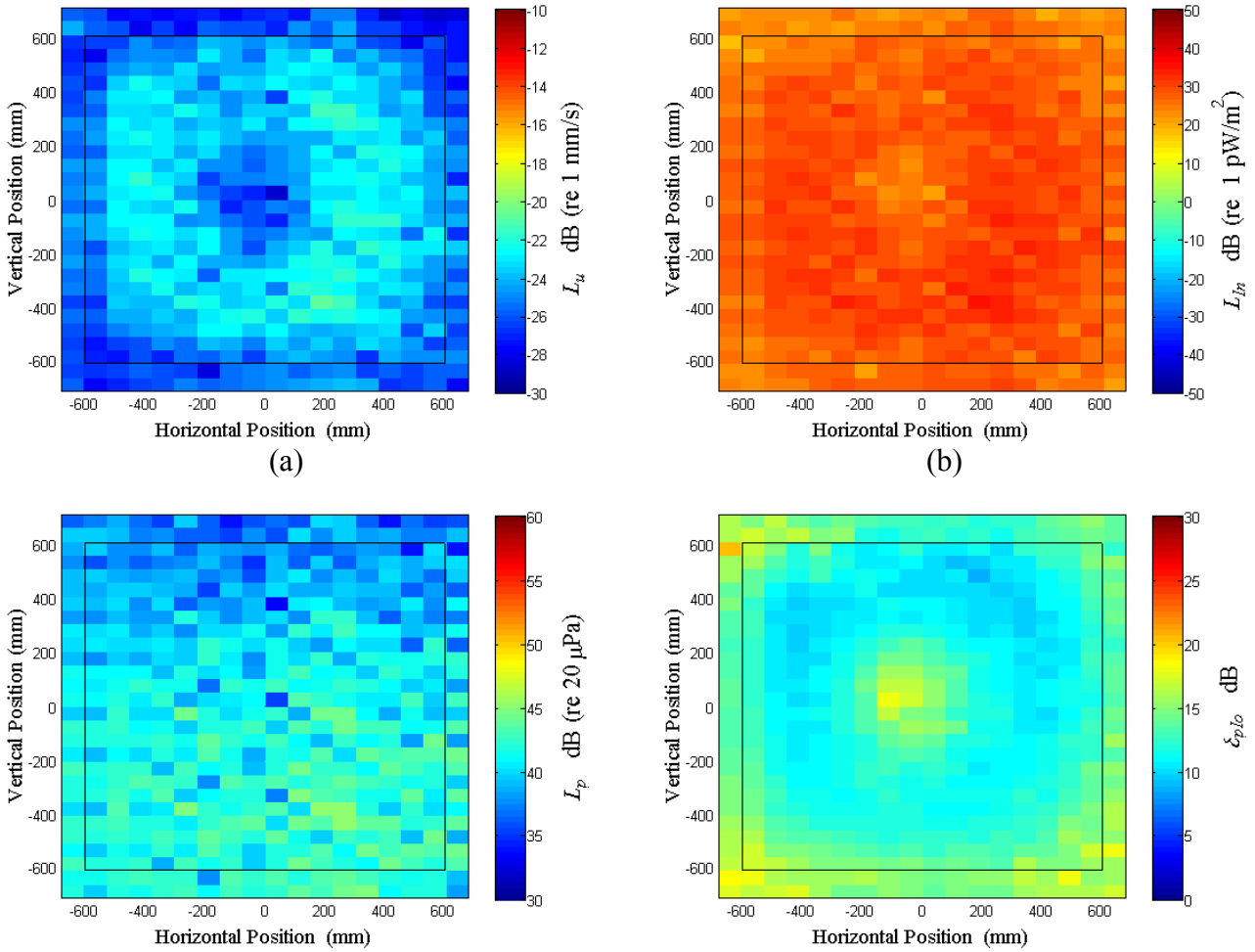

Figure B.25: Surface scan of Window B at 110 Hz (a) particle velocity level, L_u (b) normal signed sound intensity level, L_{In} (c) sound pressure level, L_p (d) pressure-residual intensity index, δ_{pIo}.

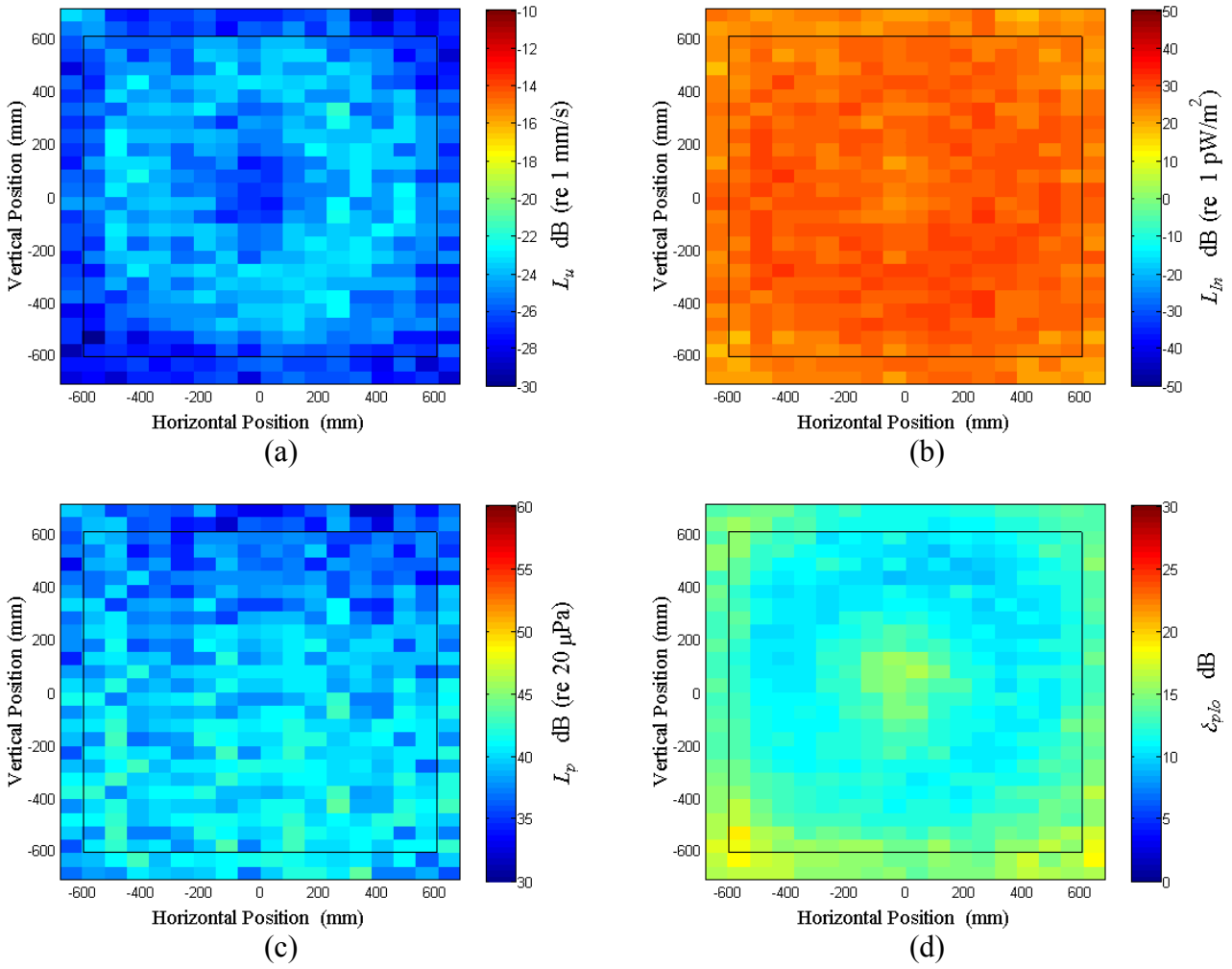

Figure B.26: Surface scan of Window B at 112.5 Hz (a) particle velocity level, L_u (b) normal signed sound intensity level, L_{In} (c) sound pressure level, L_p (d) pressure-residual intensity index, δ_{pIo}.

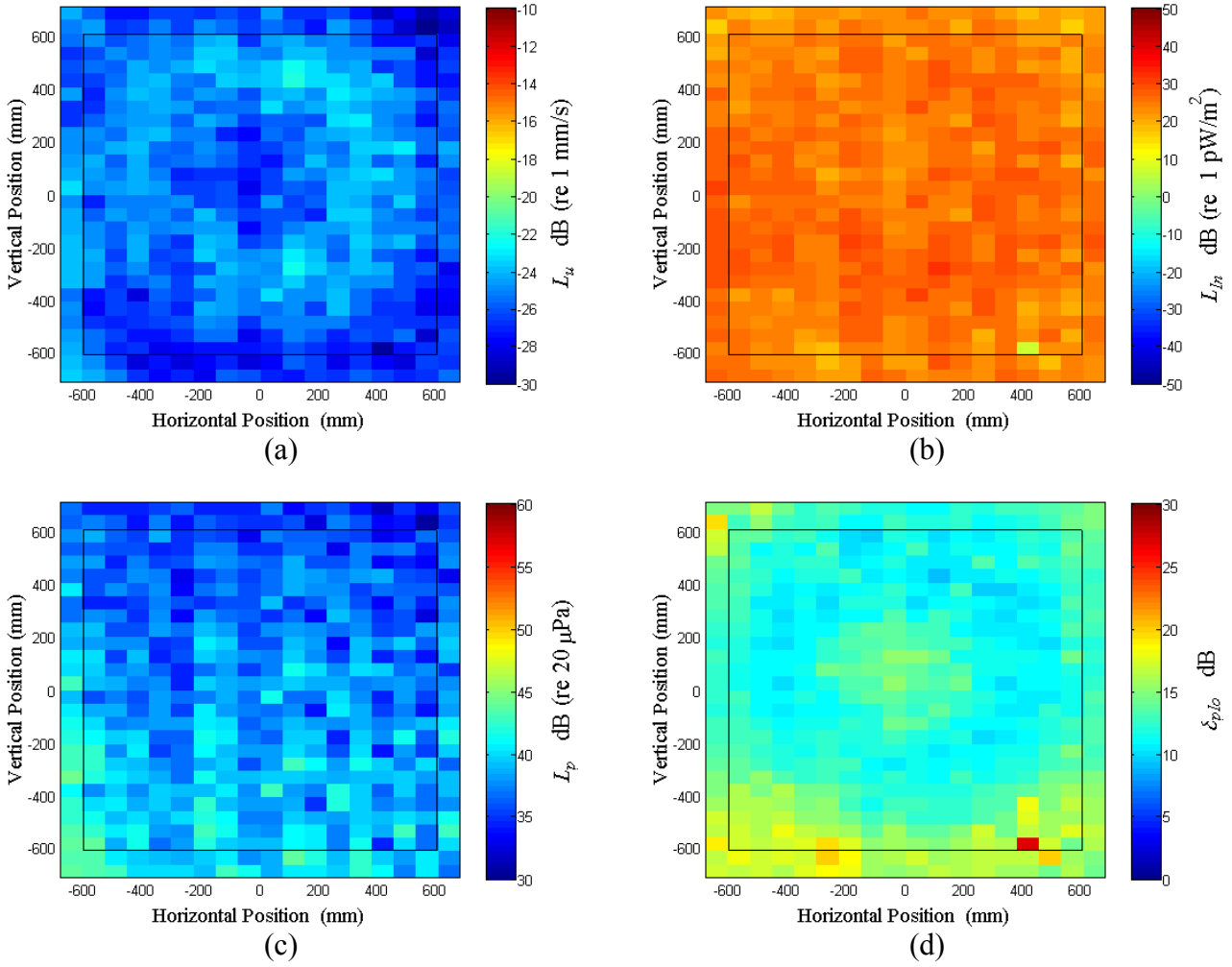

Figure B.27: Surface scan of Window B at 115 Hz (a) particle velocity level, L_u (b) normal signed sound intensity level, L_{In} (c) sound pressure level, L_p (d) pressure-residual intensity index, δ_{pIo}.

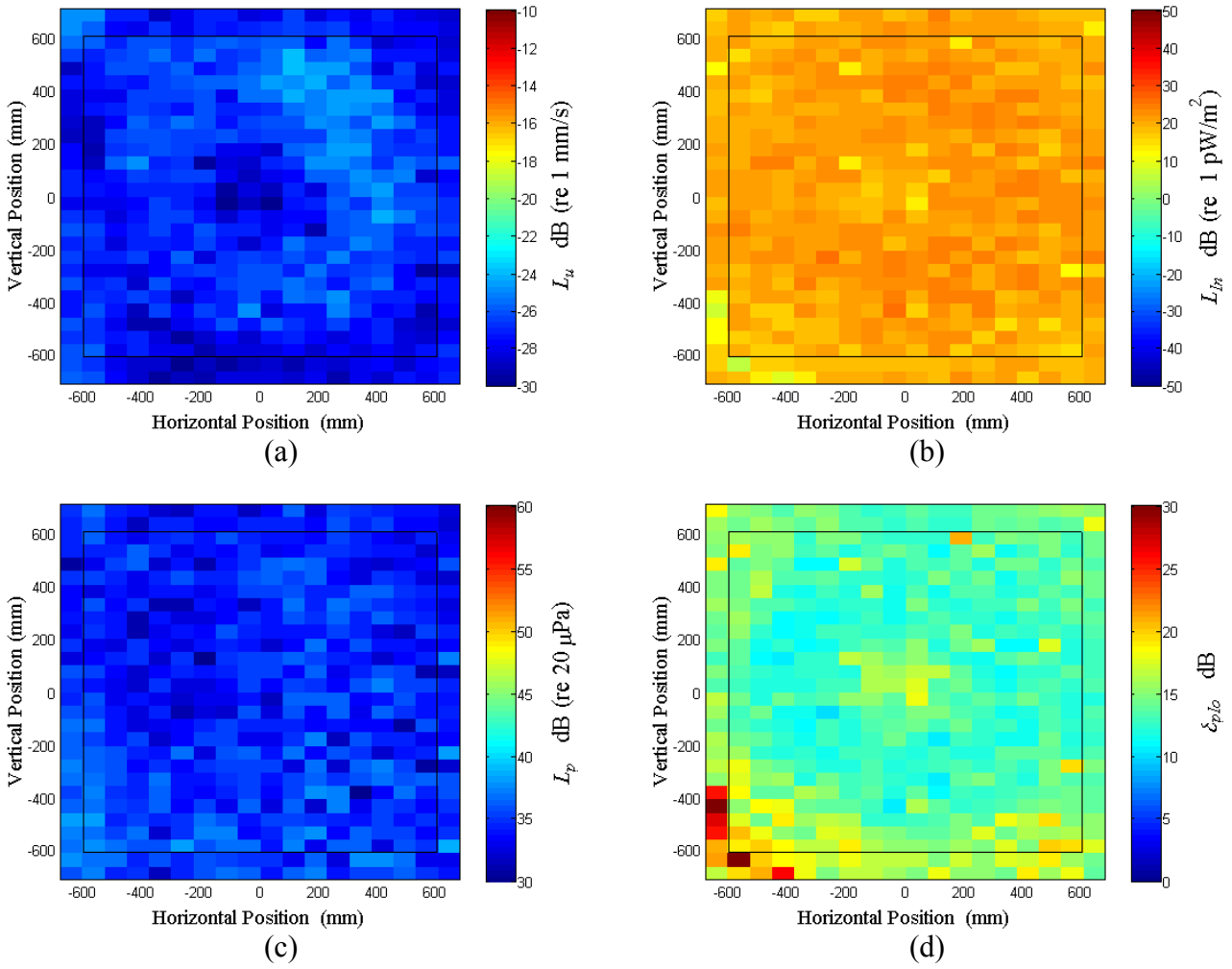

Figure B.28: Surface scan of Window B at 117.5 Hz (a) particle velocity level, L_u (b) normal signed sound intensity level, L_{In} (c) sound pressure level, L_p (d) pressure-residual intensity index, δ_{pIo}.

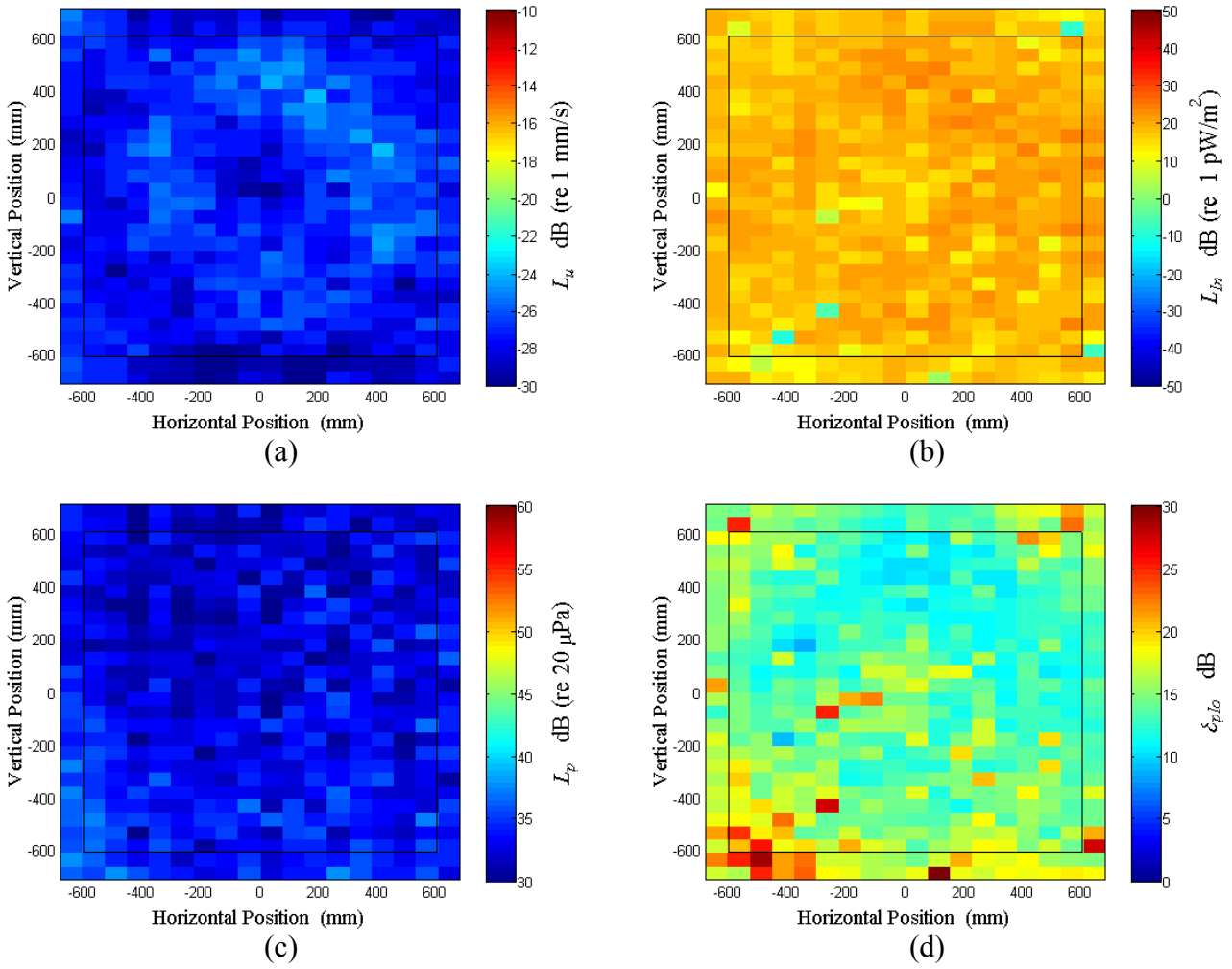

Figure B.29: Surface scan of Window B at 120 Hz (a) particle velocity level, L_u (b) normal signed sound intensity level, L_{In} (c) sound pressure level, L_p (d) pressure-residual intensity index, δ_{pIo}.

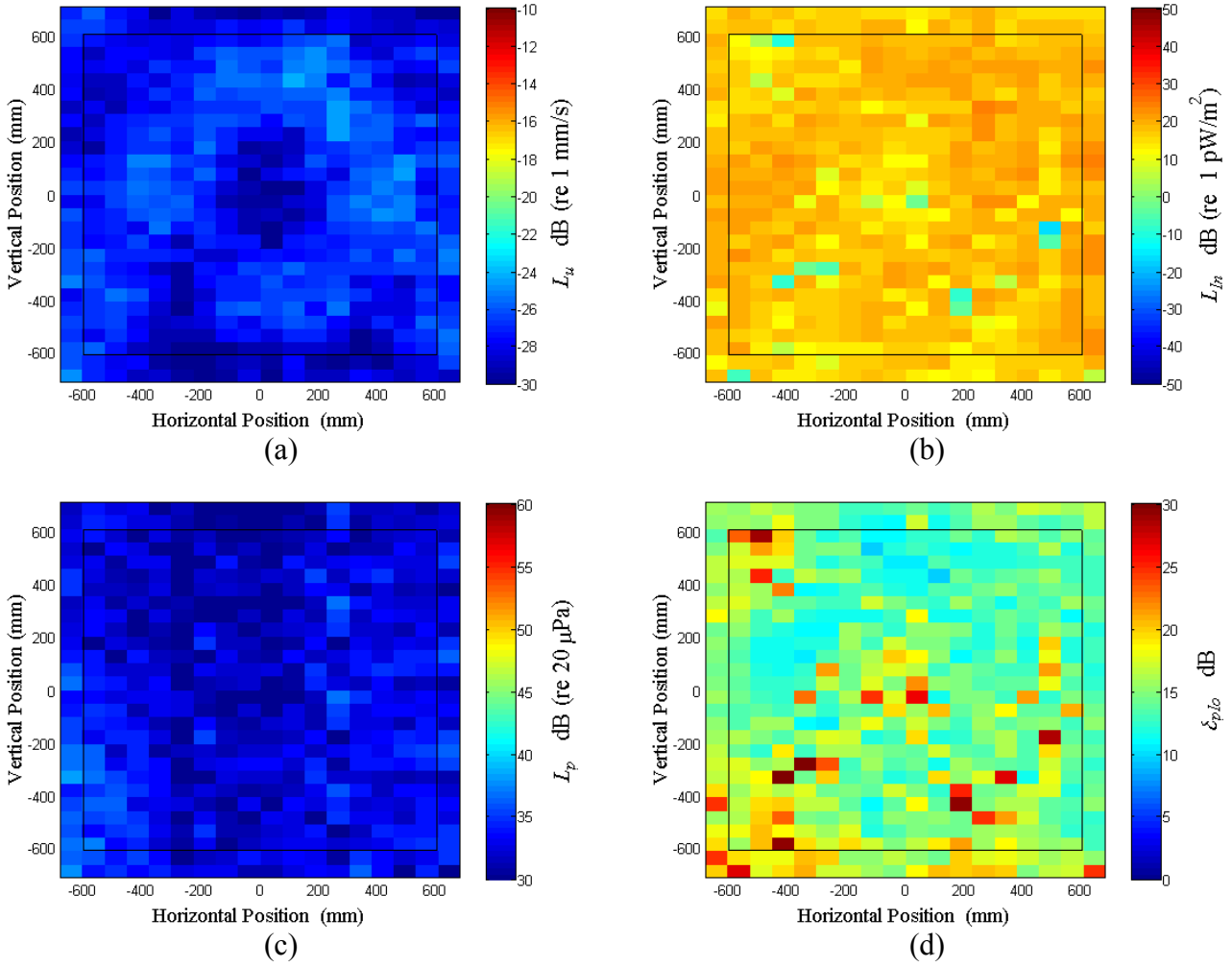

Figure B.30: Surface scan of Window B at 122.5 Hz (a) particle velocity level, L_u (b) normal signed sound intensity level, L_{In} (c) sound pressure level, L_p (d) pressure-residual intensity index, δ_{pIo}.

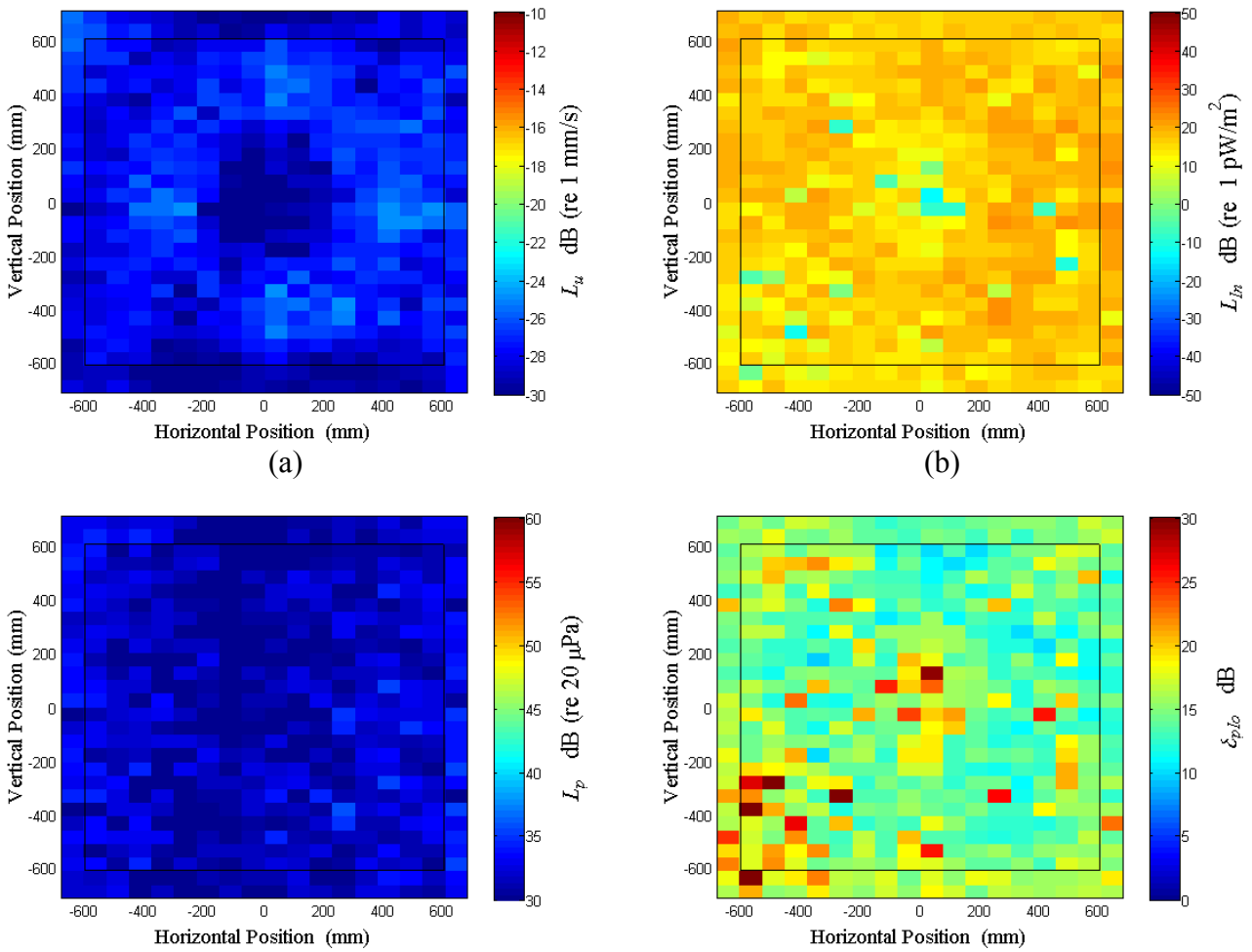

Figure B.31: Surface scan of Window B at 125 Hz (a) particle velocity level, L_u (b) normal signed sound intensity level, L_{In} (c) sound pressure level, L_p (d) pressure-residual intensity index, δ_{pIo}.

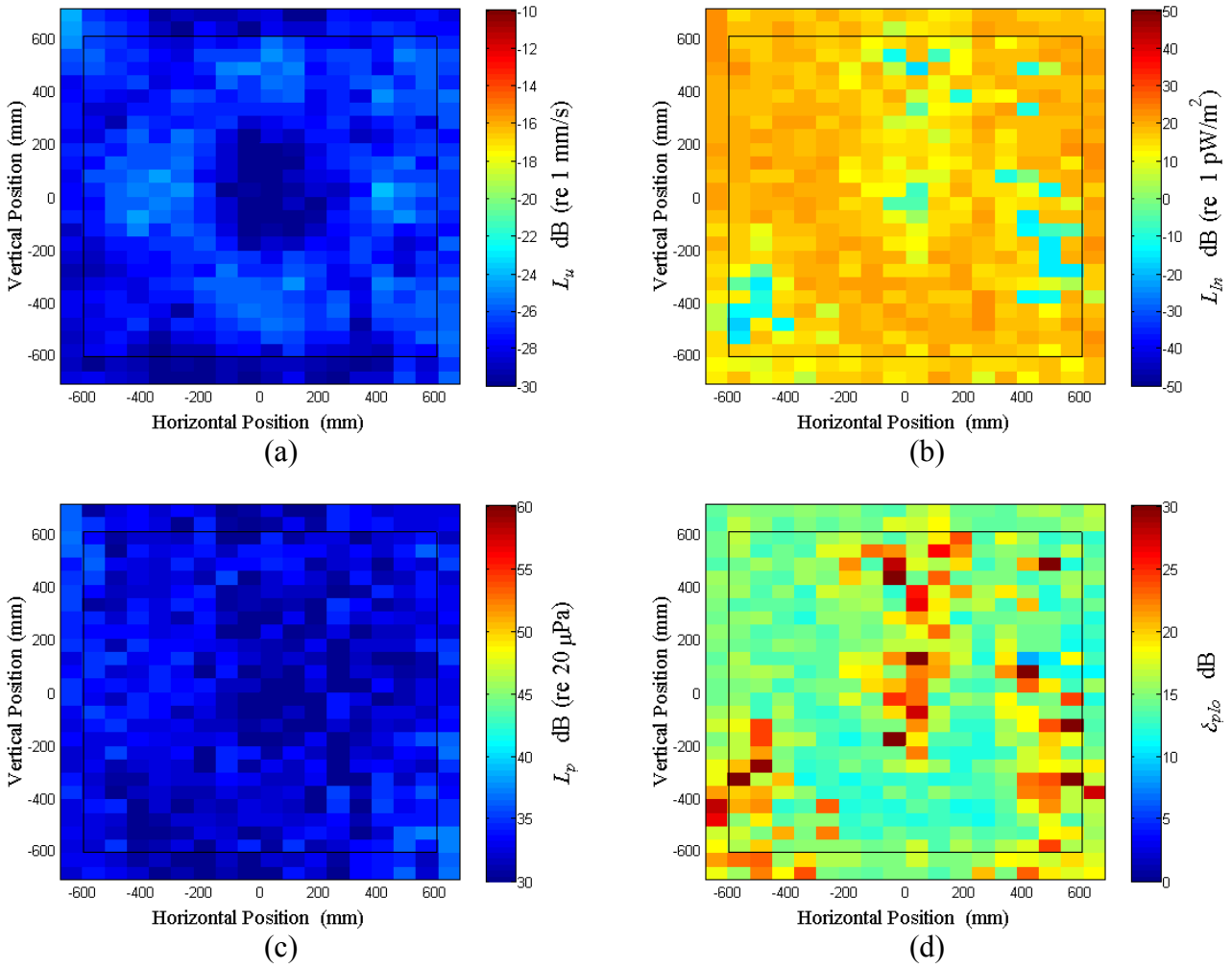

Figure B.32: Surface scan of Window B at 127.5 Hz (a) particle velocity level, L_u (b) normal signed sound intensity level, L_{In} (c) sound pressure level, L_p (d) pressure-residual intensity index, δ_{pIo}.

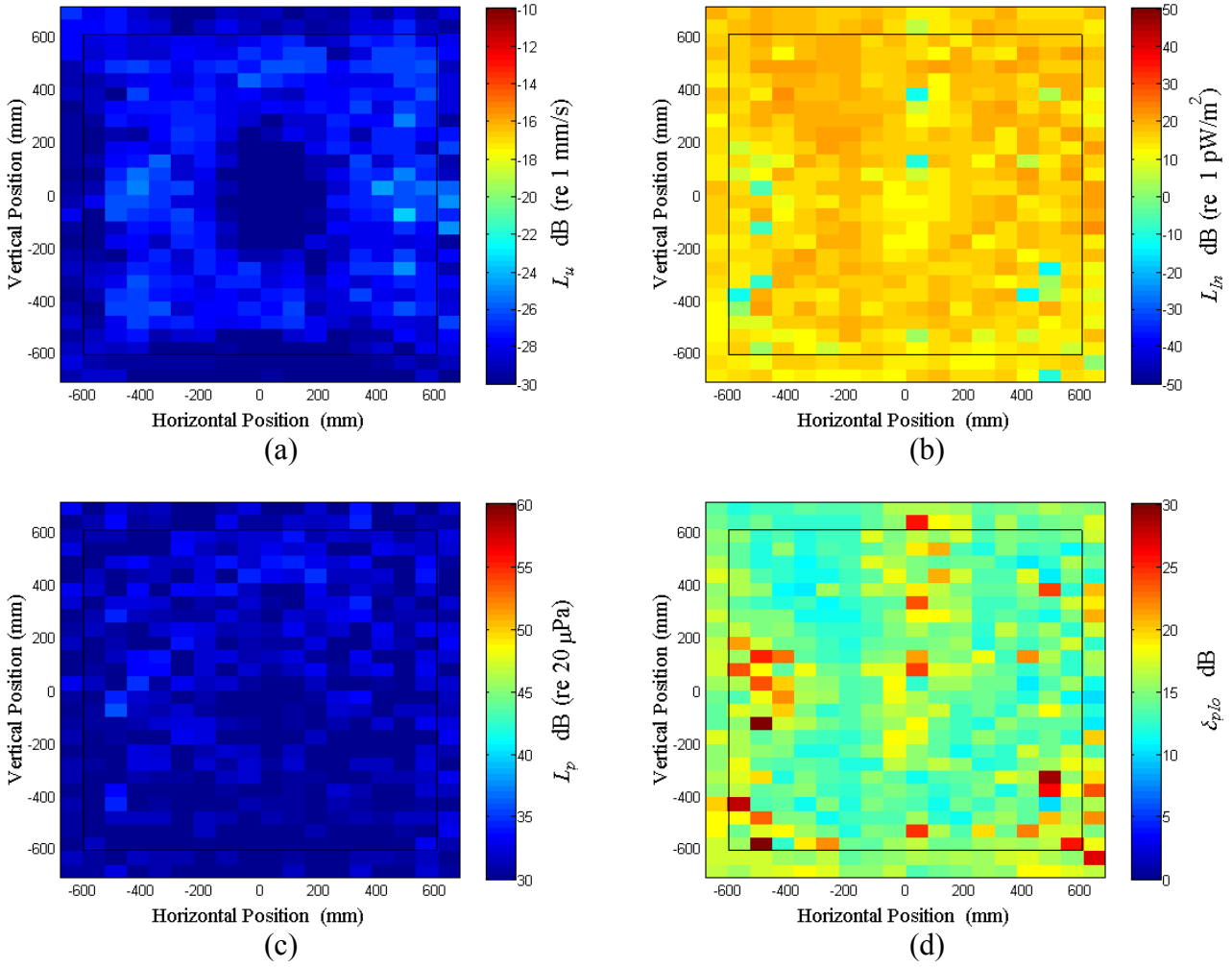

Figure B.33: Surface scan of Window B at 130 Hz (a) particle velocity level, L_u (b) normal signed sound intensity level, L_{In} (c) sound pressure level, L_p (d) pressure-residual intensity index, δ_{pIo}.

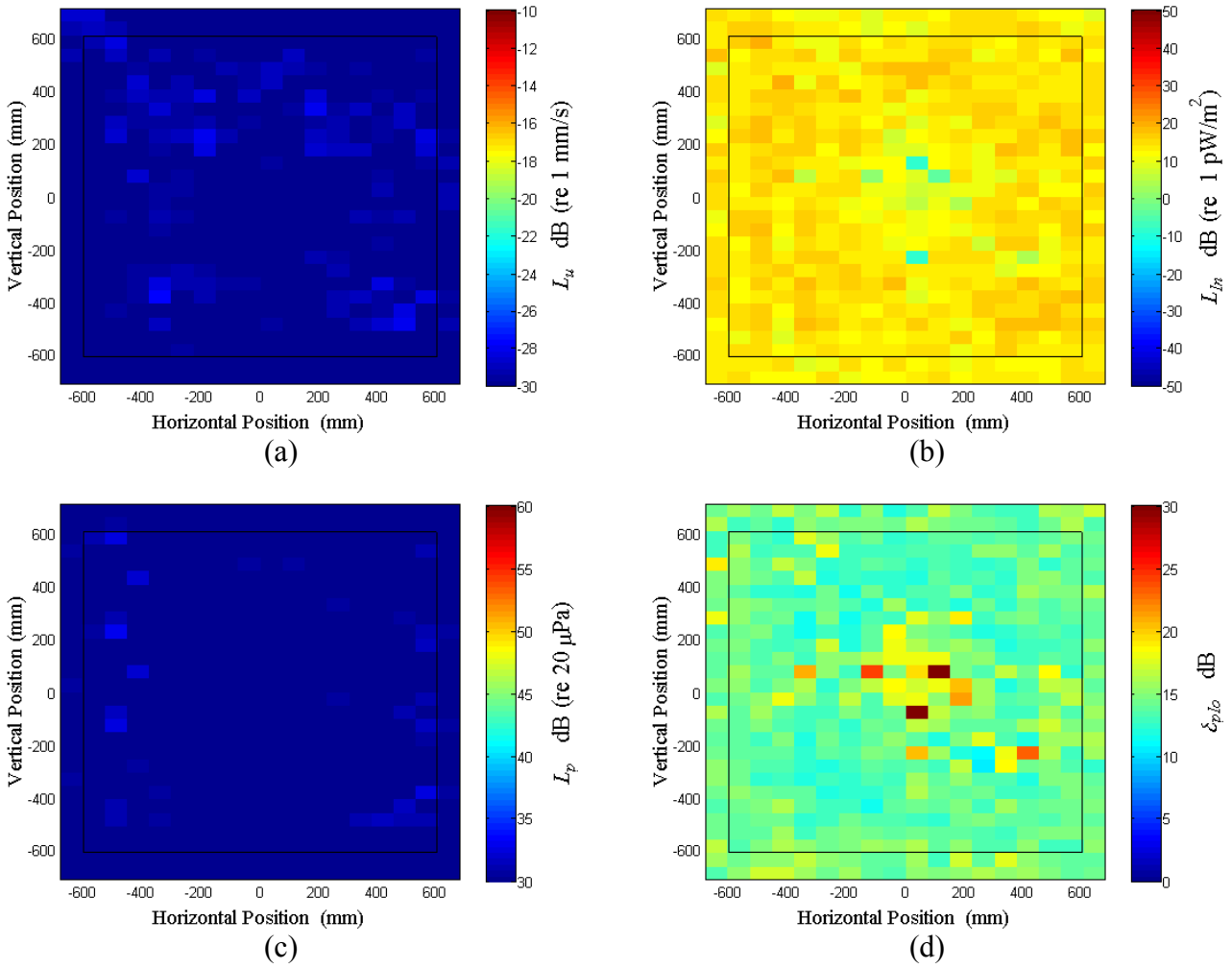

Figure B.34: Surface scan of Window B at 140 Hz (a) particle velocity level, L_u (b) normal signed sound intensity level, L_{In} (c) sound pressure level, L_p (d) pressure-residual intensity index, δ_{pIo}.

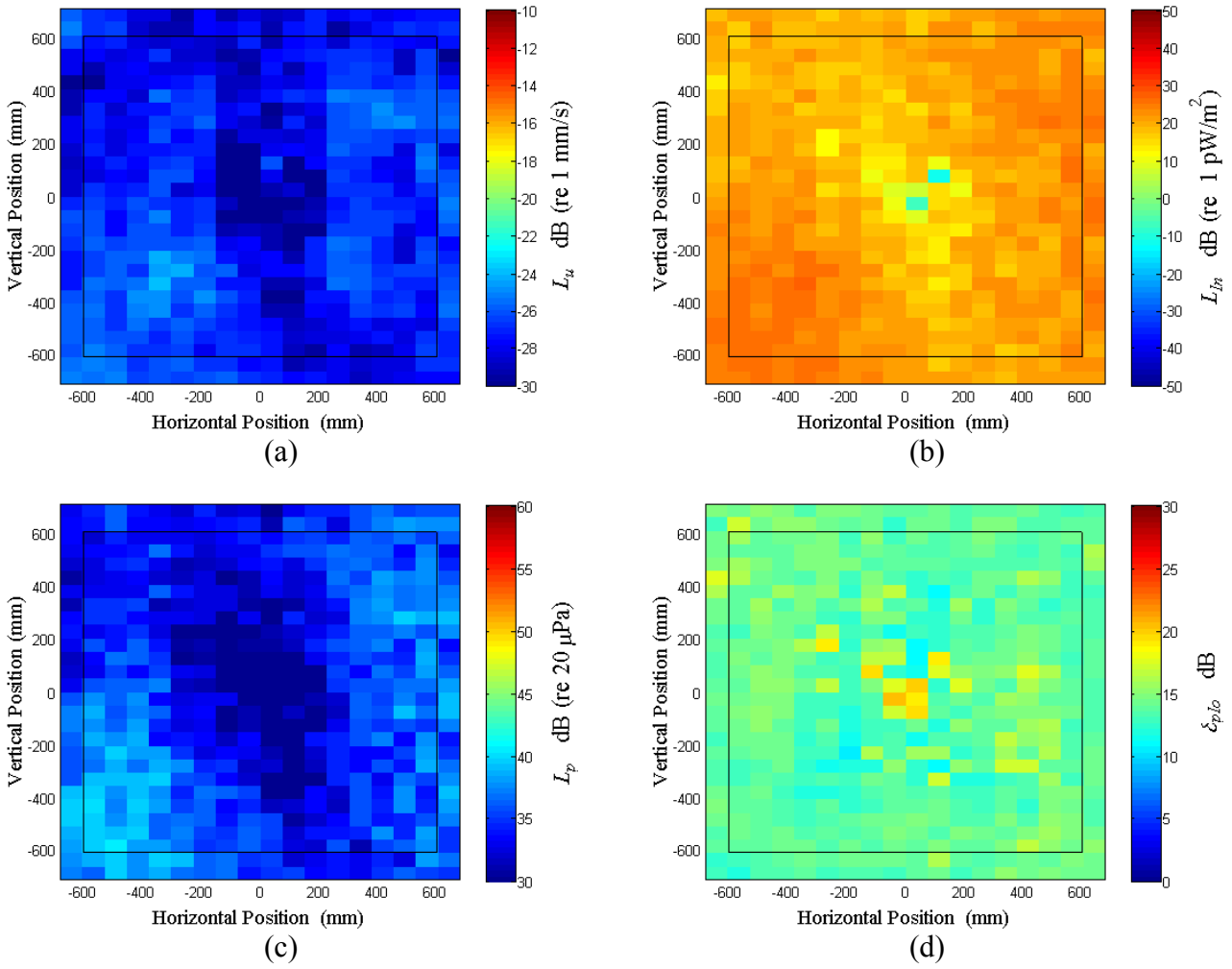

Figure B.35: Surface scan of Window B at 150 Hz (a) particle velocity level, L_u (b) normal signed sound intensity level, L_{In} (c) sound pressure level, L_p (d) pressure-residual intensity index, δ_{pIo}.

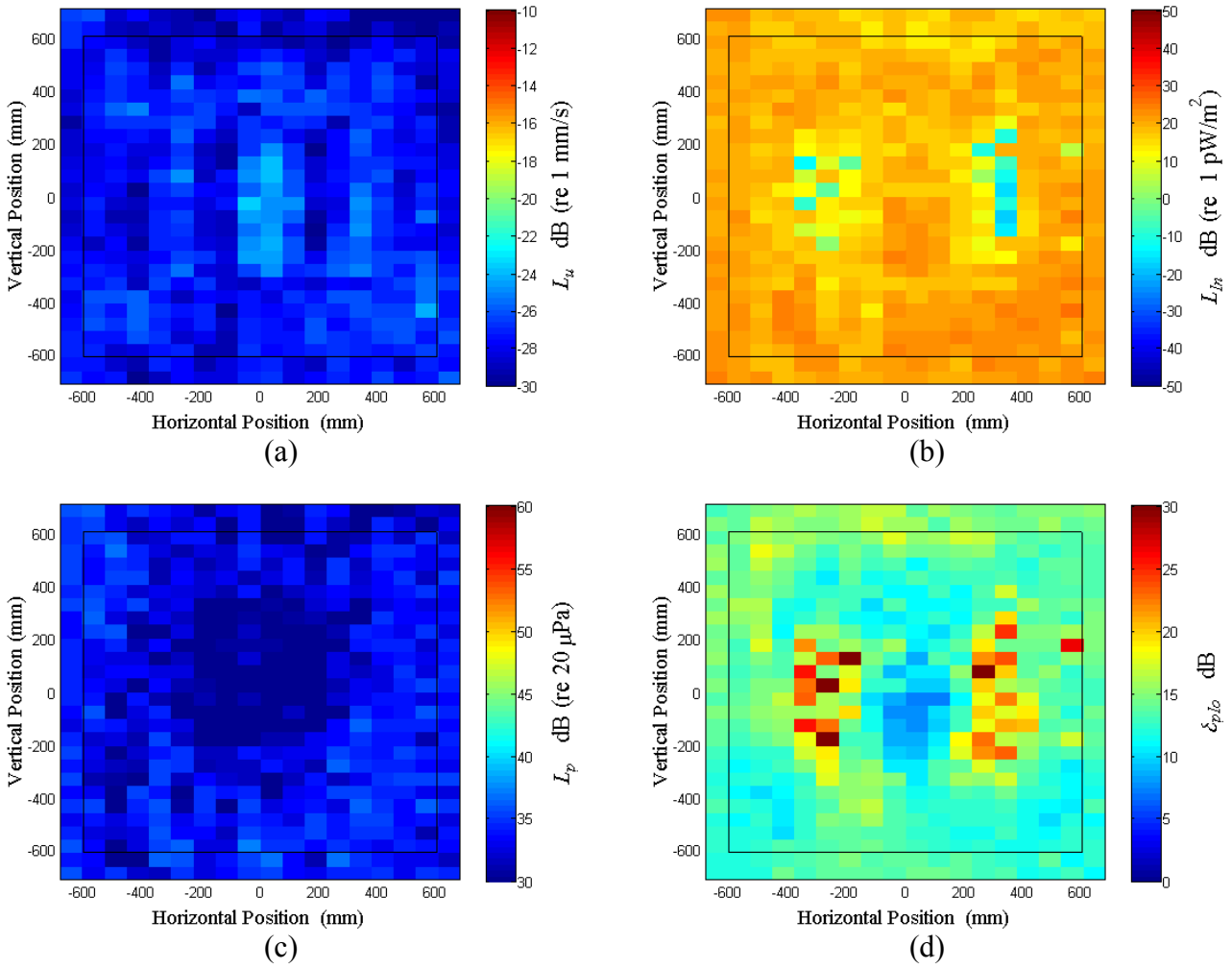

Figure B.36: Surface scan of Window B at 160 Hz (a) particle velocity level, L_u (b) normal signed sound intensity level, L_{In} (c) sound pressure level, L_p (d) pressure-residual intensity index, δ_{pIo}.

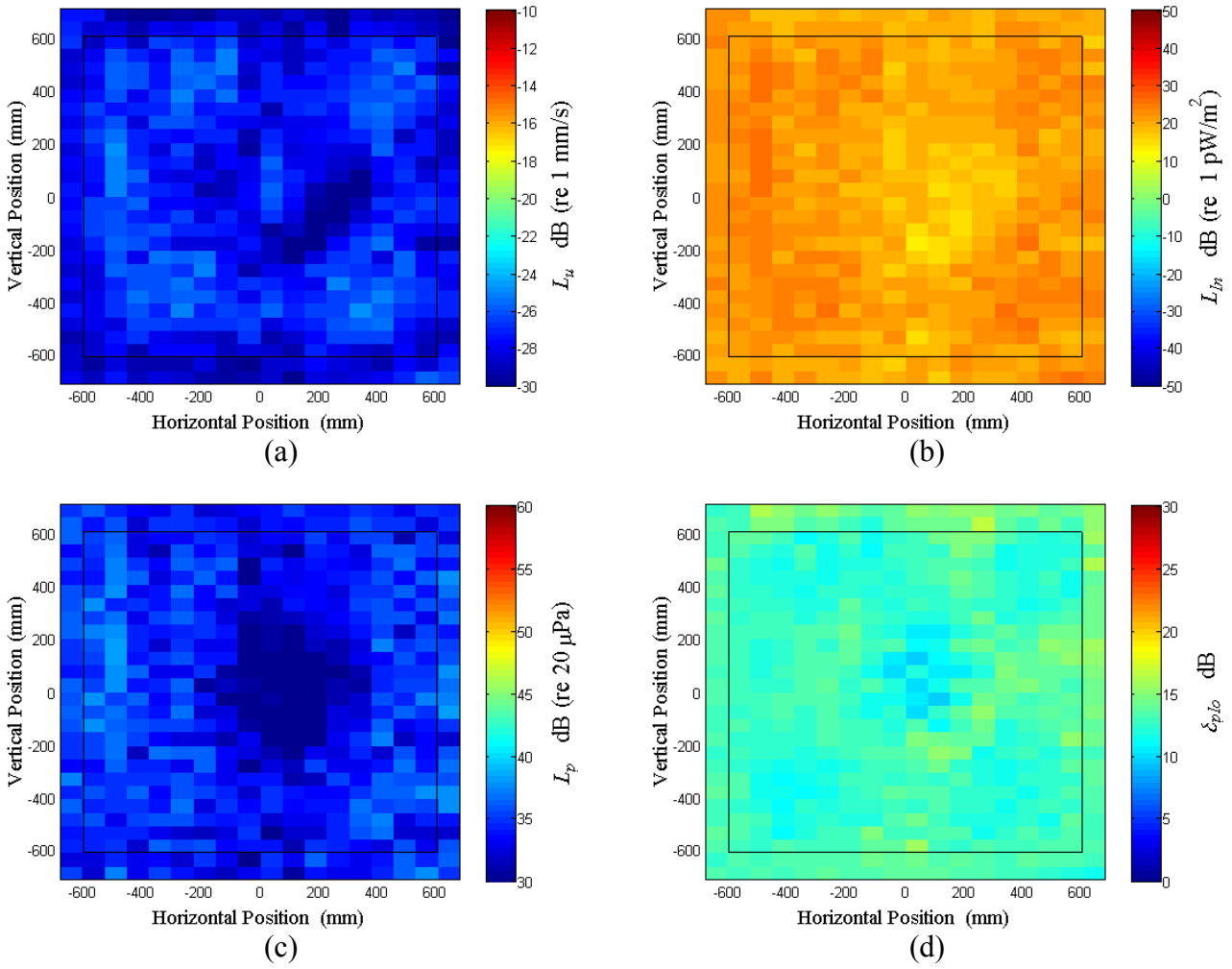

Figure B.37: Surface scan of Window B at 170 Hz (a) particle velocity level, L_u (b) normal signed sound intensity level, L_{In} (c) sound pressure level, L_p (d) pressure-residual intensity index, δ_{pIo}.

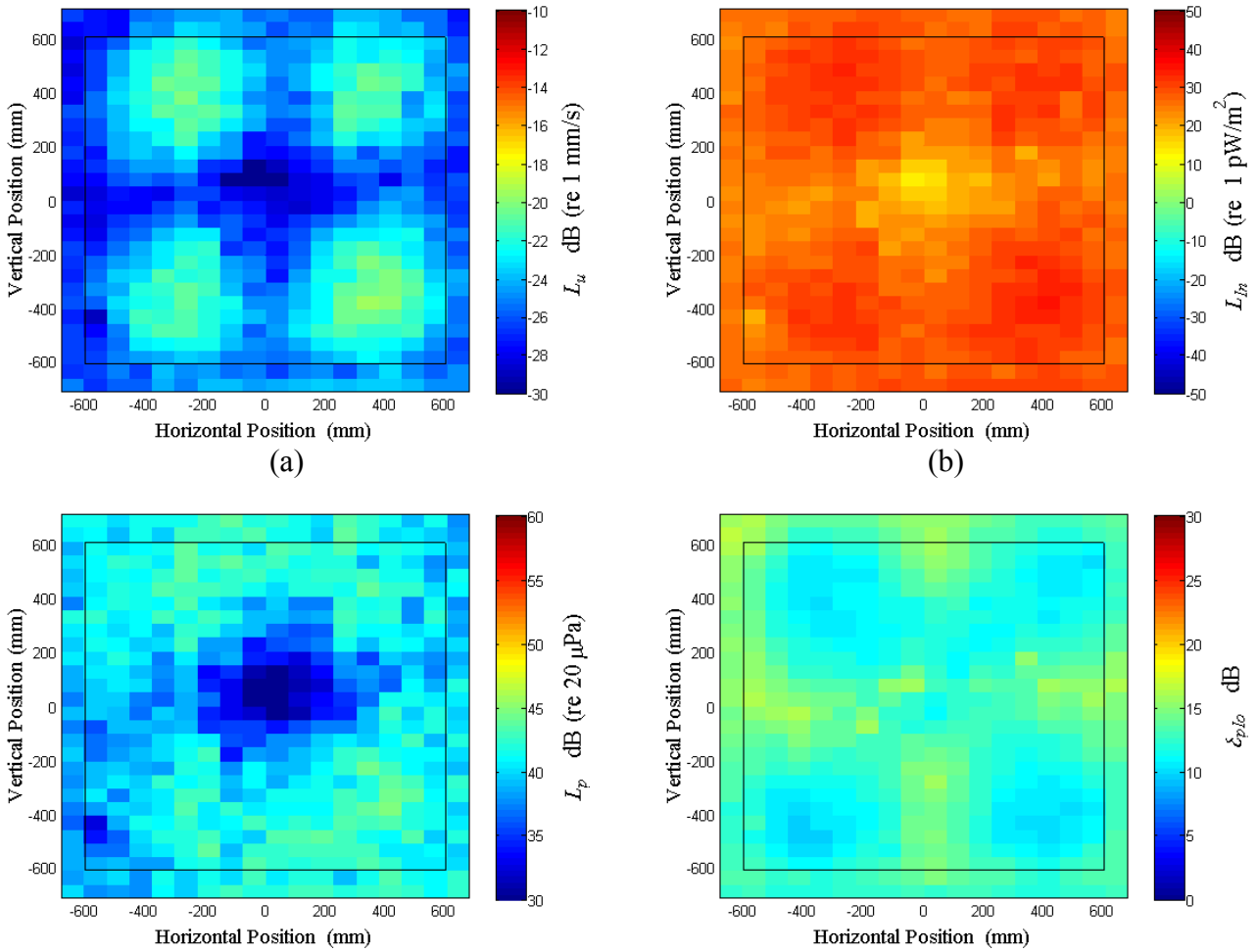

Figure B.38: Surface scan of Window B at 180 Hz (a) particle velocity level, L_u (b) normal signed sound intensity level, L_{In} (c) sound pressure level, L_p (d) pressure-residual intensity index, δ_{pIo}.

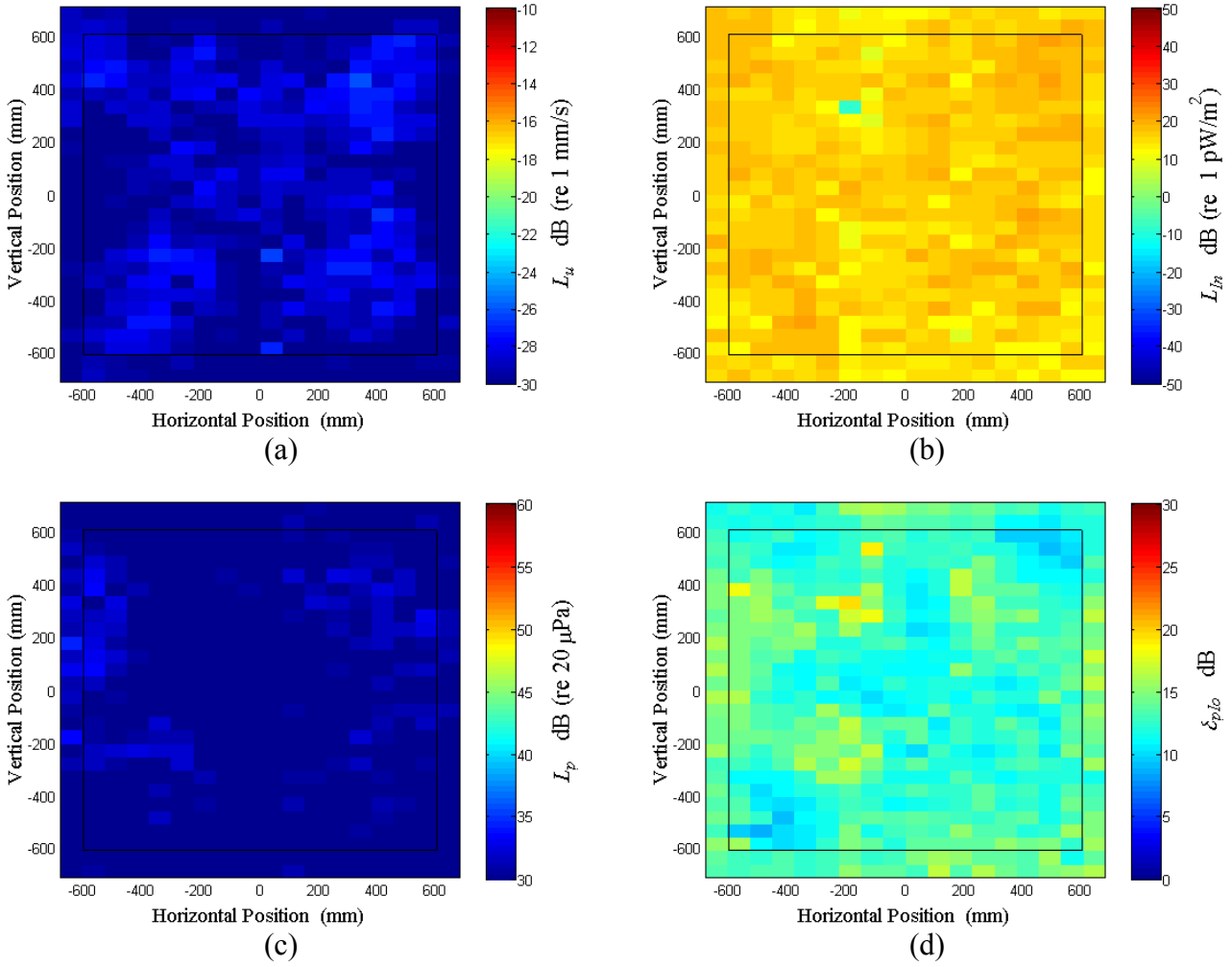

Figure B.39: Surface scan of Window B at 190 Hz (a) particle velocity level, L_u (b) normal signed sound intensity level, L_{In} (c) sound pressure level, L_p (d) pressure-residual intensity index, δ_{pIo}.

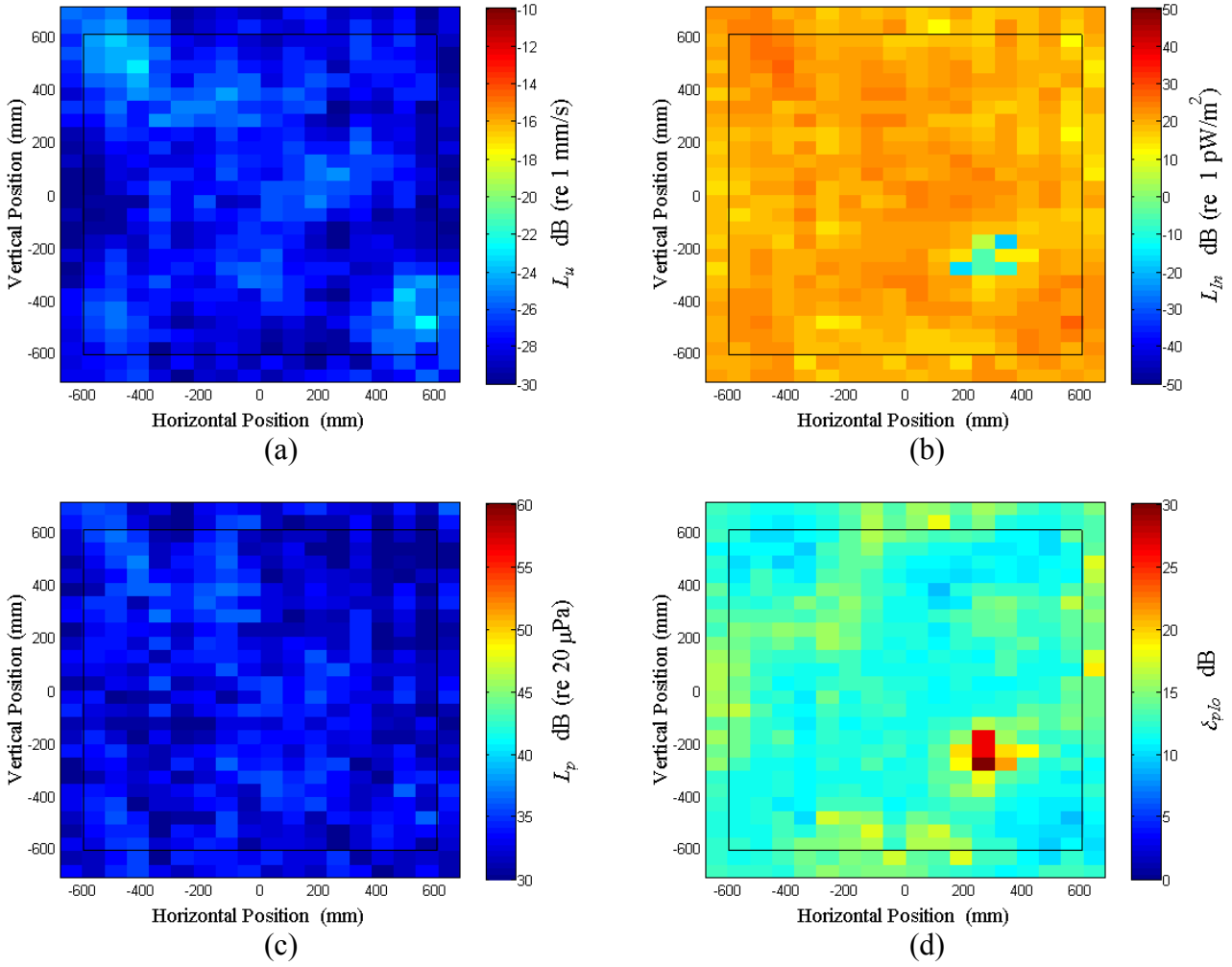

Figure B.40: Surface scan of Window B at 200 Hz (a) particle velocity level, L_u (b) normal signed sound intensity level, L_{In} (c) sound pressure level, L_p (d) pressure-residual intensity index, δ_{pIo}.

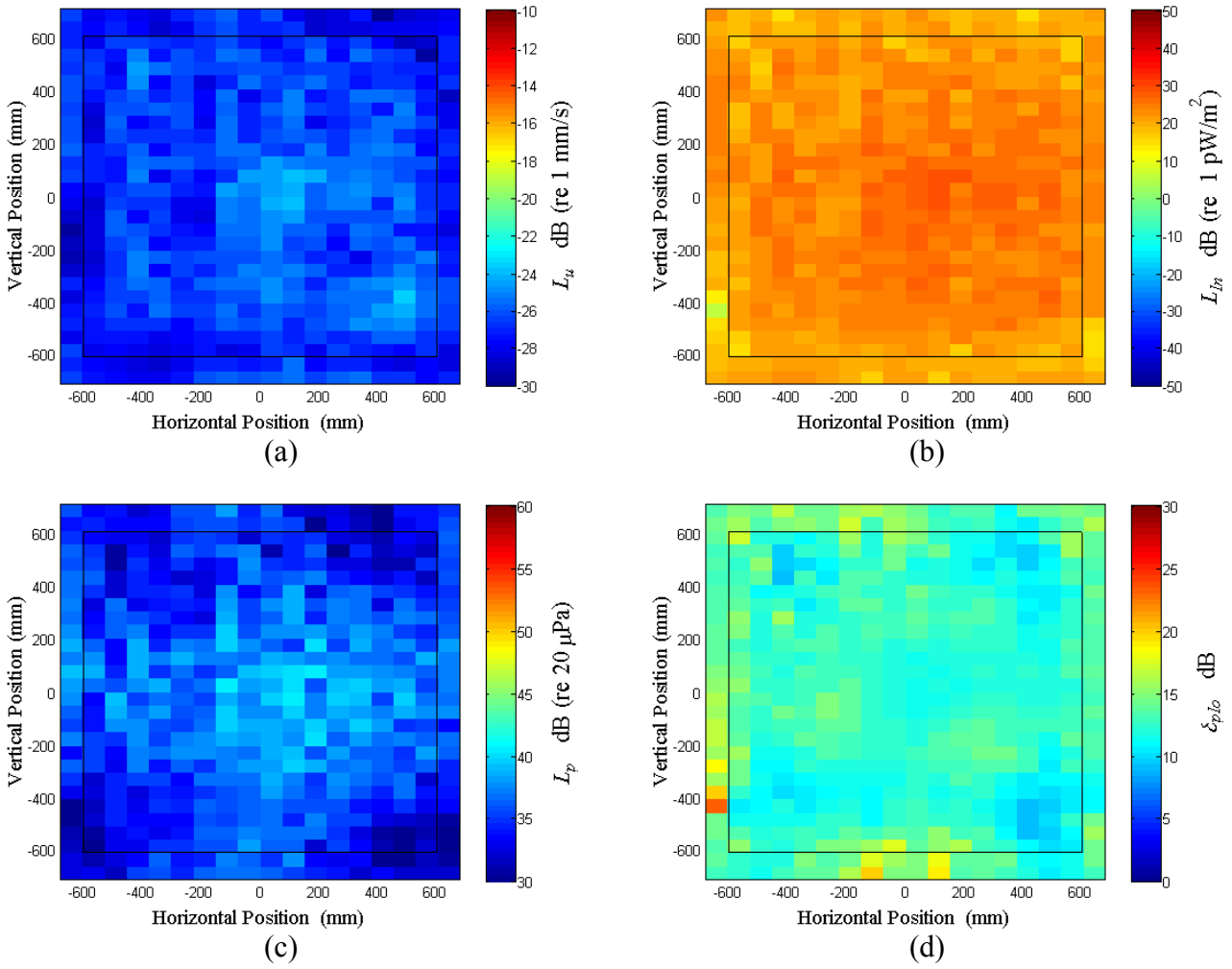

Figure B.41: Surface scan of Window B at 210 Hz (a) particle velocity level, L_u (b) normal signed sound intensity level, L_{In} (c) sound pressure level, L_p (d) pressure-residual intensity index, δ_{pIo}.

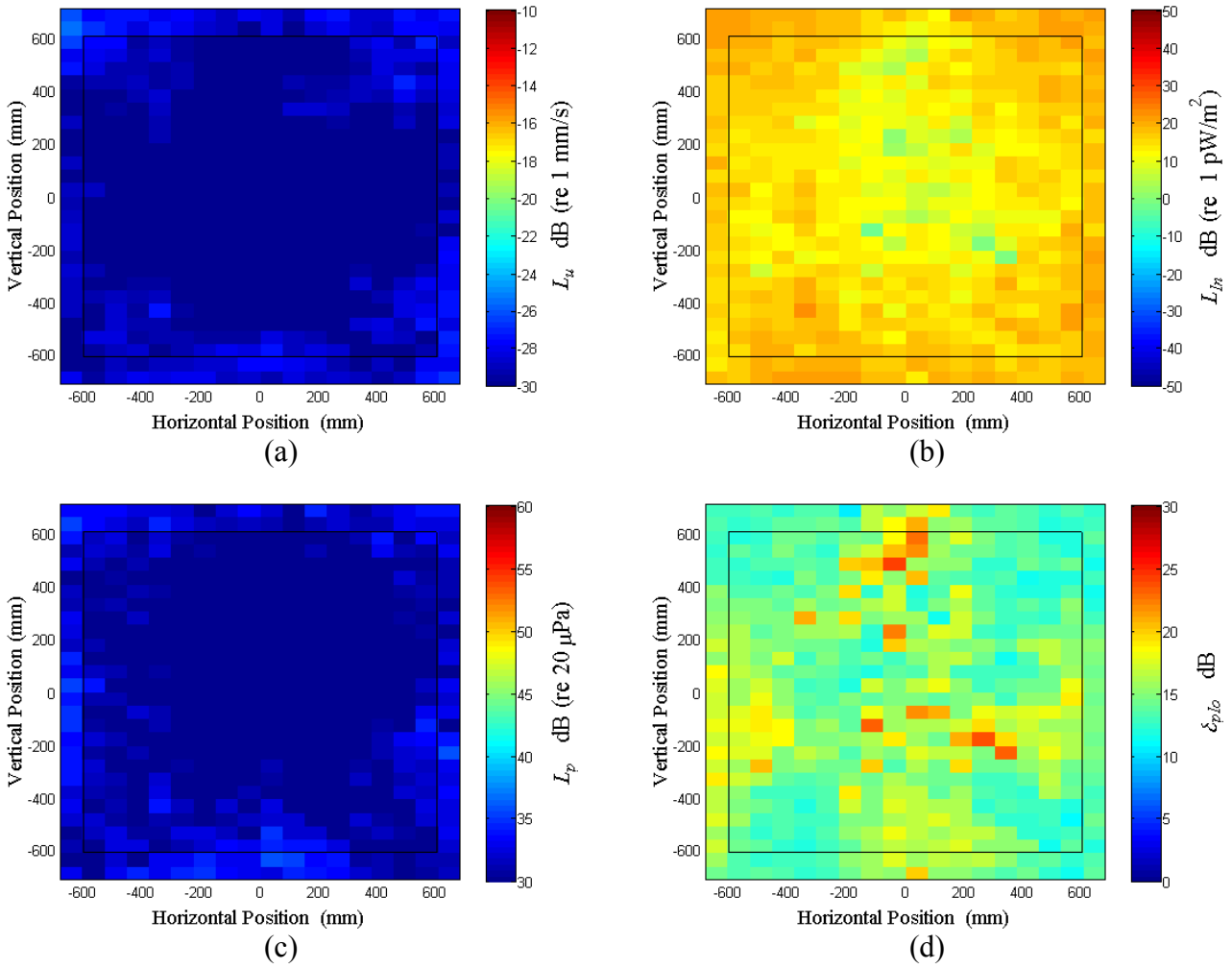

Figure B.42: Surface scan of Window B at 220 Hz (a) particle velocity level, L_u (b) normal signed sound intensity level, L_{In} (c) sound pressure level, L_p (d) pressure-residual intensity index, δ_{pIo}.

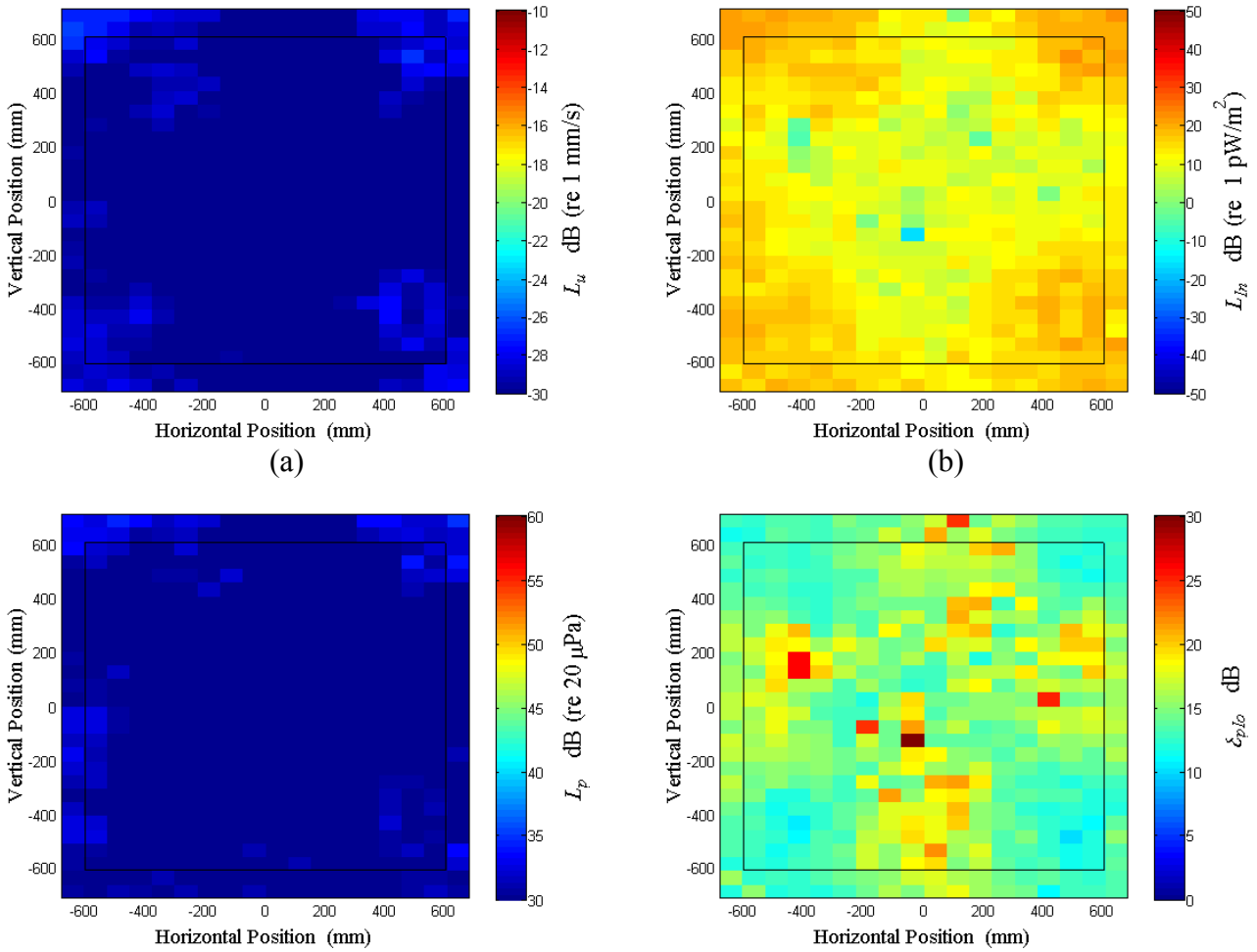

Figure B.43: Surface scan of Window B at 230 Hz (a) particle velocity level, L_u (b) normal signed sound intensity level, L_{In} (c) sound pressure level, L_p (d) pressure-residual intensity index, δ_{pIo}.

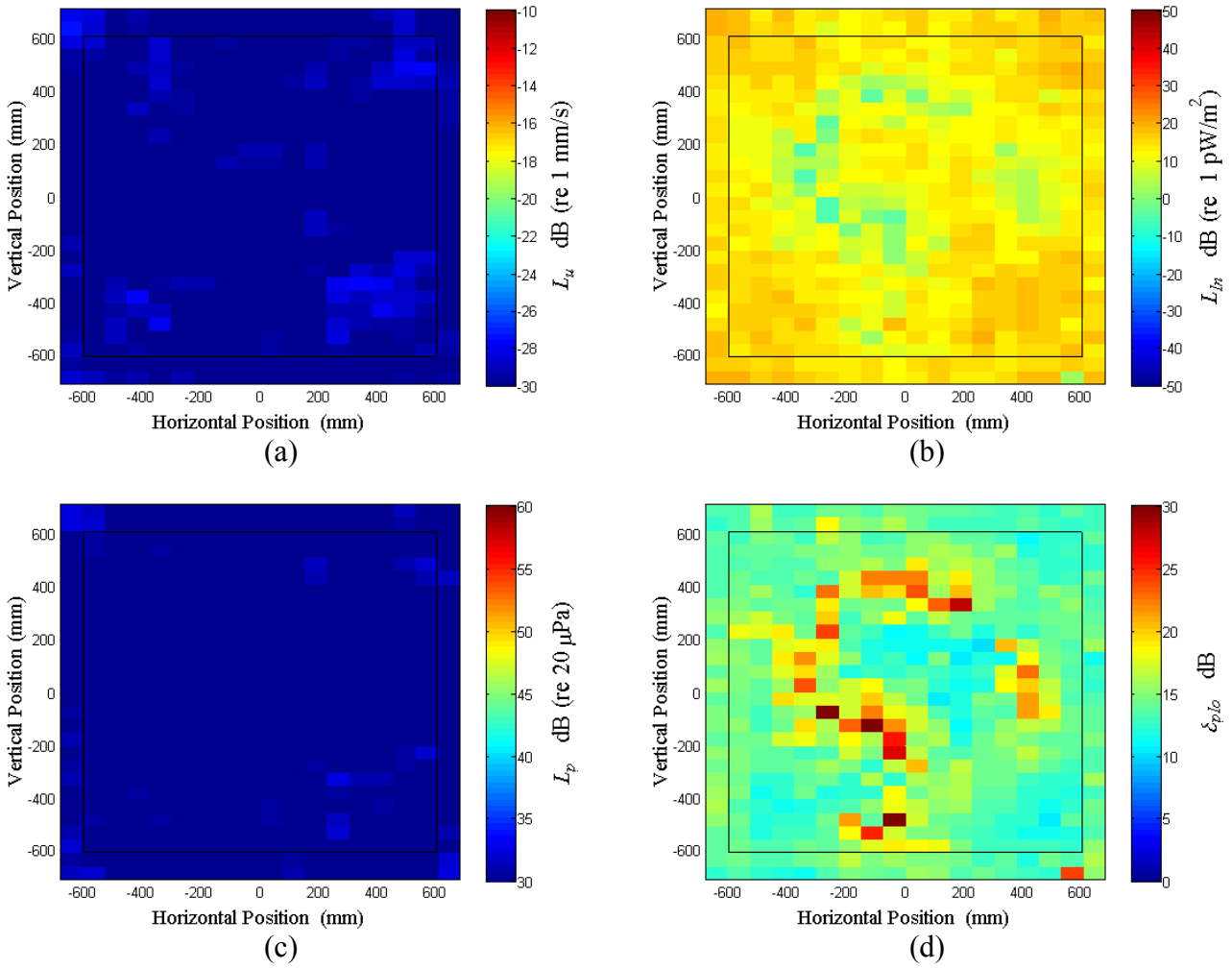

Figure B.44: Surface scan of Window B at 240 Hz (a) particle velocity level, L_u (b) normal signed sound intensity level, L_{In} (c) sound pressure level, L_p (d) pressure-residual intensity index, δ_{pIo}.

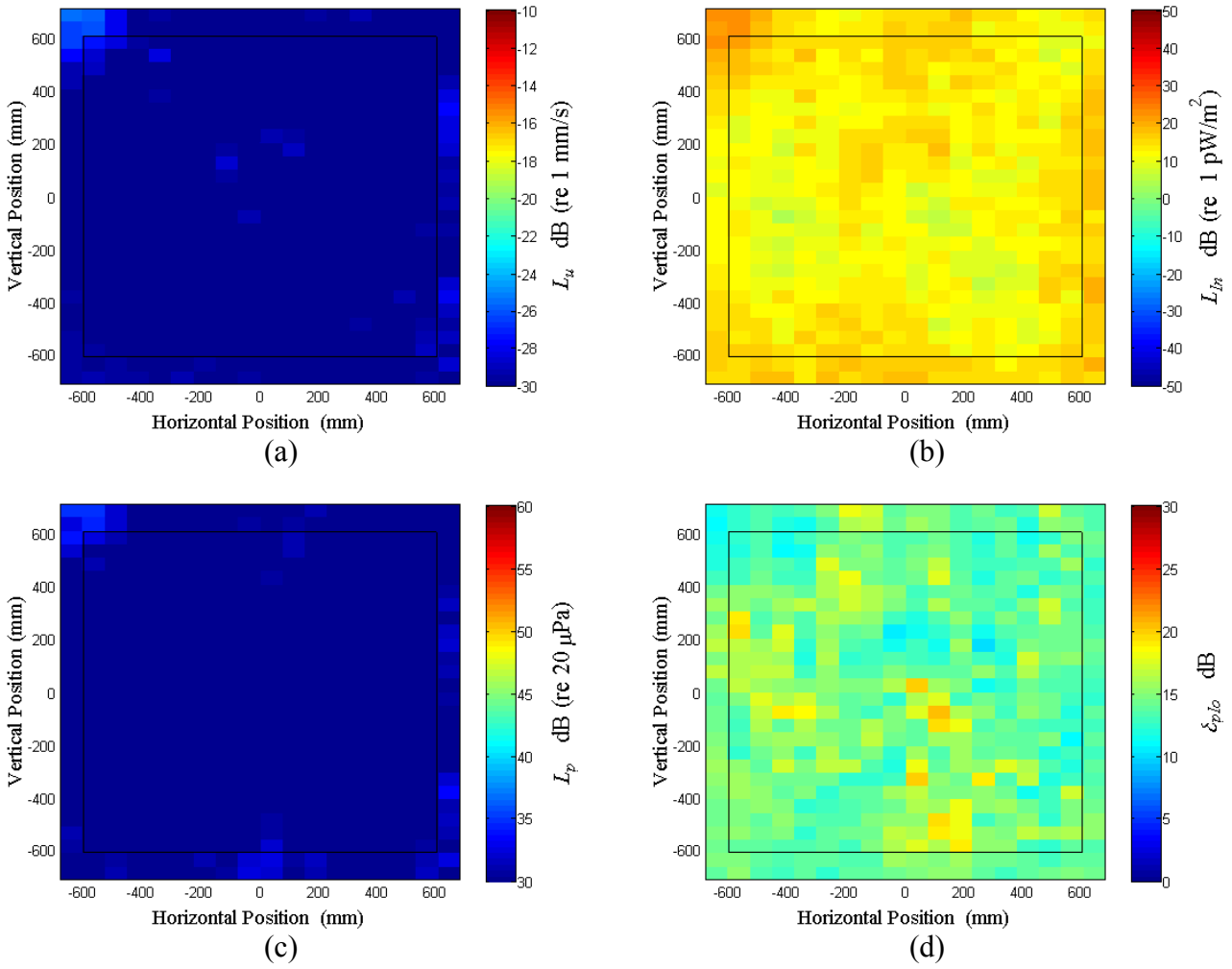

Figure B.45: Surface scan of Window B at 250 Hz (a) particle velocity level, L_u (b) normal signed sound intensity level, L_{In} (c) sound pressure level, L_p (d) pressure-residual intensity index, δ_{pIo}.

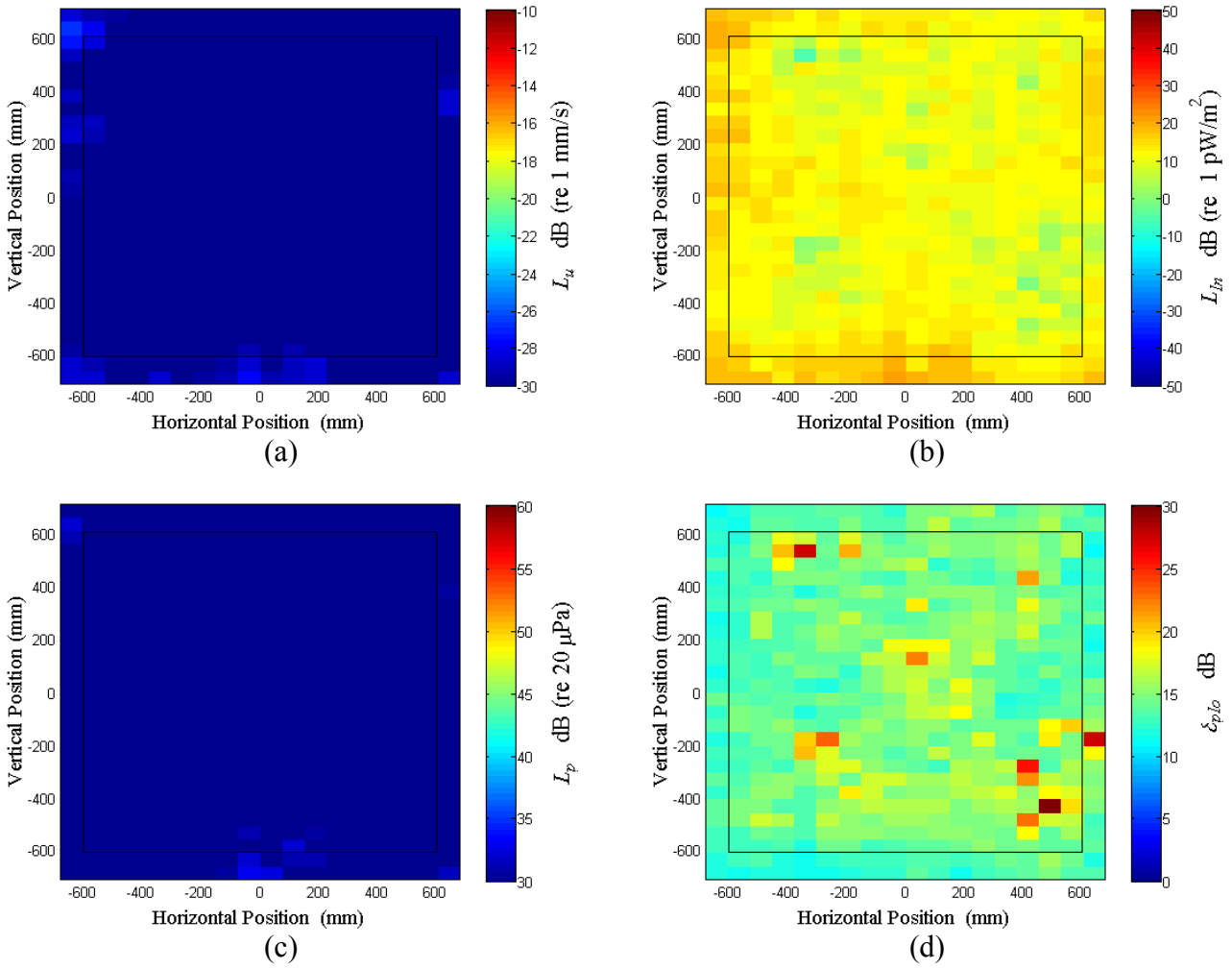

Figure B.46: Surface scan of Window B at 260 Hz (a) particle velocity level, L_u (b) normal signed sound intensity level, L_{In} (c) sound pressure level, L_p (d) pressure-residual intensity index, δ_{pIo}.

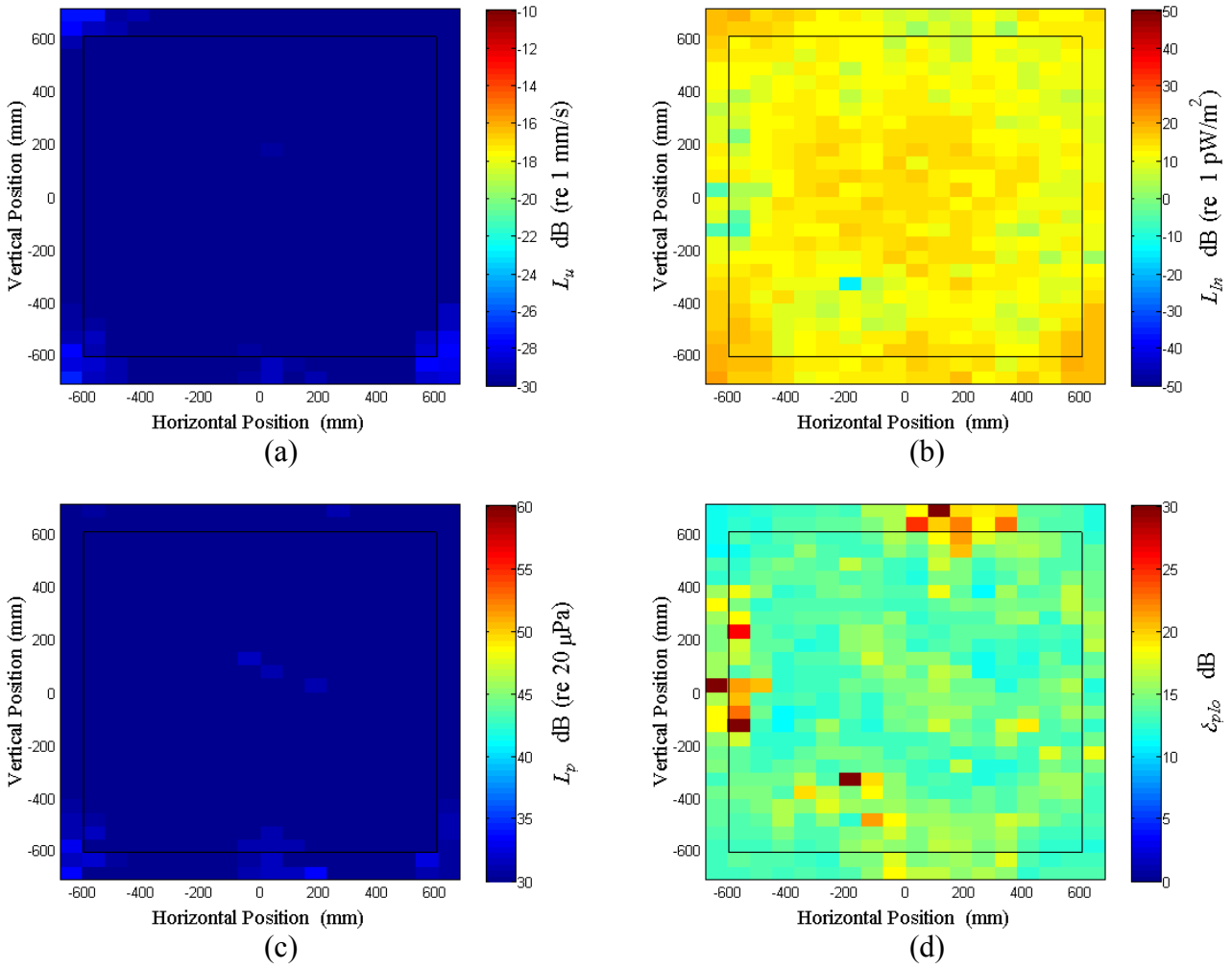

Figure B.47: Surface scan of Window B at 270 Hz (a) particle velocity level, L_u (b) normal signed sound intensity level, L_{In} (c) sound pressure level, L_p (d) pressure-residual intensity index, δ_{pIo}.

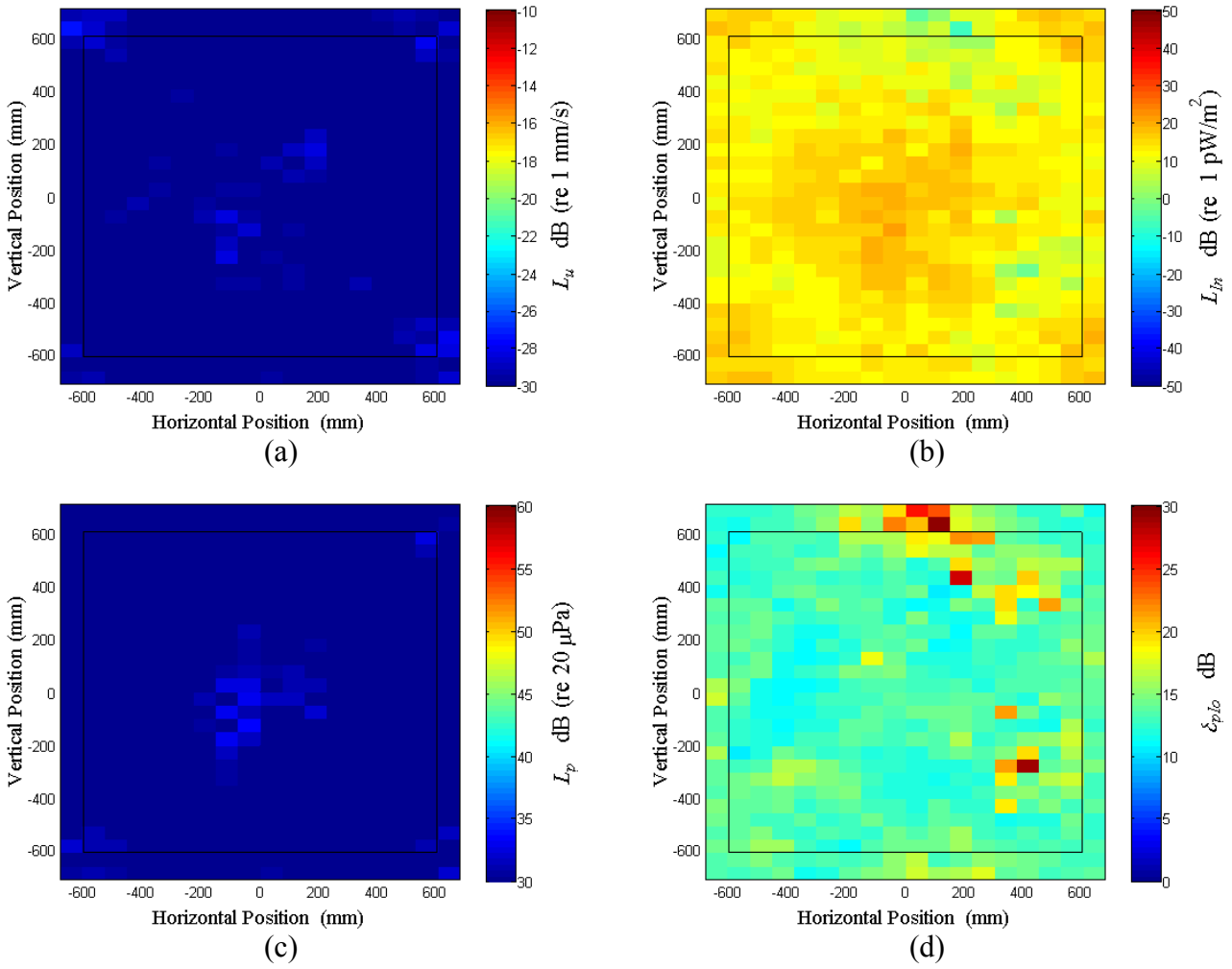

Figure B.48: Surface scan of Window B at 280 Hz (a) particle velocity level, L_u (b) normal signed sound intensity level, L_{In} (c) sound pressure level, L_p (d) pressure-residual intensity index, δ_{pIo}.

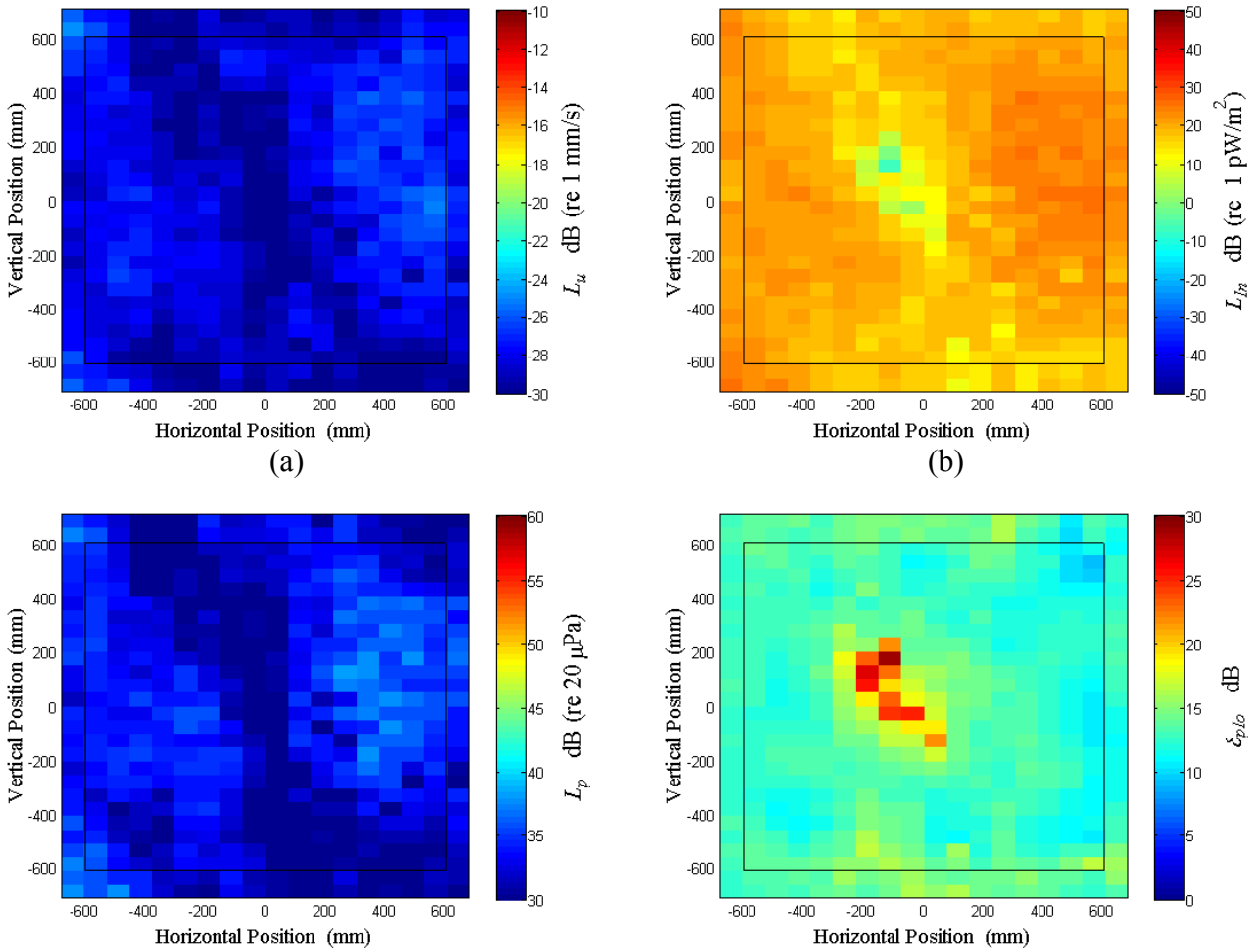

Figure B.49: Surface scan of Window B at 290 Hz (a) particle velocity level, L_u (b) normal signed sound intensity level, L_{In} (c) sound pressure level, L_p (d) pressure-residual intensity index, δ_{pIo}.

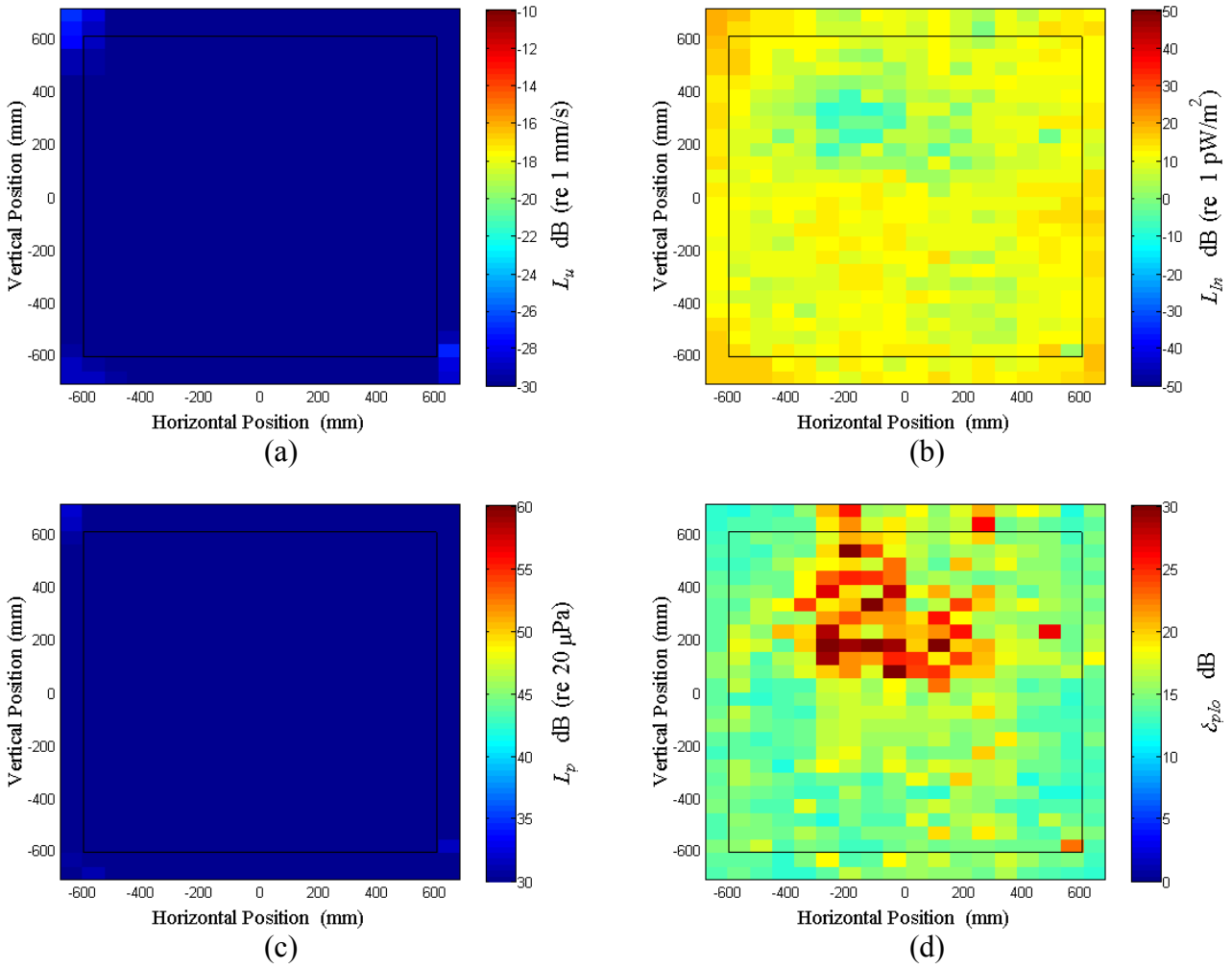

Figure B.50: Surface scan of Window B at 300 Hz (a) particle velocity level, L_u (b) normal signed sound intensity level, L_{In} (c) sound pressure level, L_p (d) pressure-residual intensity index, δ_{pIo}.

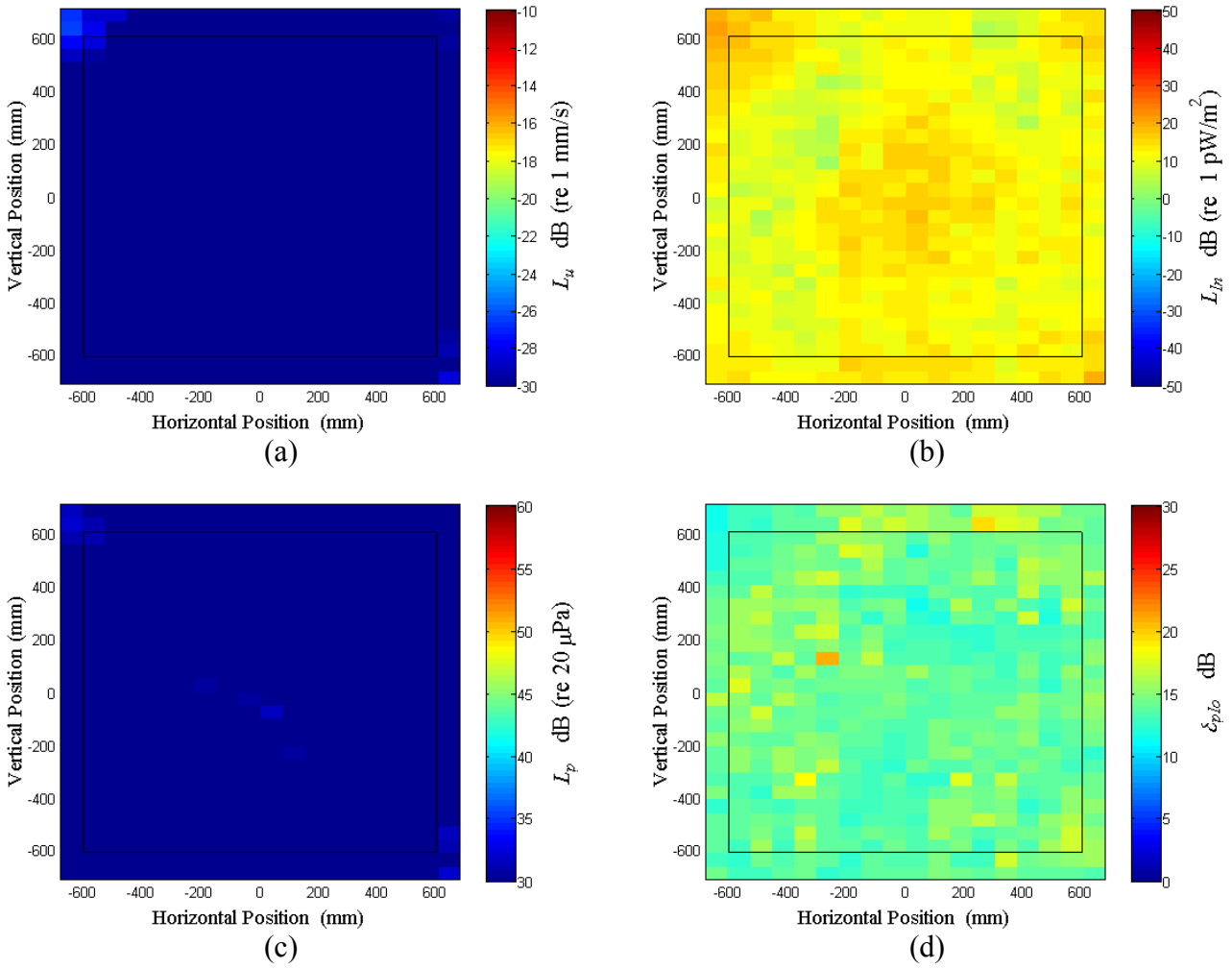

Figure B.51: Surface scan of Window B at 310 Hz (a) particle velocity level, L_u (b) normal signed sound intensity level, L_{In} (c) sound pressure level, L_p (d) pressure-residual intensity index, δ_{pIo}.

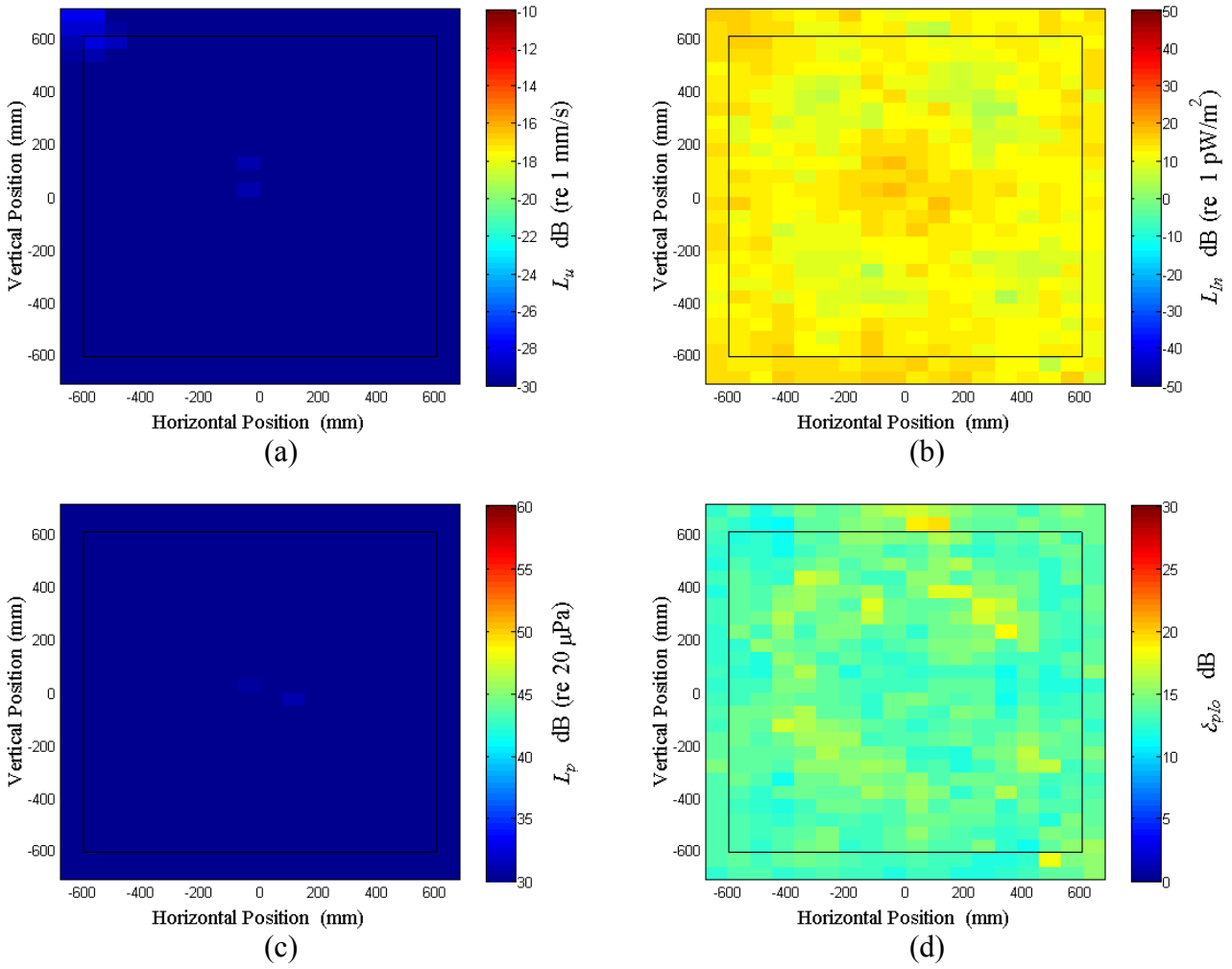

Figure B.52: Surface scan of Window B at 320 Hz (a) particle velocity level, L_u (b) normal signed sound intensity level, L_{In} (c) sound pressure level, L_p (d) pressure-residual intensity index, δ_{pIo}.

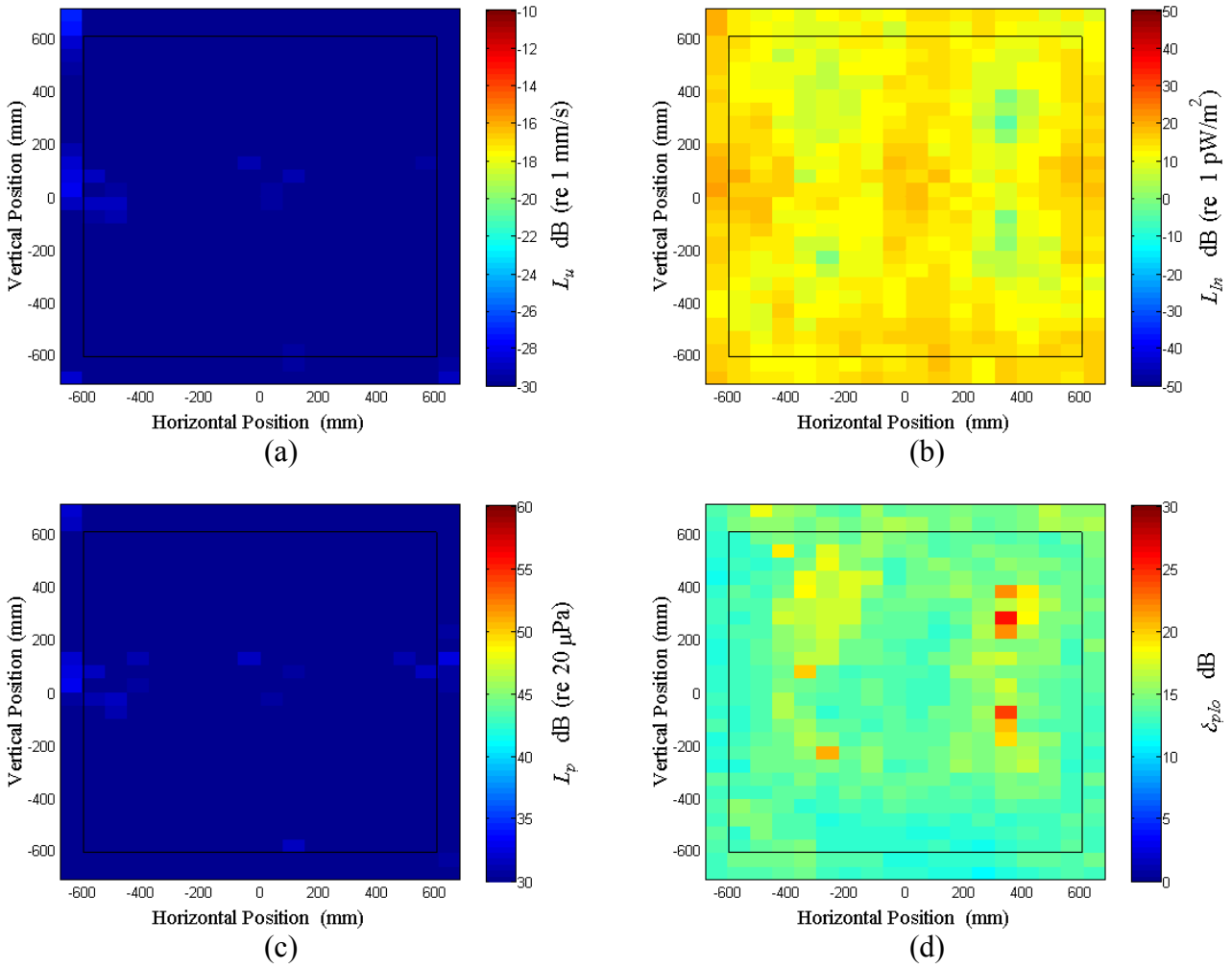

Figure B.53: Surface scan of Window B at 330 Hz (a) particle velocity level, L_u (b) normal signed sound intensity level, L_{In} (c) sound pressure level, L_p (d) pressure-residual intensity index, δ_{pIo}.

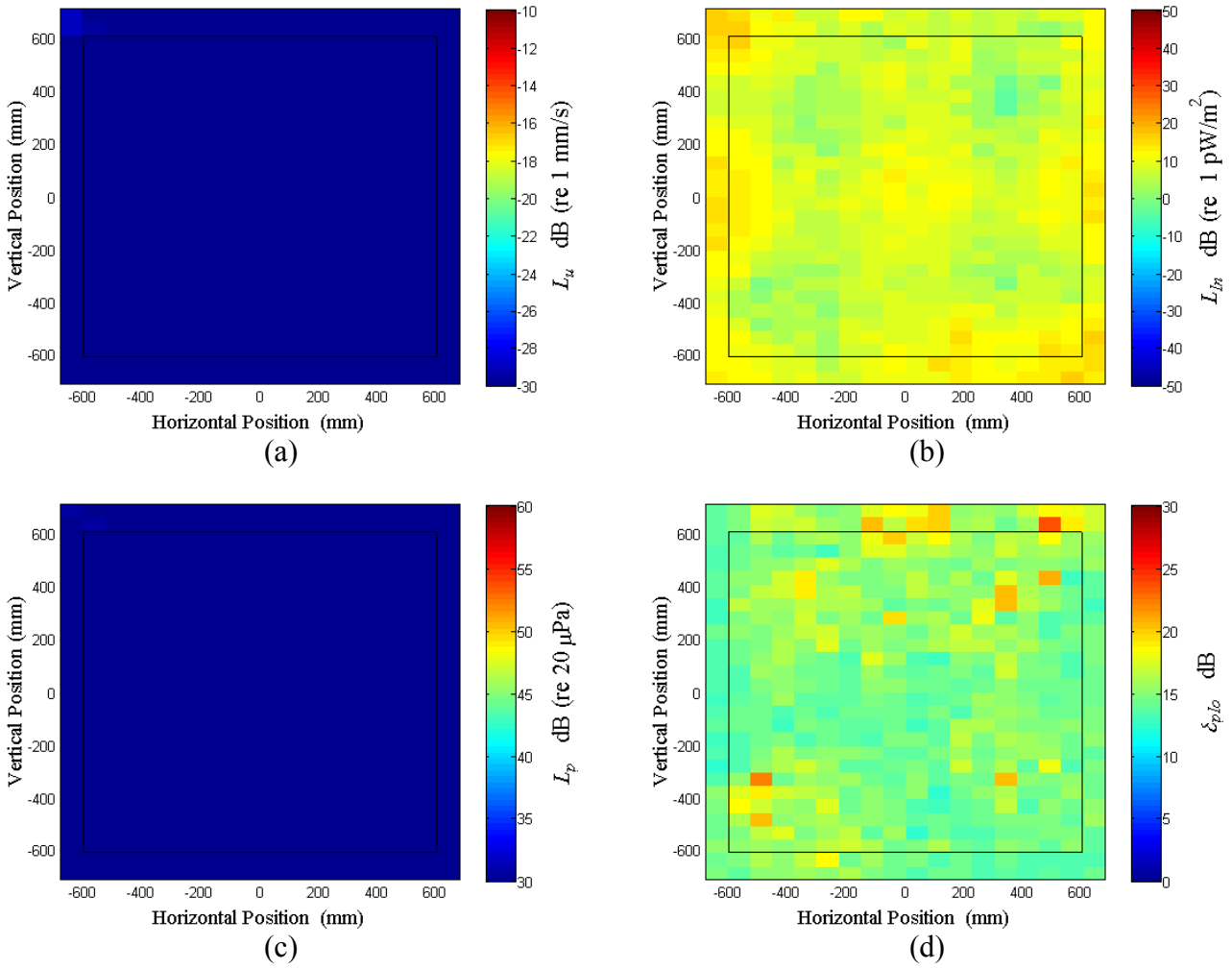

Figure B.54: Surface scan of Window B at 340 Hz (a) particle velocity level, L_u (b) normal signed sound intensity level, L_{In} (c) sound pressure level, L_p (d) pressure-residual intensity index, δ_{pIo}.

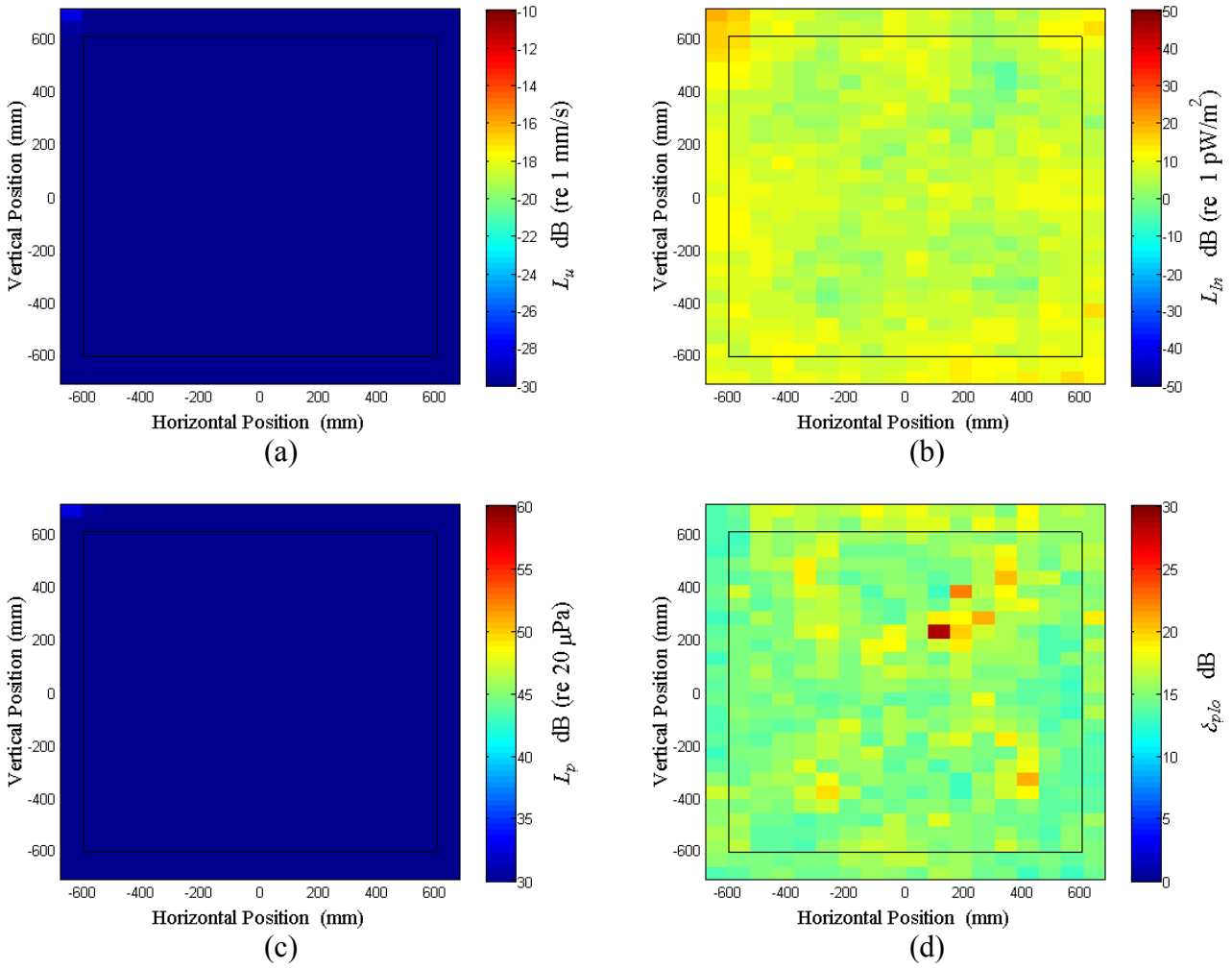

Figure B.55: Surface scan of Window B at 350 Hz (a) particle velocity level, L_u (b) normal signed sound intensity level, L_{In} (c) sound pressure level, L_p (d) pressure-residual intensity index, δ_{pIo}.

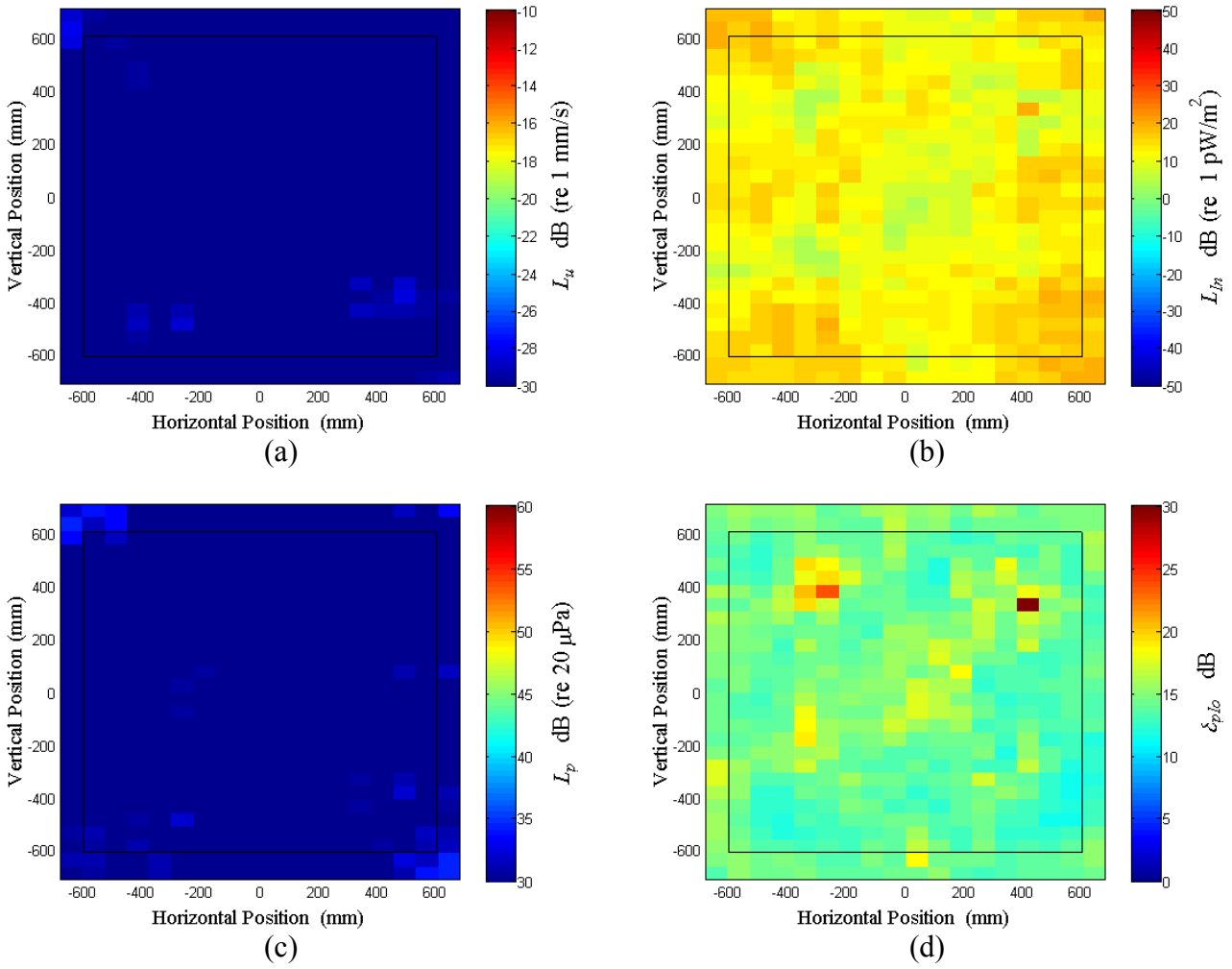

Figure B.56: Surface scan of Window B at 360 Hz (a) particle velocity level, L_u (b) normal signed sound intensity level, L_{In} (c) sound pressure level, L_p (d) pressure-residual intensity index, δ_{pIo}.

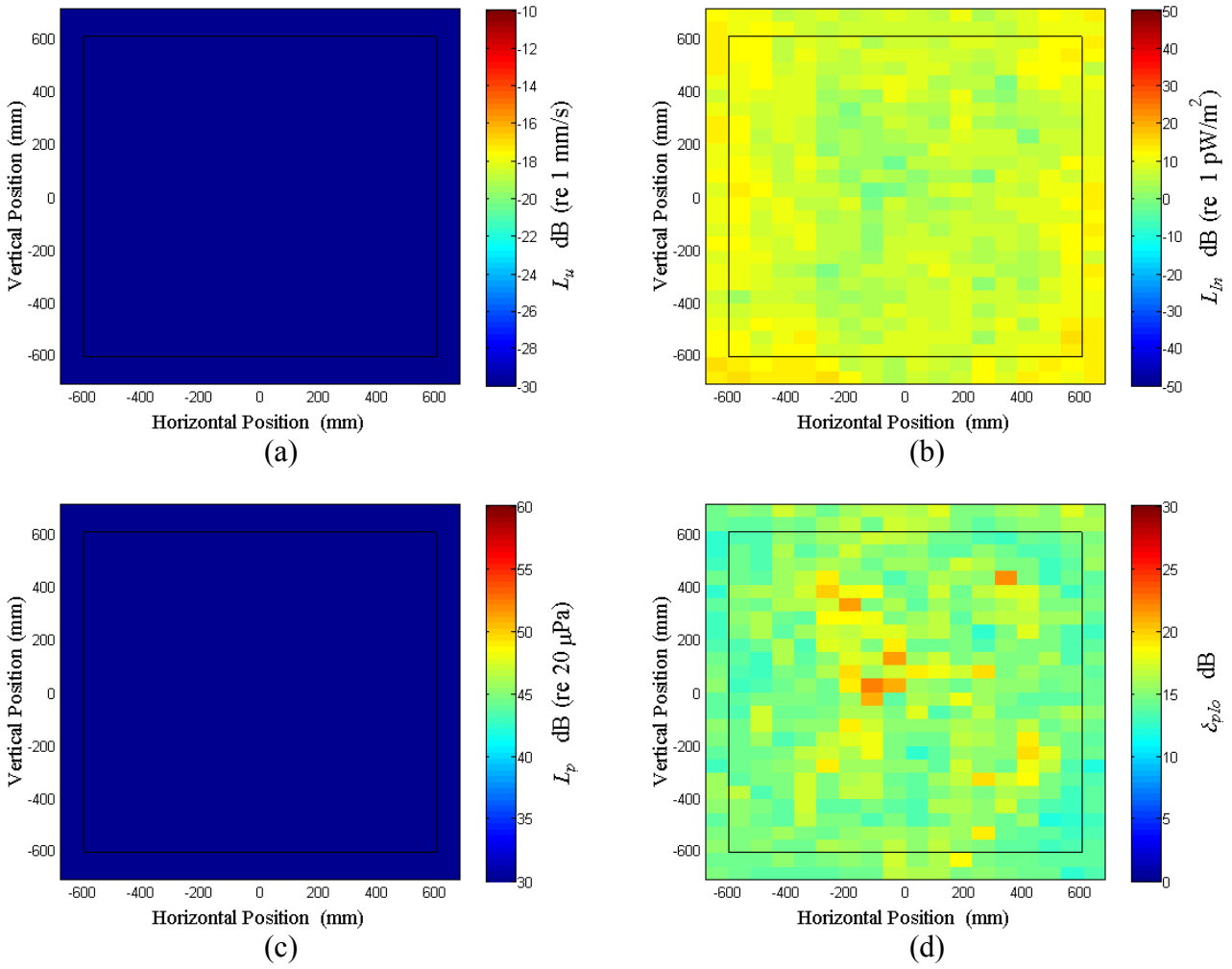

Figure B.57: Surface scan of Window B at 370 Hz (a) particle velocity level, L_u (b) normal signed sound intensity level, L_{In} (c) sound pressure level, L_p (d) pressure-residual intensity index, δ_{pIo}.

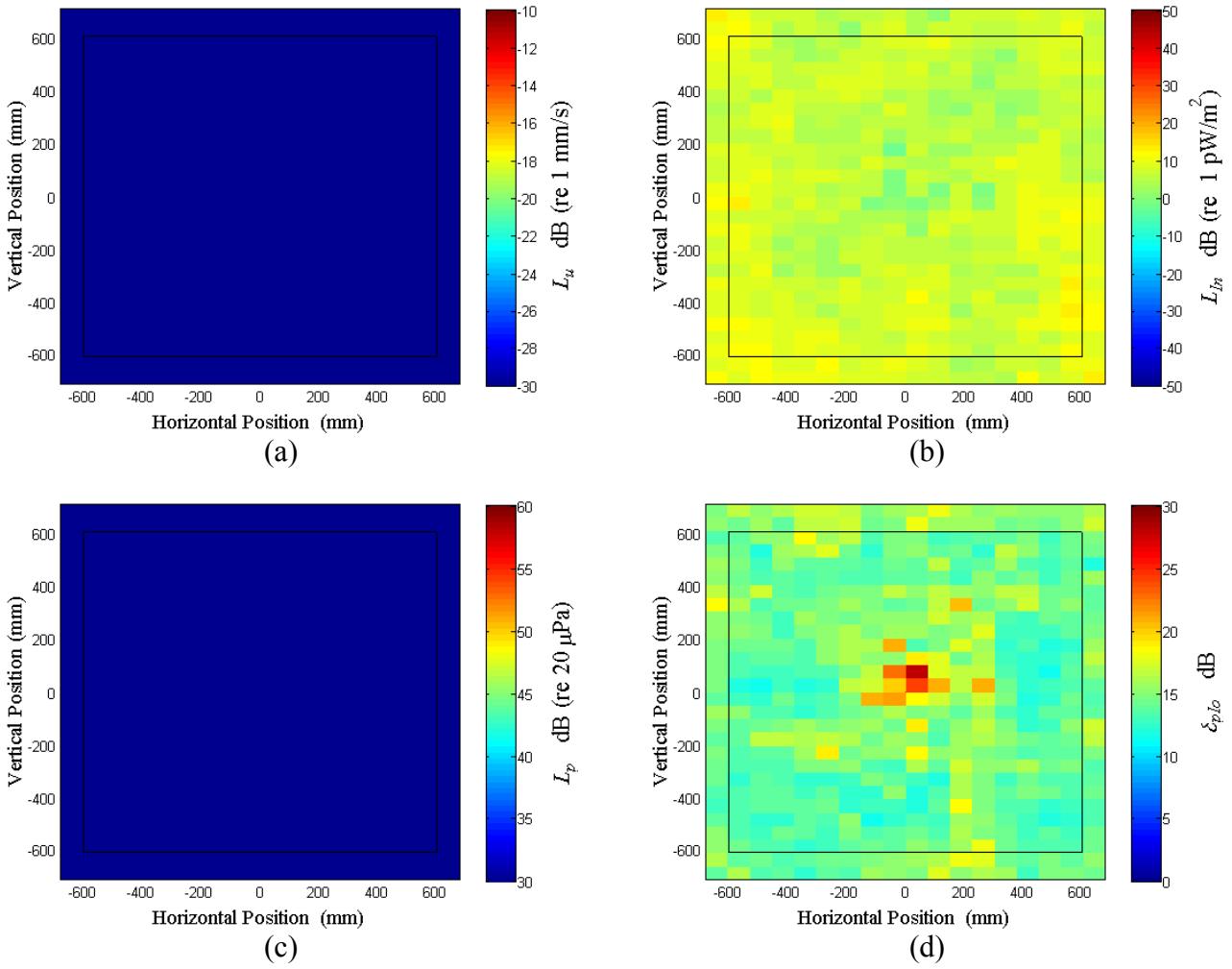

Figure B.58: Surface scan of Window B at 380 Hz (a) particle velocity level, L_u (b) normal signed sound intensity level, L_{In} (c) sound pressure level, L_p (d) pressure-residual intensity index, δ_{pIo}.

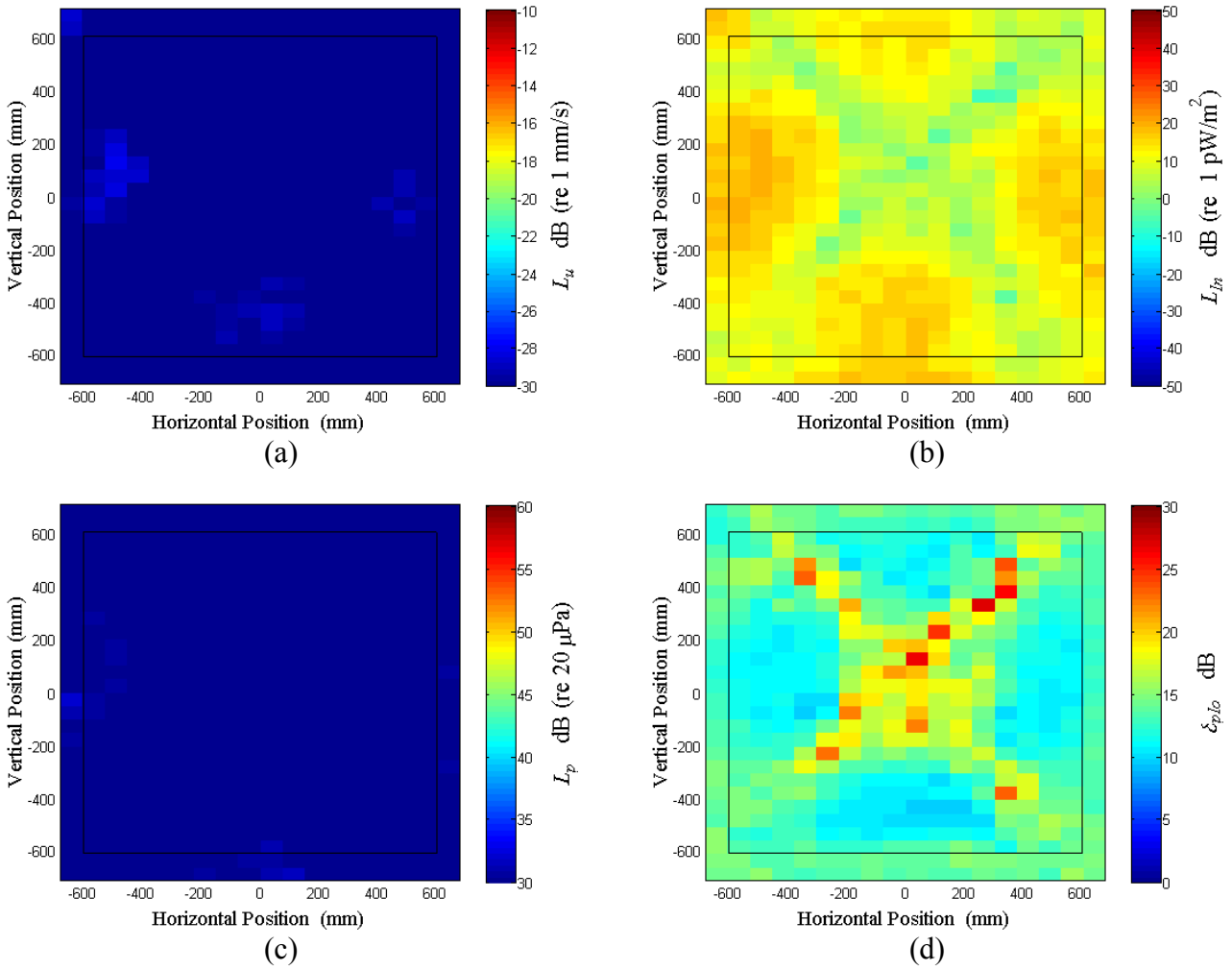

Figure B.59: Surface scan of Window B at 390 Hz (a) particle velocity level, L_u (b) normal signed sound intensity level, L_{In} (c) sound pressure level, L_p (d) pressure-residual intensity index, δ_{pIo}.

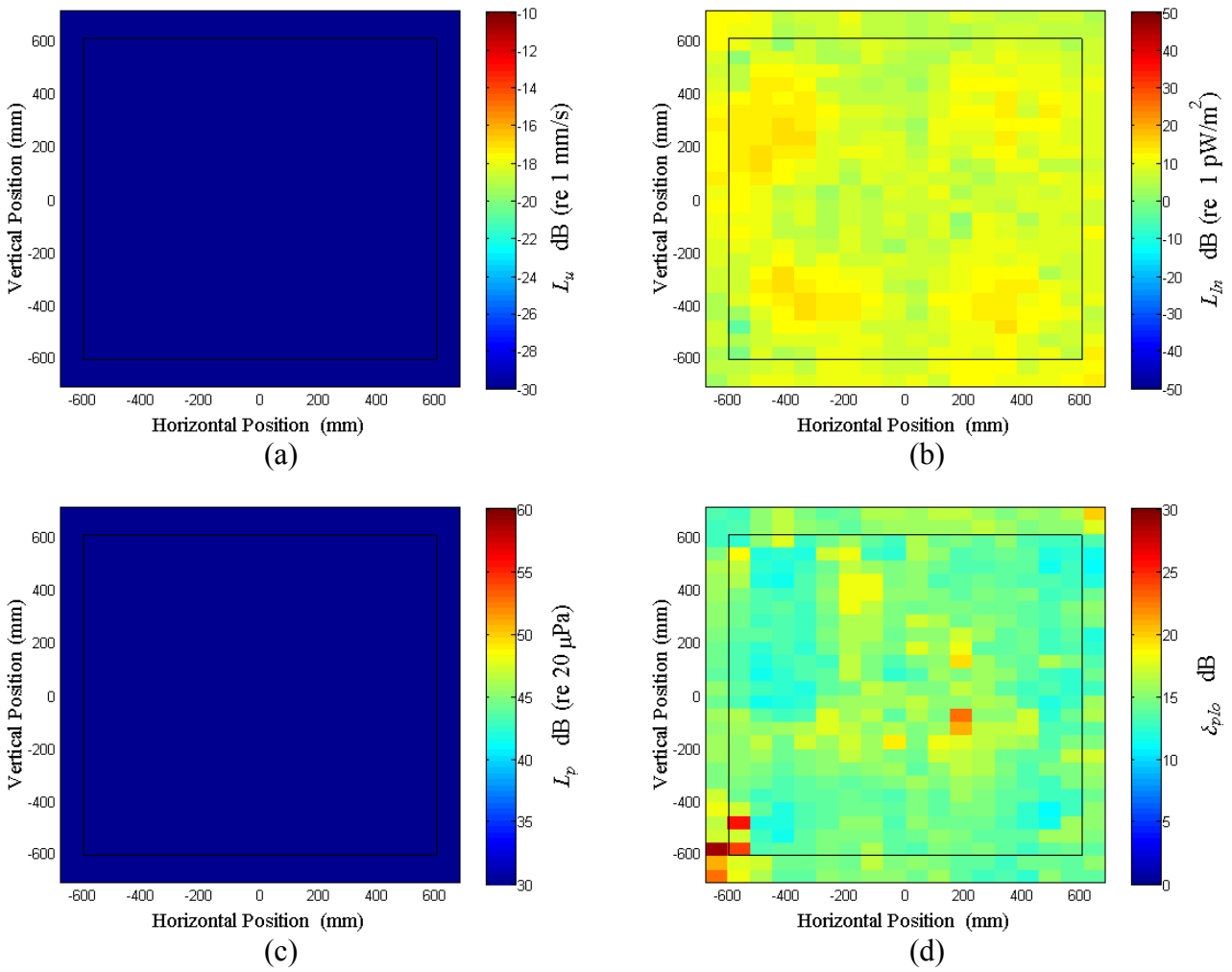

Figure B.60: Surface scan of Window B at 400 Hz (a) particle velocity level, L_u (b) normal signed sound intensity level, L_{In} (c) sound pressure level, L_p (d) pressure-residual intensity index, δ_{pIo}.

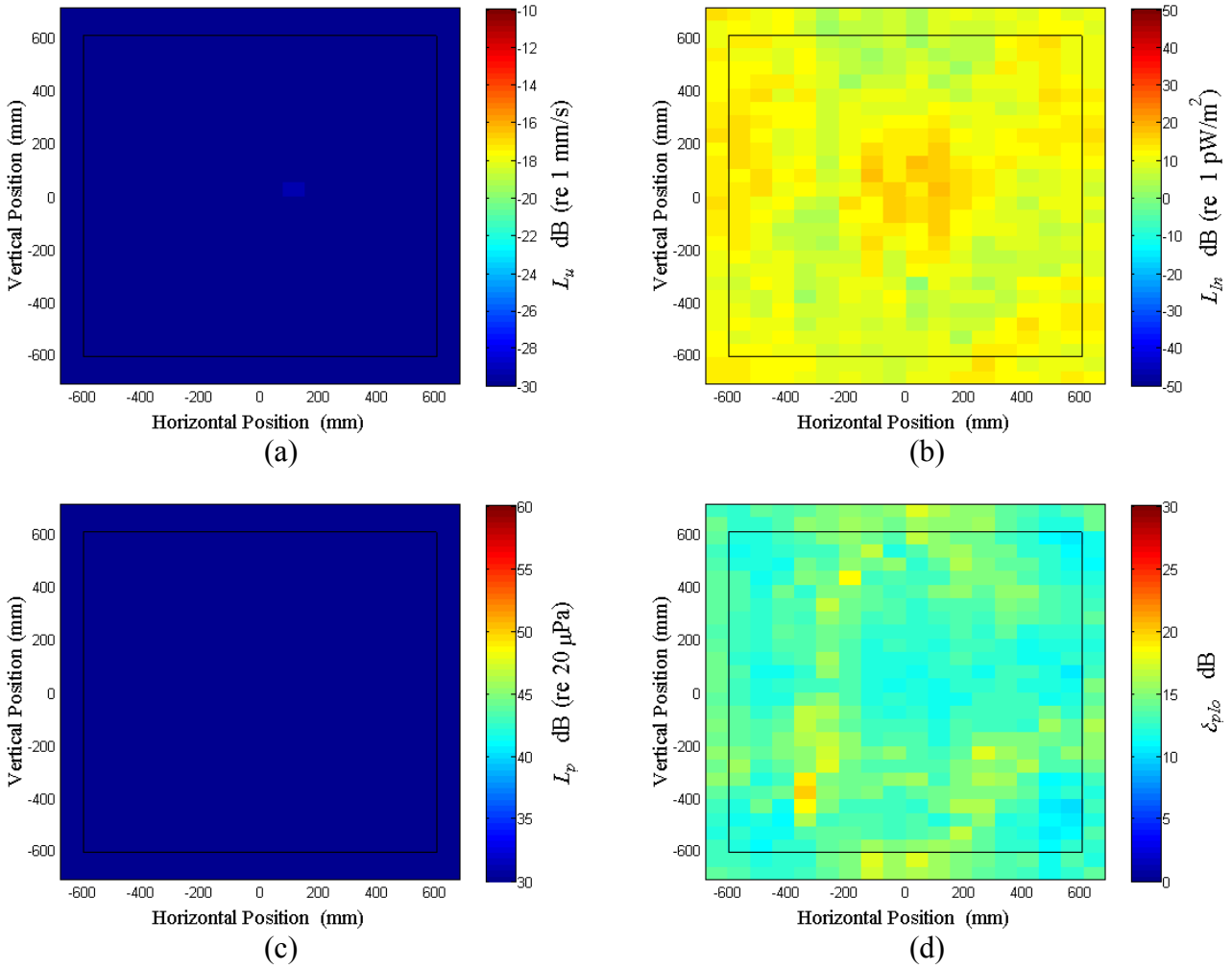

Figure B.61: Surface scan of Window B at 410 Hz (a) particle velocity level, L_u (b) normal signed sound intensity level, L_{In} (c) sound pressure level, L_p (d) pressure-residual intensity index, δ_{pIo}.

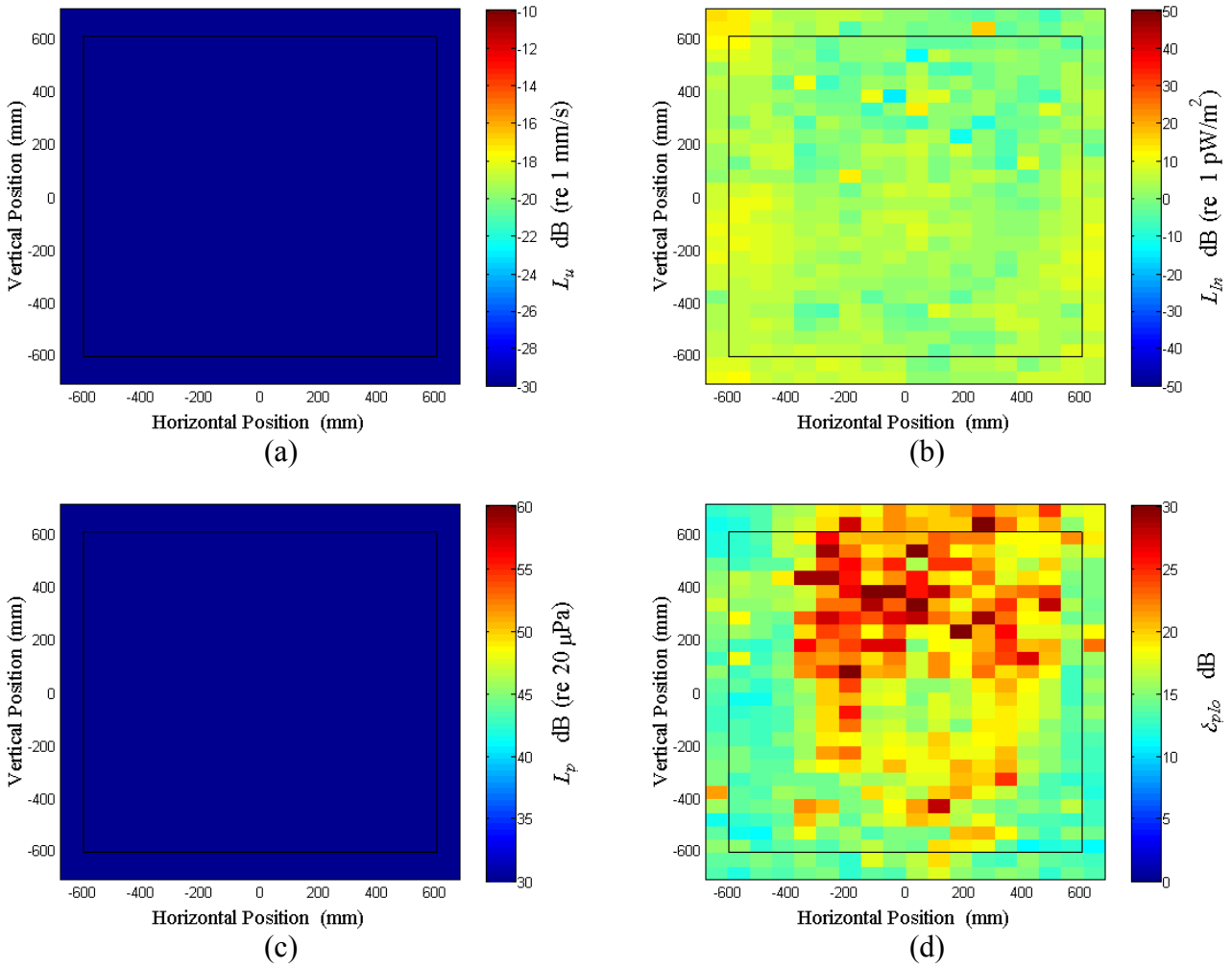

Figure B.62: Surface scan of Window B at 420 Hz (a) particle velocity level, L_u (b) normal signed sound intensity level, L_{In} (c) sound pressure level, L_p (d) pressure-residual intensity index, δ_{pIo}.

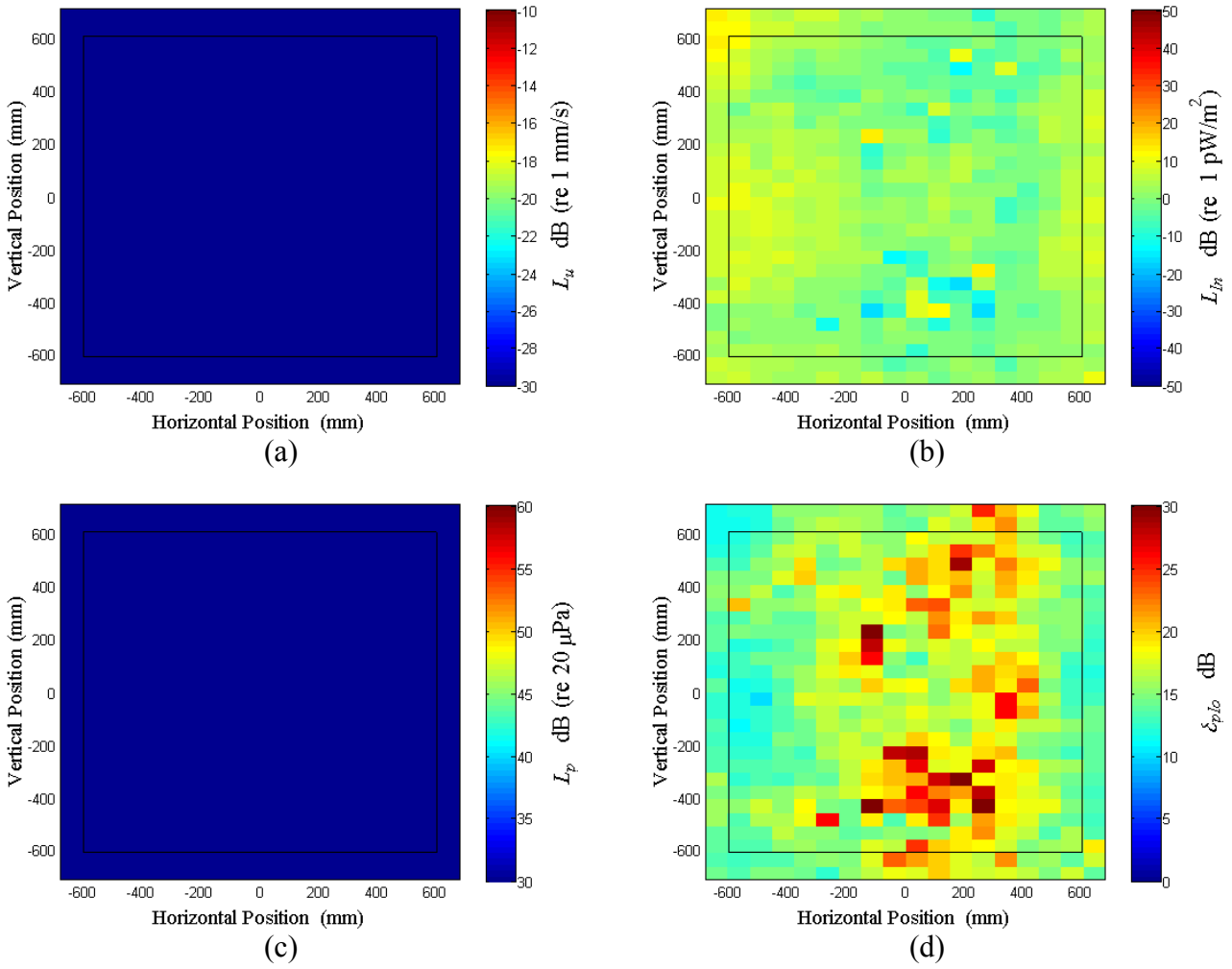

Figure B.63: Surface scan of Window B at 430 Hz (a) particle velocity level, L_u (b) normal signed sound intensity level, L_{In} (c) sound pressure level, L_p (d) pressure-residual intensity index, δ_{pIo}.

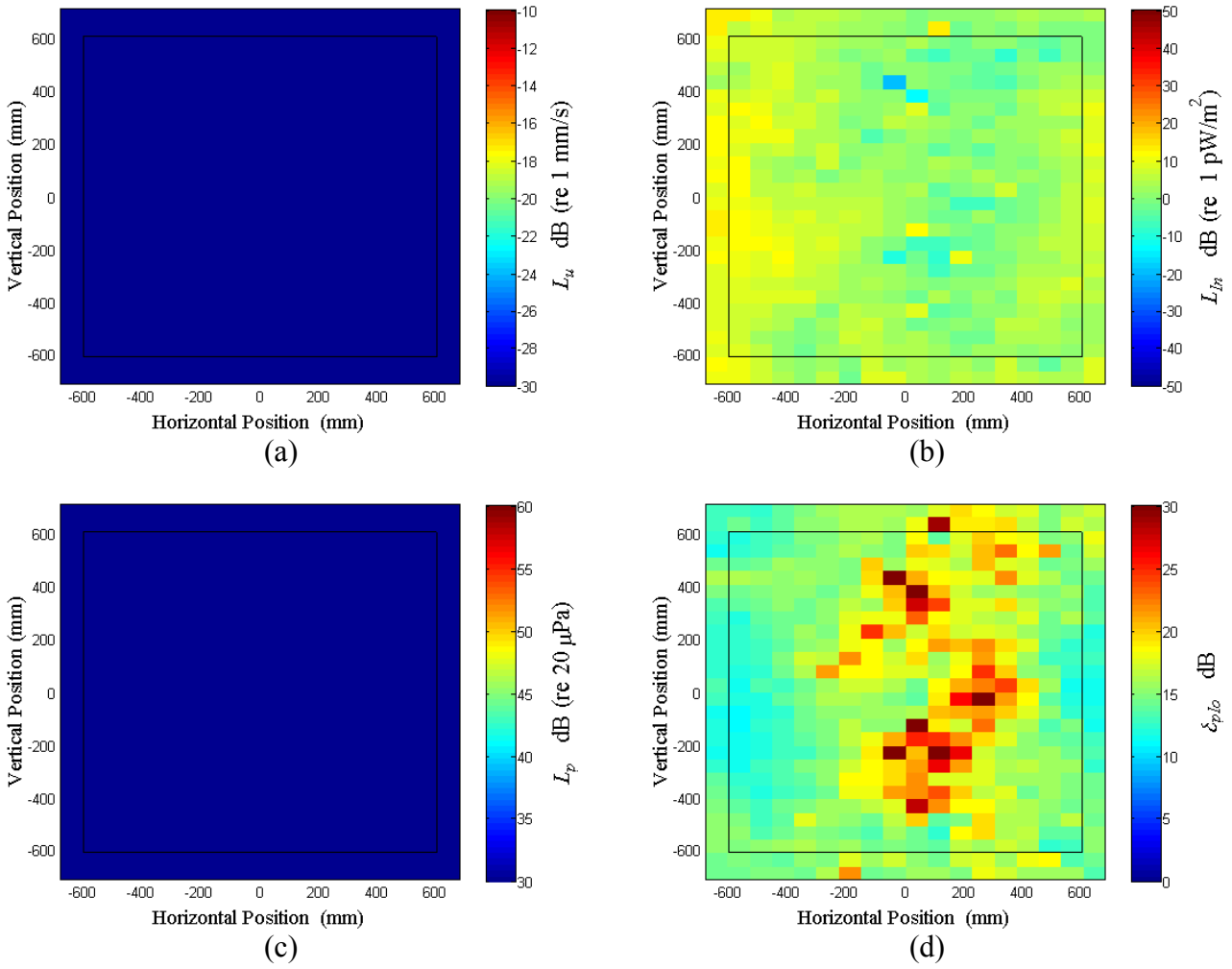

Figure B.64: Surface scan of Window B at 440 Hz (a) particle velocity level, L_u (b) normal signed sound intensity level, L_{In} (c) sound pressure level, L_p (d) pressure-residual intensity index, δ_{pIo}.

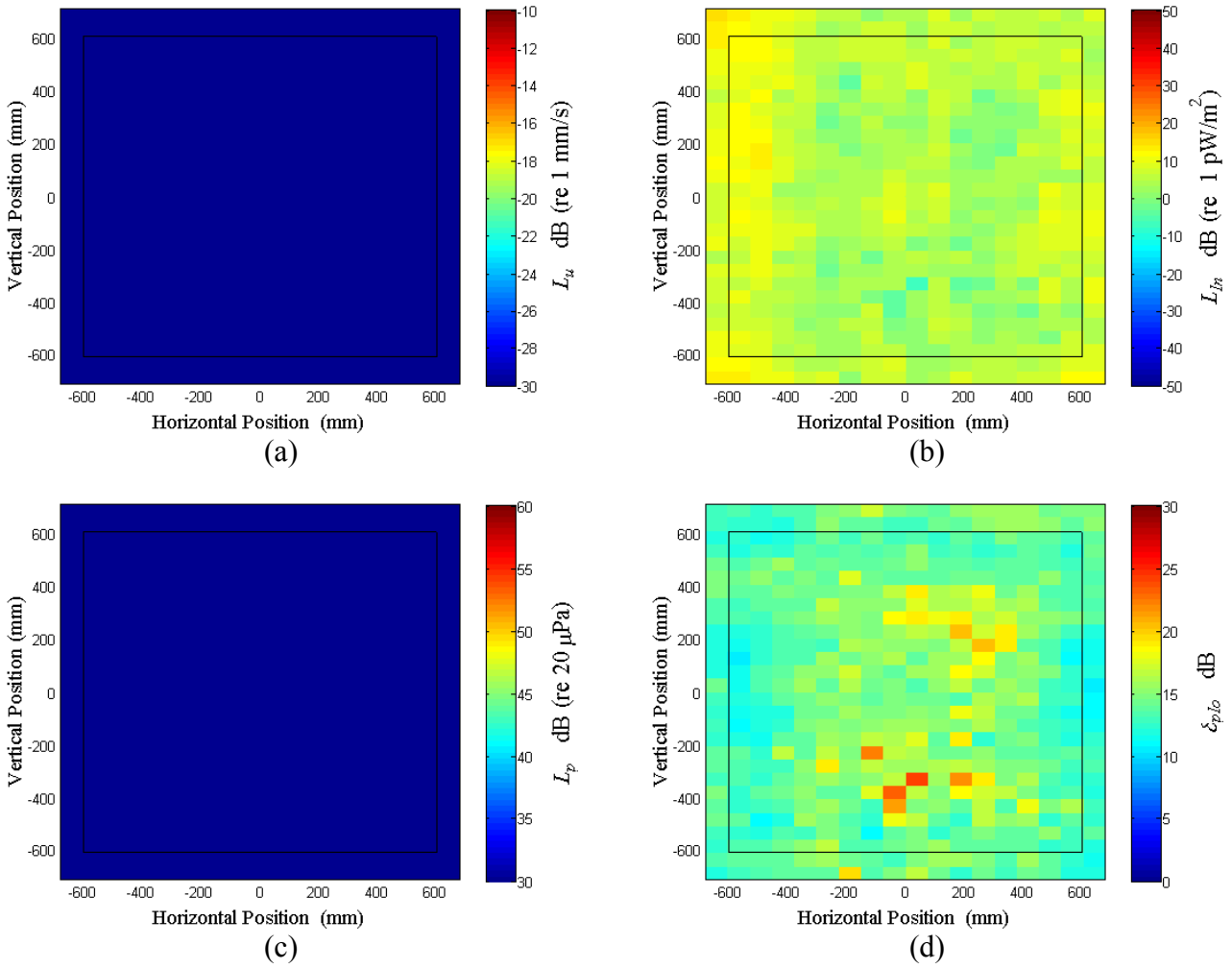

Figure B.65: Surface scan of Window B at 450 Hz (a) particle velocity level, L_u (b) normal signed sound intensity level, L_{In} (c) sound pressure level, L_p (d) pressure-residual intensity index, δ_{pIo}.

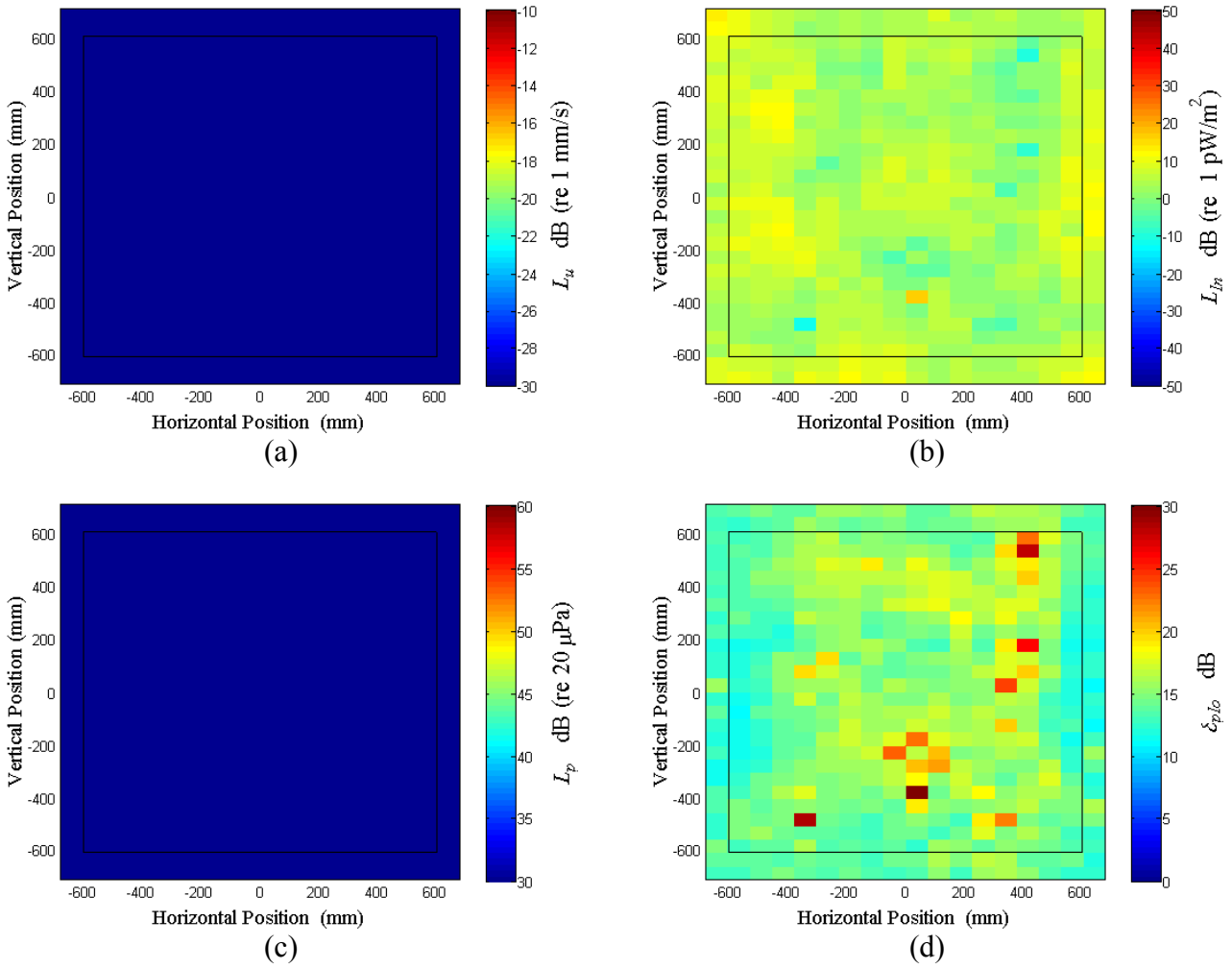

Figure B.66: Surface scan of Window B at 460 Hz (a) particle velocity level, L_u (b) normal signed sound intensity level, L_{In} (c) sound pressure level, L_p (d) pressure-residual intensity index, δ_{pIo}.

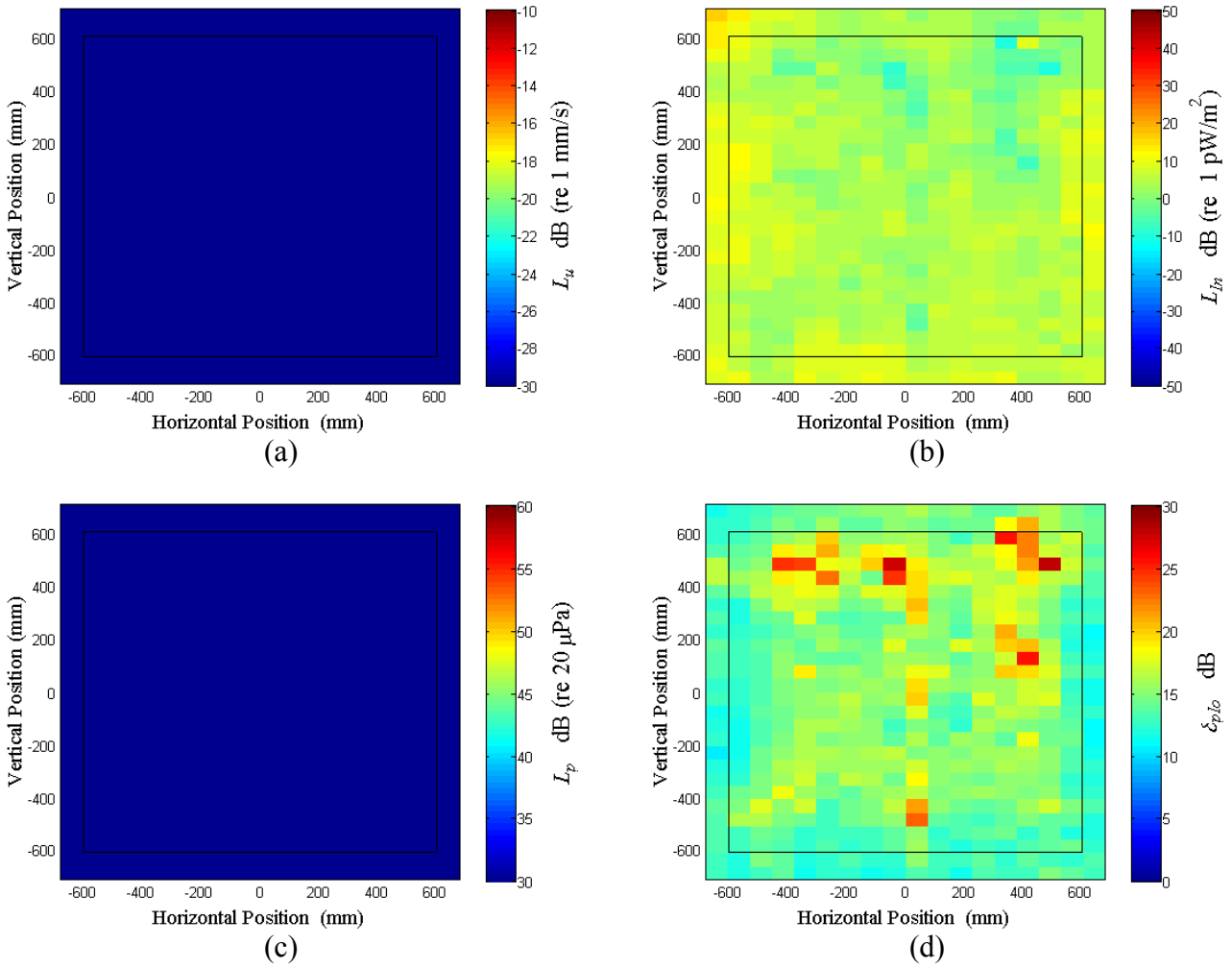

Figure B.67: Surface scan of Window B at 470 Hz (a) particle velocity level, L_u (b) normal signed sound intensity level, L_{In} (c) sound pressure level, L_p (d) pressure-residual intensity index, δ_{pIo}.

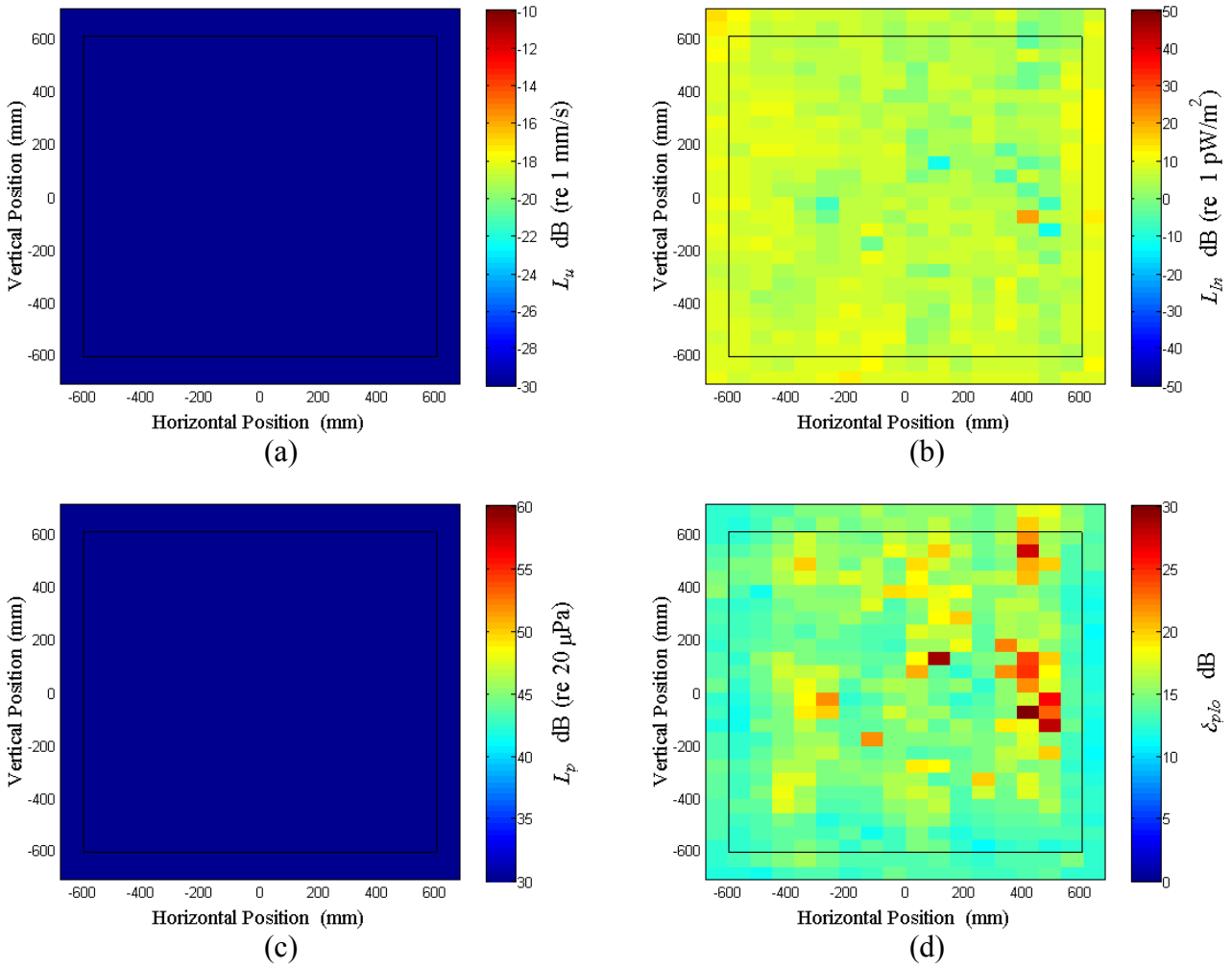

Figure B.68: Surface scan of Window B at 480 Hz (a) particle velocity level, L_u (b) normal signed sound intensity level, L_{In} (c) sound pressure level, L_p (d) pressure-residual intensity index, δ_{pIo}.

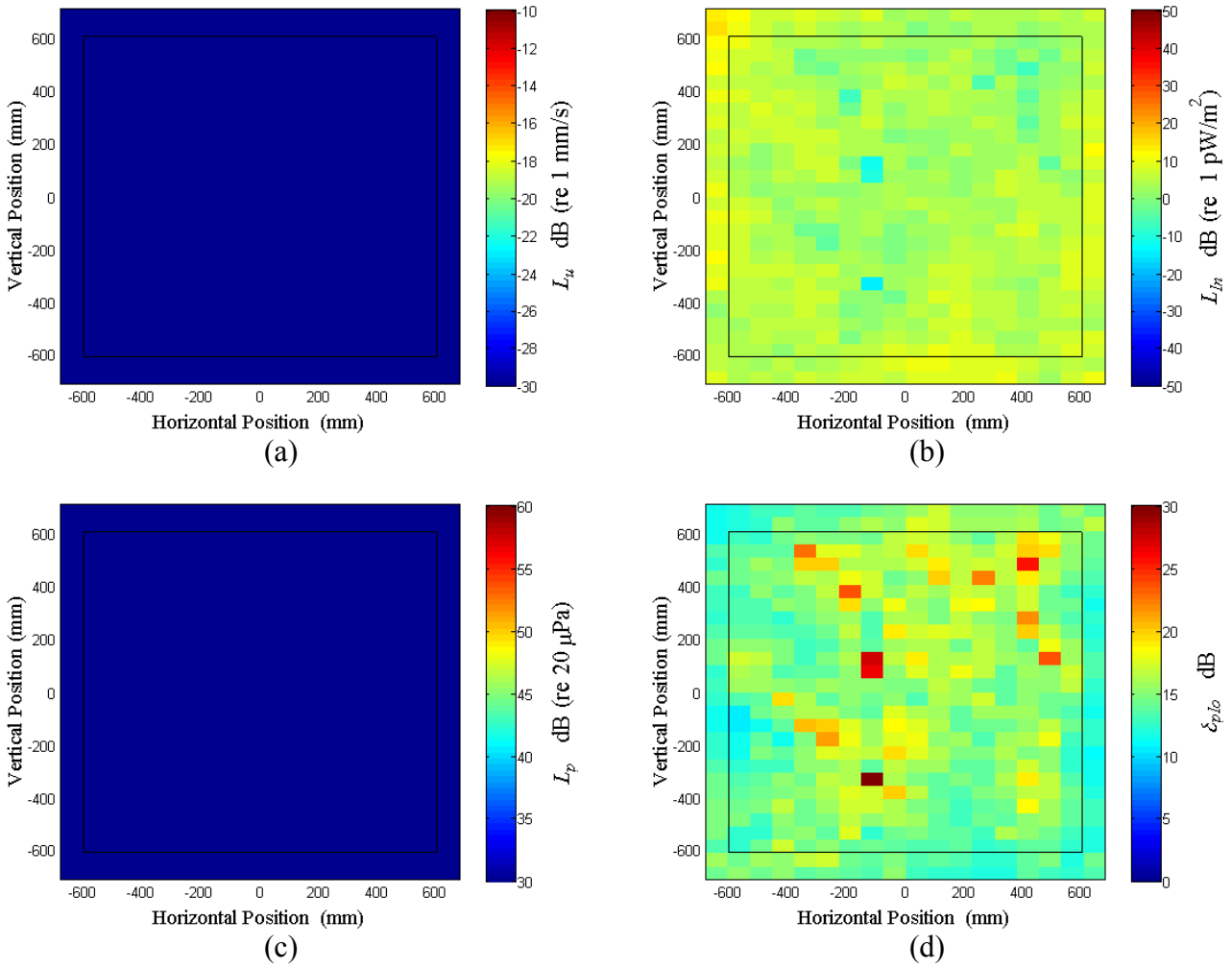

Figure B.69: Surface scan of Window B at 490 Hz (a) particle velocity level, L_u (b) normal signed sound intensity level, L_{In} (c) sound pressure level, L_p (d) pressure-residual intensity index, δ_{pIo}.

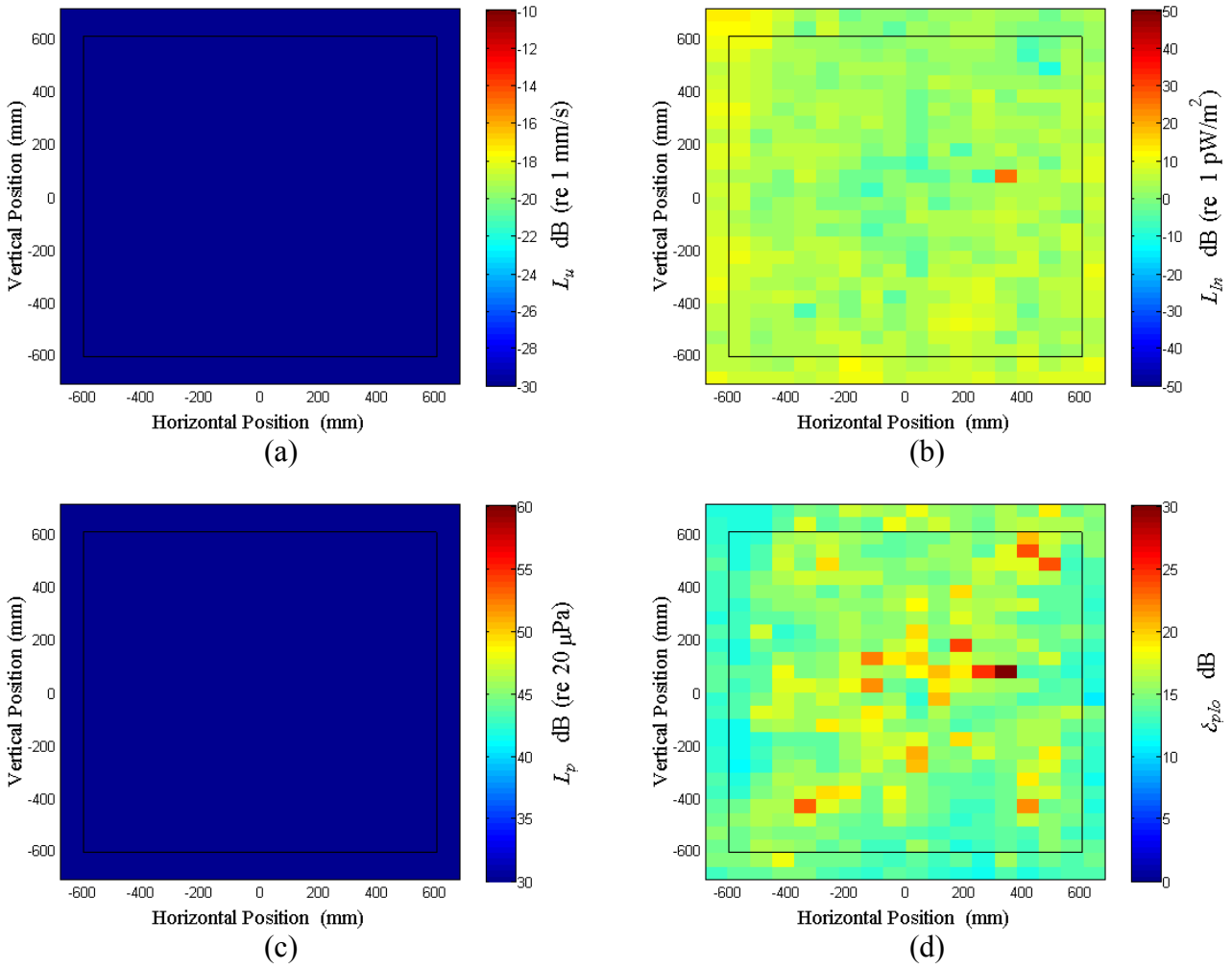

Figure B.70: Surface scan of Window B at 500 Hz (a) particle velocity level, L_u (b) normal signed sound intensity level, L_{In} (c) sound pressure level, L_p (d) pressure-residual intensity index, δ_{pIo}.

APPENDIX C. WINDOW C

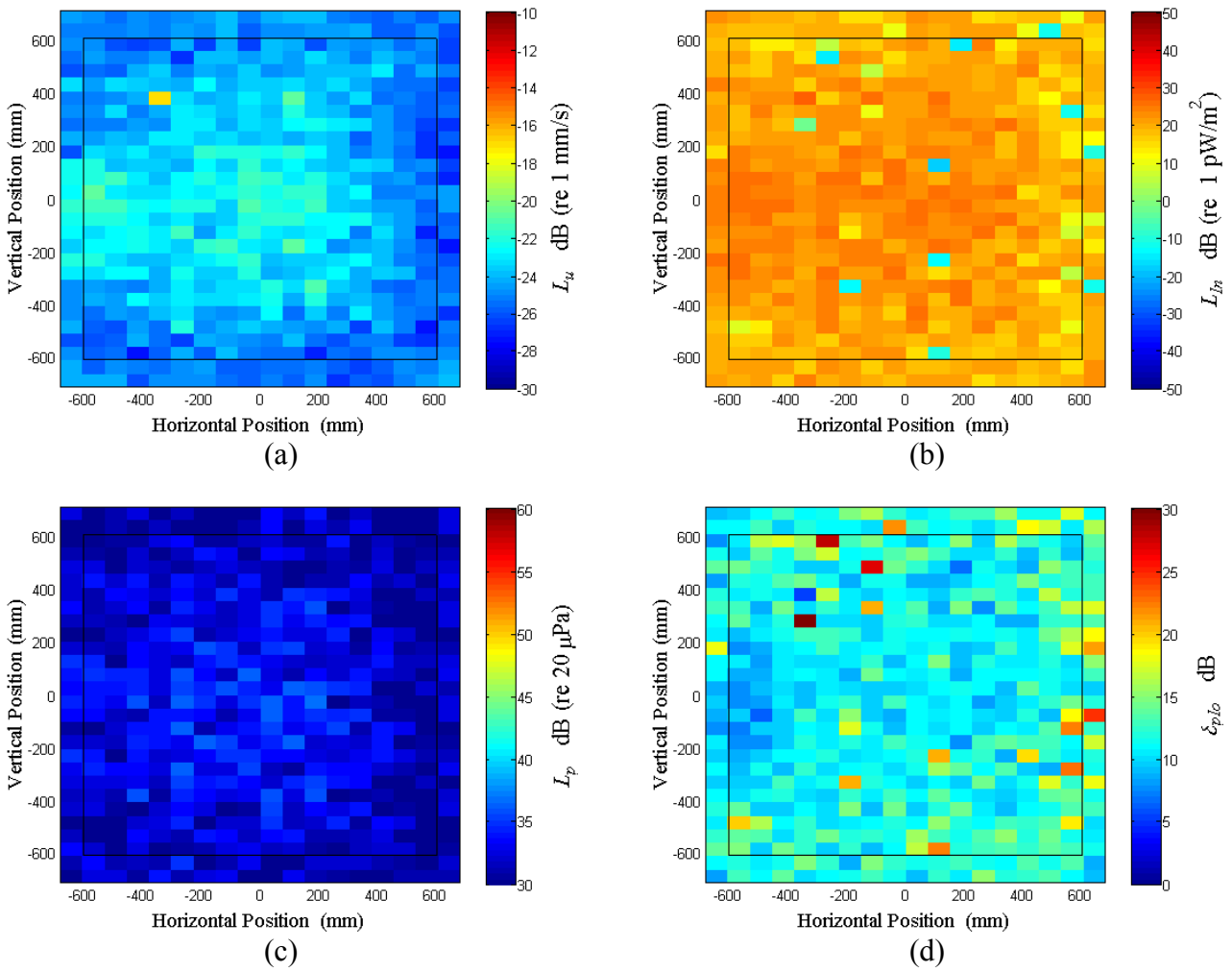

Figure C.1: Surface scan of Window C at 50 Hz (a) particle velocity level, L_u (b) normal signed sound intensity level, L_{In} (c) sound pressure level, L_p (d) pressure-residual intensity index, δ_{pIo}.

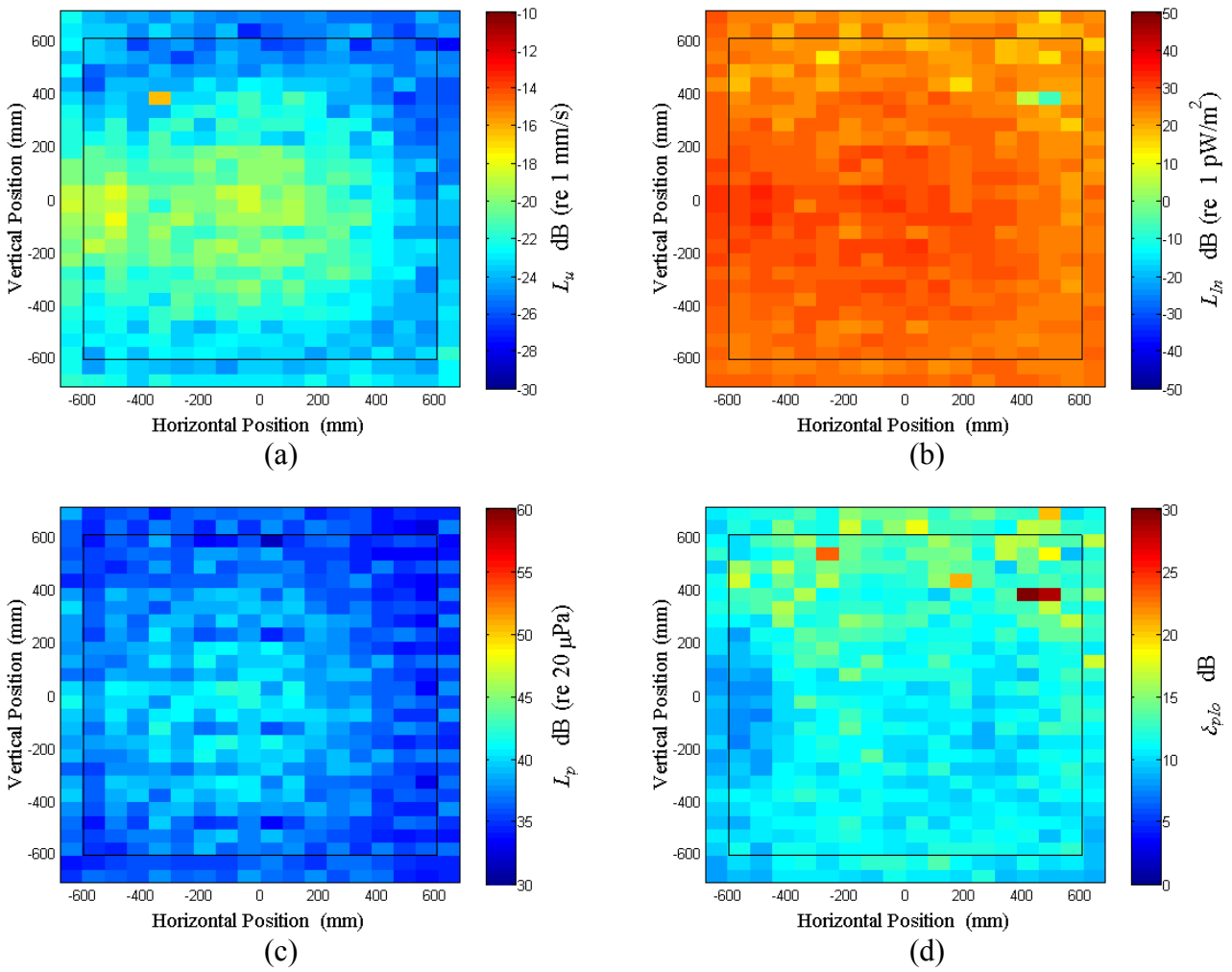

Figure C.2: Surface scan of Window C at 52.5 Hz (a) particle velocity level, L_u (b) normal signed sound intensity level, L_{In} (c) sound pressure level, L_p (d) pressure-residual intensity index, δ_{pIo}.

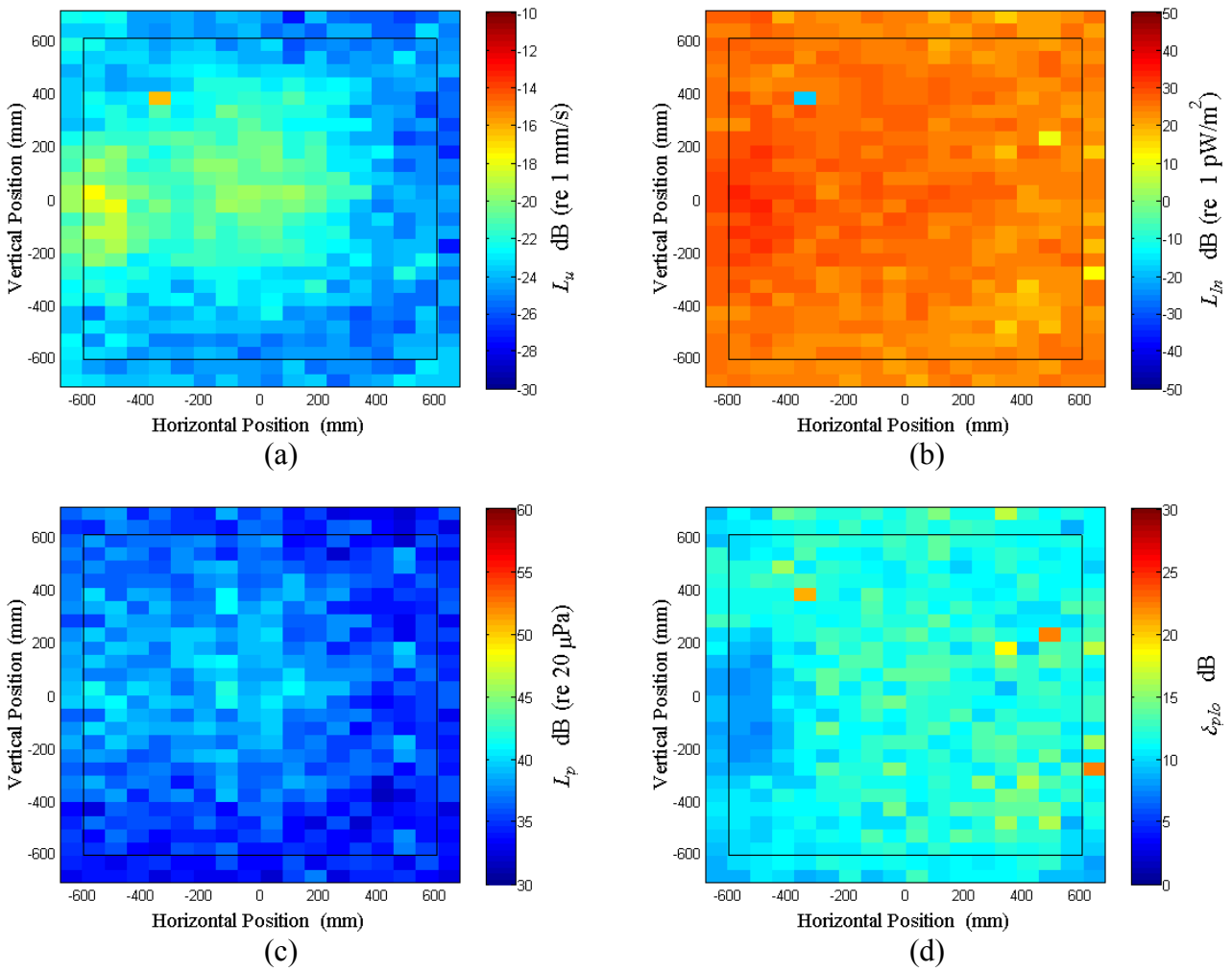

Figure C.3: Surface scan of Window C at 55 Hz (a) particle velocity level, L_u (b) normal signed sound intensity level, L_{In} (c) sound pressure level, L_p (d) pressure-residual intensity index, δ_{pIo}.

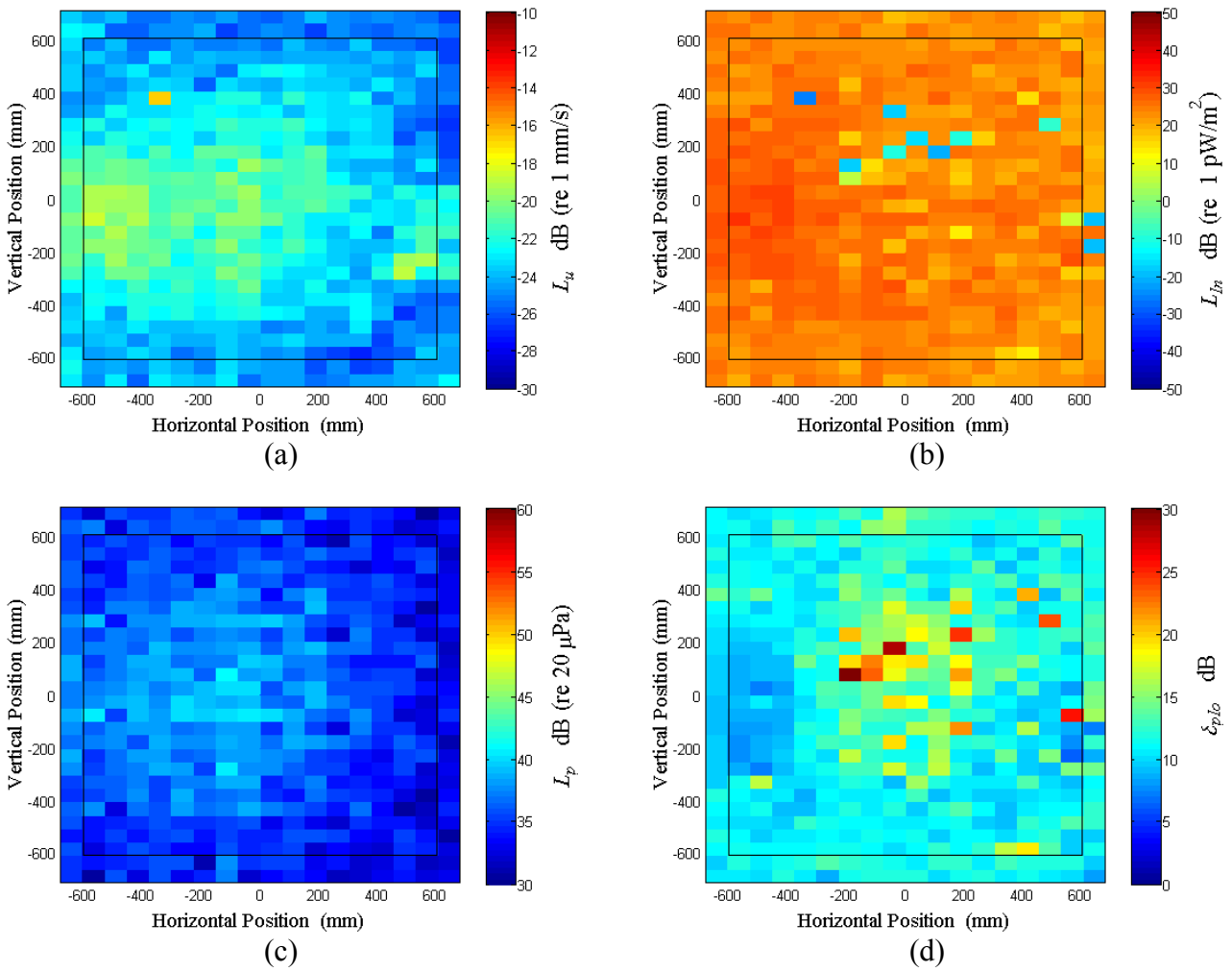

Figure C.4: Surface scan of Window C at 57.5 Hz (a) particle velocity level, L_u (b) normal signed sound intensity level, L_{In} (c) sound pressure level, L_p (d) pressure-residual intensity index, δ_{pIo}.

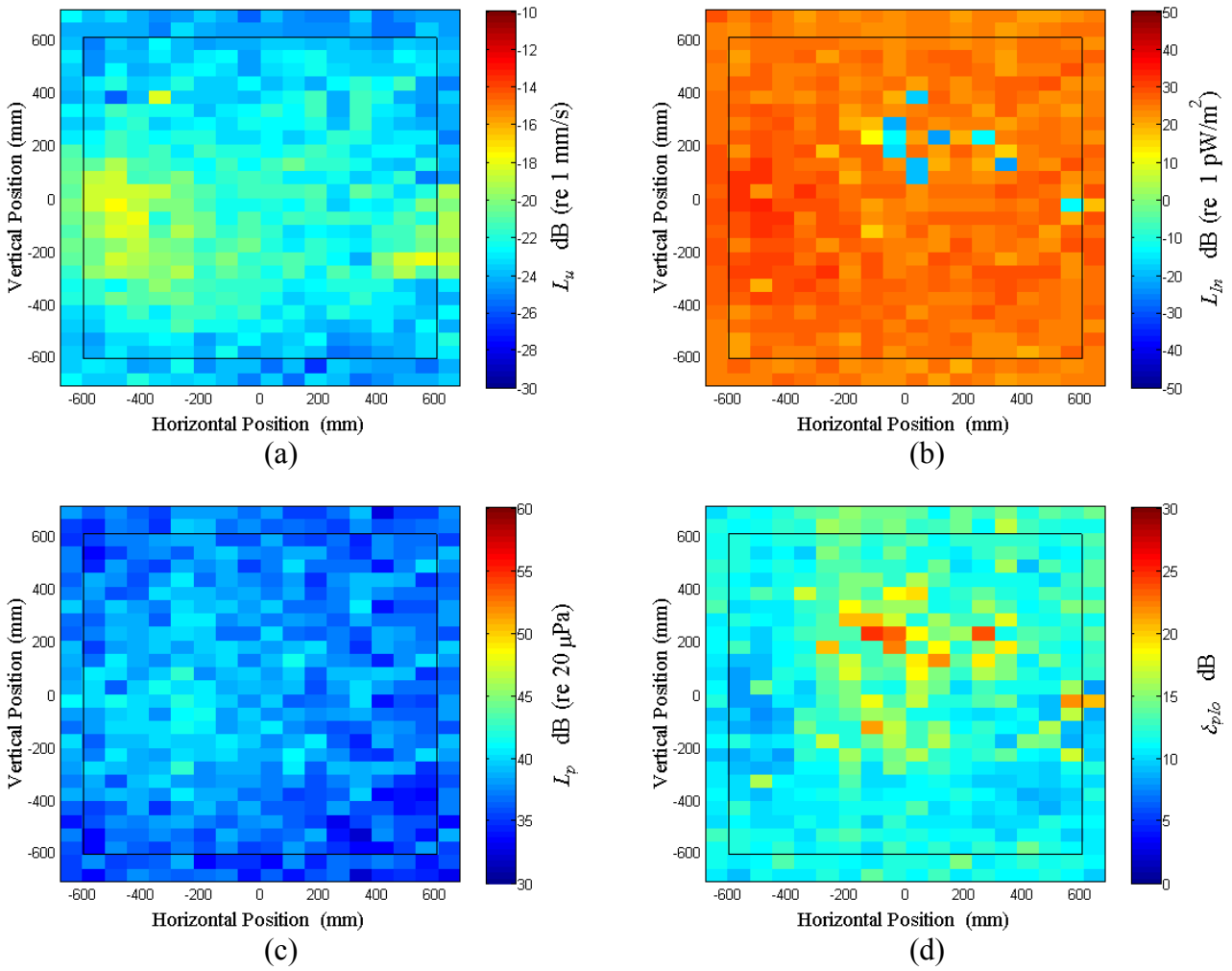

Figure C.5: Surface scan of Window C at 60 Hz (a) particle velocity level, L_u (b) normal signed sound intensity level, L_{In} (c) sound pressure level, L_p (d) pressure-residual intensity index, δ_{pIo}.

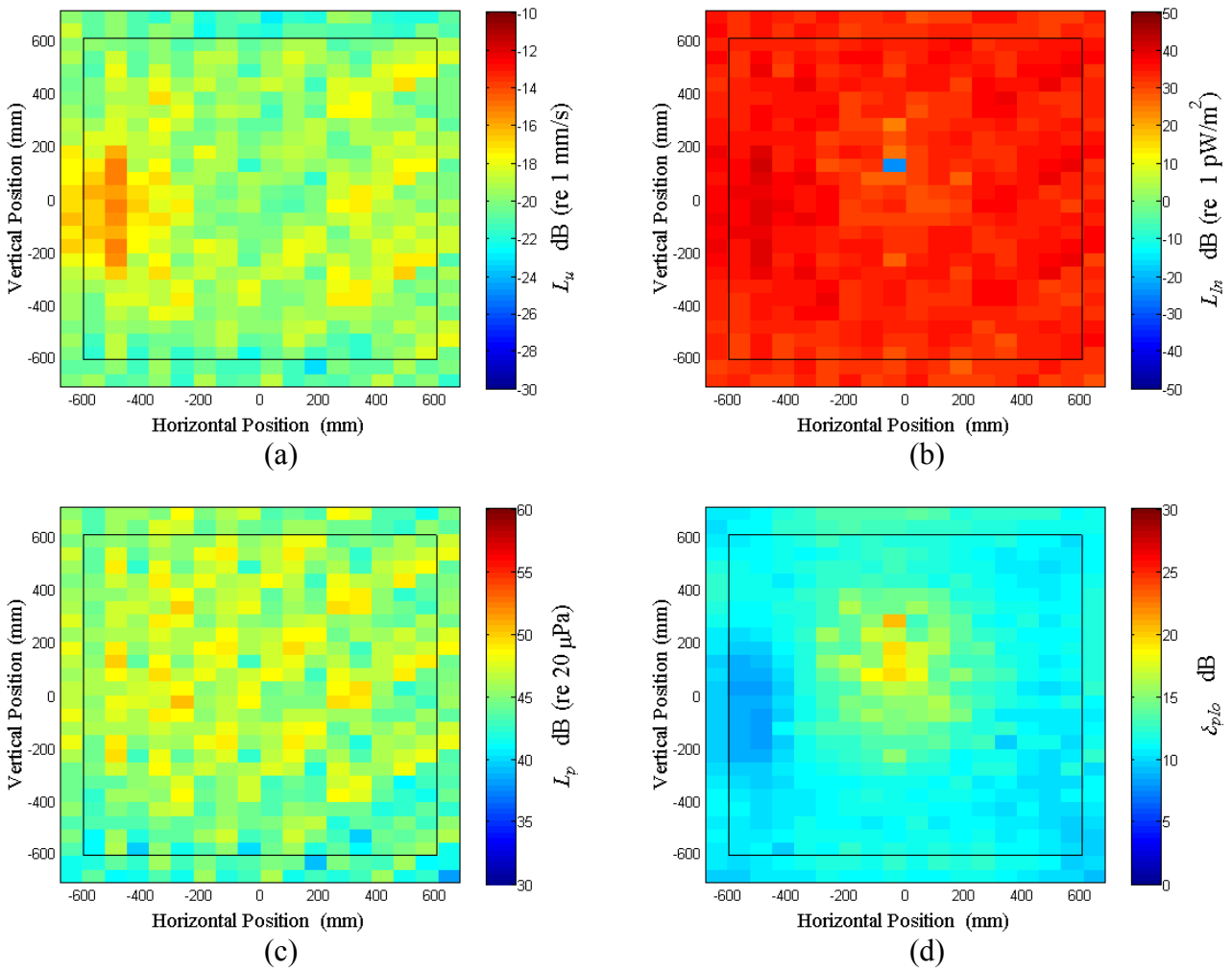

Figure C.6: Surface scan of Window C at 62.5 Hz (a) particle velocity level, L_u (b) normal signed sound intensity level, L_{In} (c) sound pressure level, L_p (d) pressure-residual intensity index, δ_{pIo}.

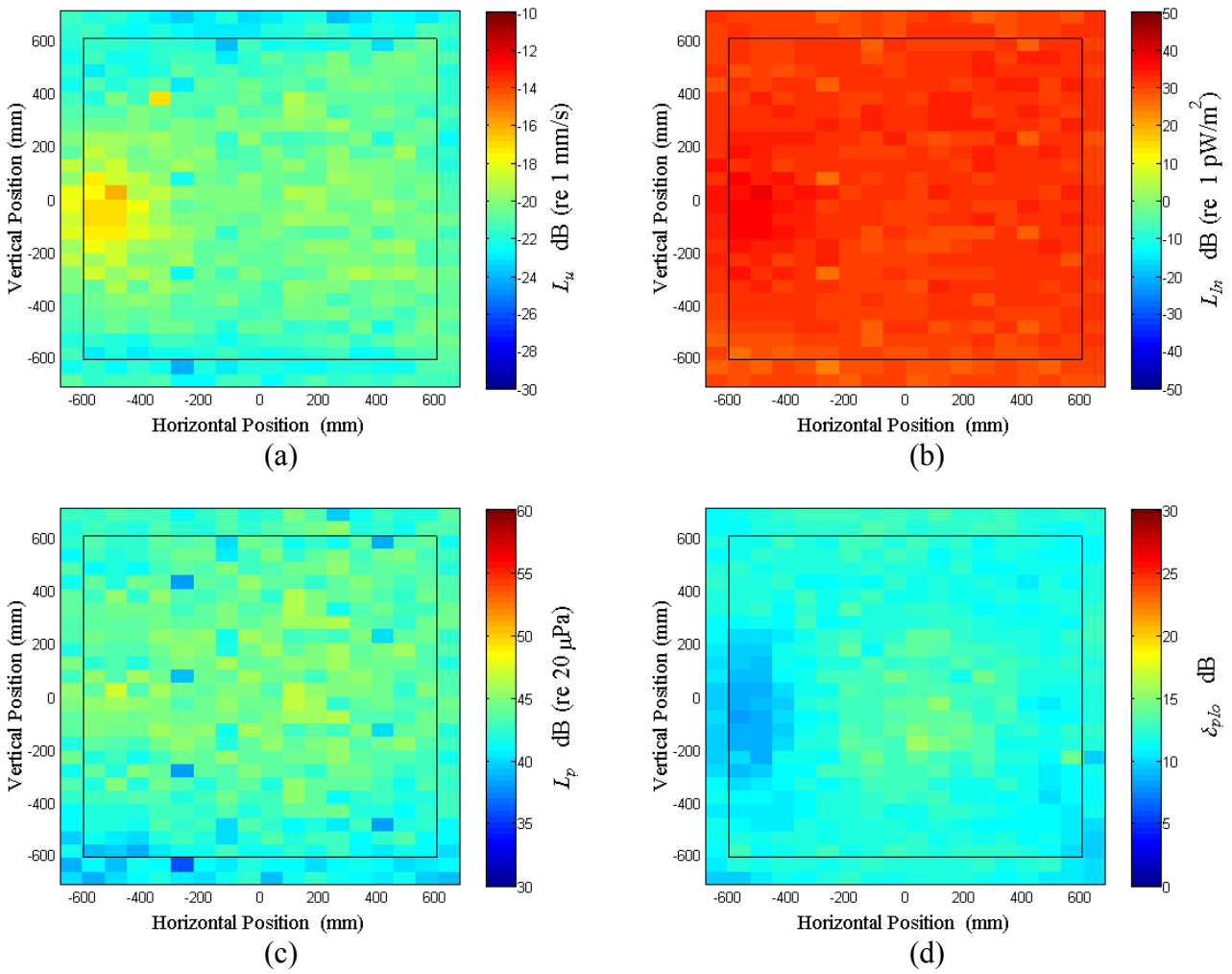

Figure C.7: Surface scan of Window C at 65 Hz (a) particle velocity level, L_u (b) normal signed sound intensity level, L_{In} (c) sound pressure level, L_p (d) pressure-residual intensity index, δ_{pIo}.

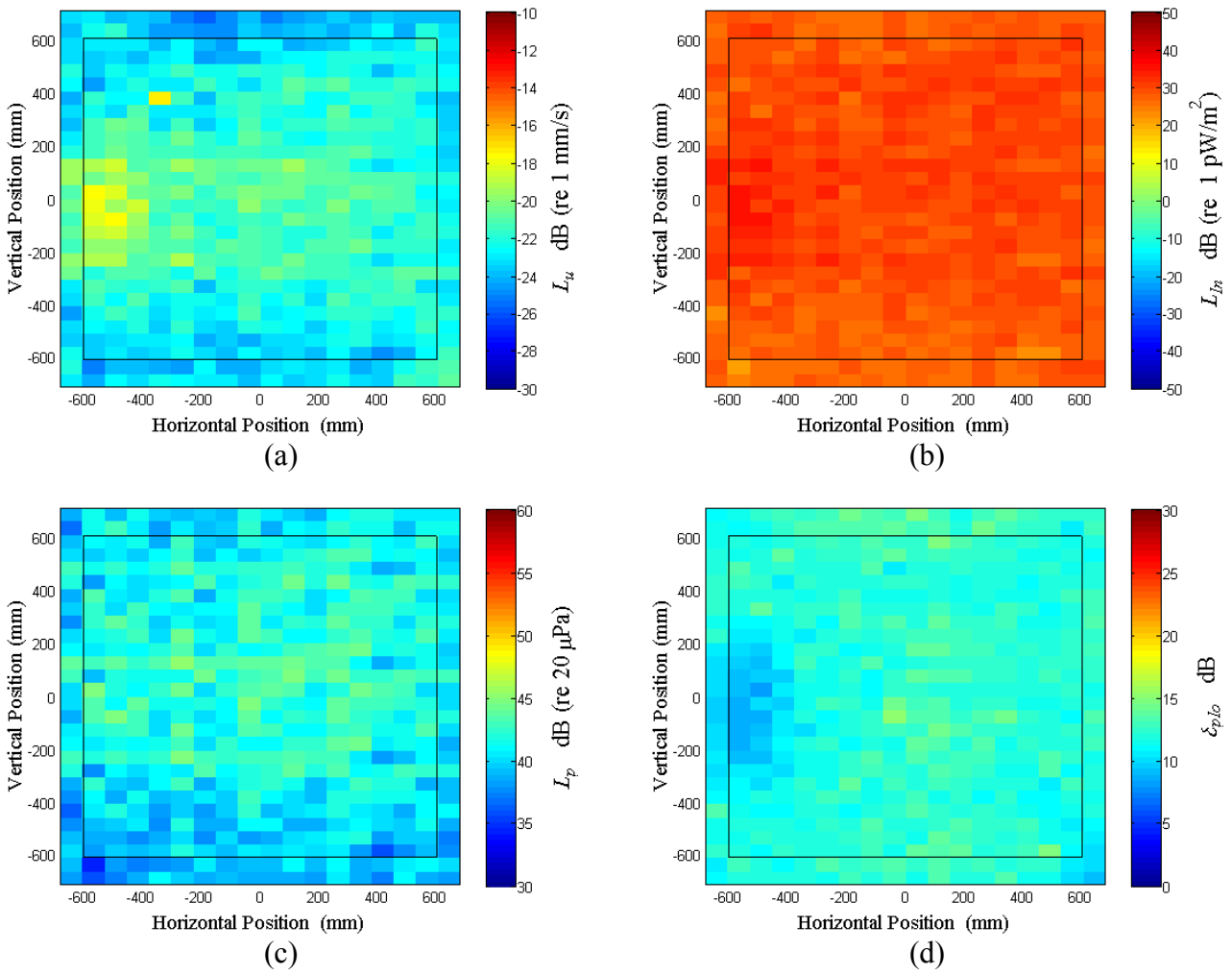

Figure C.8: Surface scan of Window C at 67.5 Hz (a) particle velocity level, L_u (b) normal signed sound intensity level, L_{In} (c) sound pressure level, L_p (d) pressure-residual intensity index, δ_{pIo}.

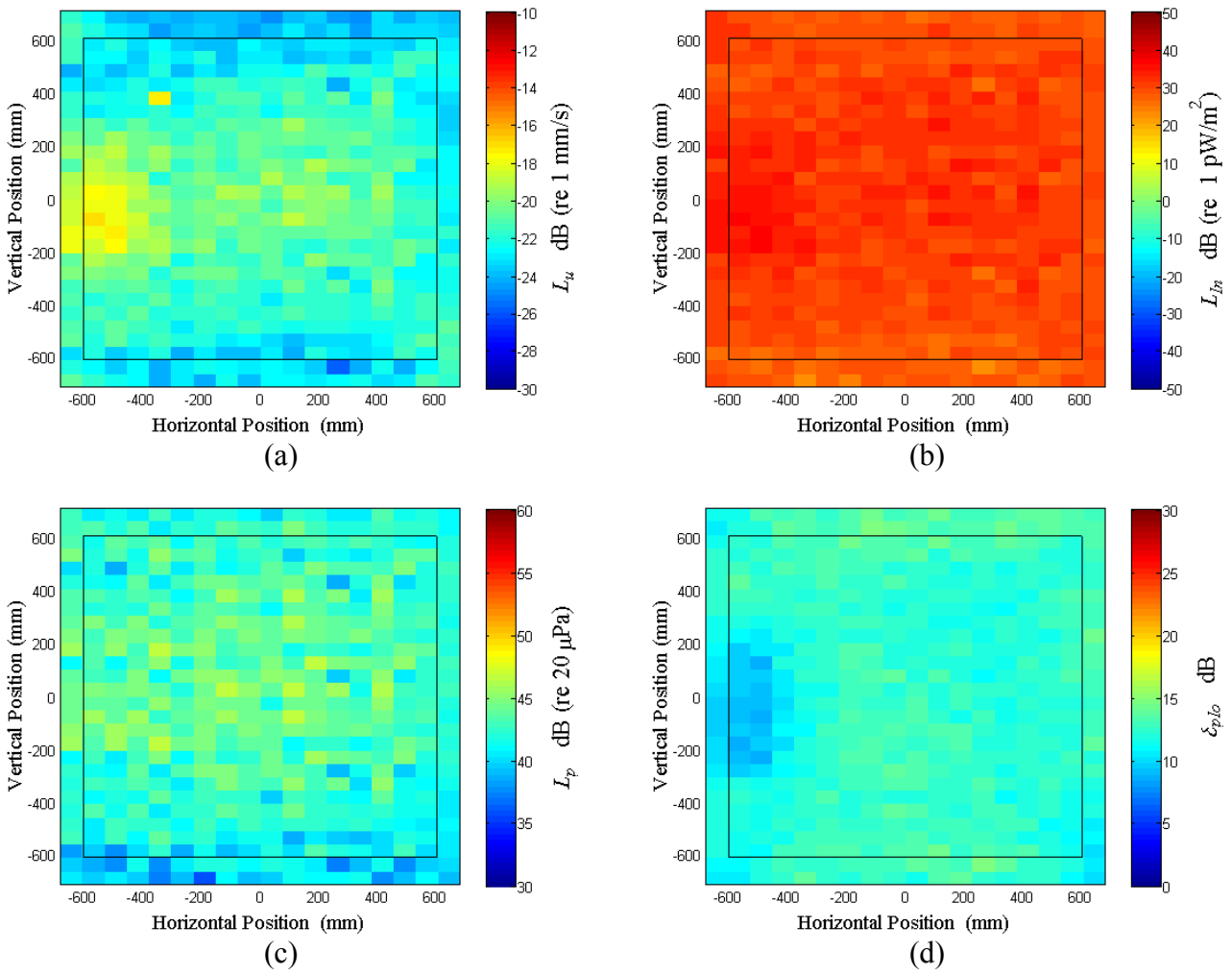

Figure C.9: Surface scan of Window C at 70 Hz (a) particle velocity level, L_u (b) normal signed sound intensity level, L_{In} (c) sound pressure level, L_p (d) pressure-residual intensity index, δ_{pIo}.

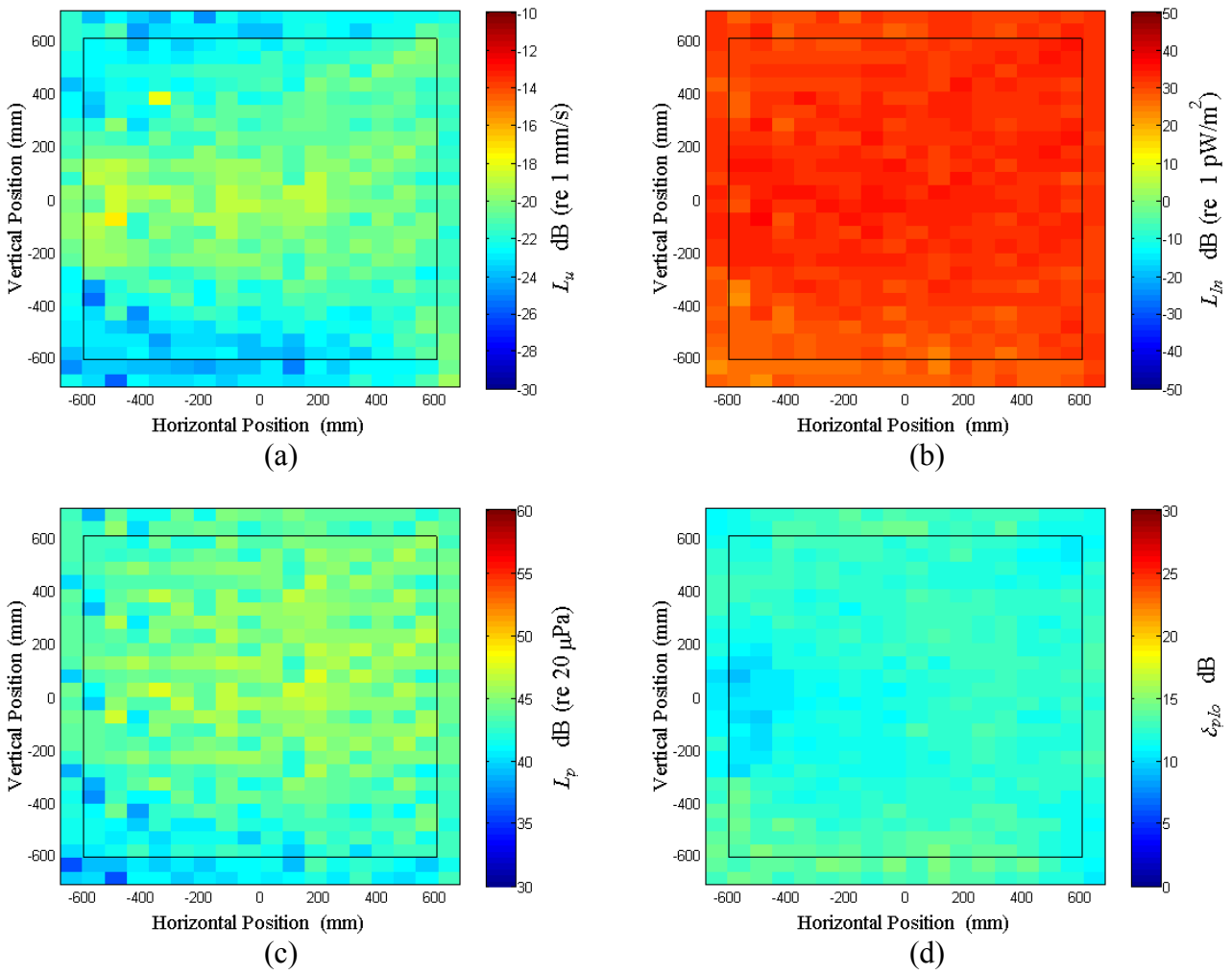

Figure C.10: Surface scan of Window C at 72.5 Hz (a) particle velocity level, L_u (b) normal signed sound intensity level, L_{In} (c) sound pressure level, L_p (d) pressure-residual intensity index, δ_{pIo}.

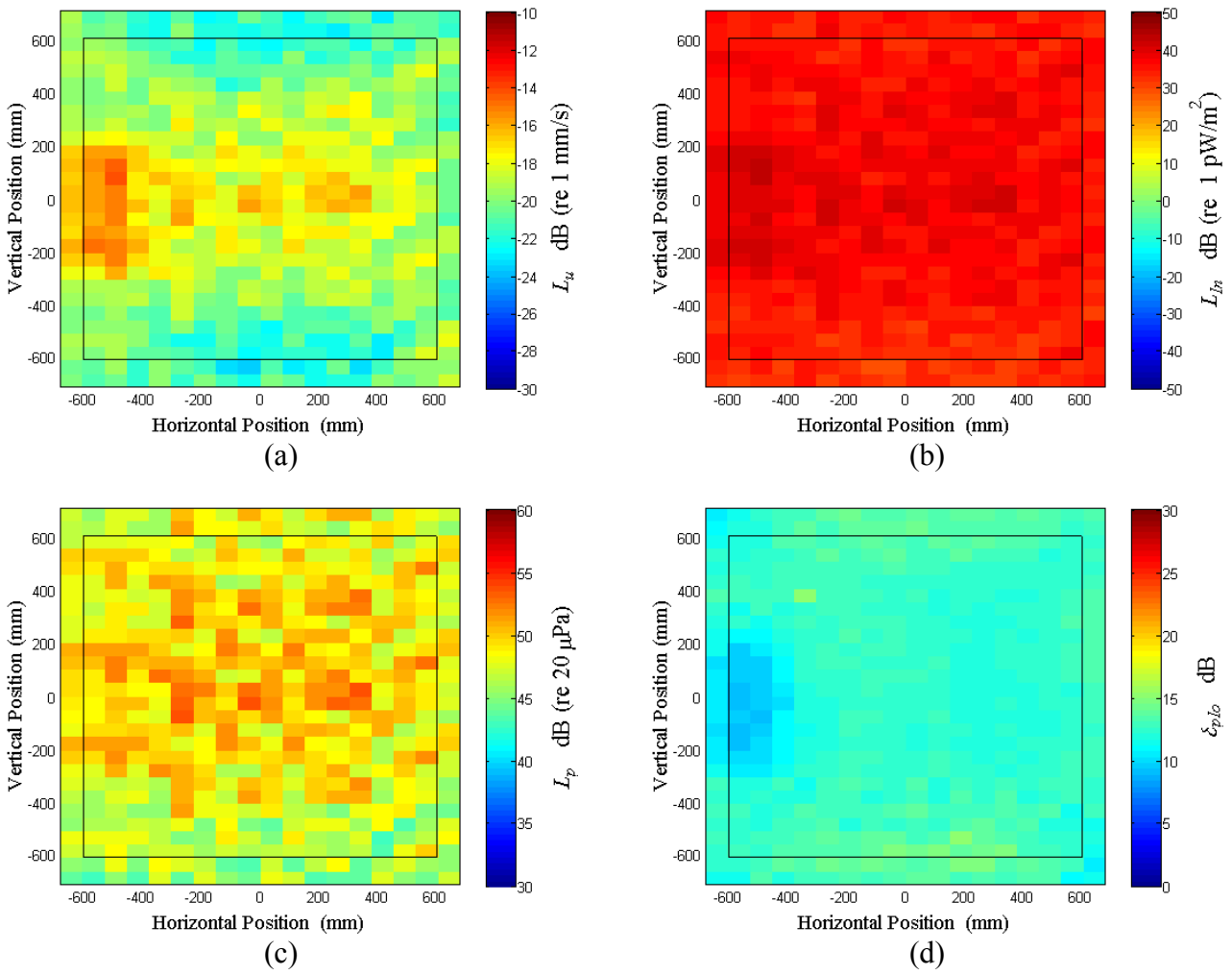

Figure C.11: Surface scan of Window C at.75 Hz (a) particle velocity level, L_u (b) normal signed sound intensity level, L_{In} (c) sound pressure level, L_p (d) pressure-residual intensity index, δ_{pIo}.

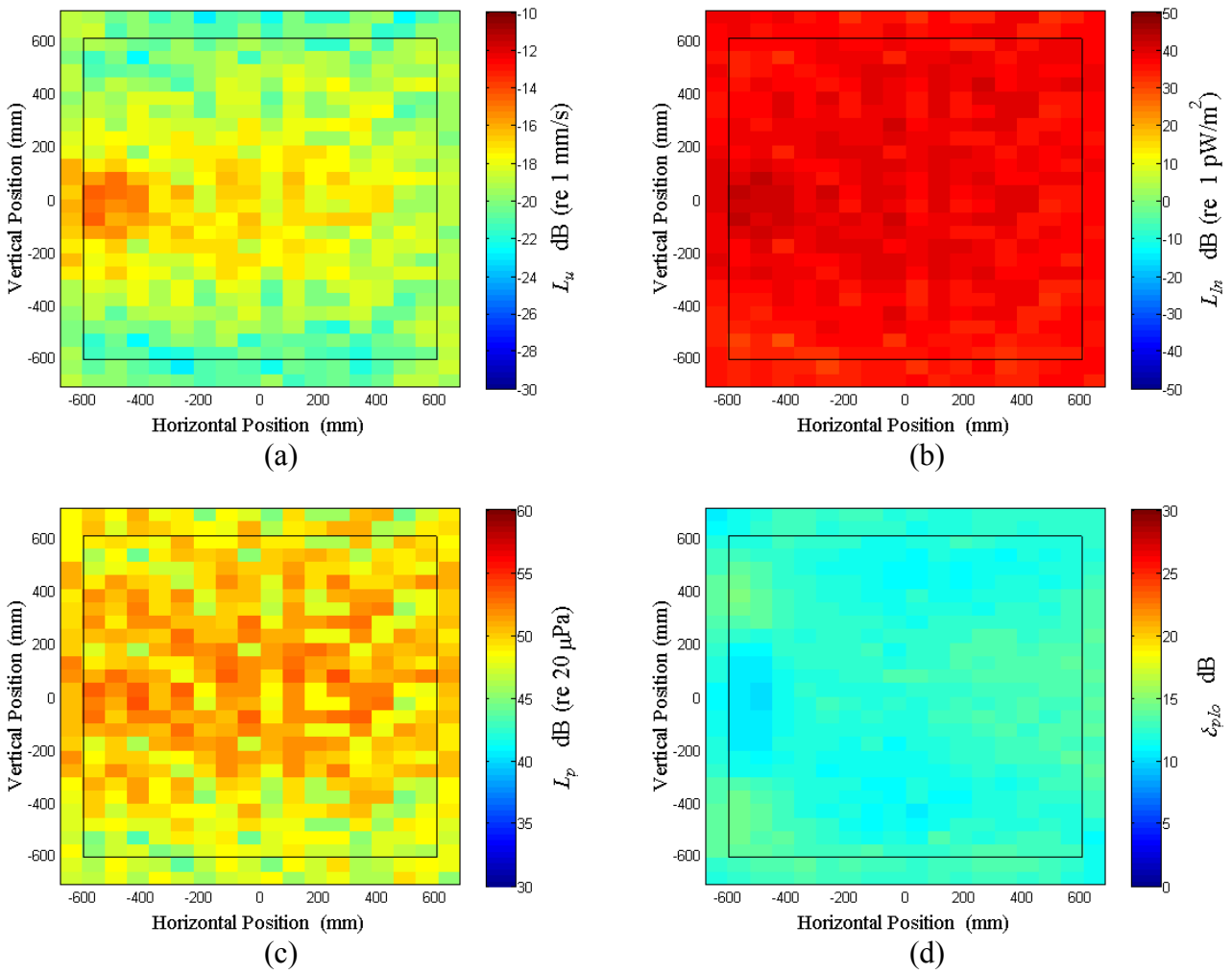

Figure C.12: Surface scan of Window C at 77.5 Hz (a) particle velocity level, L_u (b) normal signed sound intensity level, L_{In} (c) sound pressure level, L_p (d) pressure-residual intensity index, δ_{pIo}.

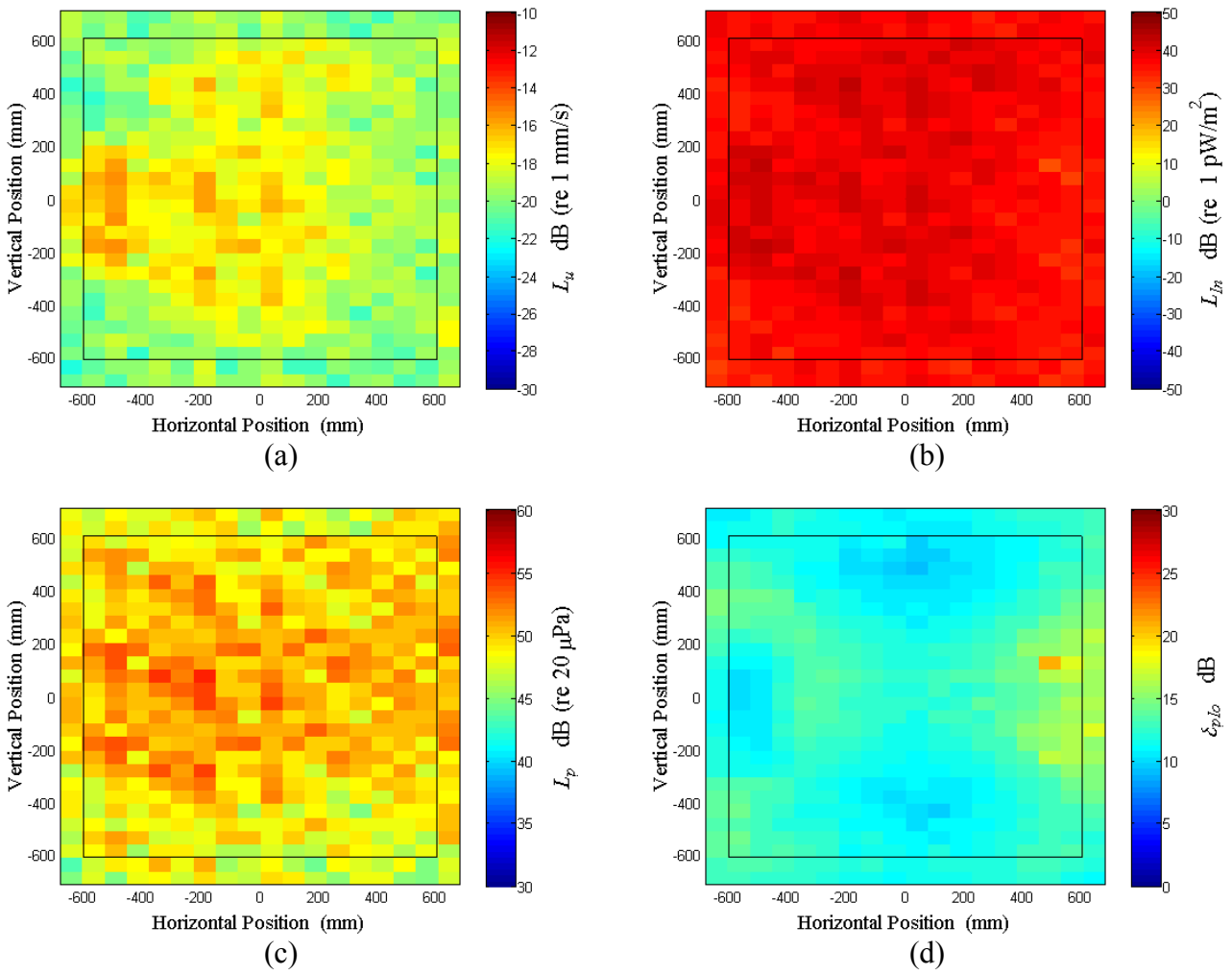

Figure C.13: Surface scan of Window C at 80 Hz (a) particle velocity level, L_u (b) normal signed sound intensity level, L_{In} (c) sound pressure level, L_p (d) pressure-residual intensity index, δ_{pIo}.

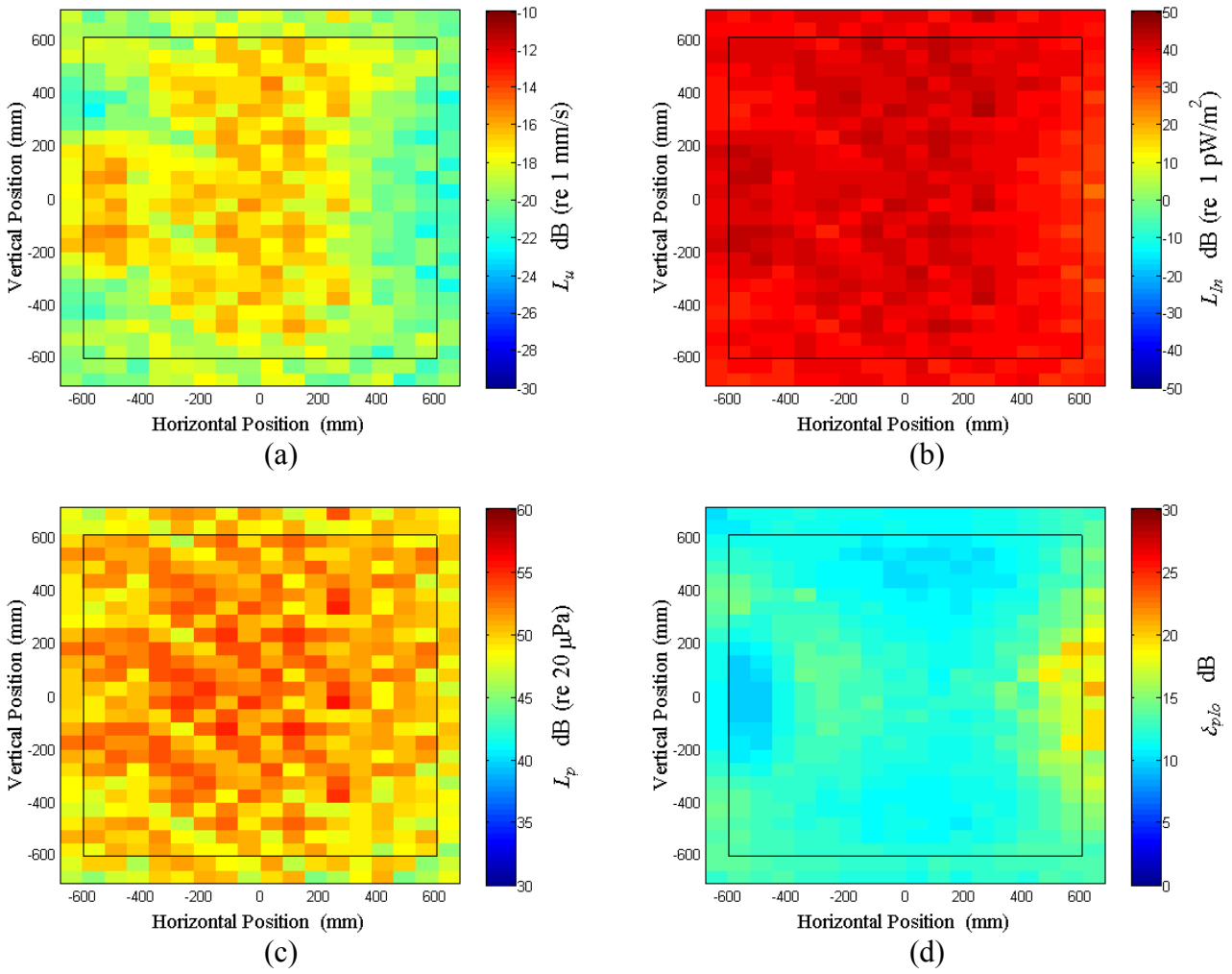

Figure C.14: Surface scan of Window C at 82.5 Hz (a) particle velocity level, L_u (b) normal signed sound intensity level, L_{In} (c) sound pressure level, L_p (d) pressure-residual intensity index, δ_{pIo}.

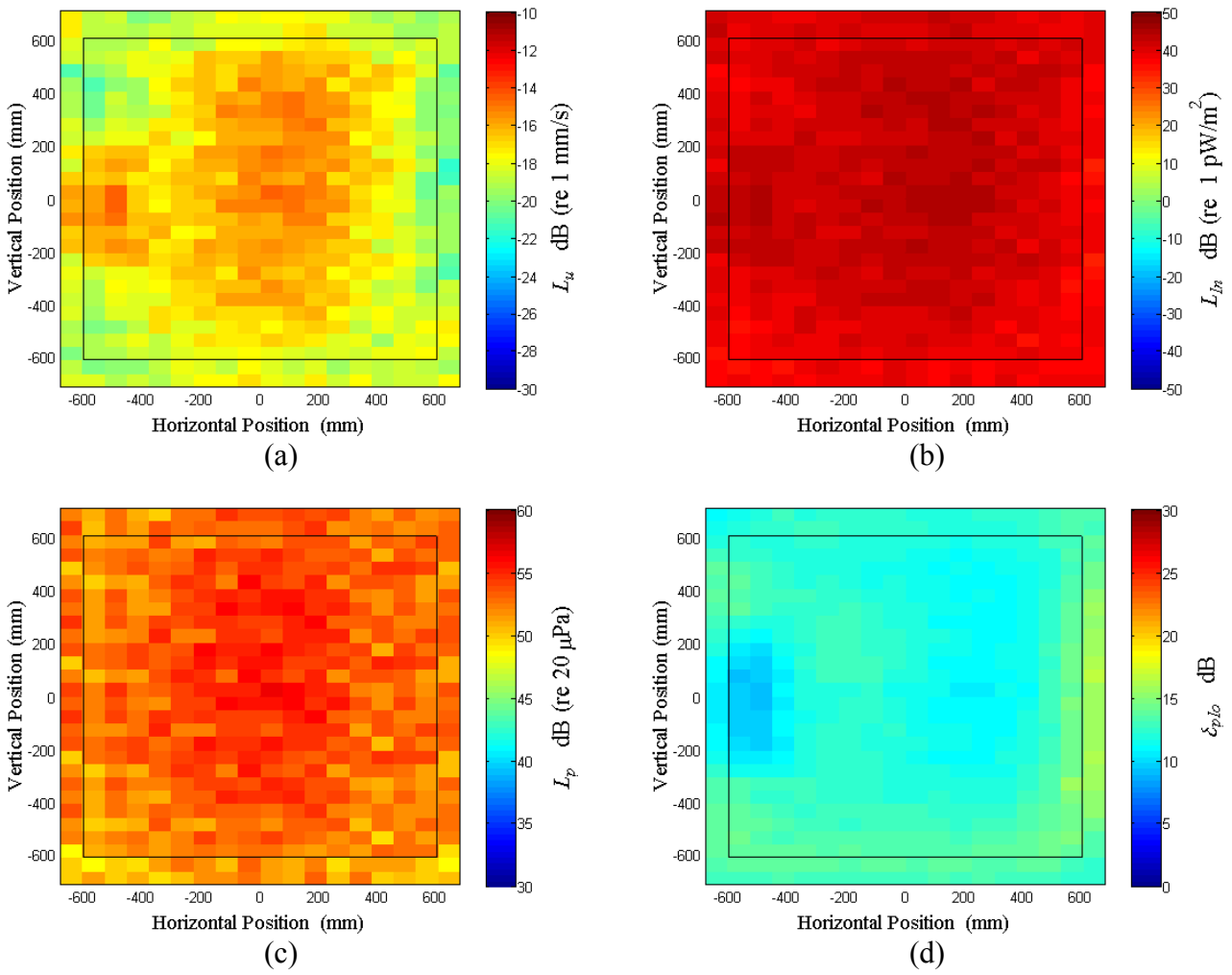

Figure C.15: Surface scan of Window C at 85 Hz (a) particle velocity level, L_u (b) normal signed sound intensity level, L_{In} (c) sound pressure level, L_p (d) pressure-residual intensity index, δ_{pIo}.

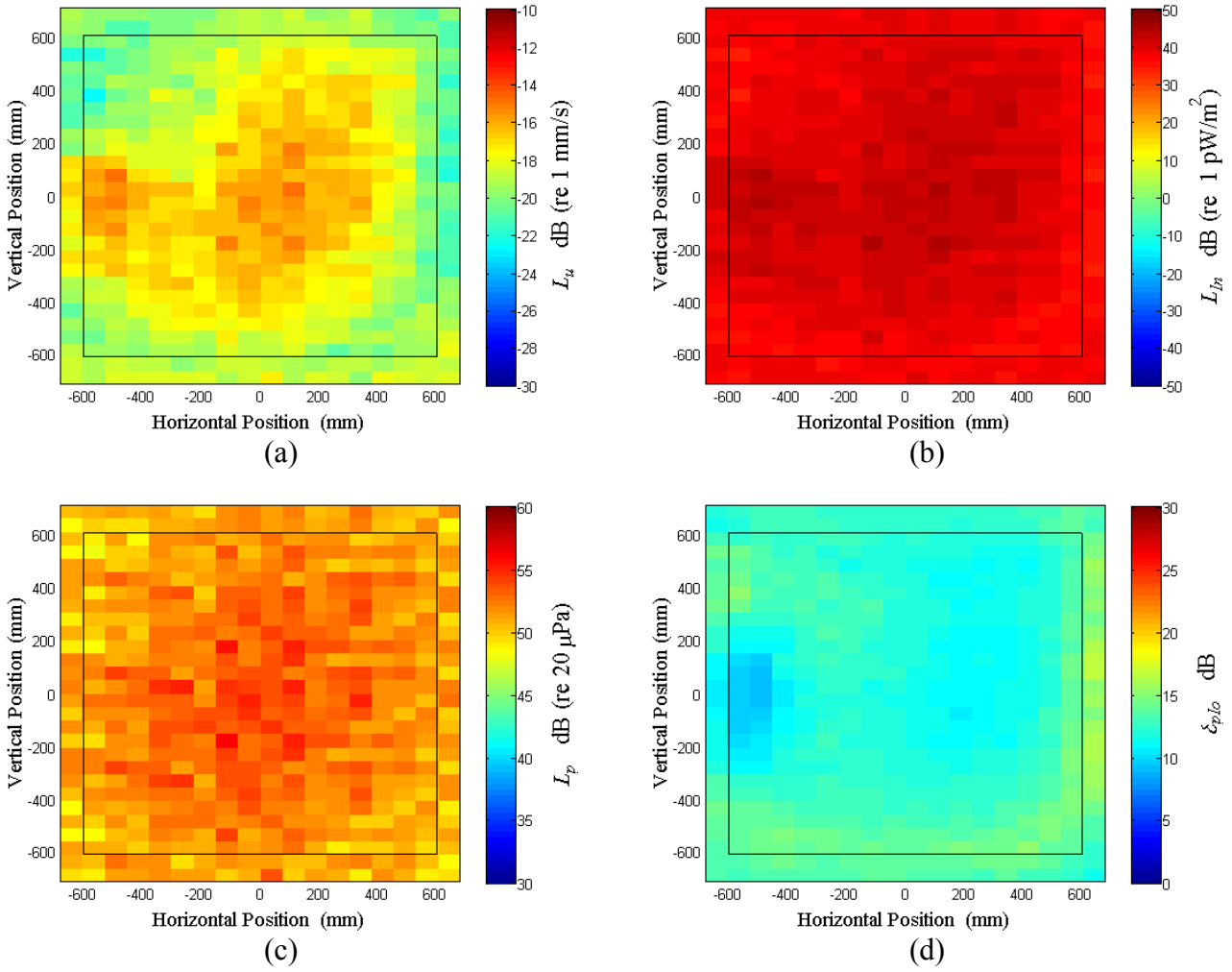

Figure C.16: Surface scan of Window C at 87.5 Hz (a) particle velocity level, L_u (b) normal signed sound intensity level, L_{In} (c) sound pressure level, L_p (d) pressure-residual intensity index, δ_{pIo}.

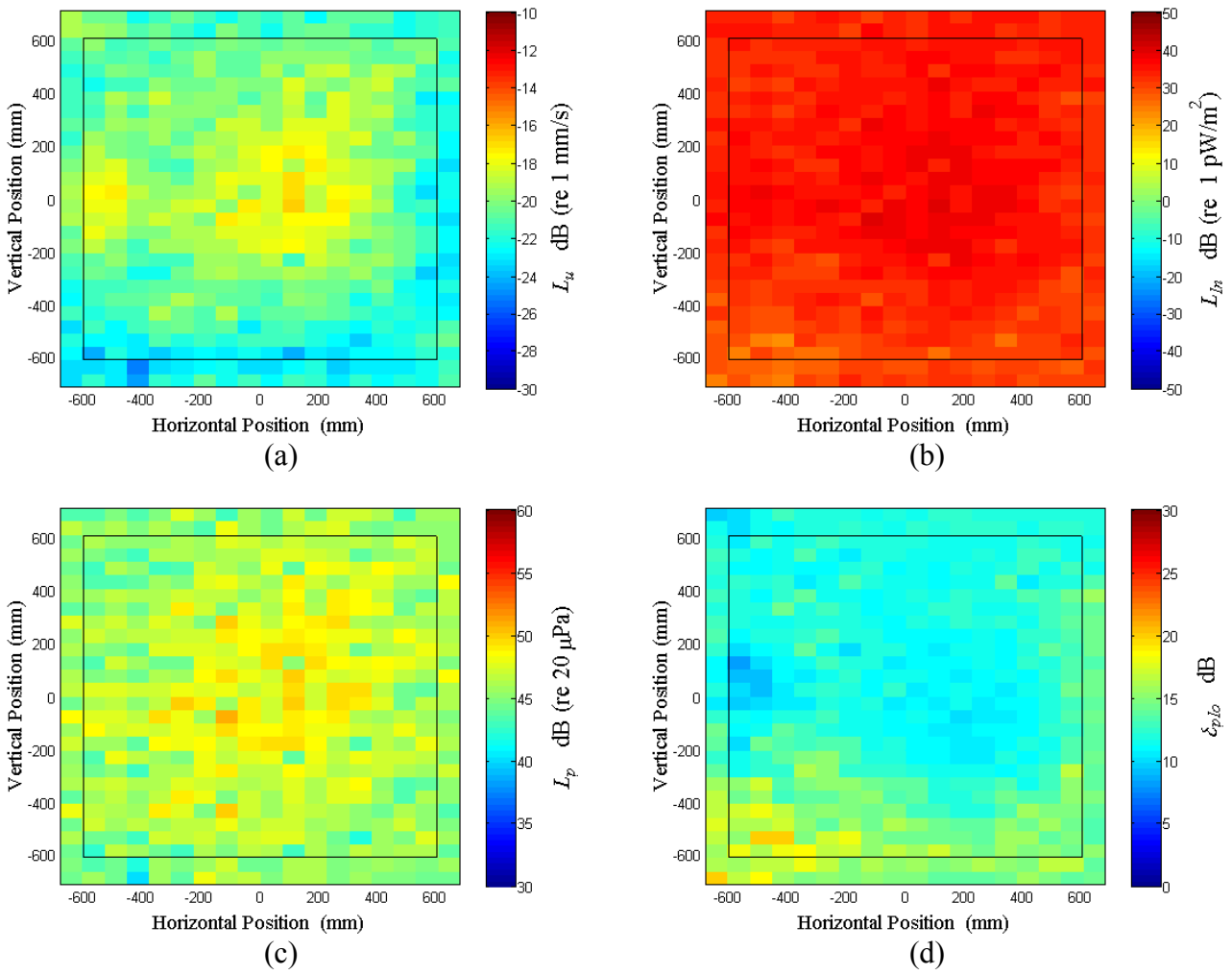

Figure C.17: Surface scan of Window C at 90 Hz (a) particle velocity level, L_u (b) normal signed sound intensity level, L_{In} (c) sound pressure level, L_p (d) pressure-residual intensity index, δ_{pIo}.

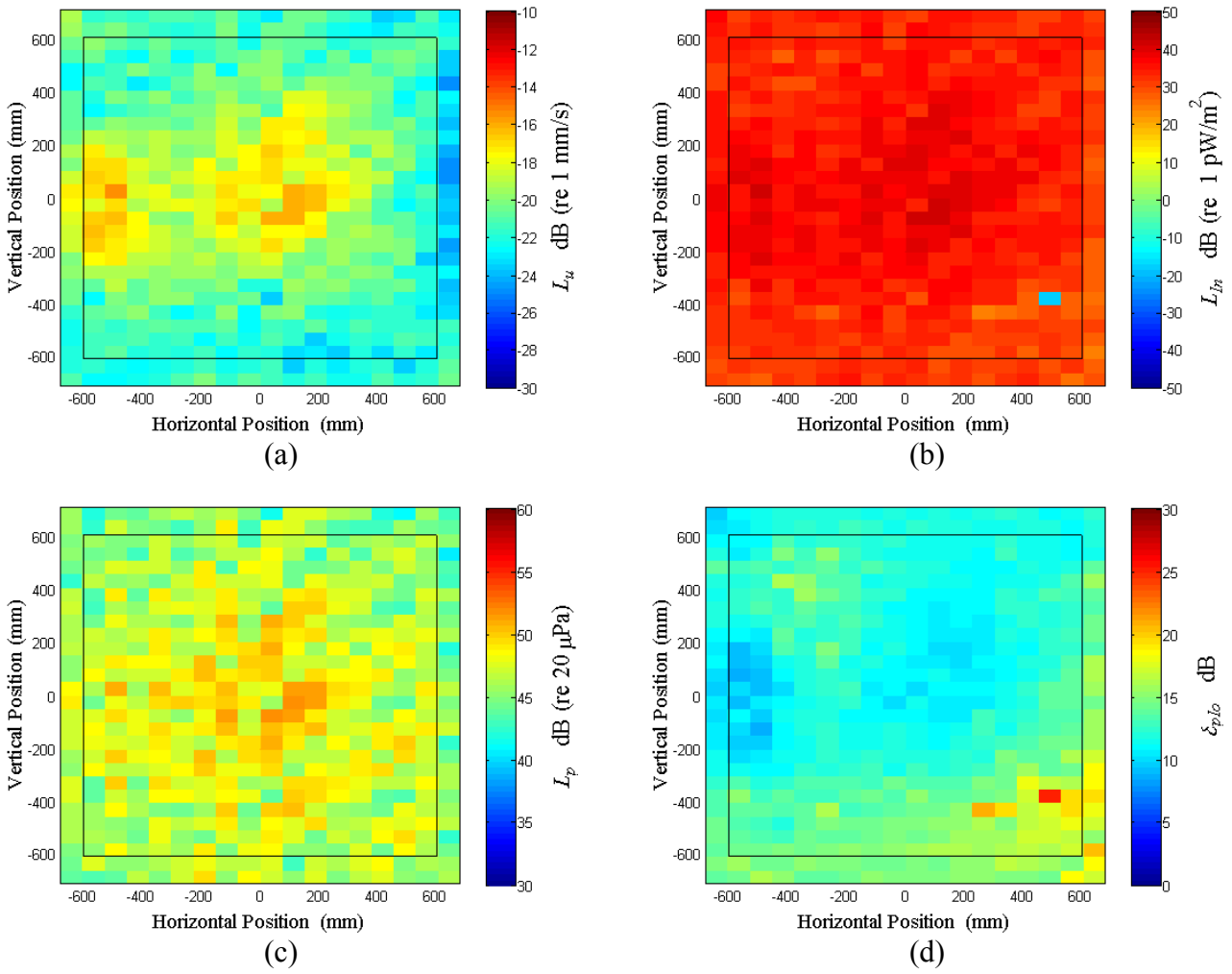

Figure C.18: Surface scan of Window C at 92.5 Hz (a) particle velocity level, L_u (b) normal signed sound intensity level, L_{In} (c) sound pressure level, L_p (d) pressure-residual intensity index, δ_{pIo}.

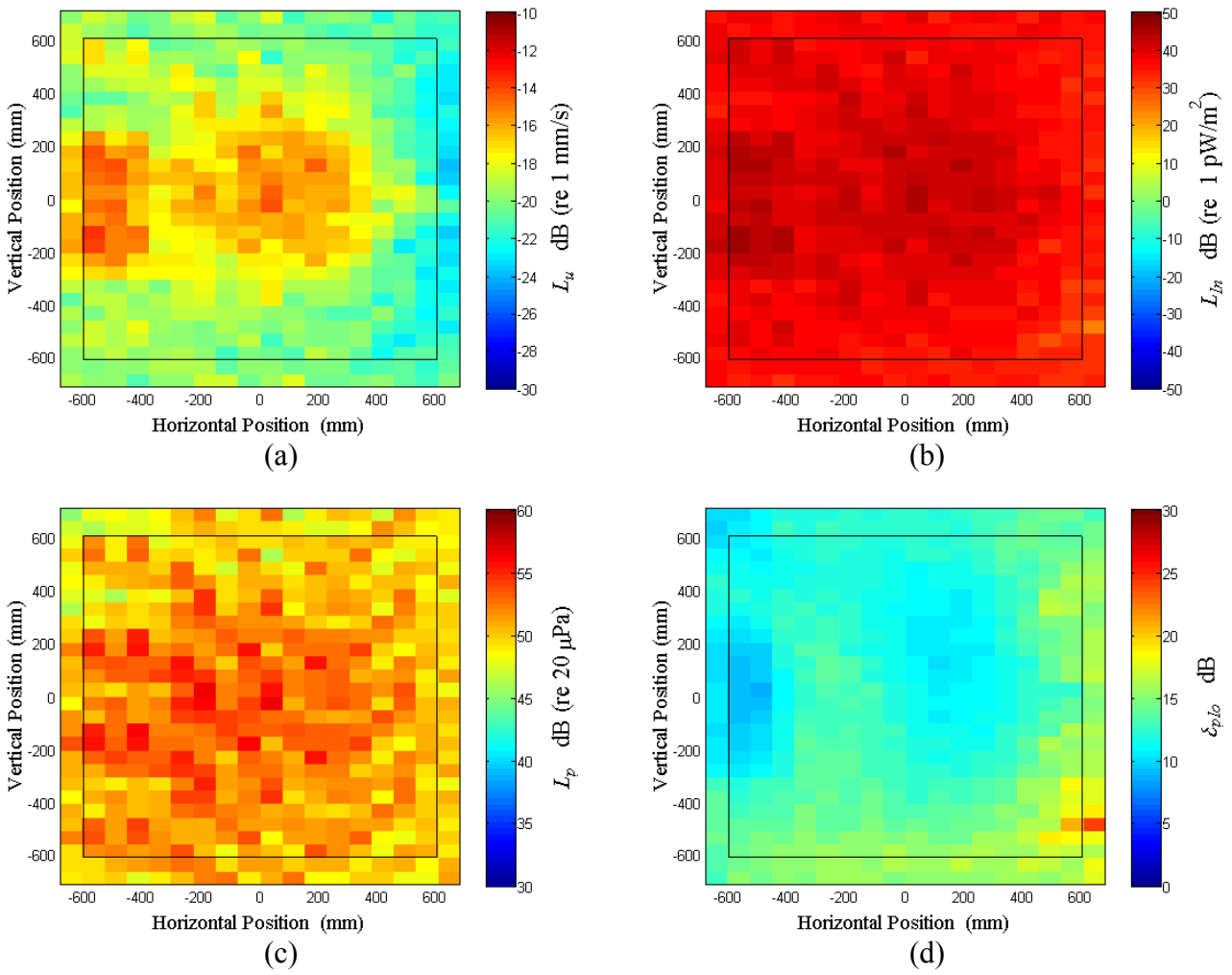

Figure C.19: Surface scan of Window C at 95 Hz (a) particle velocity level, L_u (b) normal signed sound intensity level, L_{In} (c) sound pressure level, L_p (d) pressure-residual intensity index, δ_{pIo}.

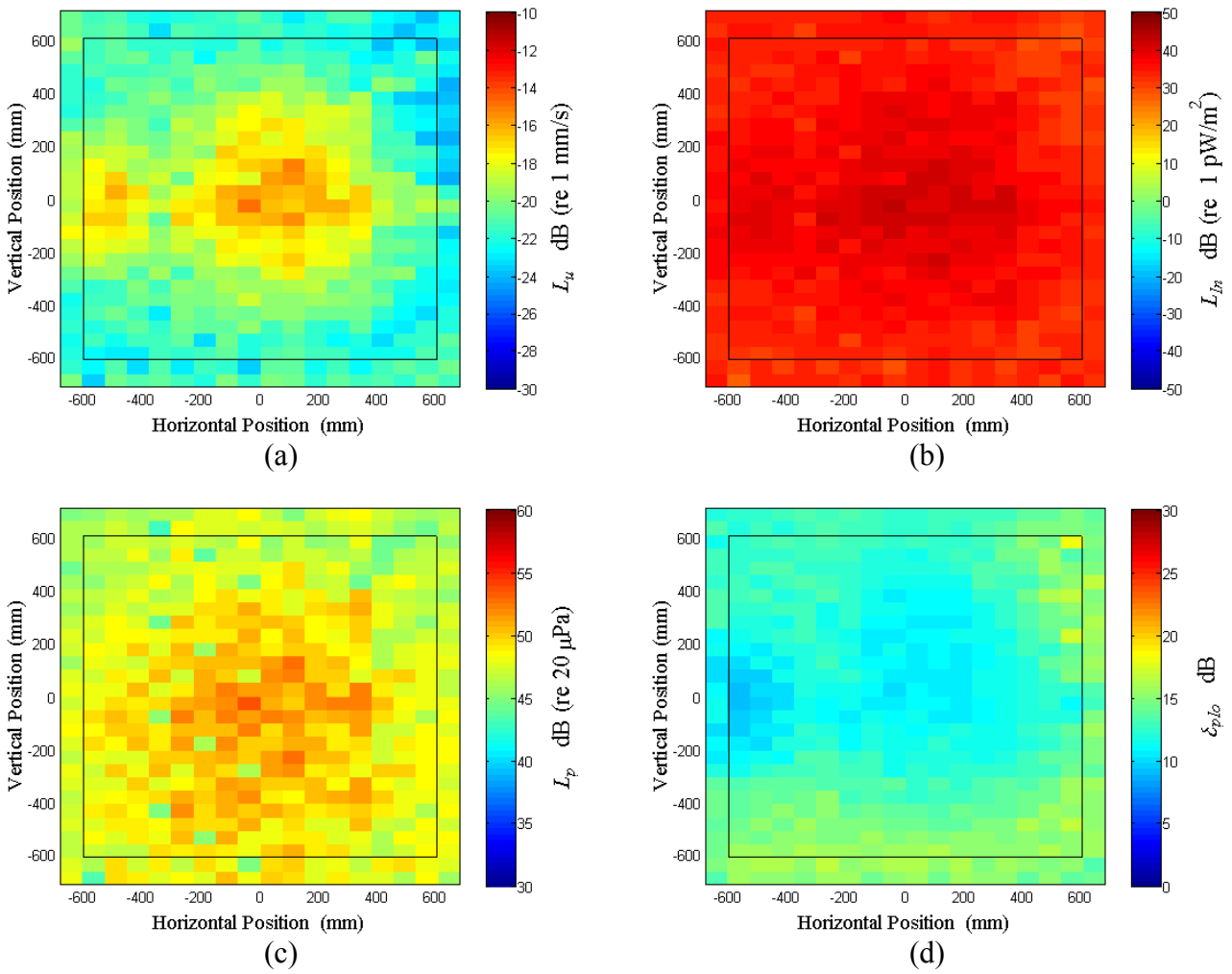

Figure C.20: Surface scan of Window C at 97.5 Hz (a) particle velocity level, L_u (b) normal signed sound intensity level, L_{In} (c) sound pressure level, L_p (d) pressure-residual intensity index, δ_{pIo}.

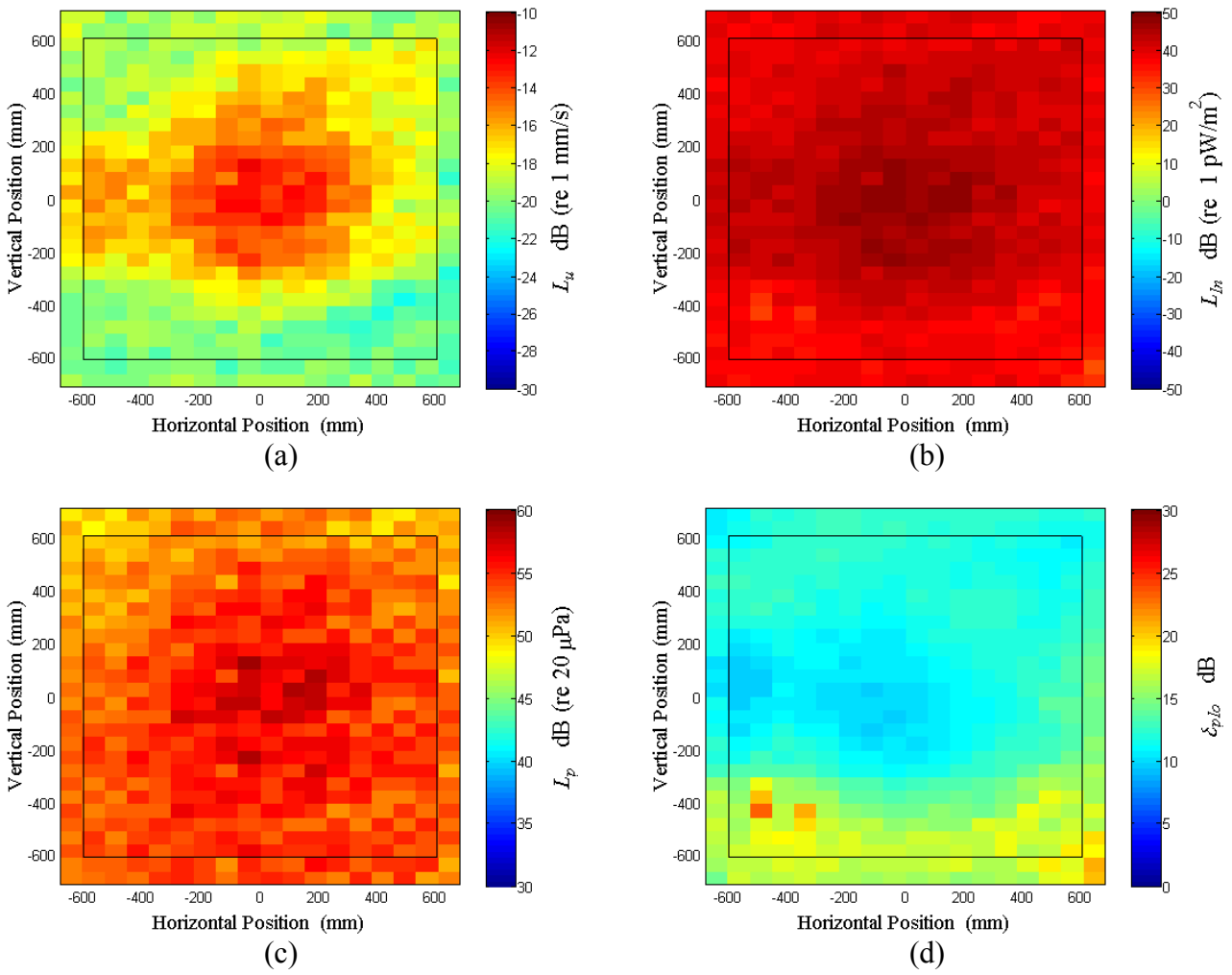

Figure C.21: Surface scan of Window C at 100 Hz (a) particle velocity level, L_u (b) normal signed sound intensity level, L_{In} (c) sound pressure level, L_p (d) pressure-residual intensity index, δ_{pIo}.

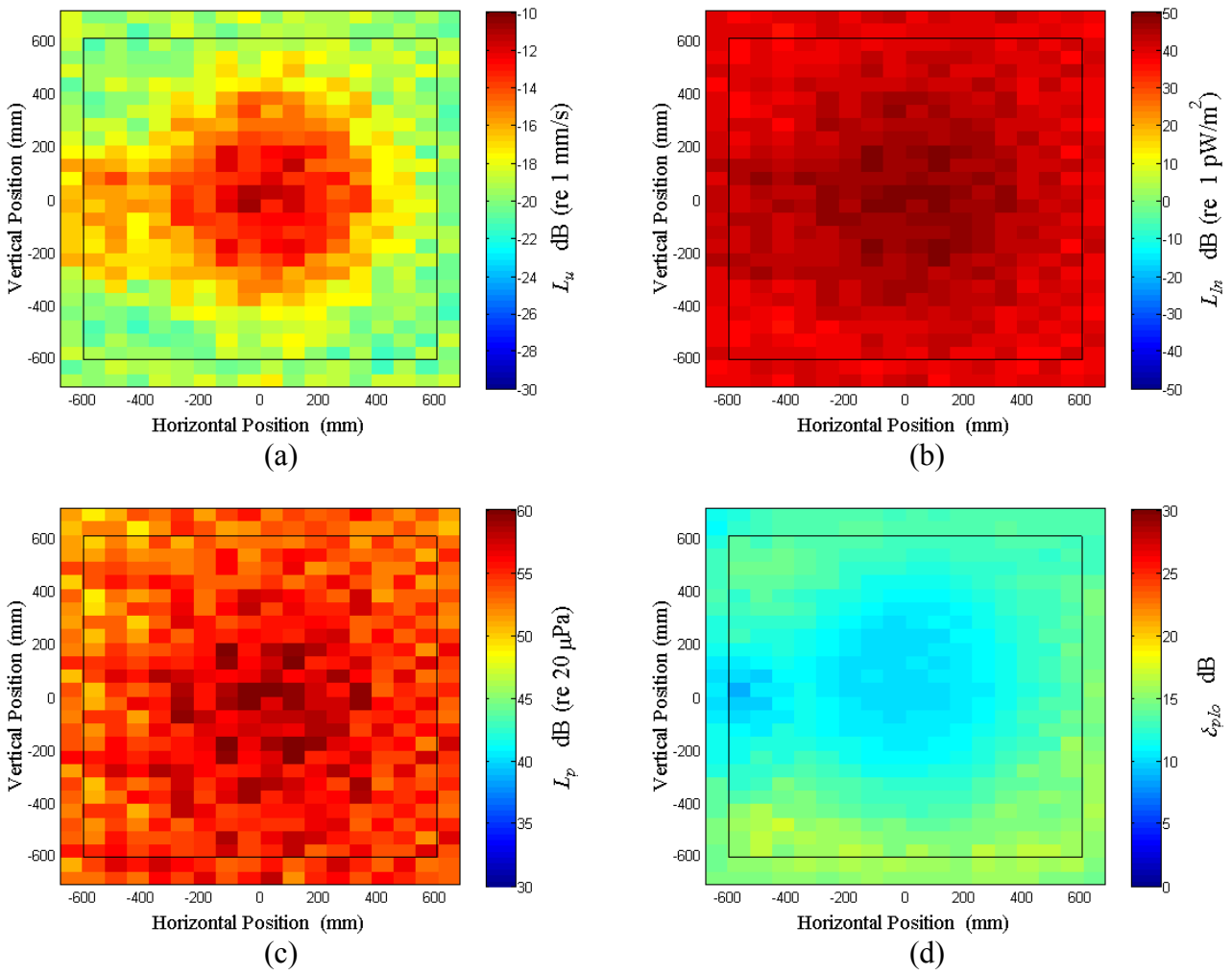

Figure C.22: Surface scan of Window C at 102.5 Hz (a) particle velocity level, L_u (b) normal signed sound intensity level, L_{In} (c) sound pressure level, L_p (d) pressure-residual intensity index, δ_{pIo}.

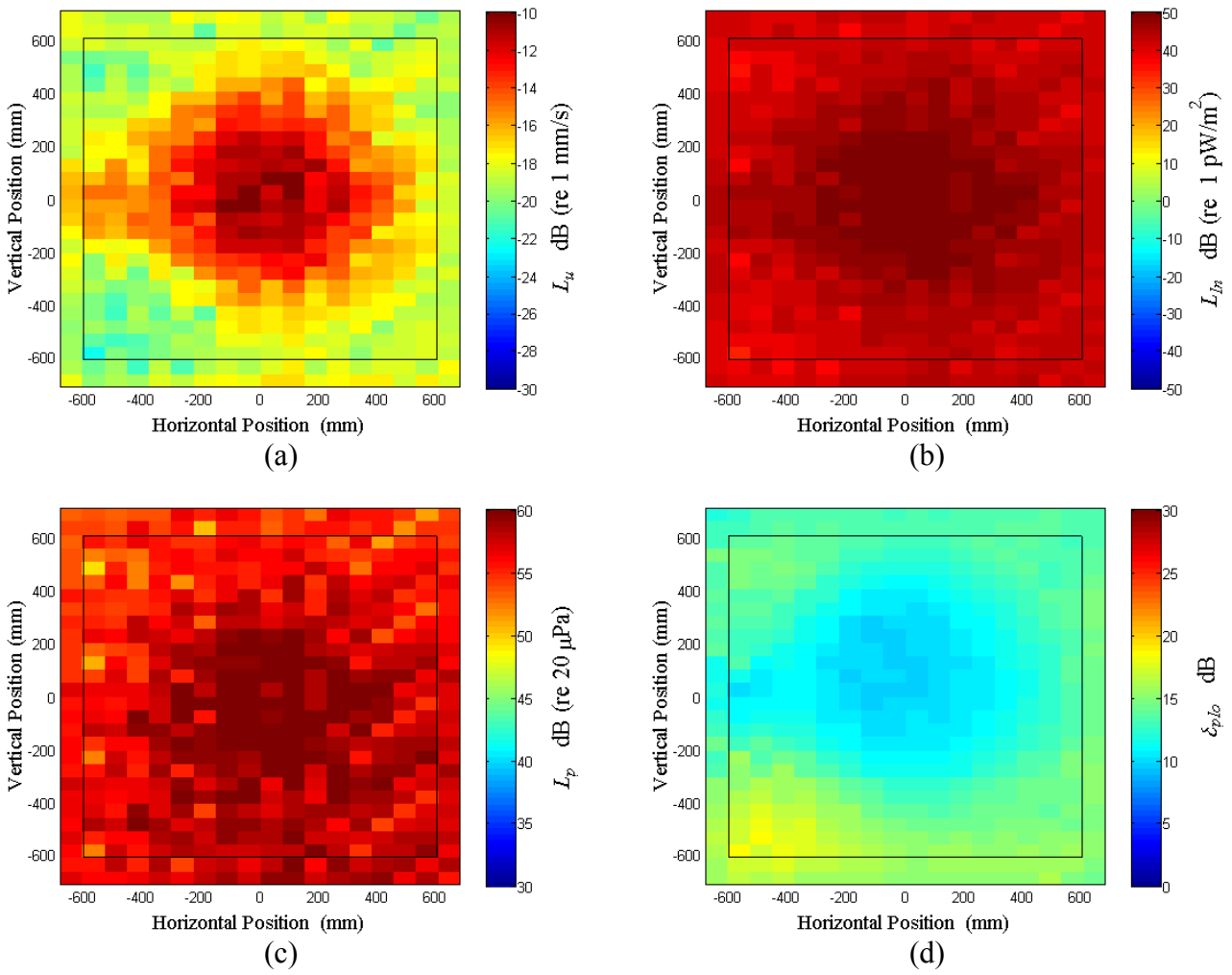

Figure C.23: Surface scan of Window C at 105 Hz (a) particle velocity level, L_u (b) normal signed sound intensity level, L_{In} (c) sound pressure level, L_p (d) pressure-residual intensity index, δ_{pIo}.

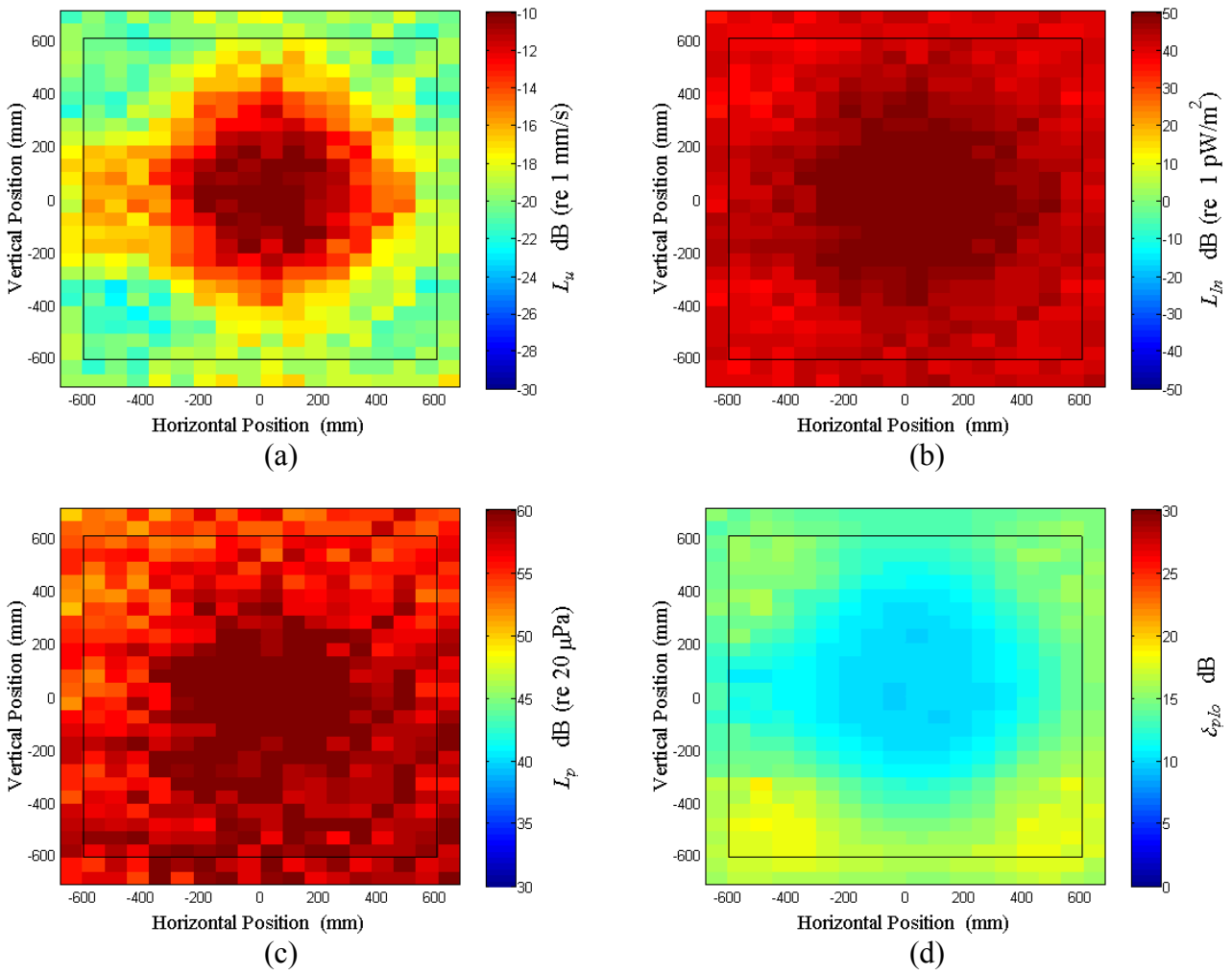

Figure C.24: Surface scan of Window C at 107.5 Hz (a) particle velocity level, L_u (b) normal signed sound intensity level, L_{In} (c) sound pressure level, L_p (d) pressure-residual intensity index, δ_{pIo}.

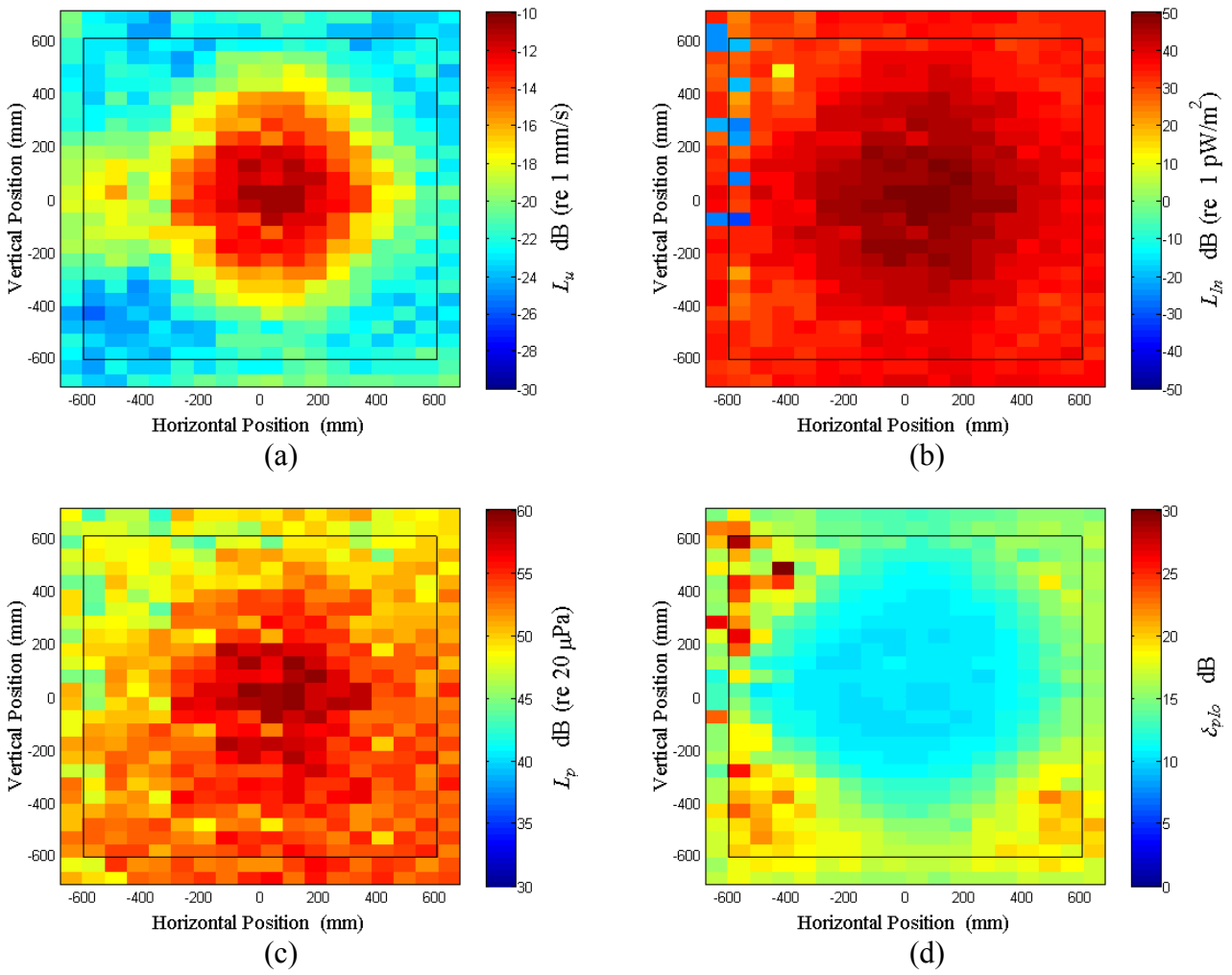

Figure C.25: Surface scan of Window C at 110 Hz (a) particle velocity level, L_u (b) normal signed sound intensity level, L_{In} (c) sound pressure level, L_p (d) pressure-residual intensity index, δ_{pIo}.

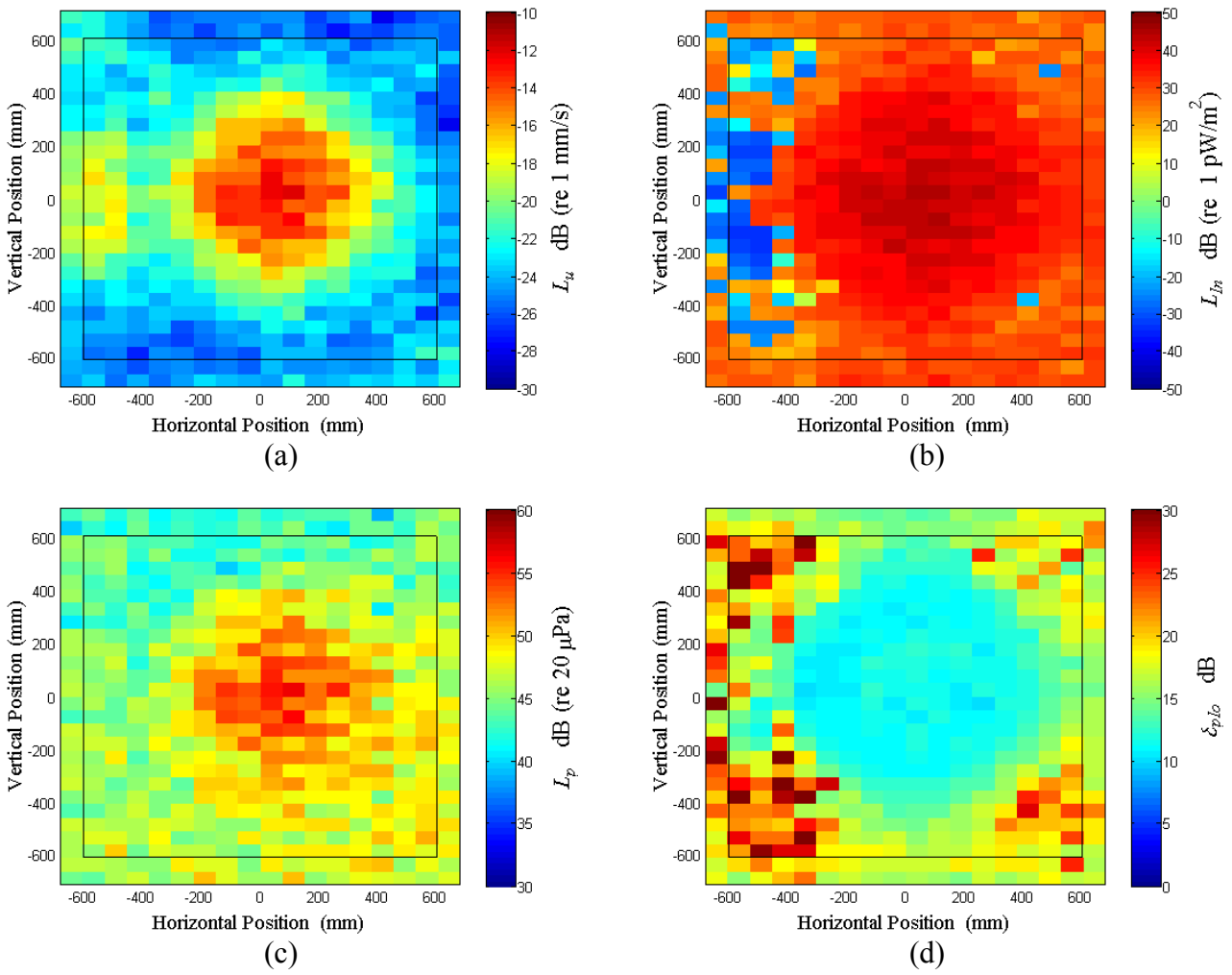

Figure C.26: Surface scan of Window C at 112.5 Hz (a) particle velocity level, L_u (b) normal signed sound intensity level, L_{In} (c) sound pressure level, L_p (d) pressure-residual intensity index, δ_{pIo}.

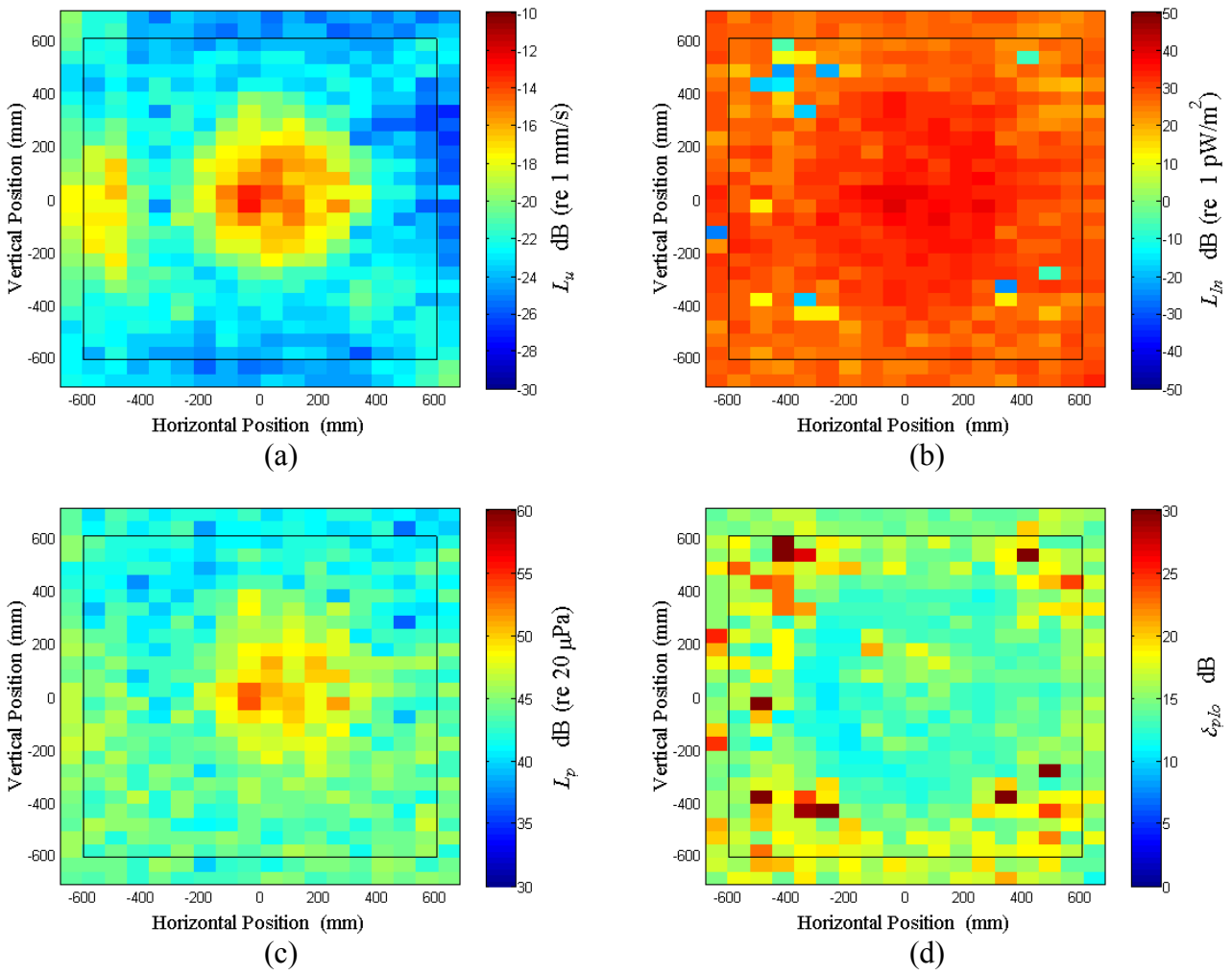

Figure C.27: Surface scan of Window C at 115 Hz (a) particle velocity level, L_u (b) normal signed sound intensity level, L_{In} (c) sound pressure level, L_p (d) pressure-residual intensity index, δ_{pIo}.

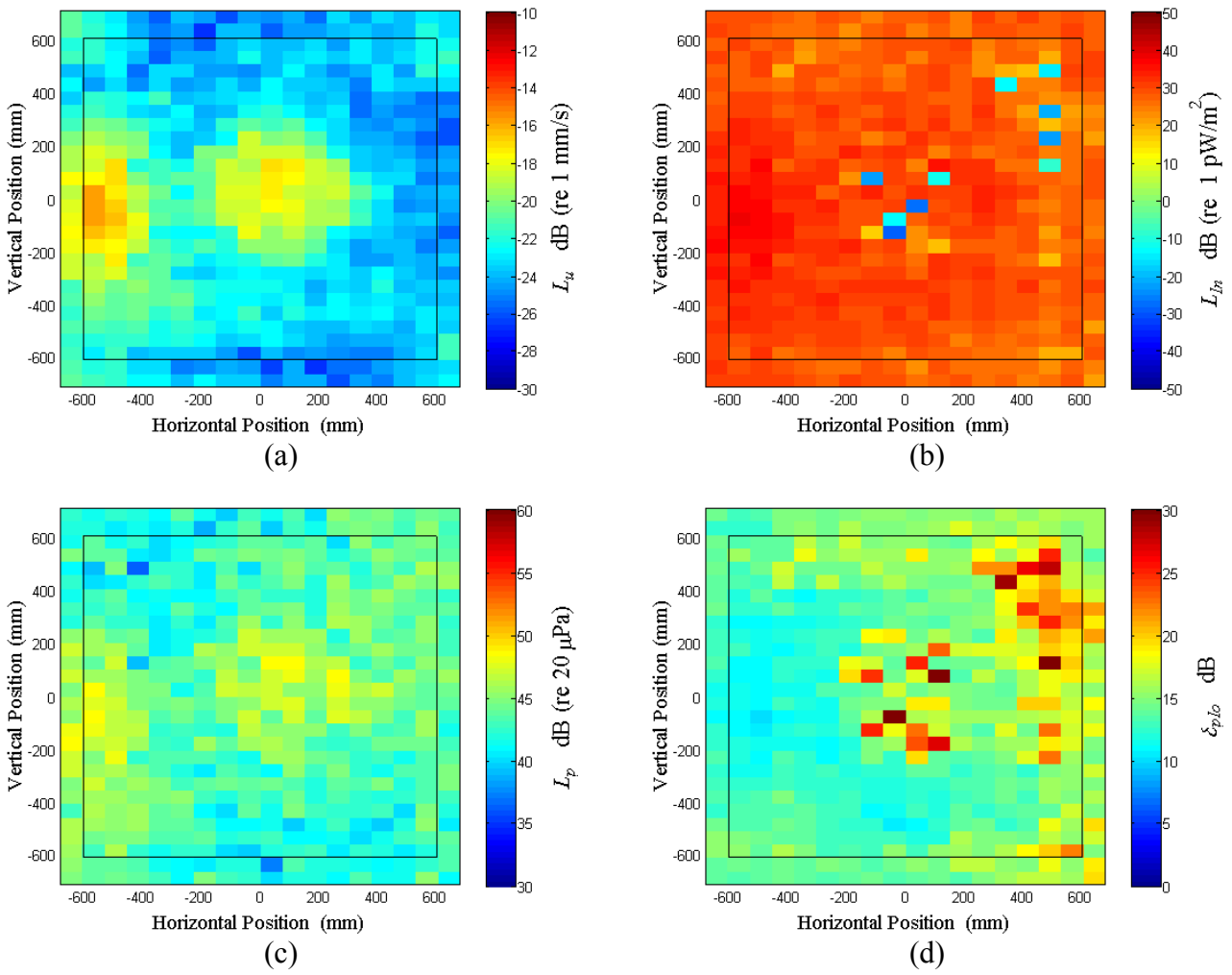

Figure C.28: Surface scan of Window C at 117.5 Hz (a) particle velocity level, L_u (b) normal signed sound intensity level, L_{In} (c) sound pressure level, L_p (d) pressure-residual intensity index, δ_{pIo}.

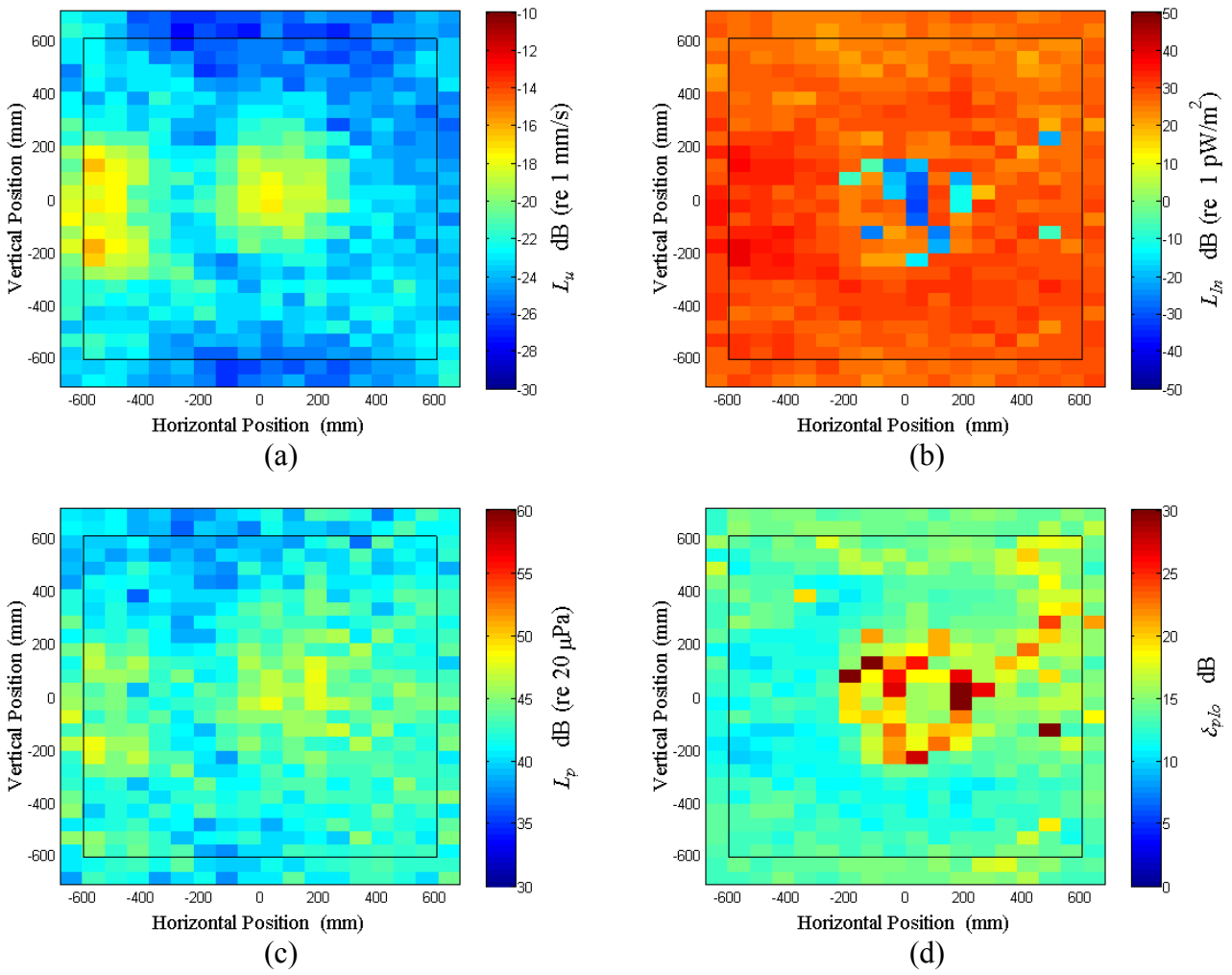

Figure C.29: Surface scan of Window C at 120 Hz (a) particle velocity level, L_u (b) normal signed sound intensity level, L_{In} (c) sound pressure level, L_p (d) pressure-residual intensity index, δ_{pIo}.

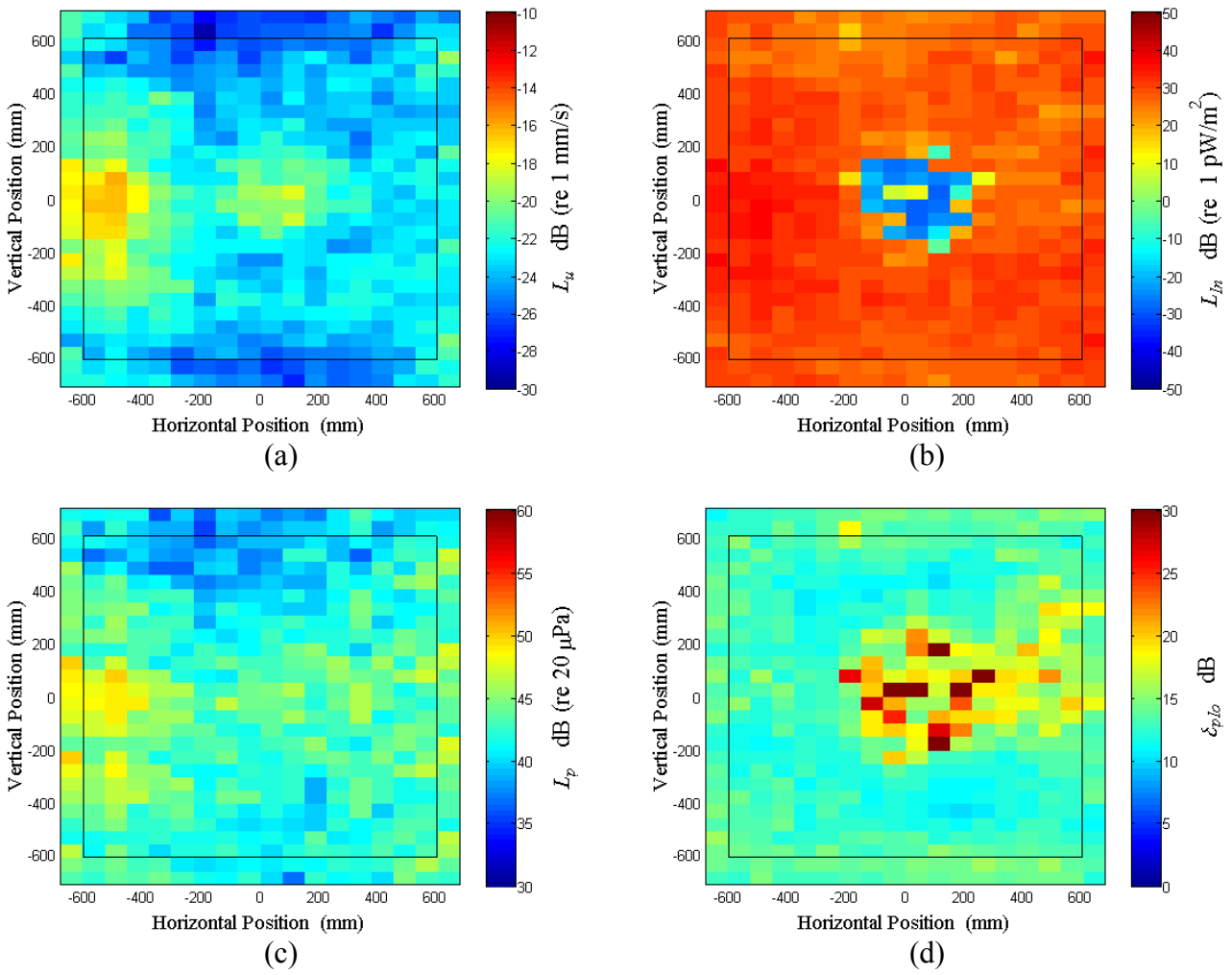

Figure C.30: Surface scan of Window C at 122.5 Hz (a) particle velocity level, L_u (b) normal signed sound intensity level, L_{In} (c) sound pressure level, L_p (d) pressure-residual intensity index, δ_{pIo}.

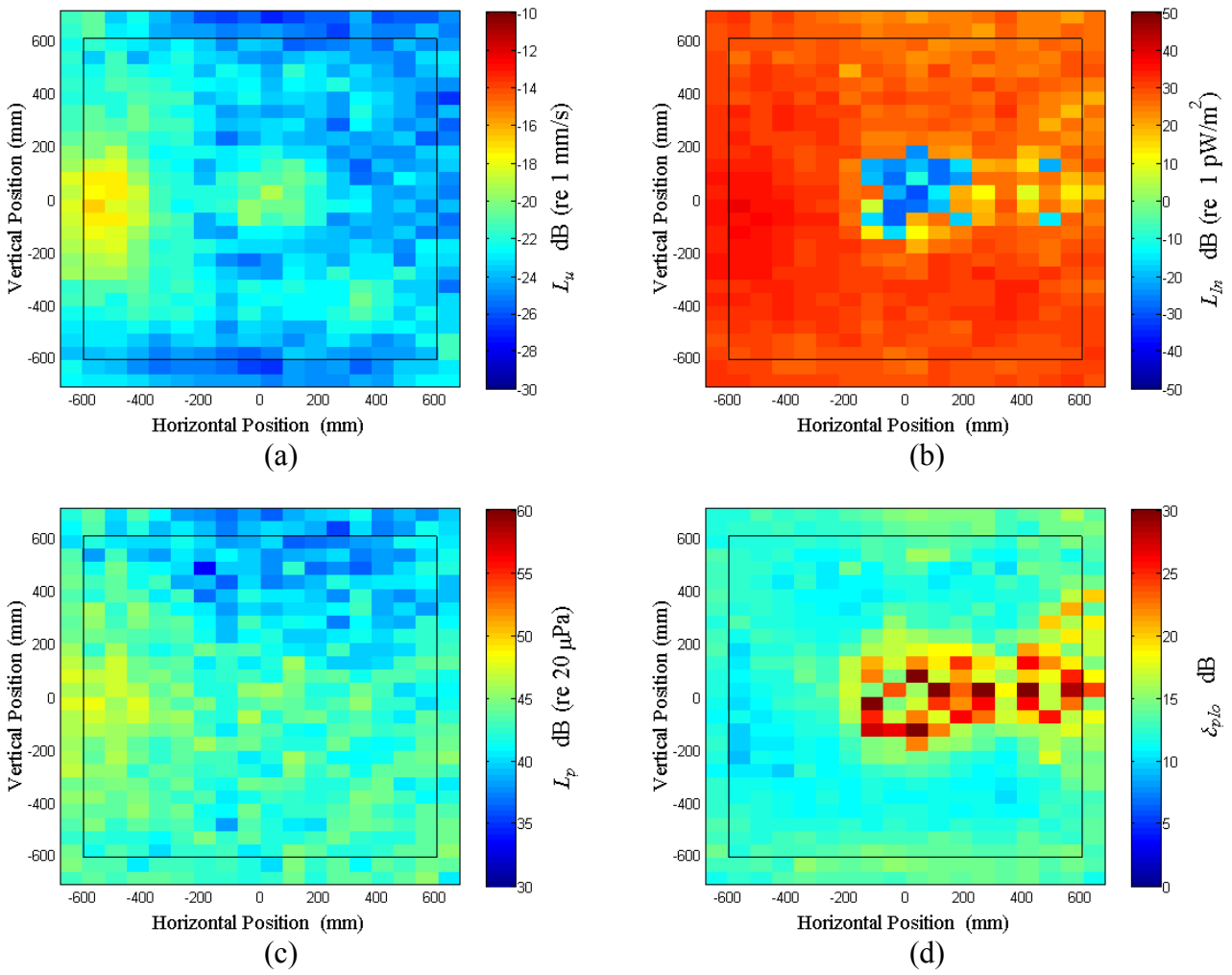

Figure C.31: Surface scan of Window C at 125 Hz (a) particle velocity level, L_u (b) normal signed sound intensity level, L_{In} (c) sound pressure level, L_p (d) pressure-residual 12ntensity index, δ_{pIo}.

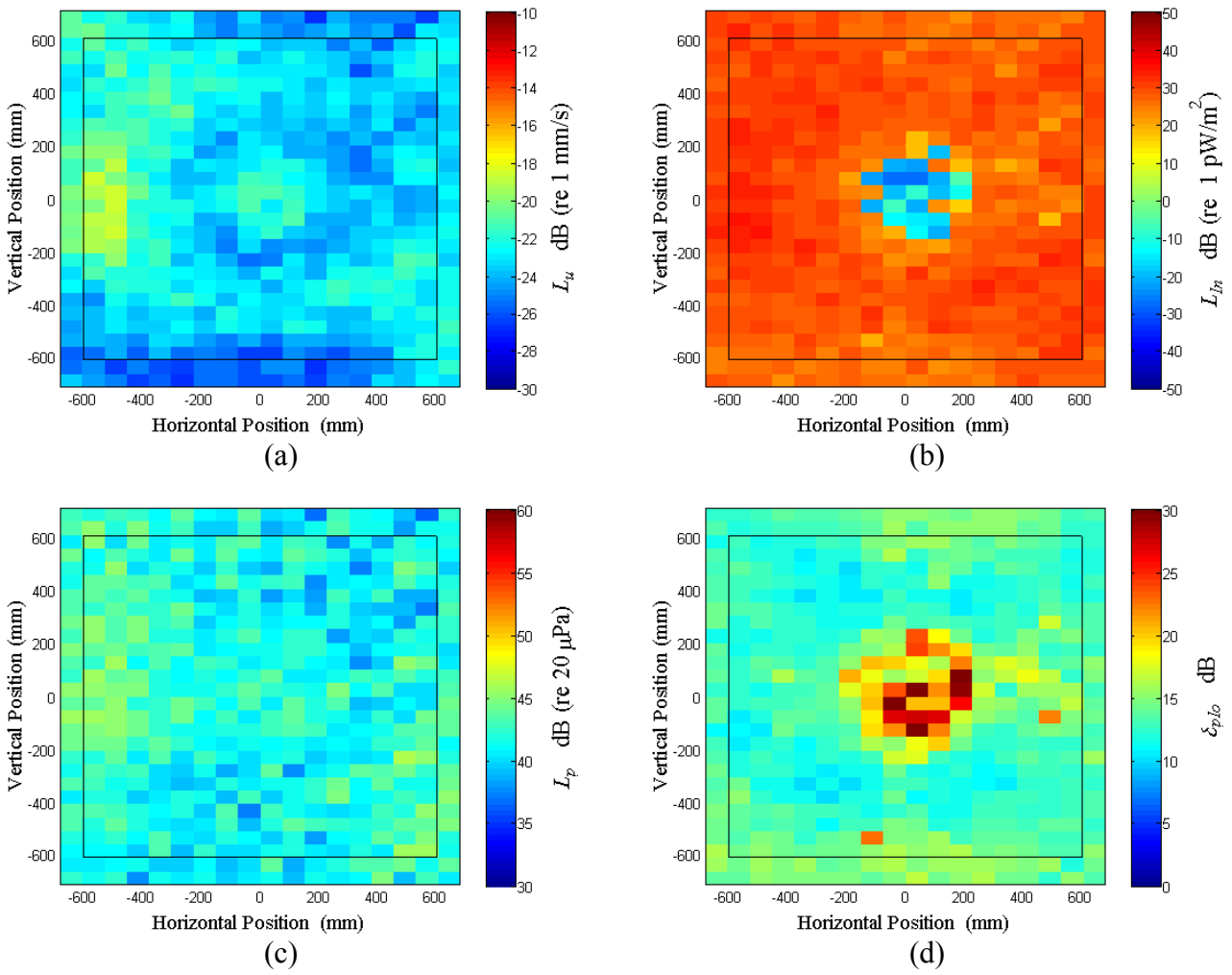

Figure C.32: Surface scan of Window C at 127.5 Hz (a) particle velocity level, L_u (b) normal signed sound intensity level, L_{In} (c) sound pressure level, L_p (d) pressure-residual intensity index, δ_{pIo}.

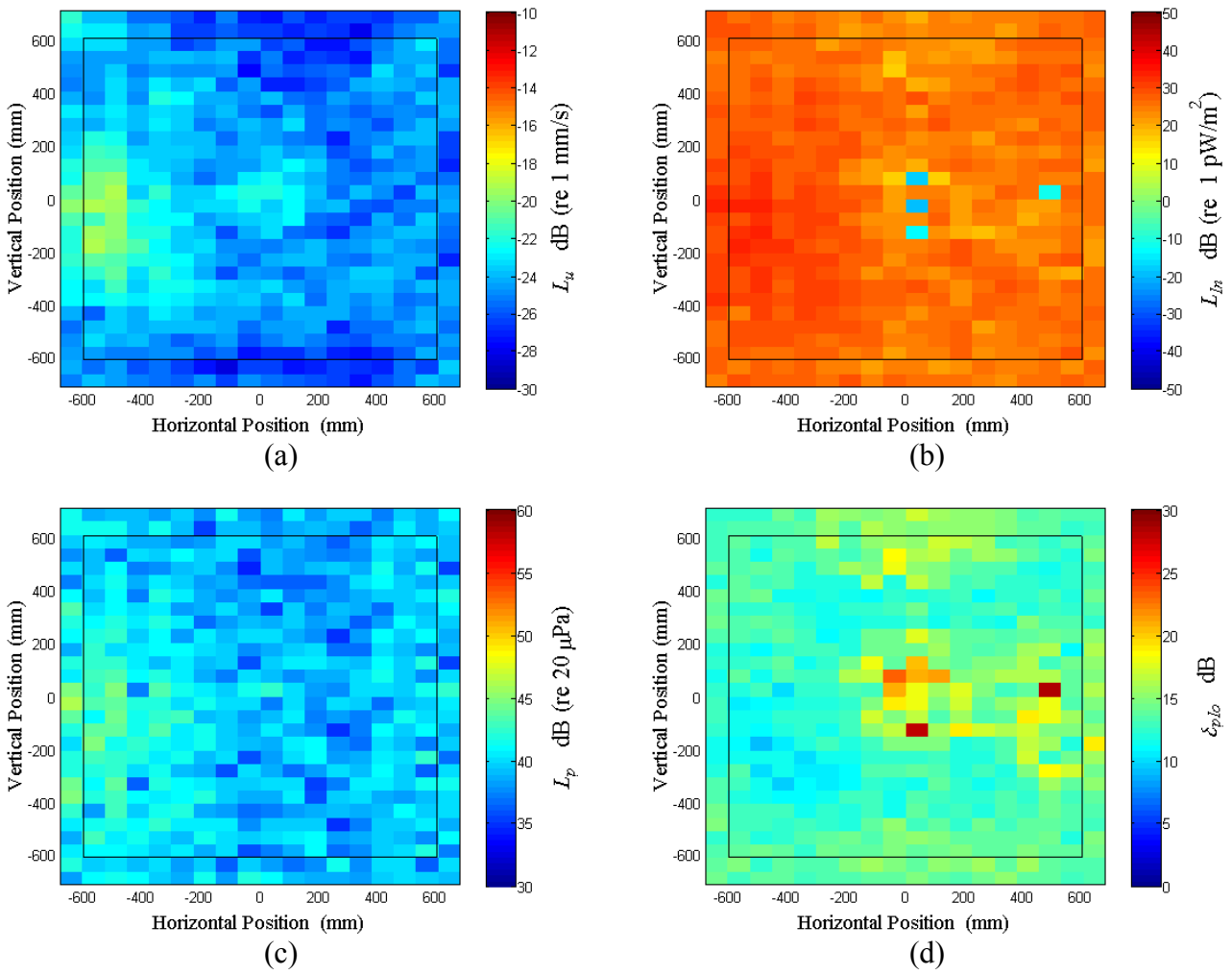

Figure C.33: Surface scan of Window C at 130 Hz (a) particle velocity level, L_u (b) normal signed sound intensity level, L_{In} (c) sound pressure level, L_p (d) pressure-residual intensity index, δ_{pIo}.

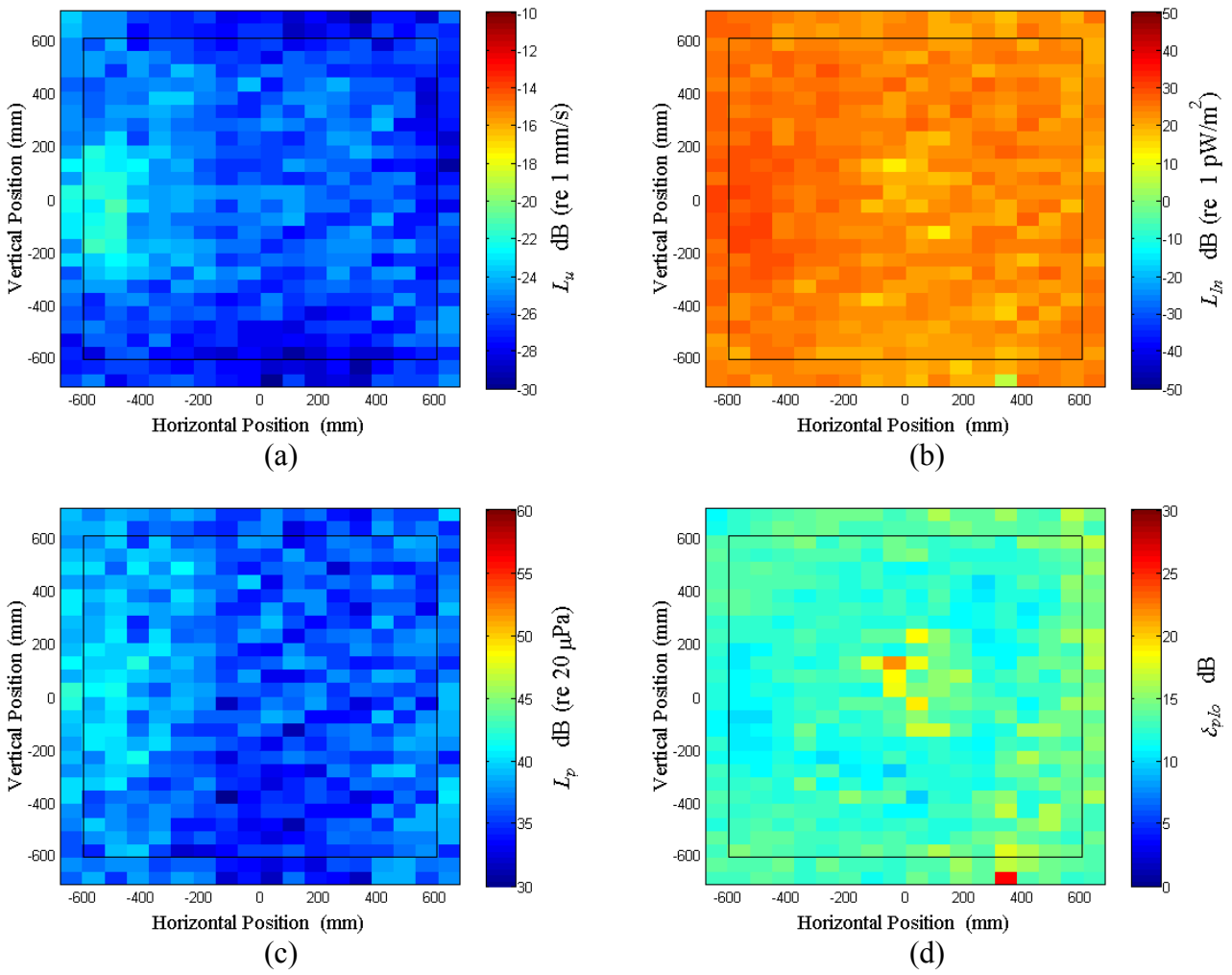

Figure C.34: Surface scan of Window C at 140 Hz (a) particle velocity level, L_u (b) normal signed sound intensity level, L_{In} (c) sound pressure level, L_p (d) pressure-residual intensity index, δ_{pIo}.

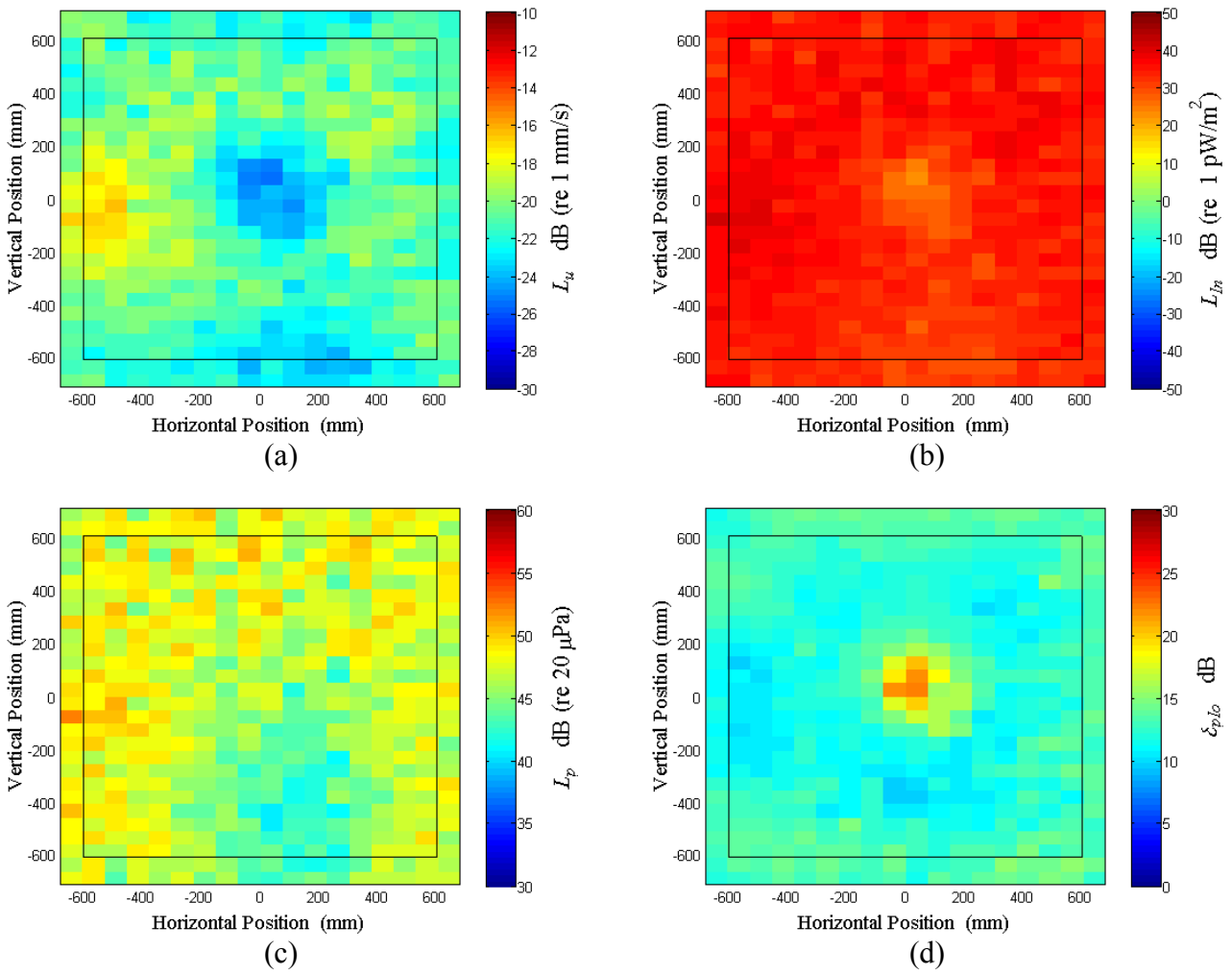

Figure C.35: Surface scan of Window C at 150 Hz (a) particle velocity level, L_u (b) normal signed sound intensity level, L_{In} (c) sound pressure level, L_p (d) pressure-residual intensity index, δ_{pIo}.

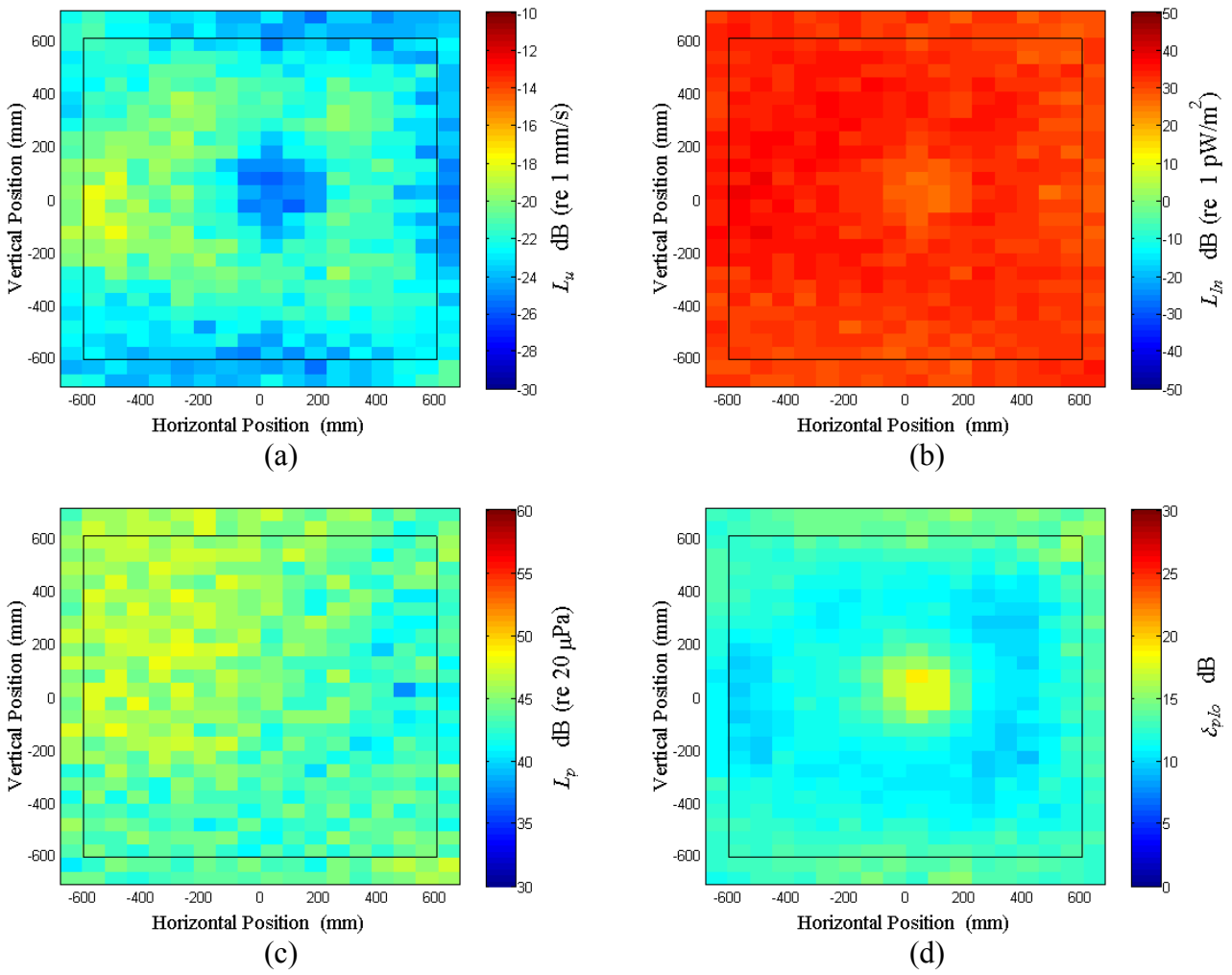

Figure C.36: Surface scan of Window C at 160 Hz (a) particle velocity level, L_u (b) normal signed sound intensity level, L_{In} (c) sound pressure level, L_p (d) pressure-residual intensity index, δ_{pIo}.

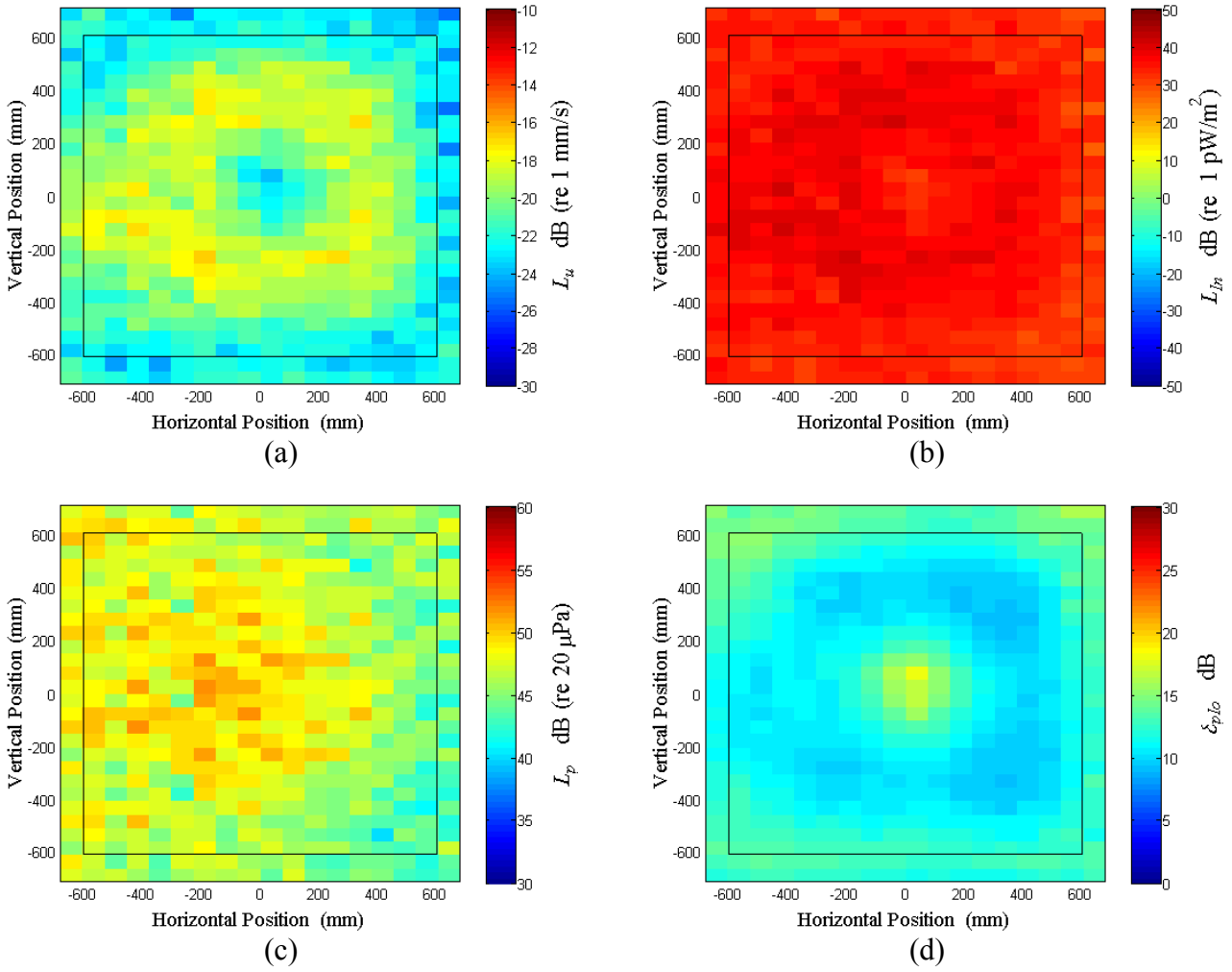

Figure C.37: Surface scan of Window C at 170 Hz (a) particle velocity level, L_u (b) normal signed sound intensity level, L_{In} (c) sound pressure level, L_p (d) pressure-residual intensity index, δ_{pIo}.

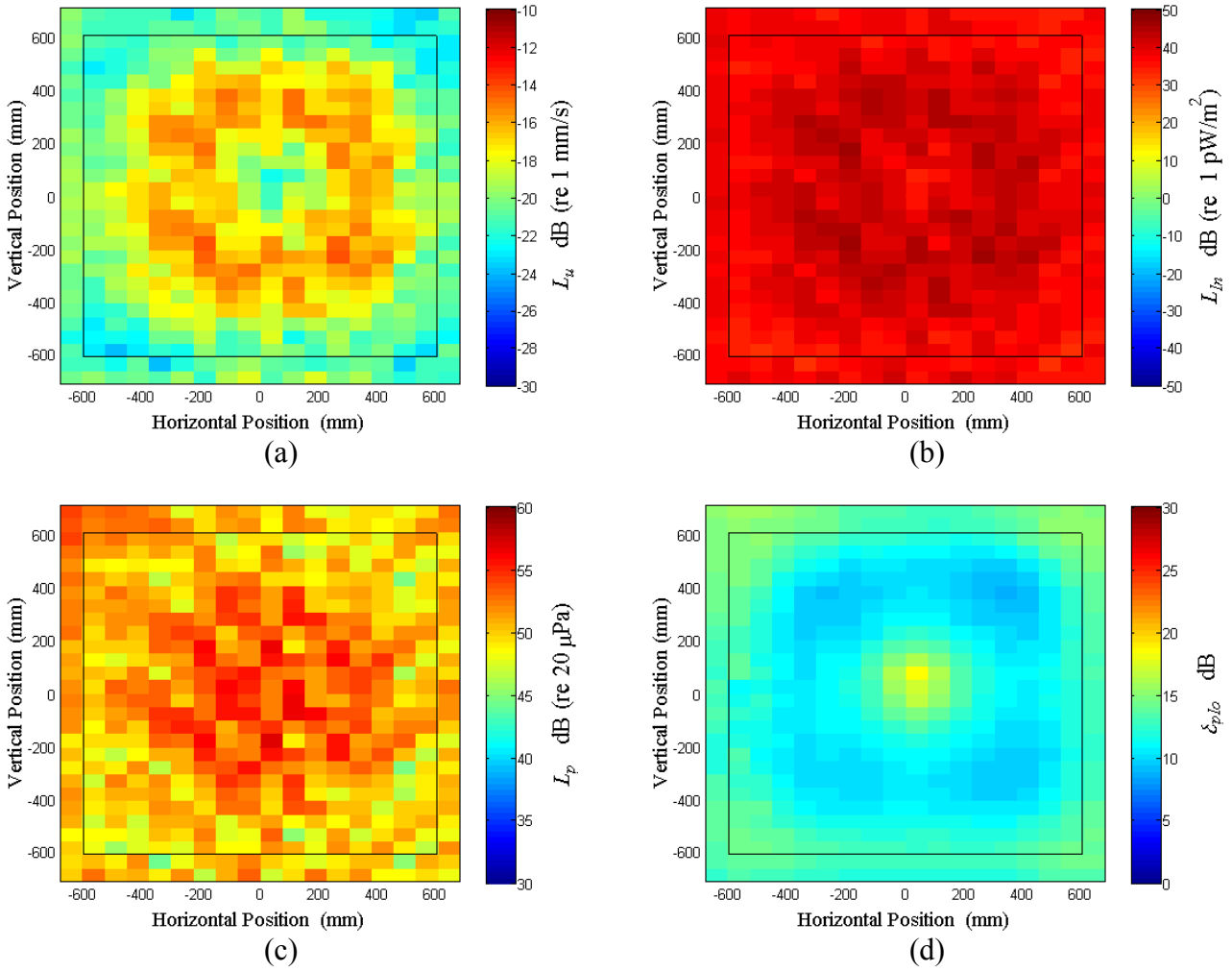

Figure C.38: Surface scan of Window C at 180 Hz (a) particle velocity level, L_u (b) normal signed sound intensity level, L_{In} (c) sound pressure level, L_p (d) pressure-residual intensity index, δ_{pIo}.

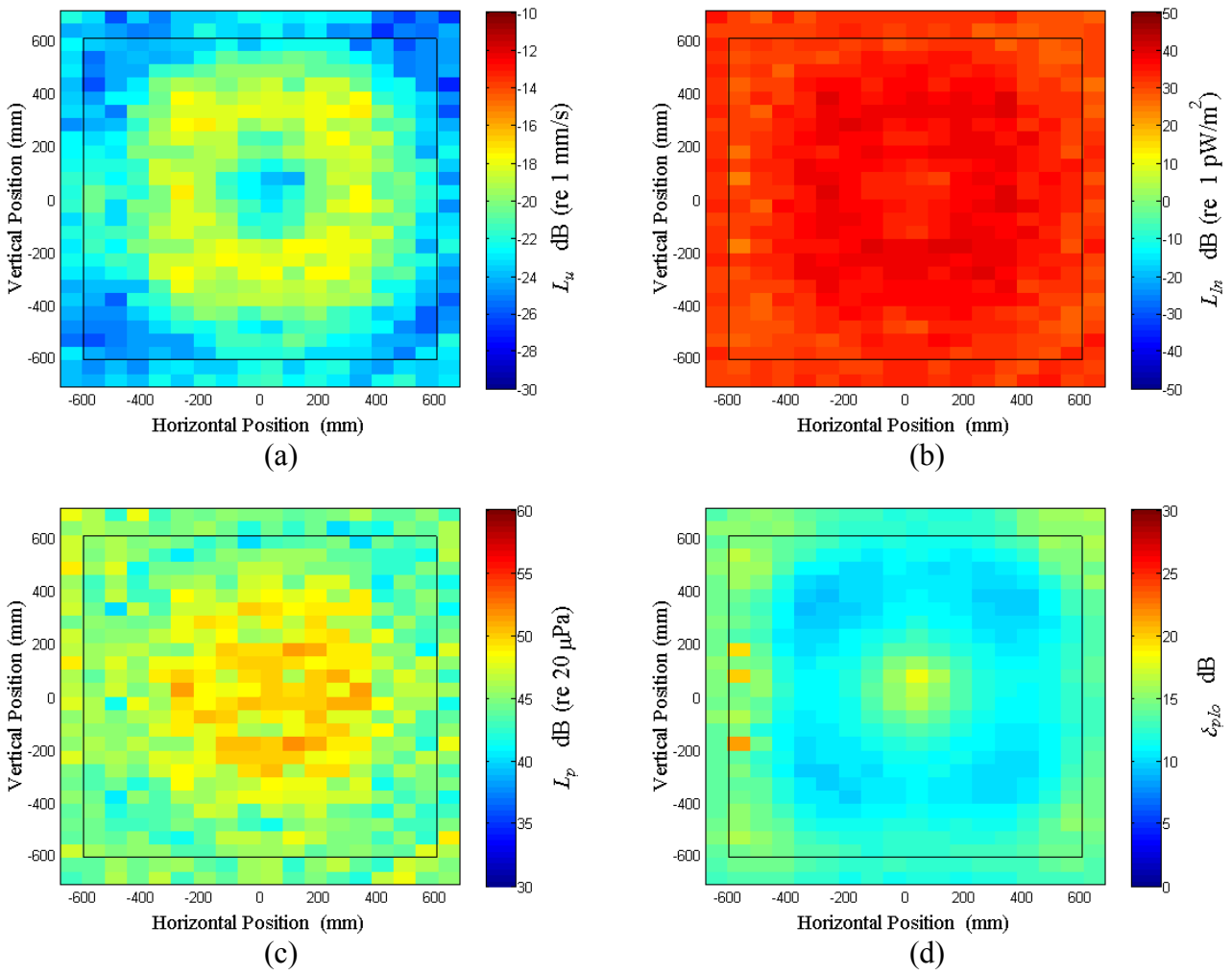

Figure C.39: Surface scan of Window C at 190 Hz (a) particle velocity level, L_u (b) normal signed sound intensity level, L_{In} (c) sound pressure level, L_p (d) pressure-residual intensity index, δ_{pIo}.

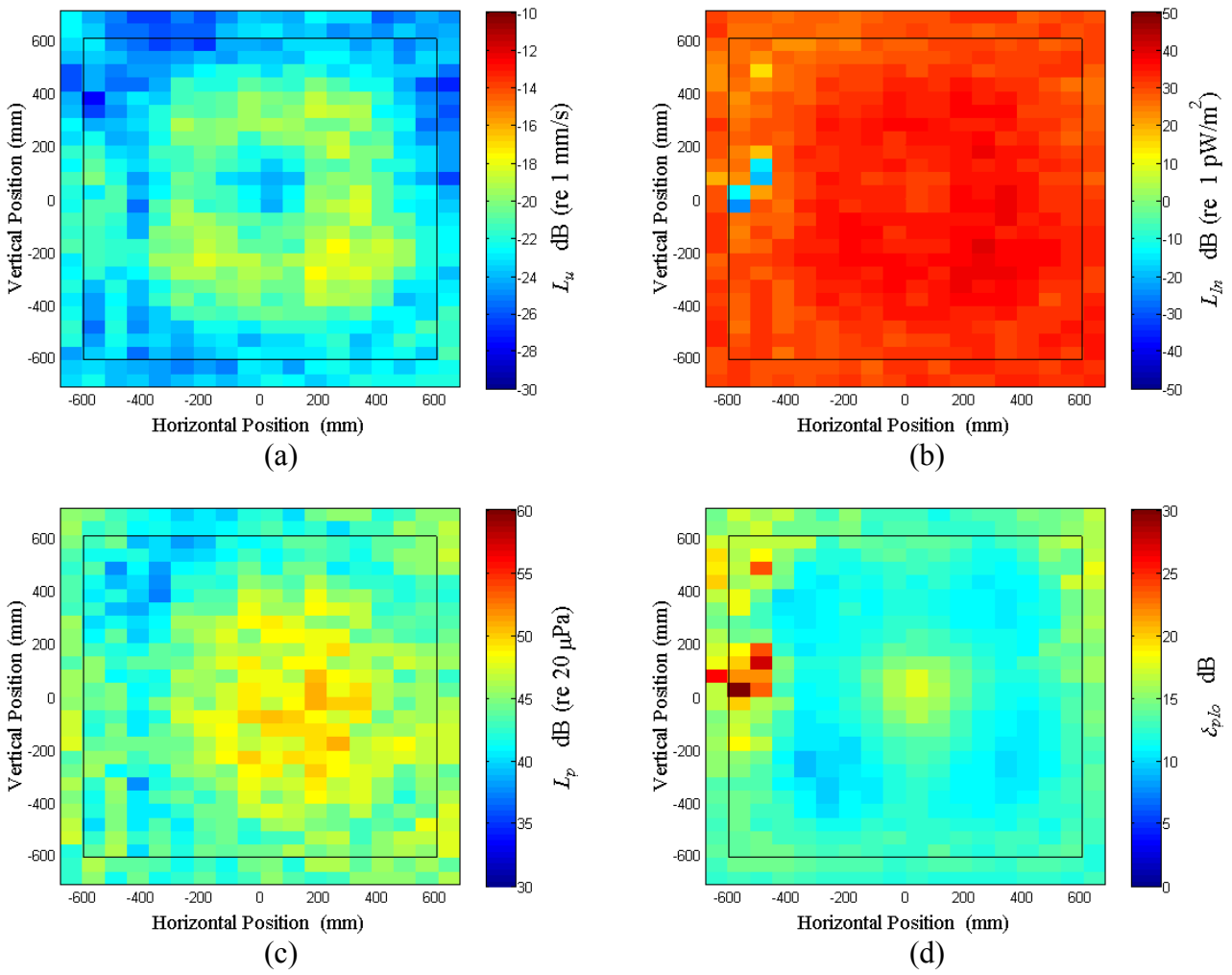

Figure C.40: Surface scan of Window C at 200 Hz (a) particle velocity level, L_u (b) normal signed sound intensity level, L_{In} (c) sound pressure level, L_p (d) pressure-residual intensity index, δ_{pIo}.

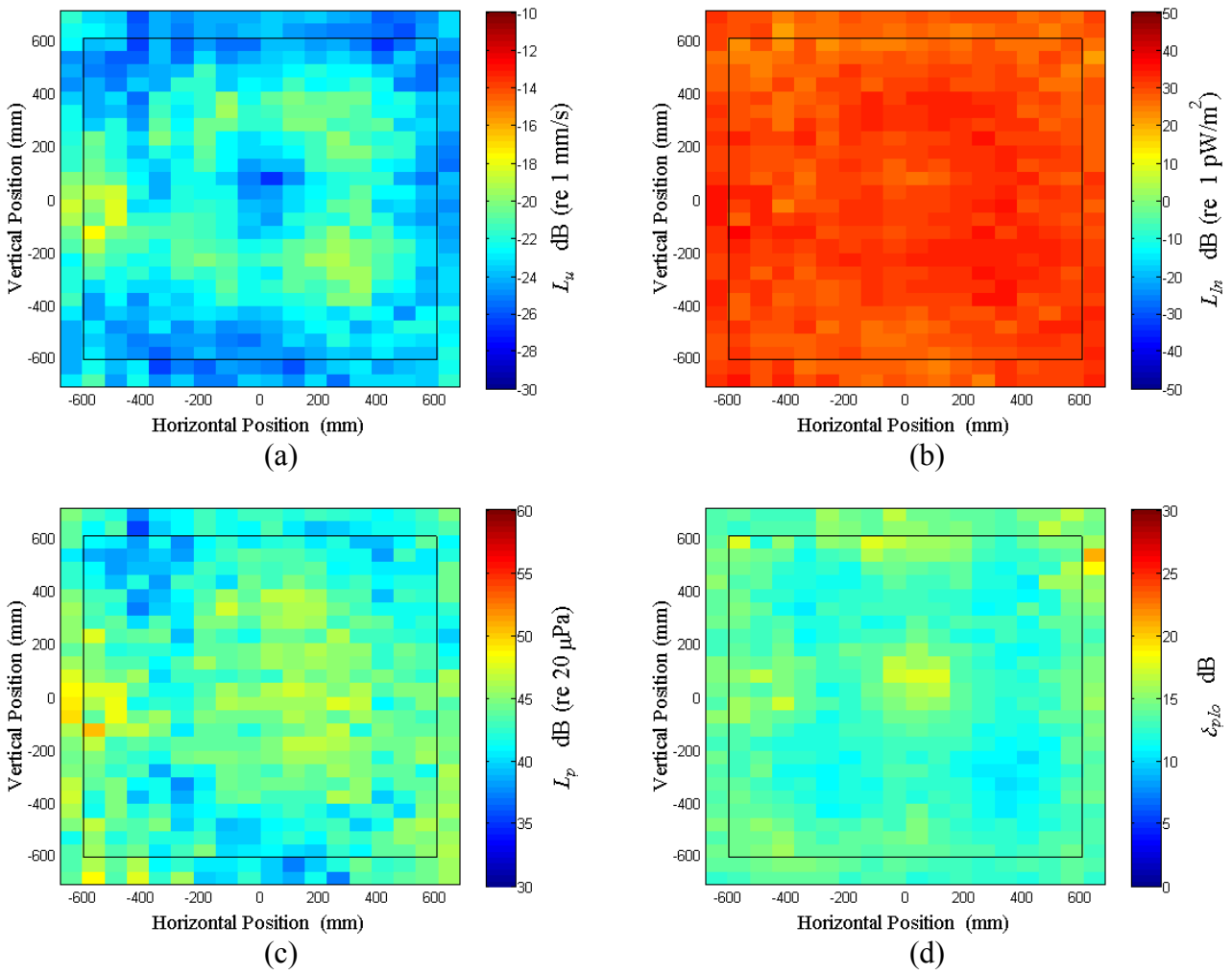

Figure C.41: Surface scan of Window C at 210 Hz (a) particle velocity level, L_u (b) normal signed sound intensity level, L_{In} (c) sound pressure level, L_p (d) pressure-residual intensity index, δ_{pIo}.

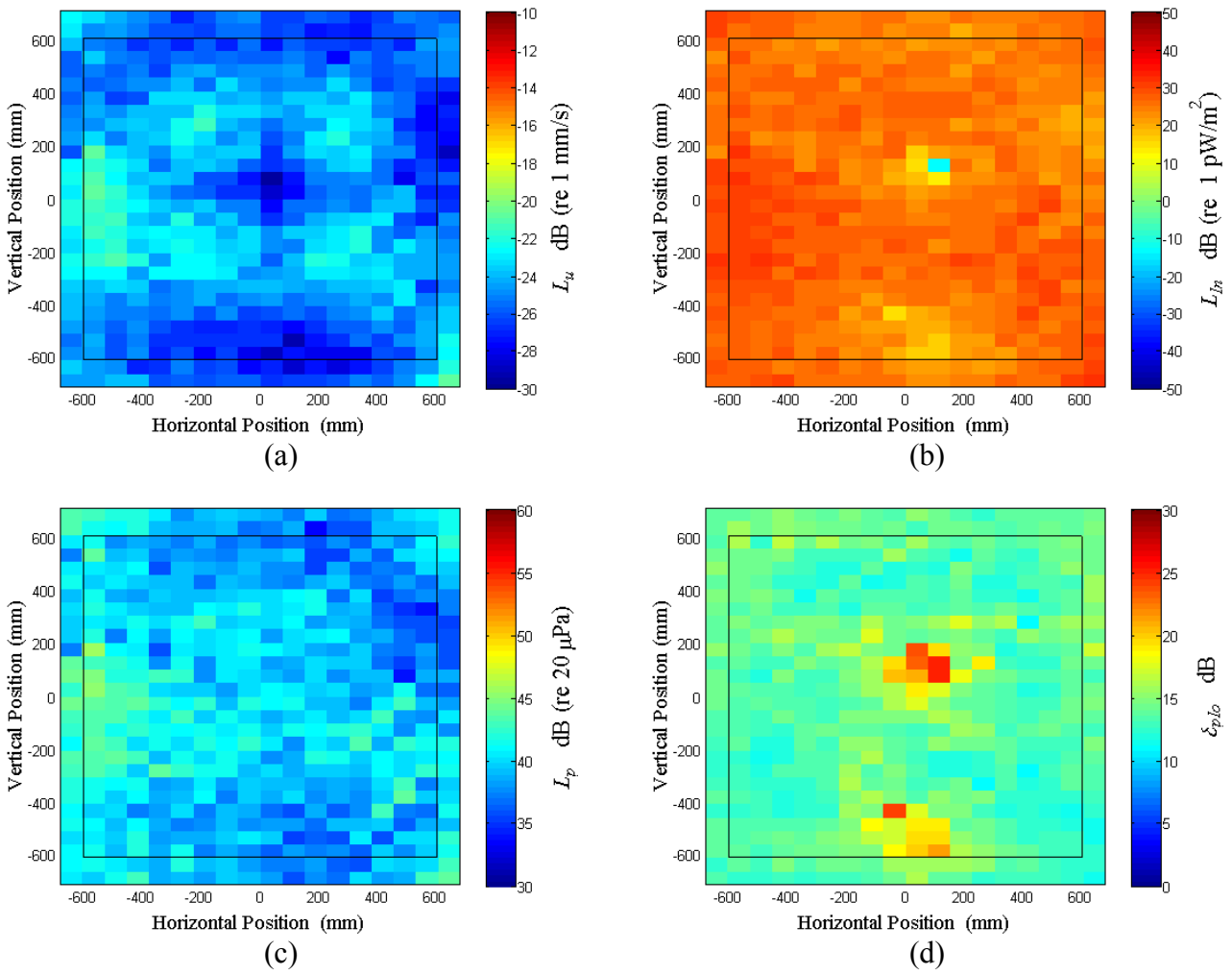

Figure C.42: Surface scan of Window C at 220 Hz (a) particle velocity level, L_u (b) normal signed sound intensity level, L_{In} (c) sound pressure level, L_p (d) pressure-residual intensity index, δ_{pIo}.

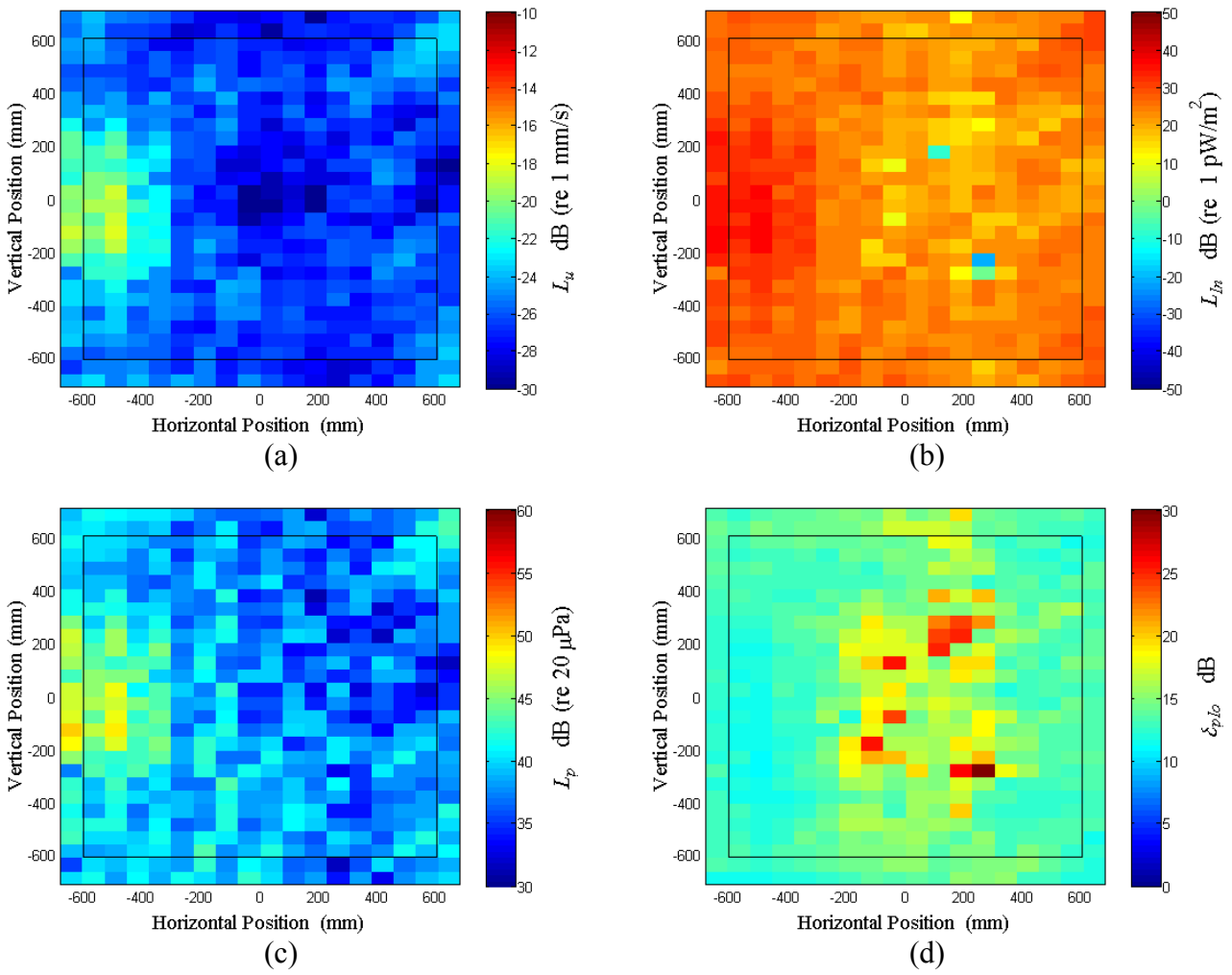

Figure C.43: Surface scan of Window C at 230 Hz (a) particle velocity level, L_u (b) normal signed sound intensity level, L_{In} (c) sound pressure level, L_p (d) pressure-residual intensity index, δ_{pIo}.

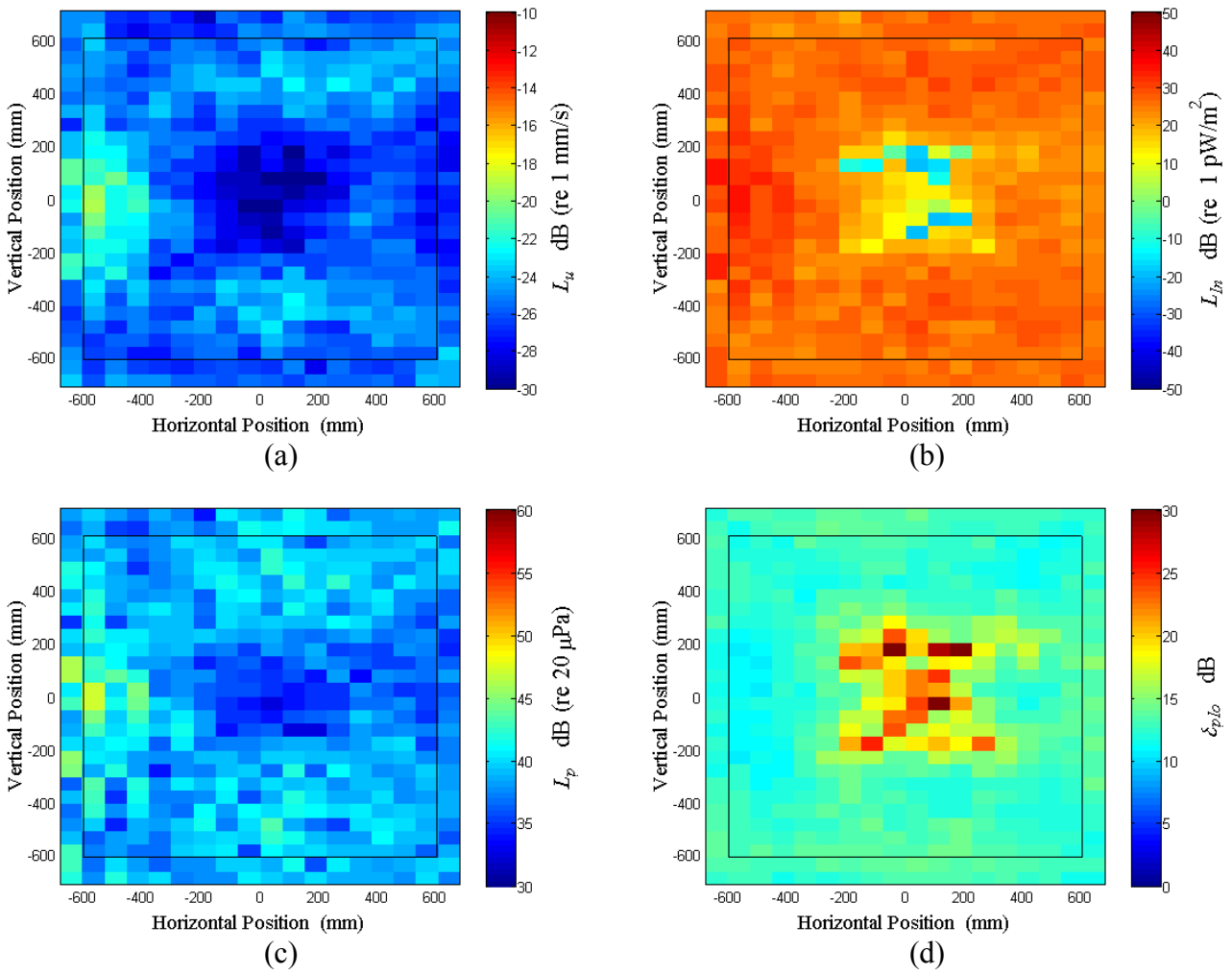

Figure C.44: Surface scan of Window C at 240 Hz (a) particle velocity level, L_u (b) normal signed sound intensity level, L_{In} (c) sound pressure level, L_p (d) pressure-residual intensity index, δ_{pIo}.

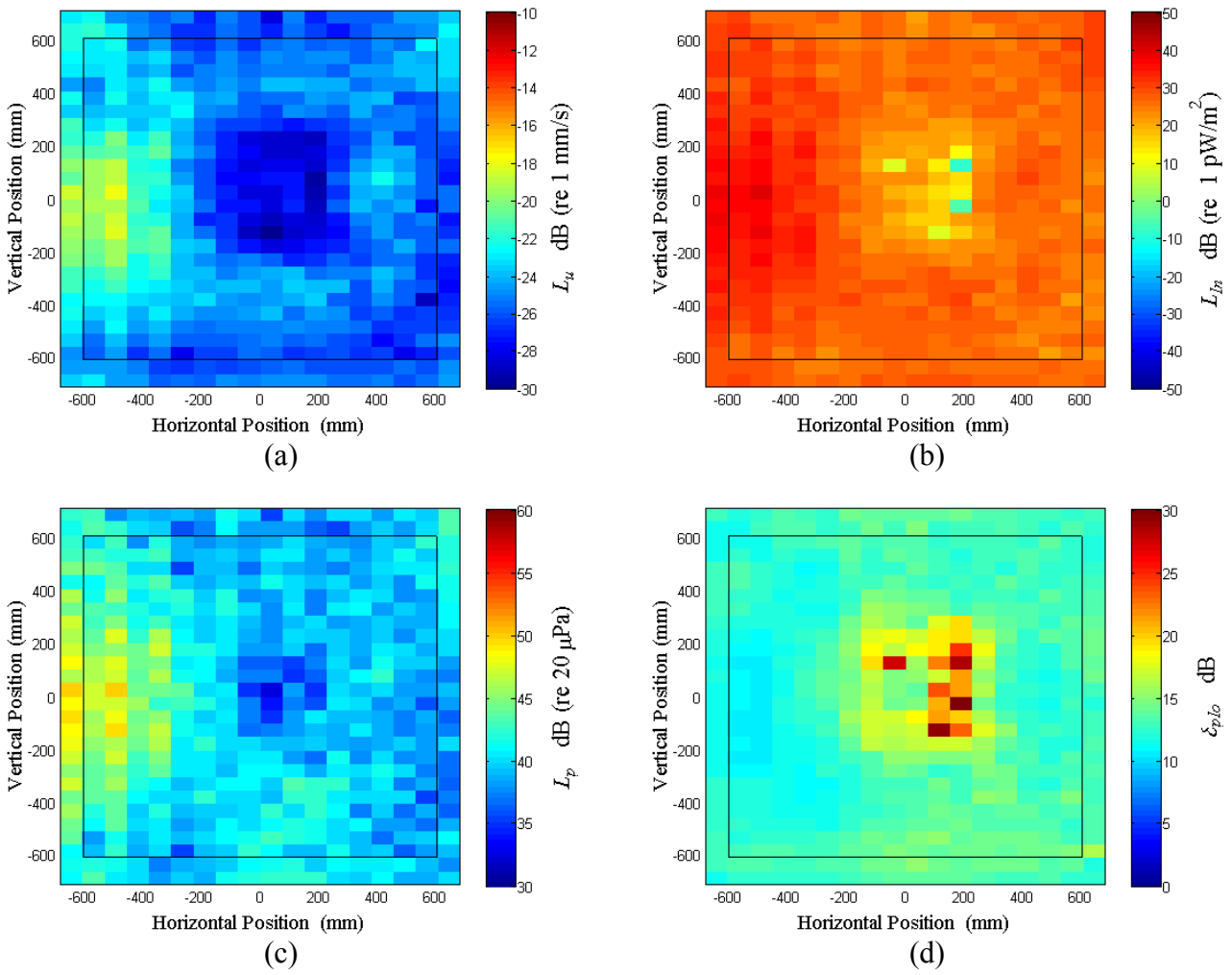

Figure C.45: Surface scan of Window C at 250 Hz (a) particle velocity level, L_u (b) normal signed sound intensity level, L_{In} (c) sound pressure level, L_p (d) pressure-residual intensity index, δ_{pIo}.

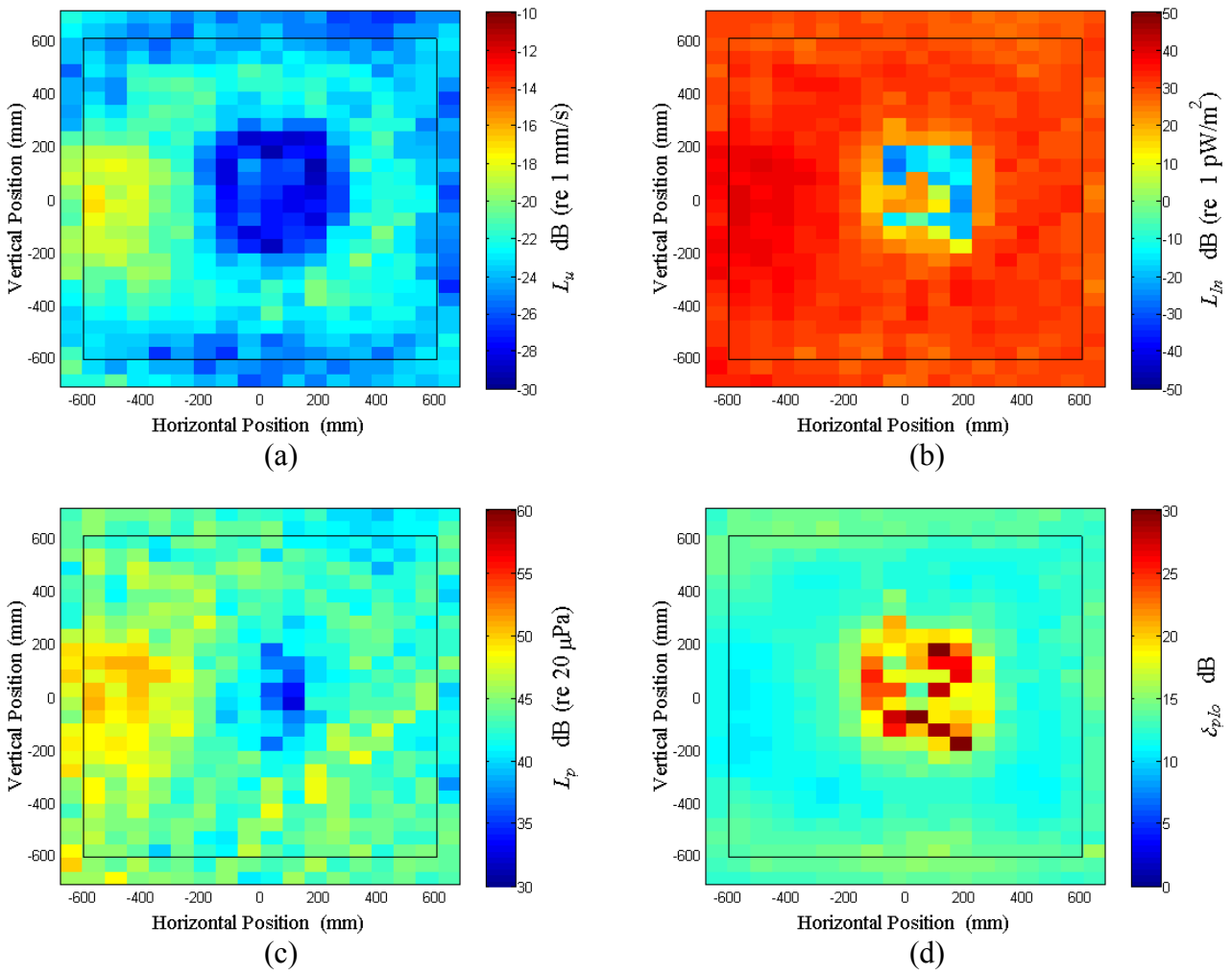

Figure C.46: Surface scan of Window C at 260 Hz (a) particle velocity level, L_u (b) normal signed sound intensity level, L_{In} (c) sound pressure level, L_p (d) pressure-residual intensity index, δ_{pIo}.

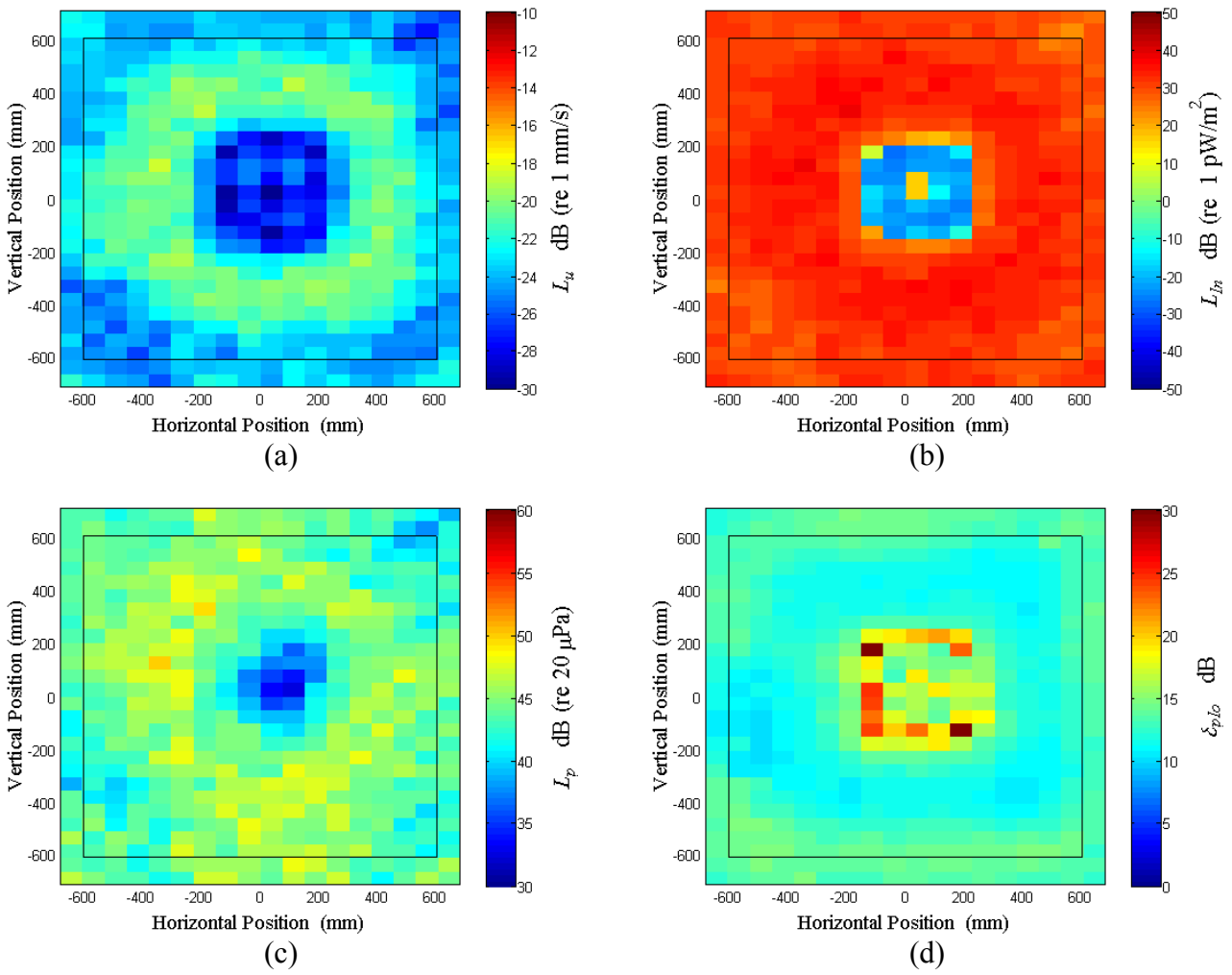

Figure C.47: Surface scan of Window C at 270 Hz (a) particle velocity level, L_u (b) normal signed sound intensity level, L_{In} (c) sound pressure level, L_p (d) pressure-residual intensity index, δ_{pIo}.

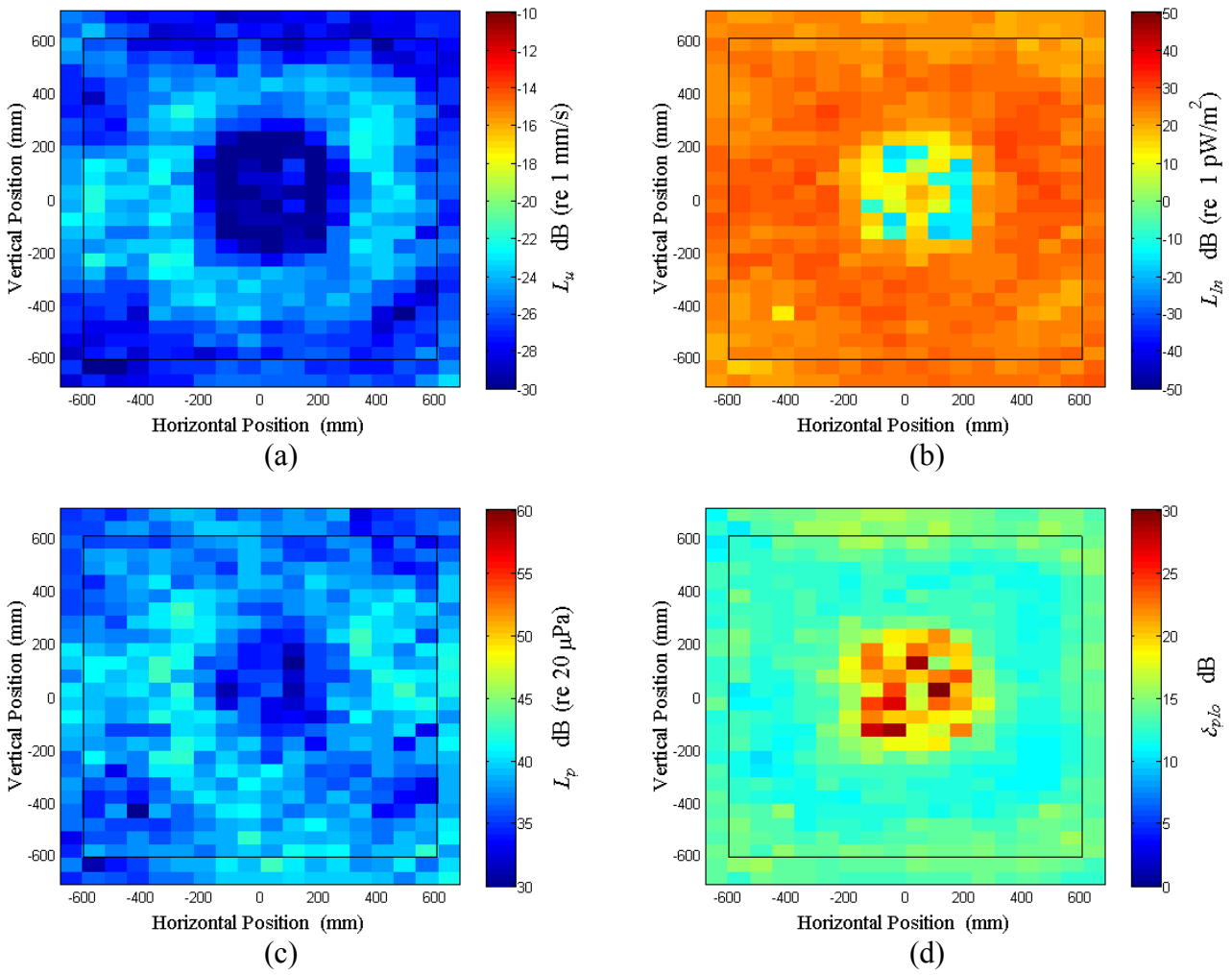

Figure C.48: Surface scan of Window C at 280 Hz (a) particle velocity level, L_u (b) normal signed sound intensity level, L_{In} (c) sound pressure level, L_p (d) pressure-residual intensity index, δ_{pIo}.

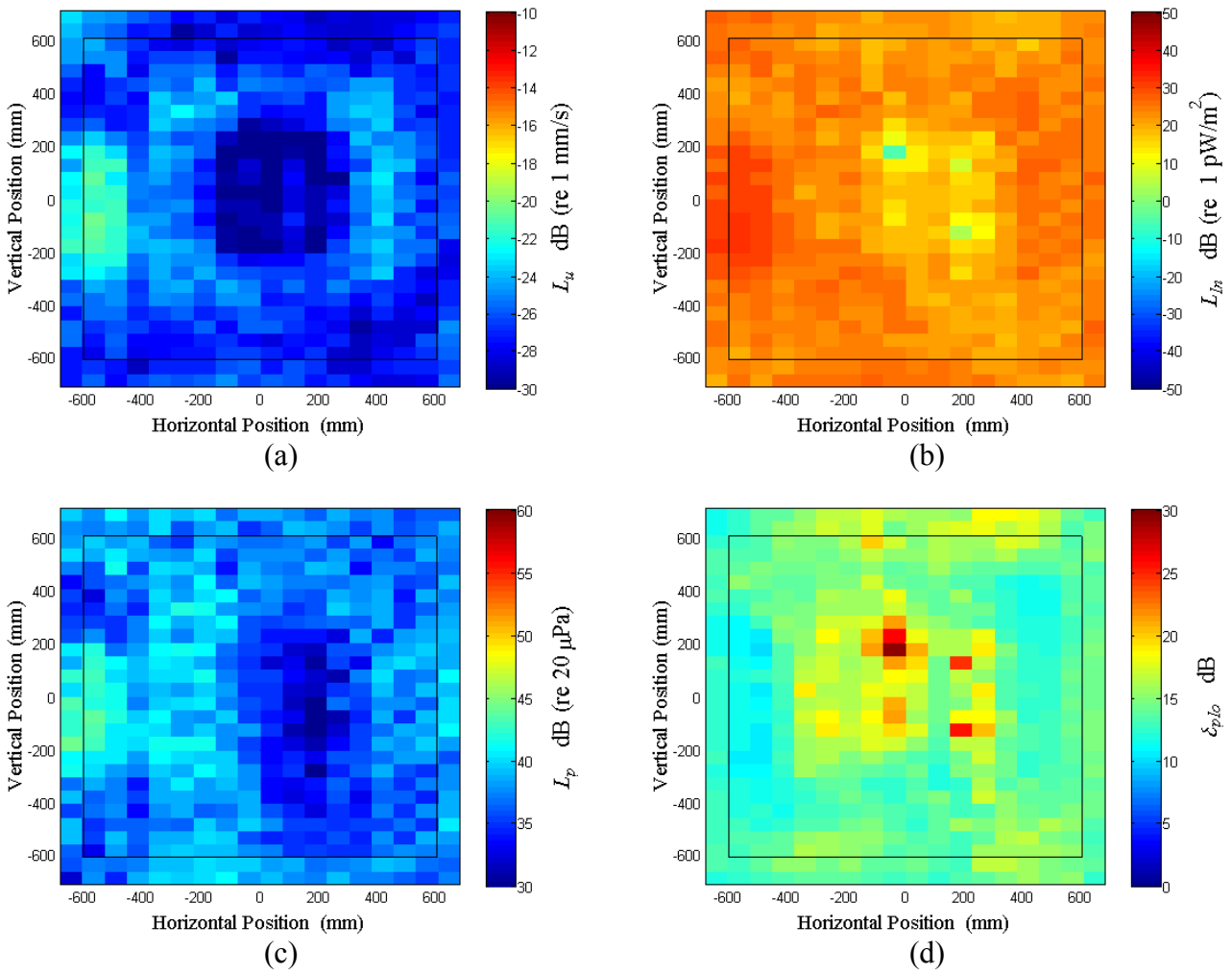

Figure C.49: Surface scan of Window C at 290 Hz (a) particle velocity level, L_u (b) normal signed sound intensity level, L_{In} (c) sound pressure level, L_p (d) pressure-residual intensity index, δ_{pIo}.

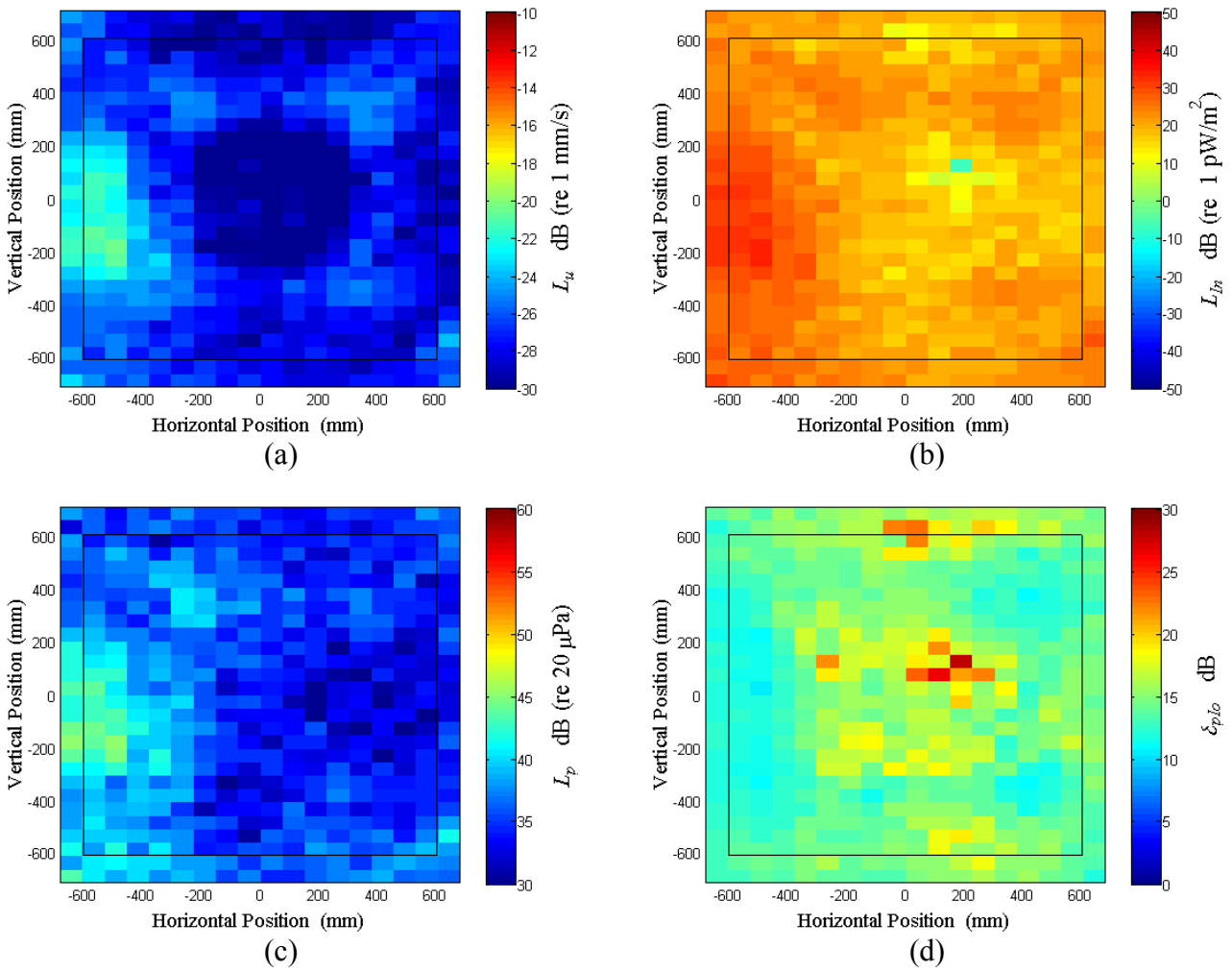

Figure C.50: Surface scan of Window C at 300 Hz (a) particle velocity level, L_u (b) normal signed sound intensity level, L_{In} (c) sound pressure level, L_p (d) pressure-residual intensity index, δ_{pIo}.

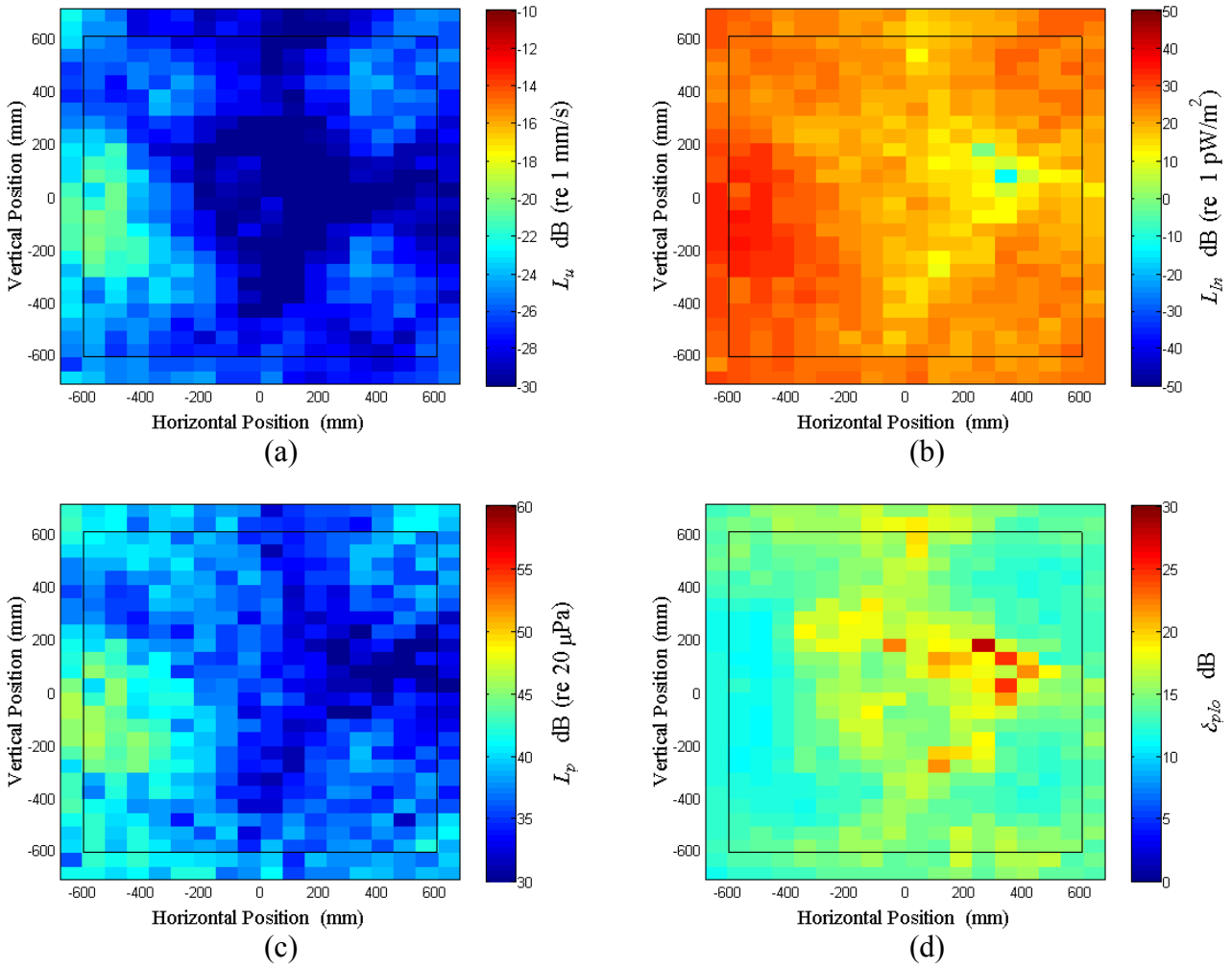

Figure C.51: Surface scan of Window C at 310 Hz (a) particle velocity level, L_u (b) normal signed sound intensity level, L_{In} (c) sound pressure level, L_p (d) pressure-residual intensity index, δ_{pIo}.

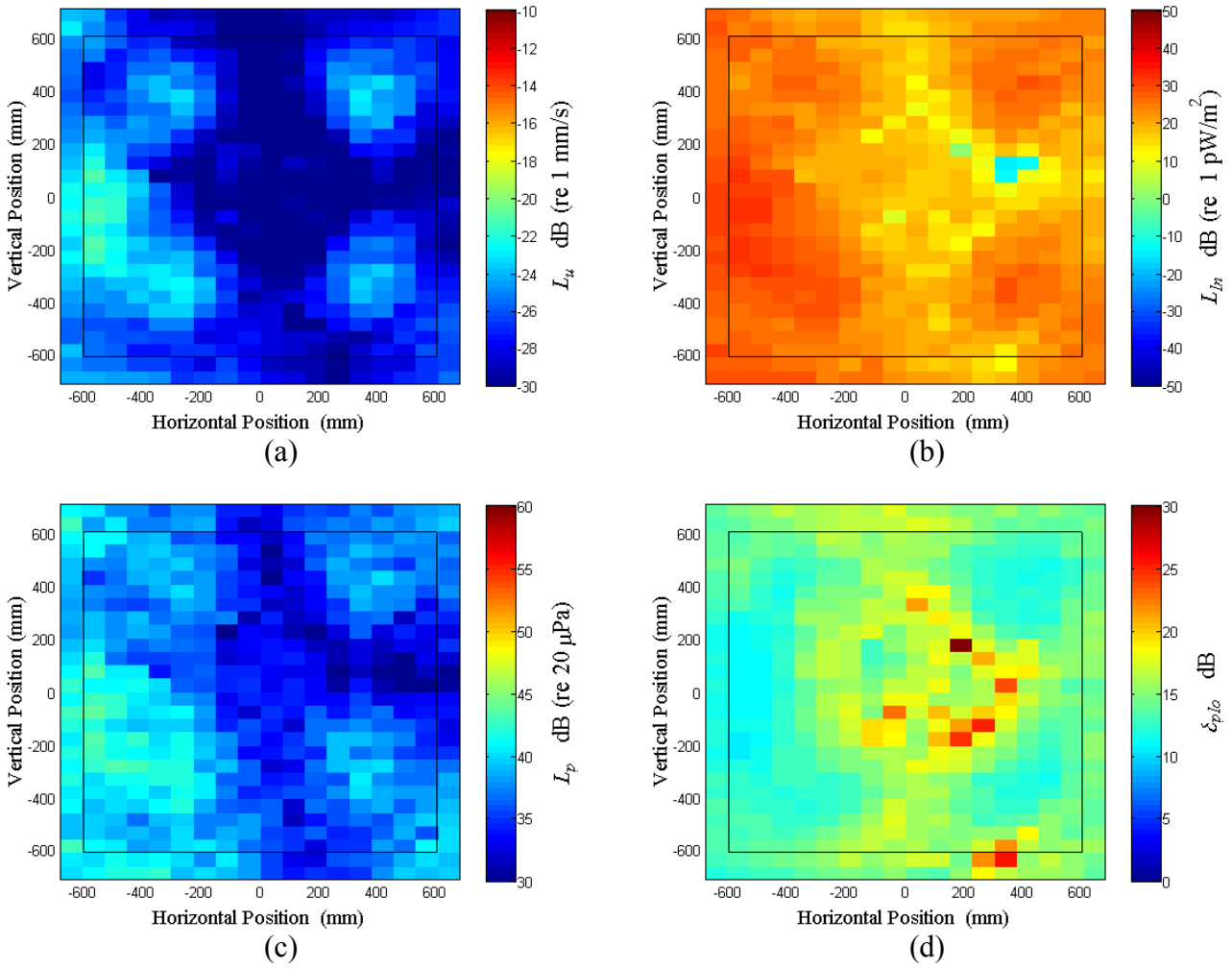

Figure C.52: Surface scan of Window C at 320 Hz (a) particle velocity level, L_u (b) normal signed sound intensity level, L_{In} (c) sound pressure level, L_p (d) pressure-residual intensity index, δ_{pIo}.

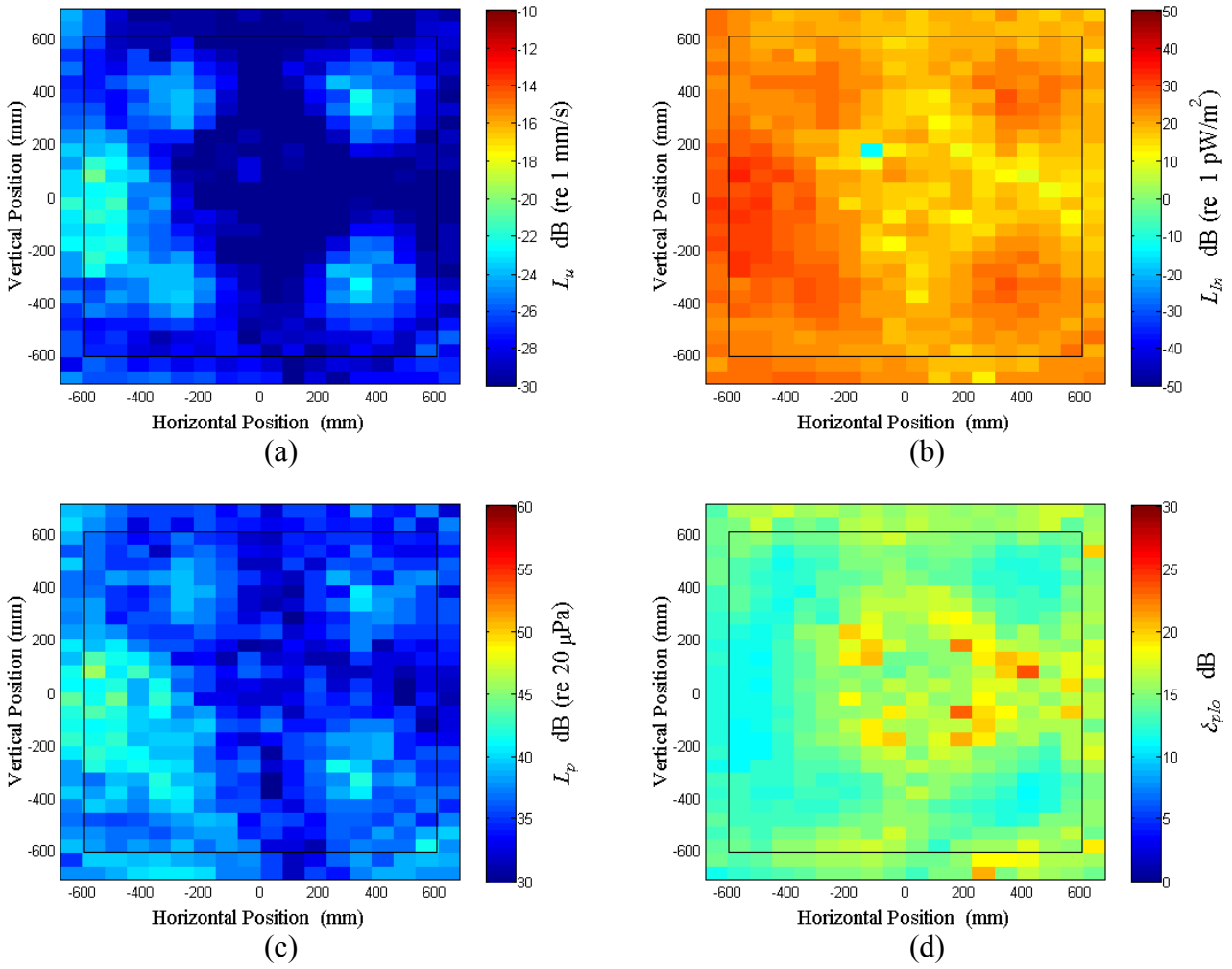

Figure C.53: Surface scan of Window C at 330 Hz (a) particle velocity level, L_u (b) normal signed sound intensity level, L_{In} (c) sound pressure level, L_p (d) pressure-residual intensity index, δ_{pIo}.

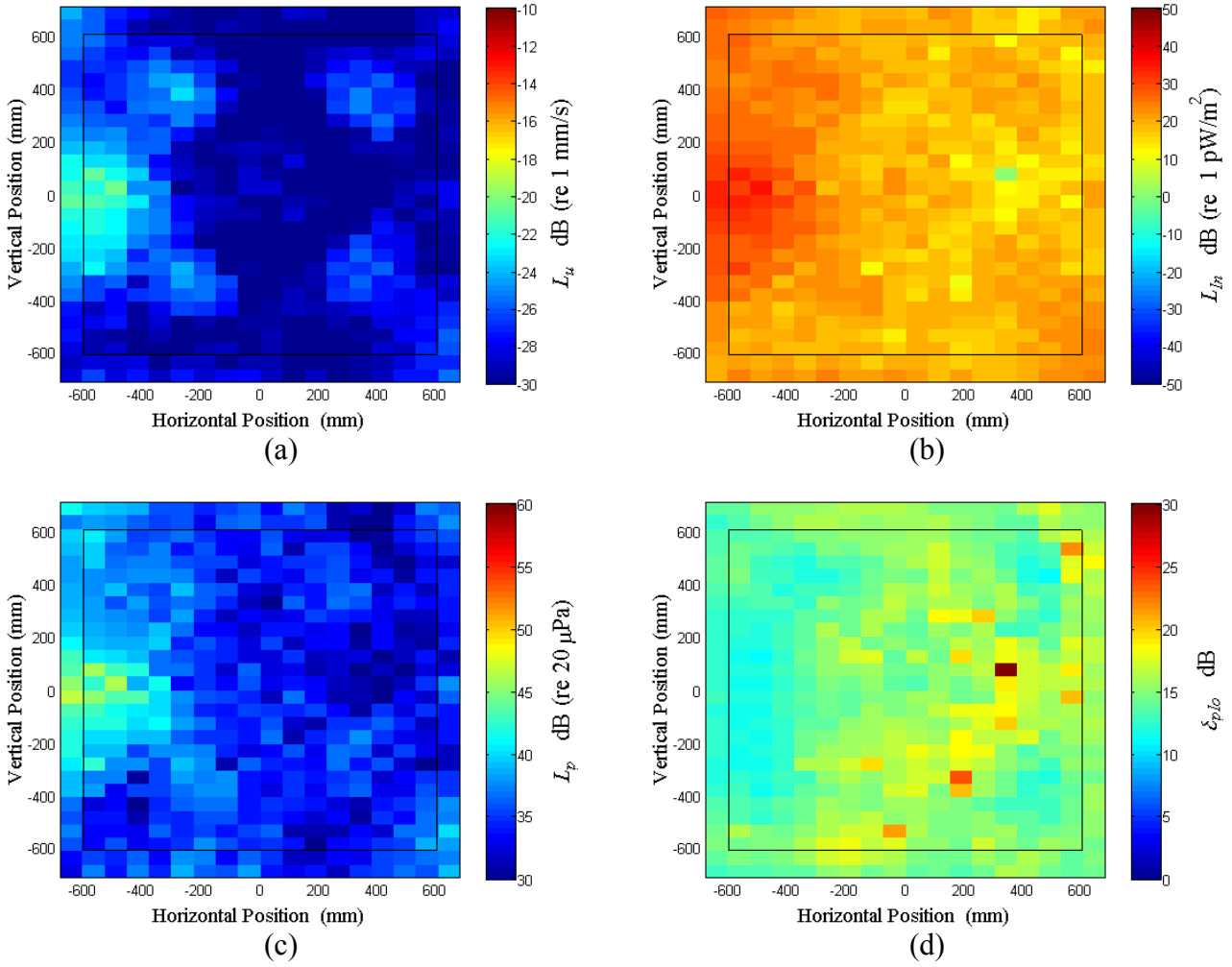

Figure C.54: Surface scan of Window C at 340 Hz (a) particle velocity level, L_u (b) normal signed sound intensity level, L_{In} (c) sound pressure level, L_p (d) pressure-residual intensity index, δ_{pIo}.

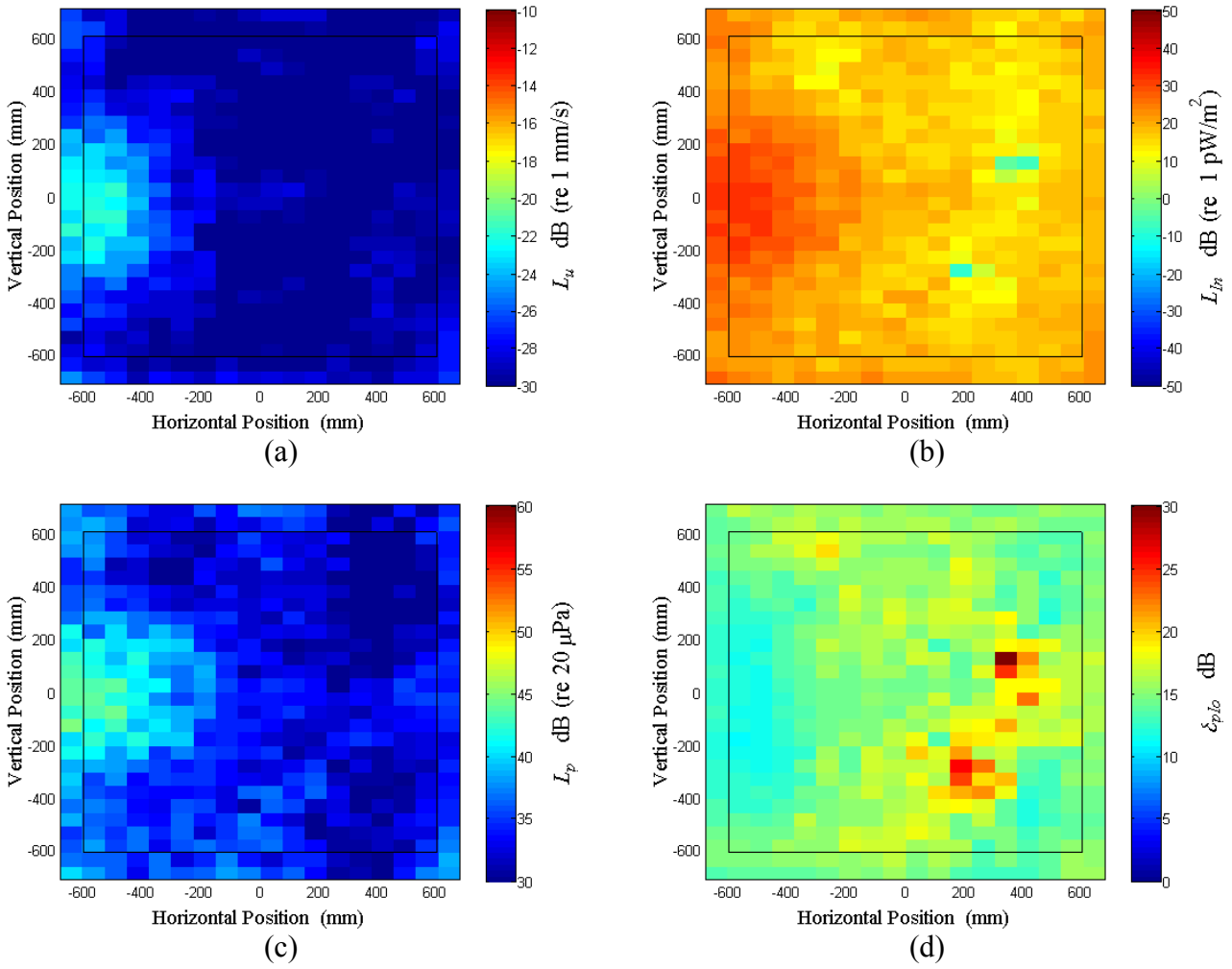

Figure C.55: Surface scan of Window C at 350 Hz (a) particle velocity level, L_u (b) normal signed sound intensity level, L_{In} (c) sound pressure level, L_p (d) pressure-residual intensity index, δ_{pIo}.

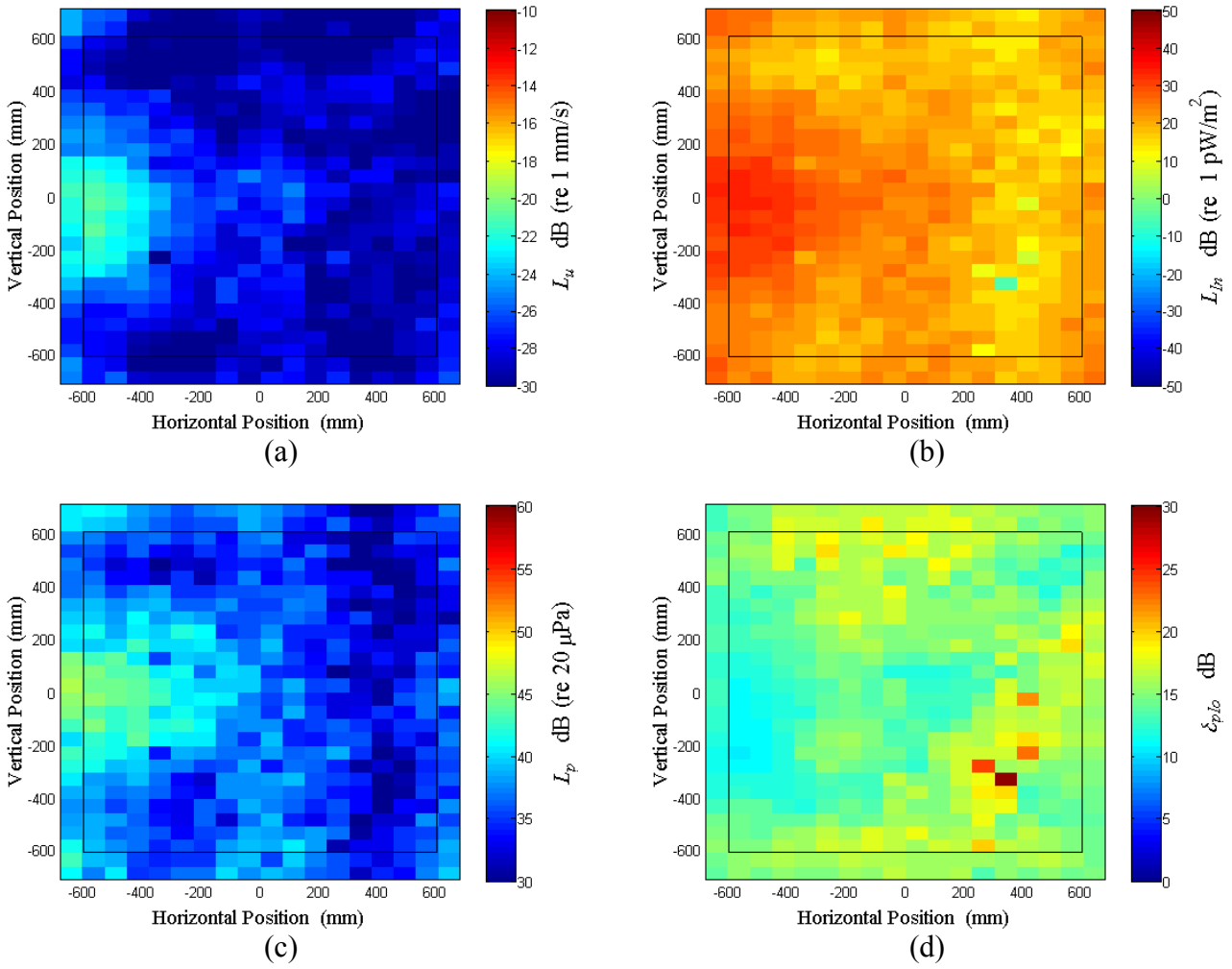

Figure C.56: Surface scan of Window C at 360 Hz (a) particle velocity level, L_u (b) normal signed sound intensity level, L_{In} (c) sound pressure level, L_p (d) pressure-residual intensity index, δ_{pIo}.

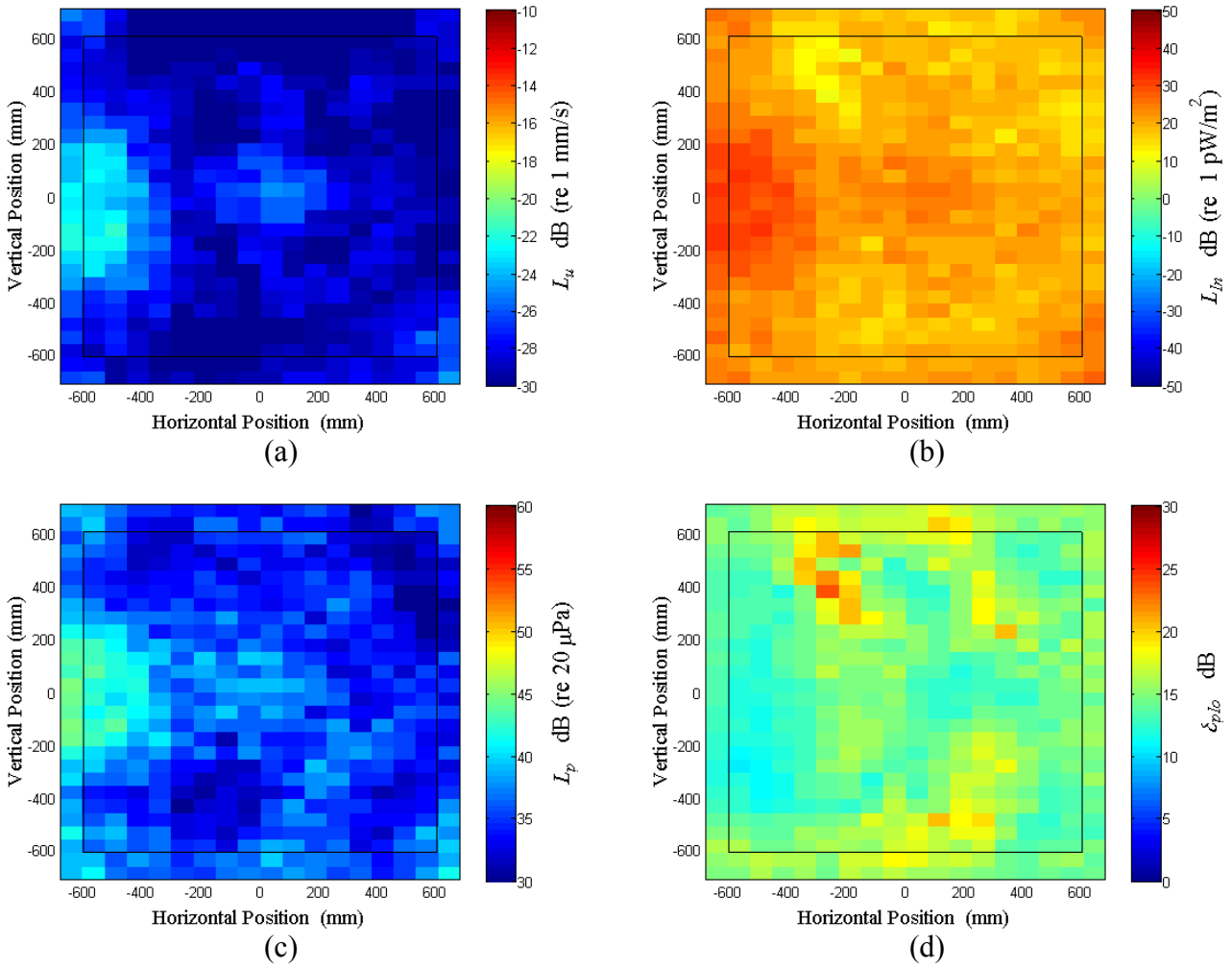

Figure C.57: Surface scan of Window C at 370 Hz (a) particle velocity level, L_u (b) normal signed sound intensity level, L_{In} (c) sound pressure level, L_p (d) pressure-residual intensity index, δ_{pIo}.

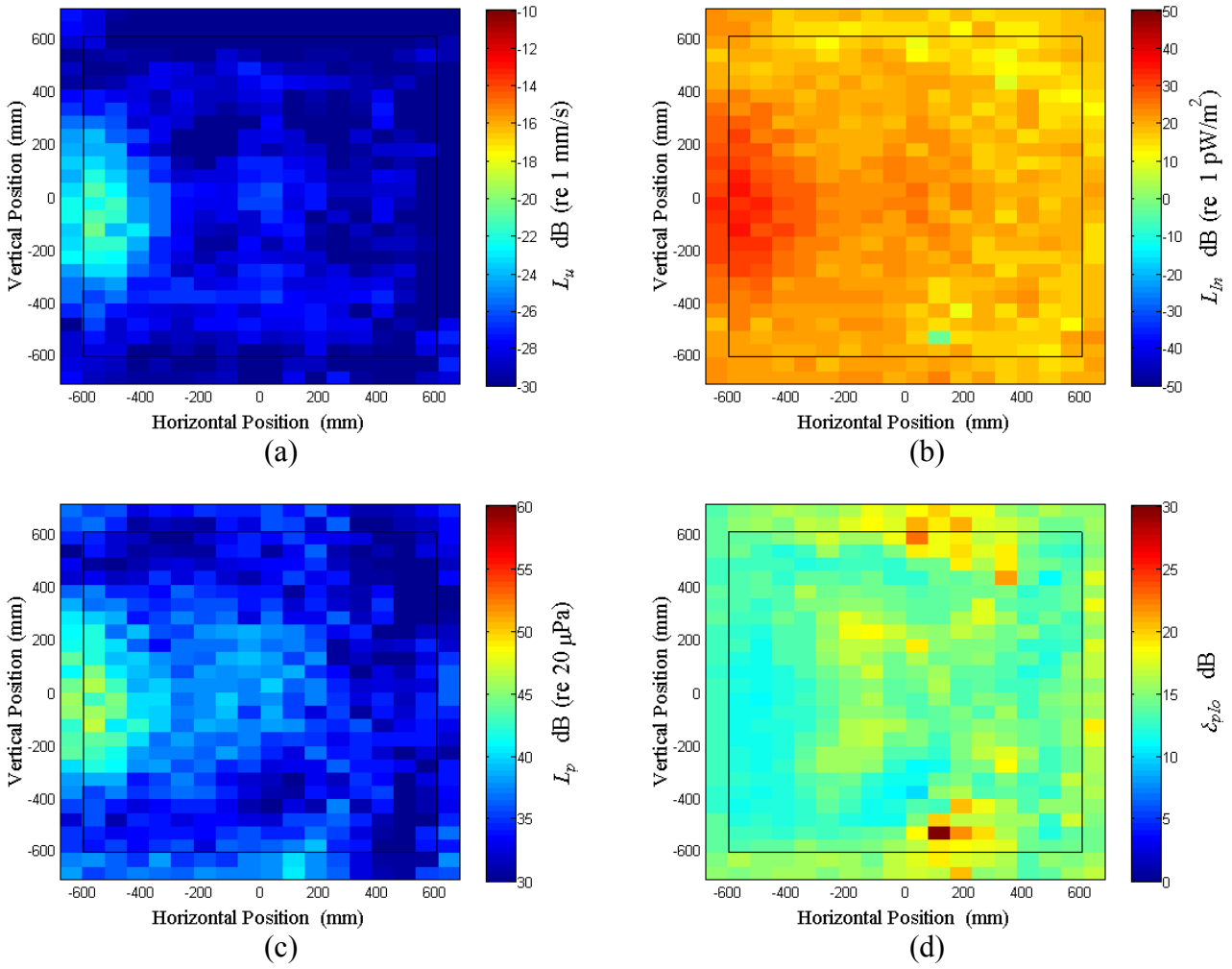

Figure C.58: Surface scan of Window C at 380 Hz (a) particle velocity level, L_u (b) normal signed sound intensity level, L_{In} (c) sound pressure level, L_p (d) pressure-residual intensity index, δ_{pIo}.

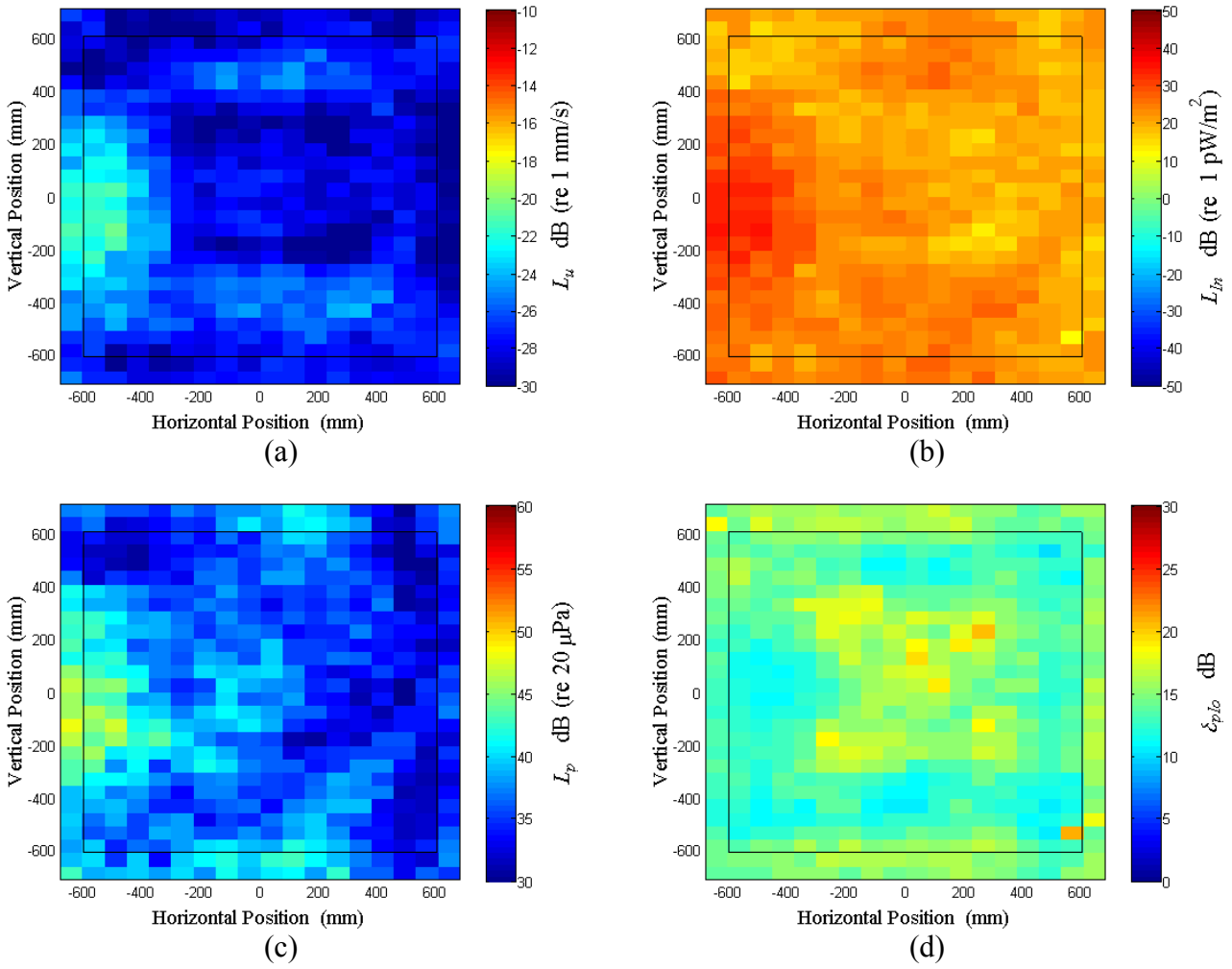

Figure C.59: Surface scan of Window C at 390 Hz (a) particle velocity level, L_u (b) normal signed sound intensity level, L_{In} (c) sound pressure level, L_p (d) pressure-residual intensity index, δ_{pIo}.

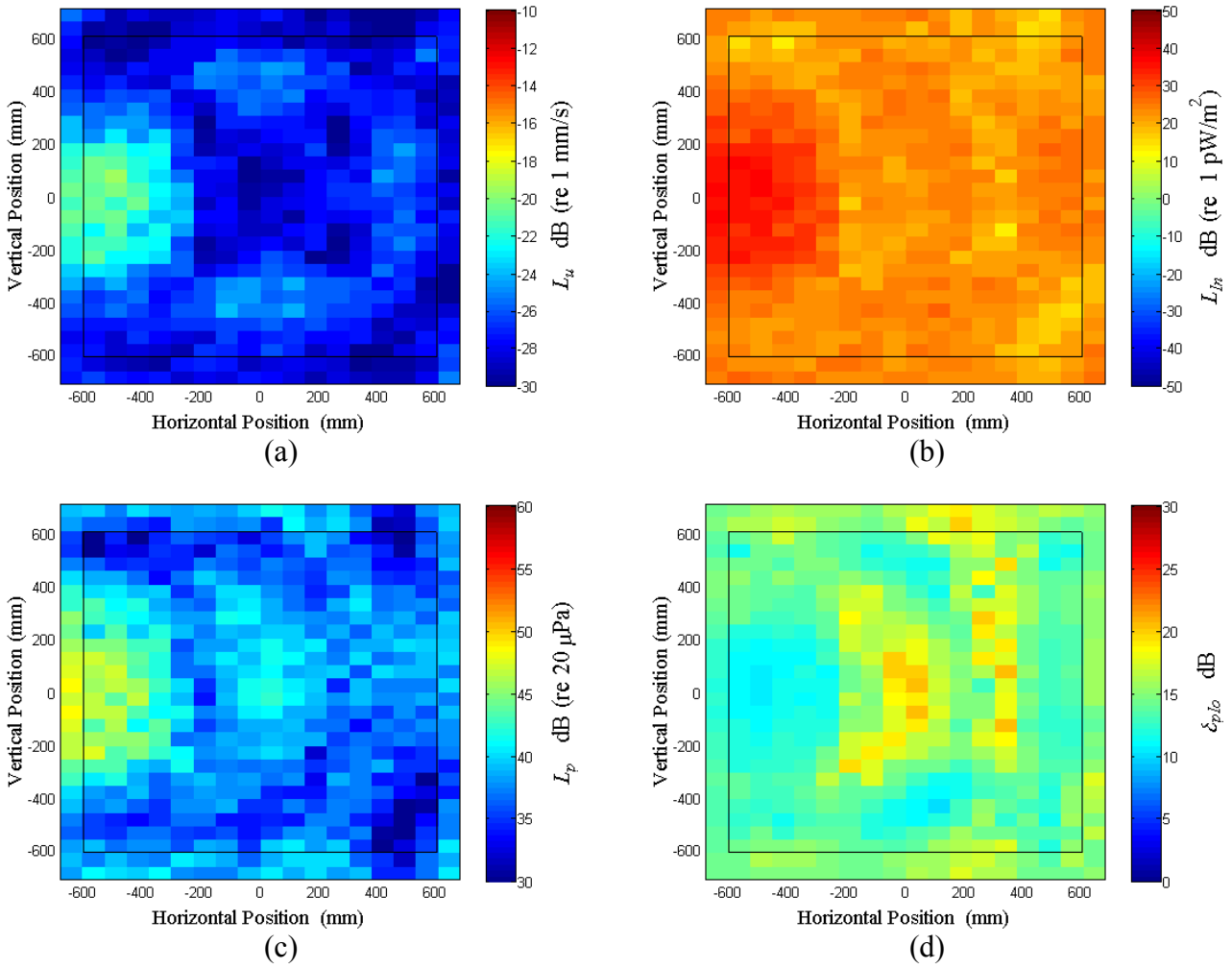

Figure C.60: Surface scan of Window C at 400 Hz (a) particle velocity level, L_u (b) normal signed sound intensity level, L_{In} (c) sound pressure level, L_p (d) pressure-residual intensity index, δ_{pIo}.

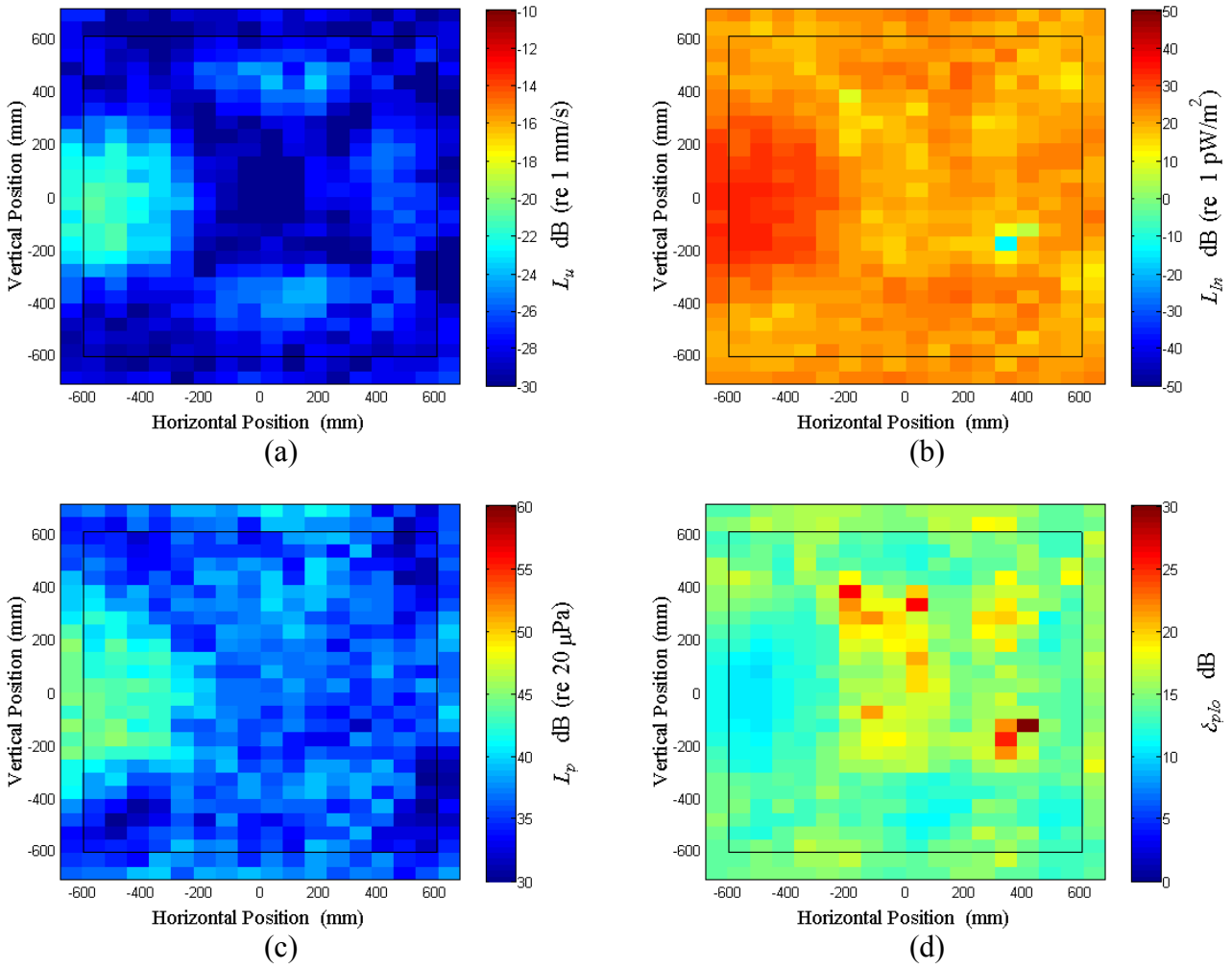

Figure C.61: Surface scan of Window C at 410 Hz (a) particle velocity level, L_u (b) normal signed sound intensity level, L_{In} (c) sound pressure level, L_p (d) pressure-residual intensity index, δ_{pIo}.

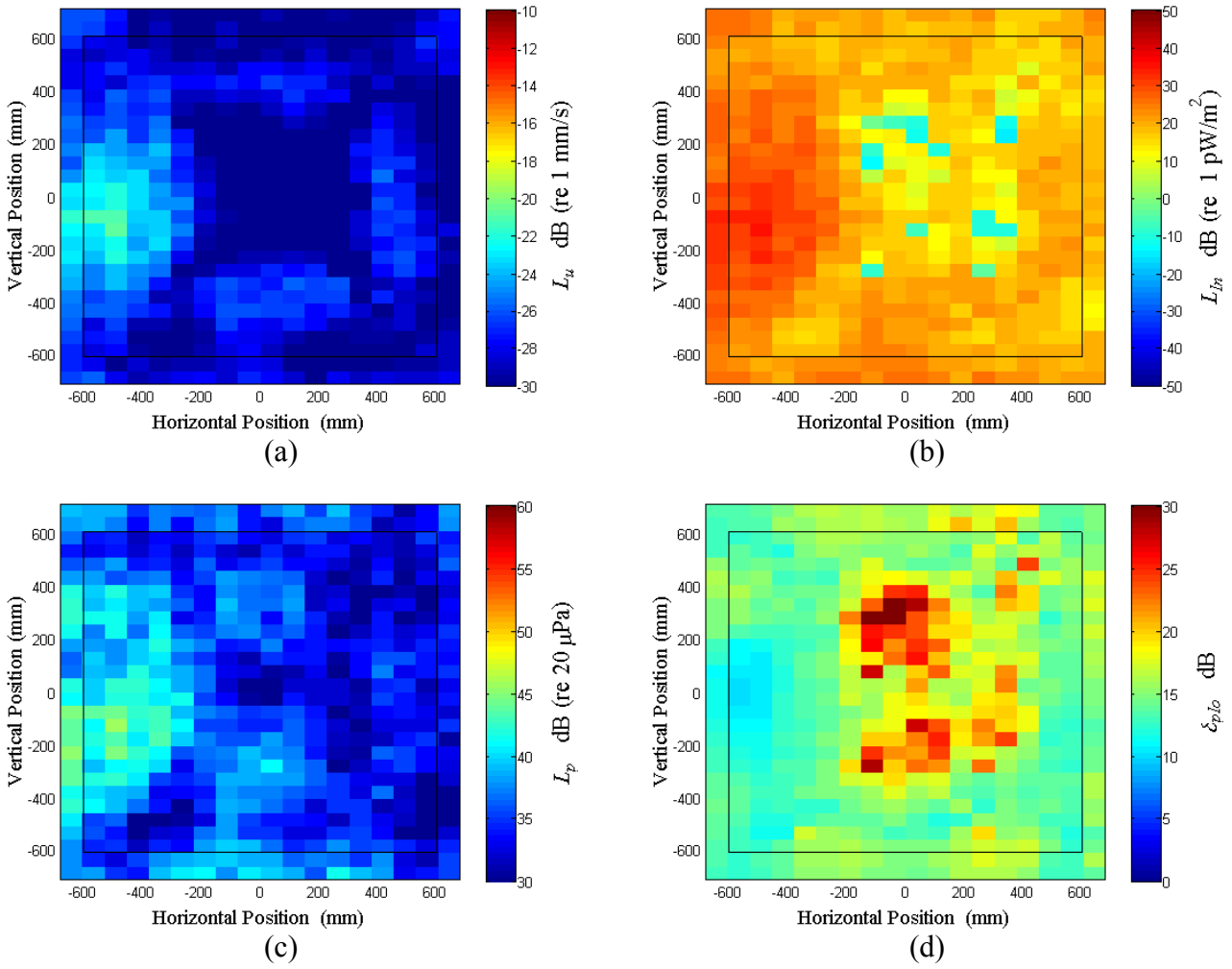

Figure C.62: Surface scan of Window C at 420 Hz (a) particle velocity level, L_u (b) normal signed sound intensity level, L_{In} (c) sound pressure level, L_p (d) pressure-residual intensity index, δ_{pIo}.

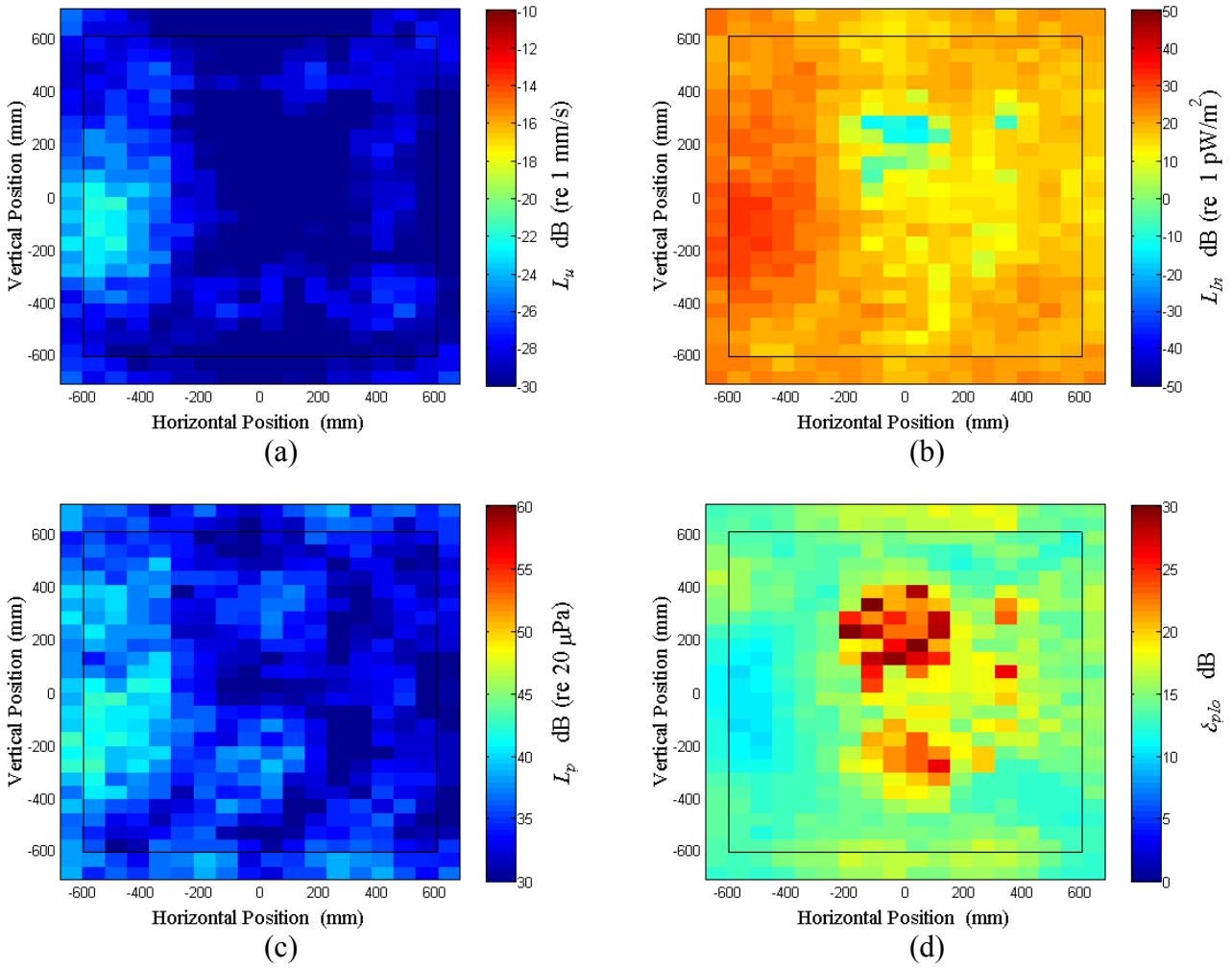

Figure C.63: Surface scan of Window C at 430 Hz (a) particle velocity level, L_u (b) normal signed sound intensity level, L_{In} (c) sound pressure level, L_p (d) pressure-residual intensity index, δ_{pIo}.

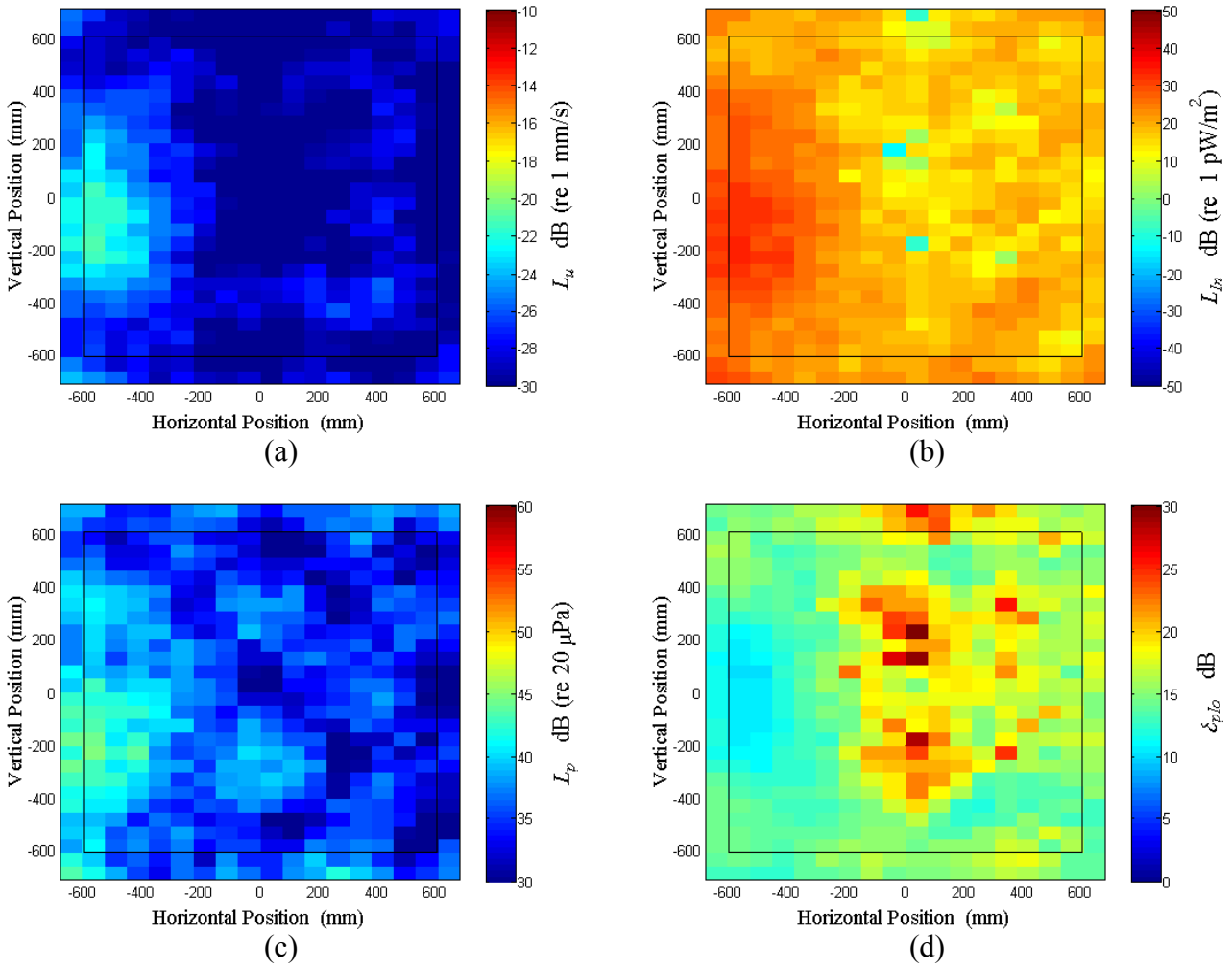

Figure C.64: Surface scan of Window C at 440 Hz (a) particle velocity level, L_u (b) normal signed sound intensity level, L_{In} (c) sound pressure level, L_p (d) pressure-residual intensity index, δ_{pIo}.

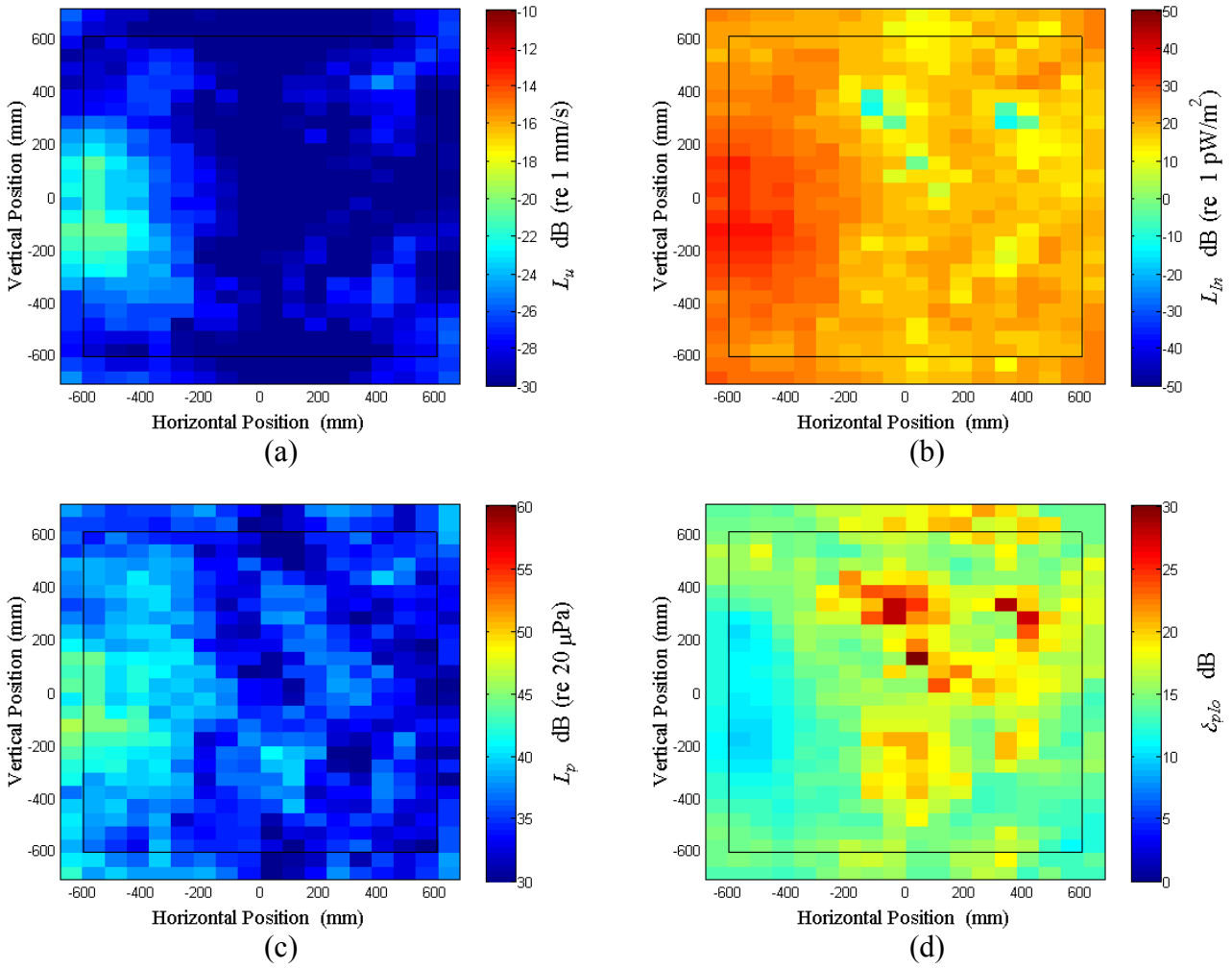

Figure C.65: Surface scan of Window C at 450 Hz (a) particle velocity level, L_u (b) normal signed sound intensity level, L_{In} (c) sound pressure level, L_p (d) pressure-residual intensity index, δ_{pIo}.

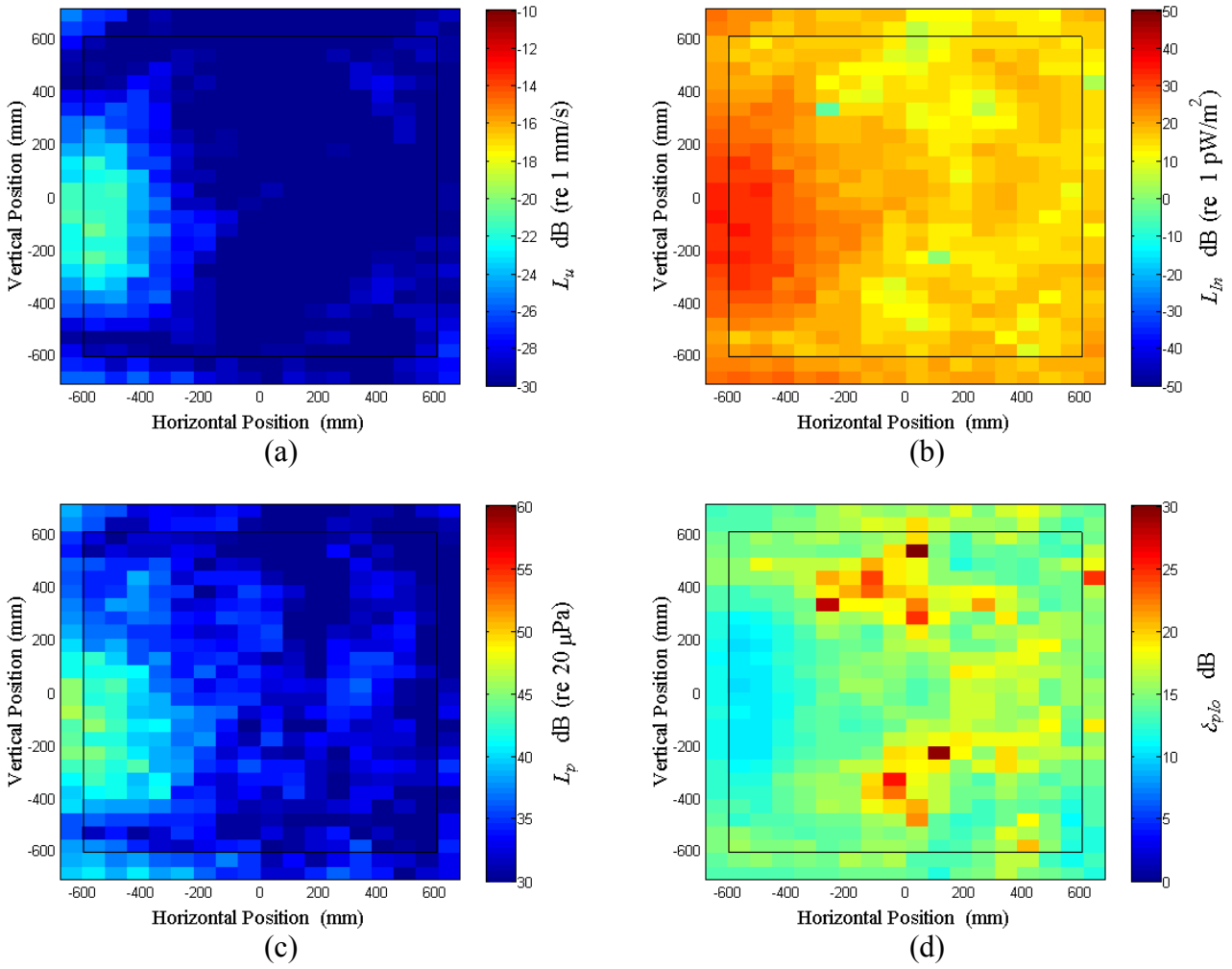

Figure C.66: Surface scan of Window C at 460 Hz (a) particle velocity level, L_u (b) normal signed sound intensity level, L_{In} (c) sound pressure level, L_p (d) pressure-residual intensity index, δ_{pIo}.

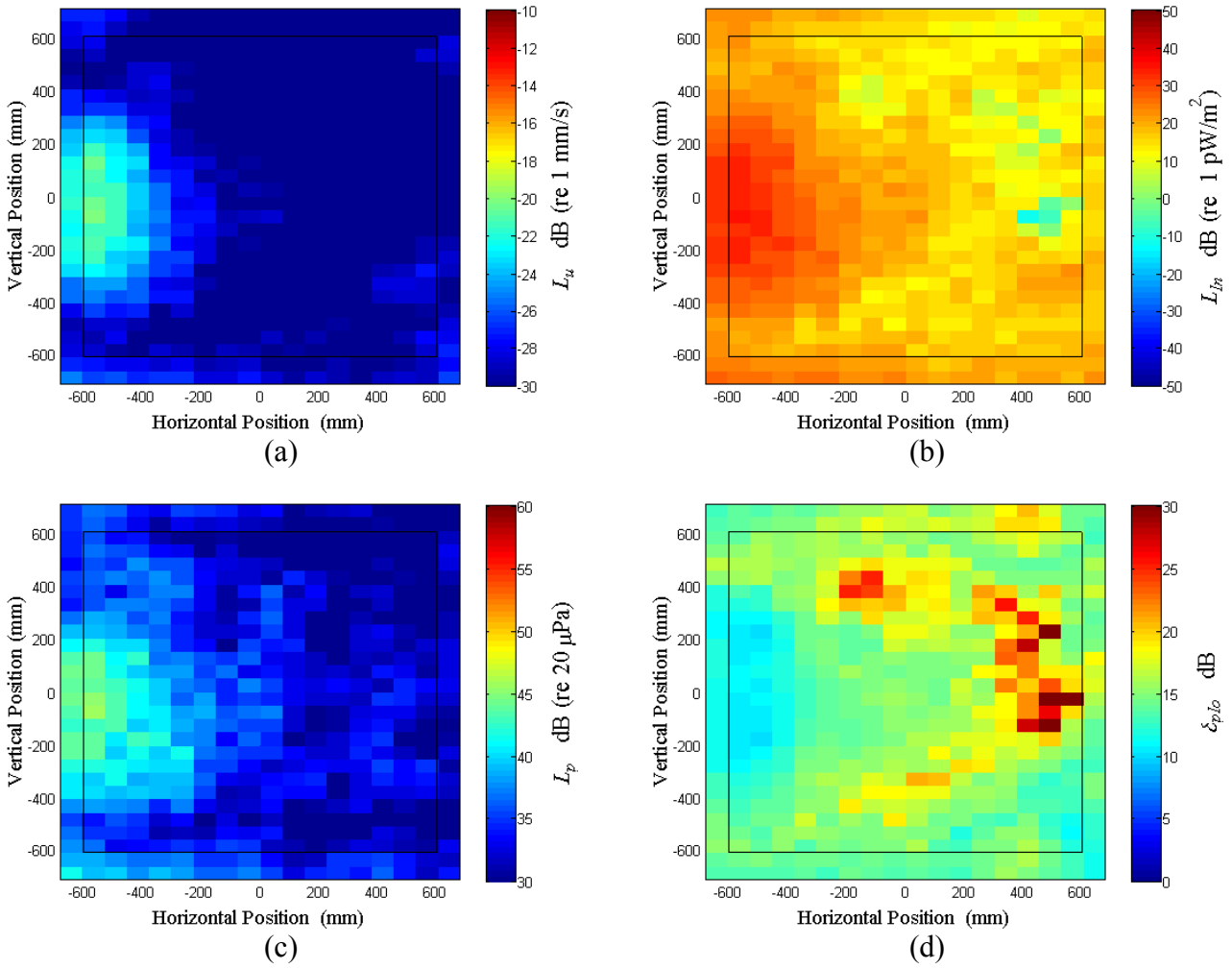

Figure C.67: Surface scan of Window C at 470 Hz (a) particle velocity level, L_u (b) normal signed sound intensity level, L_{In} (c) sound pressure level, L_p (d) pressure-residual intensity index, δ_{pIo}.

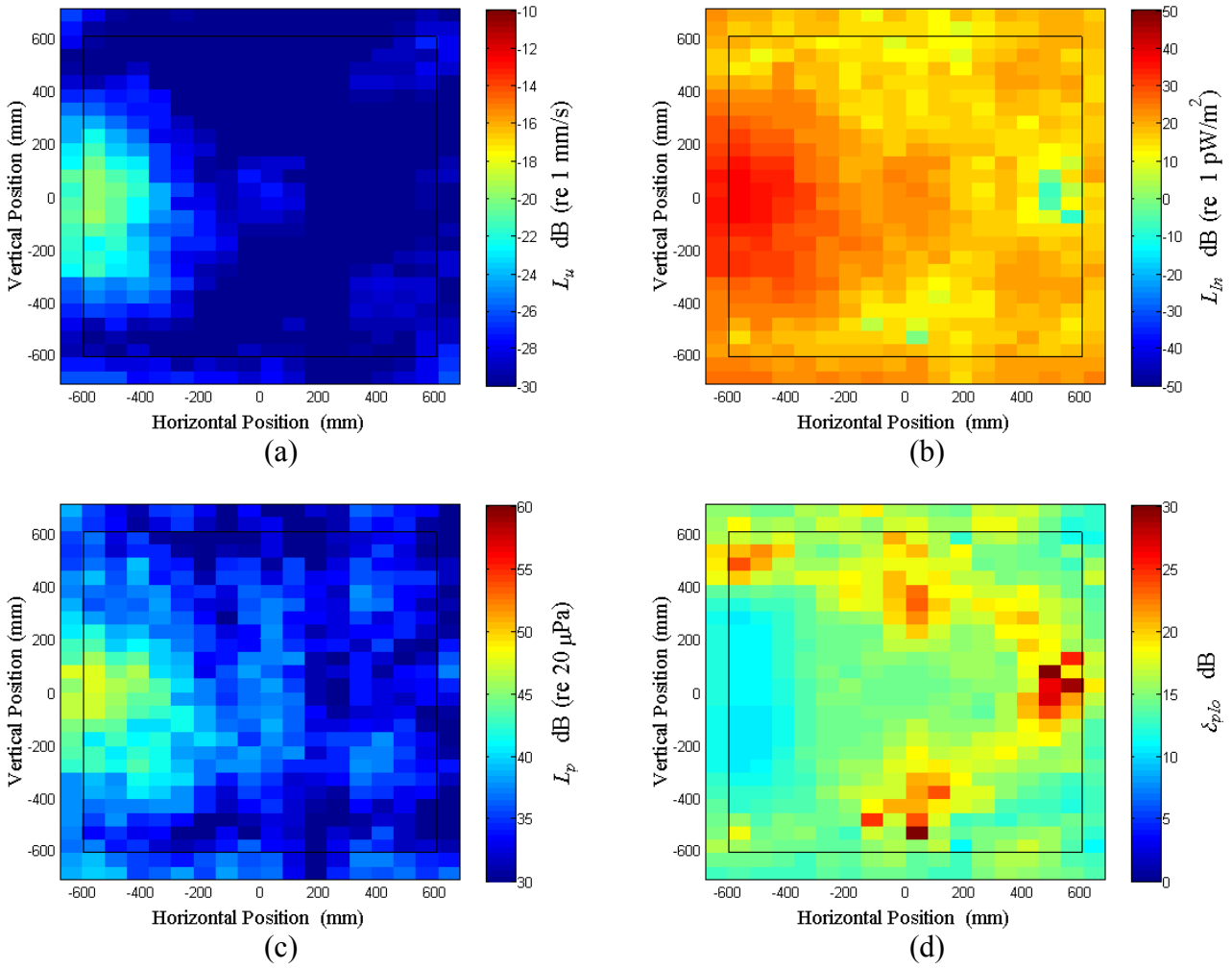

Figure C.68: Surface scan of Window C at 480 Hz (a) particle velocity level, L_u (b) normal signed sound intensity level, L_{In} (c) sound pressure level, L_p (d) pressure-residual intensity index, δ_{pIo}.

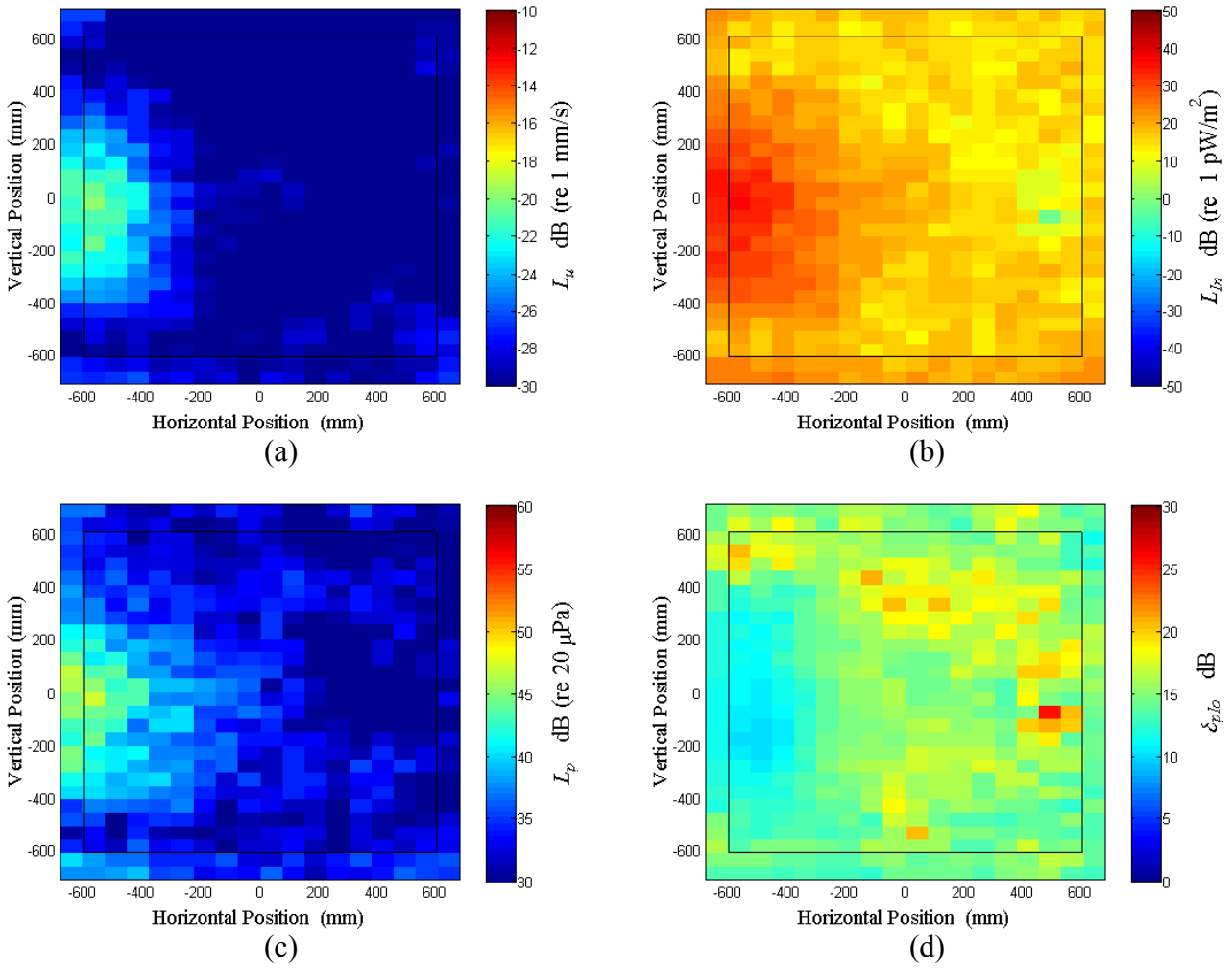

Figure C.69: Surface scan of Window C at 490 Hz (a) particle velocity level, L_u (b) normal signed sound intensity level, L_{In} (c) sound pressure level, L_p (d) pressure-residual intensity index, δ_{pIo}.

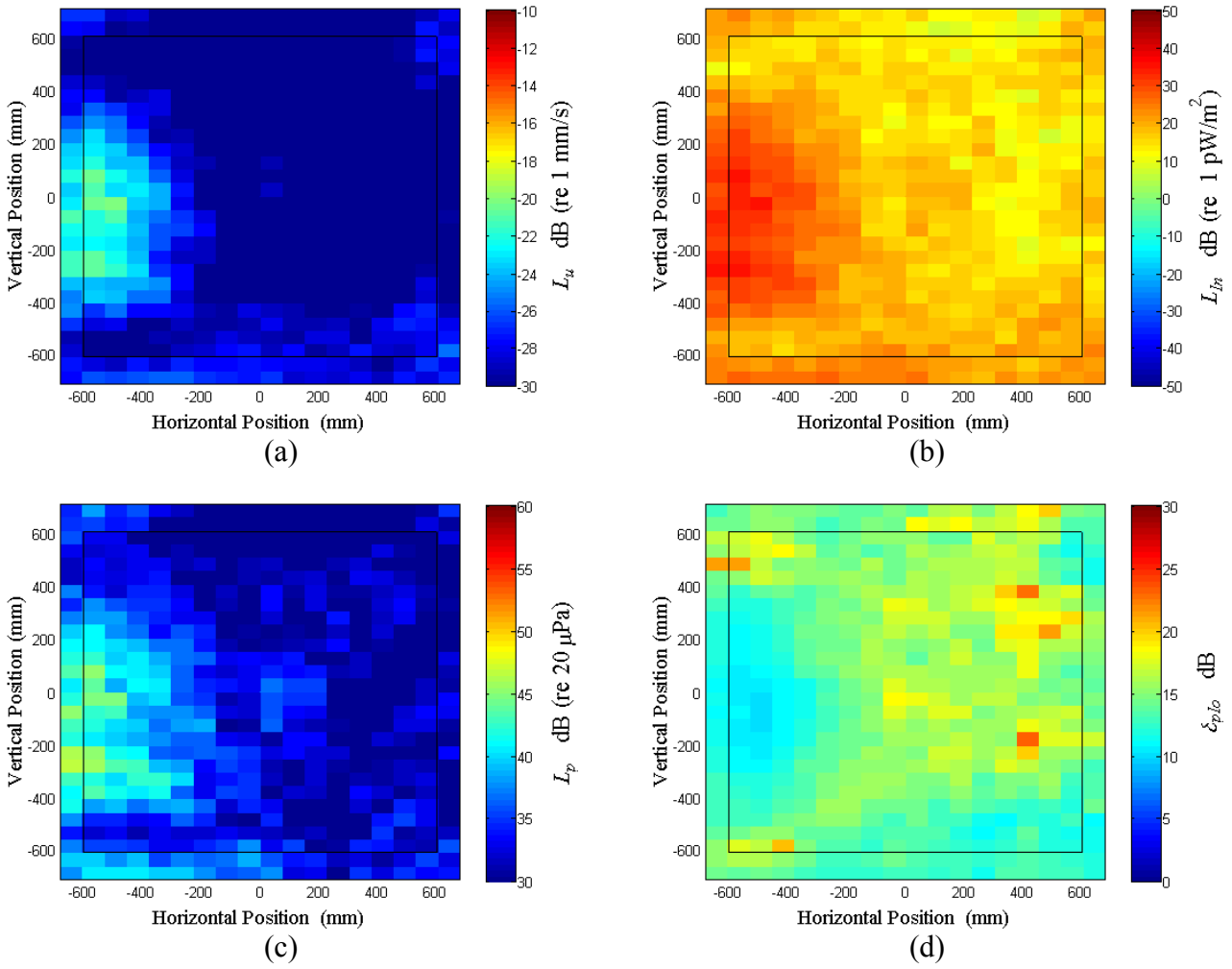

Figure C.70: Surface scan of Window C at 500 Hz (a) particle velocity level, L_u (b) normal signed sound intensity level, L_{In} (c) sound pressure level, L_p (d) pressure-residual intensity index, δ_{pIo}.

APPENDIX D. WINDOW D

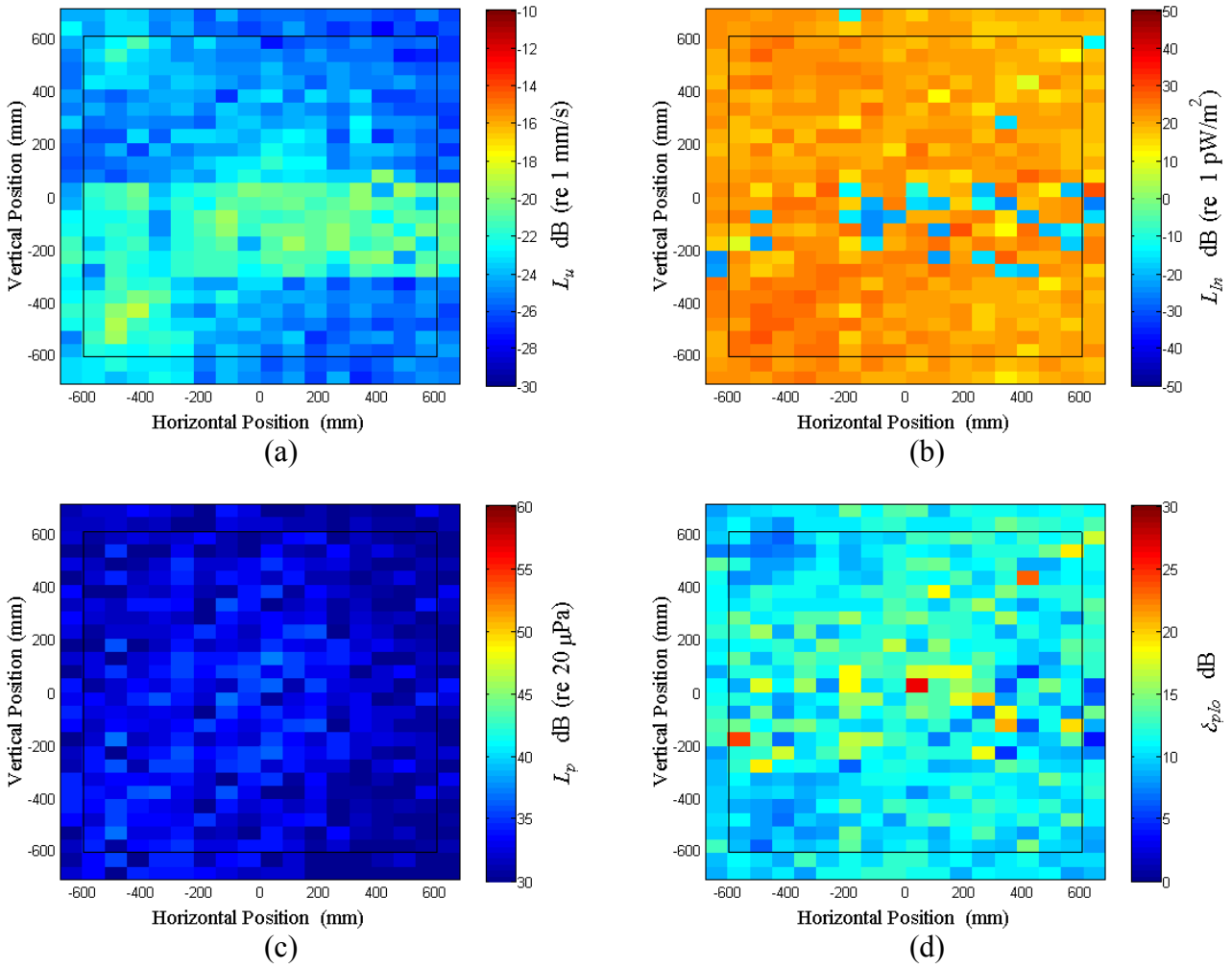

Figure D.1: Surface scan of Window D at 50 Hz (a) particle velocity level, L_u (b) normal signed sound intensity level, L_{In} (c) sound pressure level, L_p (d) pressure-residual intensity index, δ_{pIo}.

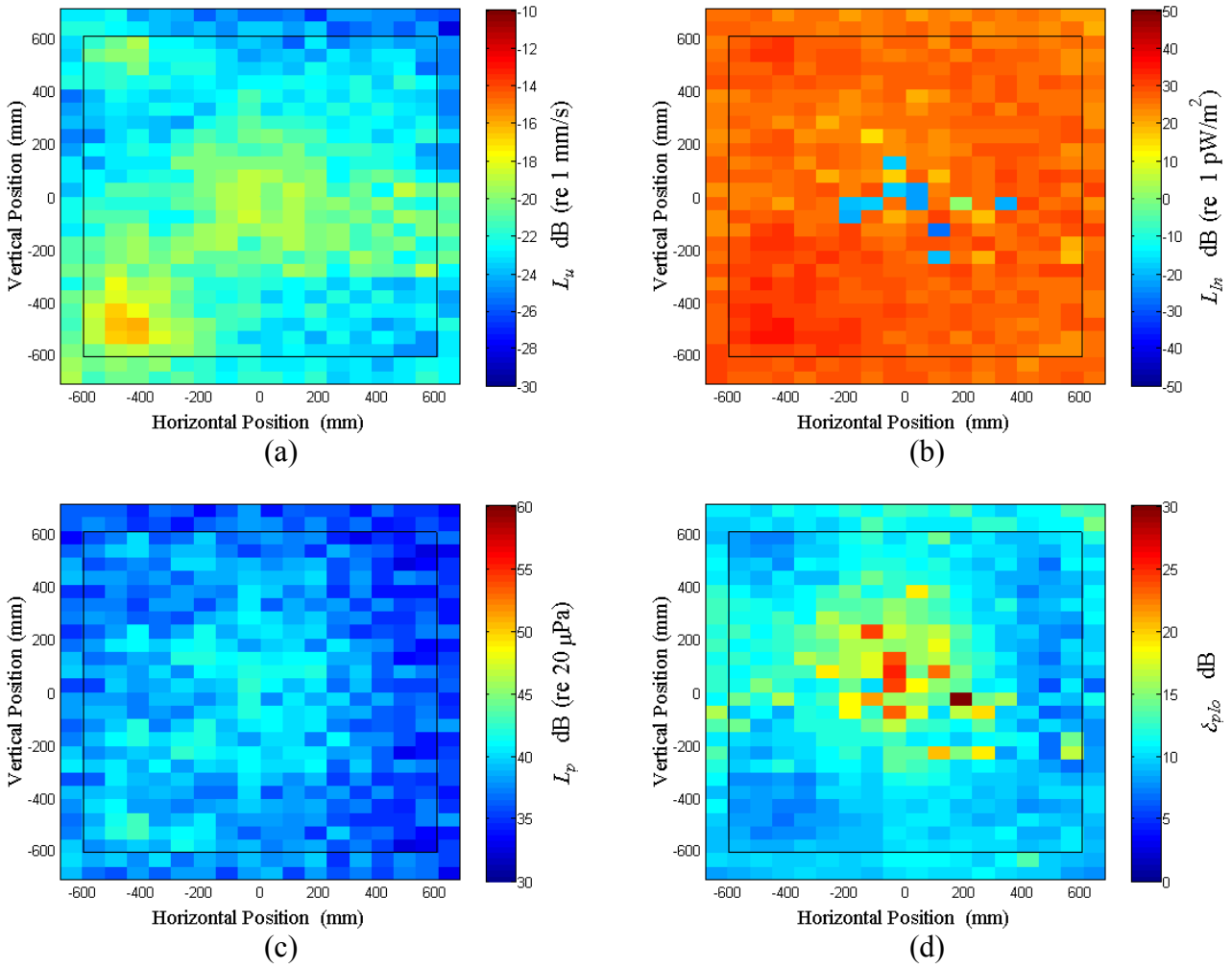

Figure D.2: Surface scan of Window D at 52.5 Hz (a) particle velocity level, L_u (b) normal signed sound intensity level, L_{In} (c) sound pressure level, L_p (d) pressure-residual intensity index, δ_{pIo}.

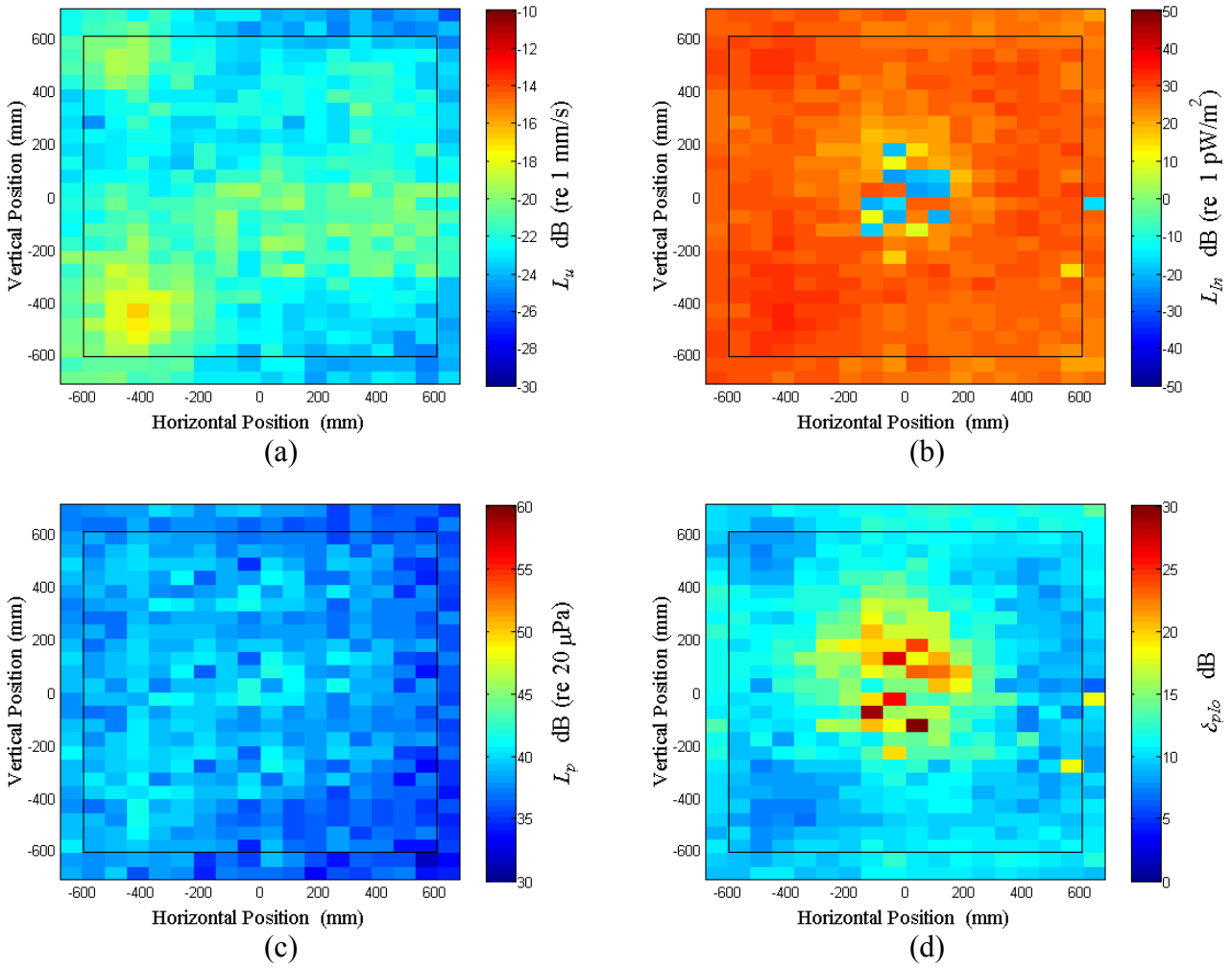

Figure D.3: Surface scan of Window D at 55 Hz (a) particle velocity level, L_u (b) normal signed sound intensity level, L_{In} (c) sound pressure level, L_p (d) pressure-residual intensity index, δ_{pIo}.

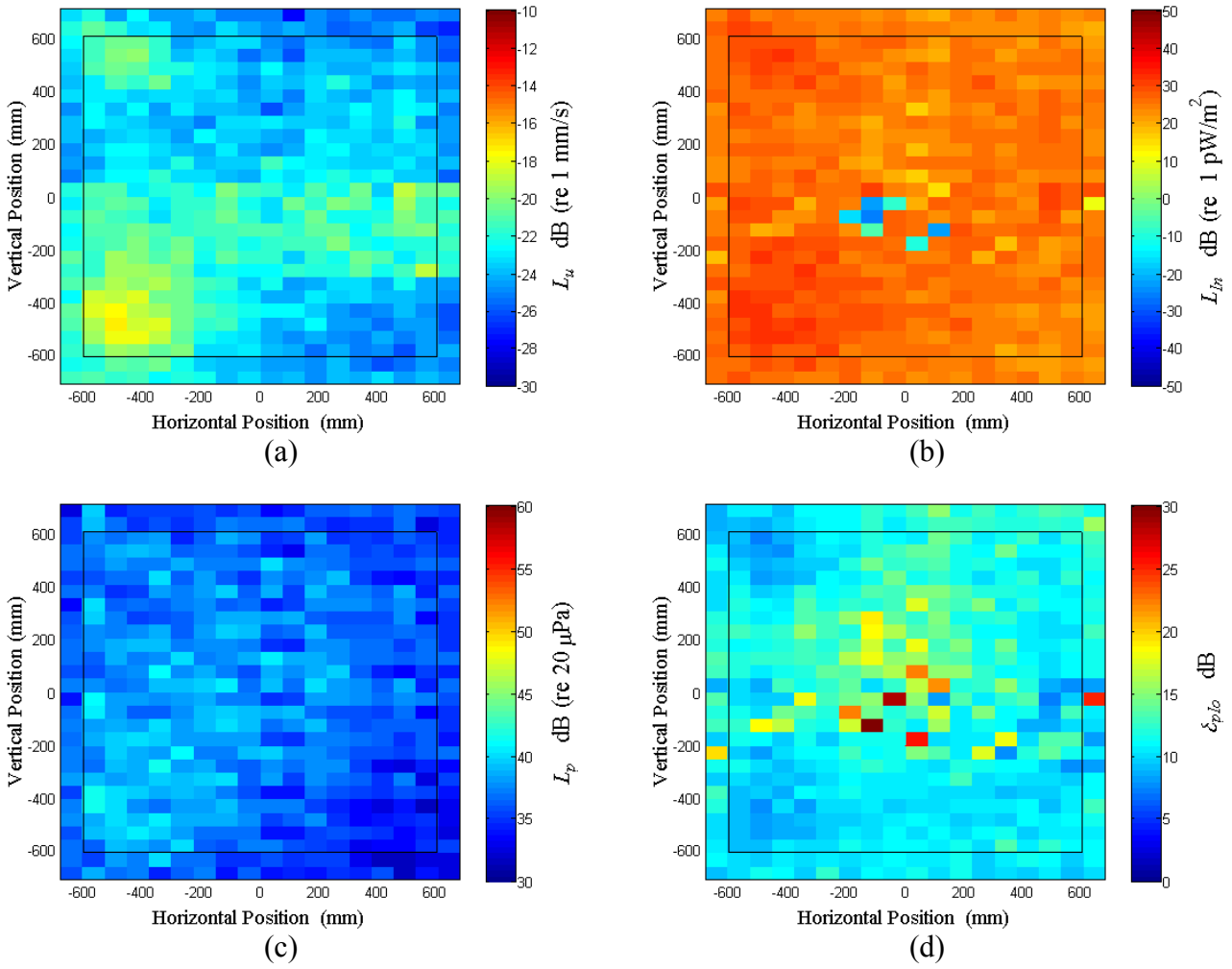

Figure D.4: Surface scan of Window D at 57.5 Hz (a) particle velocity level, L_u (b) normal signed sound intensity level, L_{In} (c) sound pressure level, L_p (d) pressure-residual intensity index, δ_{pIo}.

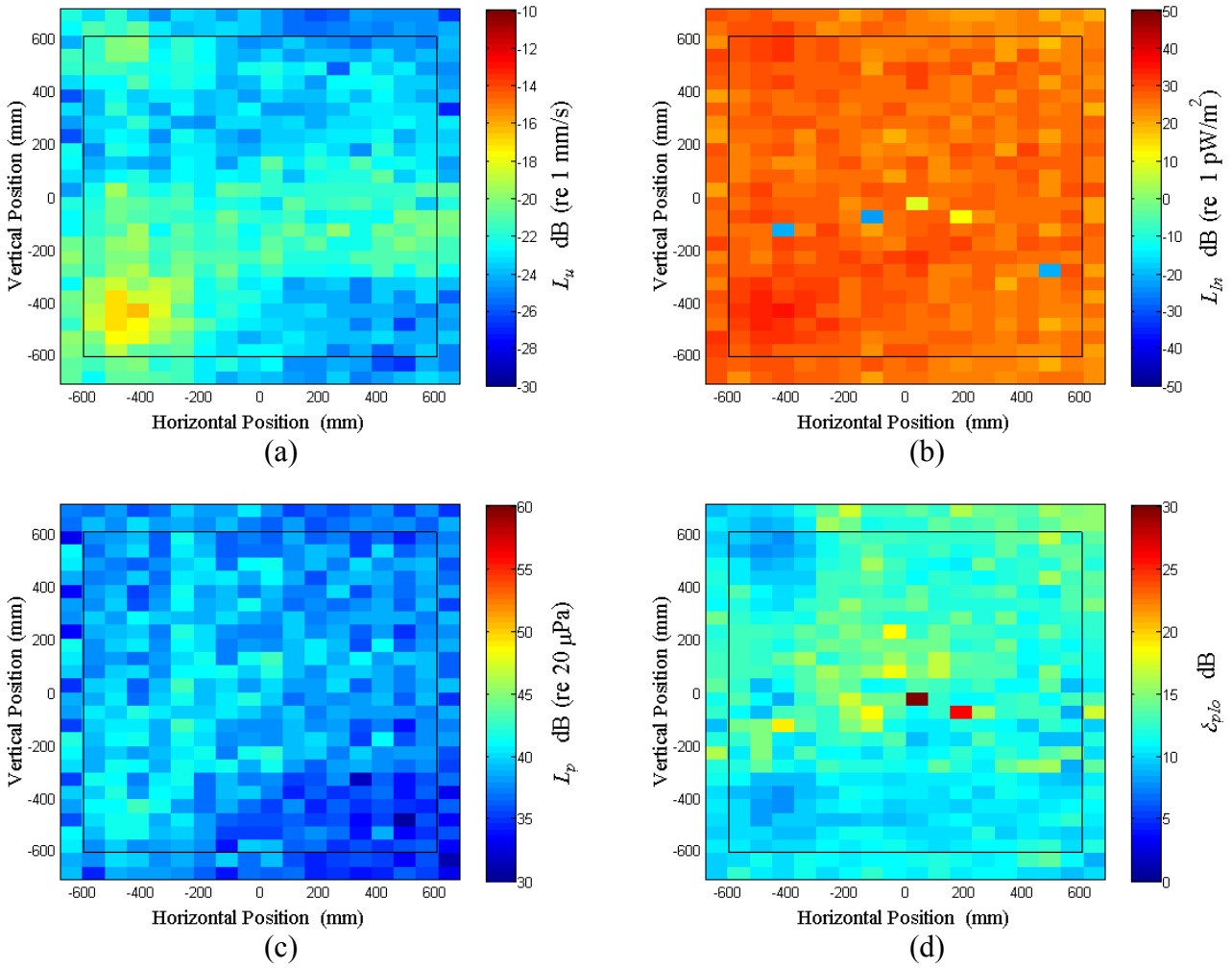

Figure D.5: Surface scan of Window D at 60 Hz (a) particle velocity level, L_u (b) normal signed sound intensity level, L_{In} (c) sound pressure level, L_p (d) pressure-residual intensity index, δ_{pIo}.

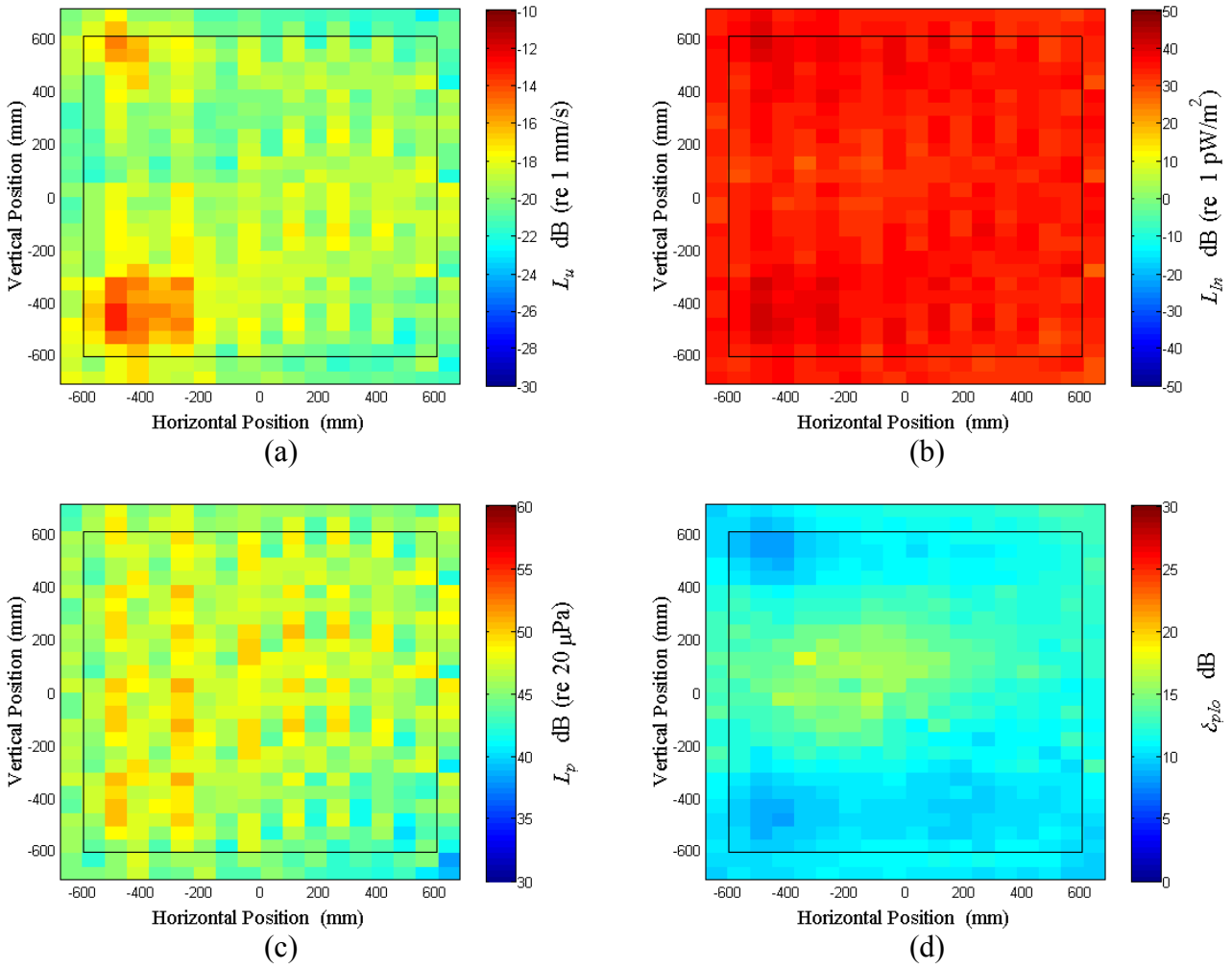

Figure D.6: Surface scan of Window D at 62.5 Hz (a) particle velocity level, L_u (b) normal signed sound intensity level, L_{In} (c) sound pressure level, L_p (d) pressure-residual intensity index, δ_{pIo}.

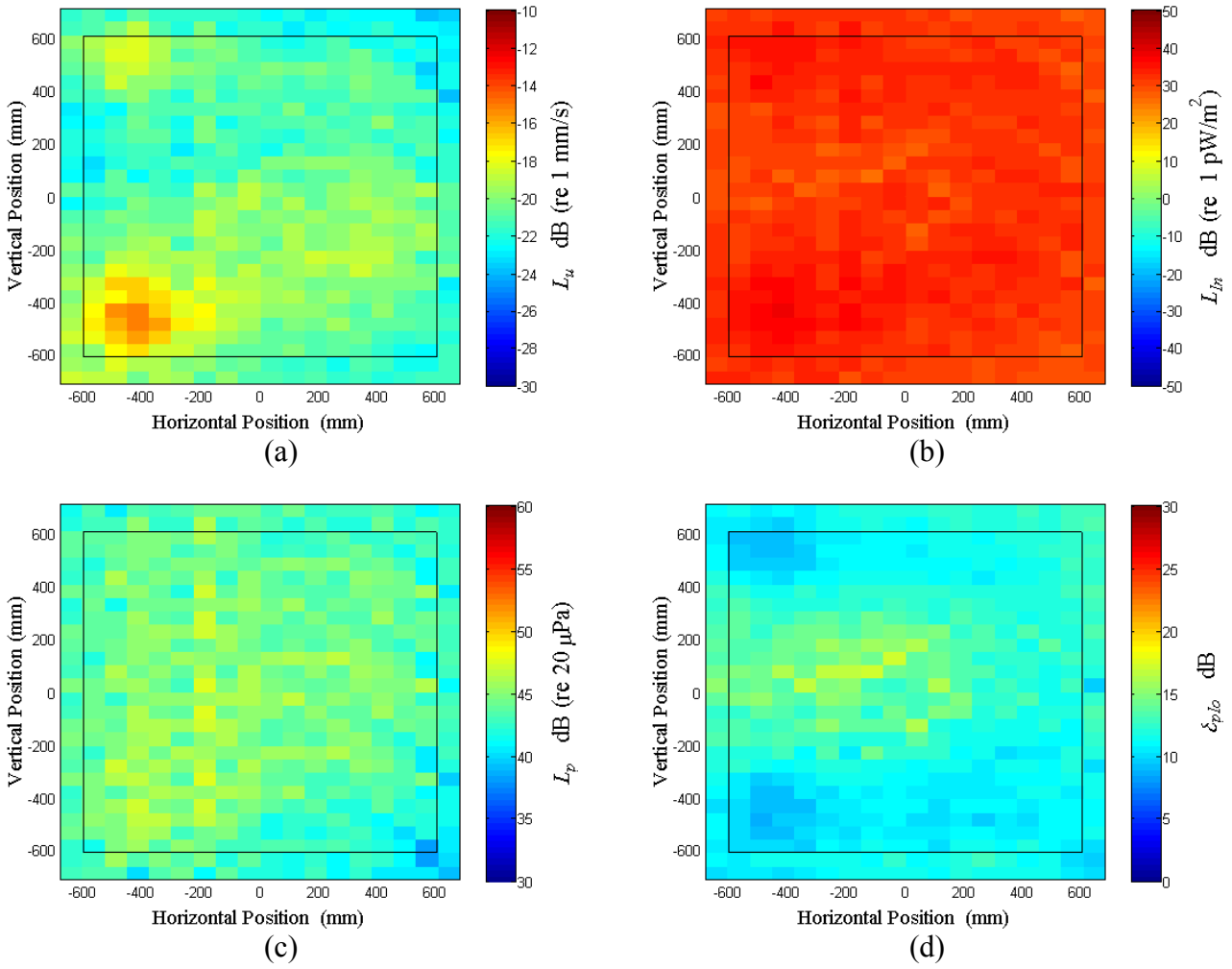

Figure D.7: Surface scan of Window D at 65 Hz (a) particle velocity level, L_u (b) normal signed sound intensity level, L_{In} (c) sound pressure level, L_p (d) pressure-residual intensity index, δ_{pIo}.

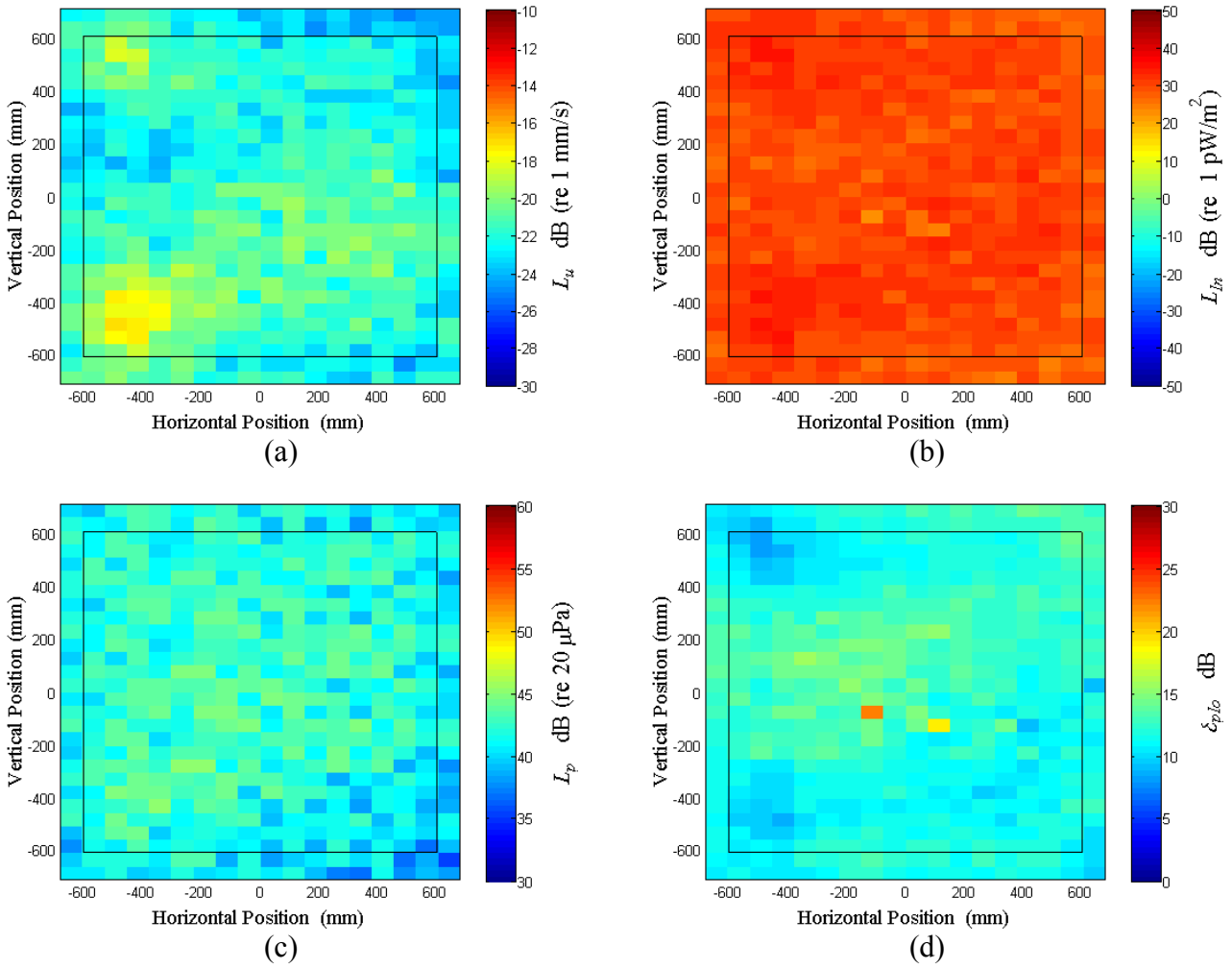

Figure D.8: Surface scan of Window D at 67.5 Hz (a) particle velocity level, L_u (b) normal signed sound intensity level, L_{In} (c) sound pressure level, L_p (d) pressure-residual intensity index, δ_{pIo}.

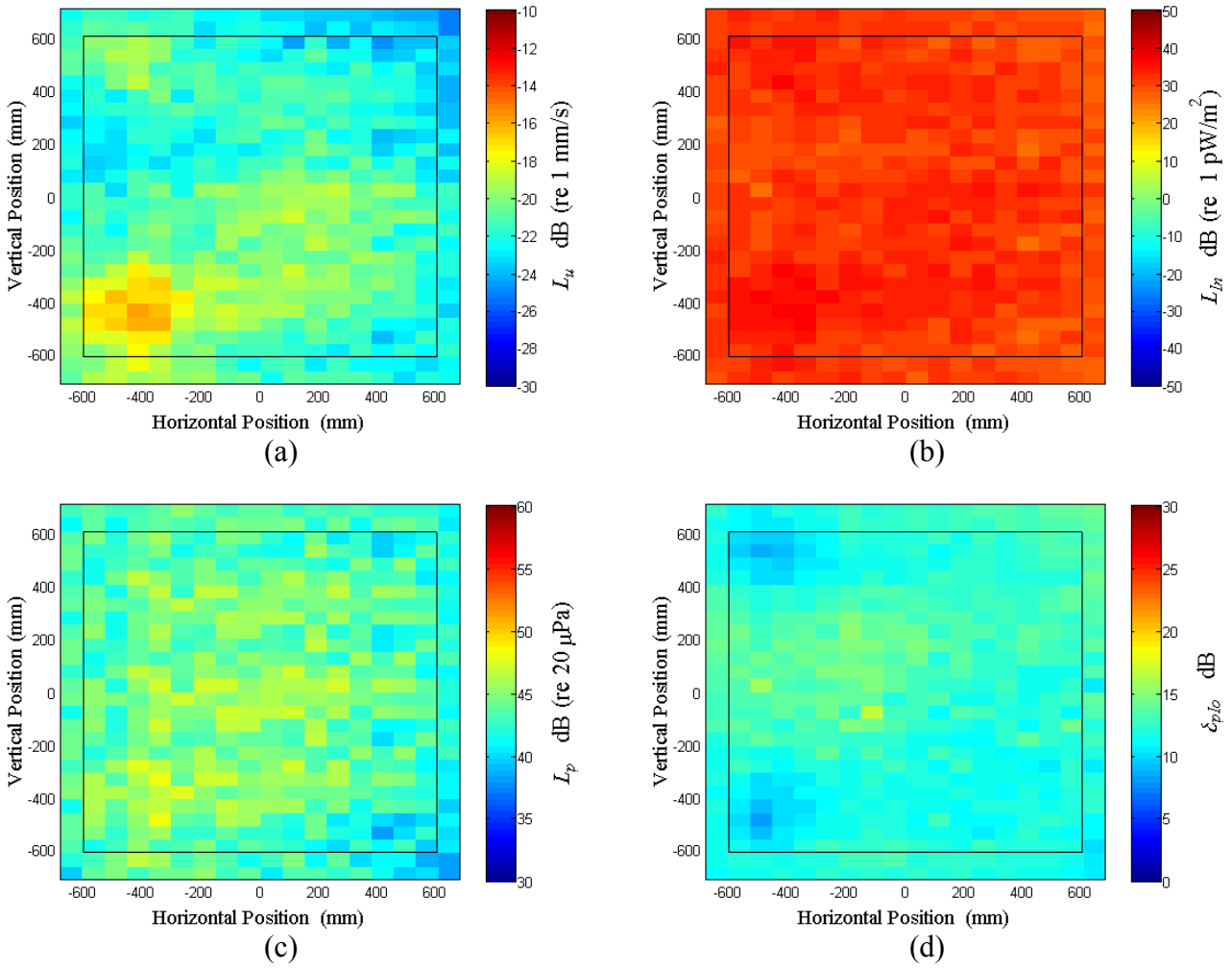

Figure D.9: Surface scan of Window D at 70 Hz (a) particle velocity level, L_u (b) normal signed sound intensity level, L_{In} (c) sound pressure level, L_p (d) pressure-residual intensity index, δ_{pIo}.

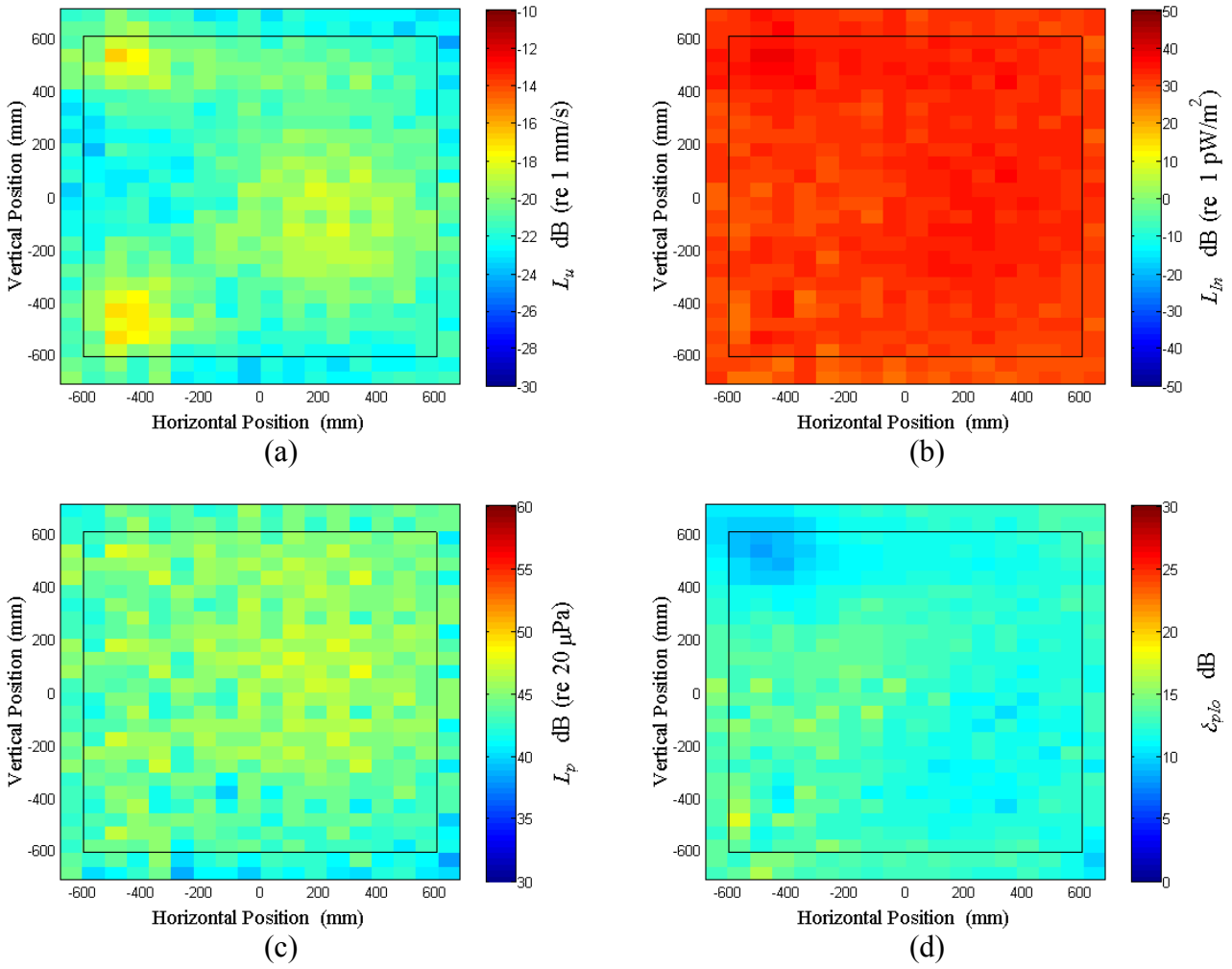

Figure D.10: Surface scan of Window D at 72.5 Hz (a) particle velocity level, L_u (b) normal signed sound intensity level, L_{In} (c) sound pressure level, L_p (d) pressure-residual intensity index, δ_{pIo}.

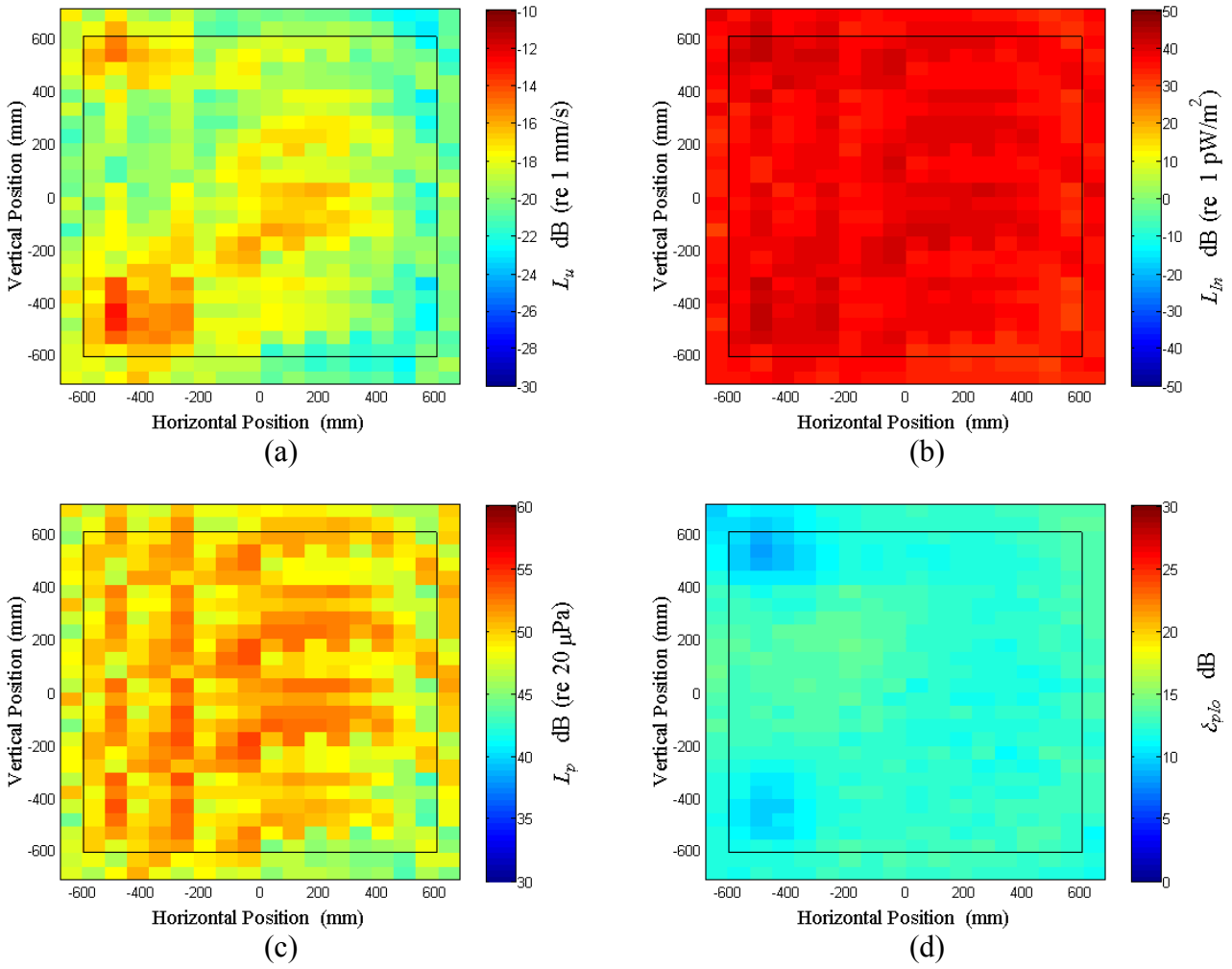

Figure D.11: Surface scan of Window D at 75 Hz (a) particle velocity level, L_u (b) normal signed sound intensity level, L_{In} (c) sound pressure level, L_p (d) pressure-residual intensity index, δ_{pIo}.

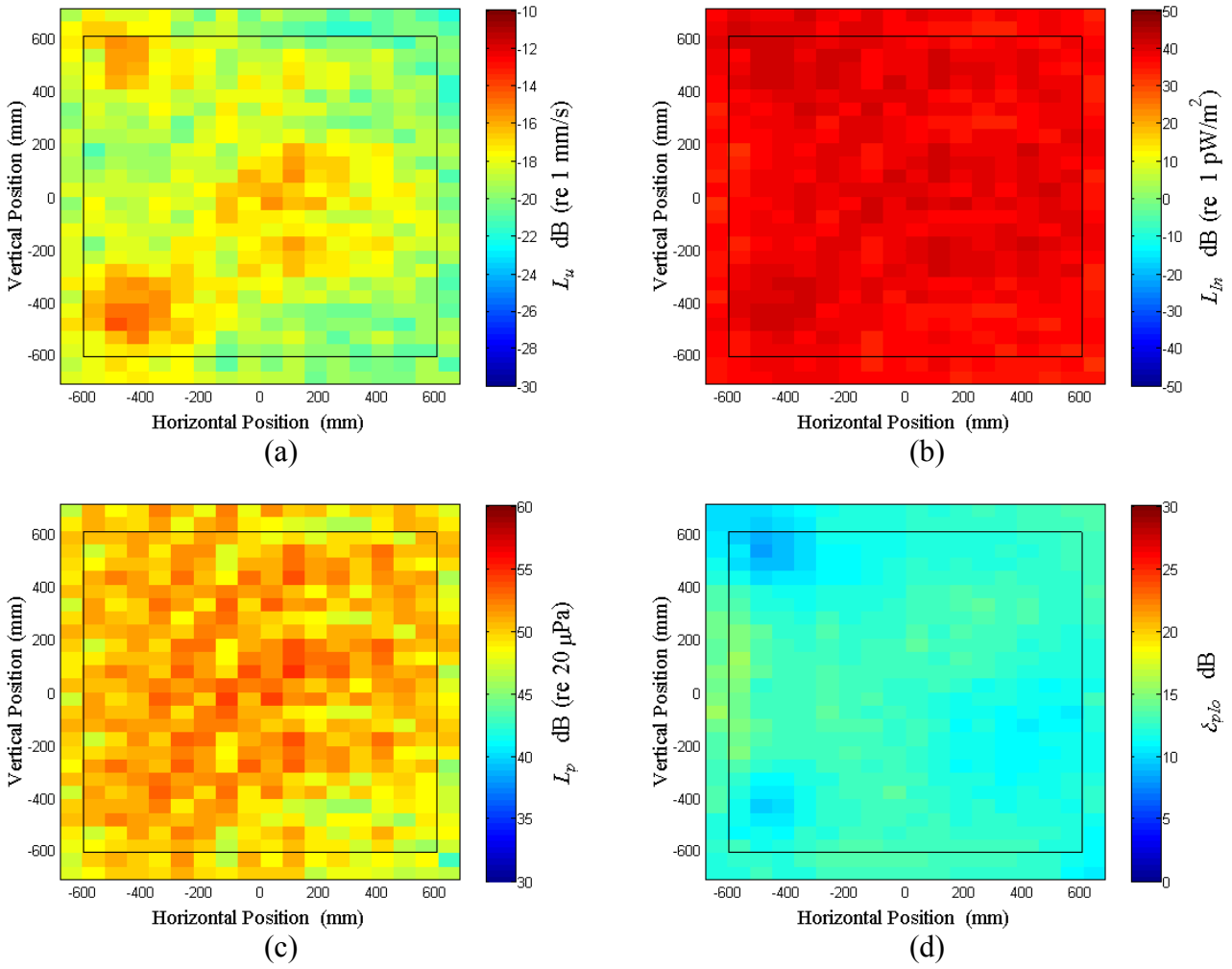

Figure D.12: Surface scan of Window D at 77.5 Hz (a) particle velocity level, L_u (b) normal signed sound intensity level, L_{In} (c) sound pressure level, L_p (d) pressure-residual intensity index, δ_{pIo}.

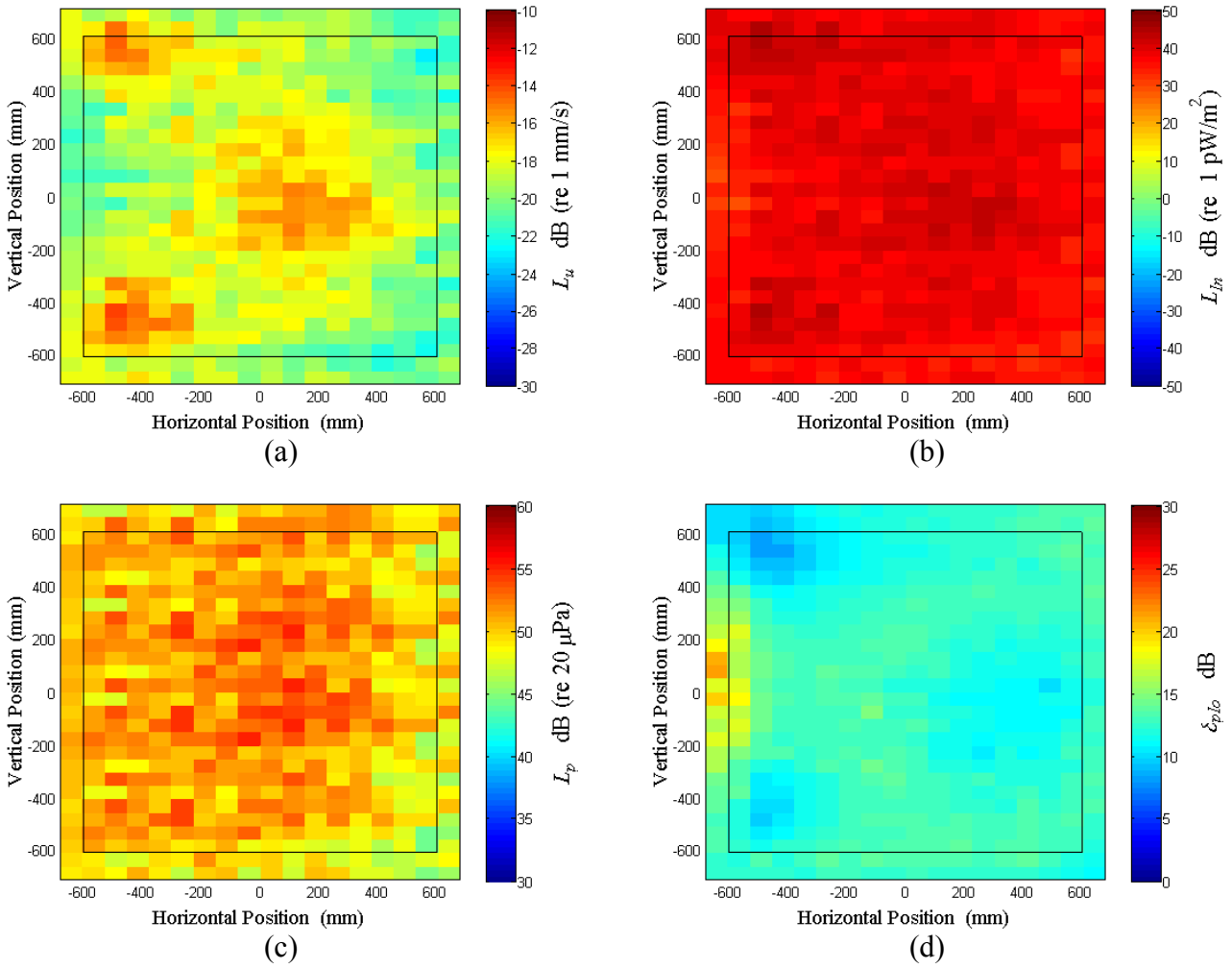

Figure D.13: Surface scan of Window D at 80 Hz (a) particle velocity level, L_u (b) normal signed sound intensity level, L_{In} (c) sound pressure level, L_p (d) pressure-residual intensity index, δ_{pIo}.

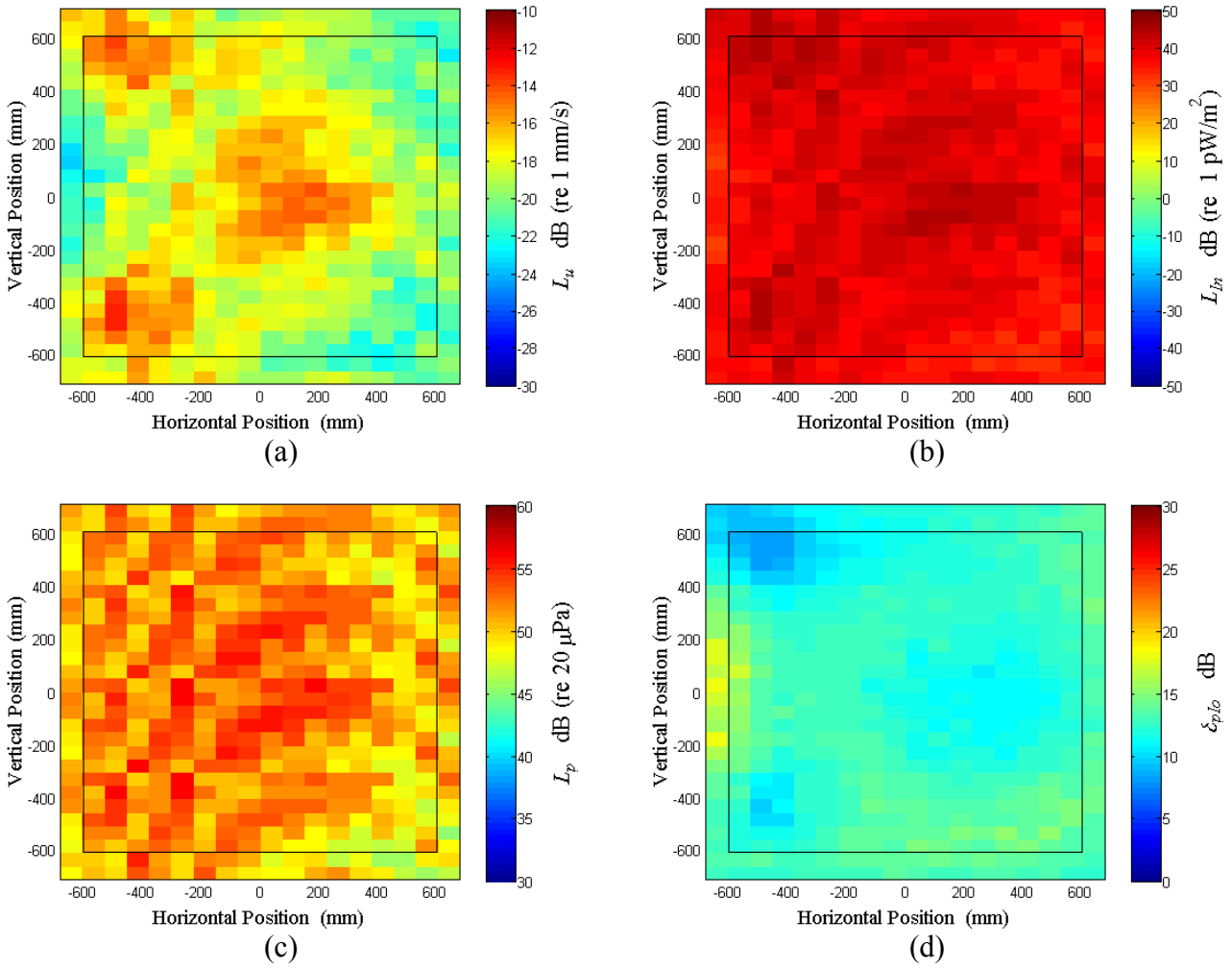

Figure D.14: Surface scan of Window D at 82.5 Hz (a) particle velocity level, L_u (b) normal signed sound intensity level, L_{In} (c) sound pressure level, L_p (d) pressure-residual intensity index, δ_{pIo}.

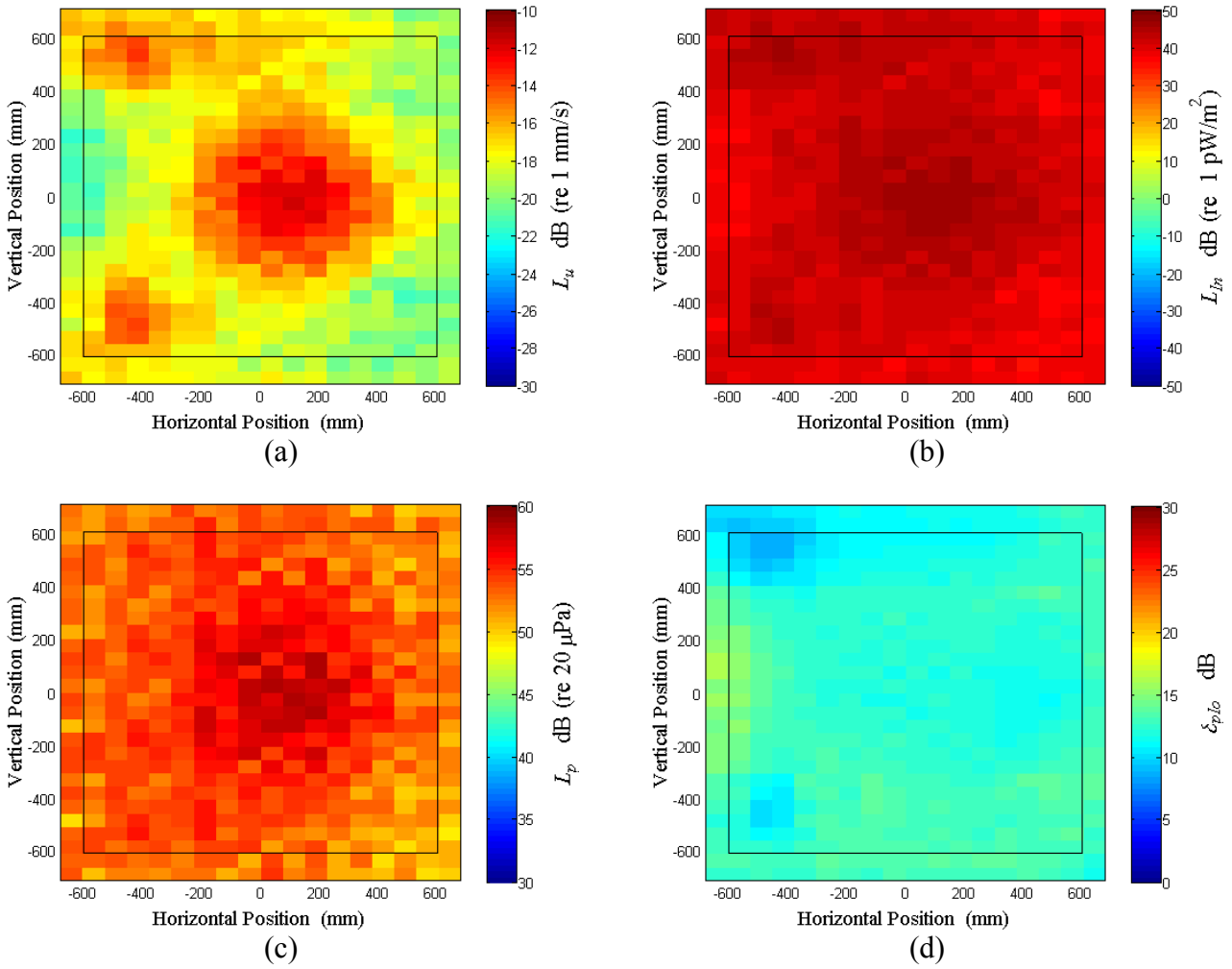

Figure D.15: Surface scan of Window D at 85 Hz (a) particle velocity level, L_u (b) normal signed sound intensity level, L_{In} (c) sound pressure level, L_p (d) pressure-residual intensity index, δ_{pIo}.

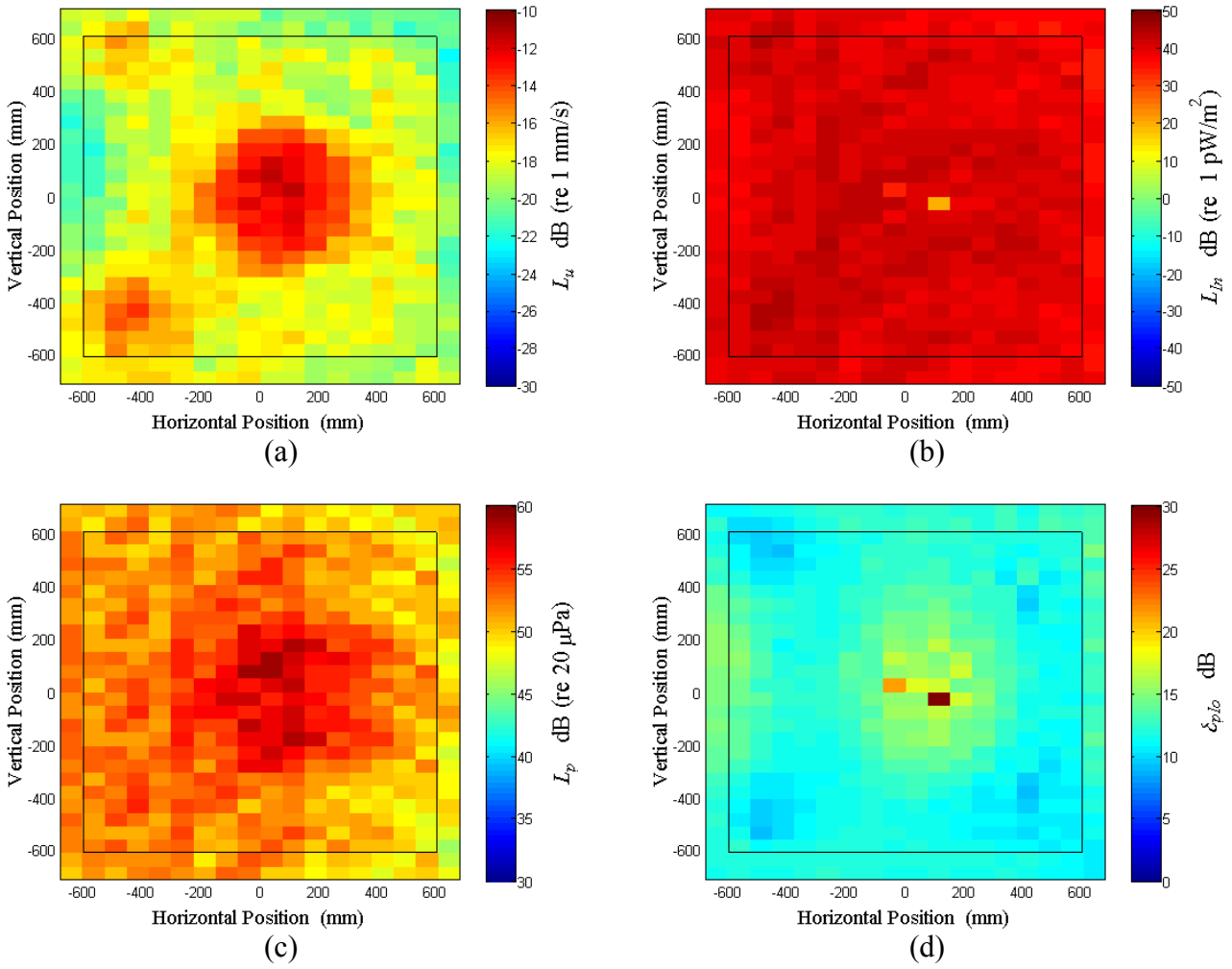

Figure D.16: Surface scan of Window D at 87.5 Hz (a) particle velocity level, L_u (b) normal signed sound intensity level, L_{In} (c) sound pressure level, L_p (d) pressure-residual intensity index, δ_{pIo}.

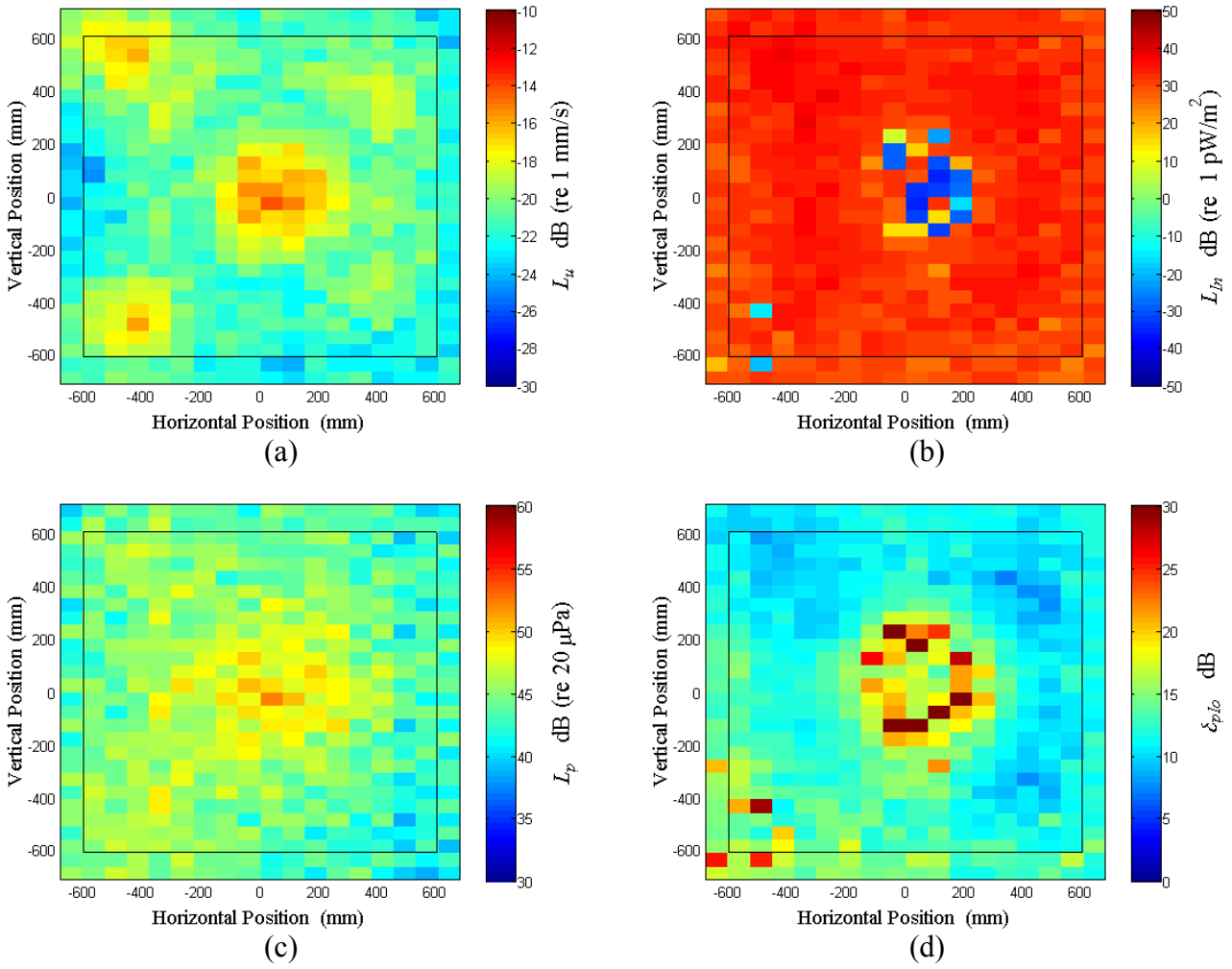

Figure D.17: Surface scan of Window D at 90 Hz (a) particle velocity level, L_u (b) normal signed sound intensity level, L_{In} (c) sound pressure level, L_p (d) pressure-residual intensity index, δ_{pIo}.

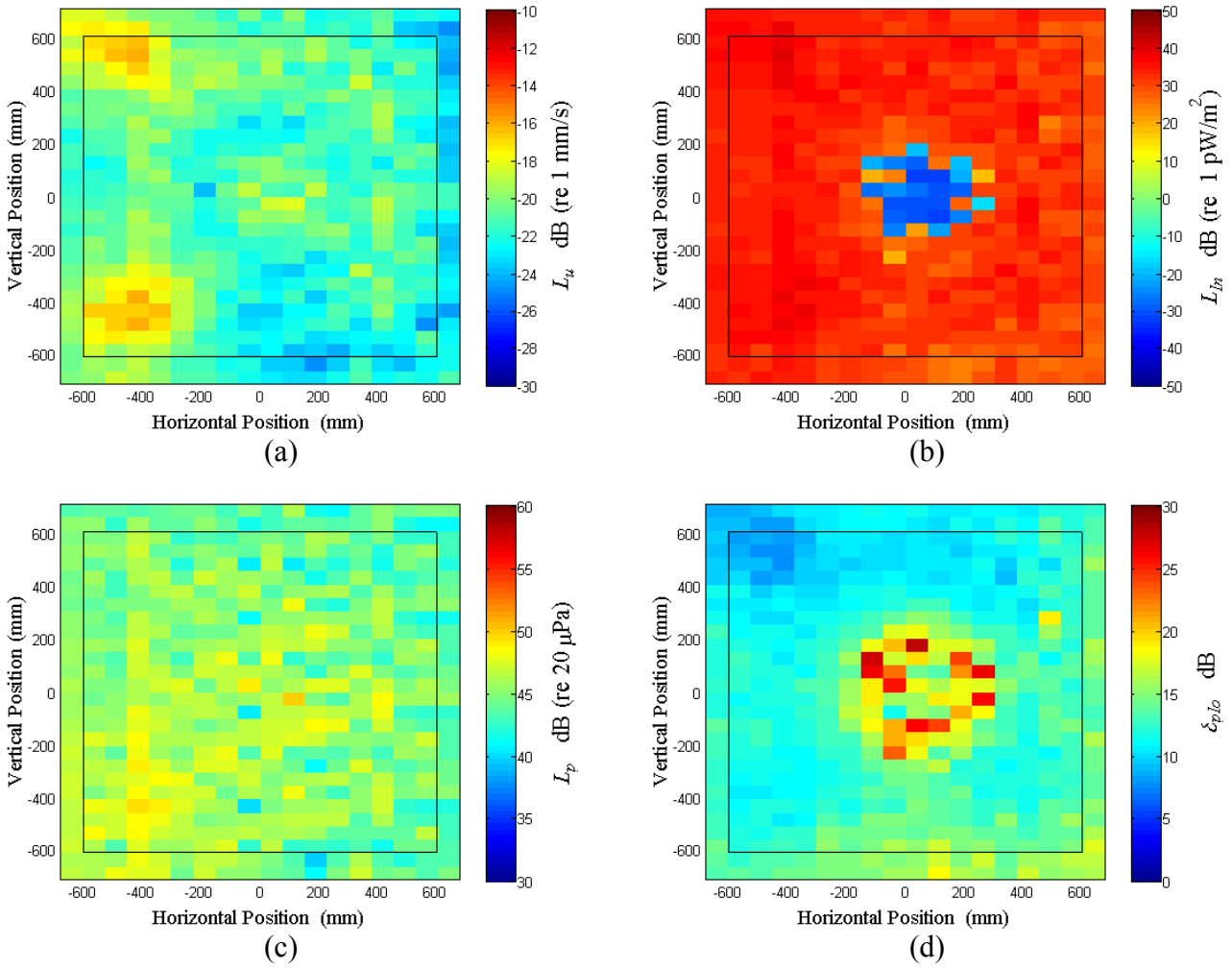

Figure D.18: Surface scan of Window D at 92.5 Hz (a) particle velocity level, L_u (b) normal signed sound intensity level, L_{In} (c) sound pressure level, L_p (d) pressure-residual intensity index, δ_{pIo}.

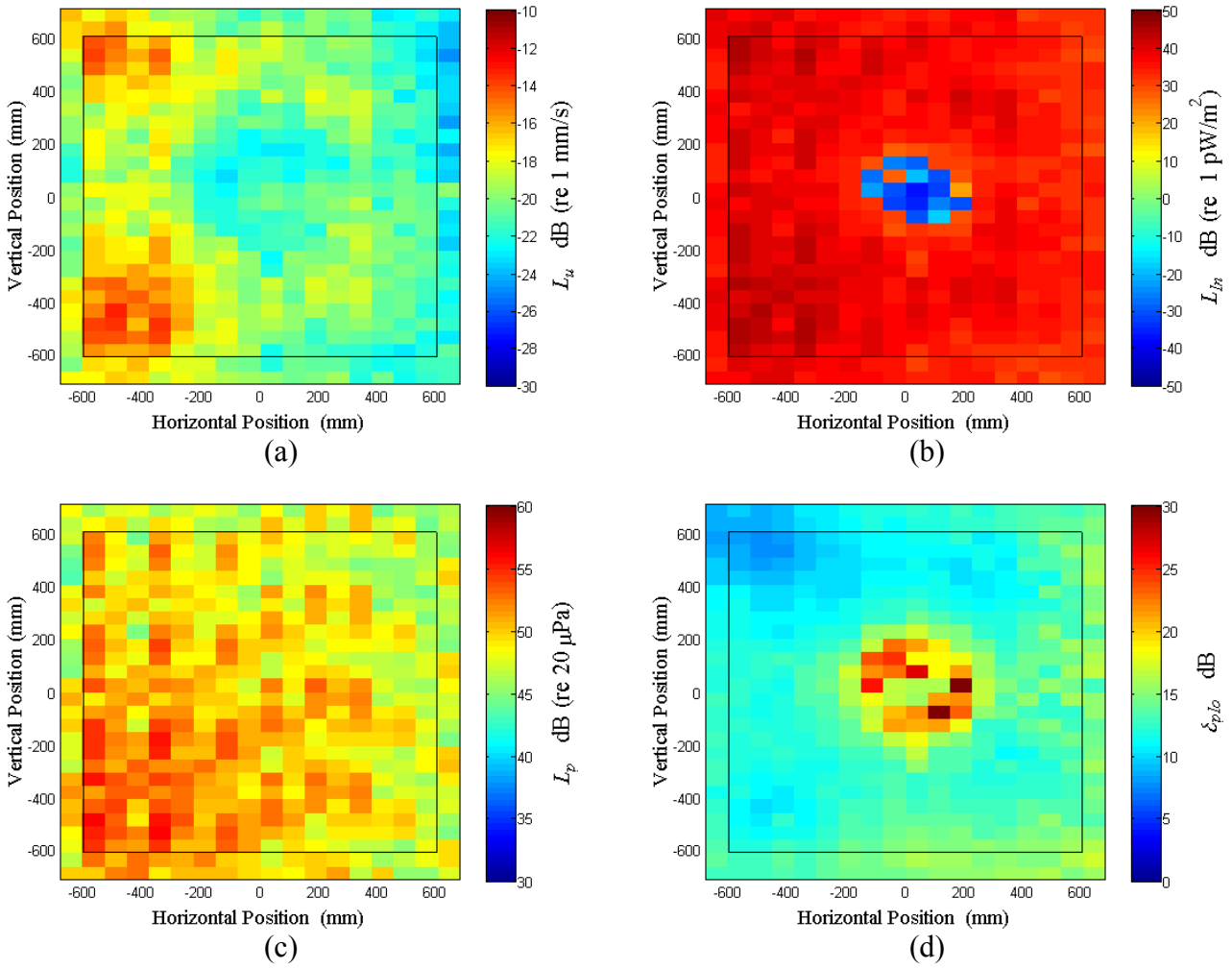

Figure D.19: Surface scan of Window D at 95 Hz (a) particle velocity level, L_u (b) normal signed sound intensity level, L_{In} (c) sound pressure level, L_p (d) pressure-residual intensity index, δ_{pIo}.

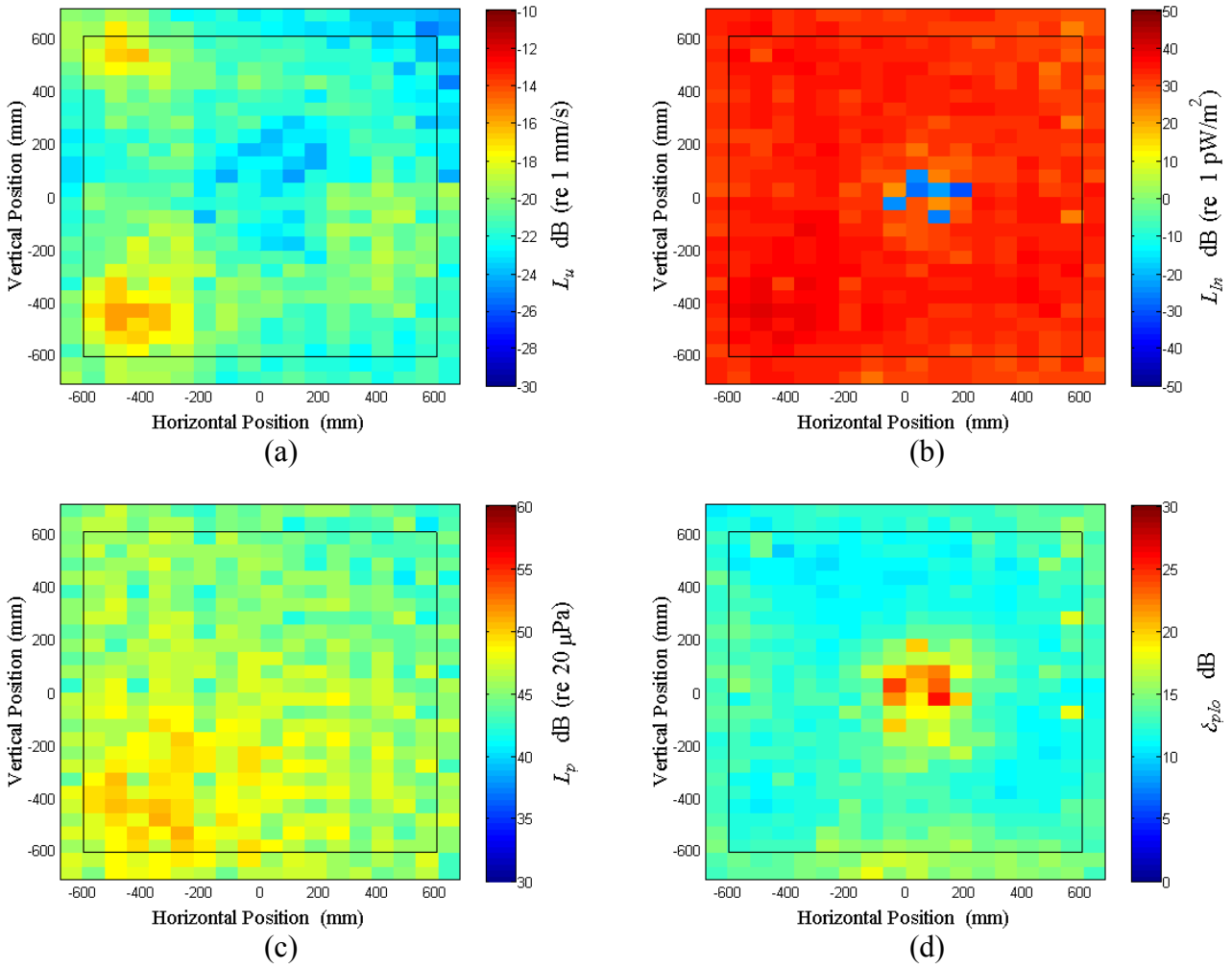

Figure D.20: Surface scan of Window D at 97.5 Hz (a) particle velocity level, L_u (b) normal signed sound intensity level, L_{In} (c) sound pressure level, L_p (d) pressure-residual intensity index, δ_{pIo}.

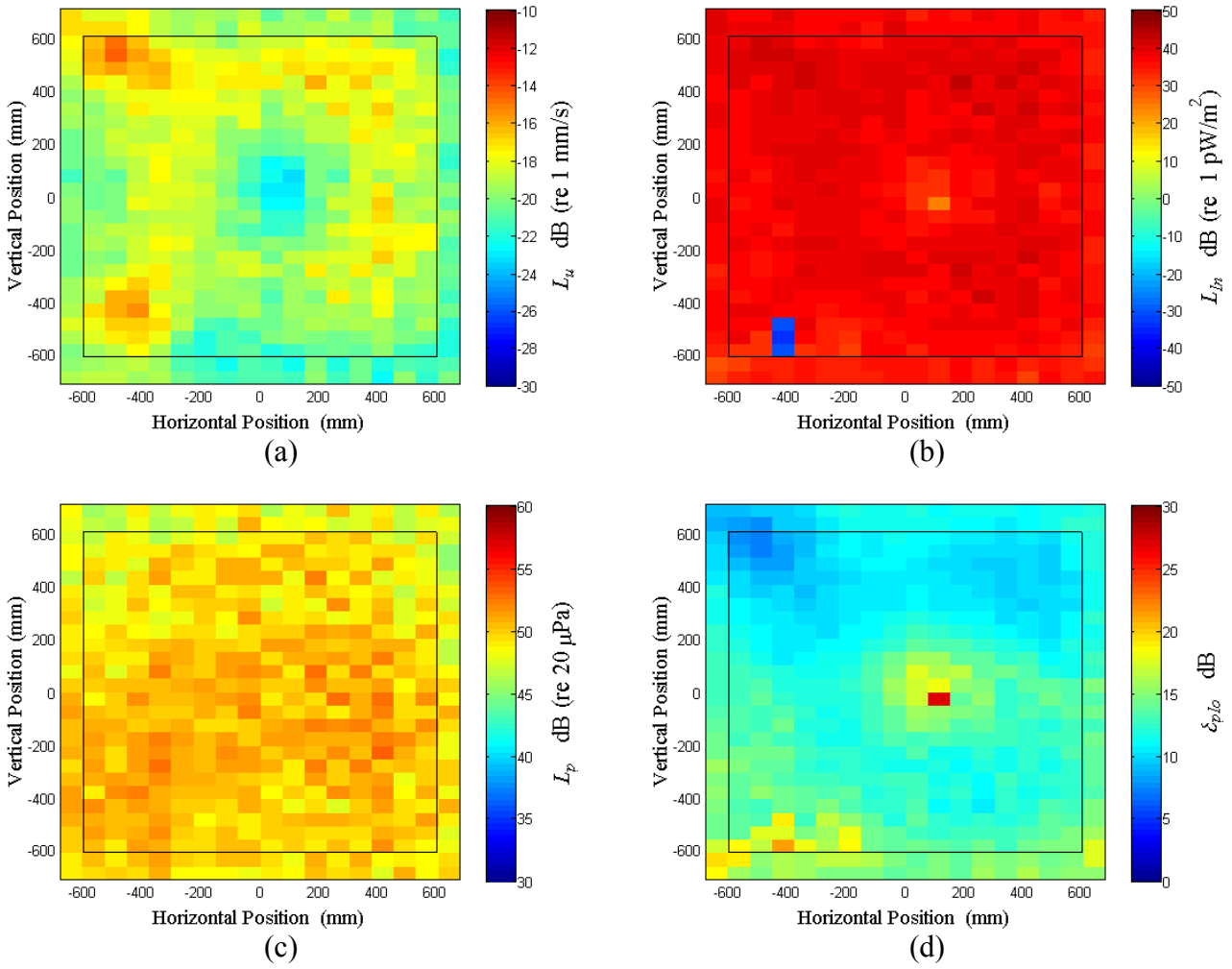

Figure D.21: Surface scan of Window D at 100 Hz (a) particle velocity level, L_u (b) normal signed sound intensity level, L_{In} (c) sound pressure level, L_p (d) pressure-residual intensity index, δ_{pIo}.

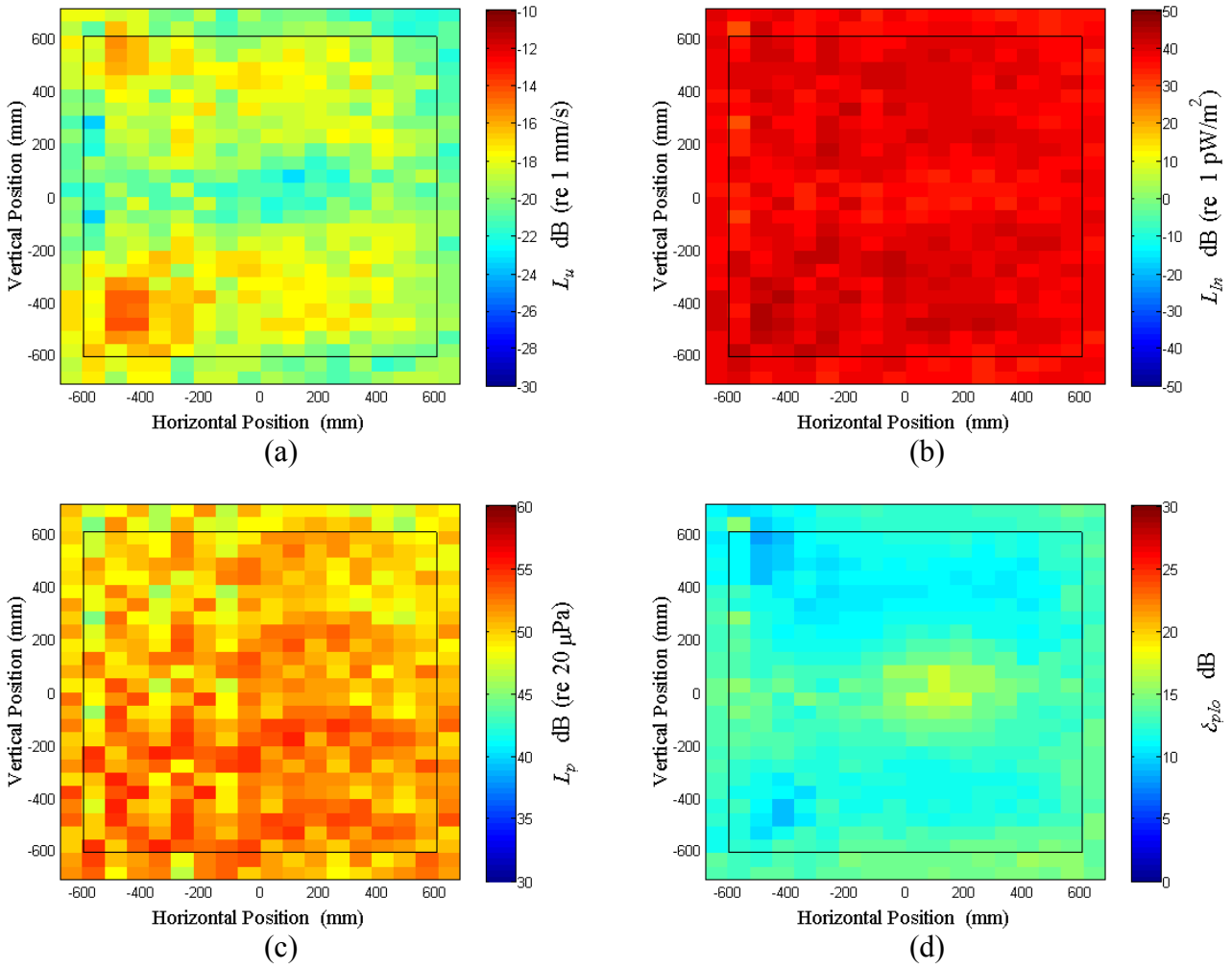

Figure D.22: Surface scan of Window D at 102.5 Hz (a) particle velocity level, L_u (b) normal signed sound intensity level, L_{In} (c) sound pressure level, L_p (d) pressure-residual intensity index, δ_{pIo}.

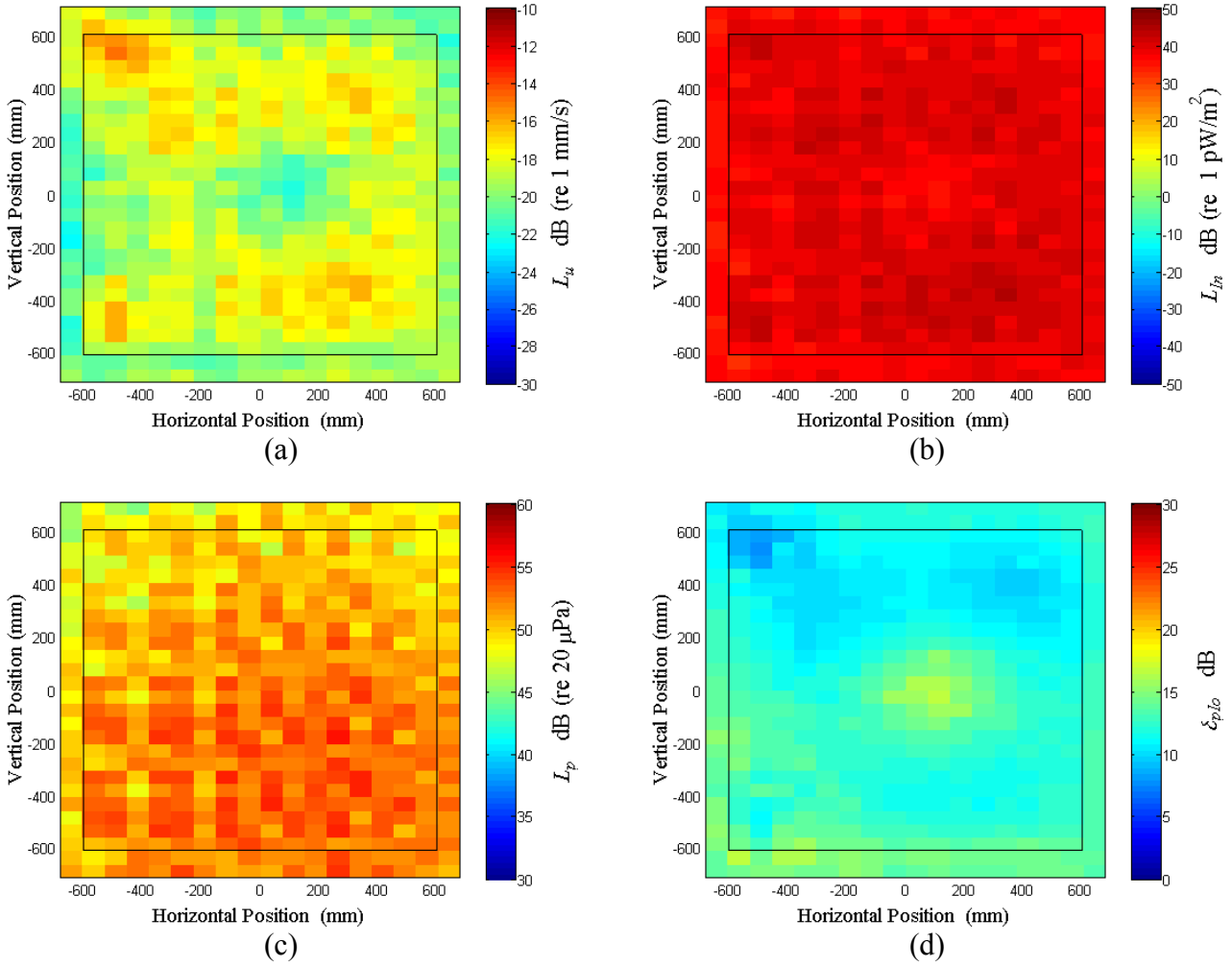

Figure D.23: Surface scan of Window D at 105 Hz (a) particle velocity level, L_u (b) normal signed sound intensity level, L_{In} (c) sound pressure level, L_p (d) pressure-residual intensity index, δ_{pIo}.

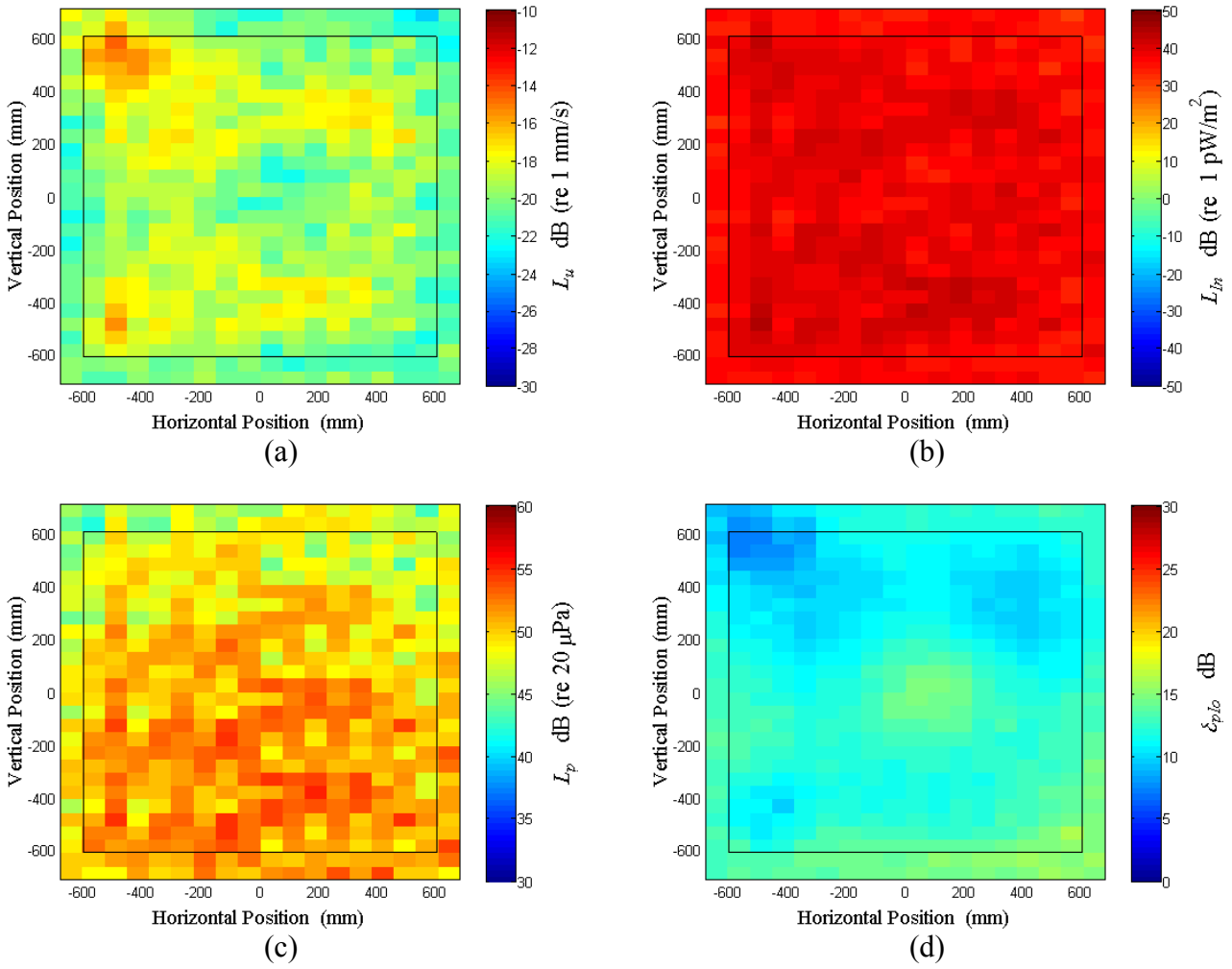

Figure D.24: Surface scan of Window D at 107.5 Hz (a) particle velocity level, L_u (b) normal signed sound intensity level, L_{In} (c) sound pressure level, L_p (d) pressure-residual intensity index, δ_{pIo}.

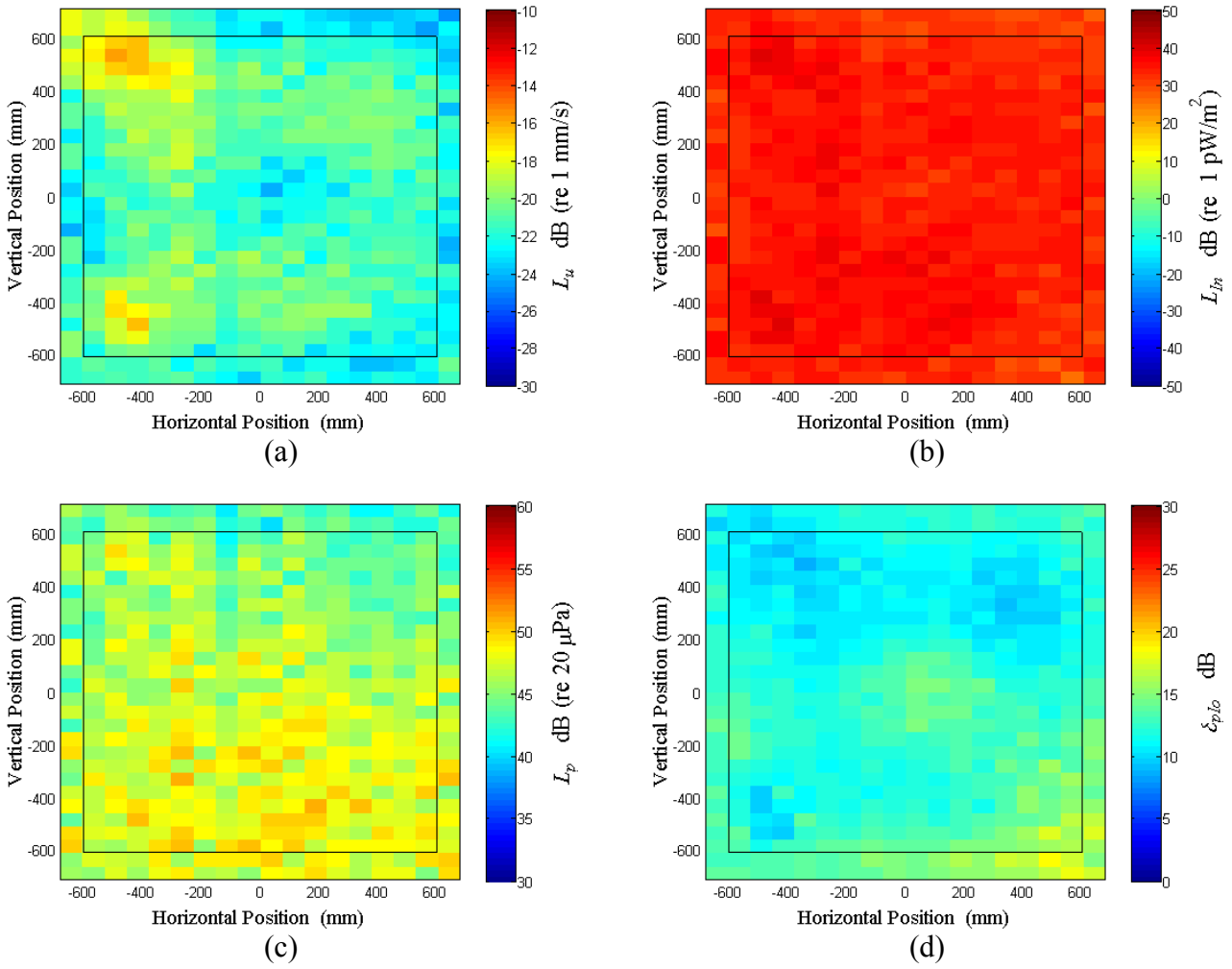

Figure D.25: Surface scan of Window D at 110 Hz (a) particle velocity level, L_u (b) normal signed sound intensity level, L_{In} (c) sound pressure level, L_p (d) pressure-residual intensity index, δ_{pIo}.

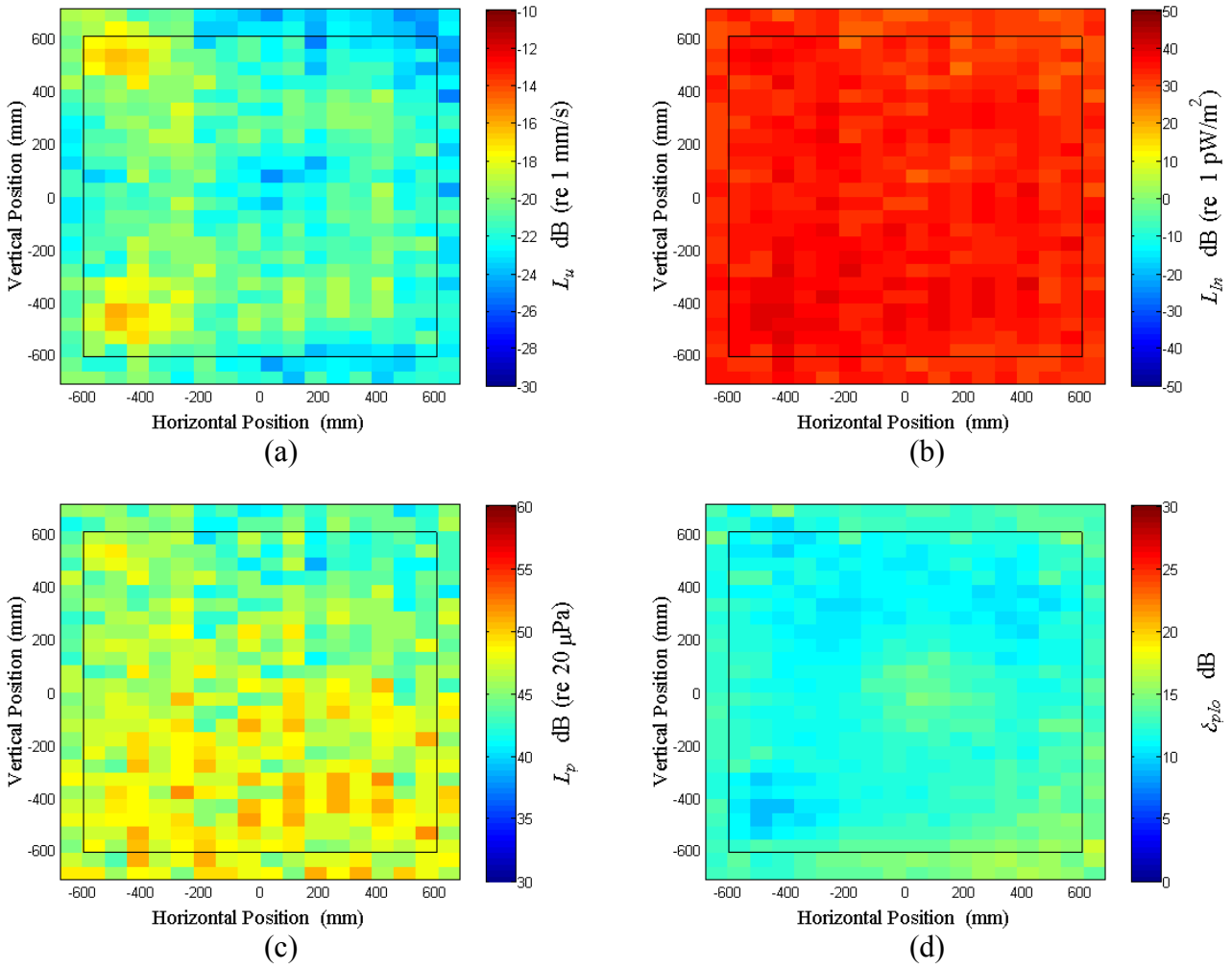

Figure D.26: Surface scan of Window D at 112.5 Hz (a) particle velocity level, L_u (b) normal signed sound intensity level, L_{In} (c) sound pressure level, L_p (d) pressure-residual intensity index, δ_{pIo}.

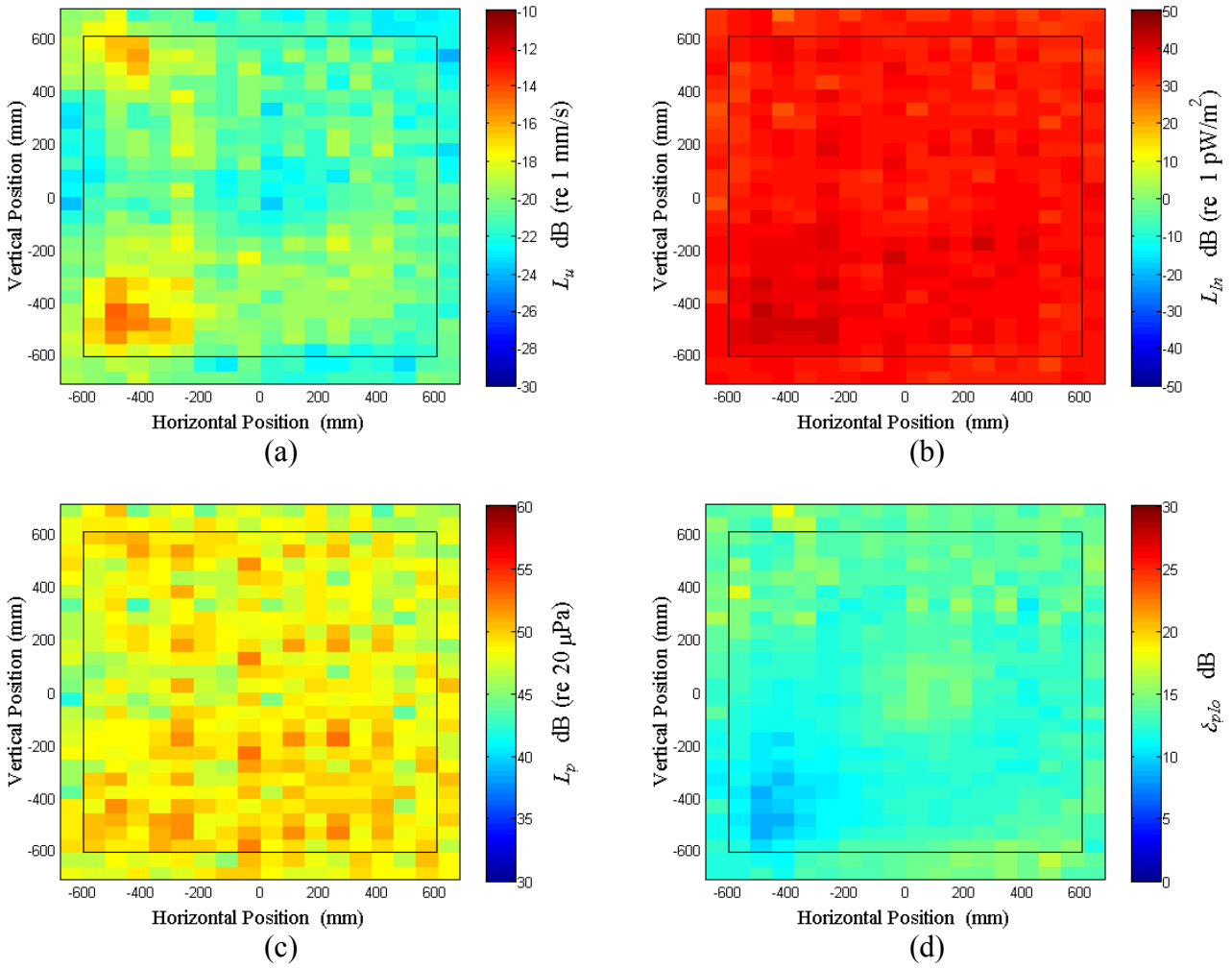

Figure D.27: Surface scan of Window D at 115 Hz (a) particle velocity level, L_u (b) normal signed sound intensity level, L_{In} (c) sound pressure level, L_p (d) pressure-residual intensity index, δ_{pIo}.

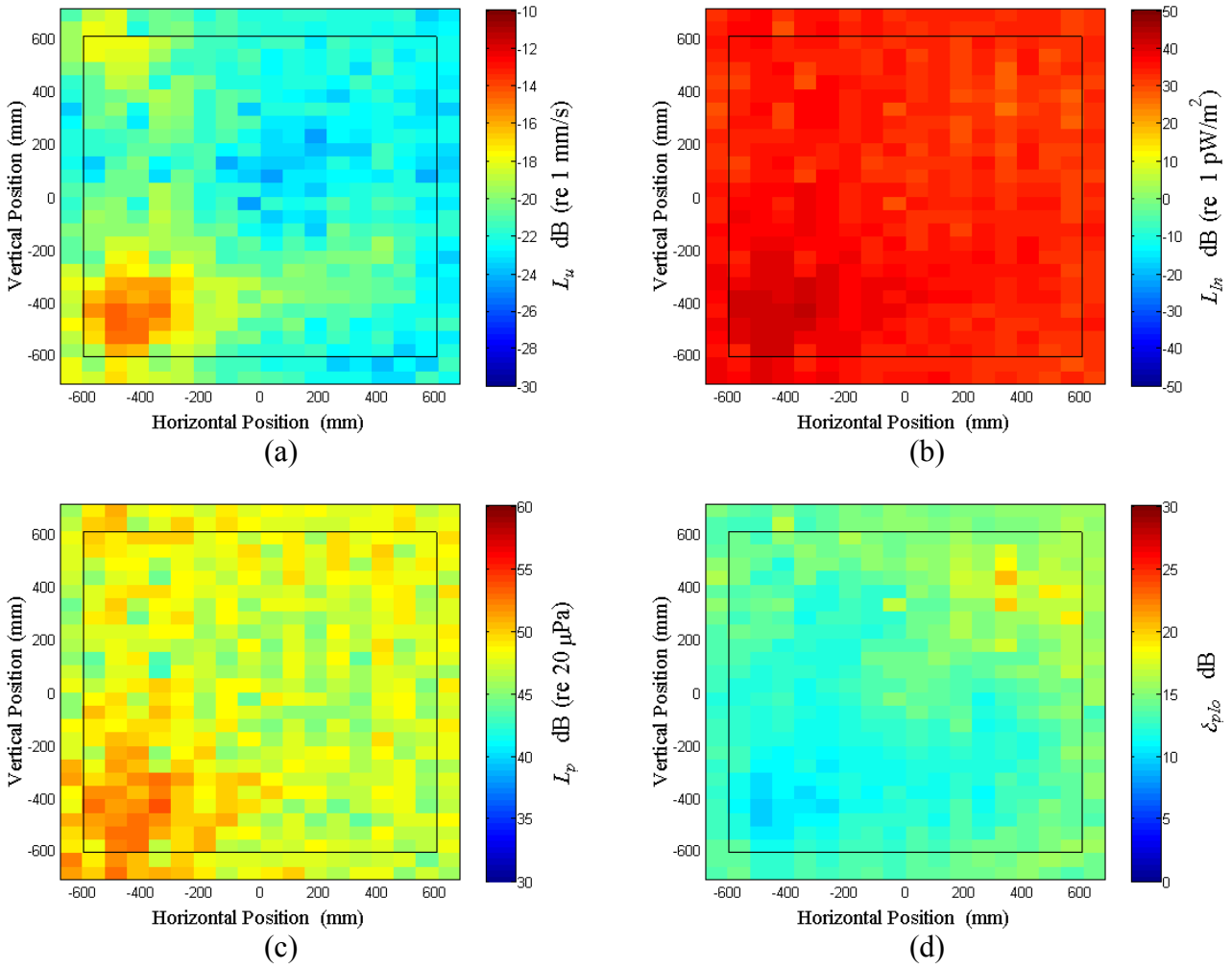

Figure D.28: Surface scan of Window D at 117.5 Hz (a) particle velocity level, L_u (b) normal signed sound intensity level, L_{In} (c) sound pressure level, L_p (d) pressure-residual intensity index, δ_{pIo}.

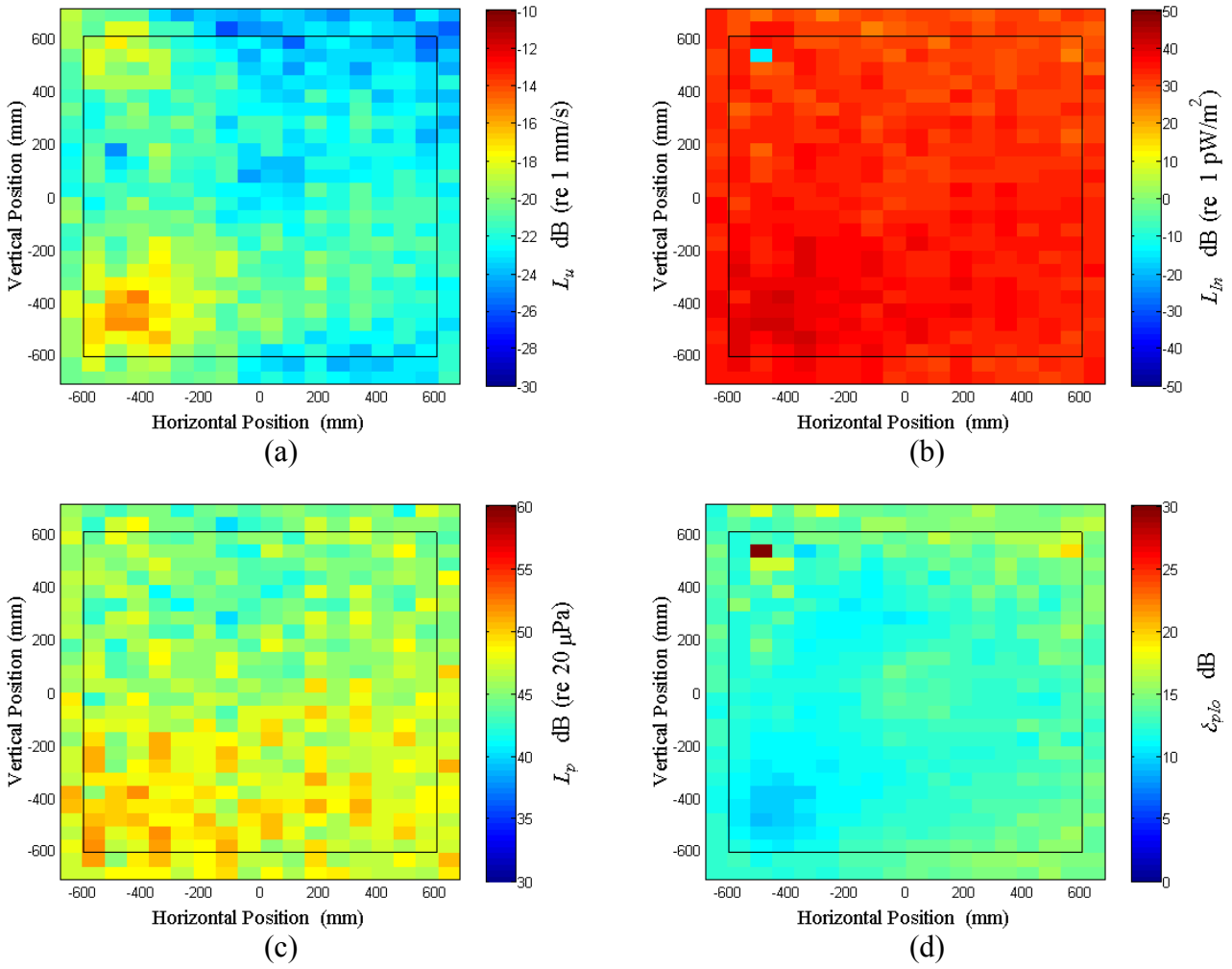

Figure D.29: Surface scan of Window D at 120 Hz (a) particle velocity level, L_u (b) normal signed sound intensity level, L_{In} (c) sound pressure level, L_p (d) pressure-residual intensity index, δ_{pIo}.

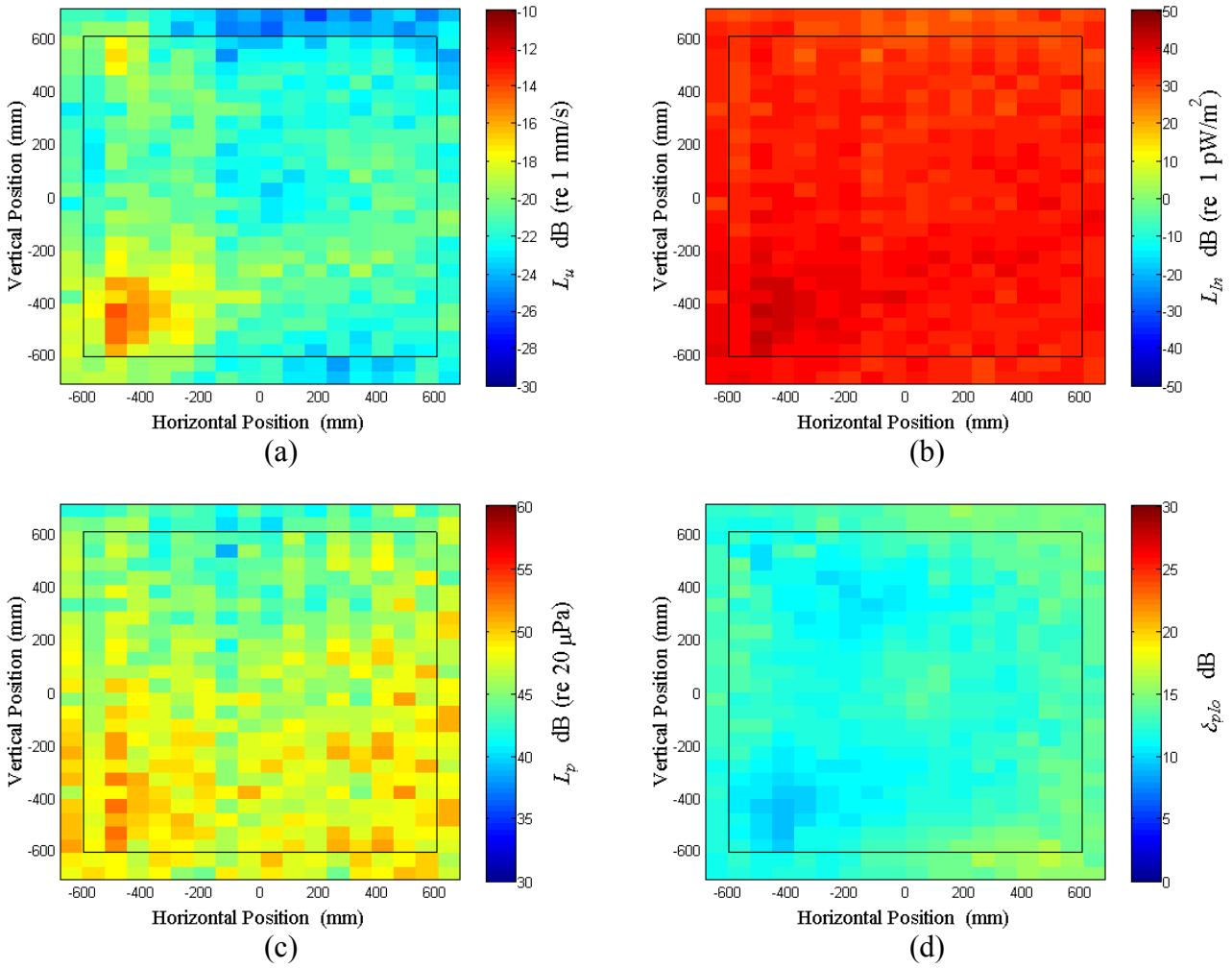

Figure D.30: Surface scan of Window D at 122.5 Hz (a) particle velocity level, L_u (b) normal signed sound intensity level, L_{In} (c) sound pressure level, L_p (d) pressure-residual intensity index, δ_{pIo}.

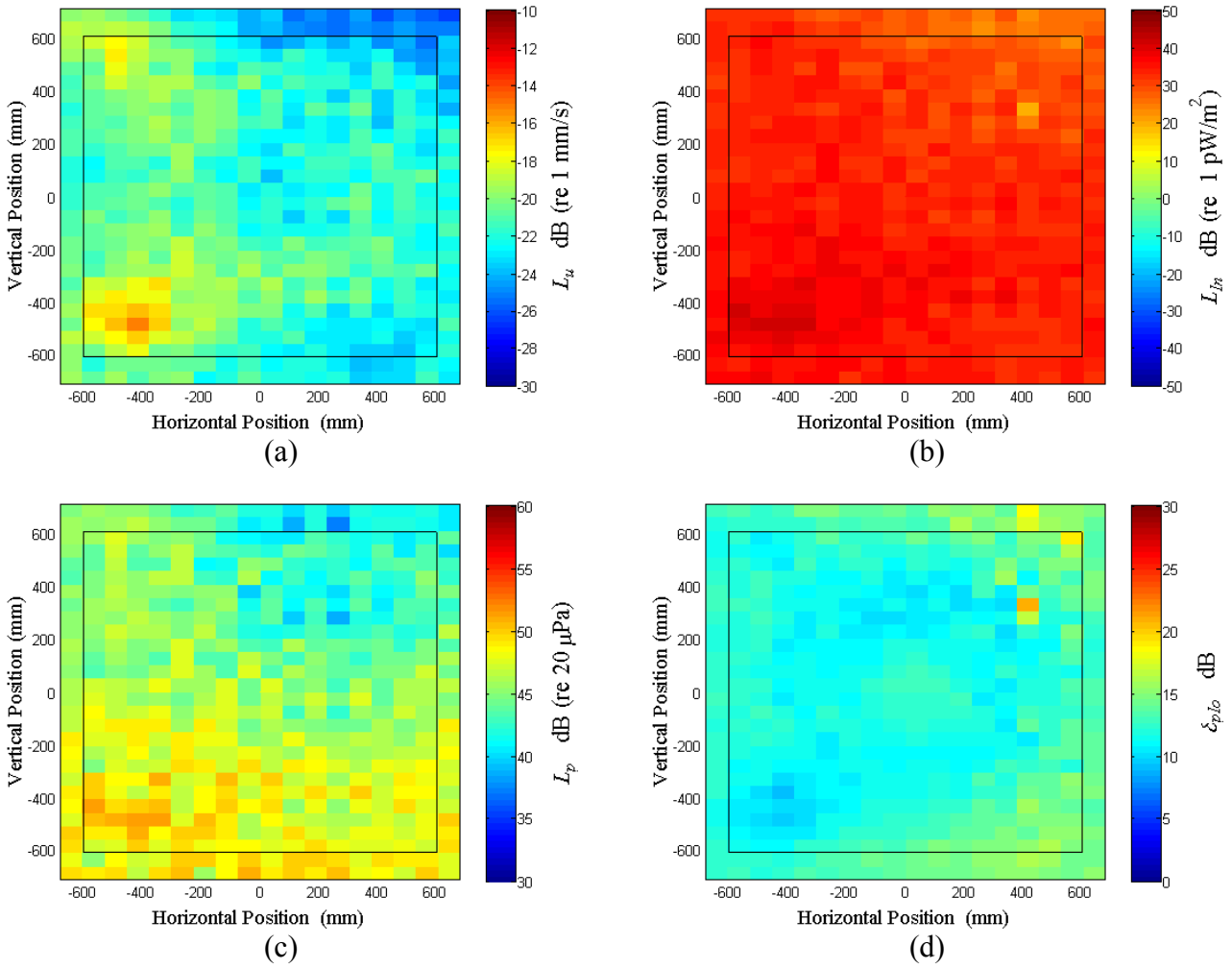

Figure D.31: Surface scan of Window D at 125 Hz (a) particle velocity level, L_u (b) normal signed sound intensity level, L_{In} (c) sound pressure level, L_p (d) pressure-residual 12ntensity index, δ_{pIo}.

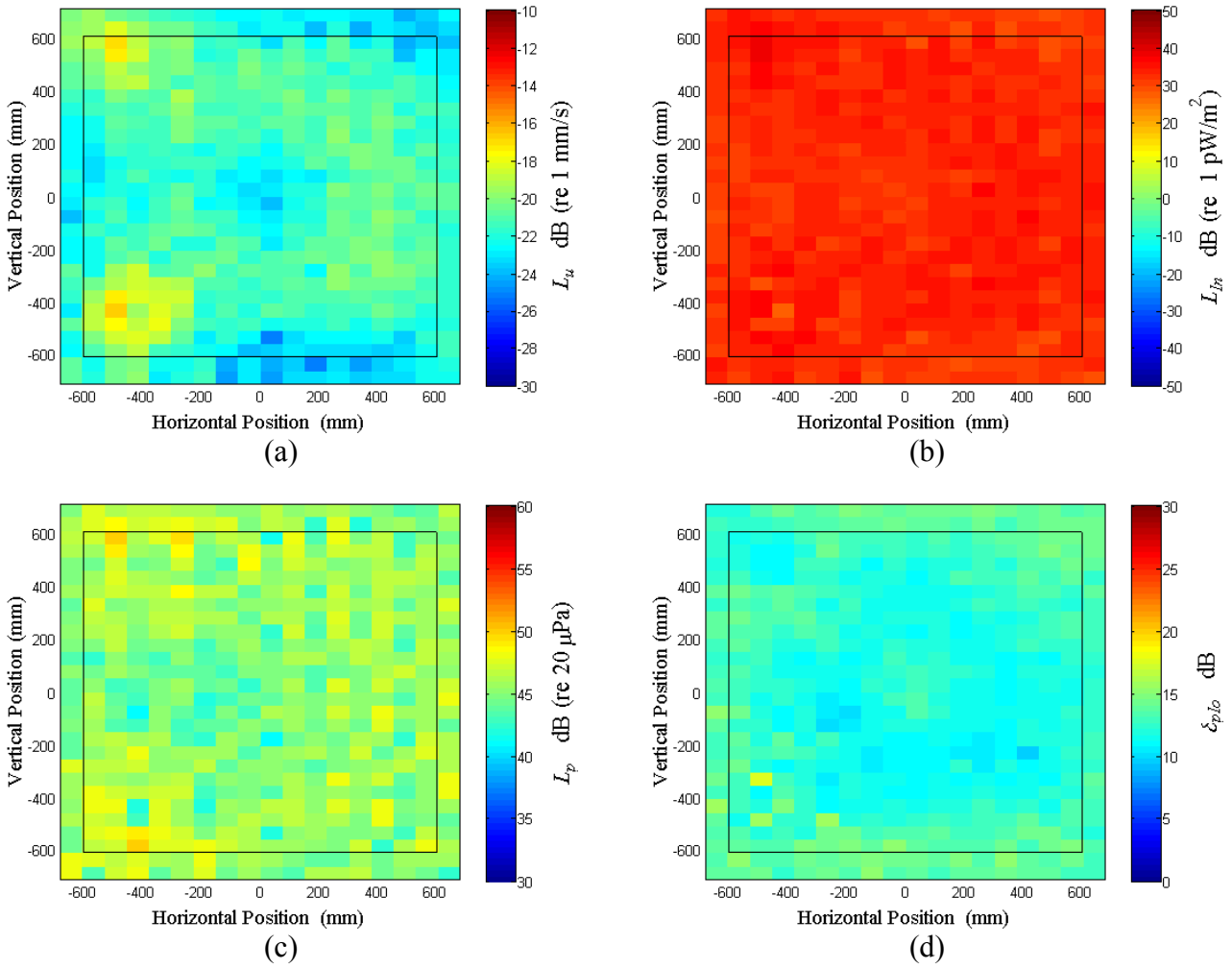

Figure D.32: Surface scan of Window D at 127.5 Hz (a) particle velocity level, L_u (b) normal signed sound intensity level, L_{In} (c) sound pressure level, L_p (d) pressure-residual intensity index, δ_{pIo}.

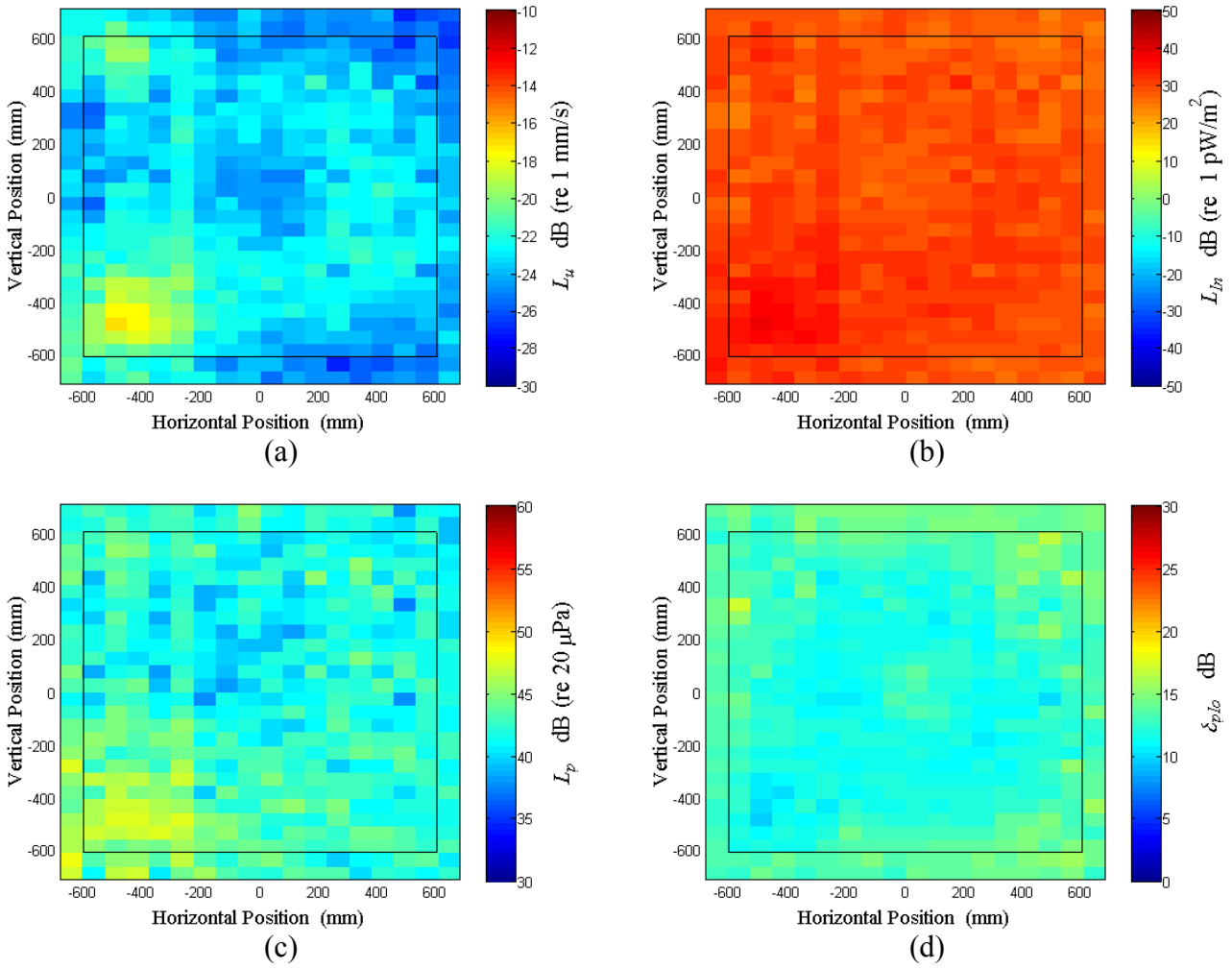

Figure D.33: Surface scan of Window D at 130 Hz (a) particle velocity level, L_u (b) normal signed sound intensity level, L_{In} (c) sound pressure level, L_p (d) pressure-residual intensity index, δ_{pIo}.

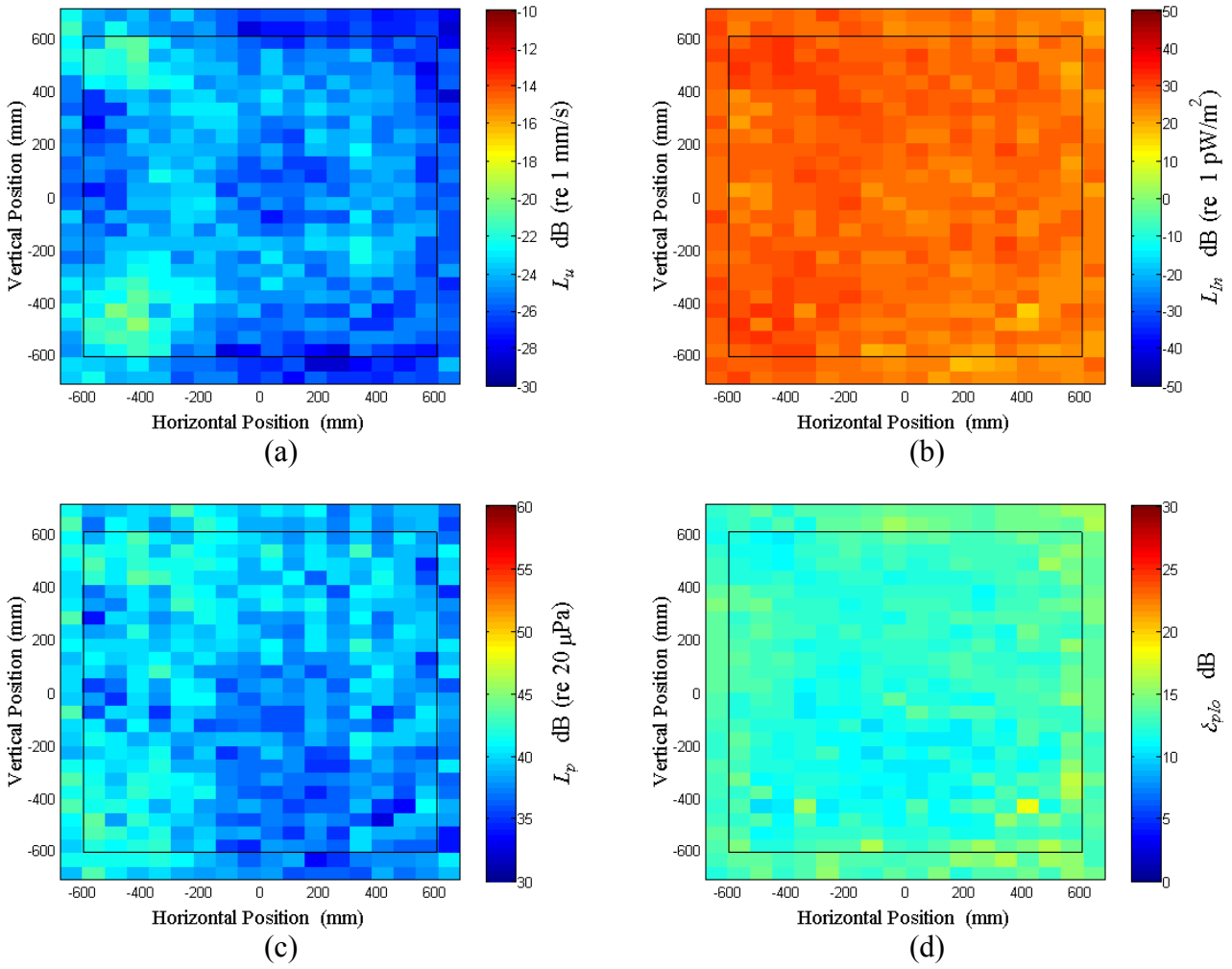

Figure D.34: Surface scan of Window D at 140 Hz (a) particle velocity level, L_u (b) normal signed sound intensity level, L_{In} (c) sound pressure level, L_p (d) pressure-residual intensity index, δ_{pIo}.

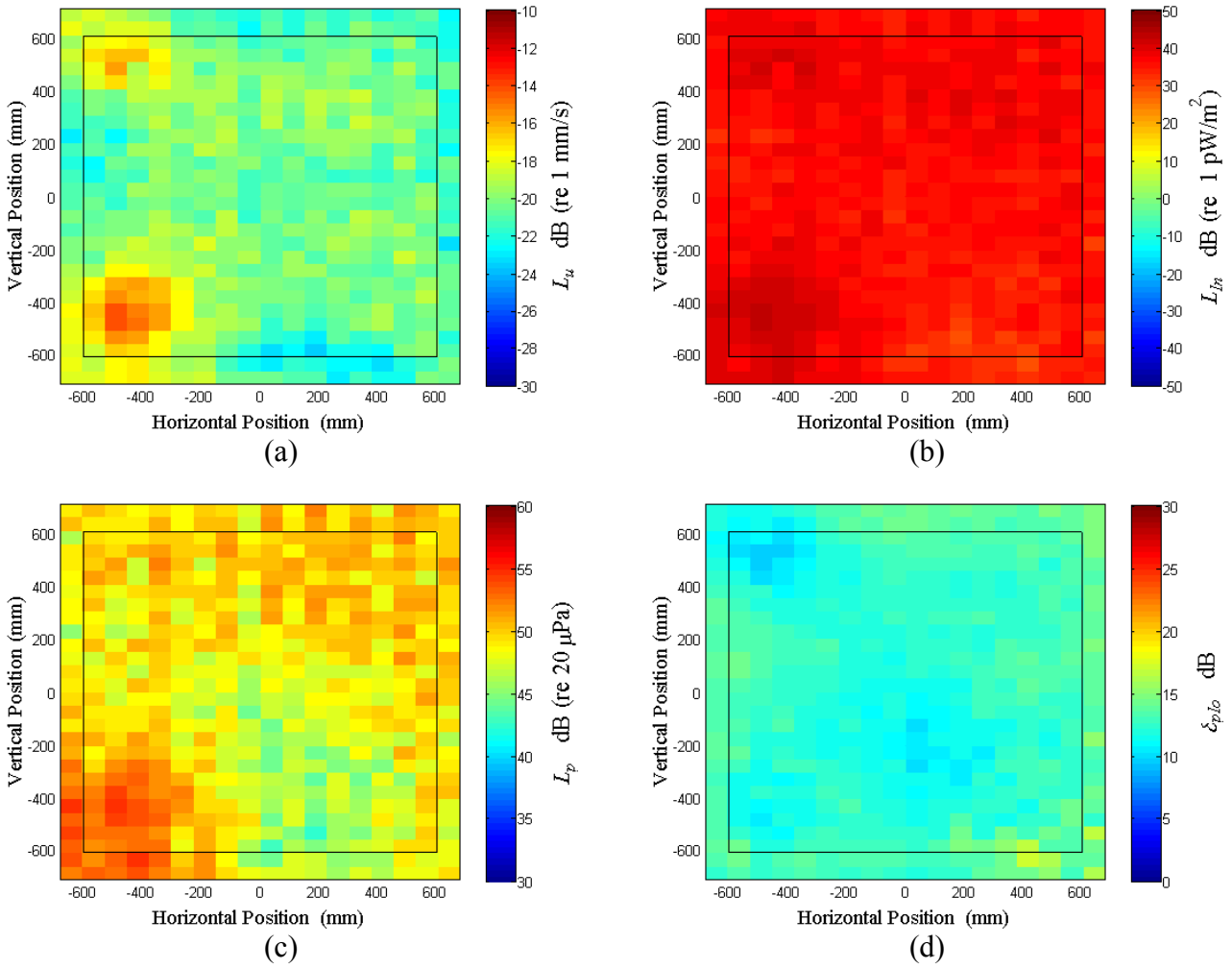

Figure D.35: Surface scan of Window D at 150 Hz (a) particle velocity level, L_u (b) normal signed sound intensity level, L_{In} (c) sound pressure level, L_p (d) pressure-residual intensity index, δ_{pIo}.

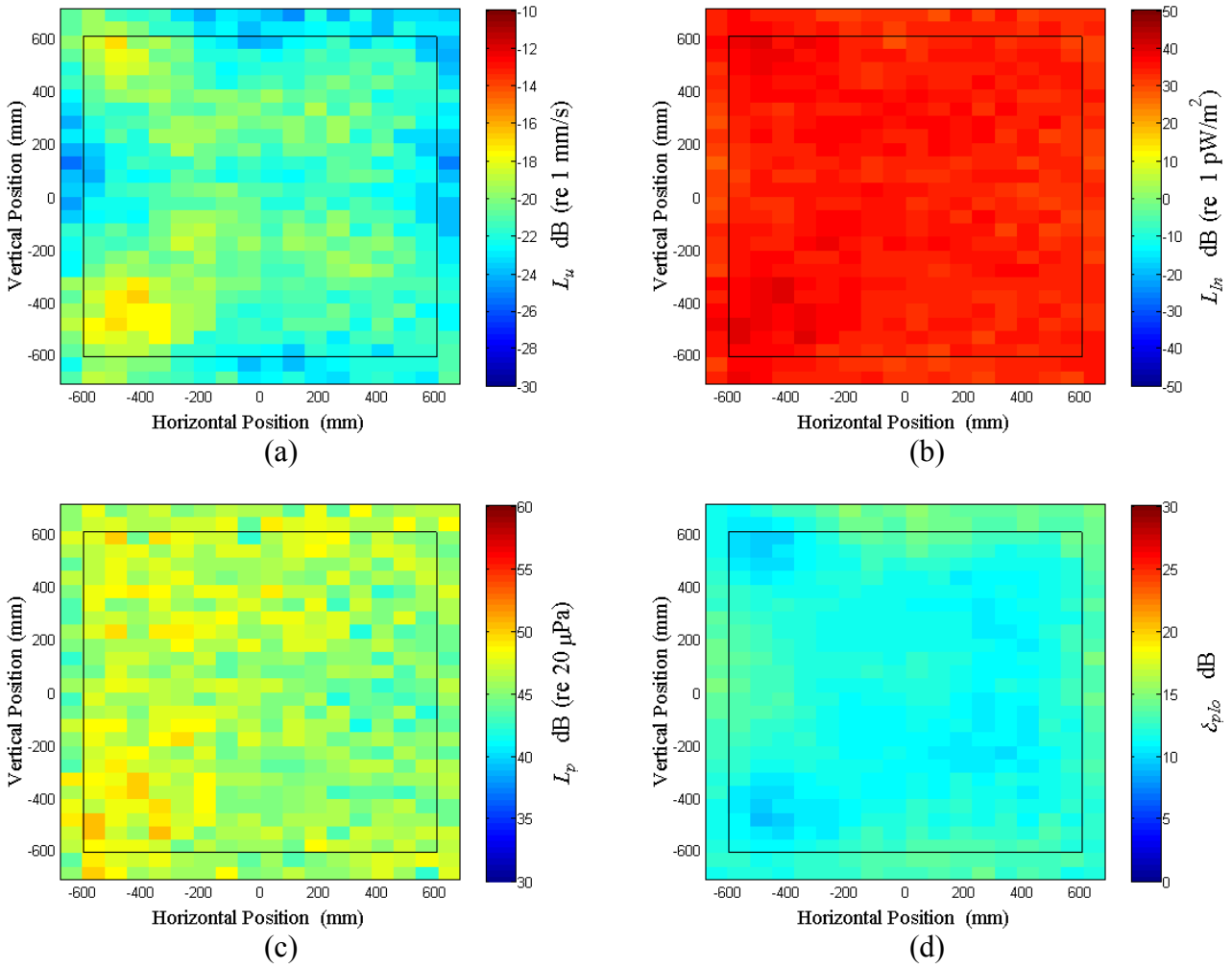

Figure D.36: Surface scan of Window D at 160 Hz (a) particle velocity level, L_u (b) normal signed sound intensity level, L_{In} (c) sound pressure level, L_p (d) pressure-residual intensity index, δ_{pIo}.

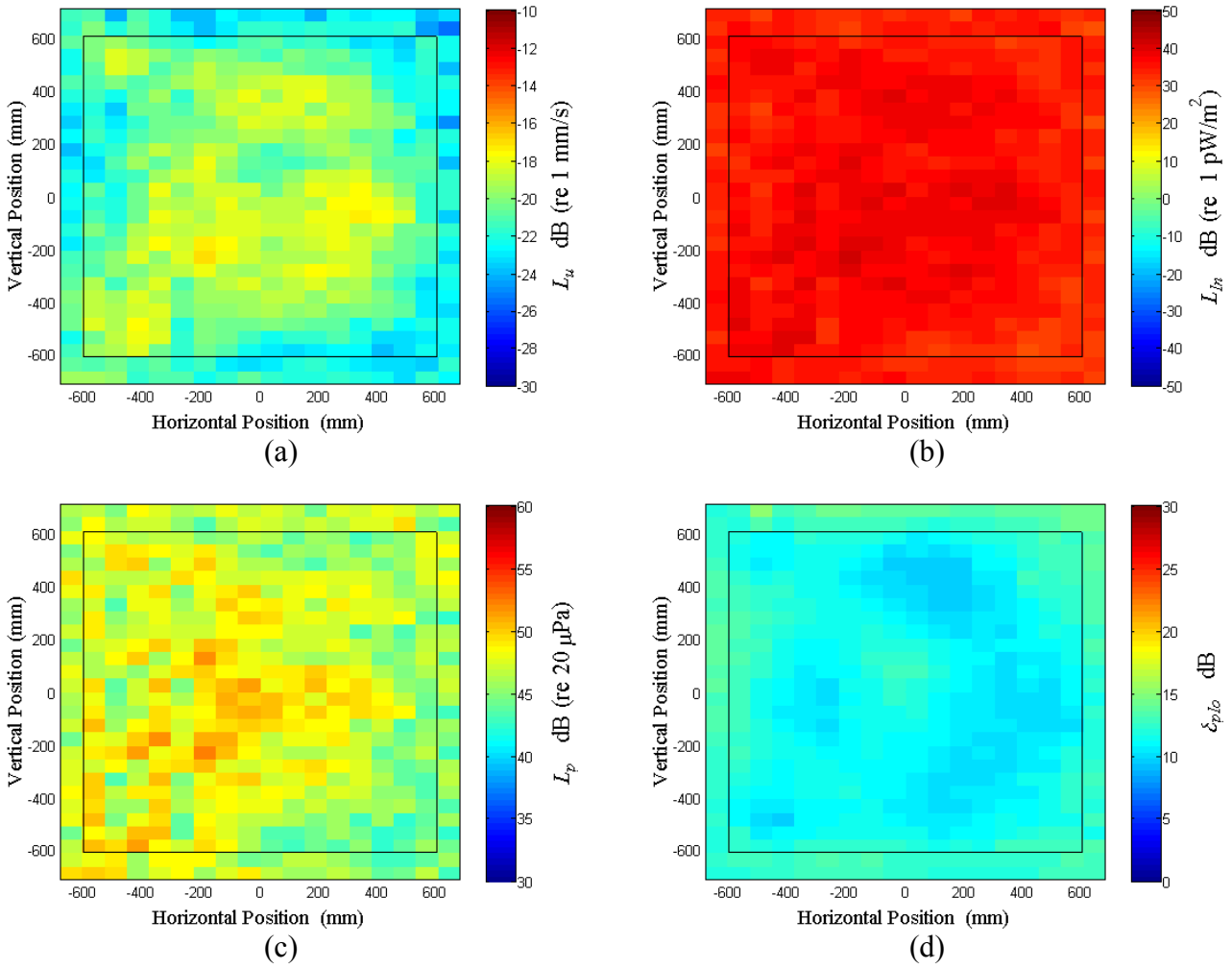

Figure D.37: Surface scan of Window D at 170 Hz (a) particle velocity level, L_u (b) normal signed sound intensity level, L_{In} (c) sound pressure level, L_p (d) pressure-residual intensity index, δ_{pIo}.

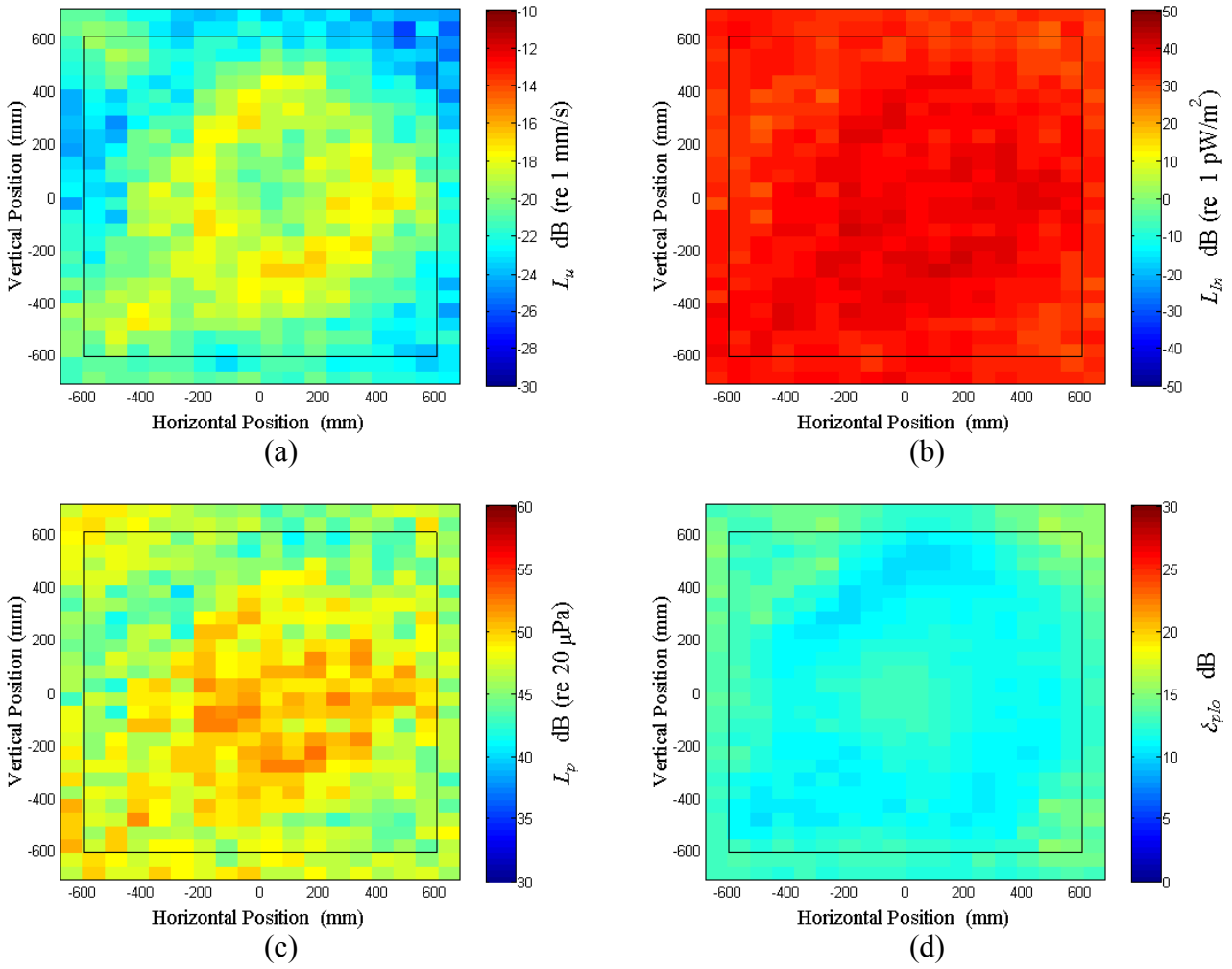

Figure D.38: Surface scan of Window D at 180 Hz (a) particle velocity level, L_u (b) normal signed sound intensity level, L_{In} (c) sound pressure level, L_p (d) pressure-residual intensity index, δ_{pIo}.

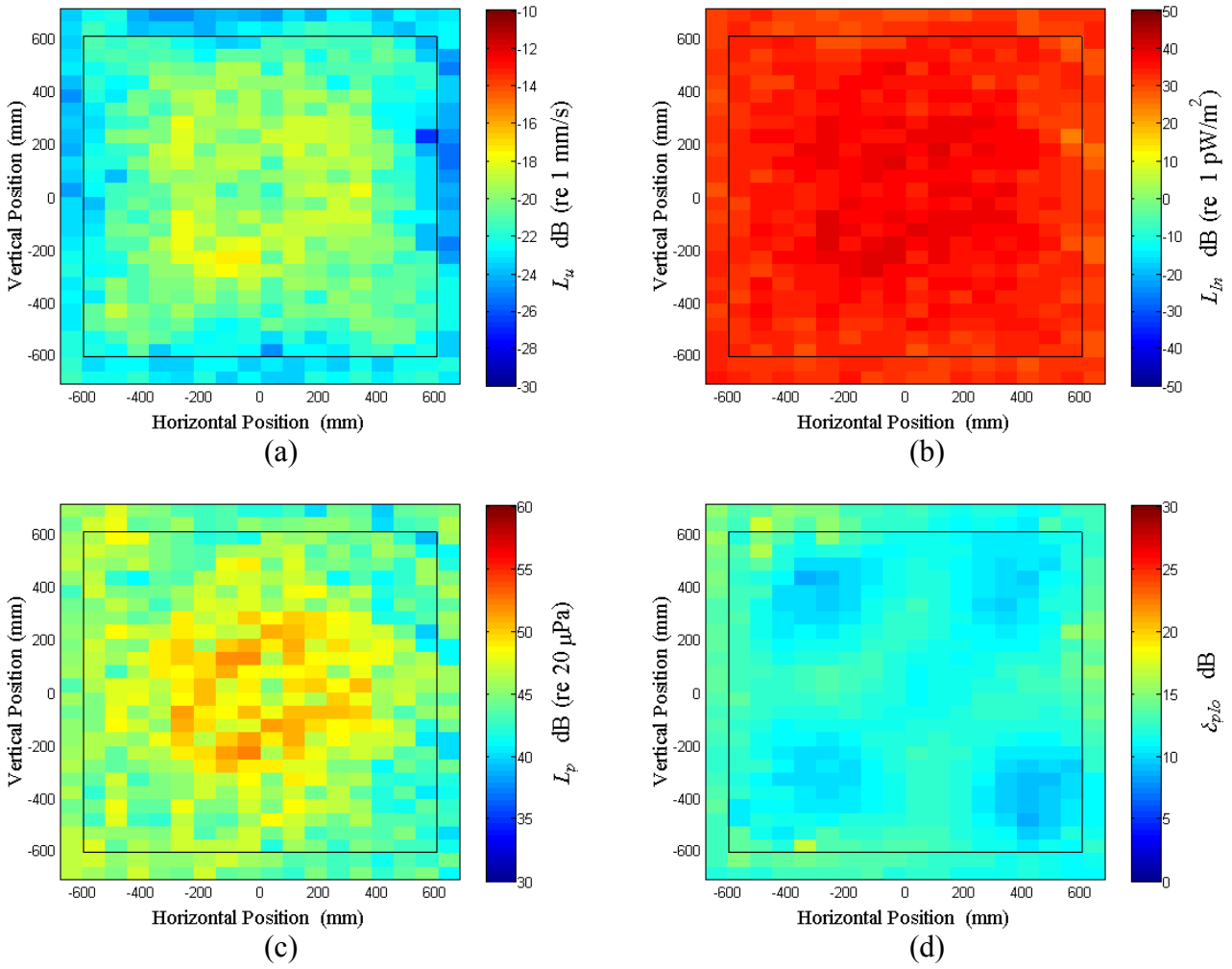

Figure D.39: Surface scan of Window D at 190 Hz (a) particle velocity level, L_u (b) normal signed sound intensity level, L_{In} (c) sound pressure level, L_p (d) pressure-residual intensity index, δ_{pIo}.

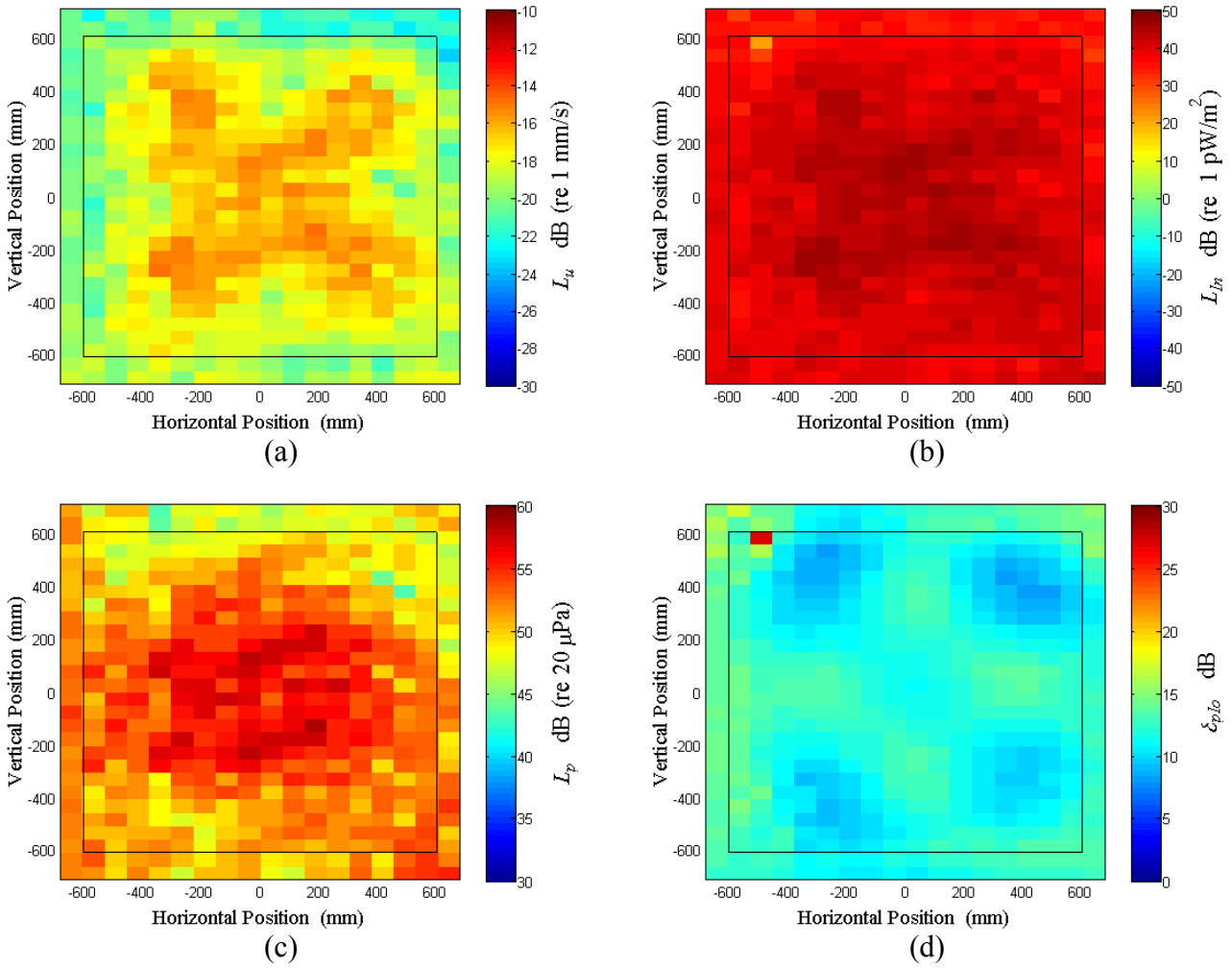

Figure D.40: Surface scan of Window D at 200 Hz (a) particle velocity level, L_u (b) normal signed sound intensity level, L_{In} (c) sound pressure level, L_p (d) pressure-residual intensity index, δ_{pIo}.

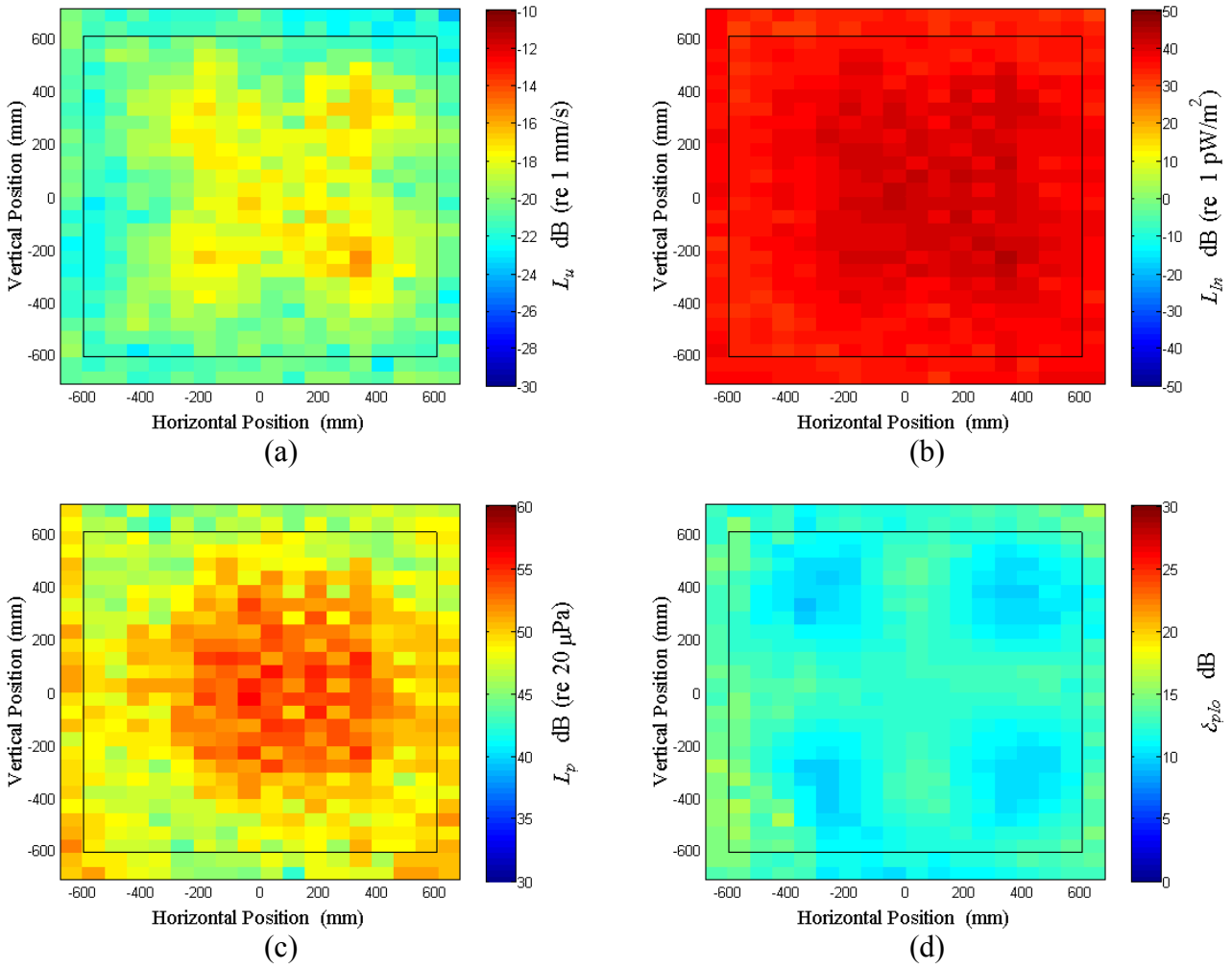

Figure D.41: Surface scan of Window D at 210 Hz (a) particle velocity level, L_u (b) normal signed sound intensity level, L_{In} (c) sound pressure level, L_p (d) pressure-residual intensity index, δ_{pIo}.

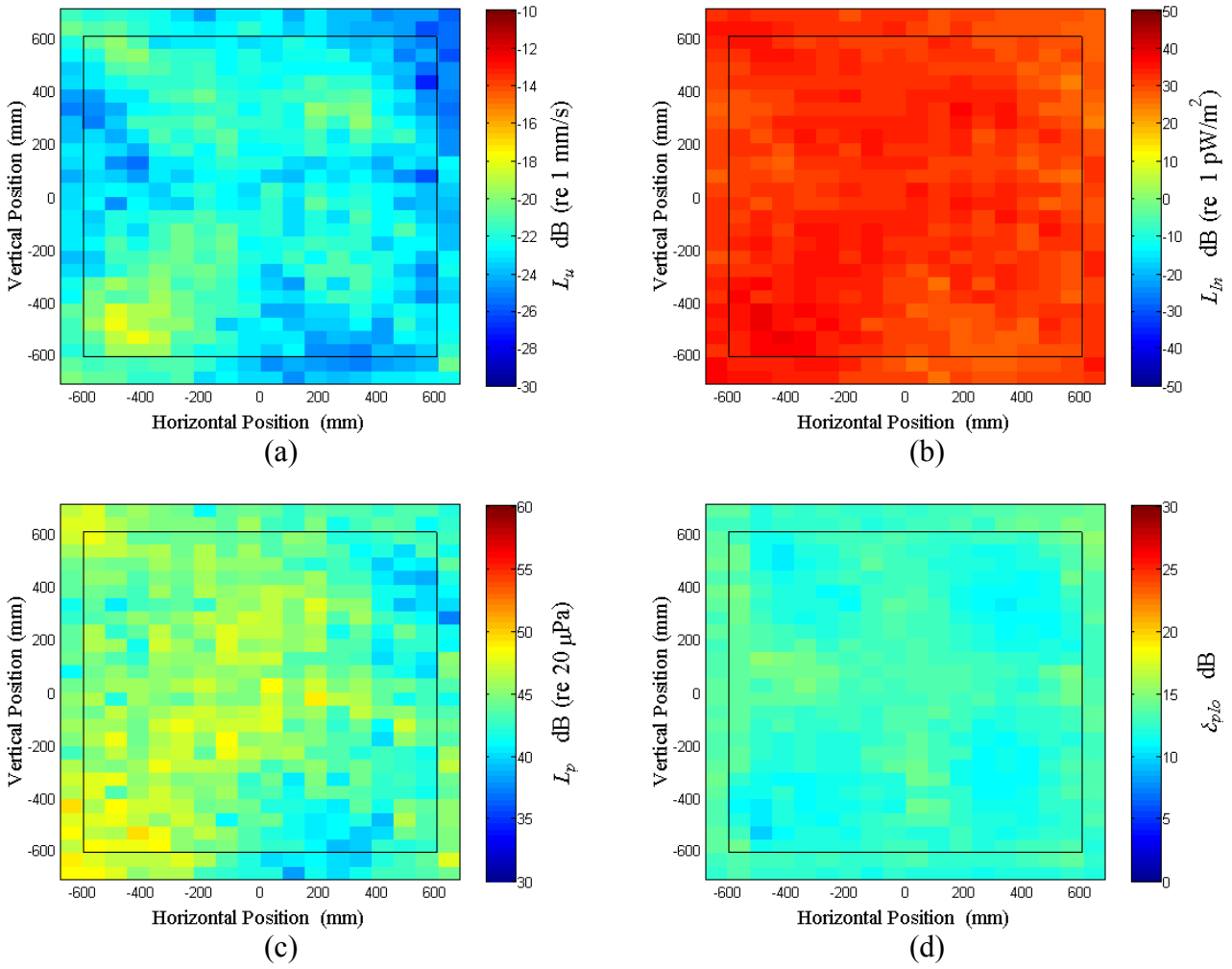

Figure D.42: Surface scan of Window D at 220 Hz (a) particle velocity level, L_u (b) normal signed sound intensity level, L_{In} (c) sound pressure level, L_p (d) pressure-residual intensity index, δ_{pIo}.

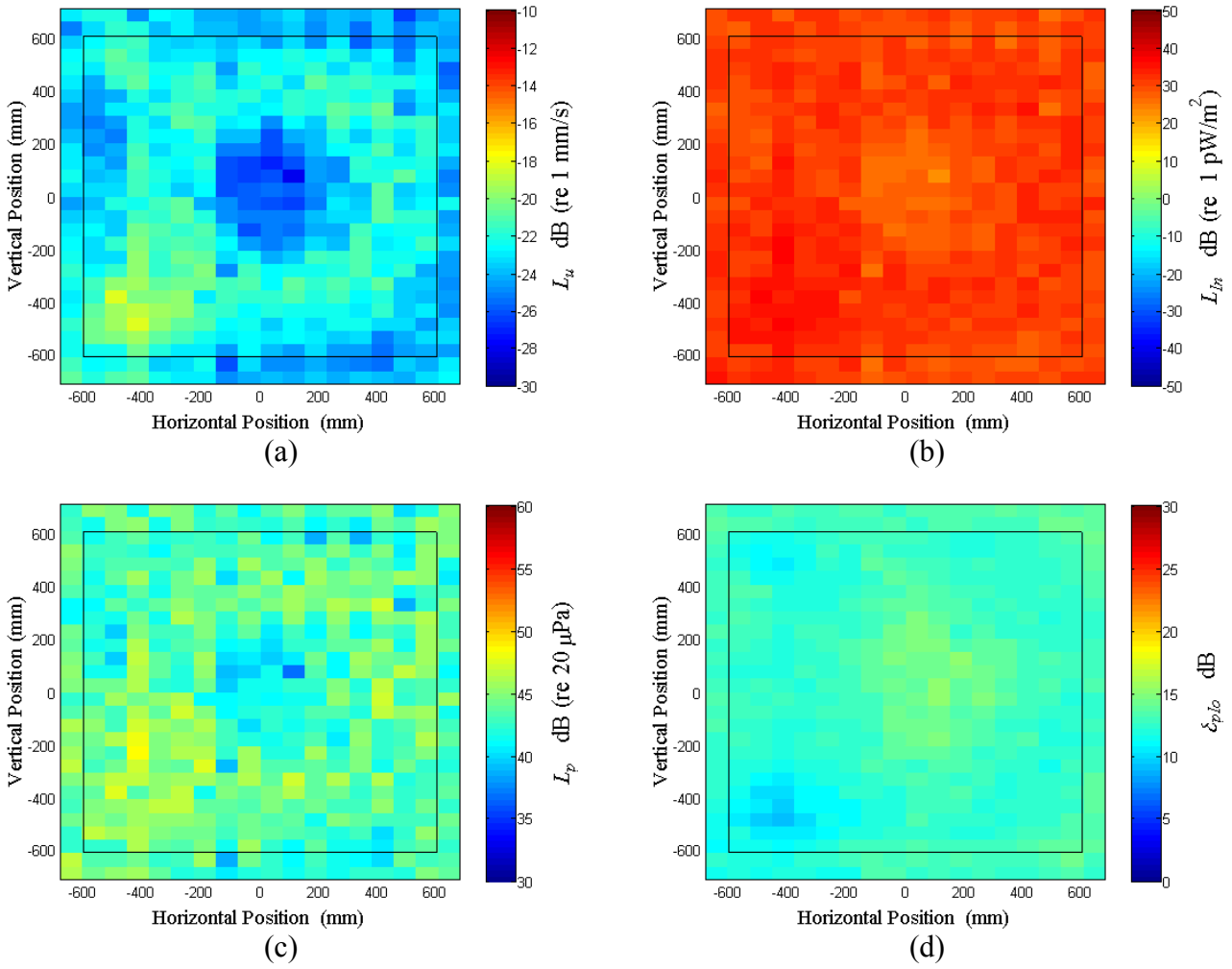

Figure D.43: Surface scan of Window D at 230 Hz (a) particle velocity level, L_u (b) normal signed sound intensity level, L_{In} (c) sound pressure level, L_p (d) pressure-residual intensity index, δ_{pIo}.

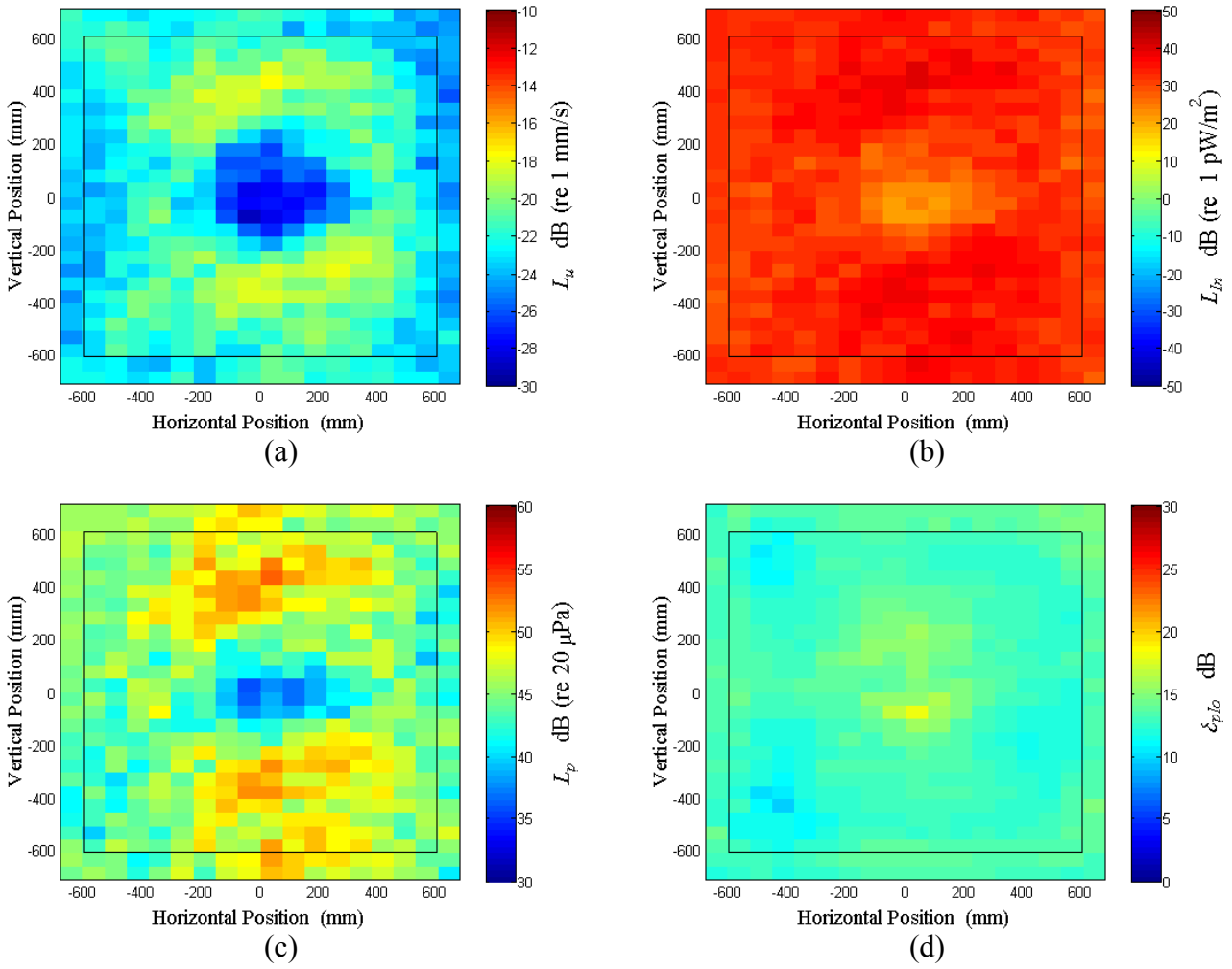

Figure D.44: Surface scan of Window D at 240 Hz (a) particle velocity level, L_u (b) normal signed sound intensity level, L_{In} (c) sound pressure level, L_p (d) pressure-residual intensity index, δ_{pIo}.

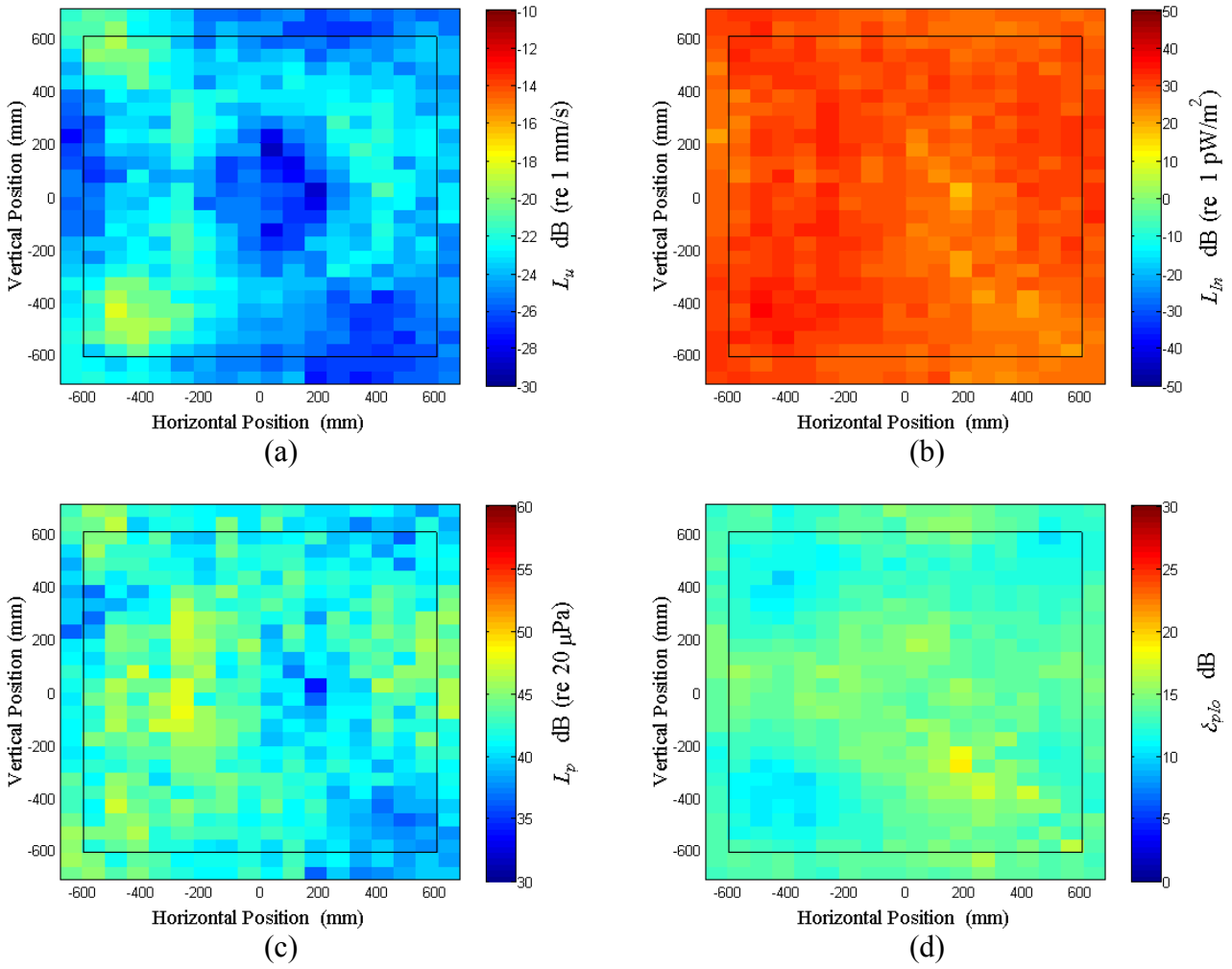

Figure D.45: Surface scan of Window D at 250 Hz (a) particle velocity level, L_u (b) normal signed sound intensity level, L_{In} (c) sound pressure level, L_p (d) pressure-residual intensity index, δ_{pIo}.

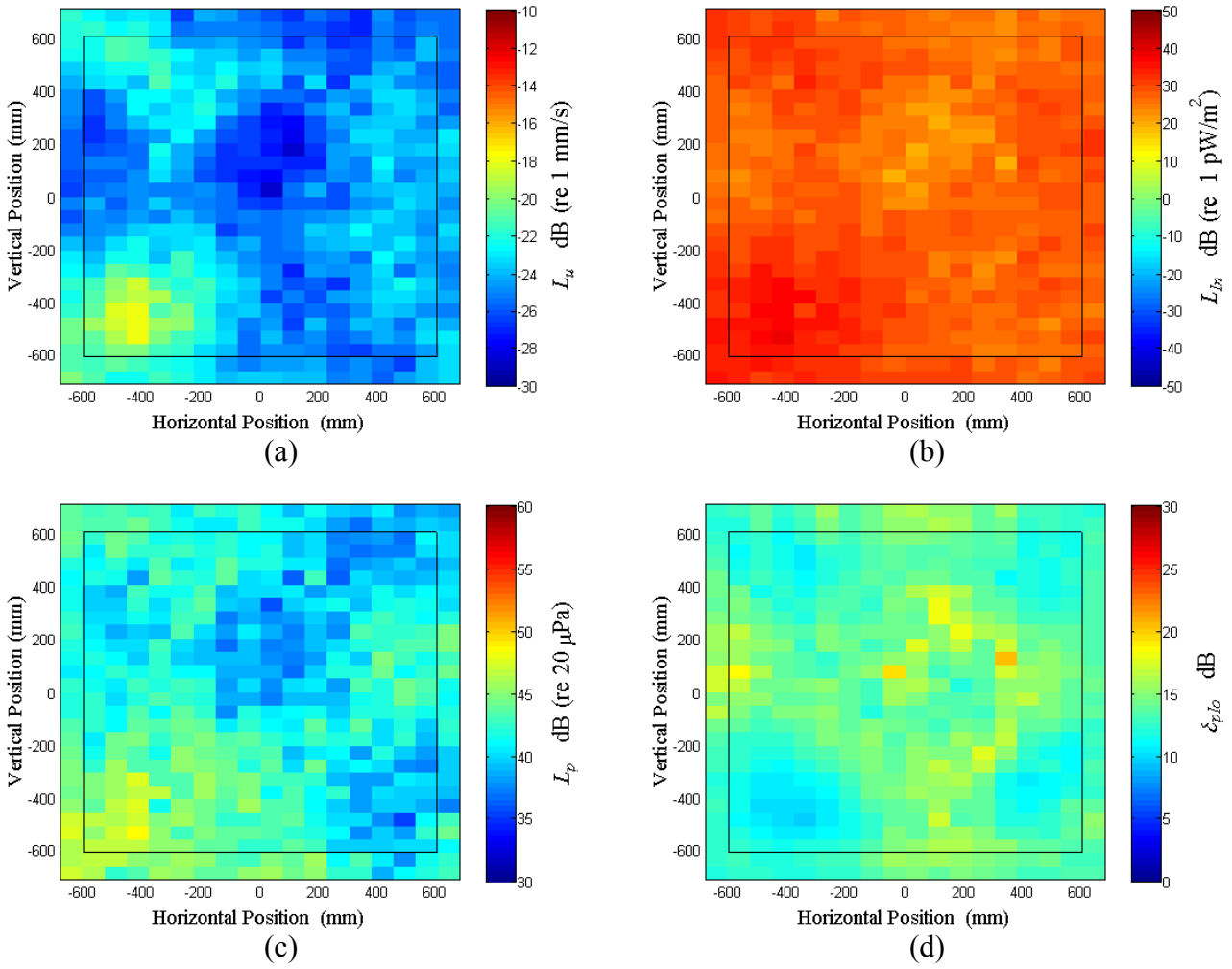

Figure D.46: Surface scan of Window D at 260 Hz (a) particle velocity level, L_u (b) normal signed sound intensity level, L_{In} (c) sound pressure level, L_p (d) pressure-residual intensity index, δ_{pIo}.

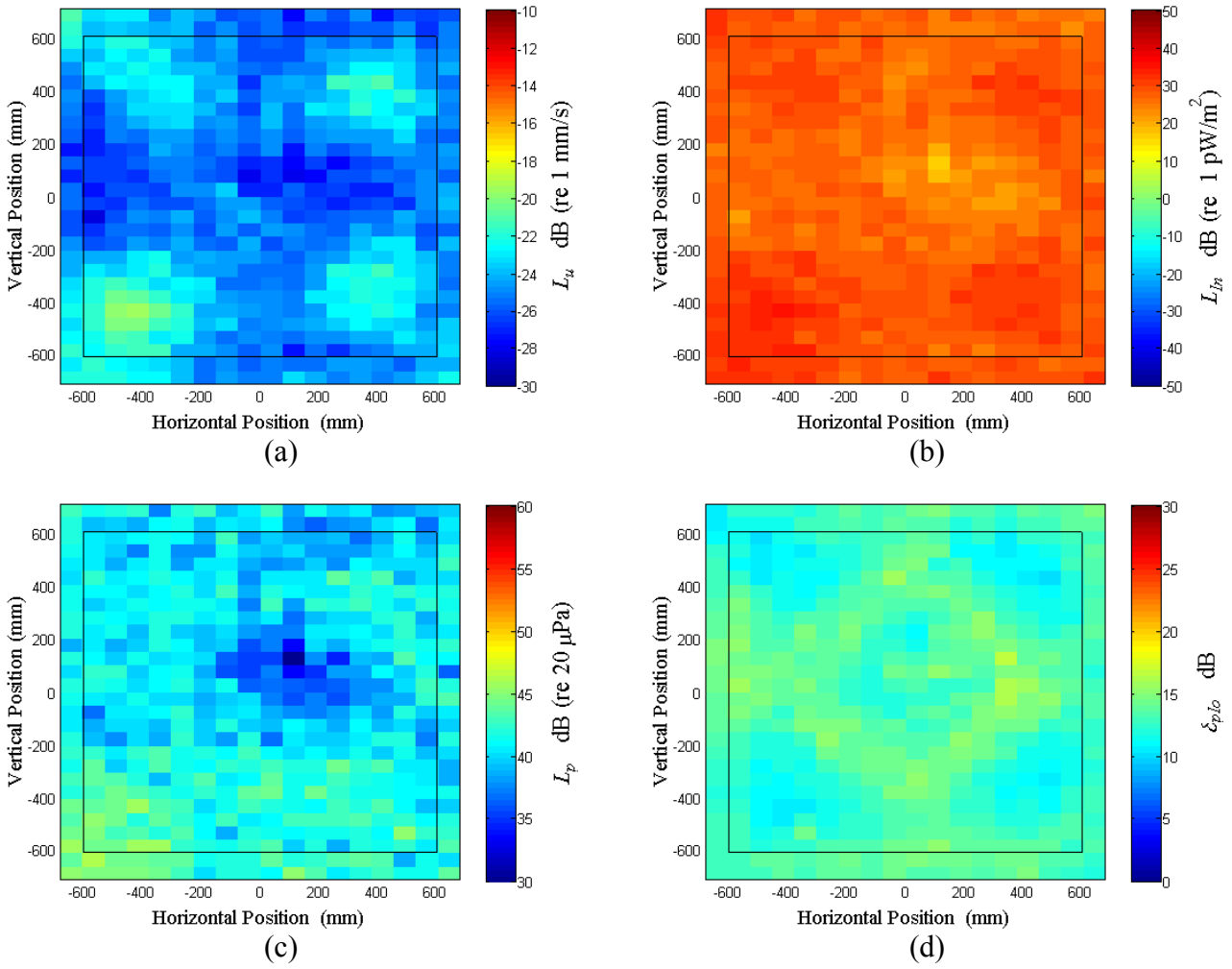

Figure D.47: Surface scan of Window D at 270 Hz (a) particle velocity level, L_u (b) normal signed sound intensity level, L_{In} (c) sound pressure level, L_p (d) pressure-residual intensity index, δ_{pIo}.

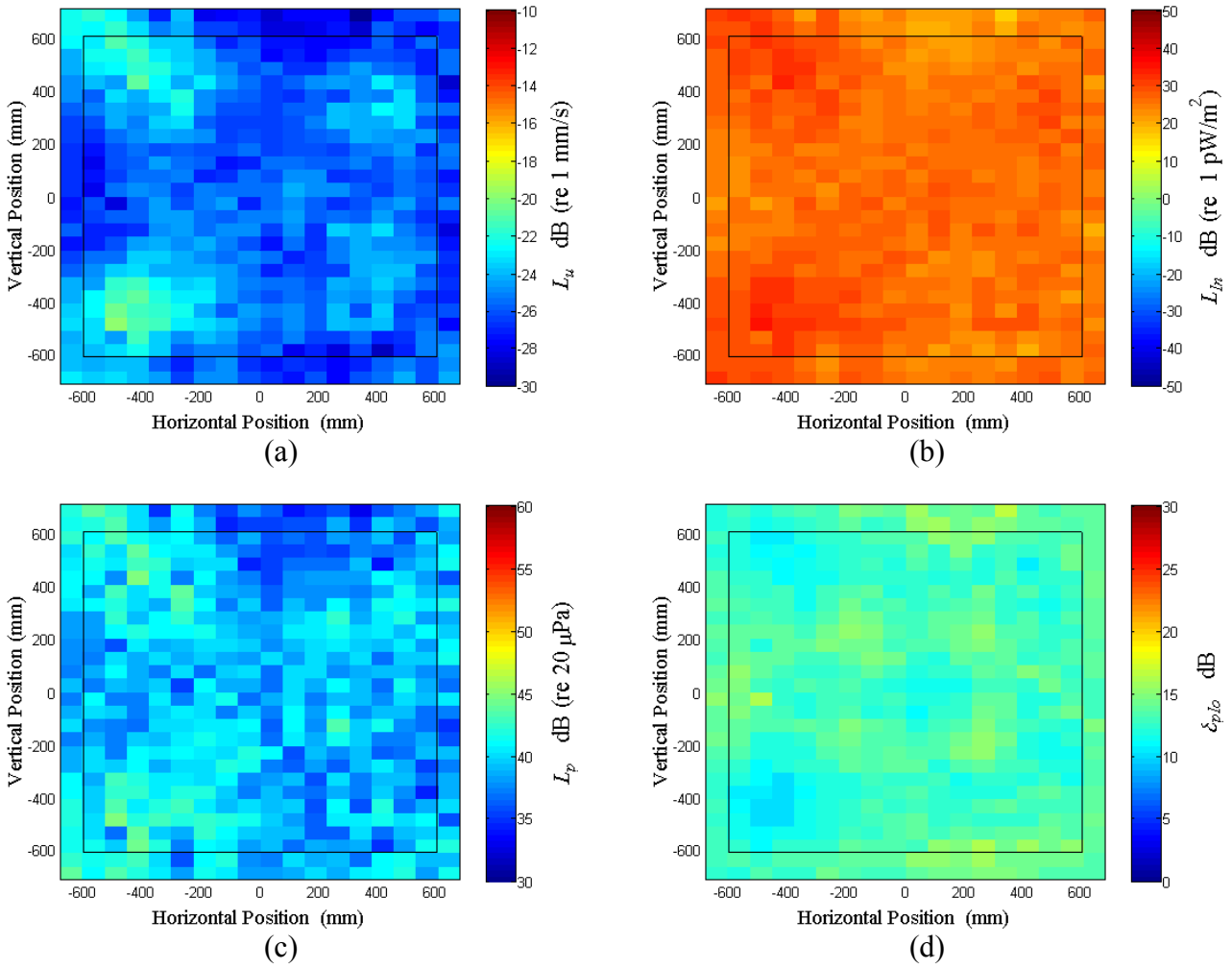

Figure D.48: Surface scan of Window D at 280 Hz (a) particle velocity level, L_u (b) normal signed sound intensity level, L_{In} (c) sound pressure level, L_p (d) pressure-residual intensity index, δ_{pIo}.

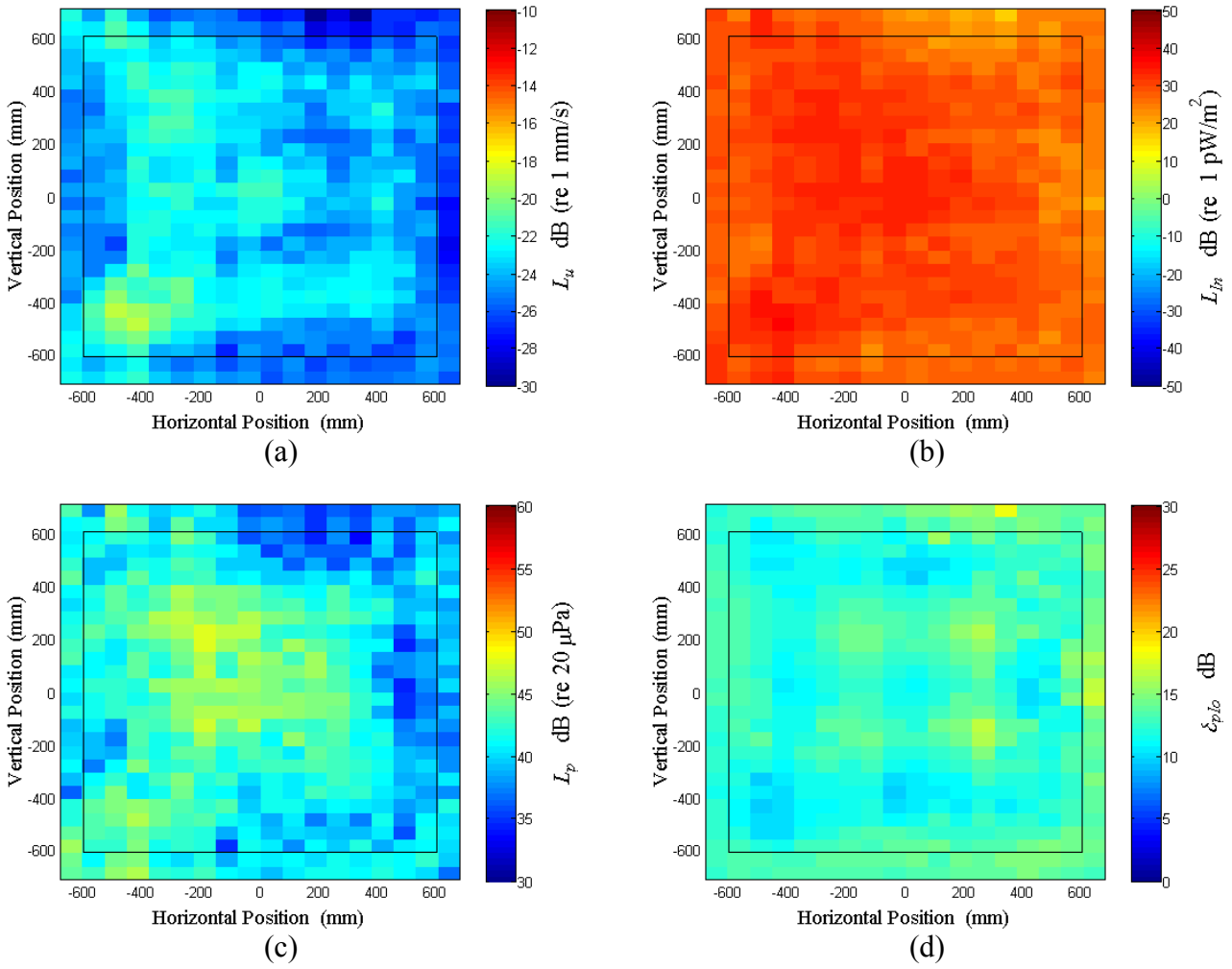

Figure D.49: Surface scan of Window D at 290 Hz (a) particle velocity level, L_u (b) normal signed sound intensity level, L_{In} (c) sound pressure level, L_p (d) pressure-residual intensity index, δ_{pIo}.

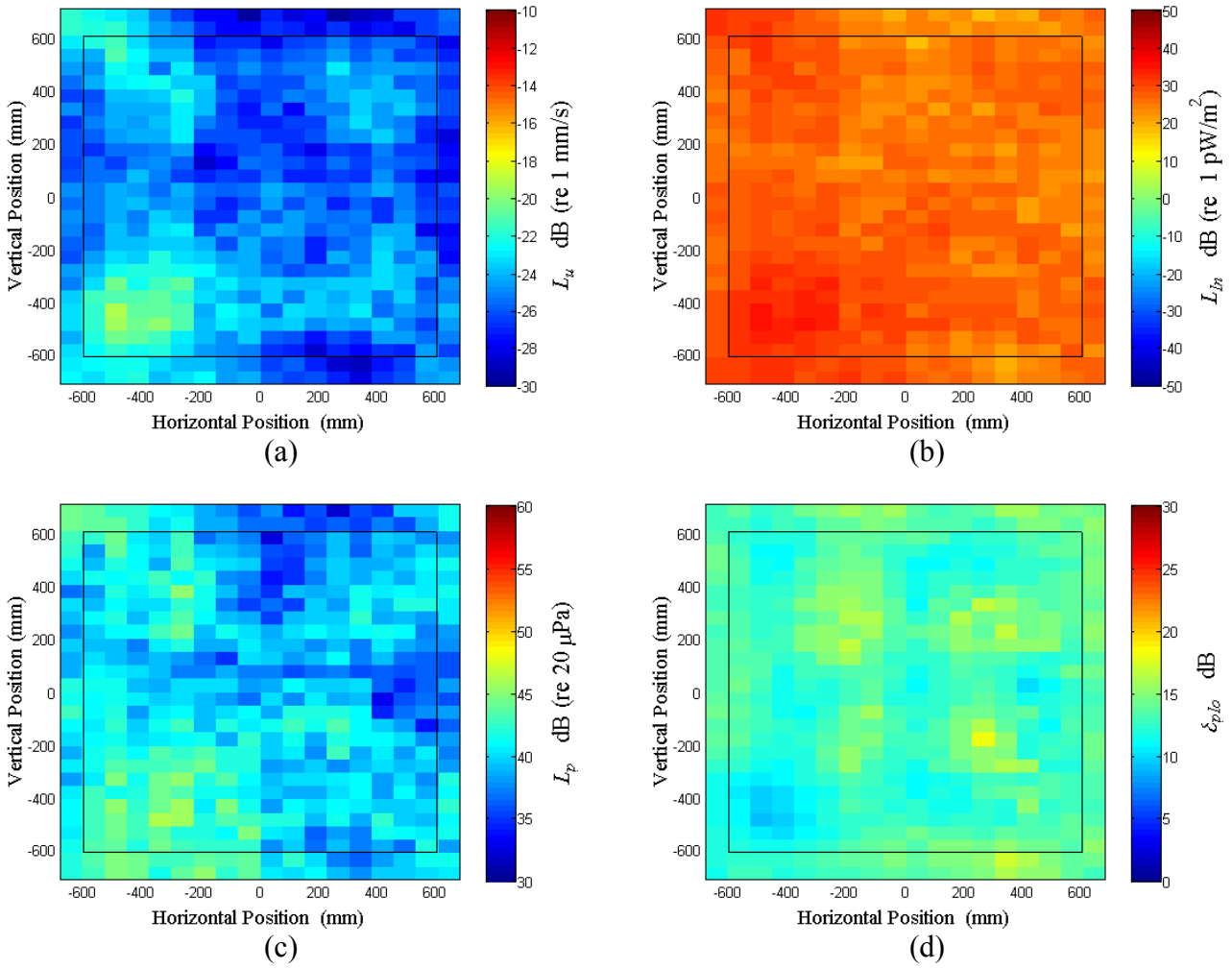

Figure D.50: Surface scan of Window D at 300 Hz (a) particle velocity level, L_u (b) normal signed sound intensity level, L_{In} (c) sound pressure level, L_p (d) pressure-residual intensity index, δ_{pIo}.

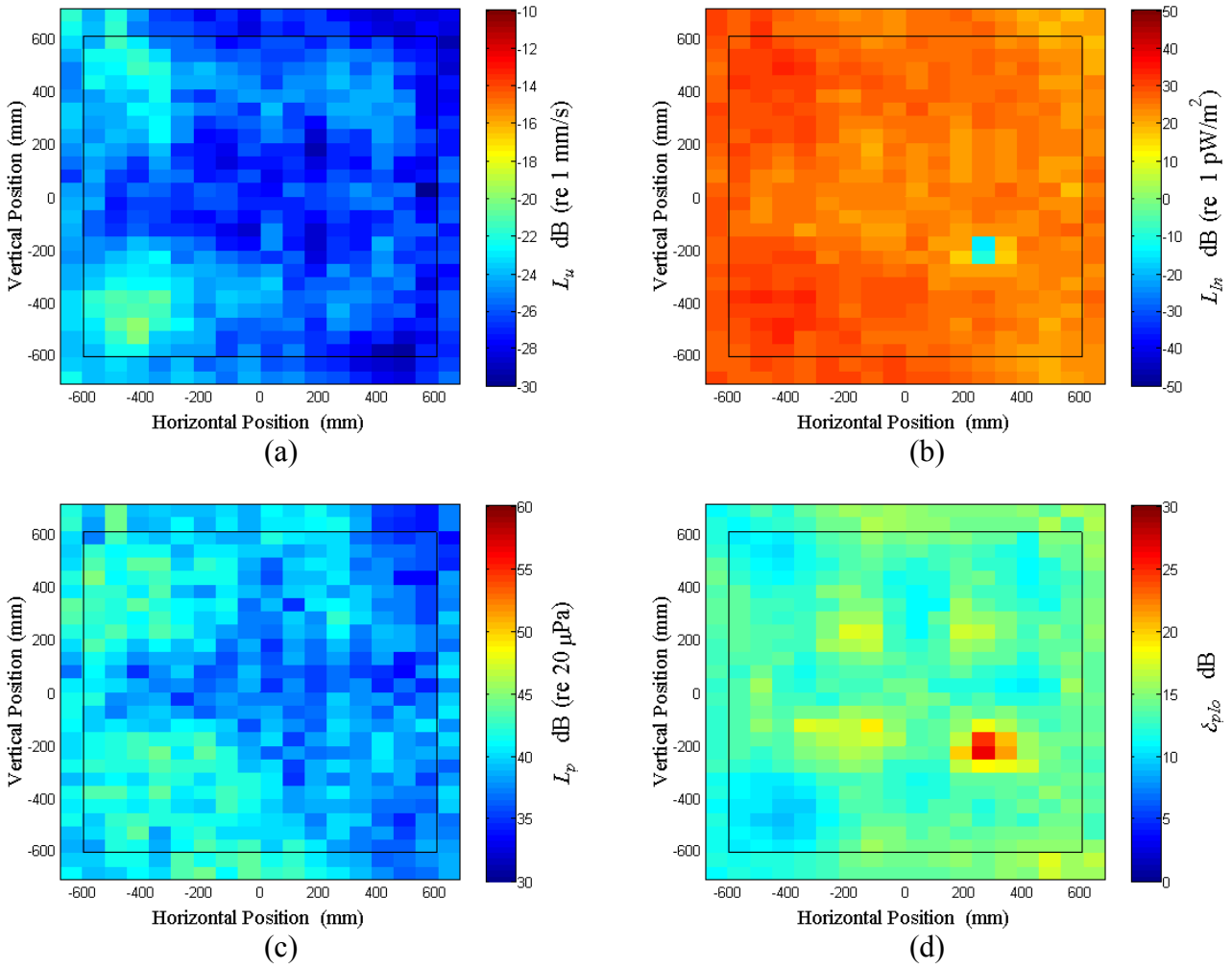

Figure D.51: Surface scan of Window D at 310 Hz (a) particle velocity level, L_u (b) normal signed sound intensity level, L_{In} (c) sound pressure level, L_p (d) pressure-residual intensity index, δ_{pIo}.

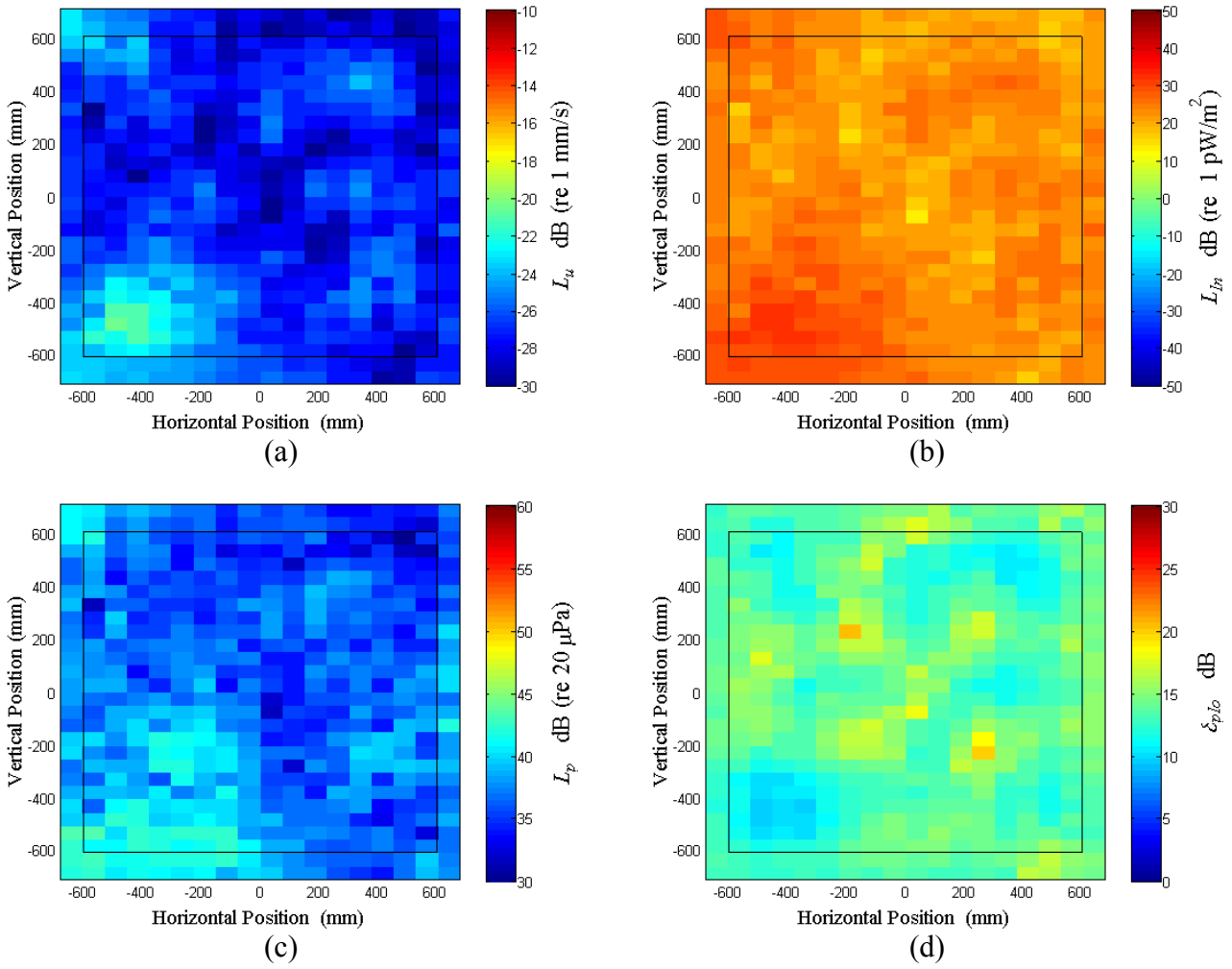

Figure D.52: Surface scan of Window D at 320 Hz (a) particle velocity level, L_u (b) normal signed sound intensity level, L_{In} (c) sound pressure level, L_p (d) pressure-residual intensity index, δ_{pIo}.

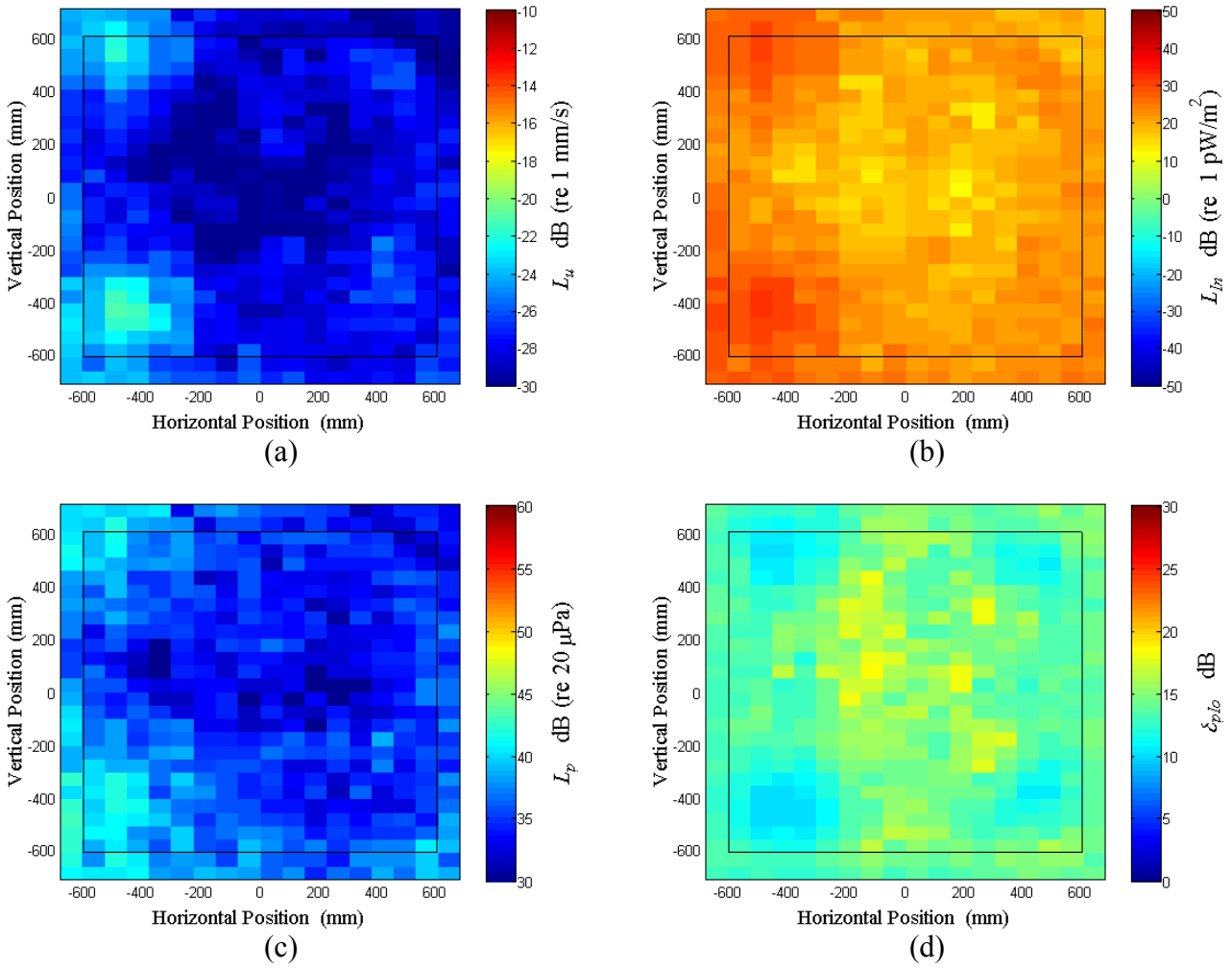

Figure D.53: Surface scan of Window D at 330 Hz (a) particle velocity level, L_u (b) normal signed sound intensity level, L_{In} (c) sound pressure level, L_p (d) pressure-residual intensity index, δ_{pIo}.

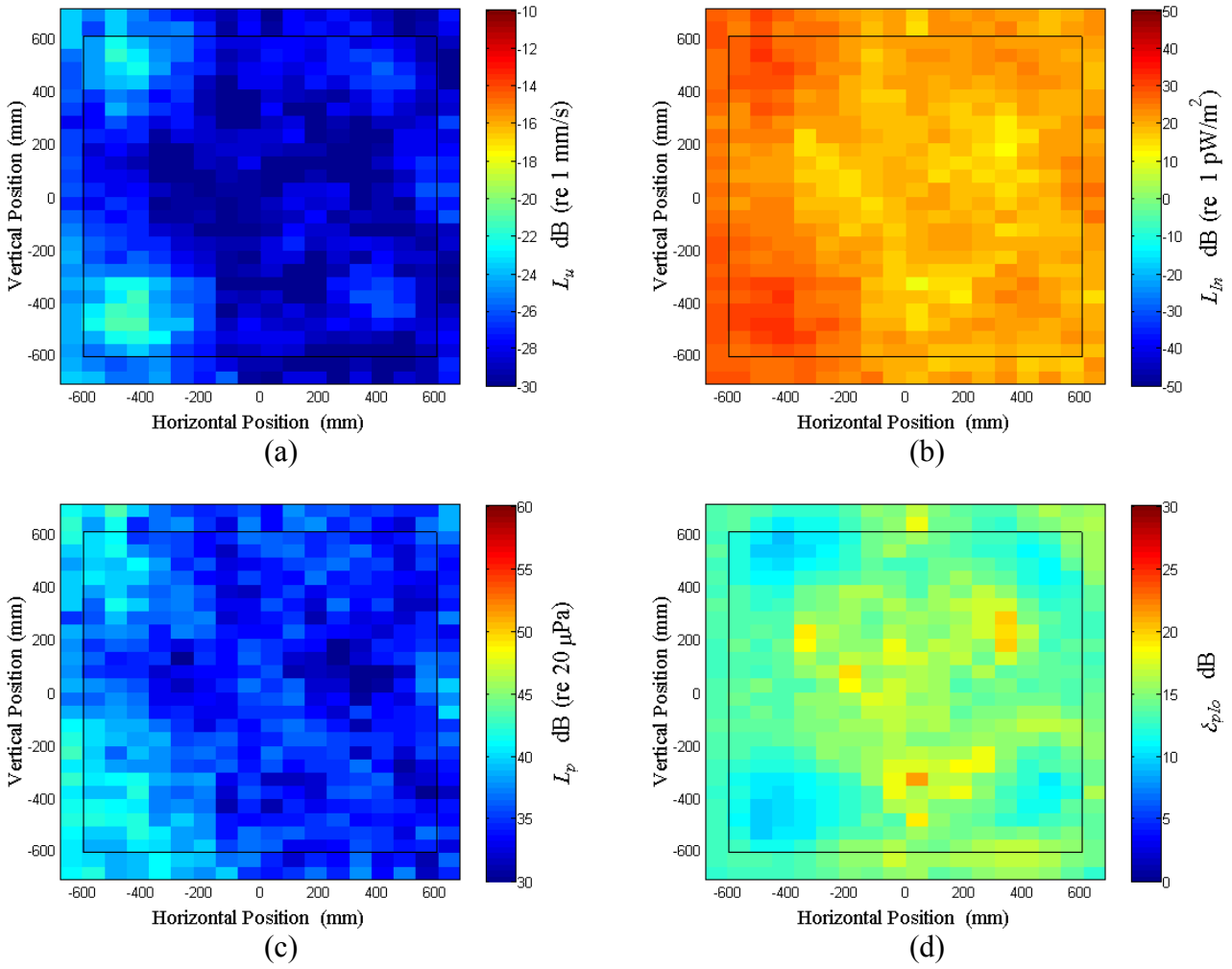

Figure D.54: Surface scan of Window D at 340 Hz (a) particle velocity level, L_u (b) normal signed sound intensity level, L_{In} (c) sound pressure level, L_p (d) pressure-residual intensity index, δ_{pIo}.

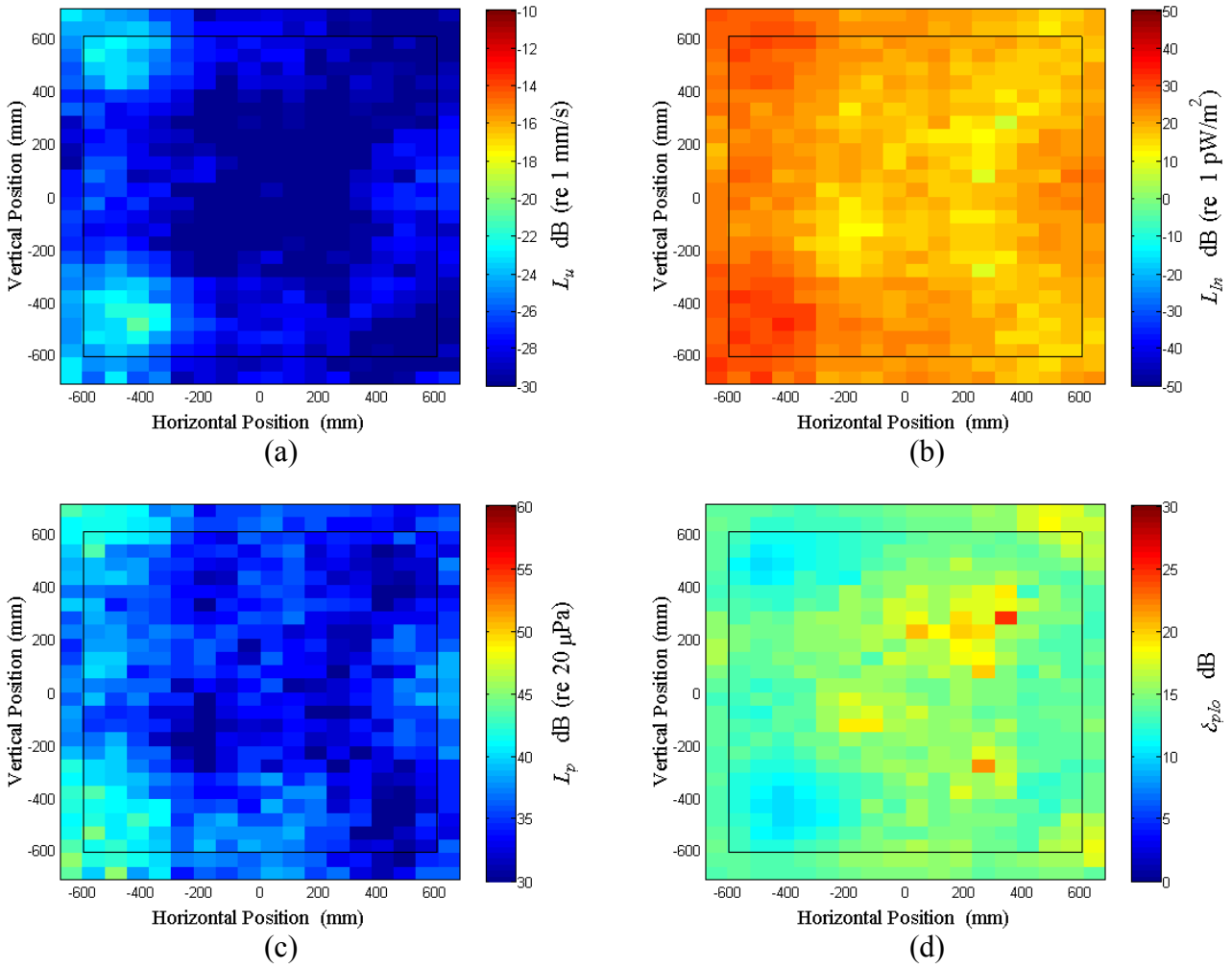

Figure D.55: Surface scan of Window D at 350 Hz (a) particle velocity level, L_u (b) normal signed sound intensity level, L_{In} (c) sound pressure level, L_p (d) pressure-residual intensity index, δ_{pIo}.

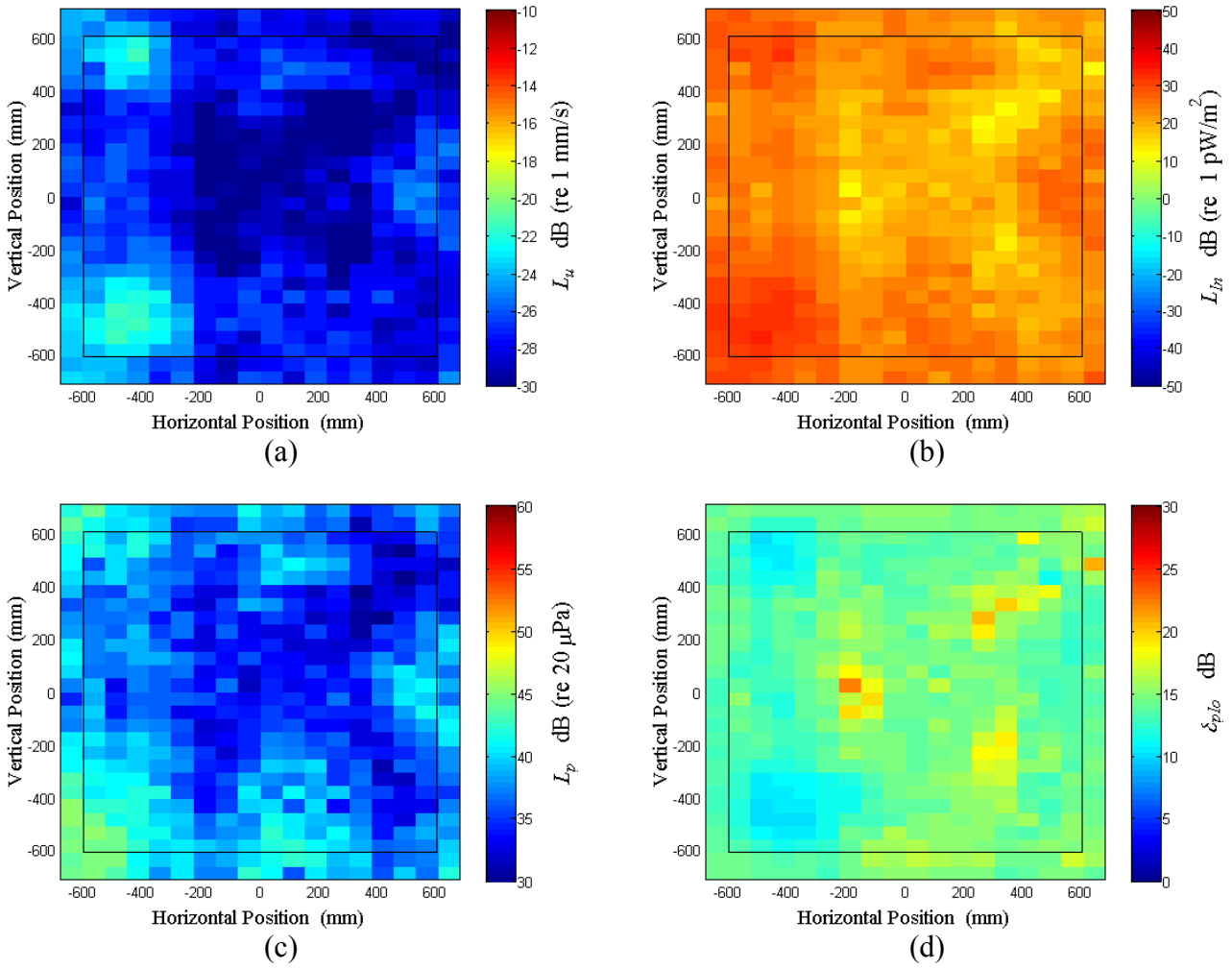

Figure D.56: Surface scan of Window D at 360 Hz (a) particle velocity level, L_u (b) normal signed sound intensity level, L_{In} (c) sound pressure level, L_p (d) pressure-residual intensity index, δ_{pIo}.

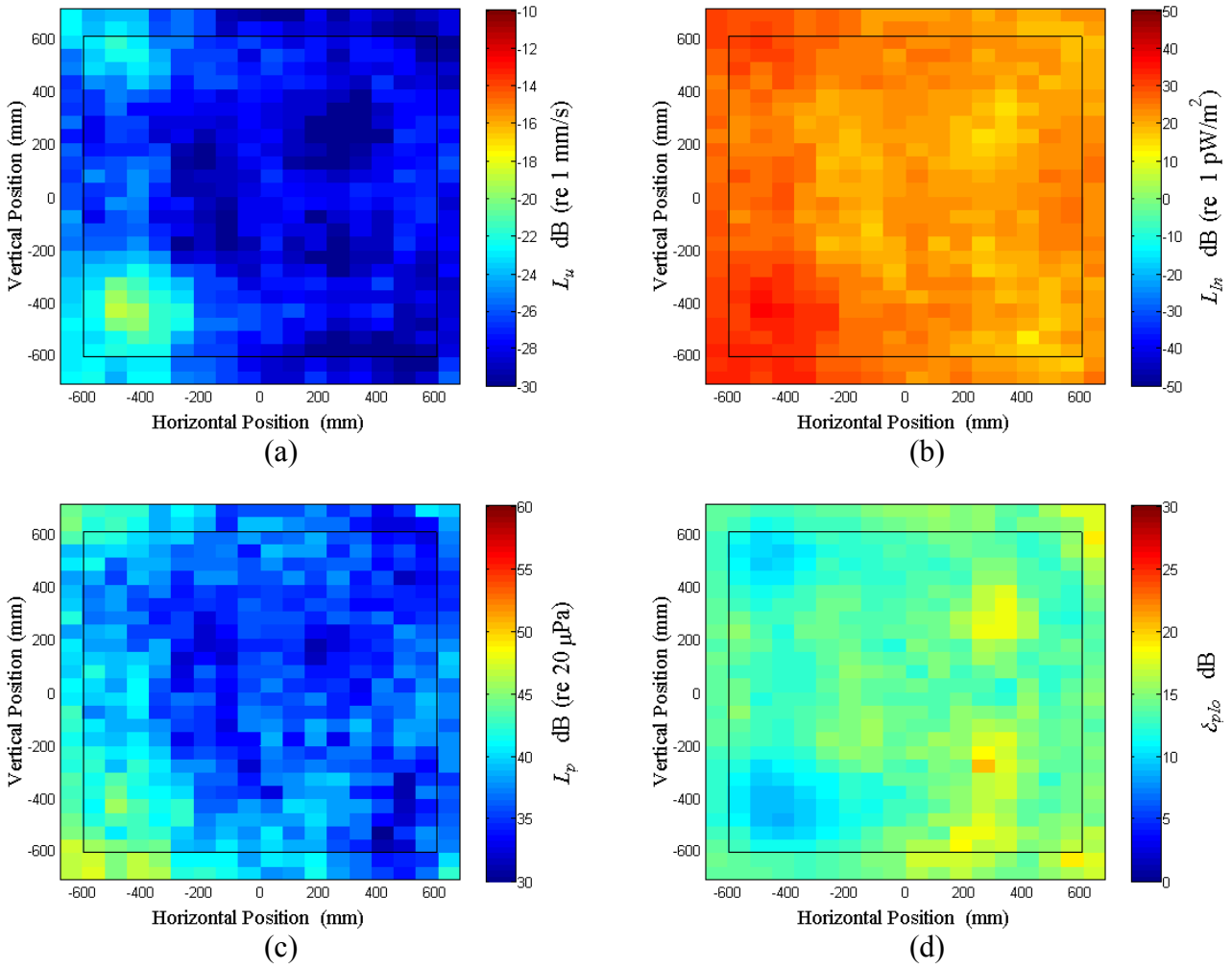

Figure D.57: Surface scan of Window D at 370 Hz (a) particle velocity level, L_u (b) normal signed sound intensity level, L_{In} (c) sound pressure level, L_p (d) pressure-residual intensity index, δ_{pIo}.

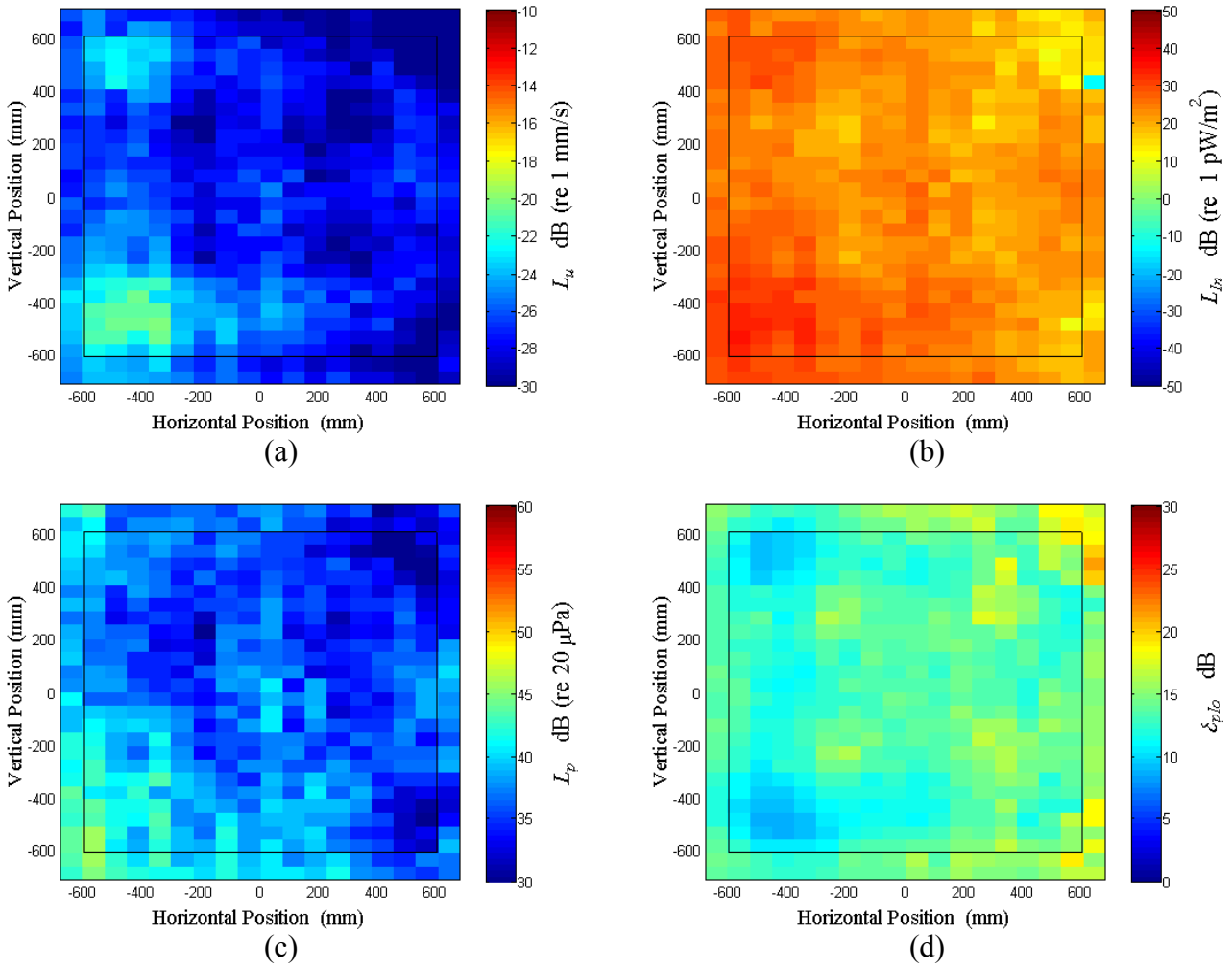

Figure D.58: Surface scan of Window D at 380 Hz (a) particle velocity level, L_u (b) normal signed sound intensity level, L_{In} (c) sound pressure level, L_p (d) pressure-residual intensity index, δ_{pIo}.

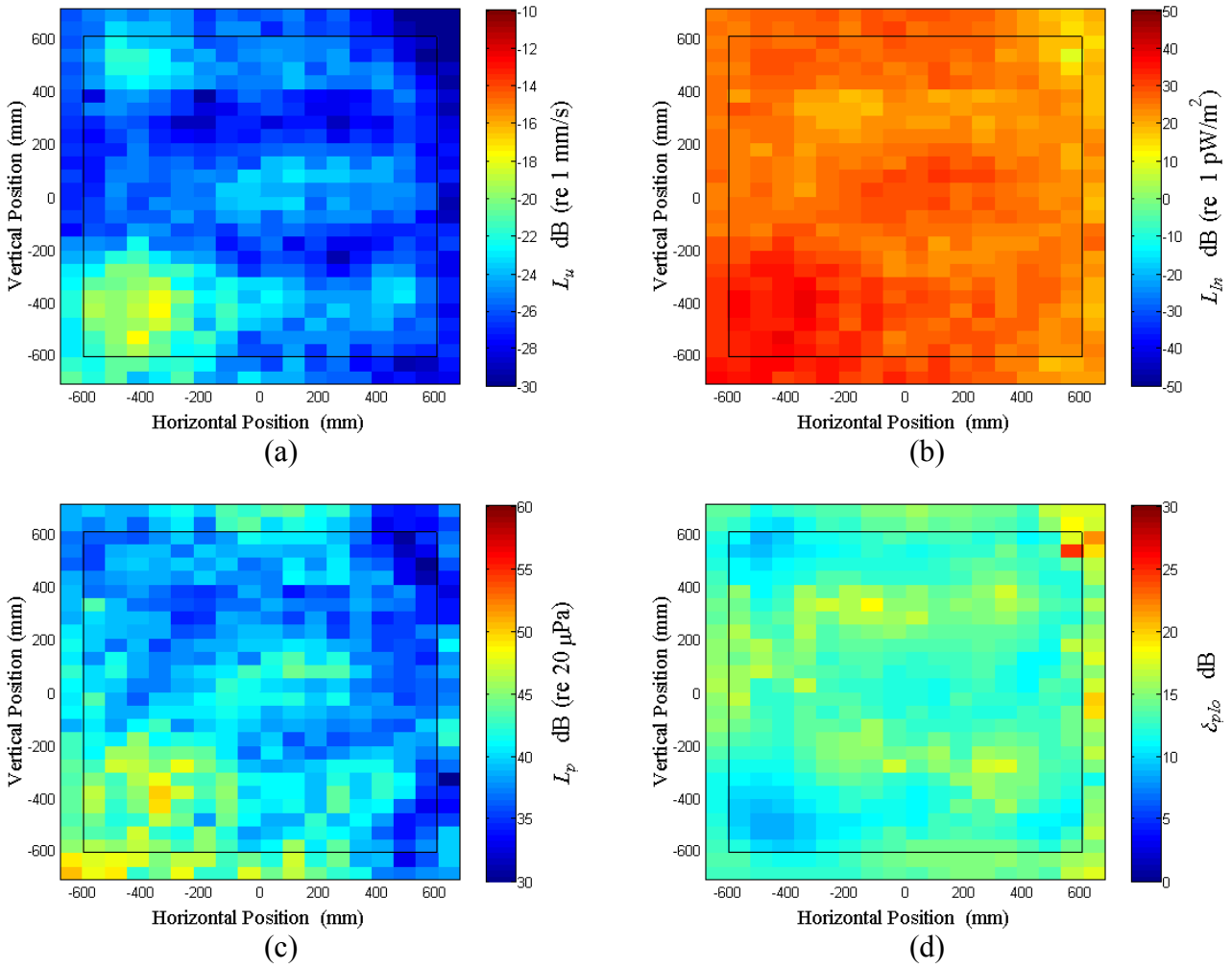

Figure D.59: Surface scan of Window D at 390 Hz (a) particle velocity level, L_u (b) normal signed sound intensity level, L_{In} (c) sound pressure level, L_p (d) pressure-residual intensity index, δ_{pIo}.

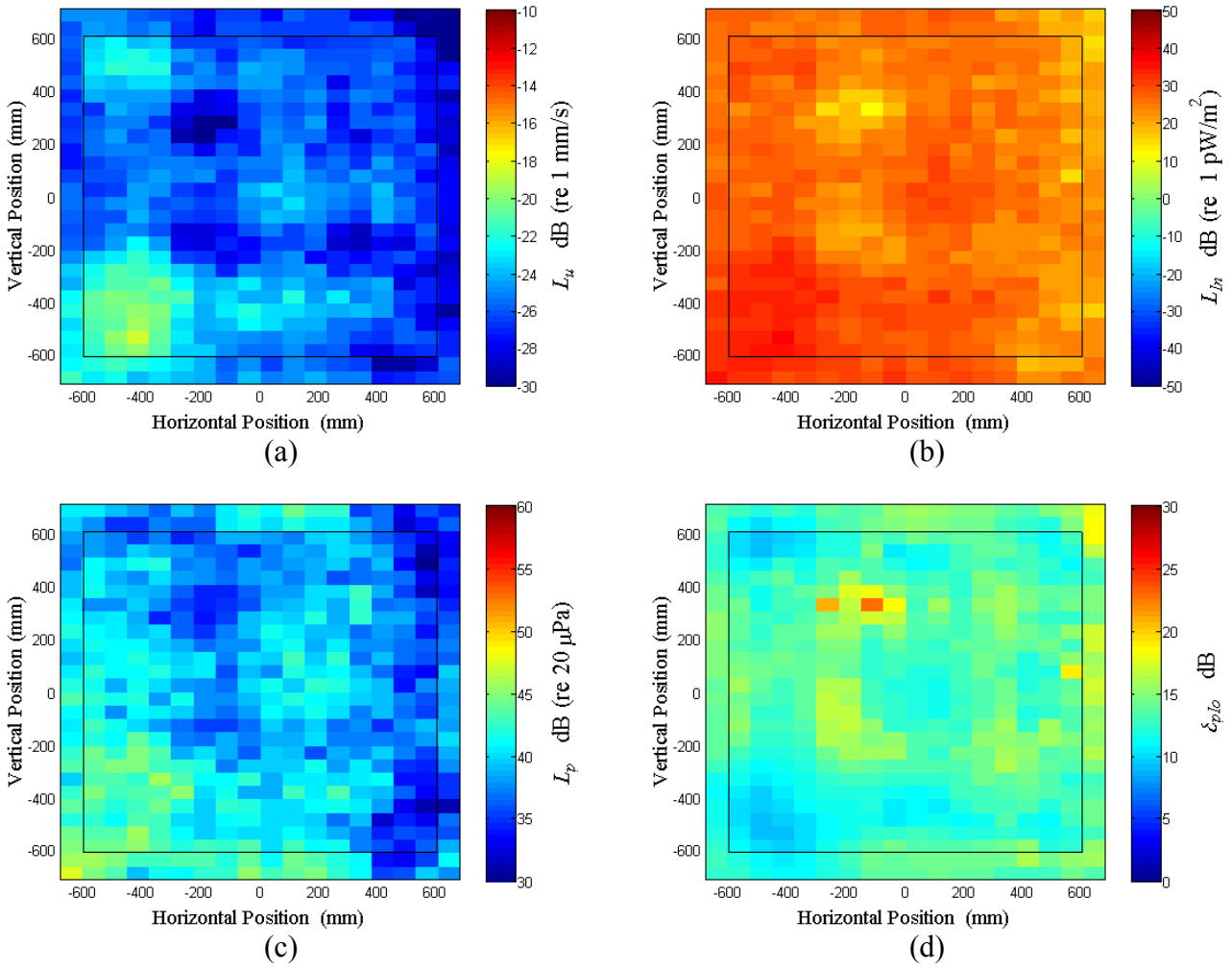

Figure D.60: Surface scan of Window D at 400 Hz (a) particle velocity level, L_u (b) normal signed sound intensity level, L_{In} (c) sound pressure level, L_p (d) pressure-residual intensity index, δ_{pIo}.

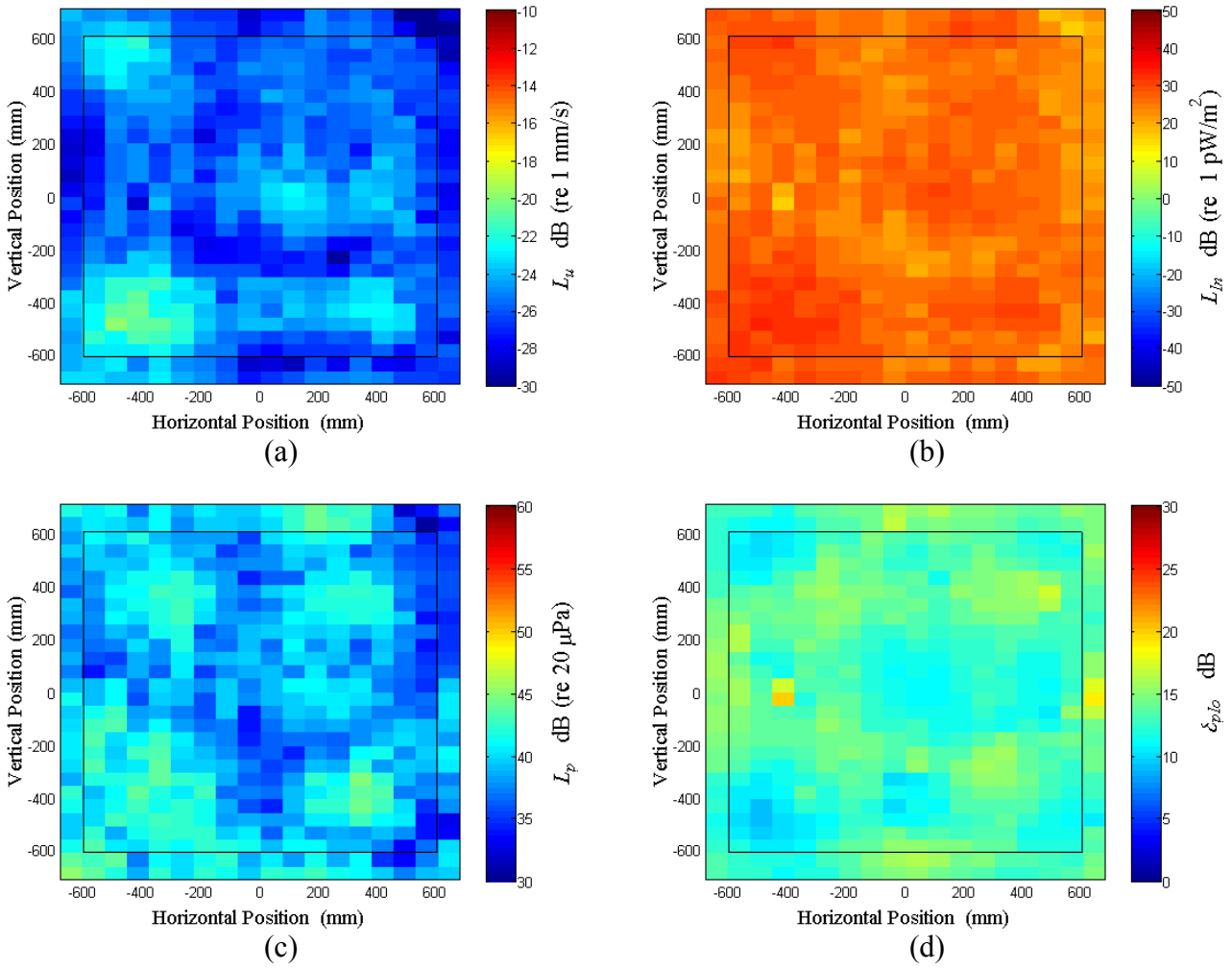

Figure D.61: Surface scan of Window D at 410 Hz (a) particle velocity level, L_u (b) normal signed sound intensity level, L_{In} (c) sound pressure level, L_p (d) pressure-residual intensity index, δ_{pIo}.

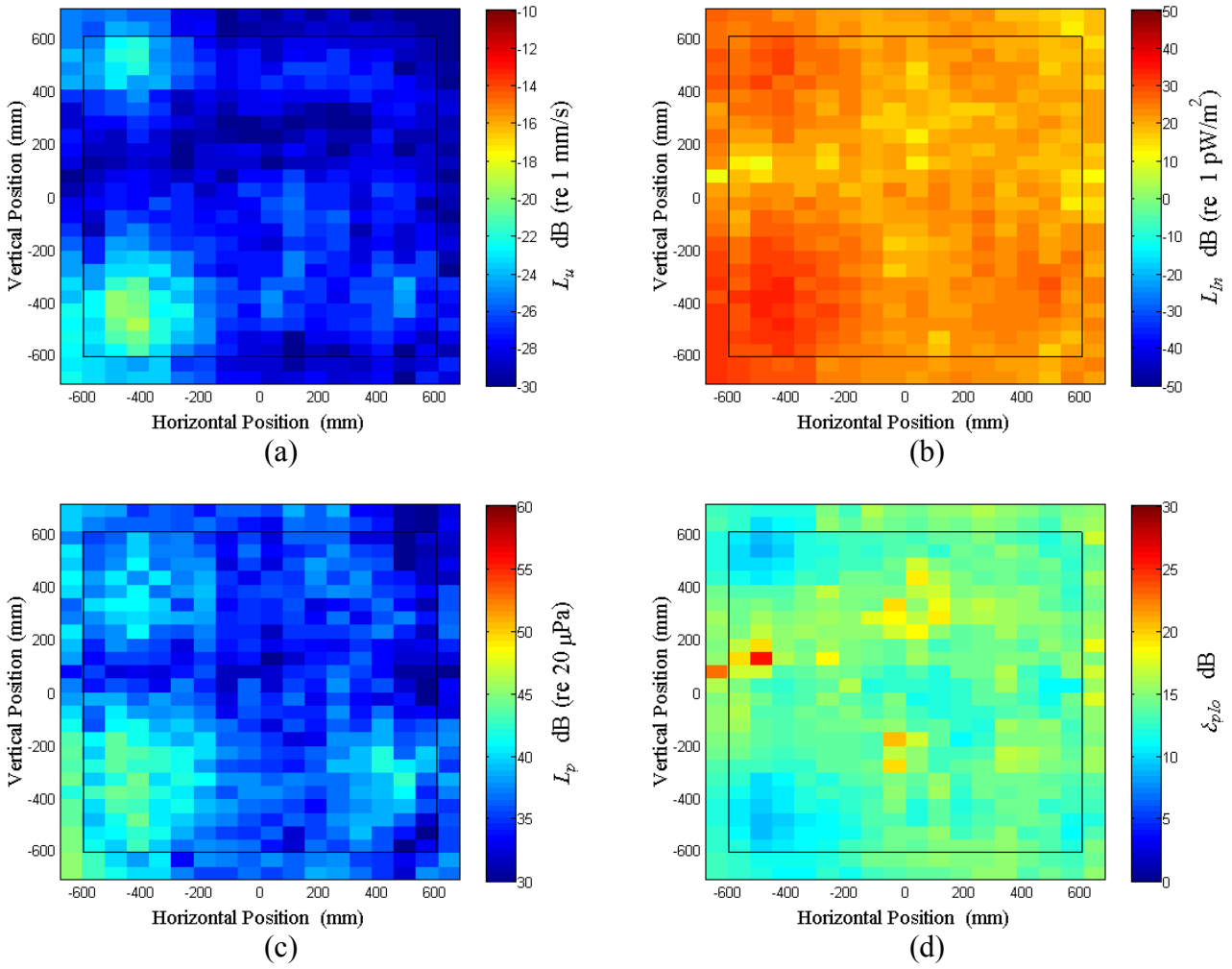

Figure D.62: Surface scan of Window D at 420 Hz (a) particle velocity level, L_u (b) normal signed sound intensity level, L_{In} (c) sound pressure level, L_p (d) pressure-residual intensity index, δ_{pIo}.

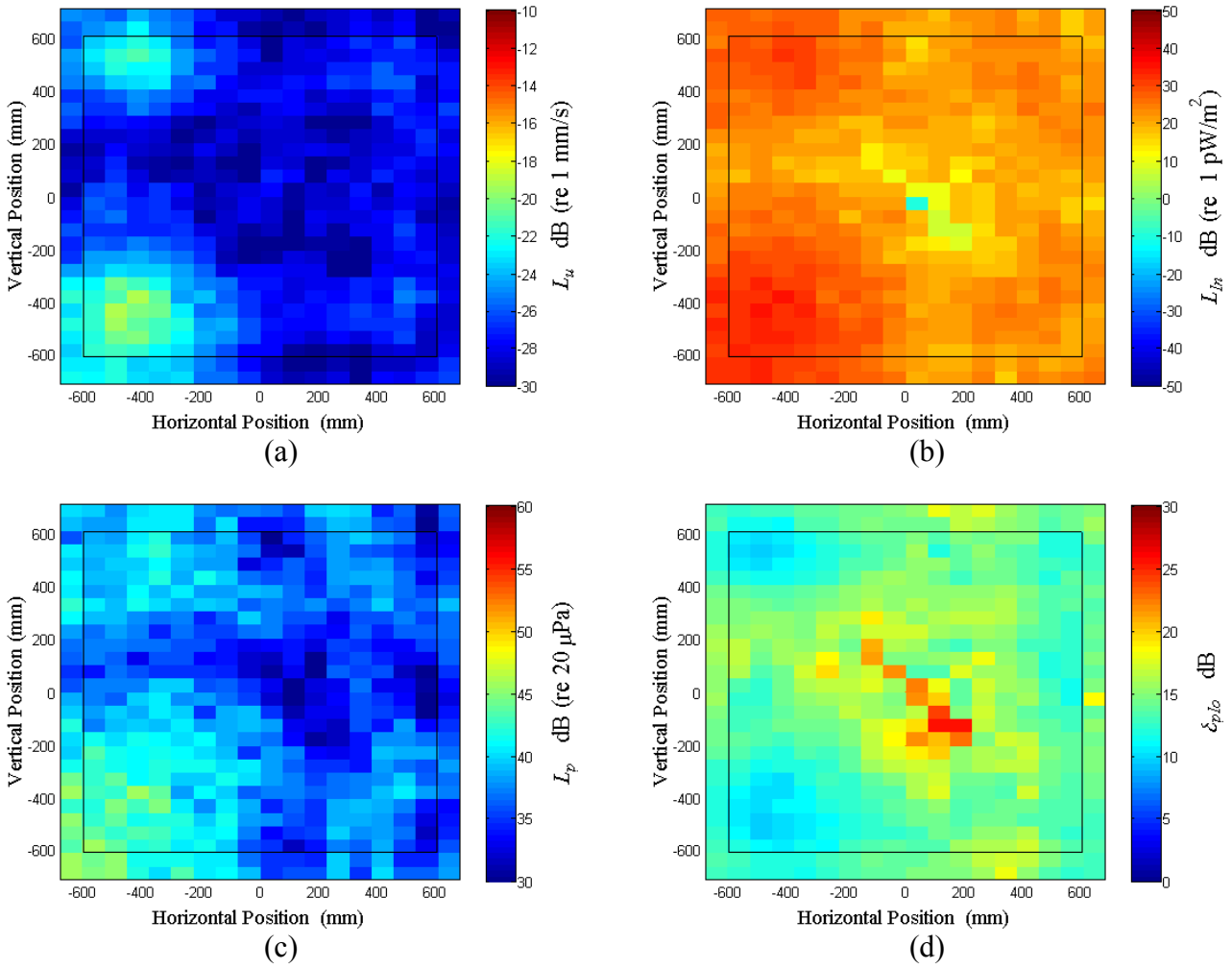

Figure D.63: Surface scan of Window D at 430 Hz (a) particle velocity level, L_u (b) normal signed sound intensity level, L_{In} (c) sound pressure level, L_p (d) pressure-residual intensity index, δ_{pIo}.

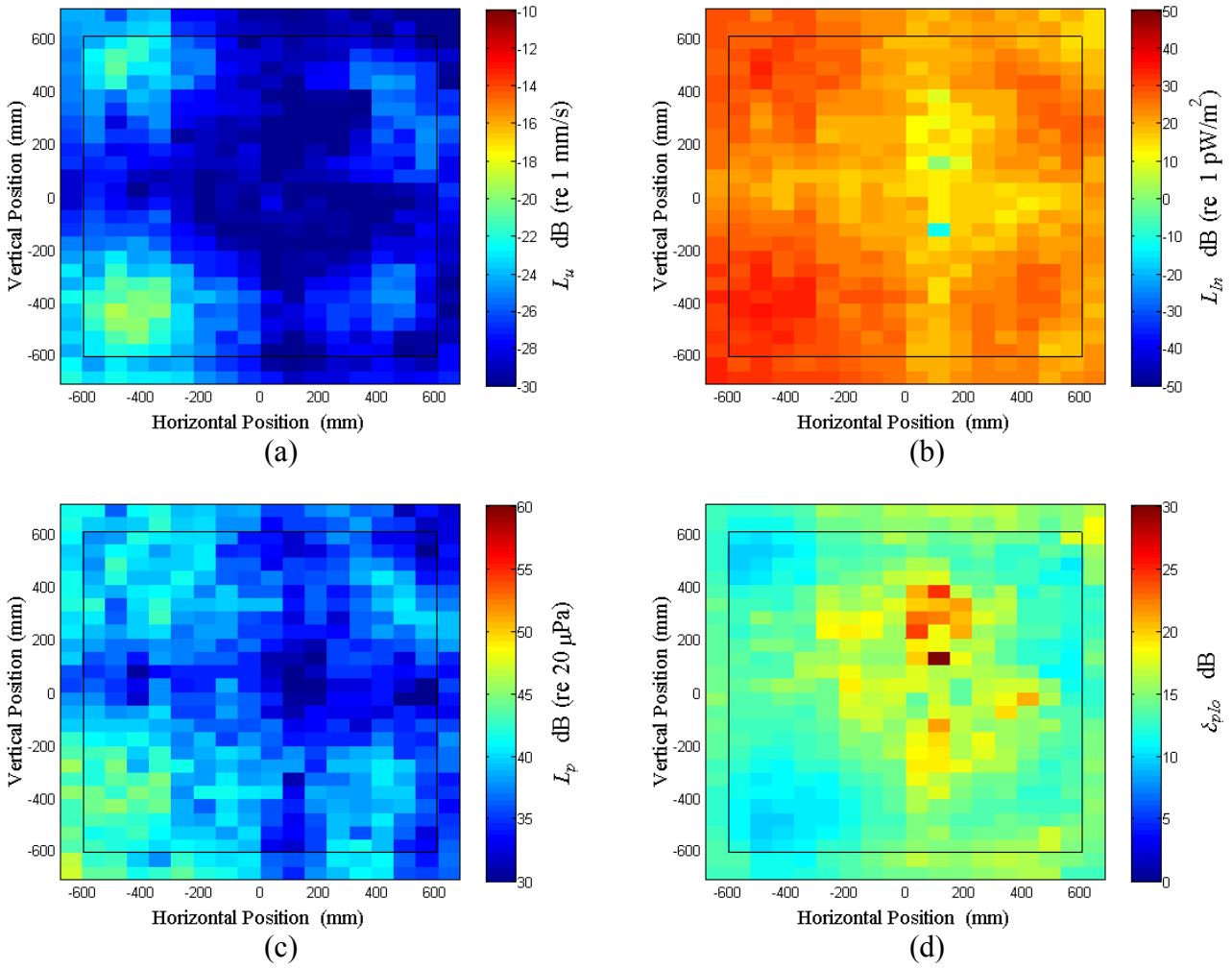

Figure D.64: Surface scan of Window D at 440 Hz (a) particle velocity level, L_u (b) normal signed sound intensity level, L_{In} (c) sound pressure level, L_p (d) pressure-residual intensity index, δ_{pIo}.

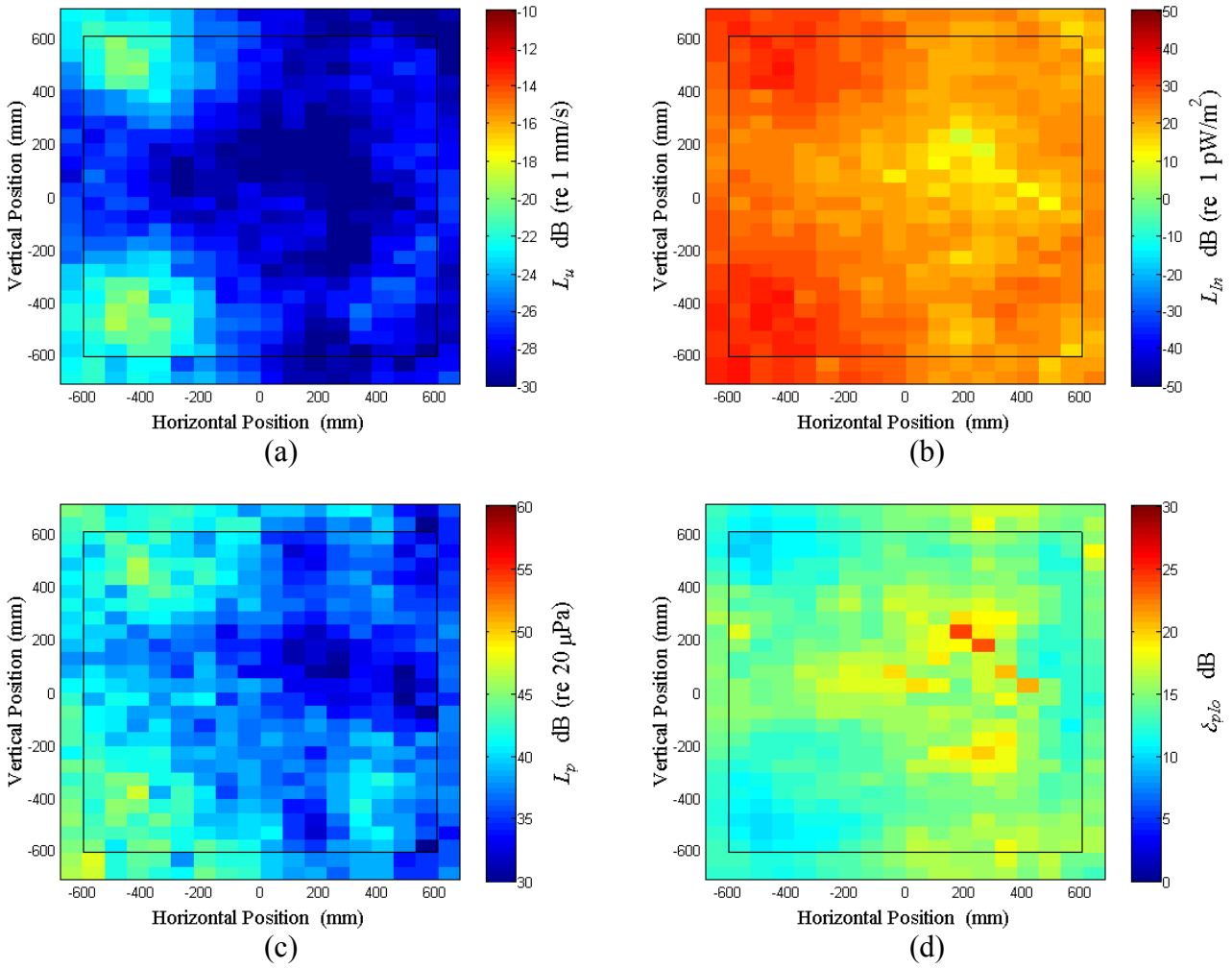

Figure D.65: Surface scan of Window D at 450 Hz (a) particle velocity level, L_u (b) normal signed sound intensity level, L_{In} (c) sound pressure level, L_p (d) pressure-residual intensity index, δ_{pIo}.

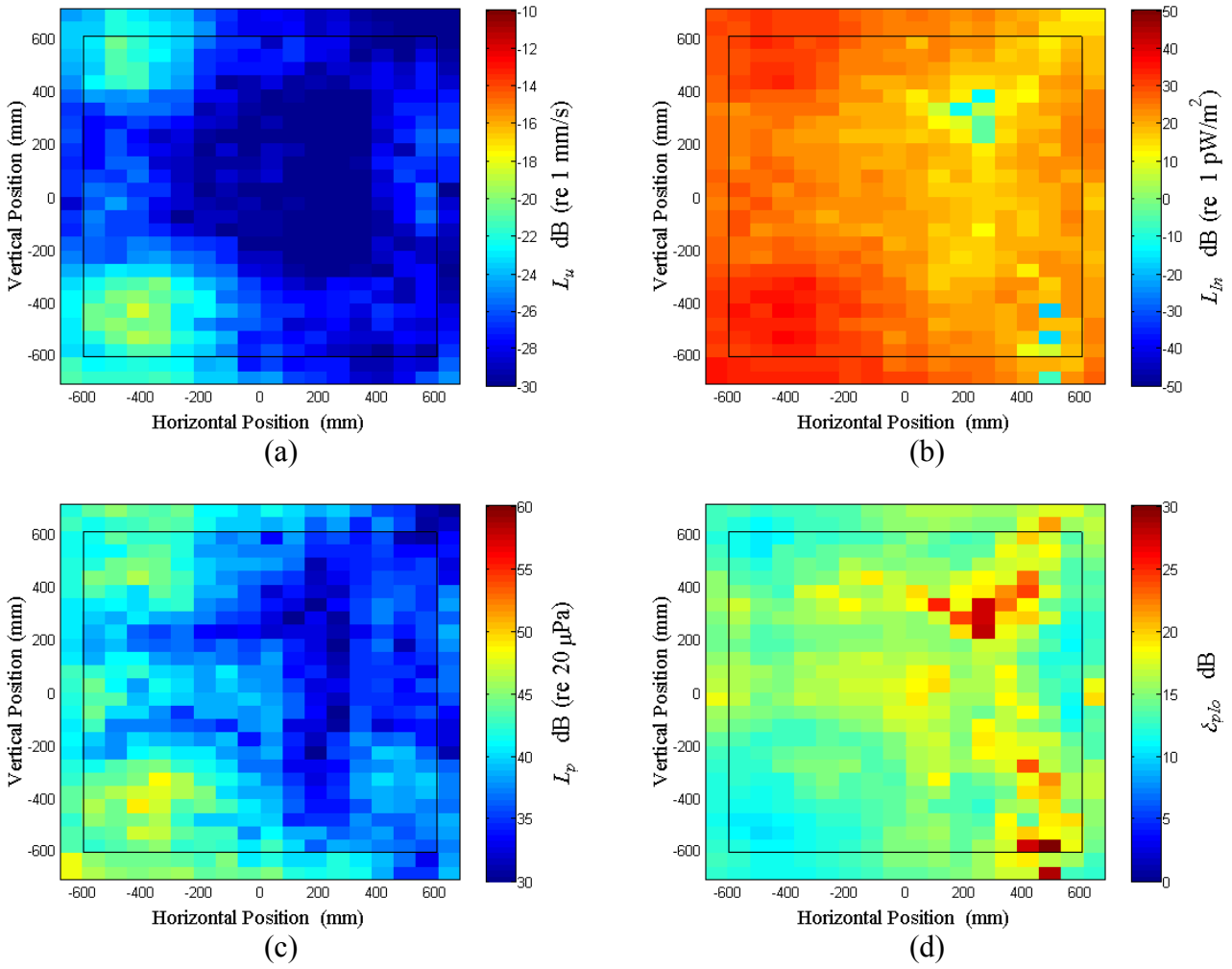

Figure D.66: Surface scan of Window D at 460 Hz (a) particle velocity level, L_u (b) normal signed sound intensity level, L_{In} (c) sound pressure level, L_p (d) pressure-residual intensity index, δ_{pIo}.

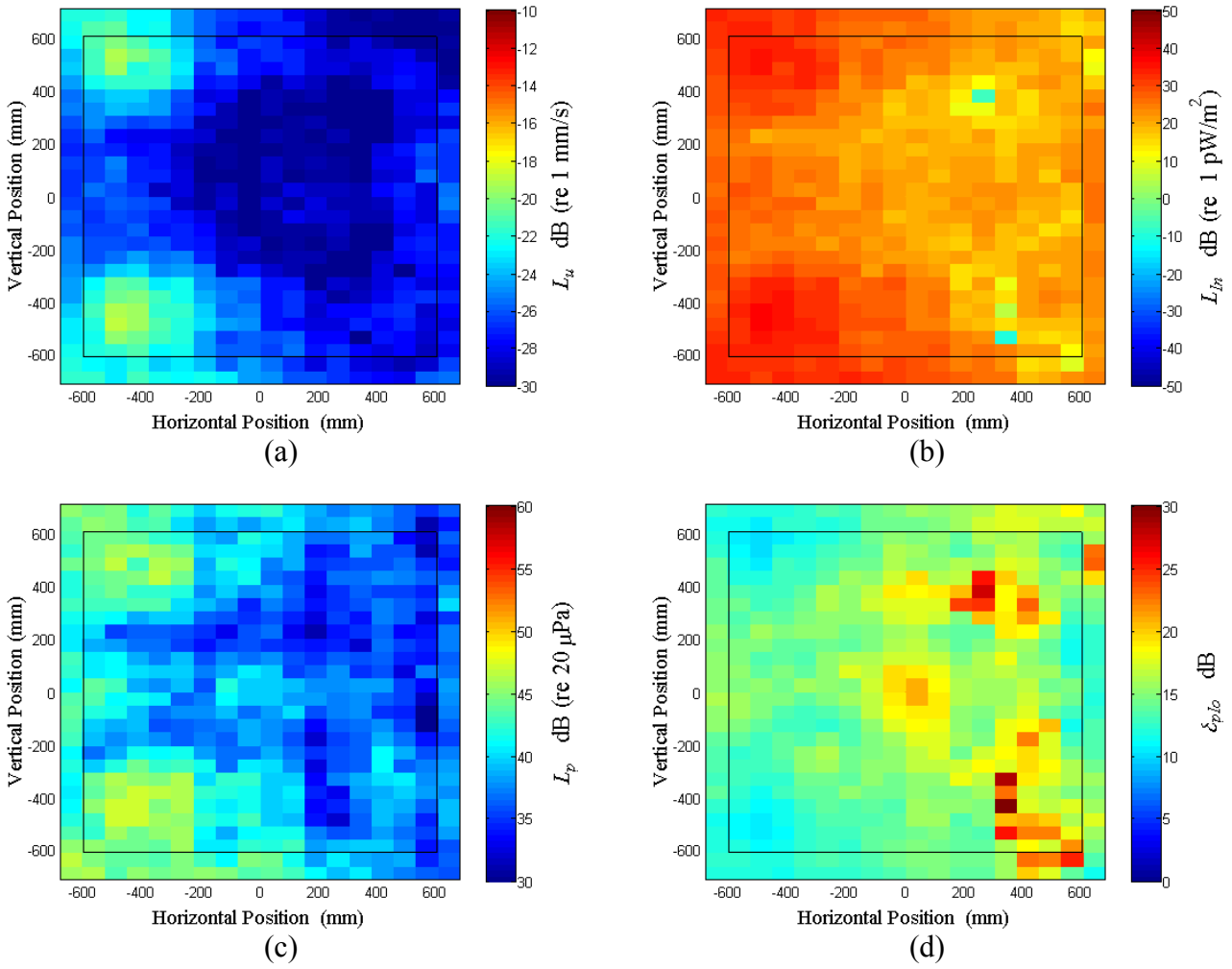

Figure D.67: Surface scan of Window D at 470 Hz (a) particle velocity level, L_u (b) normal signed sound intensity level, L_{In} (c) sound pressure level, L_p (d) pressure-residual intensity index, δ_{pIo}.

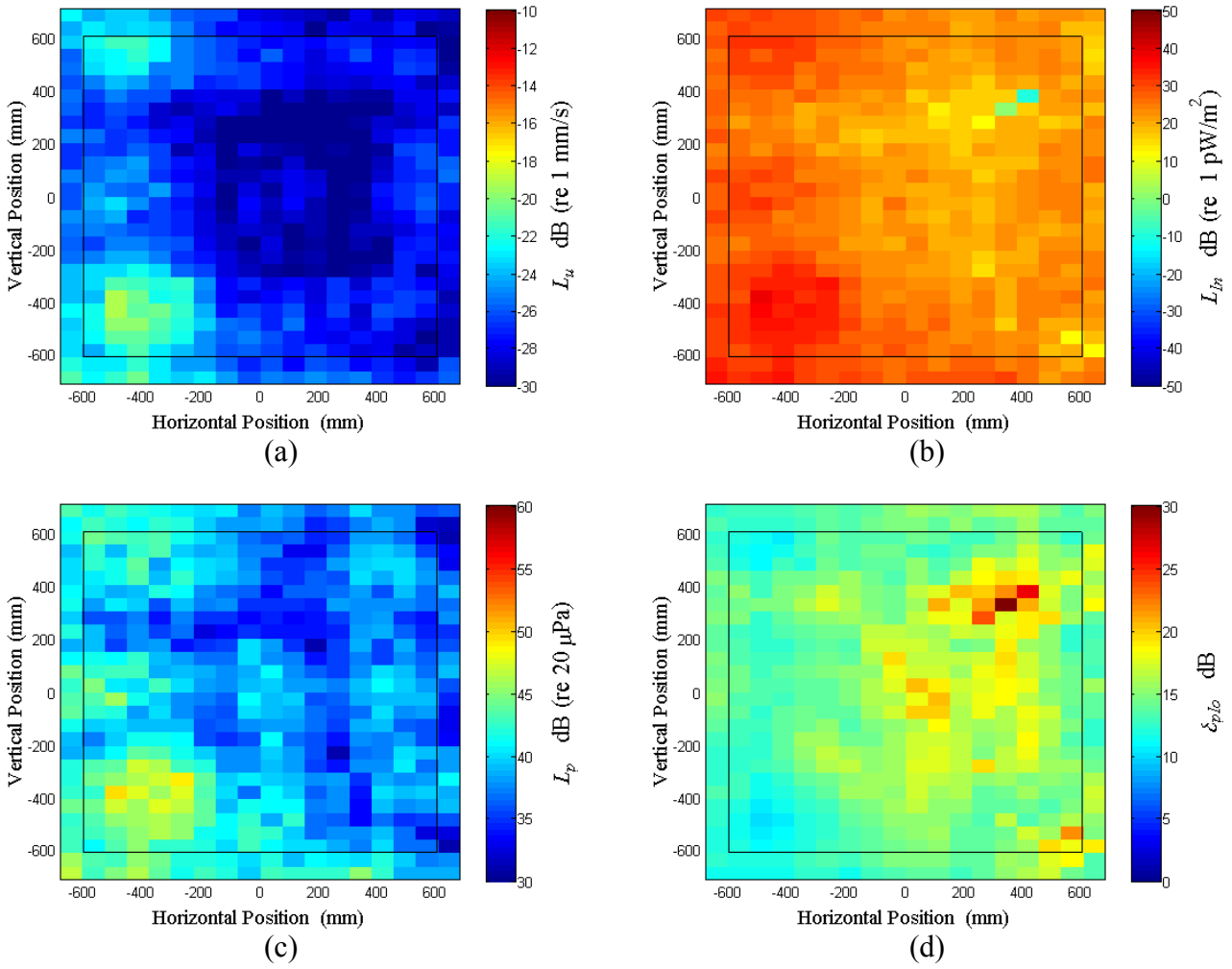

Figure D.68: Surface scan of Window D at 480 Hz (a) particle velocity level, L_u (b) normal signed sound intensity level, L_{In} (c) sound pressure level, L_p (d) pressure-residual intensity index, δ_{pIo}.

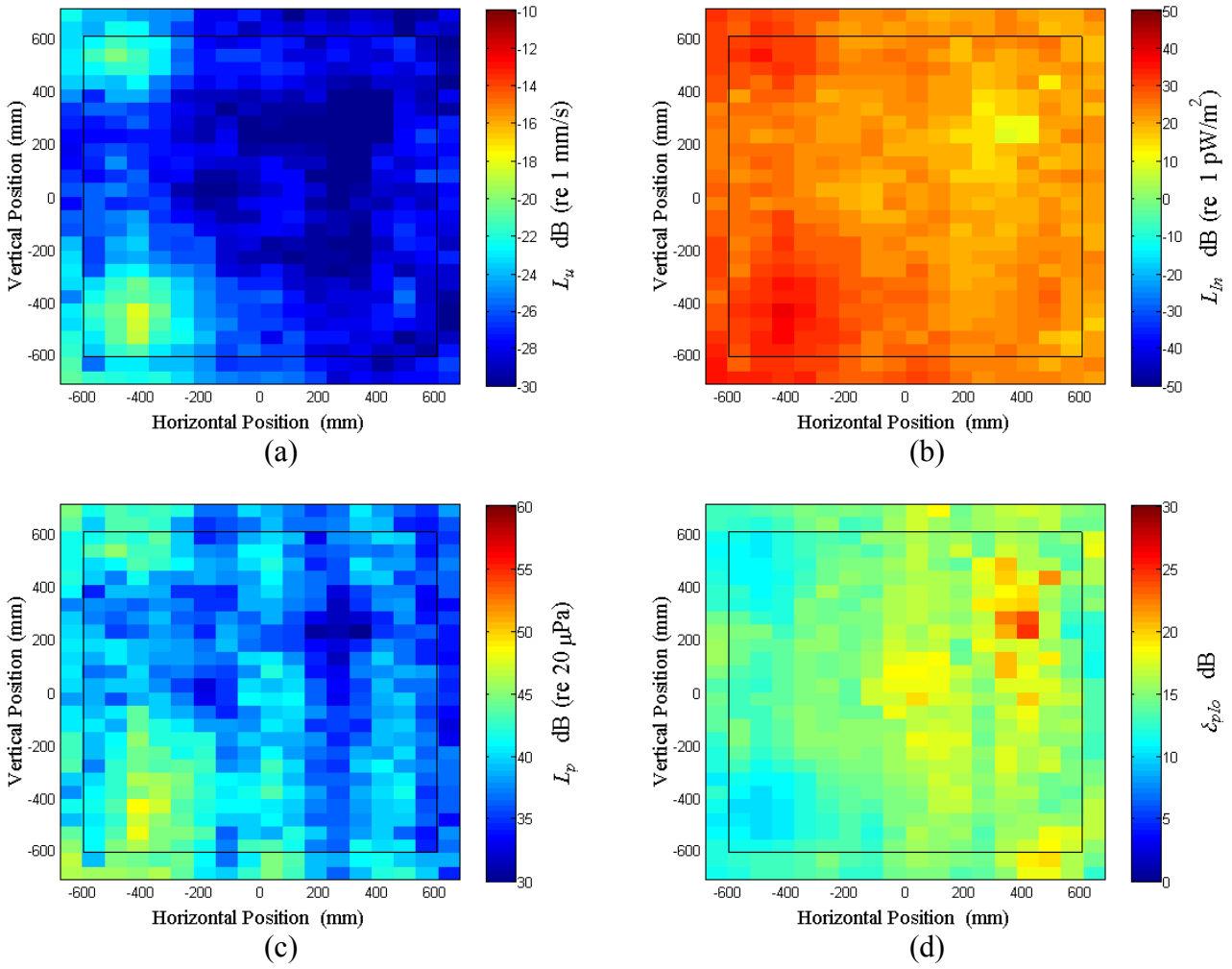

Figure D.69: Surface scan of Window D at 490 Hz (a) particle velocity level, L_u (b) normal signed sound intensity level, L_{In} (c) sound pressure level, L_p (d) pressure-residual intensity index, δ_{pIo}.

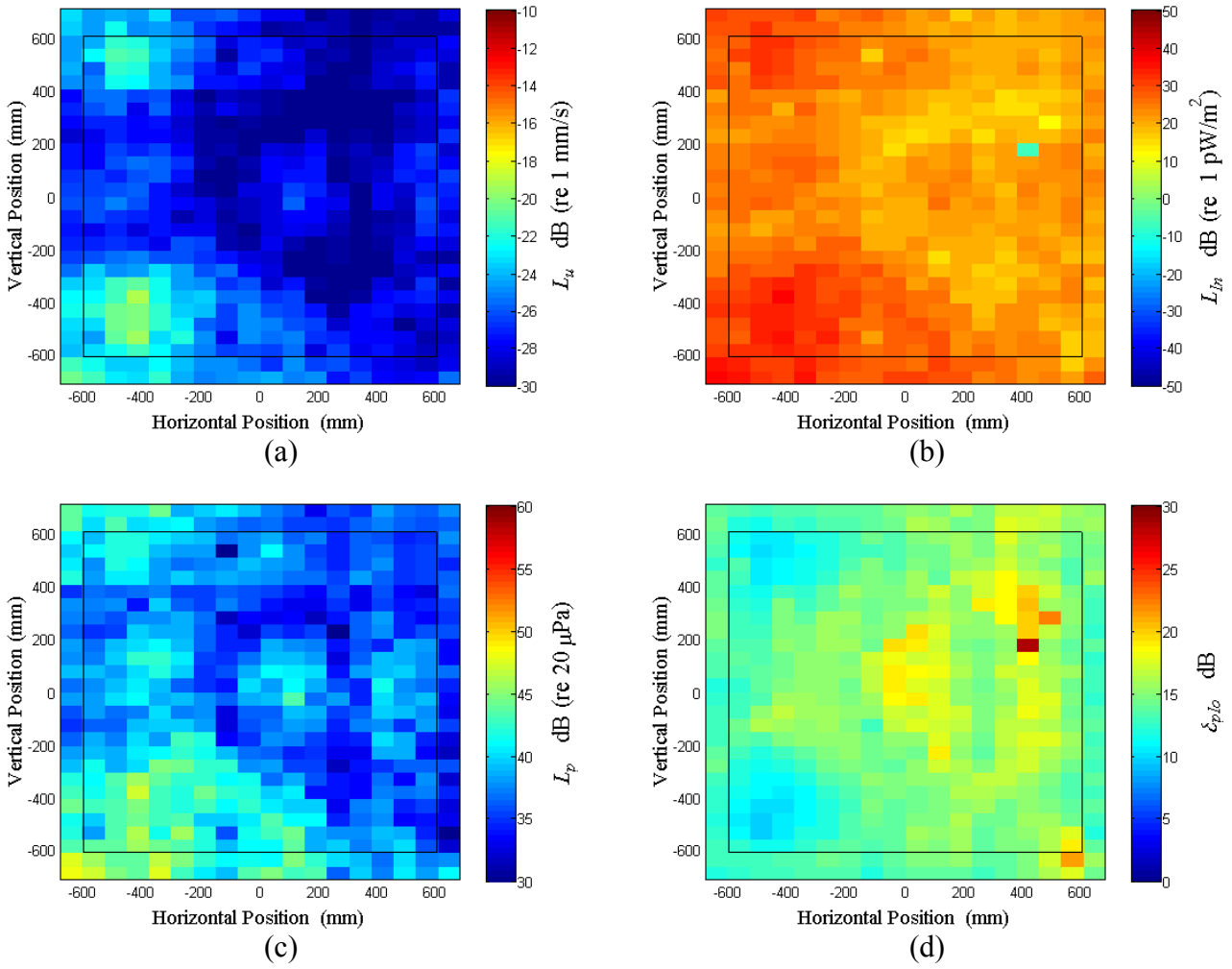

Figure D.70: Surface scan of Window D at 500 Hz (a) particle velocity level, L_u (b) normal signed sound intensity level, L_{In} (c) sound pressure level, L_p (d) pressure-residual intensity index, δ_{pIo}.

APPENDIX E. WINDOW E

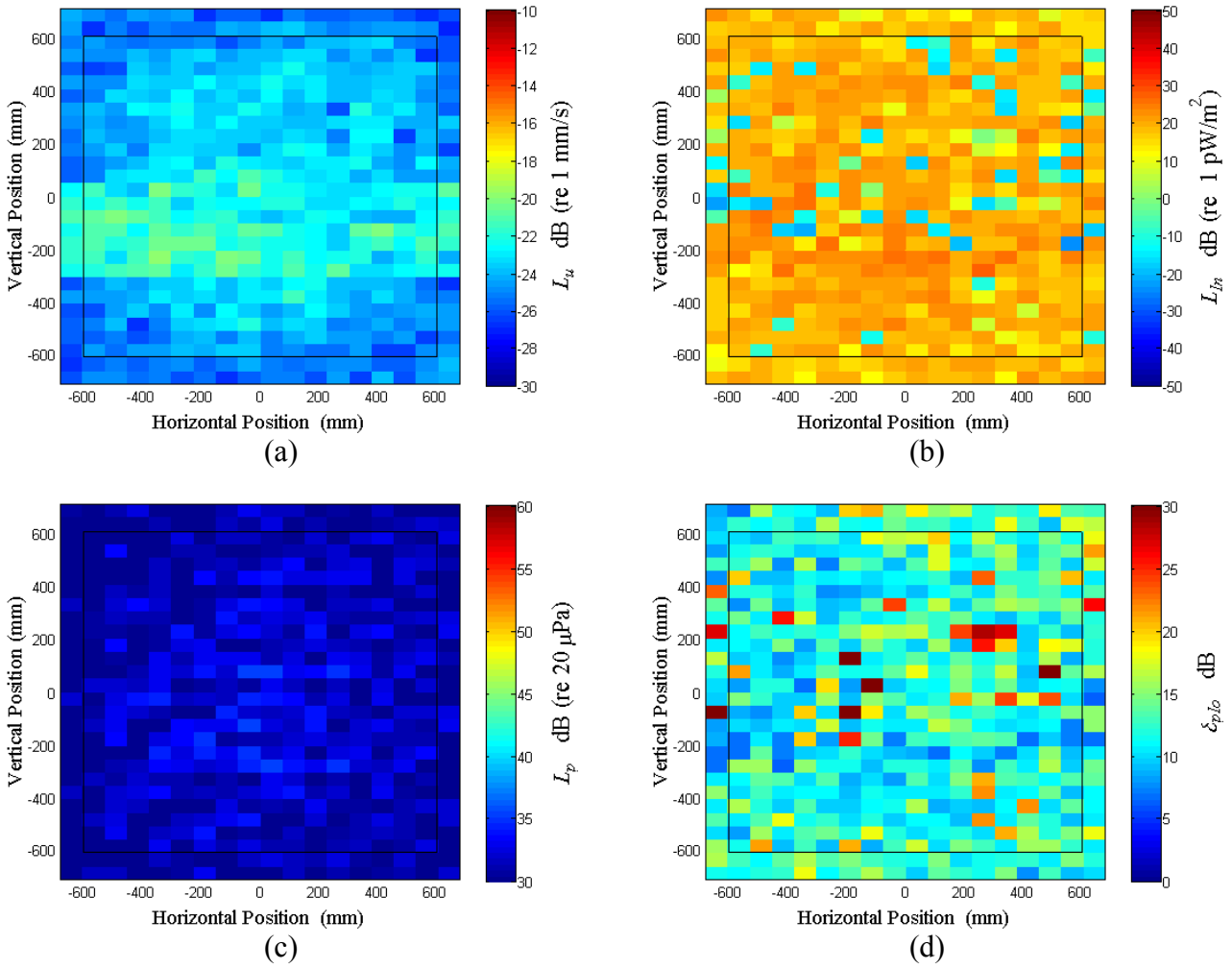

Figure E.1: Surface scan of Window E at 50 Hz (a) particle velocity level, L_u (b) normal signed sound intensity level, L_{In} (c) sound pressure level, L_p (d) pressure-residual intensity index, δ_{pIo}.

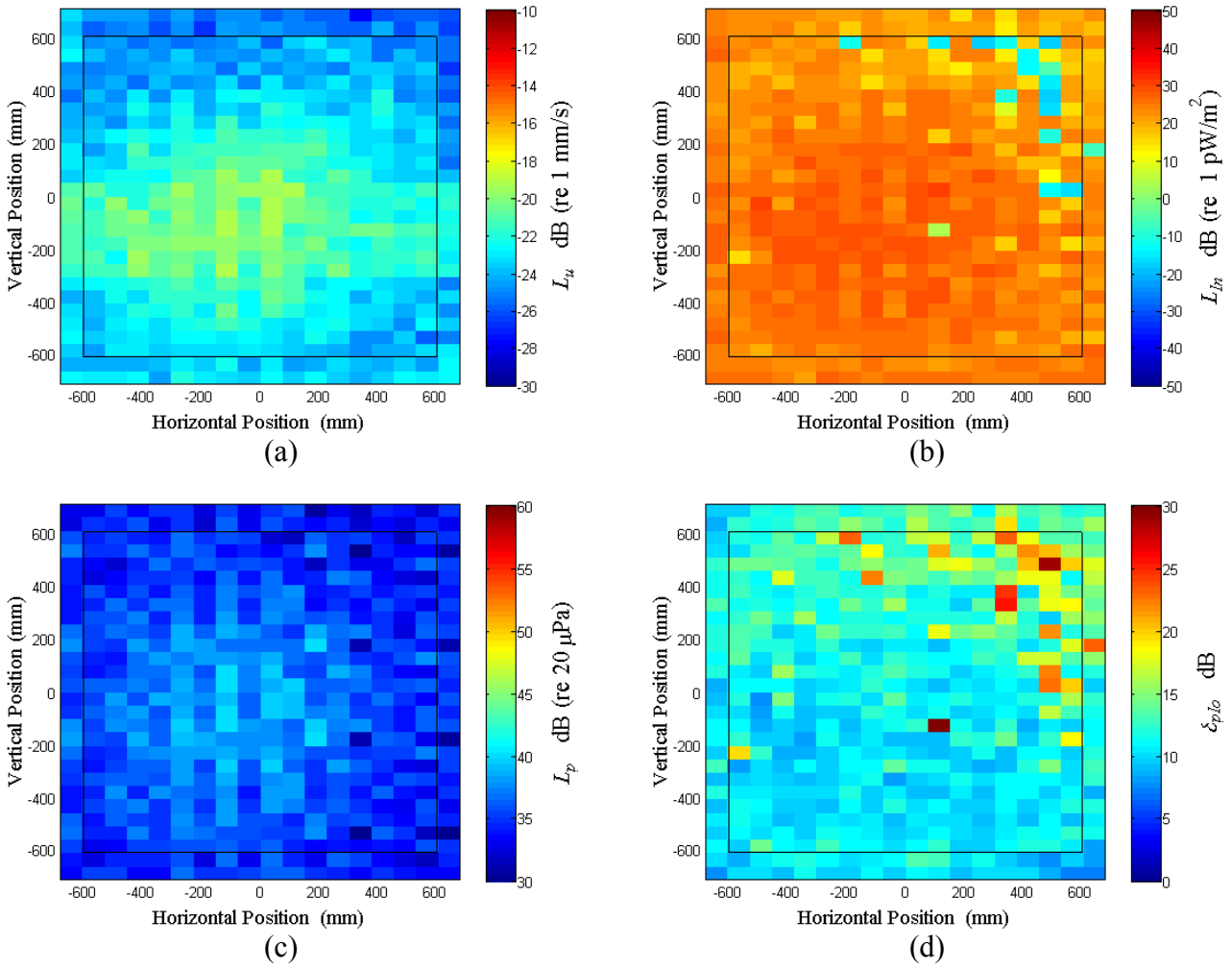

Figure E.2: Surface scan of Window E at 52.5 Hz (a) particle velocity level, L_u (b) normal signed sound intensity level, L_{In} (c) sound pressure level, L_p (d) pressure-residual intensity index, δ_{pIo}.

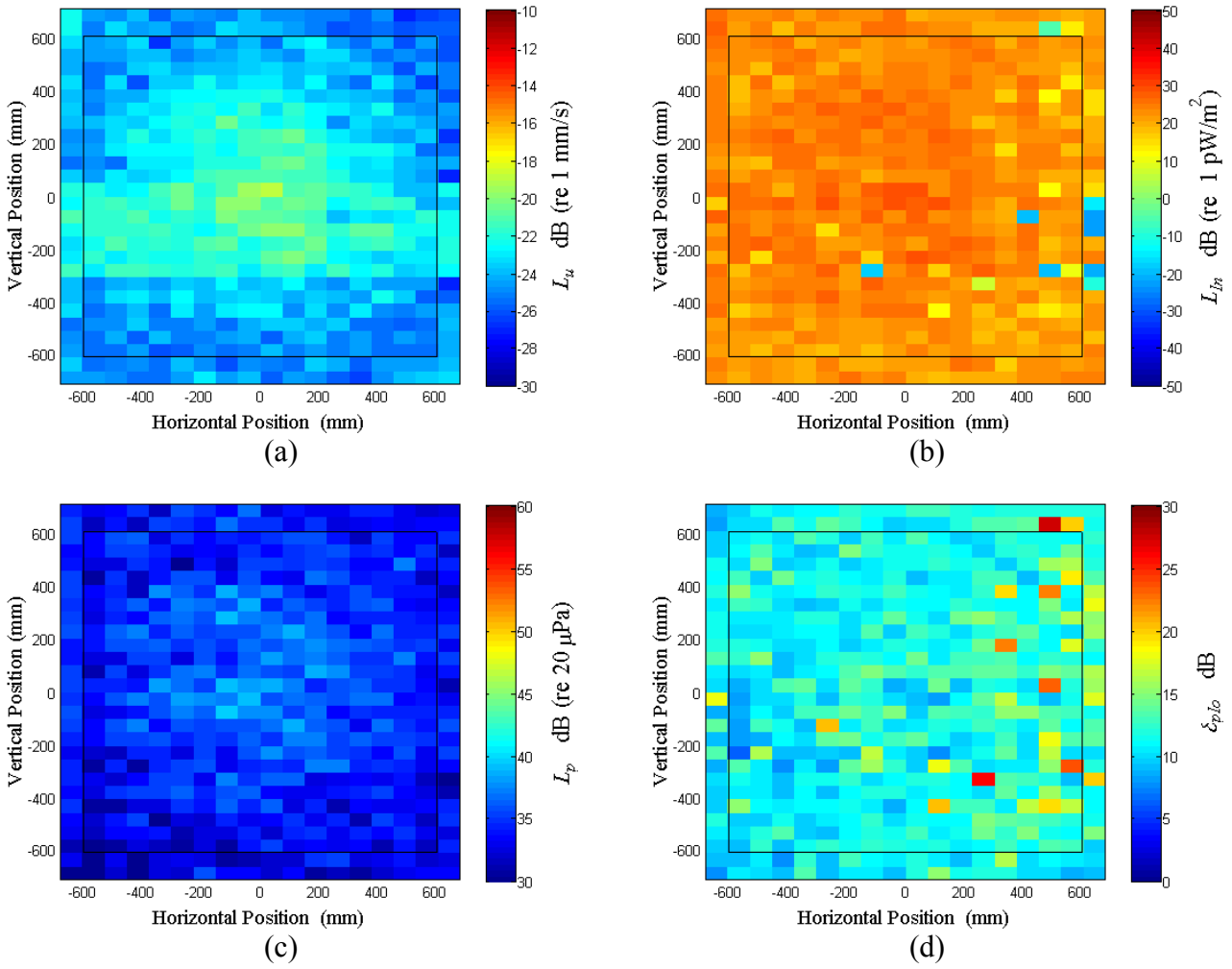

Figure E.3: Surface scan of Window E at 55 Hz (a) particle velocity level, L_u (b) normal signed sound intensity level, L_{In} (c) sound pressure level, L_p (d) pressure-residual intensity index, δ_{pIo}.

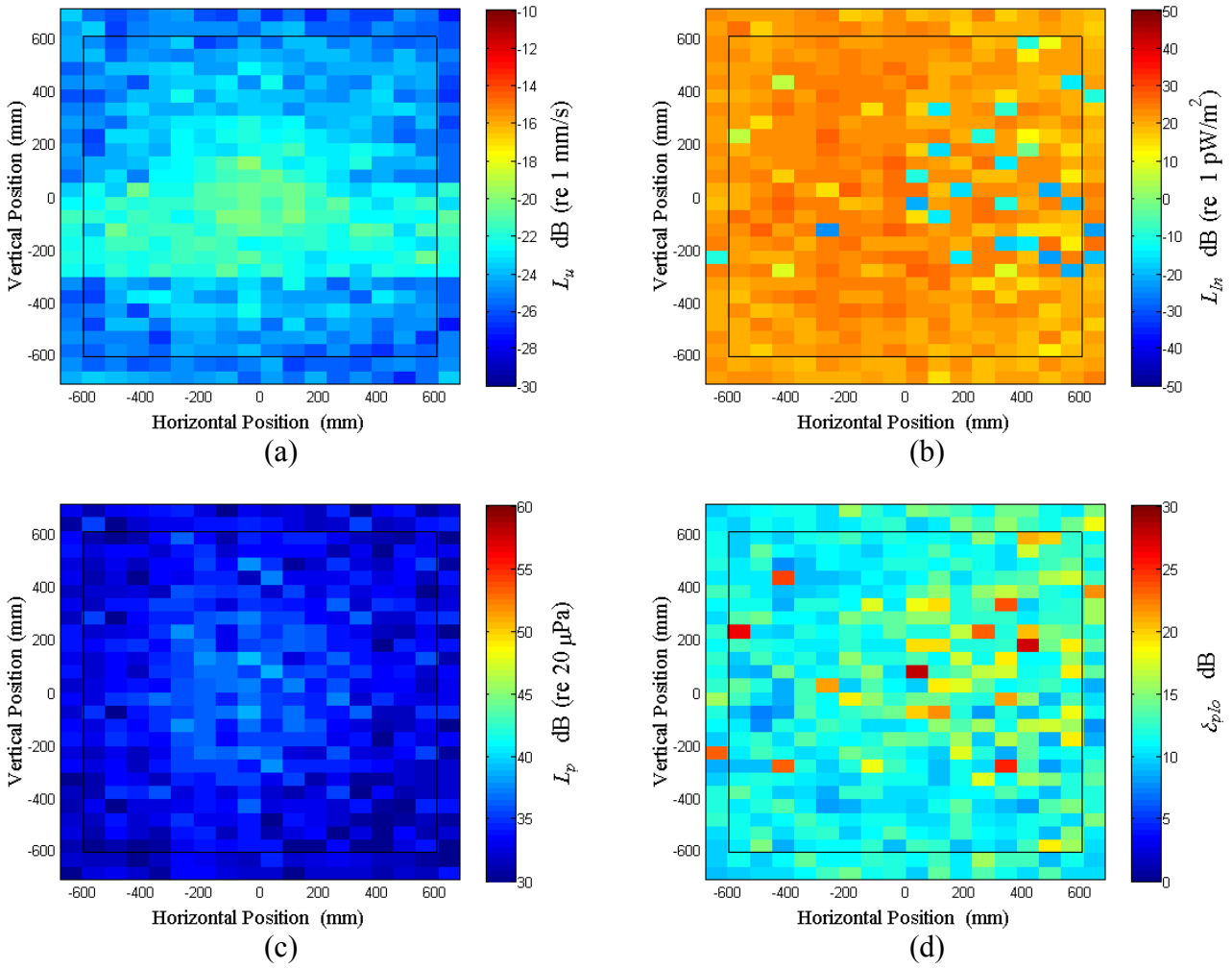

Figure E.4: Surface scan of Window E at 57.5 Hz (a) particle velocity level, L_u (b) normal signed sound intensity level, L_{In} (c) sound pressure level, L_p (d) pressure-residual intensity index, δ_{pIo}.

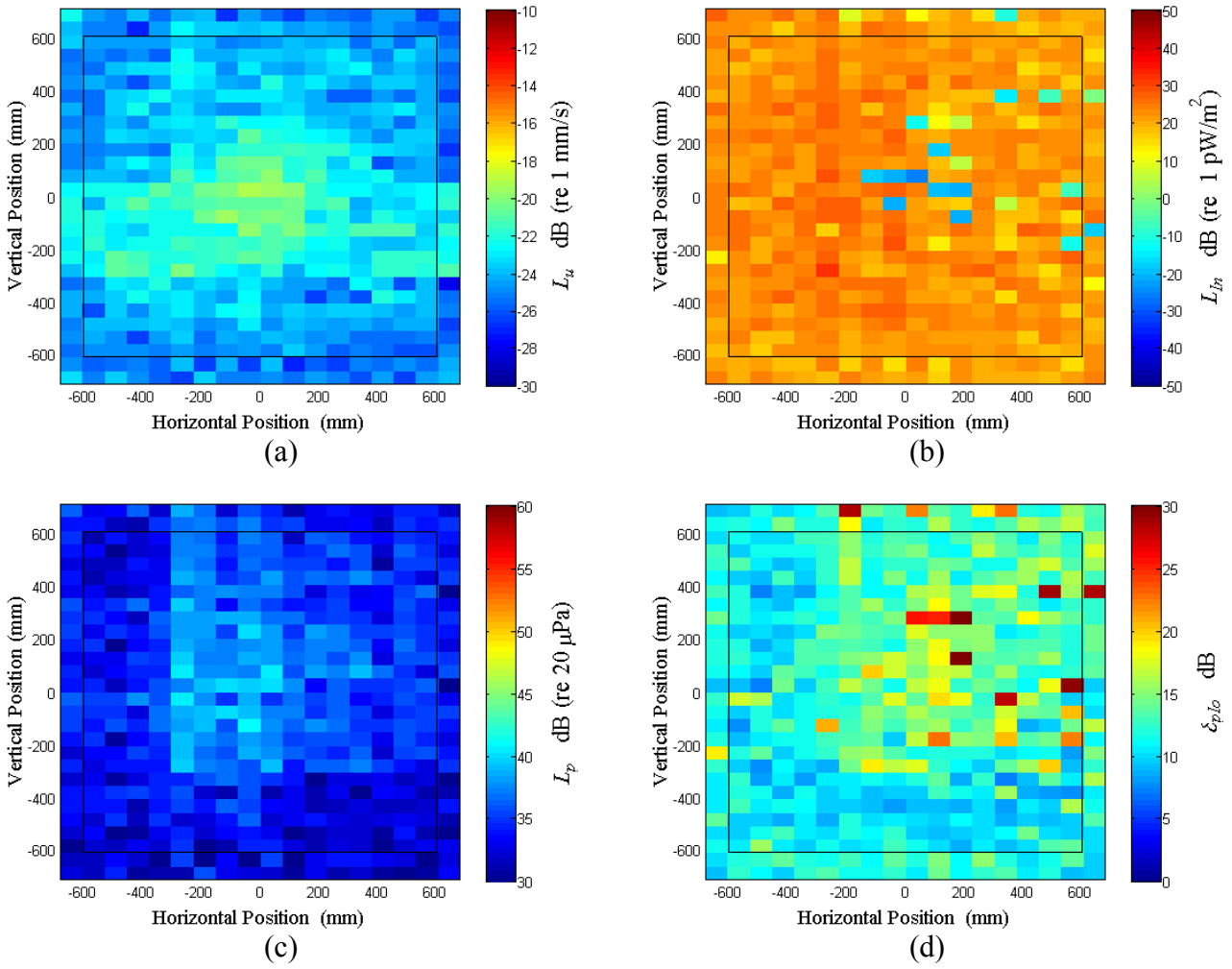

Figure E.5: Surface scan of Window E at 60 Hz (a) particle velocity level, L_u (b) normal signed sound intensity level, L_{In} (c) sound pressure level, L_p (d) pressure-residual intensity index, δ_{pIo}.

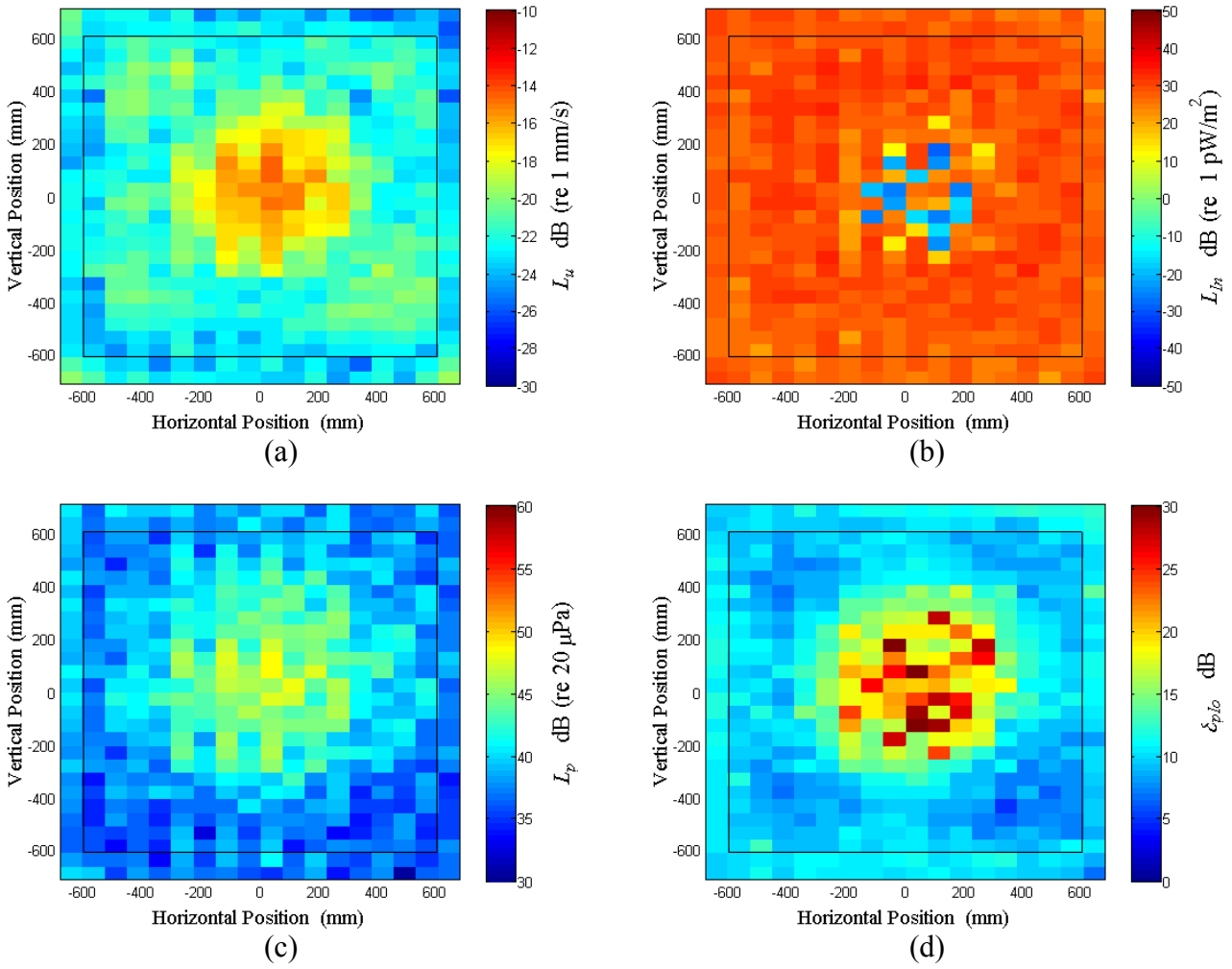

Figure E.6: Surface scan of Window E at 62.5 Hz (a) particle velocity level, L_u (b) normal signed sound intensity level, L_{In} (c) sound pressure level, L_p (d) pressure-residual intensity index, δ_{pIo}.

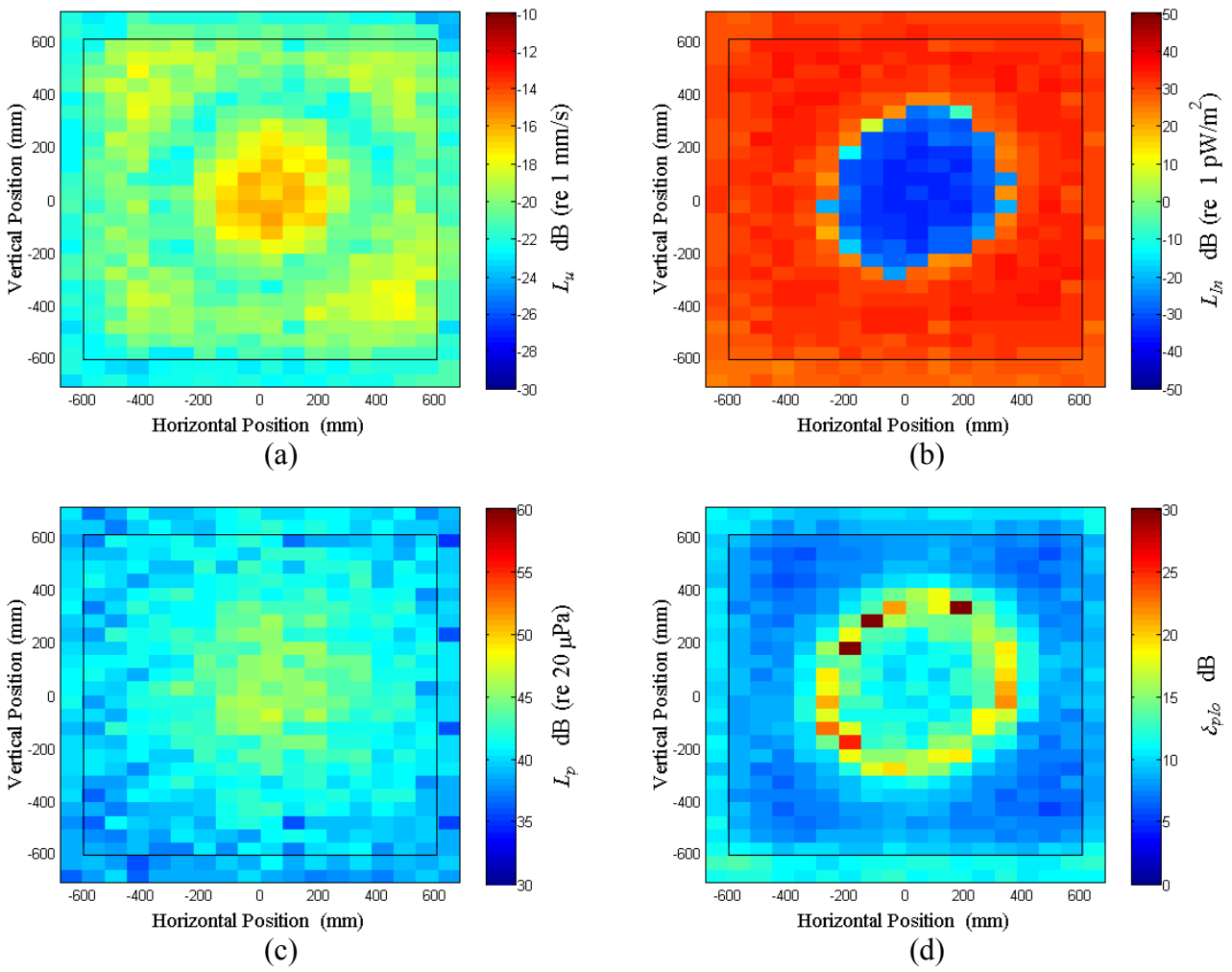

Figure E.7: Surface scan of Window E at 65 Hz (a) particle velocity level, L_u (b) normal signed sound intensity level, L_{In} (c) sound pressure level, L_p (d) pressure-residual intensity index, δ_{pIo}.

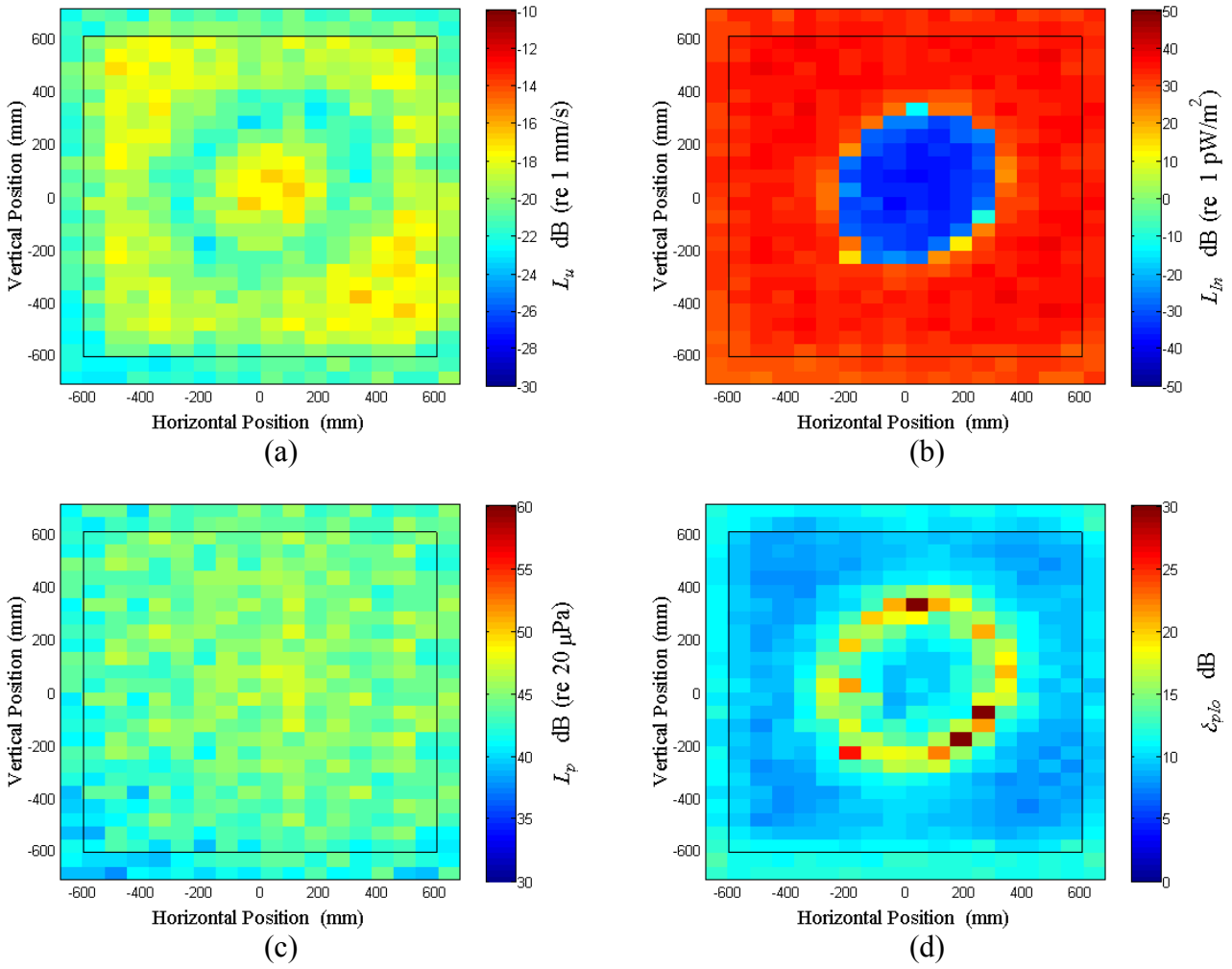

Figure E.8: Surface scan of Window E at 67.5 Hz (a) particle velocity level, L_u (b) normal signed sound intensity level, L_{In} (c) sound pressure level, L_p (d) pressure-residual intensity index, δ_{pIo}.

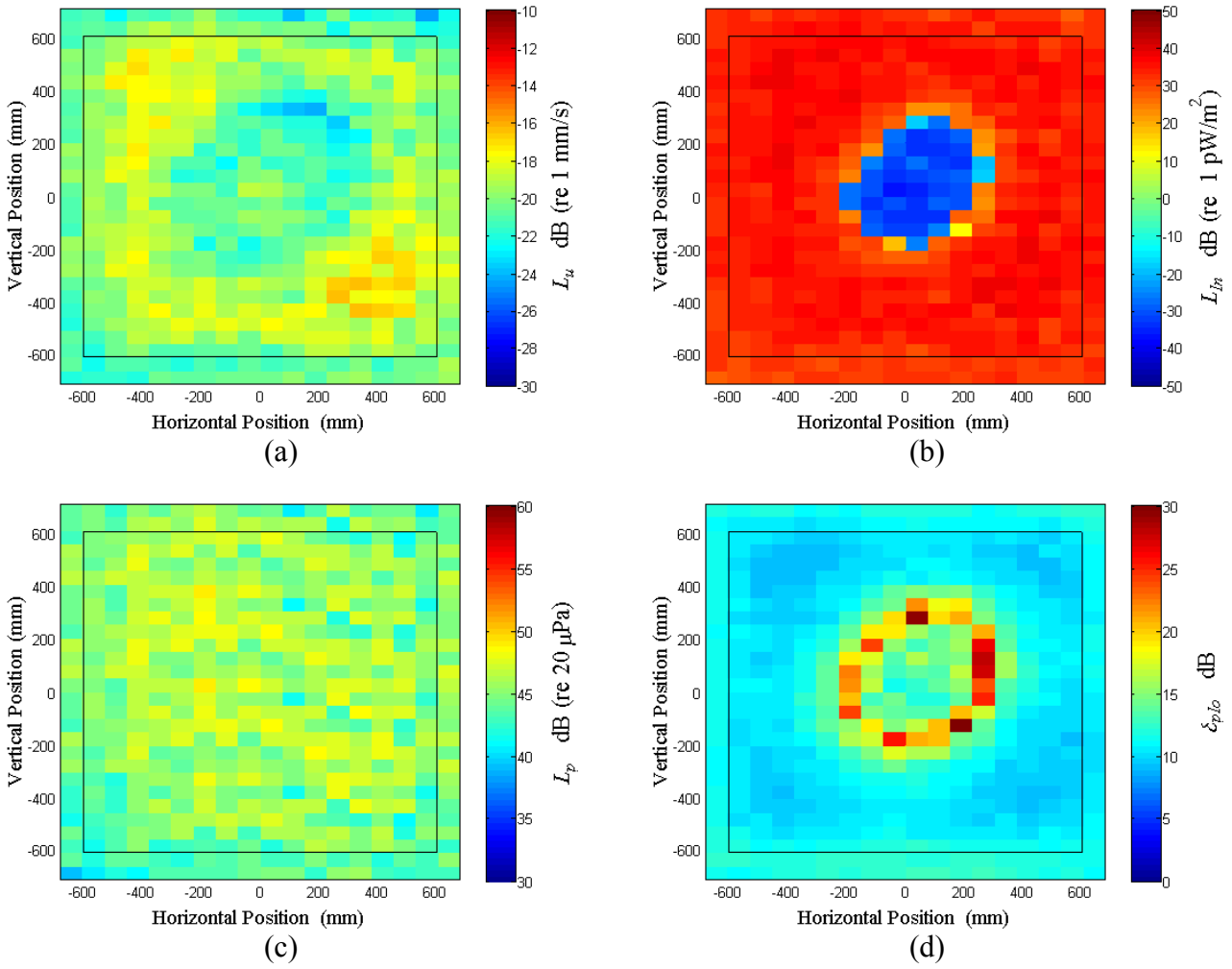

Figure E.9: Surface scan of Window E at 70 Hz (a) particle velocity level, L_u (b) normal signed sound intensity level, L_{In} (c) sound pressure level, L_p (d) pressure-residual intensity index, δ_{pIo}.

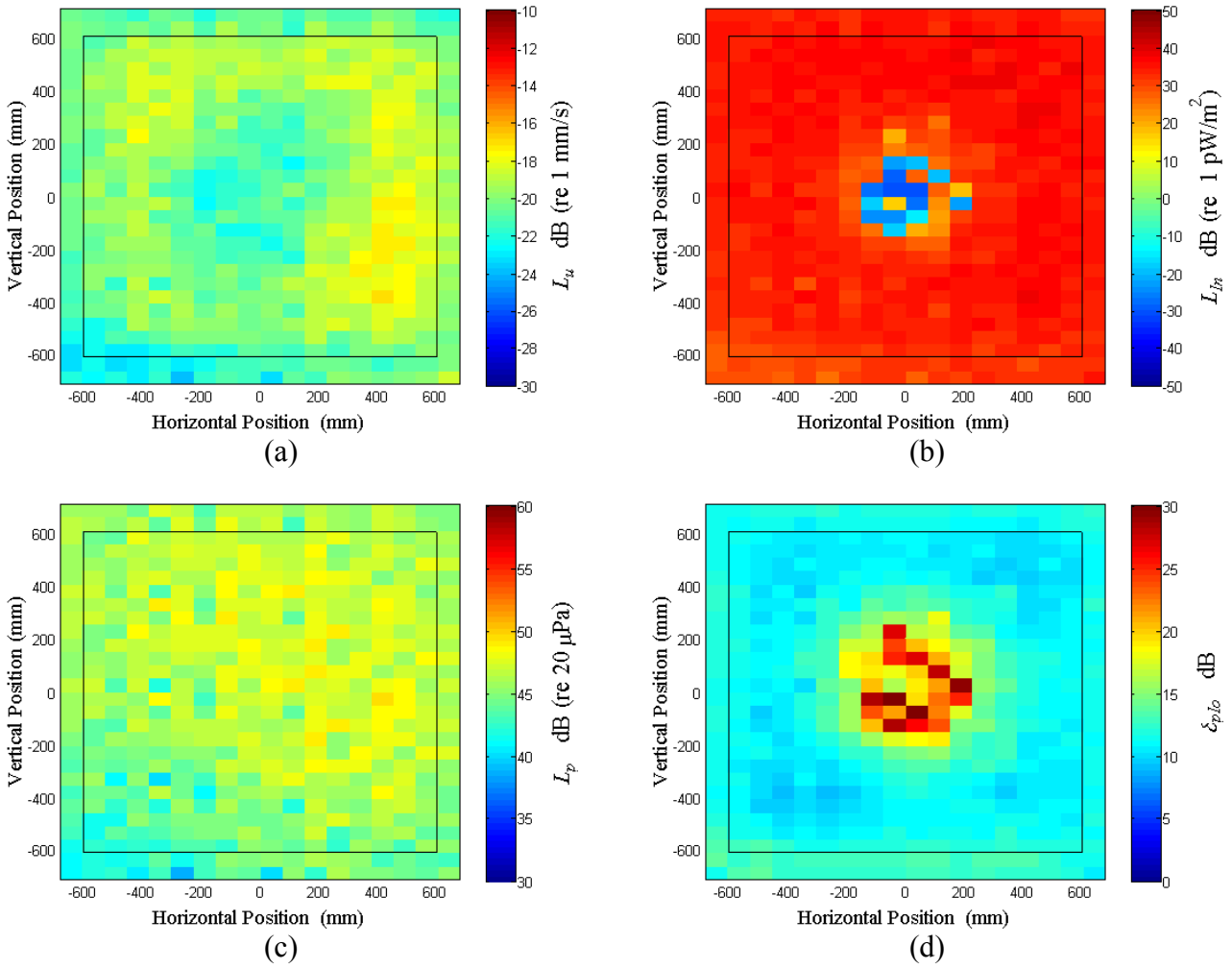

Figure E.10: Surface scan of Window E at 72.5 Hz (a) particle velocity level, L_u (b) normal signed sound intensity level, L_{In} (c) sound pressure level, L_p (d) pressure-residual intensity index, δ_{pIo}.

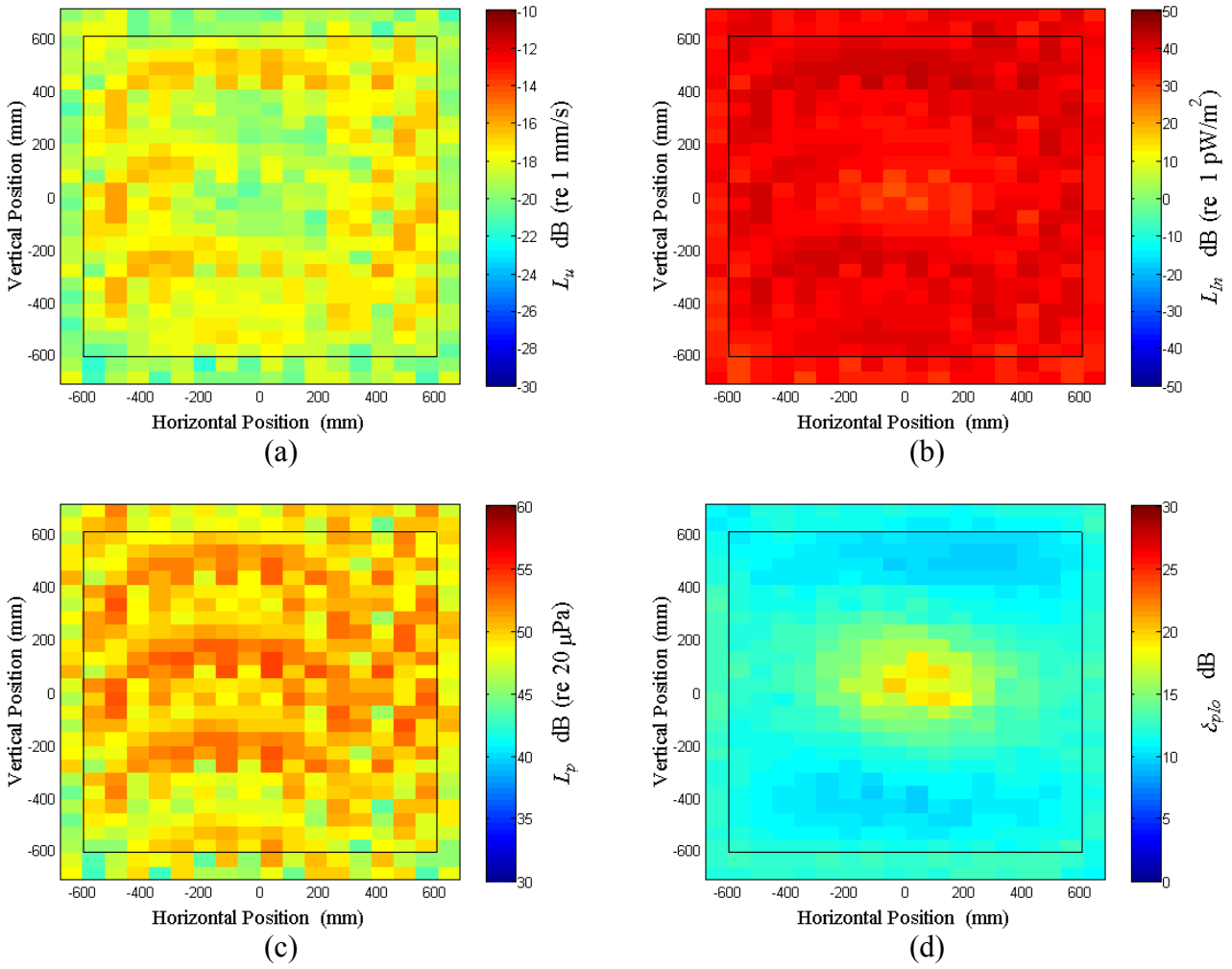

Figure E.11: Surface scan of Window E at.75 Hz (a) particle velocity level, L_u (b) normal signed sound intensity level, L_{In} (c) sound pressure level, L_p (d) pressure-residual intensity index, δ_{pIo}.

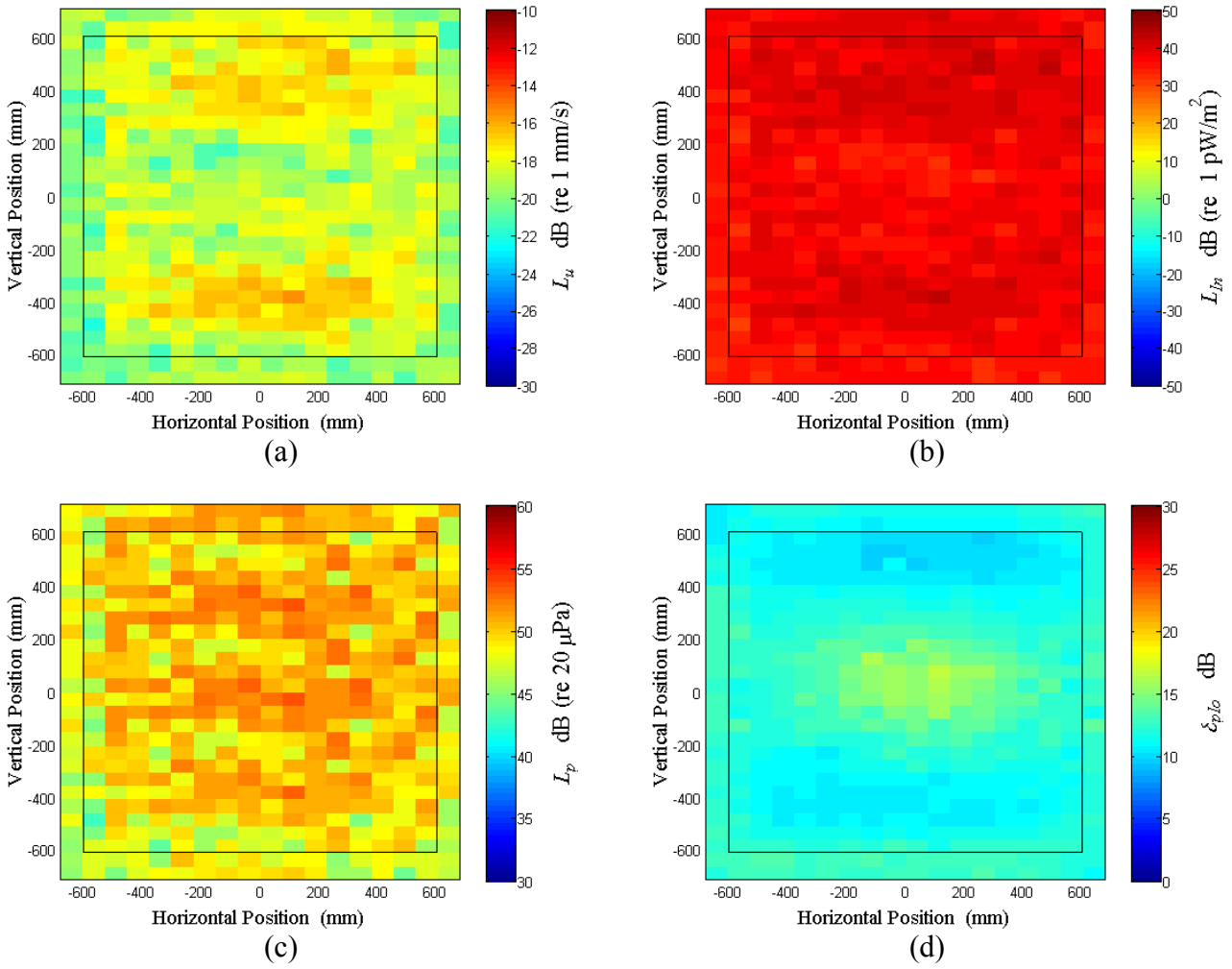

Figure E.12: Surface scan of Window E at 77.5 Hz (a) particle velocity level, L_u (b) normal signed sound intensity level, L_{In} (c) sound pressure level, L_p (d) pressure-residual intensity index, δ_{pIo}.

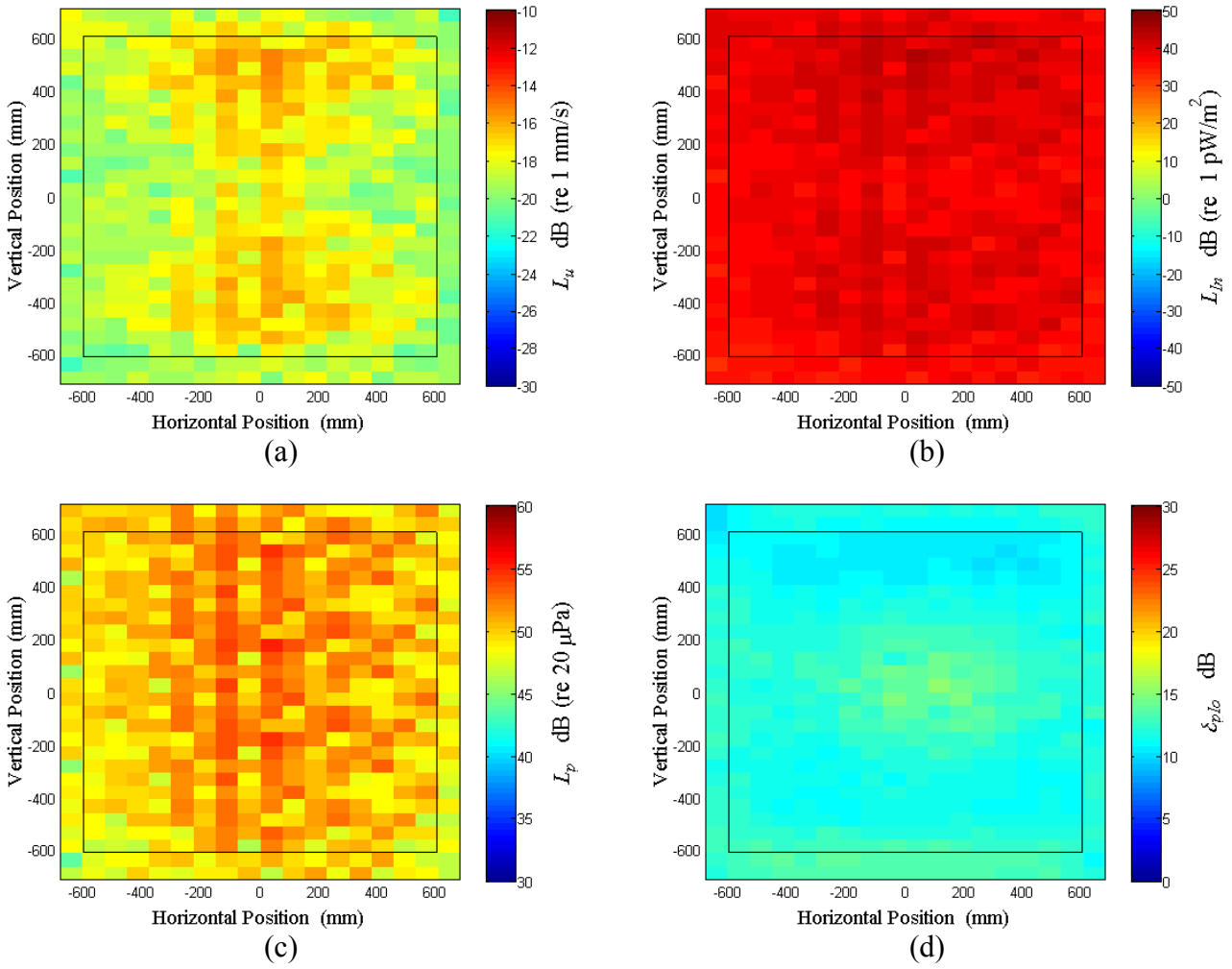

Figure E.13: Surface scan of Window E at 80 Hz (a) particle velocity level, L_u (b) normal signed sound intensity level, L_{In} (c) sound pressure level, L_p (d) pressure-residual intensity index, δ_{pIo}.

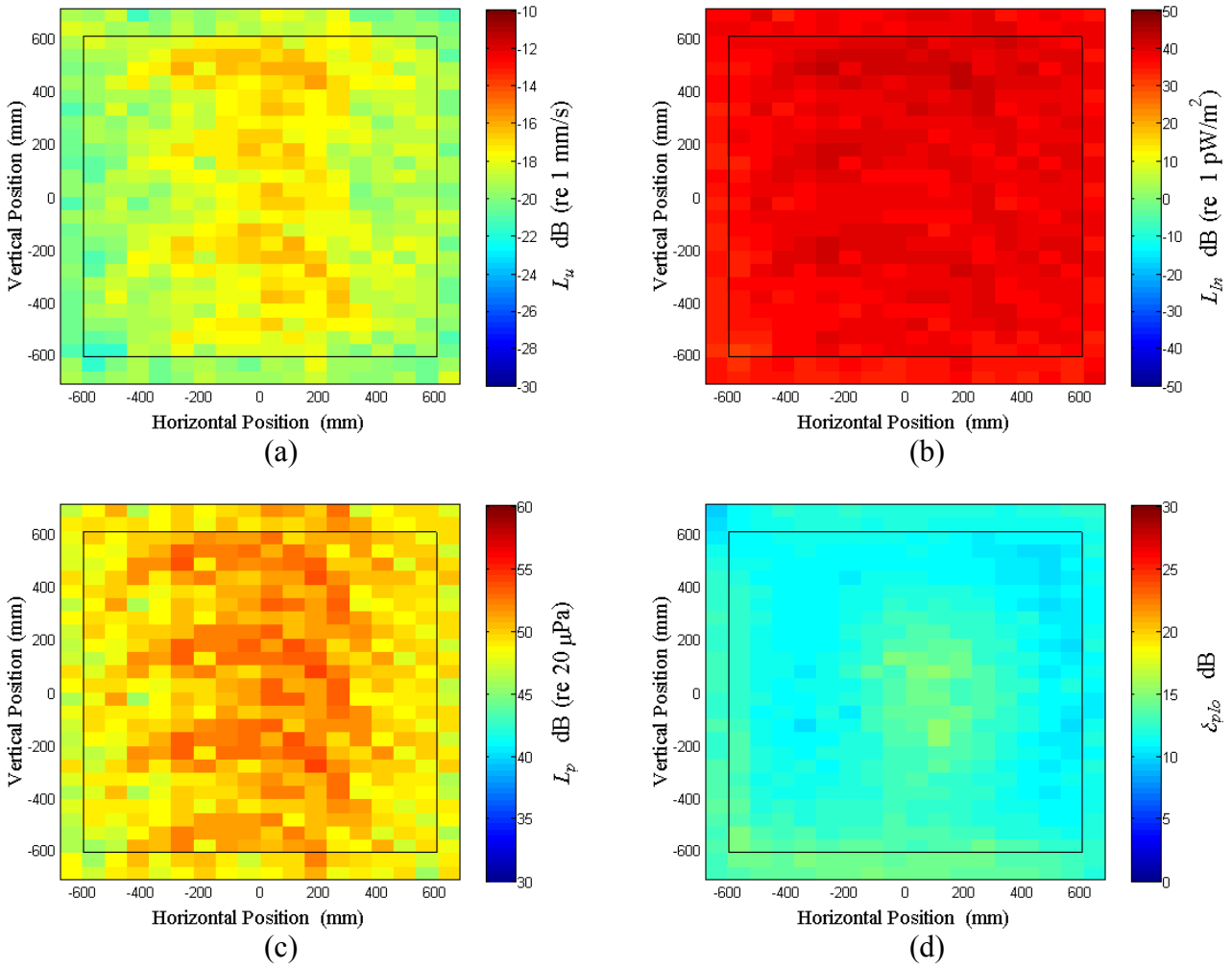

Figure E.14: Surface scan of Window E at 82.5 Hz (a) particle velocity level, L_u (b) normal signed sound intensity level, L_{In} (c) sound pressure level, L_p (d) pressure-residual intensity index, δ_{pIo}.

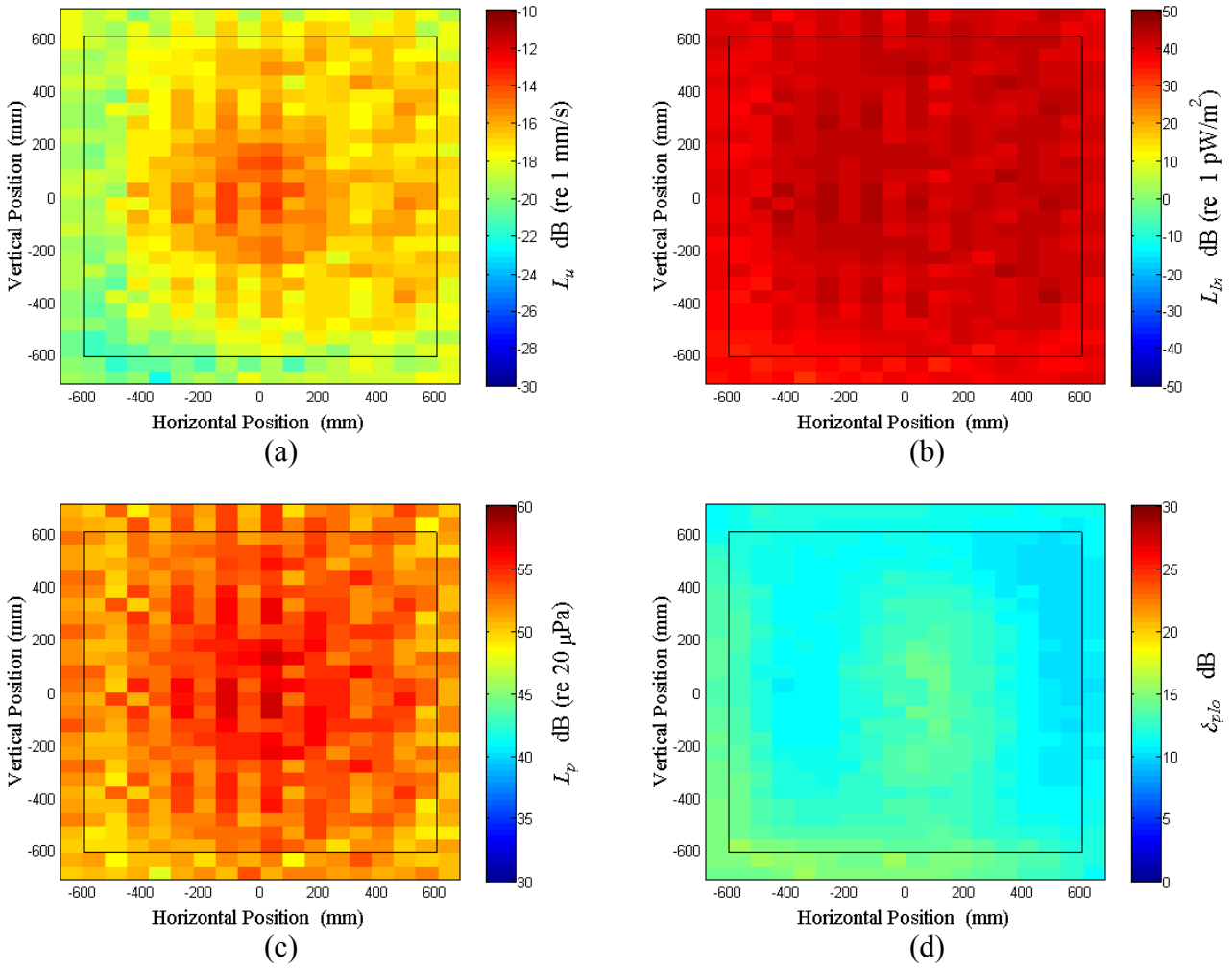

Figure E.15: Surface scan of Window E at 85 Hz (a) particle velocity level, L_u (b) normal signed sound intensity level, L_{In} (c) sound pressure level, L_p (d) pressure-residual intensity index, δ_{pIo}.

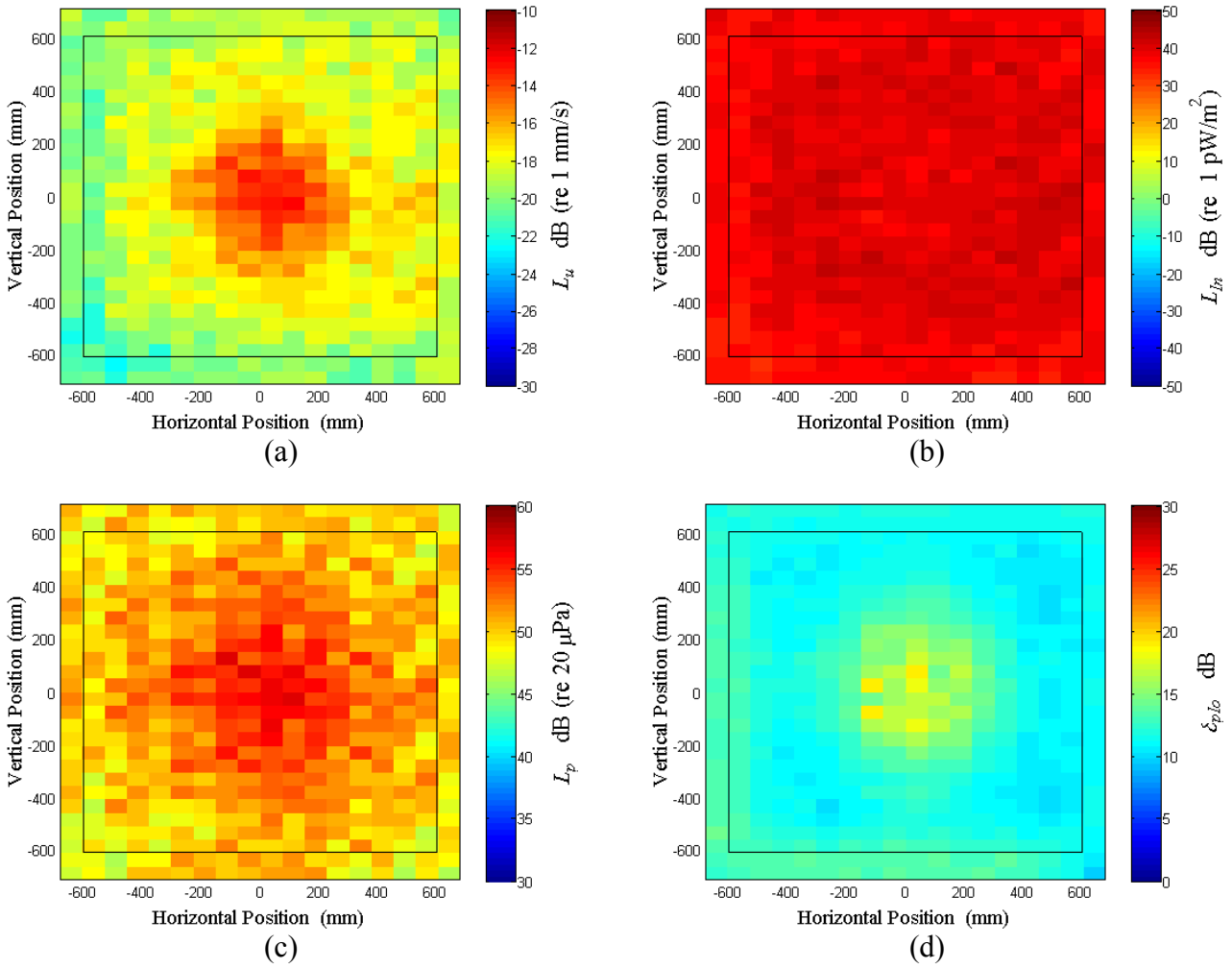

Figure E.16: Surface scan of Window E at 87.5 Hz (a) particle velocity level, L_u (b) normal signed sound intensity level, L_{In} (c) sound pressure level, L_p (d) pressure-residual intensity index, δ_{pIo}.

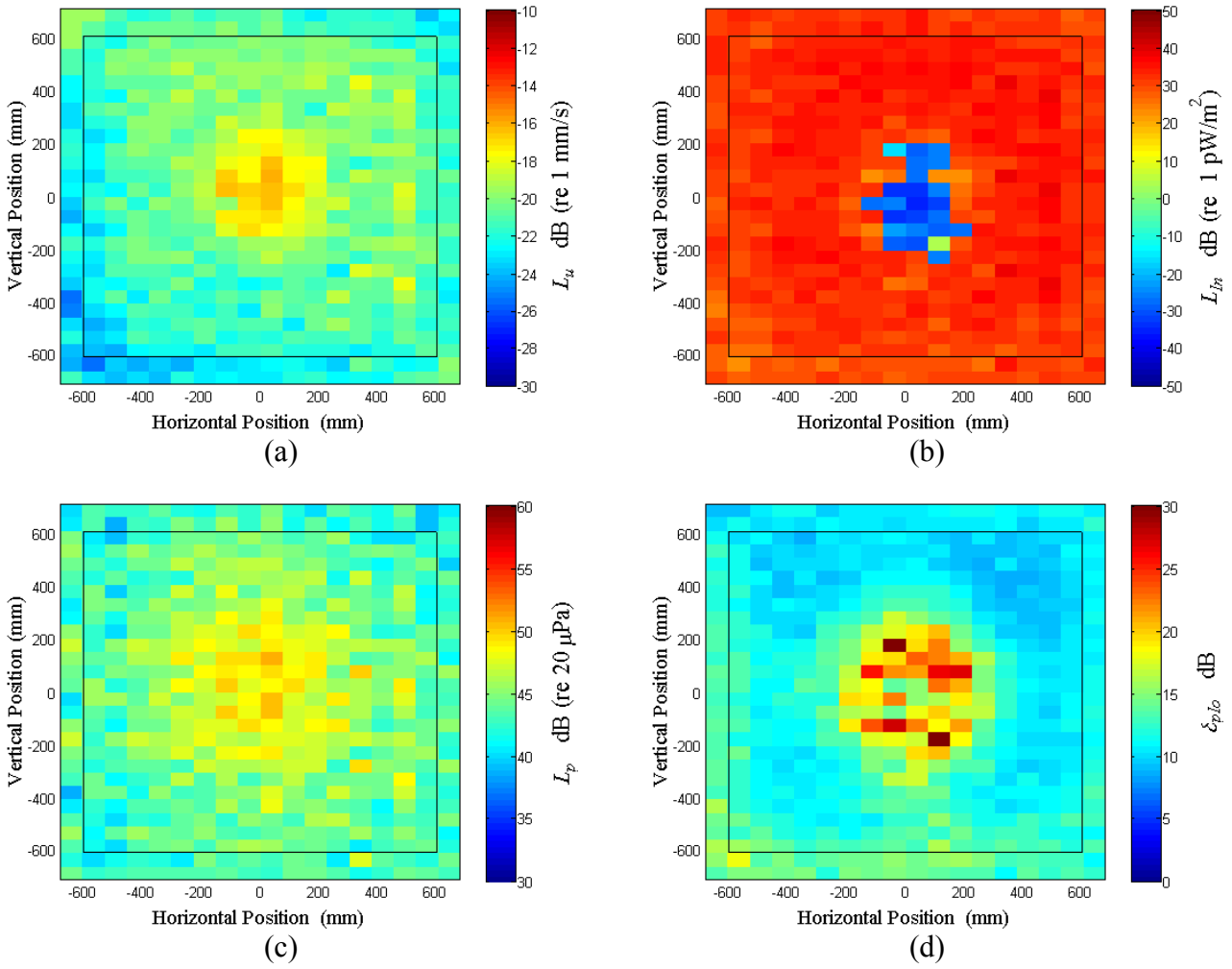

Figure E.17: Surface scan of Window E at 90 Hz (a) particle velocity level, L_u (b) normal signed sound intensity level, L_{In} (c) sound pressure level, L_p (d) pressure-residual intensity index, δ_{pIo}.

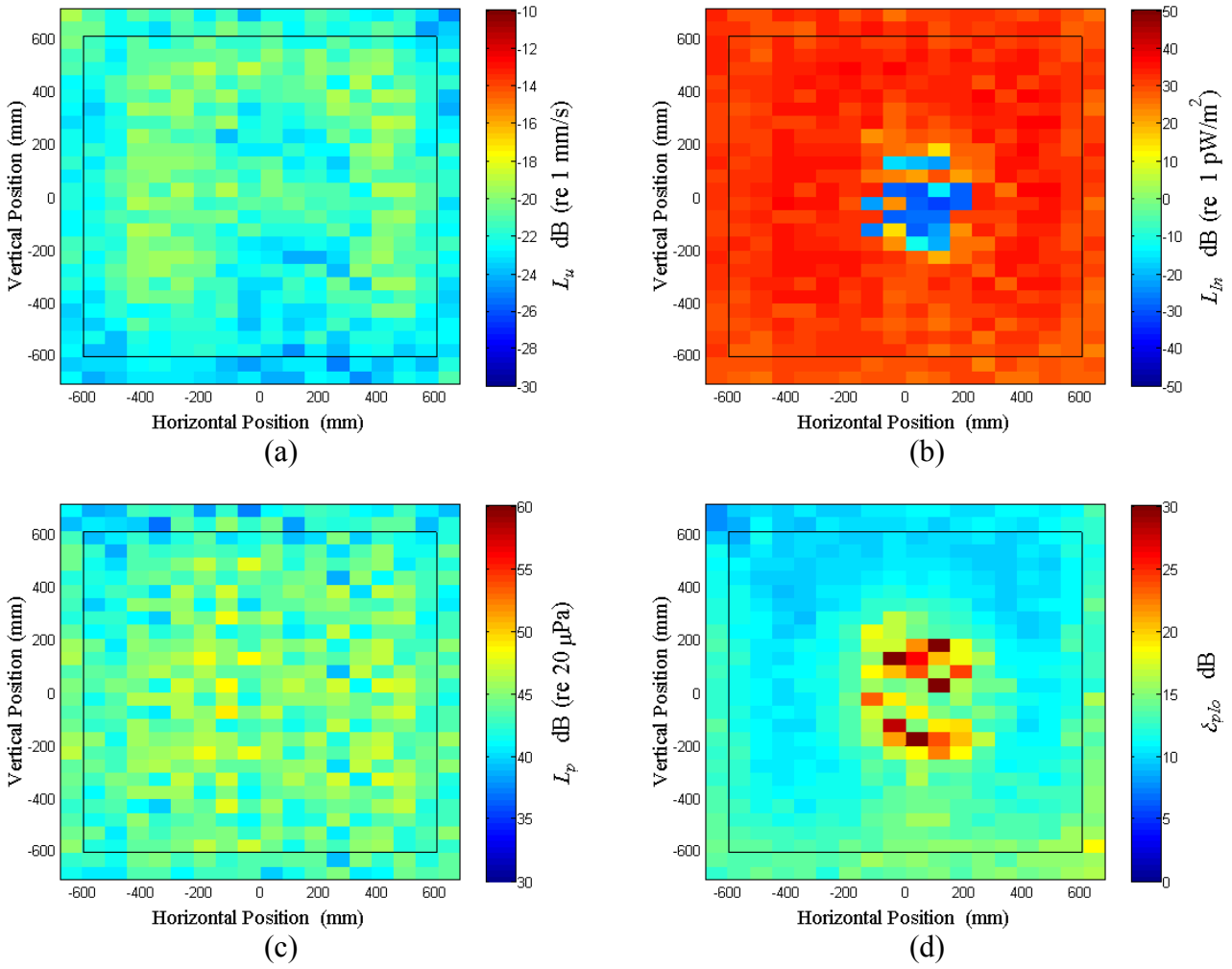

Figure E.18: Surface scan of Window E at 92.5 Hz (a) particle velocity level, L_u (b) normal signed sound intensity level, L_{In} (c) sound pressure level, L_p (d) pressure-residual intensity index, δ_{pIo}.

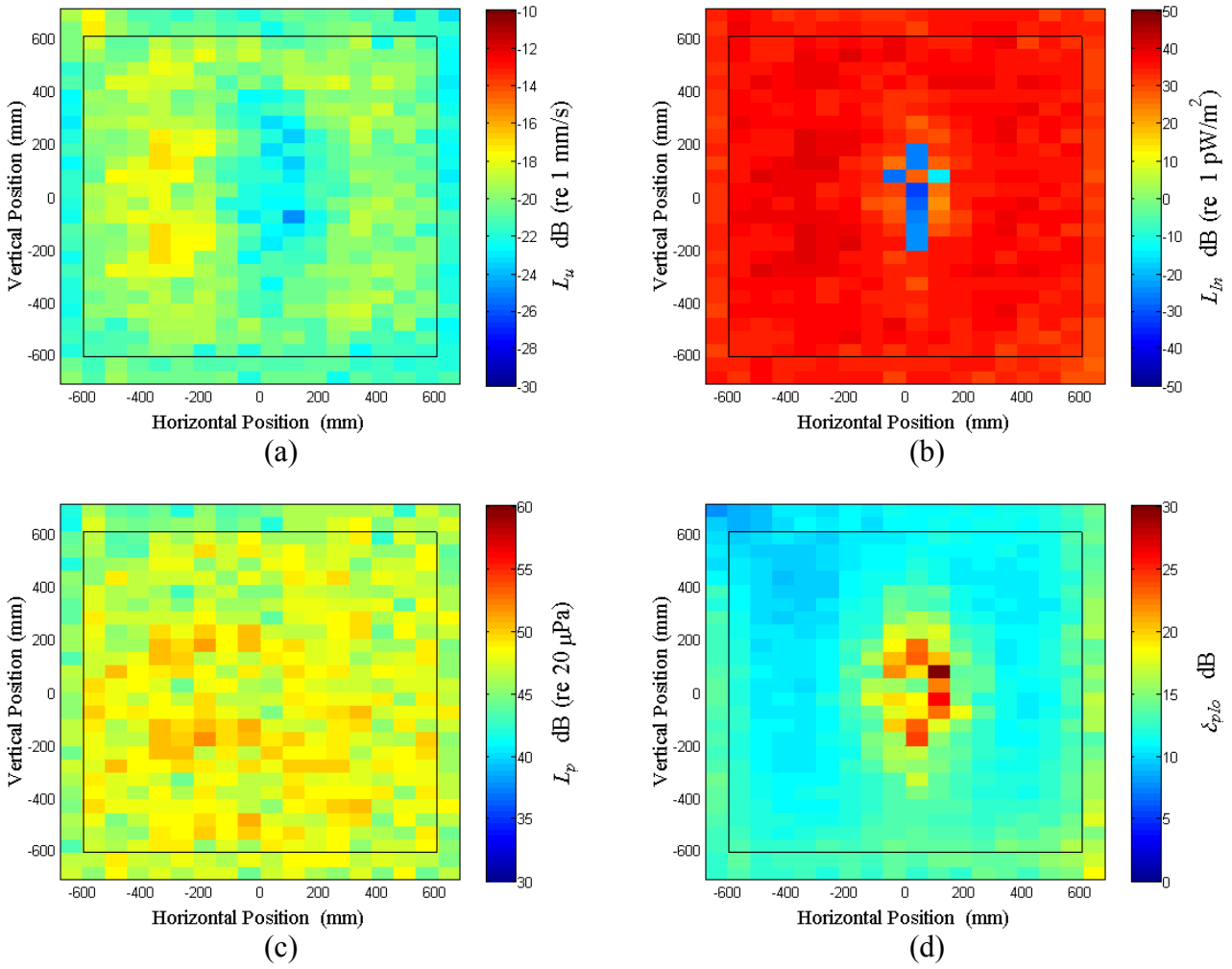

Figure E.19: Surface scan of Window E at 95 Hz (a) particle velocity level, L_u (b) normal signed sound intensity level, L_{In} (c) sound pressure level, L_p (d) pressure-residual intensity index, δ_{pIo}.

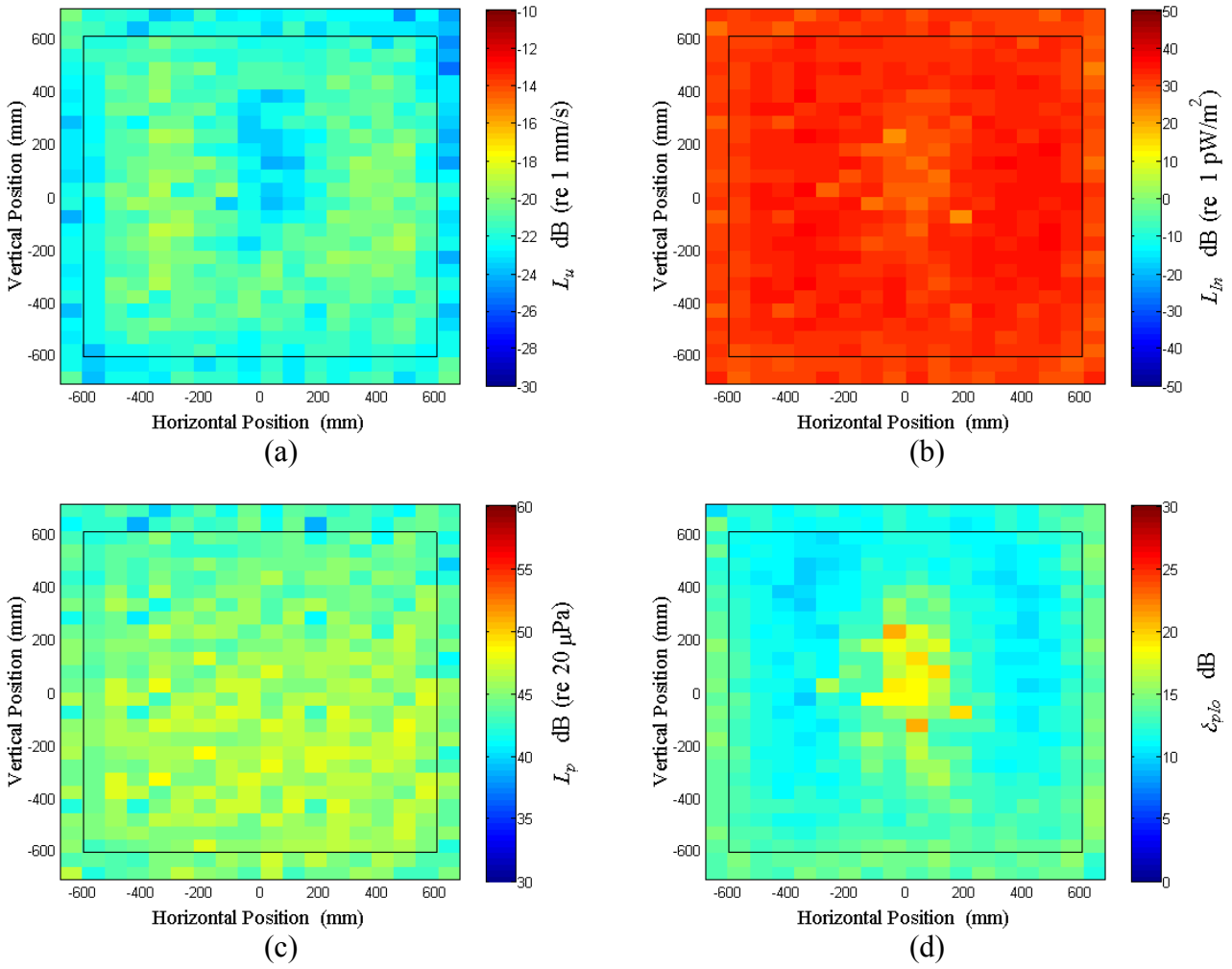

Figure E.20: Surface scan of Window E at 97.5 Hz (a) particle velocity level, L_u (b) normal signed sound intensity level, L_{In} (c) sound pressure level, L_p (d) pressure-residual intensity index, δ_{pIo}.

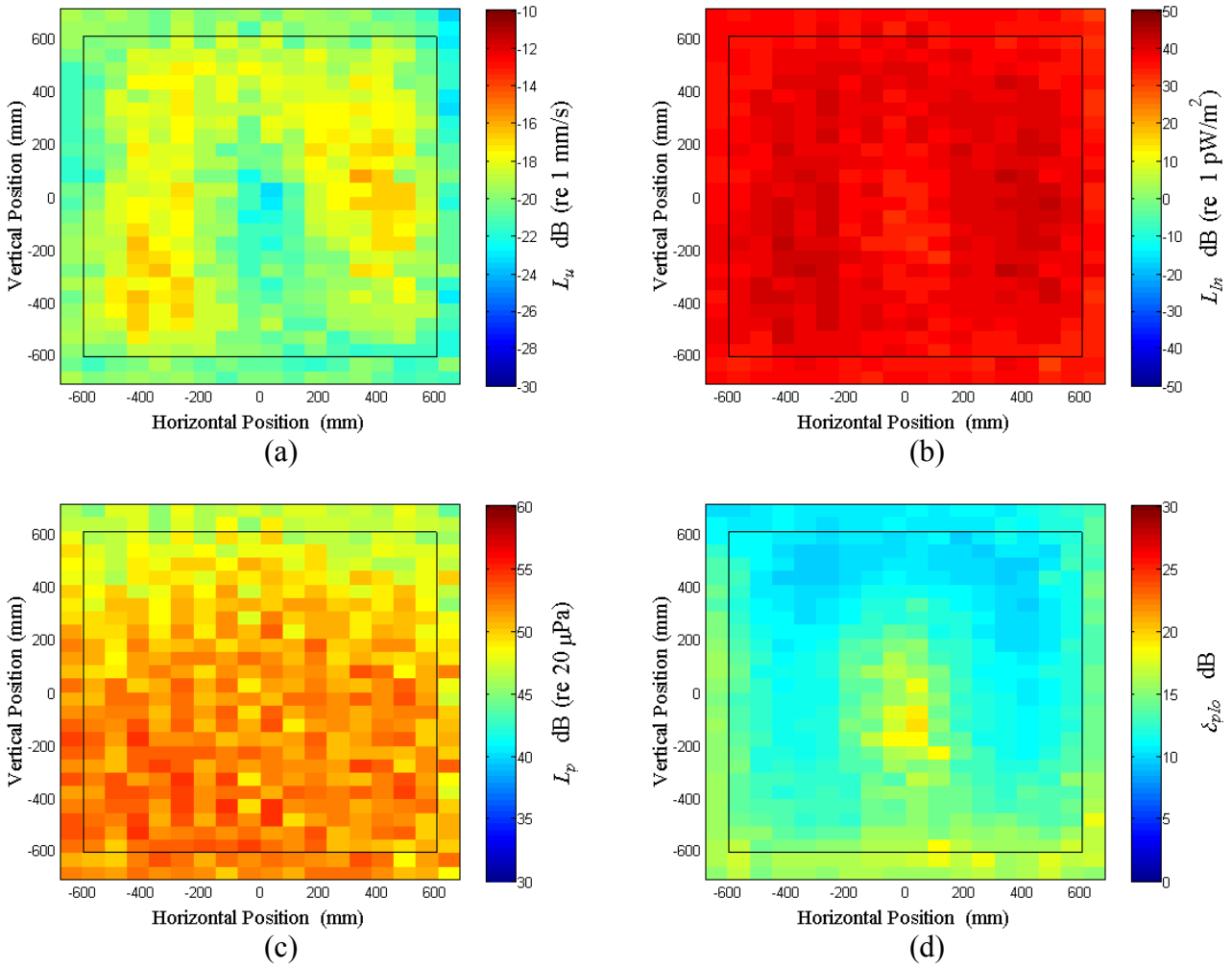

Figure E.21: Surface scan of Window E at 100 Hz (a) particle velocity level, L_u (b) normal signed sound intensity level, L_{In} (c) sound pressure level, L_p (d) pressure-residual intensity index, δ_{pIo}.

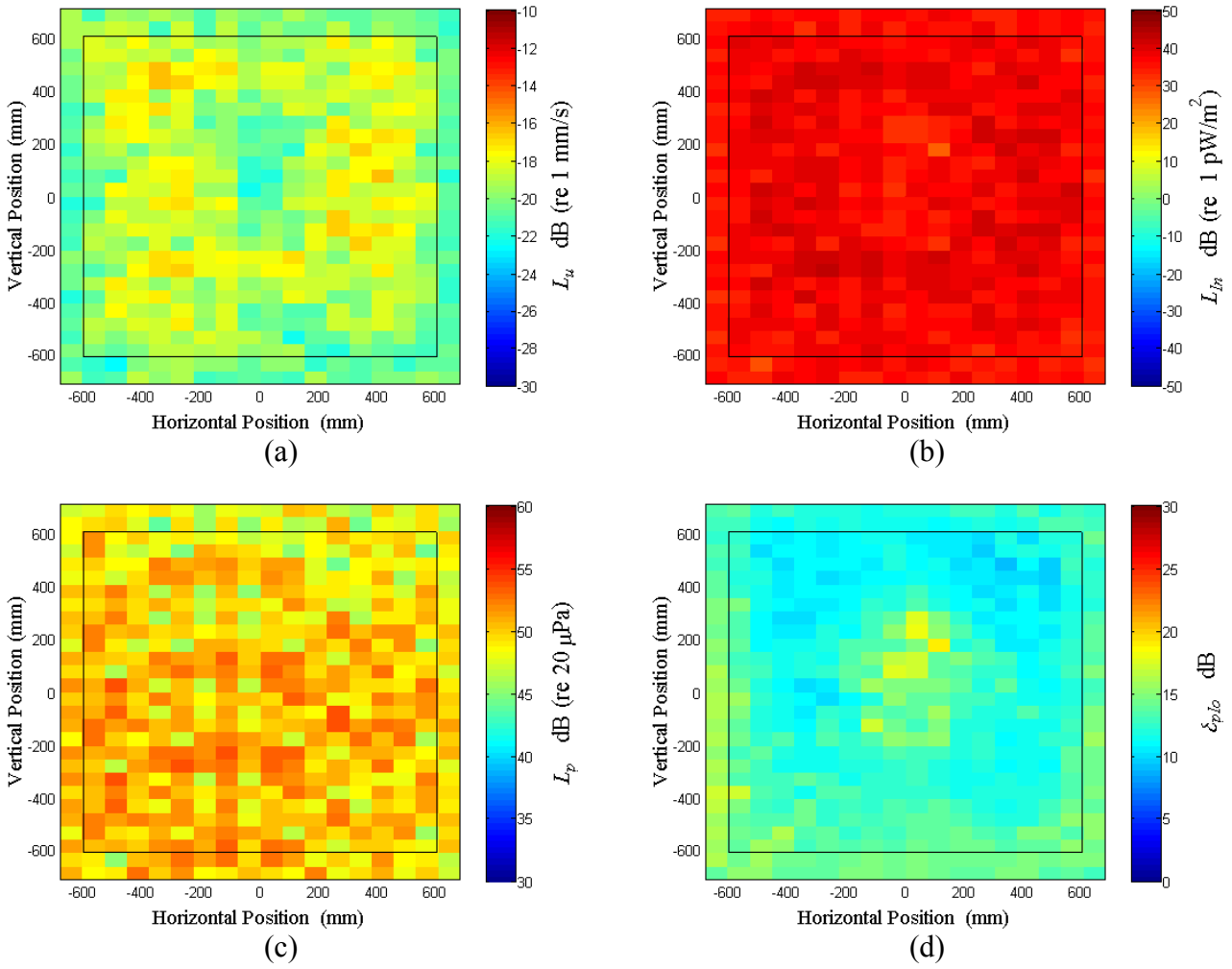

Figure E.22: Surface scan of Window E at 102.5 Hz (a) particle velocity level, L_u (b) normal signed sound intensity level, L_{In} (c) sound pressure level, L_p (d) pressure-residual intensity index, δ_{pIo}.

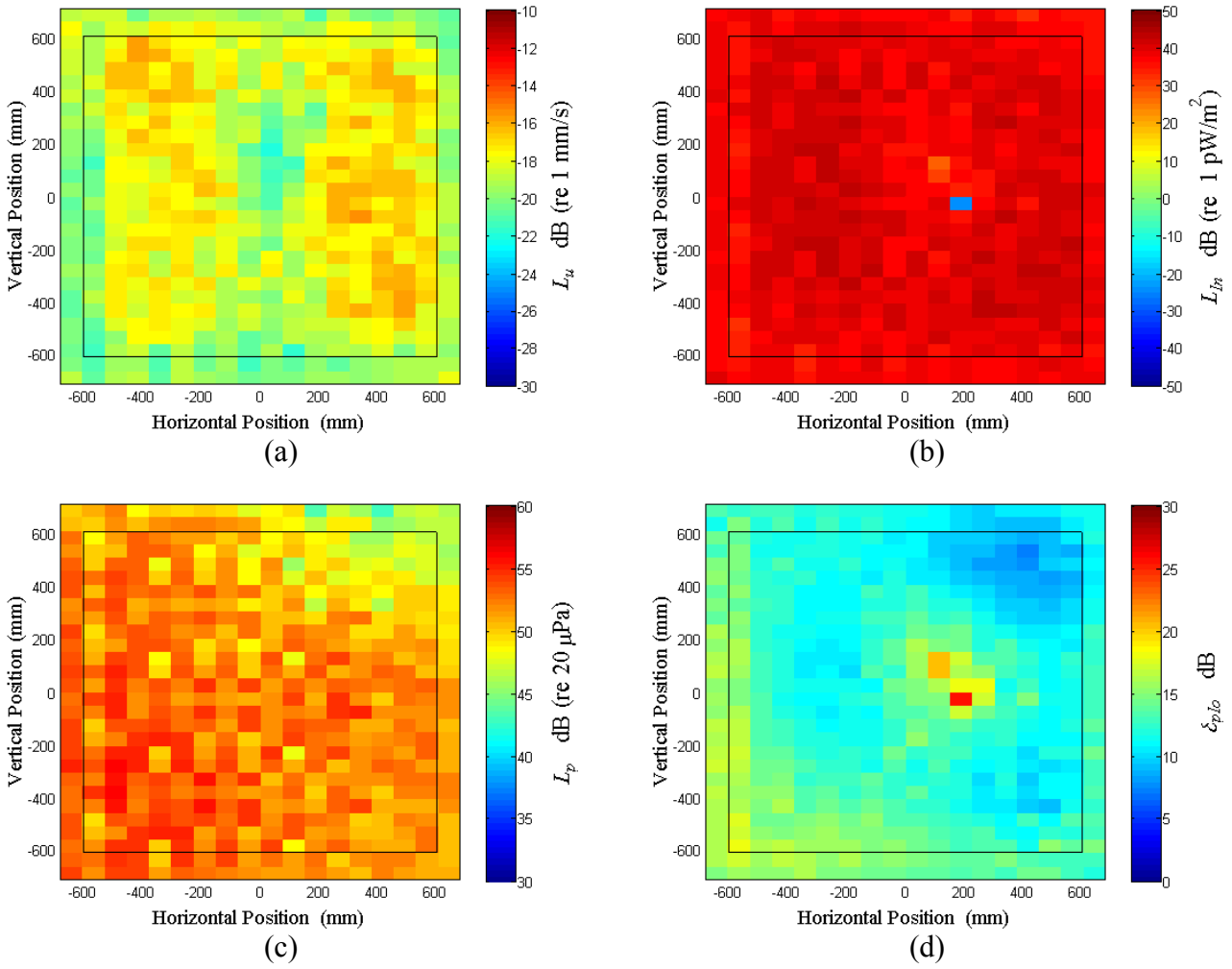

Figure E.23: Surface scan of Window E at 105 Hz (a) particle velocity level, L_u (b) normal signed sound intensity level, L_{In} (c) sound pressure level, L_p (d) pressure-residual intensity index, δ_{pIo}.

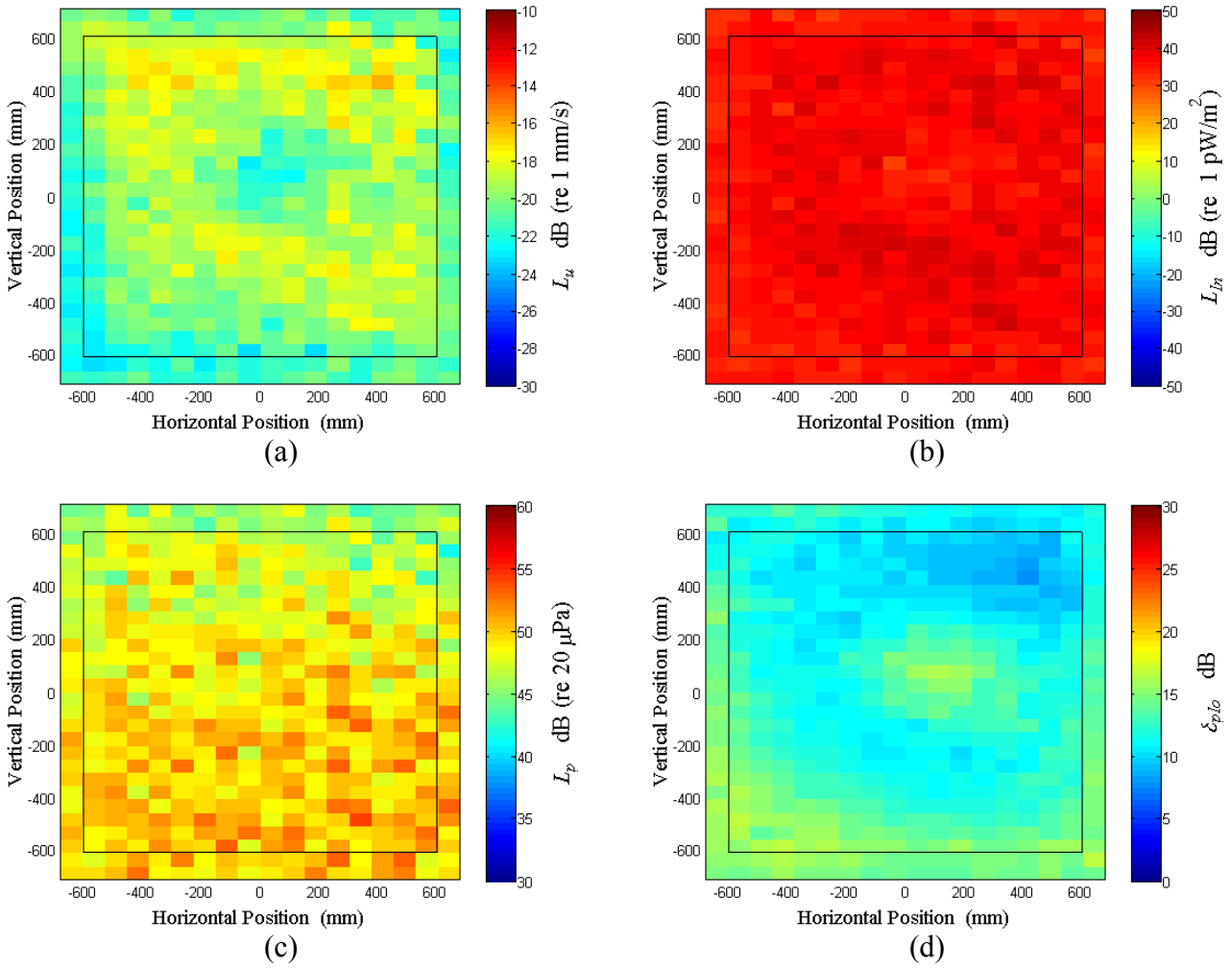

Figure E.24: Surface scan of Window E at 107.5 Hz (a) particle velocity level, L_u (b) normal signed sound intensity level, L_{In} (c) sound pressure level, L_p (d) pressure-residual intensity index, δ_{pIo}.

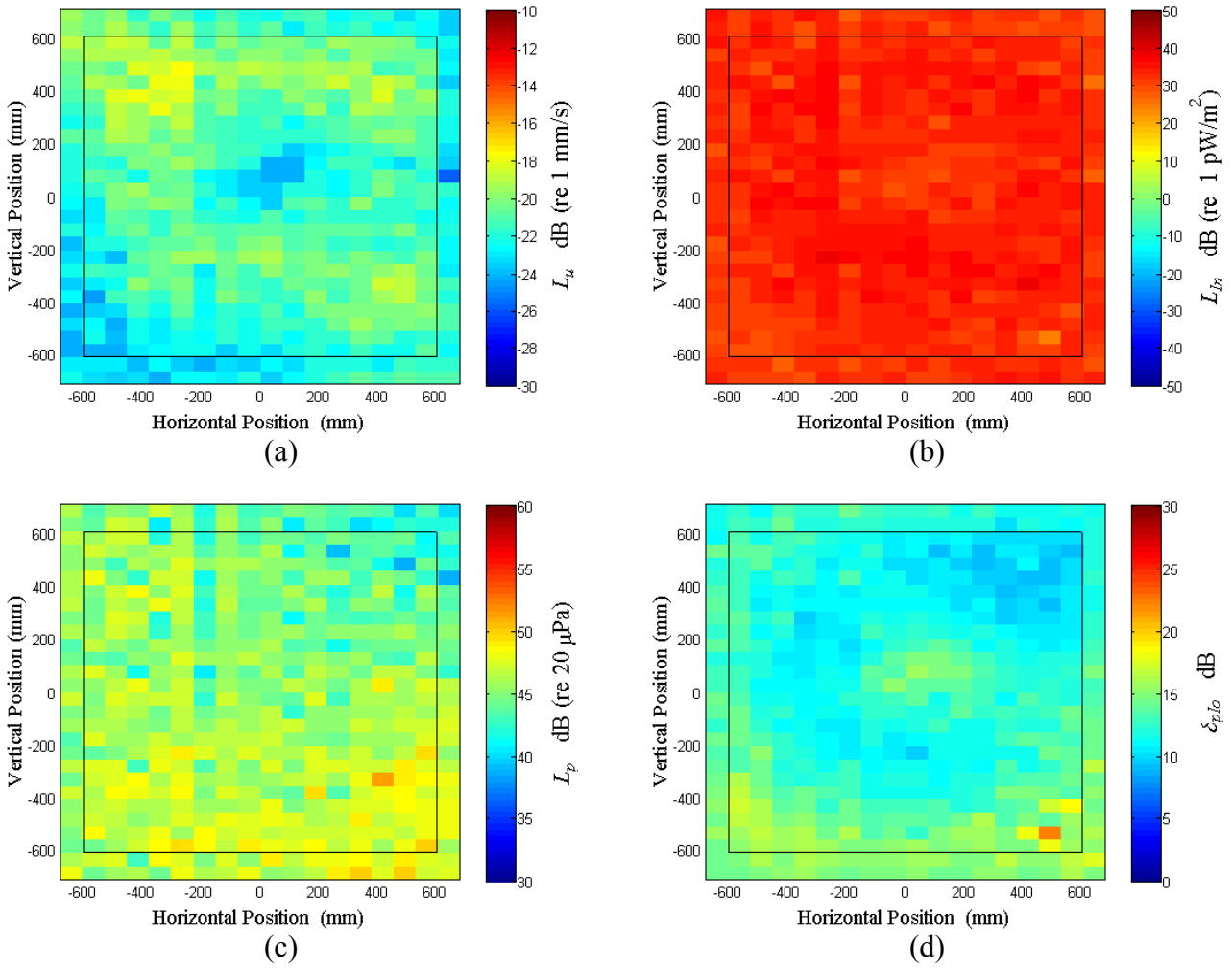

Figure E.25: Surface scan of Window E at 110 Hz (a) particle velocity level, L_u (b) normal signed sound intensity level, L_{In} (c) sound pressure level, L_p (d) pressure-residual intensity index, δ_{pIo}.

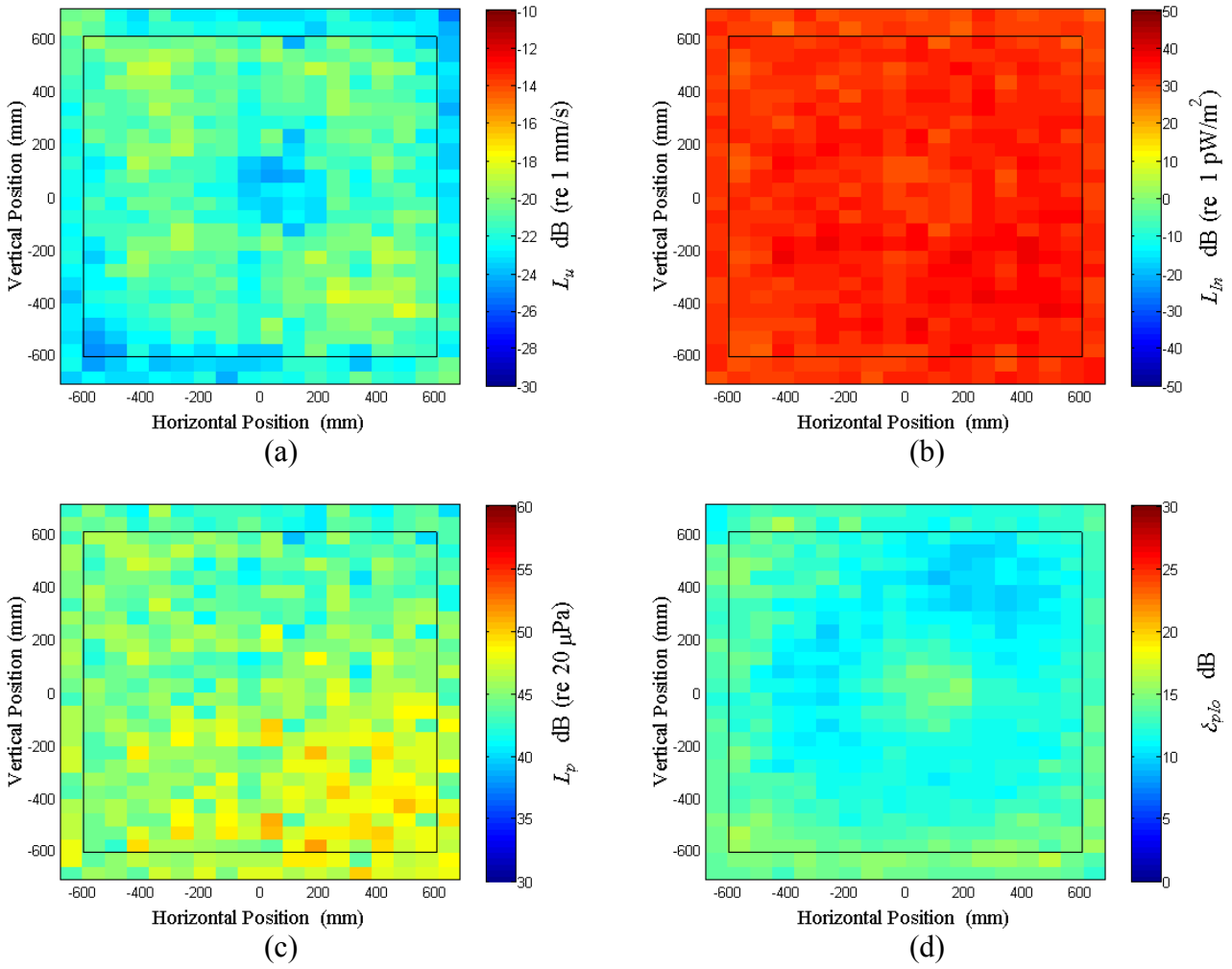

Figure E.26: Surface scan of Window E at 112.5 Hz (a) particle velocity level, L_u (b) normal signed sound intensity level, L_{In} (c) sound pressure level, L_p (d) pressure-residual intensity index, δ_{pIo}.

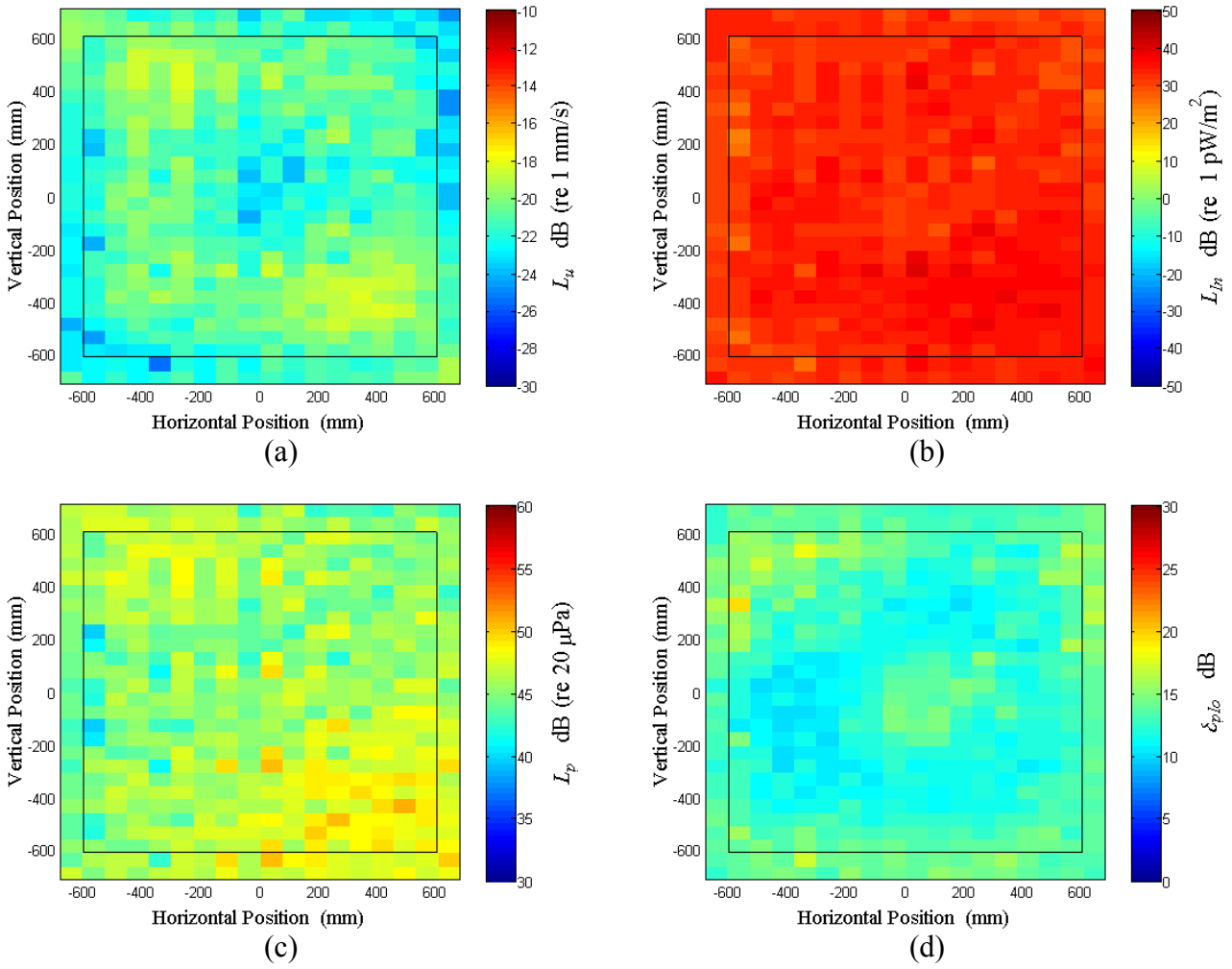

Figure E.27: Surface scan of Window E at 115 Hz (a) particle velocity level, L_u (b) normal signed sound intensity level, L_{In} (c) sound pressure level, L_p (d) pressure-residual intensity index, δ_{pIo}.

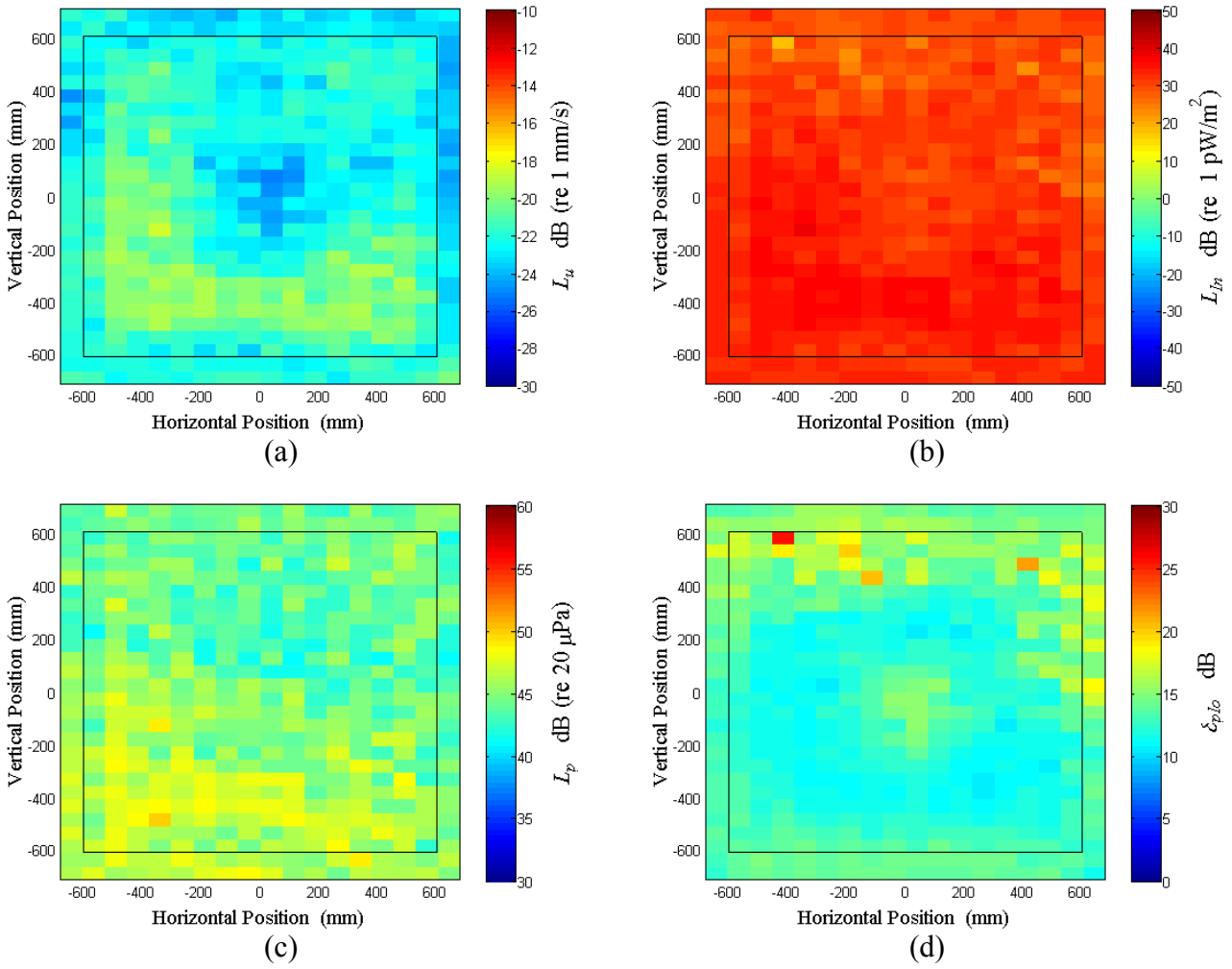

Figure E.28: Surface scan of Window E at 117.5 Hz (a) particle velocity level, L_u (b) normal signed sound intensity level, L_{In} (c) sound pressure level, L_p (d) pressure-residual intensity index, δ_{pIo}.

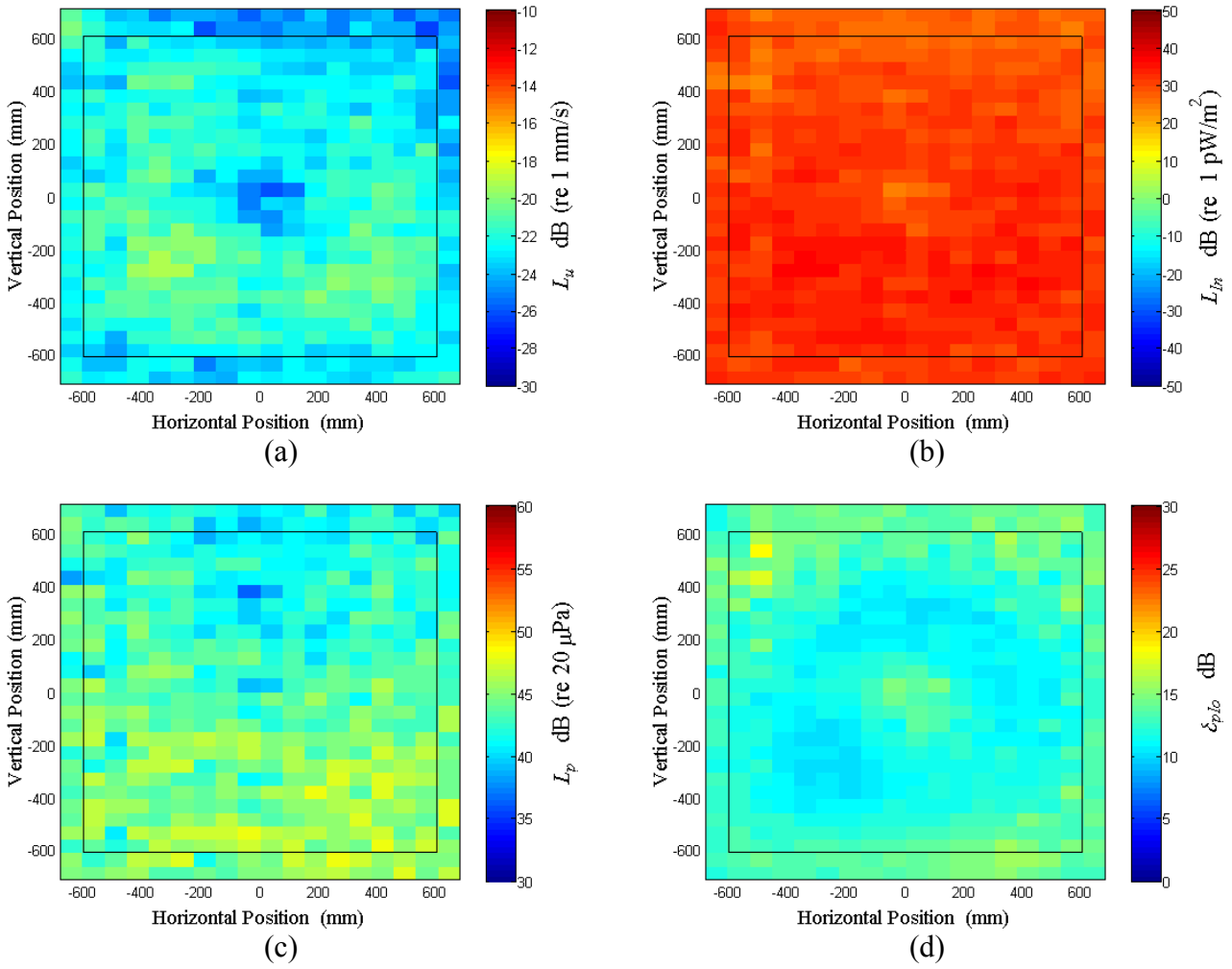

Figure E.29: Surface scan of Window E at 120 Hz (a) particle velocity level, L_u (b) normal signed sound intensity level, L_{In} (c) sound pressure level, L_p (d) pressure-residual intensity index, δ_{pIo}.

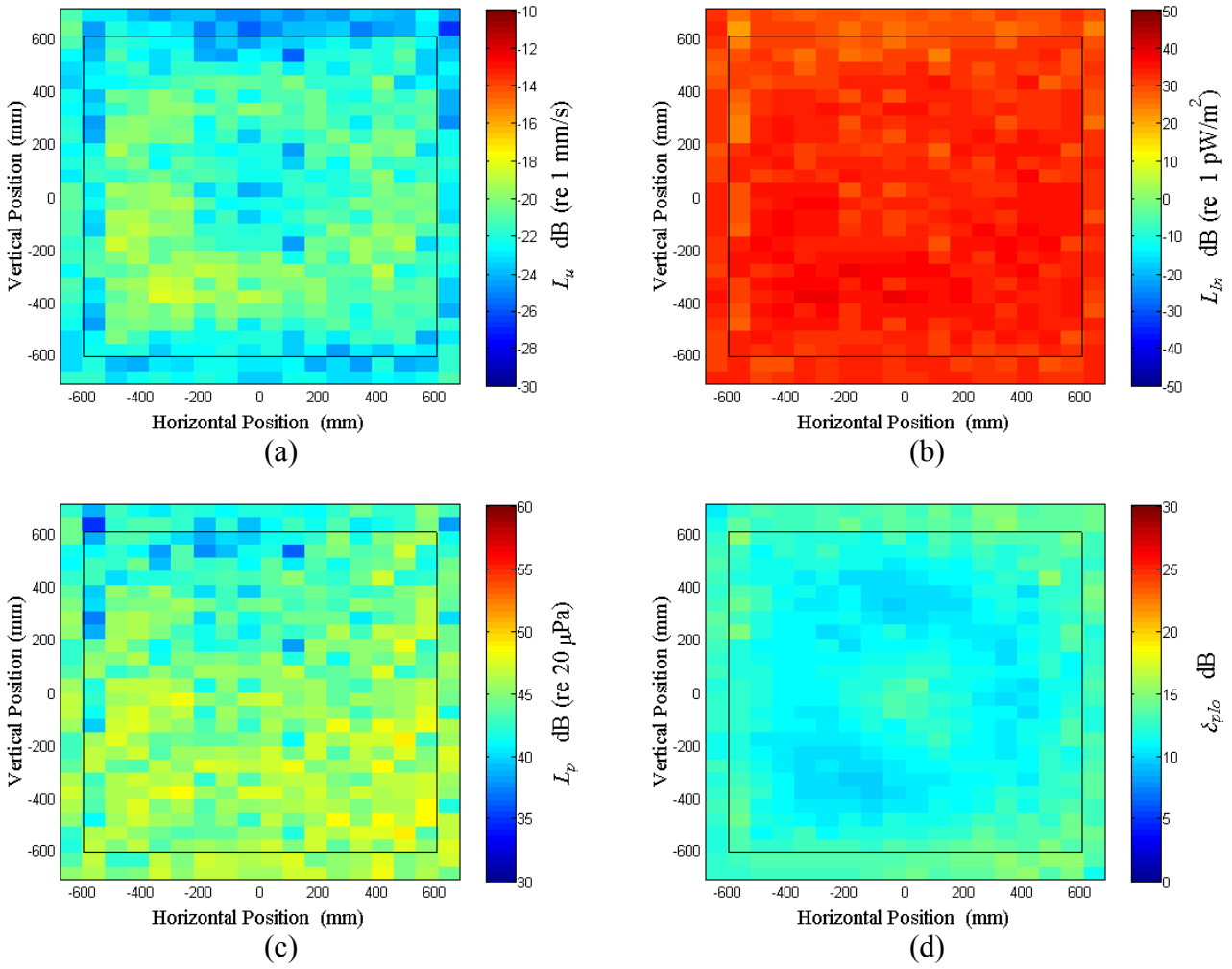

Figure E.30: Surface scan of Window E at 122.5 Hz (a) particle velocity level, L_u (b) normal signed sound intensity level, L_{In} (c) sound pressure level, L_p (d) pressure-residual intensity index, δ_{pIo}.

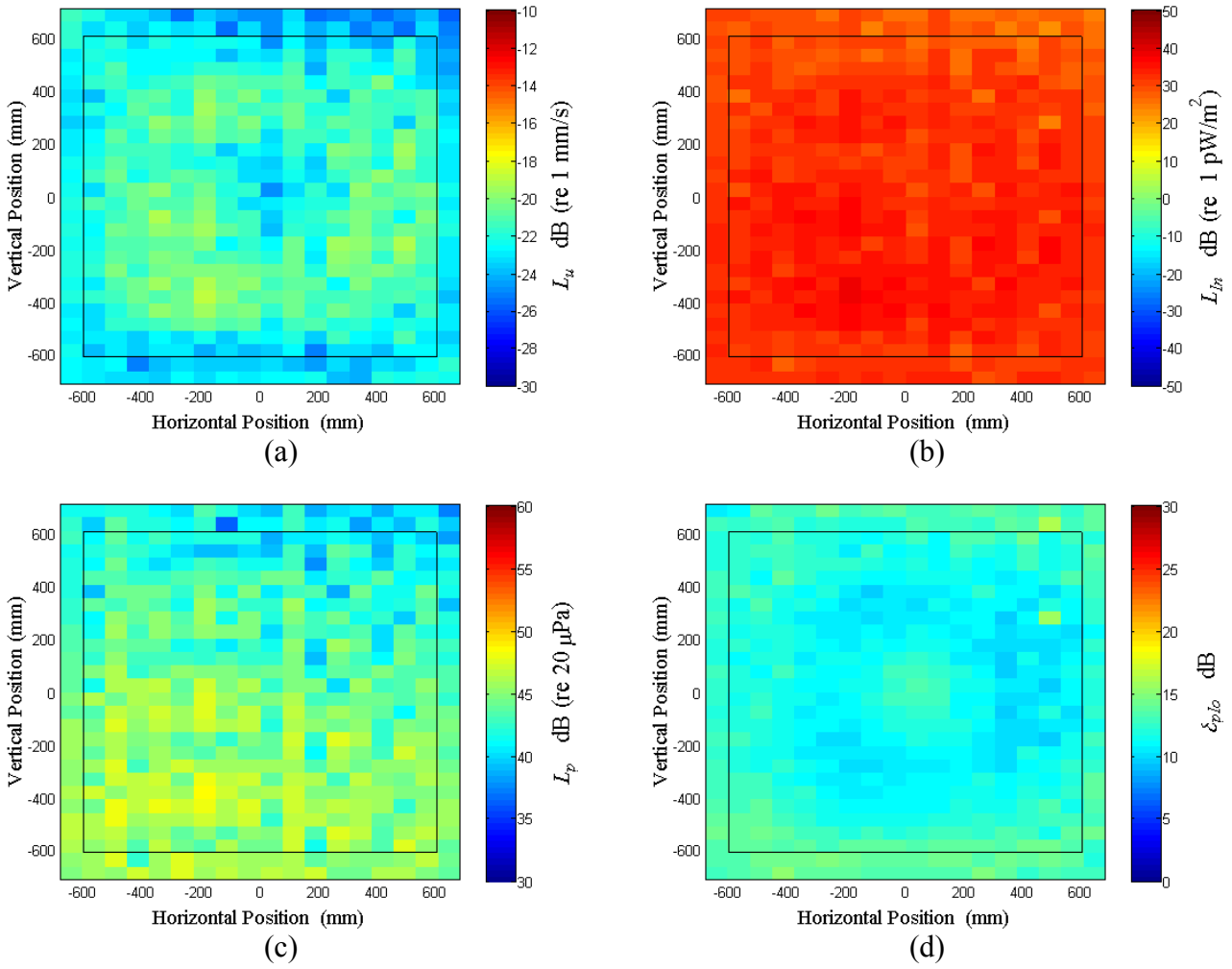

Figure E.31: Surface scan of Window E at 125 Hz (a) particle velocity level, L_u (b) normal signed sound intensity level, L_{In} (c) sound pressure level, L_p (d) pressure-residual 12ntensity index, δ_{pIo}.

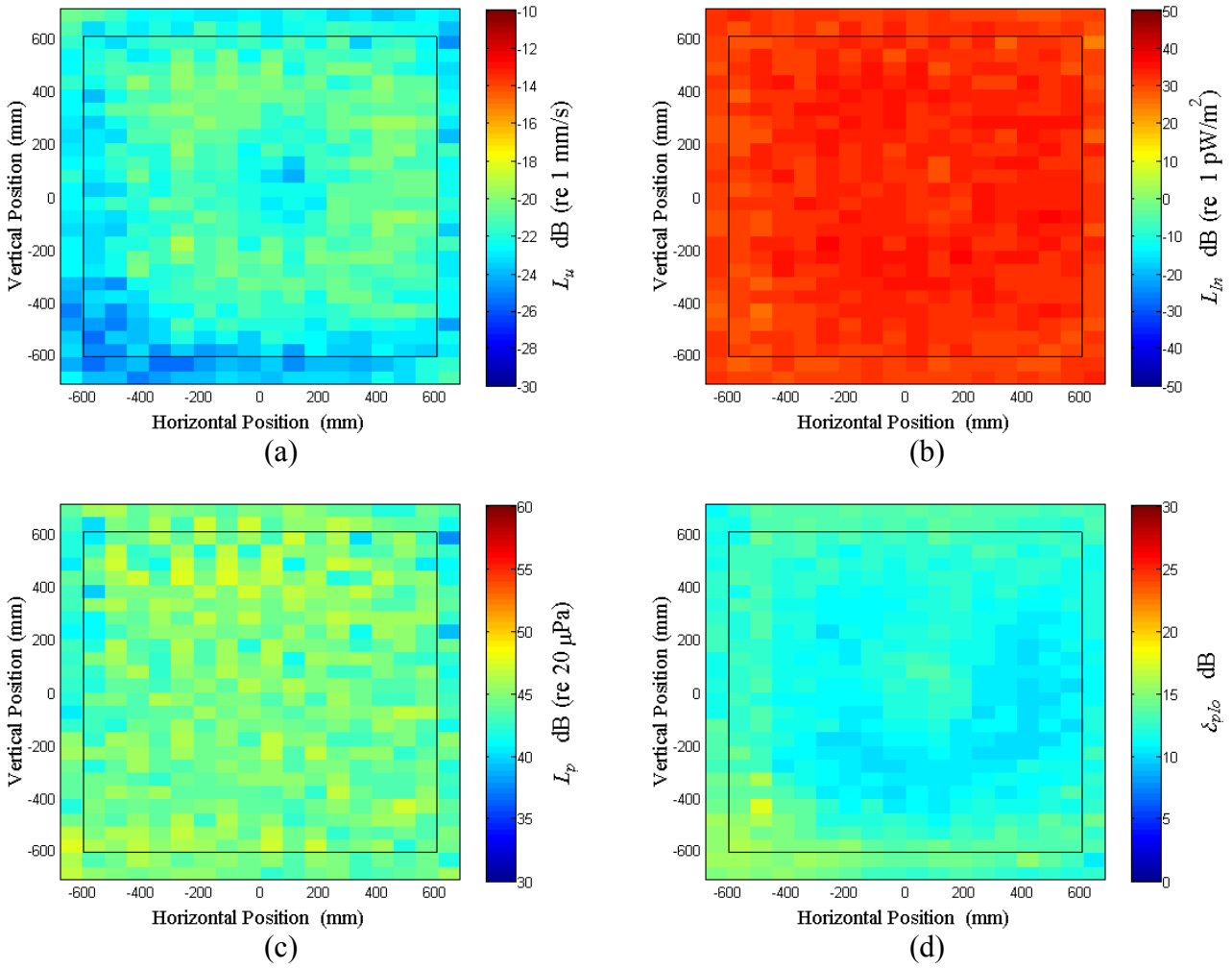

Figure E.32: Surface scan of Window E at 127.5 Hz (a) particle velocity level, L_u (b) normal signed sound intensity level, L_{In} (c) sound pressure level, L_p (d) pressure-residual intensity index, δ_{pIo}.

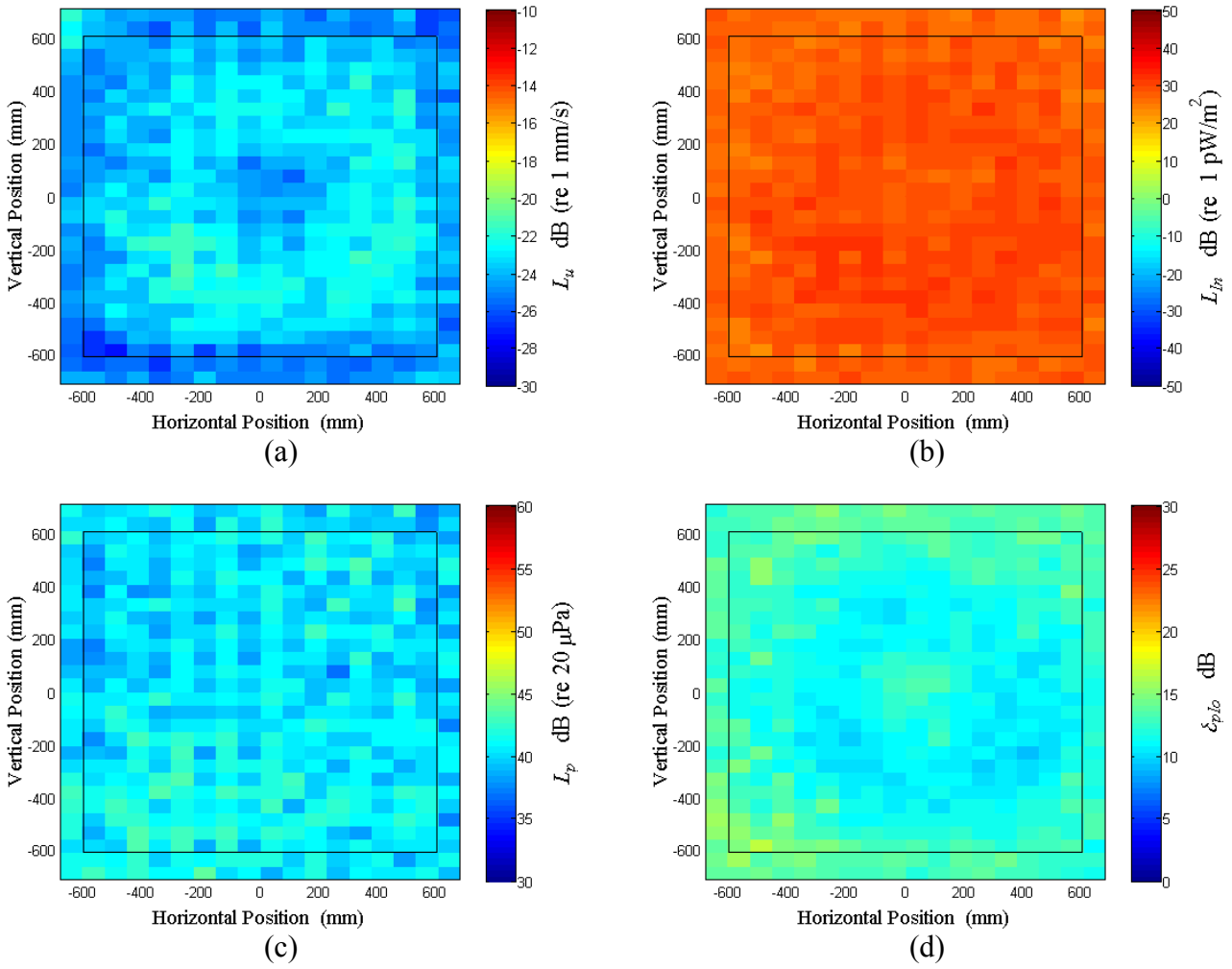

Figure E.33: Surface scan of Window E at 130 Hz (a) particle velocity level, L_u (b) normal signed sound intensity level, L_{In} (c) sound pressure level, L_p (d) pressure-residual intensity index, δ_{pIo}.

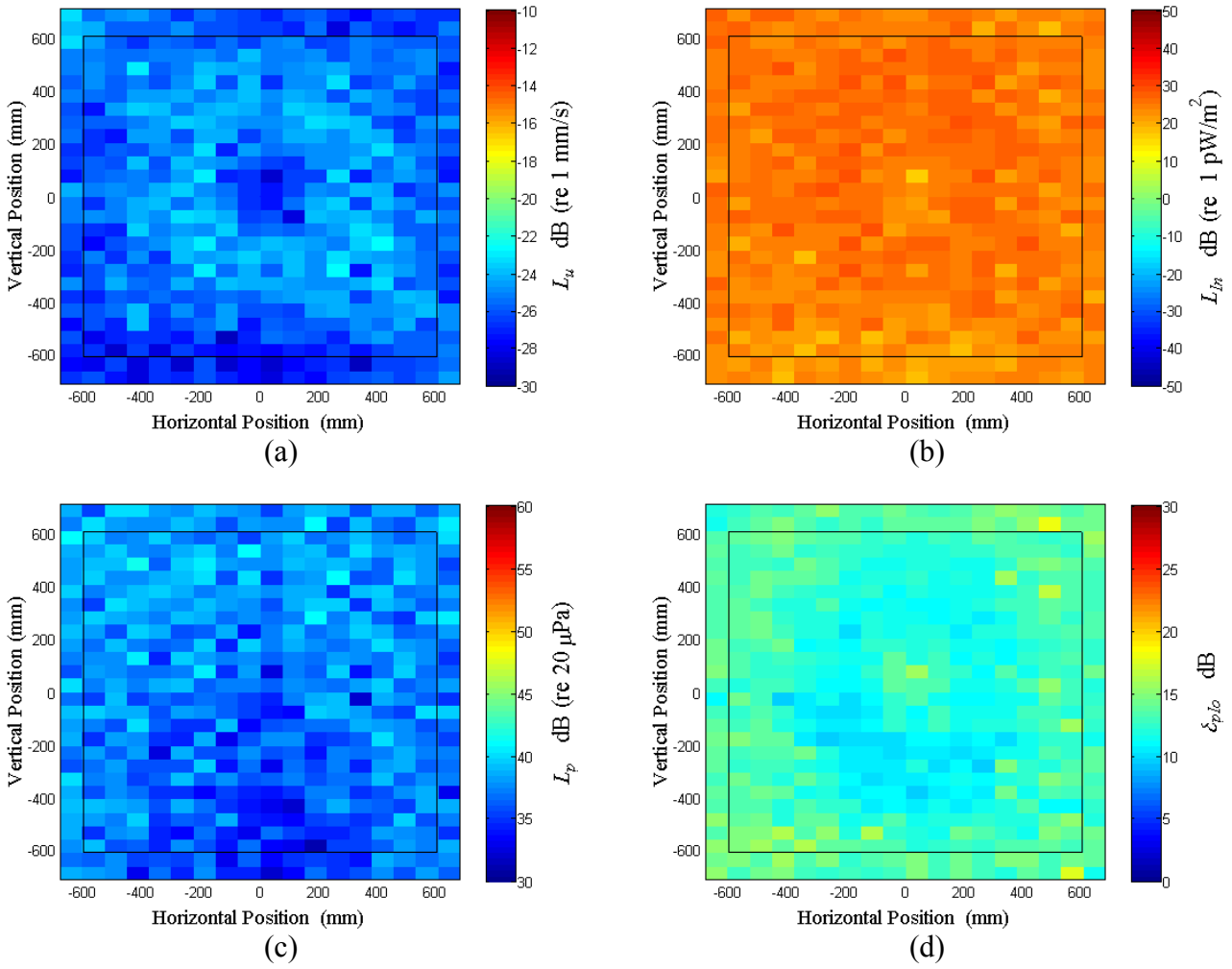

Figure E.34: Surface scan of Window E at 140 Hz (a) particle velocity level, L_u (b) normal signed sound intensity level, L_{In} (c) sound pressure level, L_p (d) pressure-residual intensity index, δ_{pIo}.

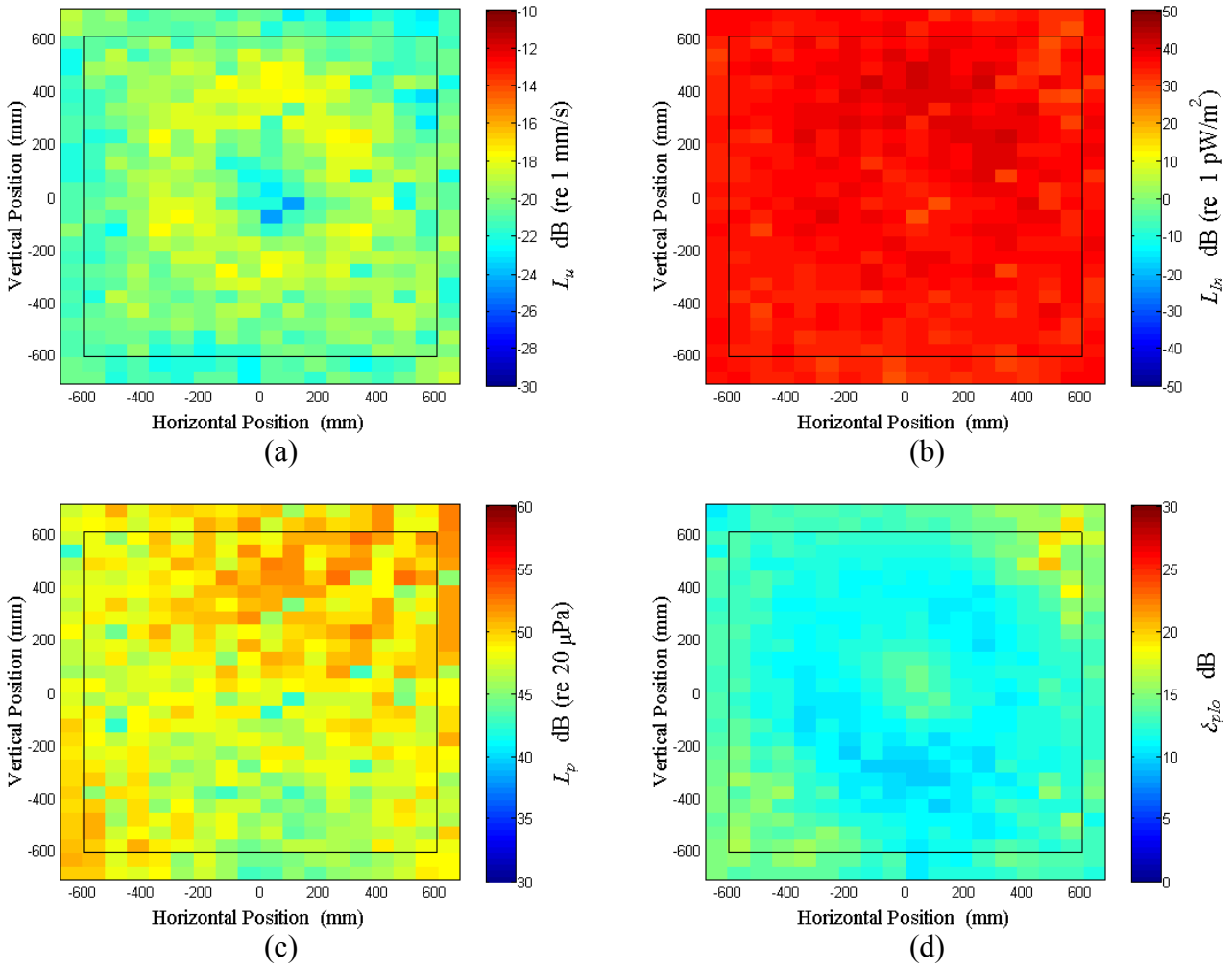

Figure E.35: Surface scan of Window E at 150 Hz (a) particle velocity level, L_u (b) normal signed sound intensity level, L_{In} (c) sound pressure level, L_p (d) pressure-residual intensity index, δ_{pIo}.

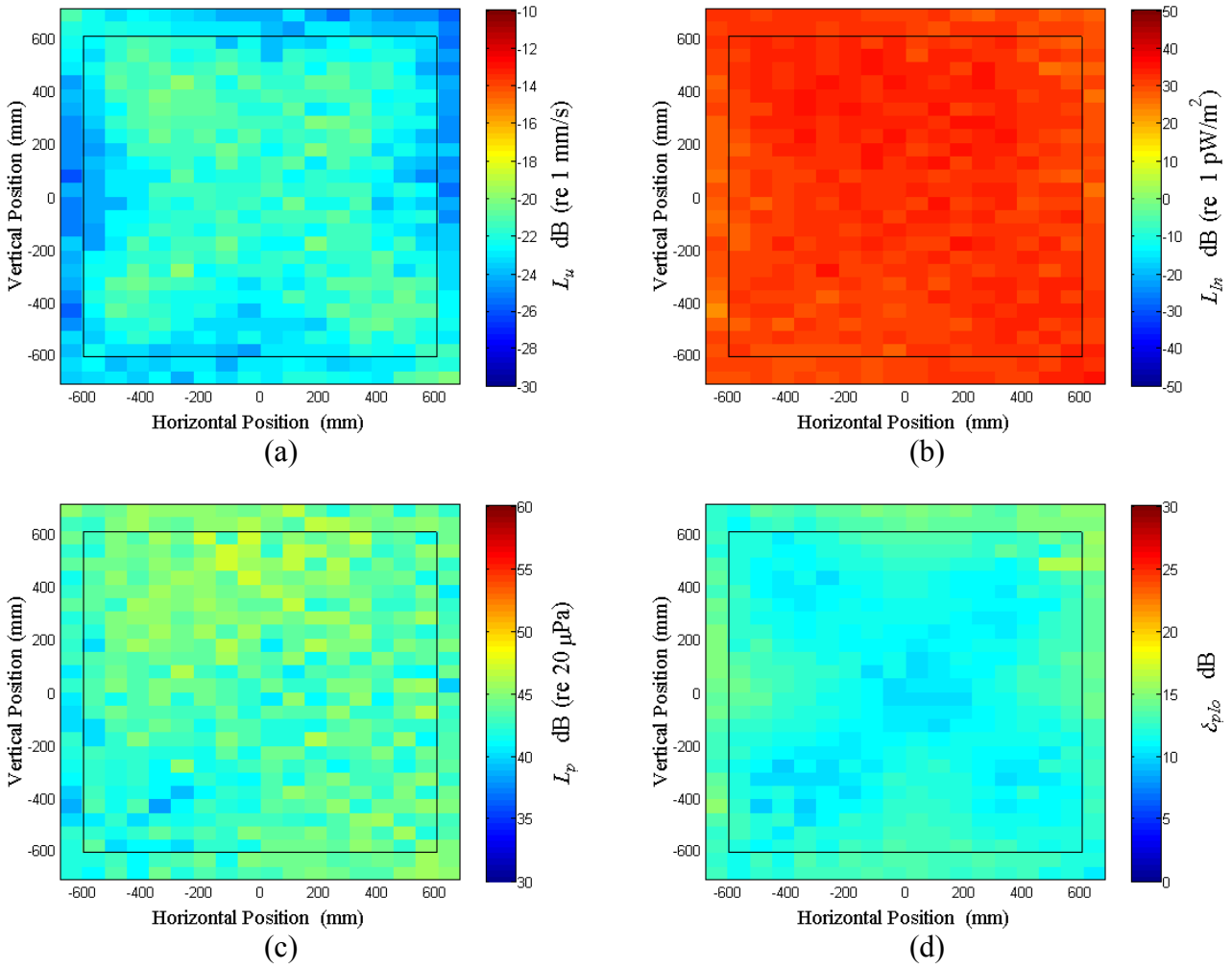

Figure E.36: Surface scan of Window E at 160 Hz (a) particle velocity level, L_u (b) normal signed sound intensity level, L_{In} (c) sound pressure level, L_p (d) pressure-residual intensity index, δ_{pIo}.

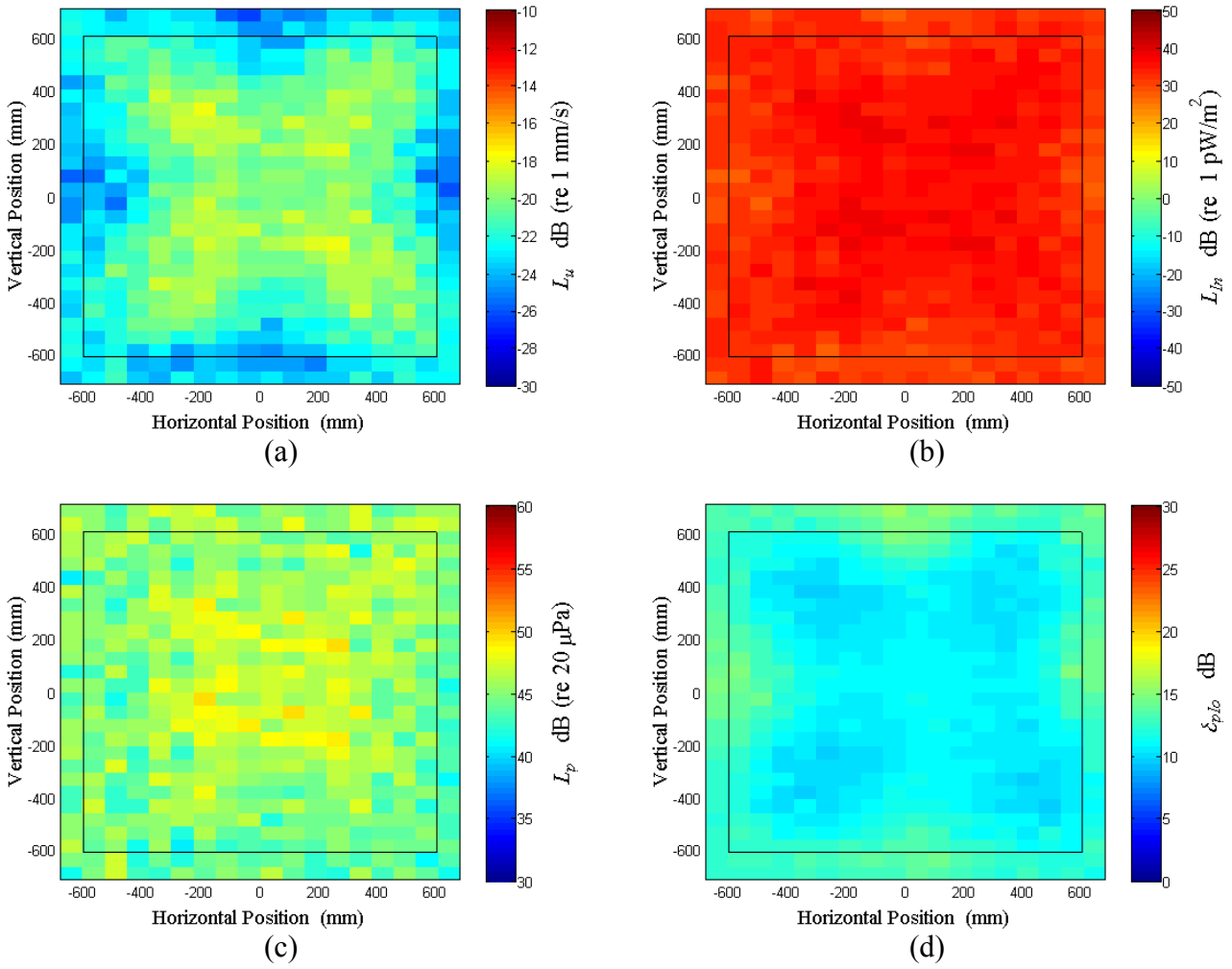

Figure E.37: Surface scan of Window E at 170 Hz (a) particle velocity level, L_u (b) normal signed sound intensity level, L_{In} (c) sound pressure level, L_p (d) pressure-residual intensity index, δ_{pIo}.

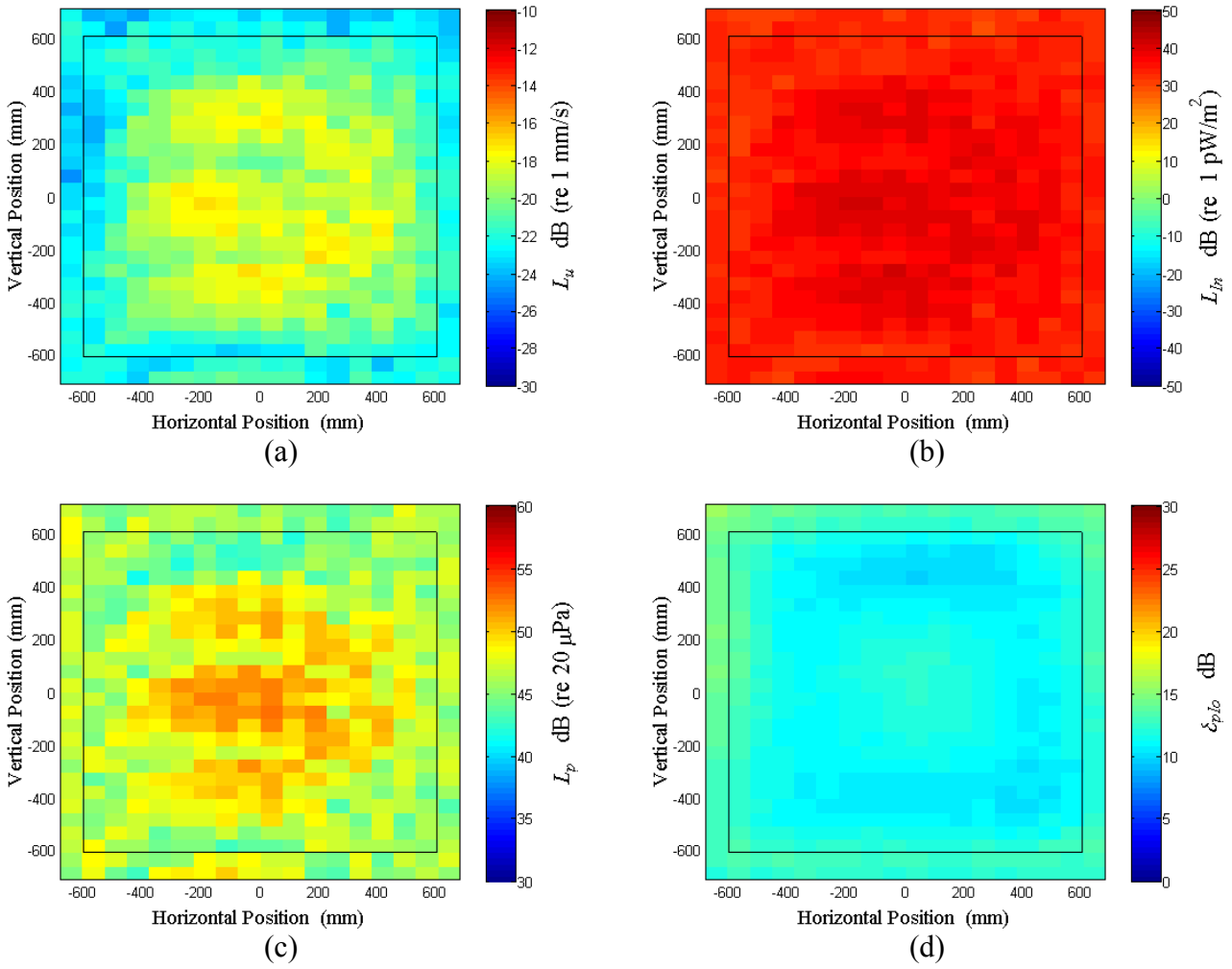

Figure E.38: Surface scan of Window E at 180 Hz (a) particle velocity level, L_u (b) normal signed sound intensity level, L_{In} (c) sound pressure level, L_p (d) pressure-residual intensity index, δ_{pIo}.

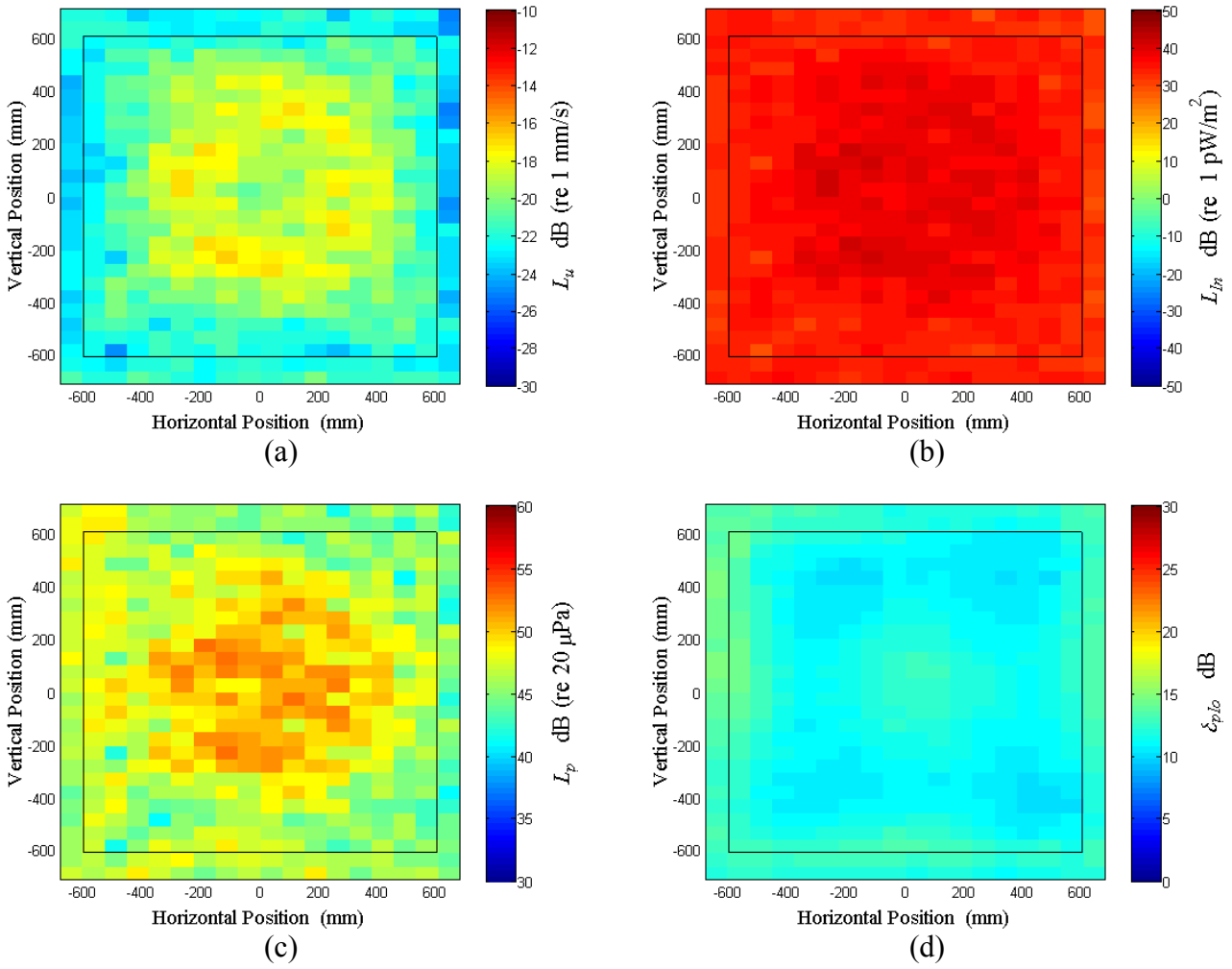

Figure E.39: Surface scan of Window E at 190 Hz (a) particle velocity level, L_u (b) normal signed sound intensity level, L_{In} (c) sound pressure level, L_p (d) pressure-residual intensity index, δ_{pIo}.

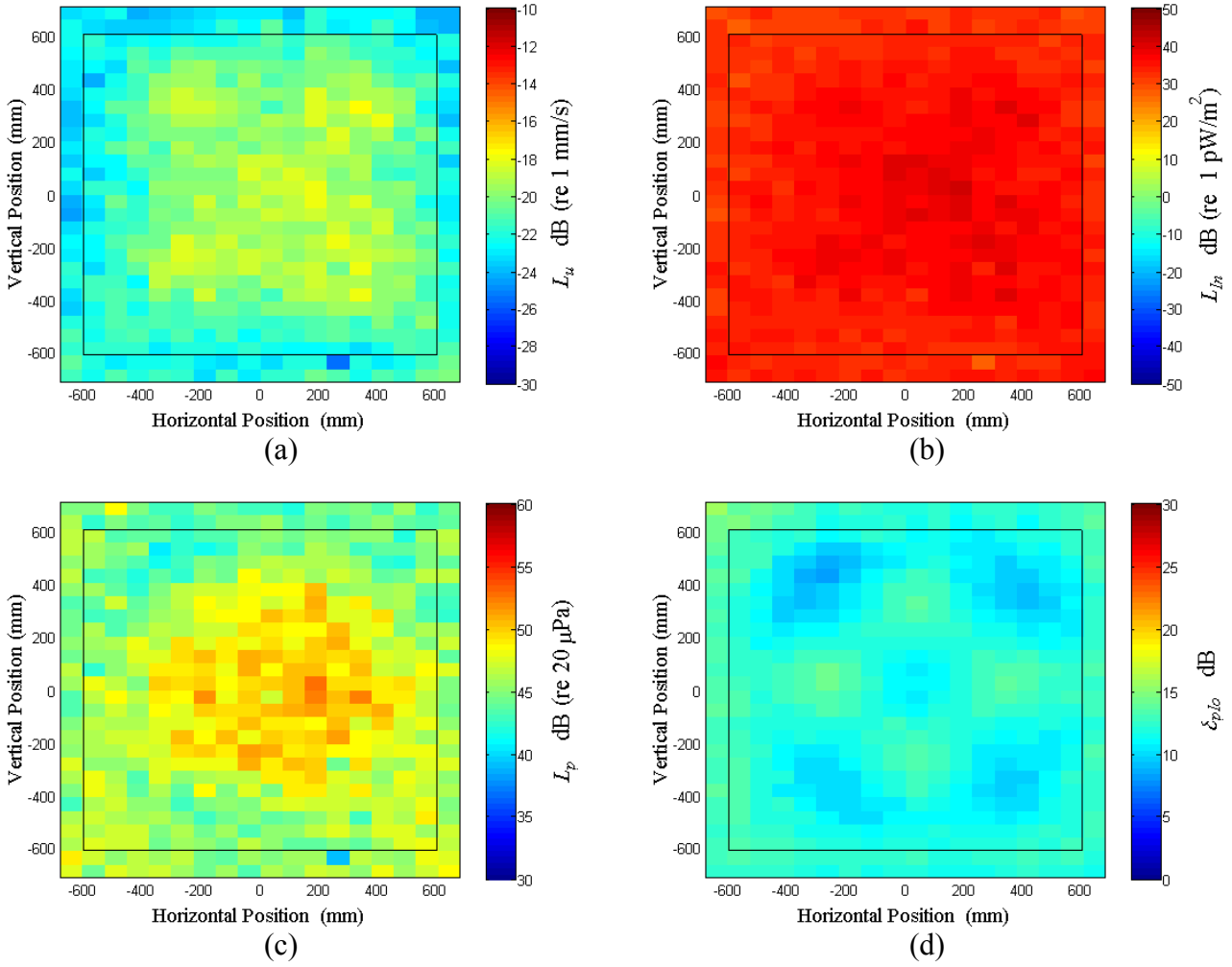

Figure E.40: Surface scan of Window E at 200 Hz (a) particle velocity level, L_u (b) normal signed sound intensity level, L_{In} (c) sound pressure level, L_p (d) pressure-residual intensity index, δ_{pIo}.

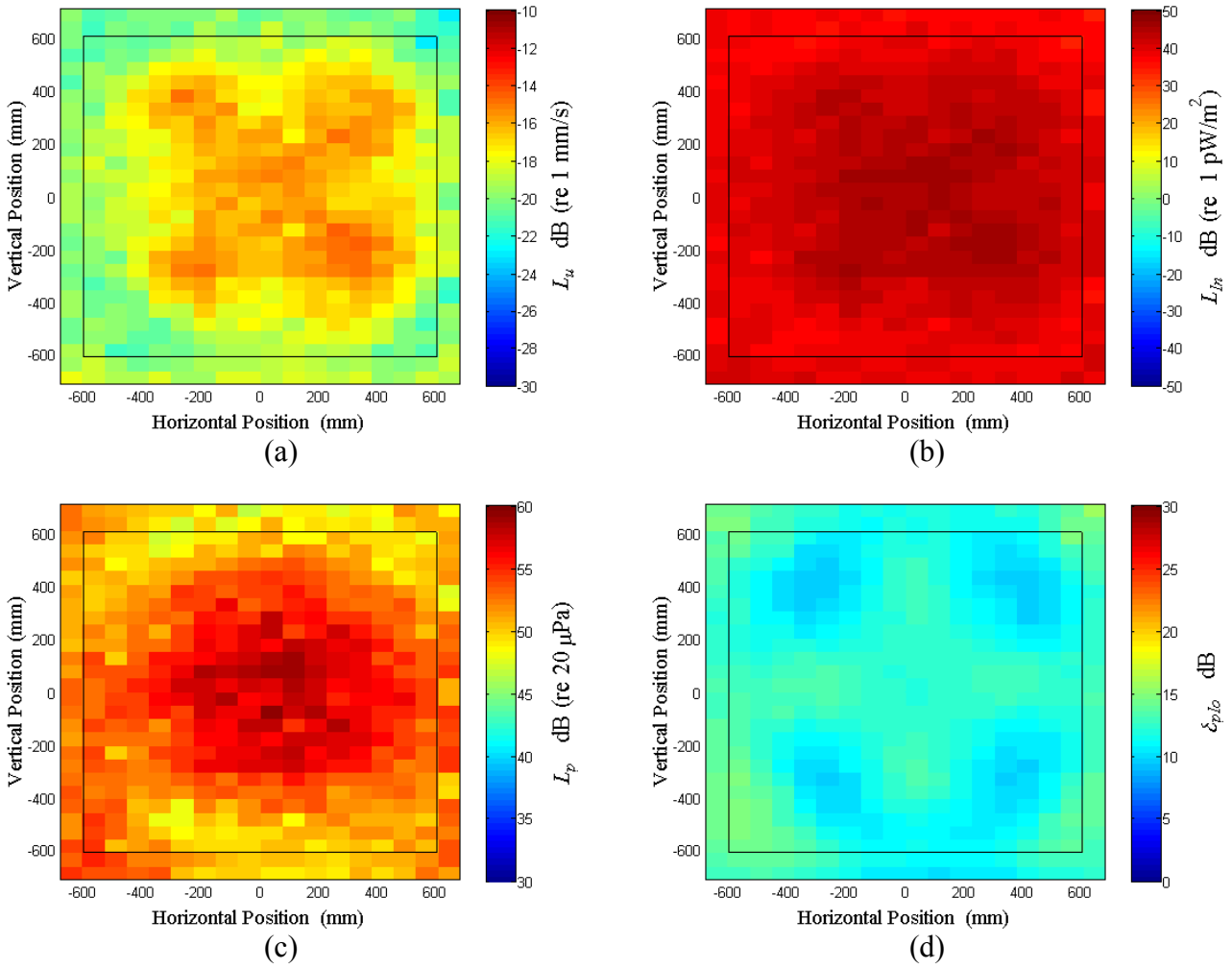

Figure E.41: Surface scan of Window E at 210 Hz (a) particle velocity level, L_u (b) normal signed sound intensity level, L_{In} (c) sound pressure level, L_p (d) pressure-residual intensity index, δ_{pIo}.

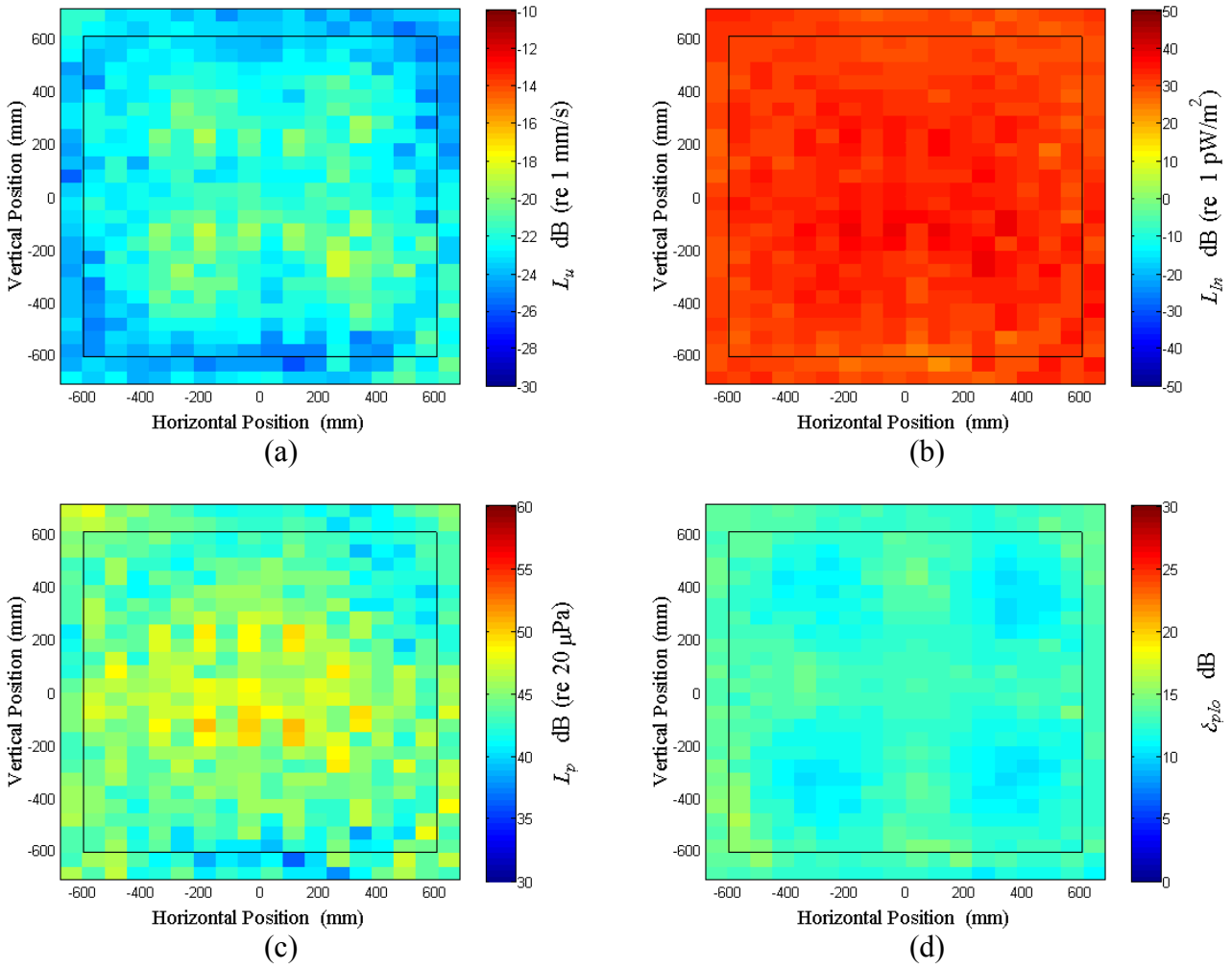

Figure E.42: Surface scan of Window E at 220 Hz (a) particle velocity level, L_u (b) normal signed sound intensity level, L_{In} (c) sound pressure level, L_p (d) pressure-residual intensity index, δ_{pIo}.

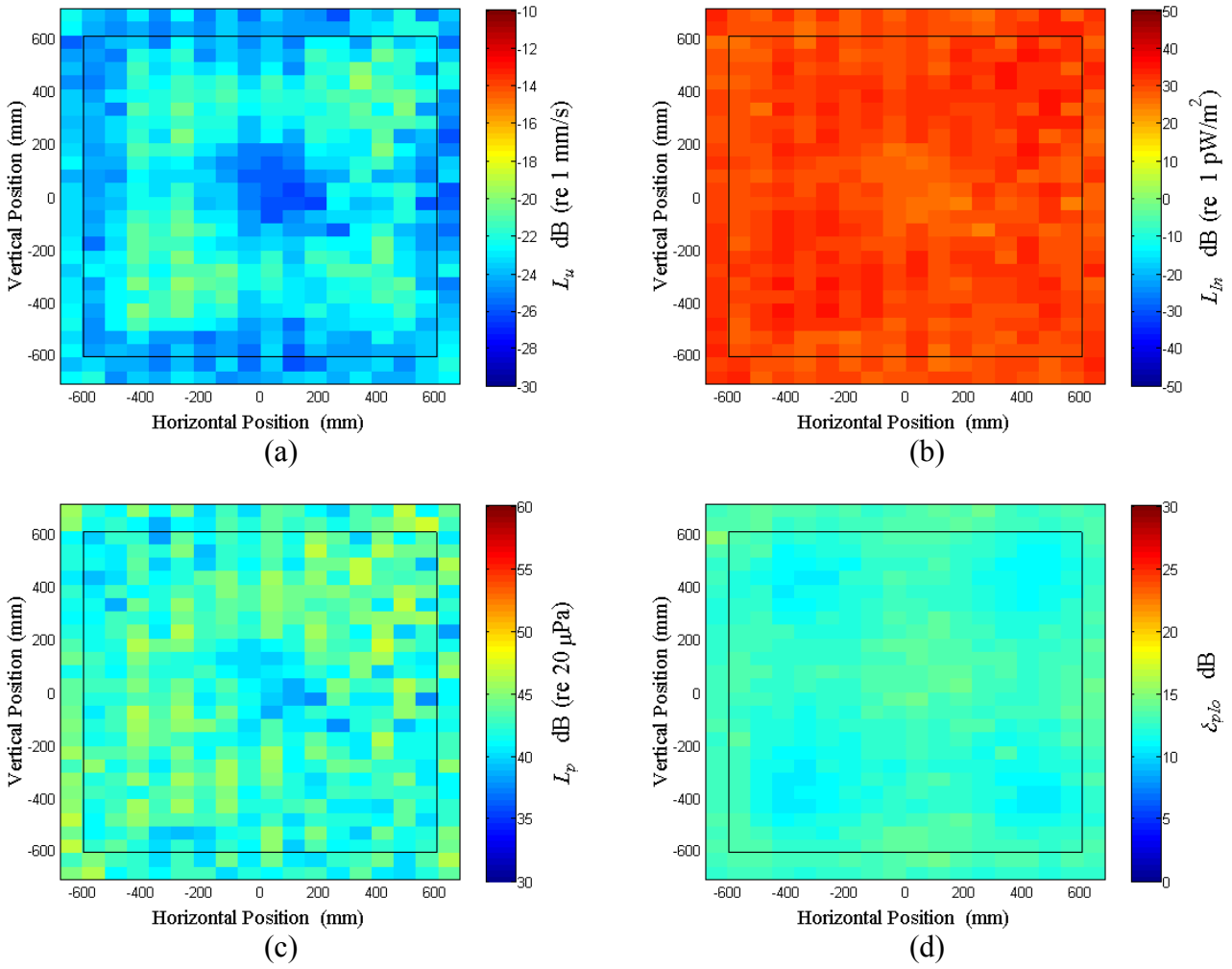

Figure E.43: Surface scan of Window E at 230 Hz (a) particle velocity level, L_u (b) normal signed sound intensity level, L_{In} (c) sound pressure level, L_p (d) pressure-residual intensity index, δ_{pIo}.

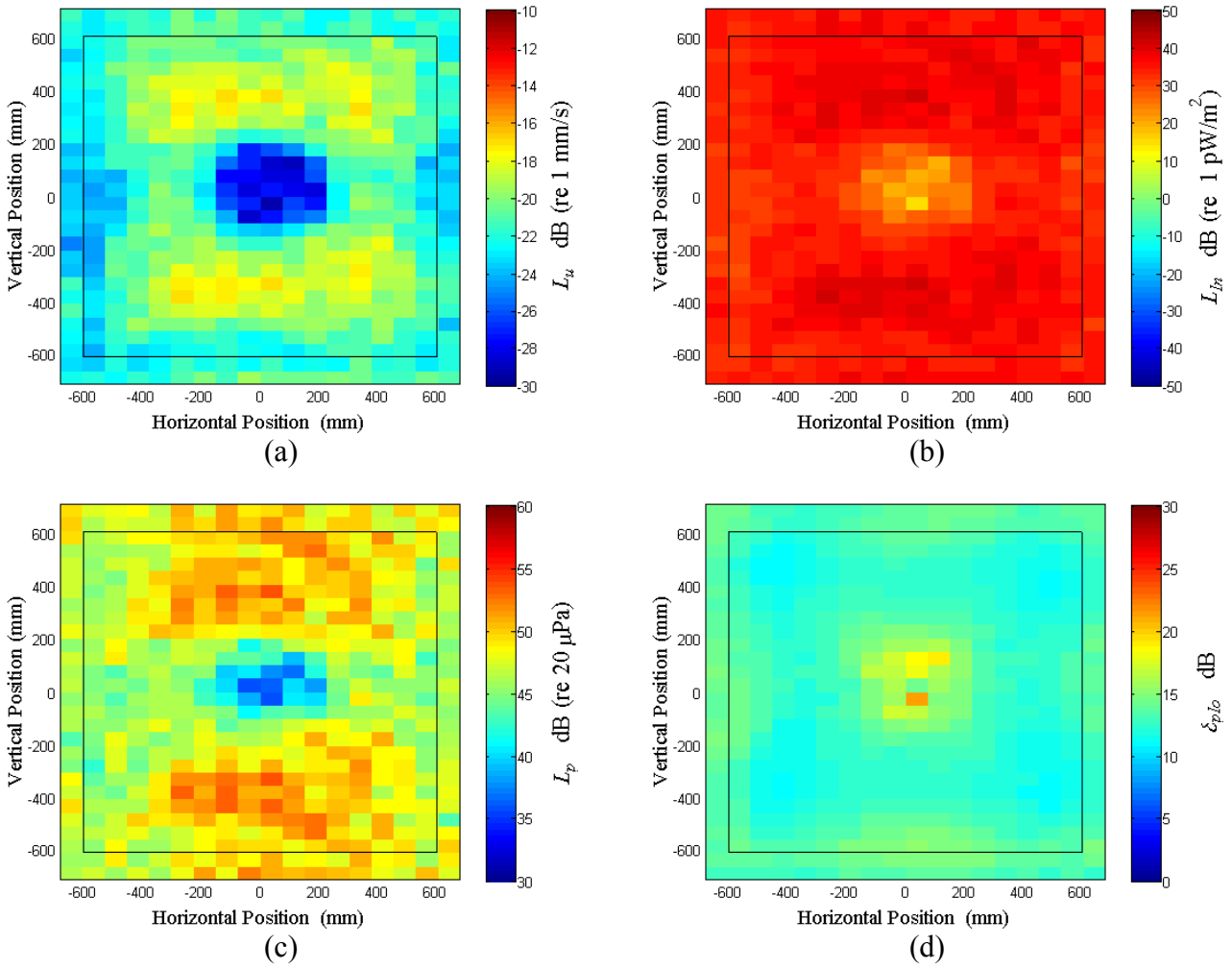

Figure E.44: Surface scan of Window E at 240 Hz (a) particle velocity level, L_u (b) normal signed sound intensity level, L_{In} (c) sound pressure level, L_p (d) pressure-residual intensity index, δ_{pIo}.

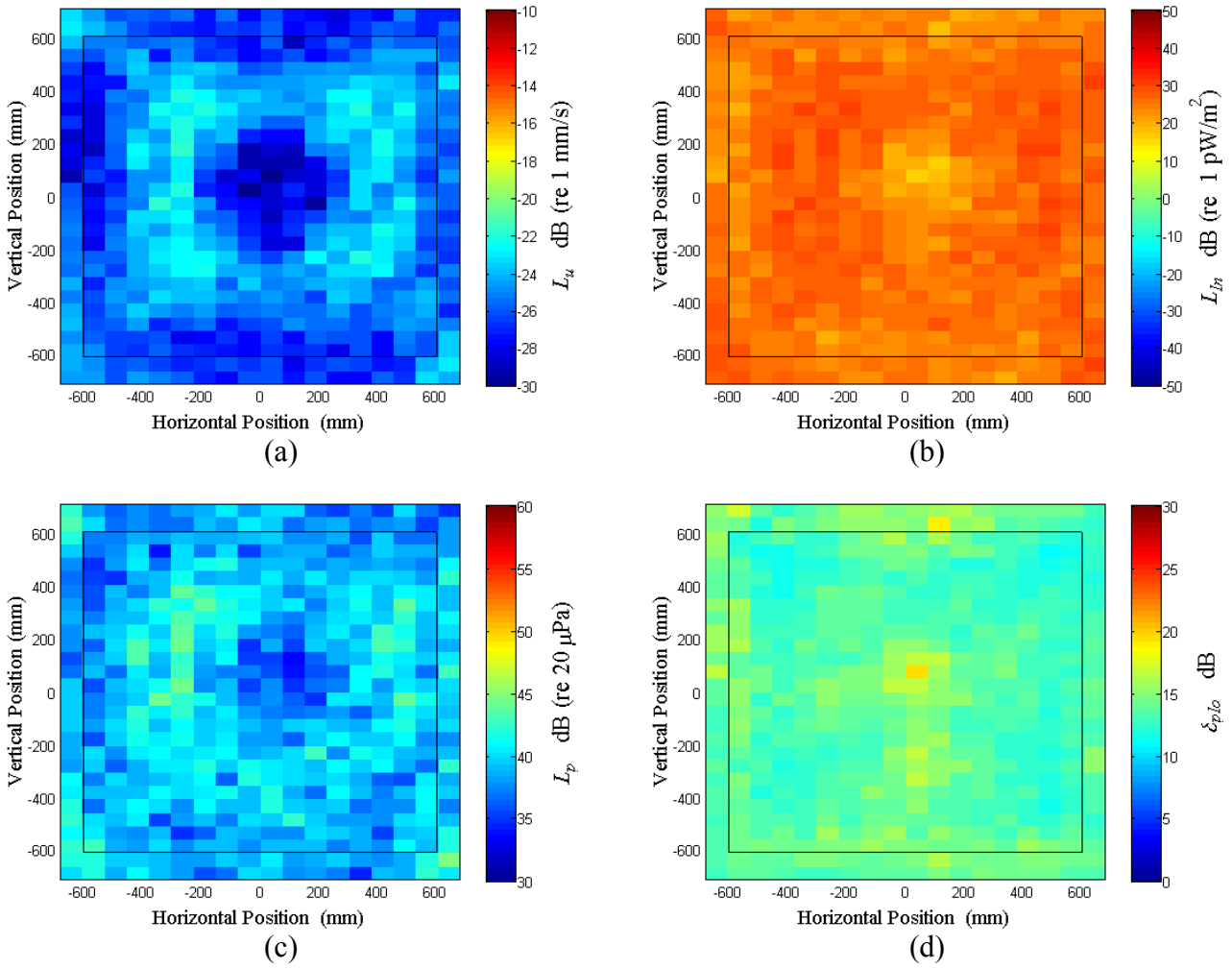

Figure E.45: Surface scan of Window E at 250 Hz (a) particle velocity level, L_u (b) normal signed sound intensity level, L_{In} (c) sound pressure level, L_p (d) pressure-residual intensity index, δ_{pIo}.

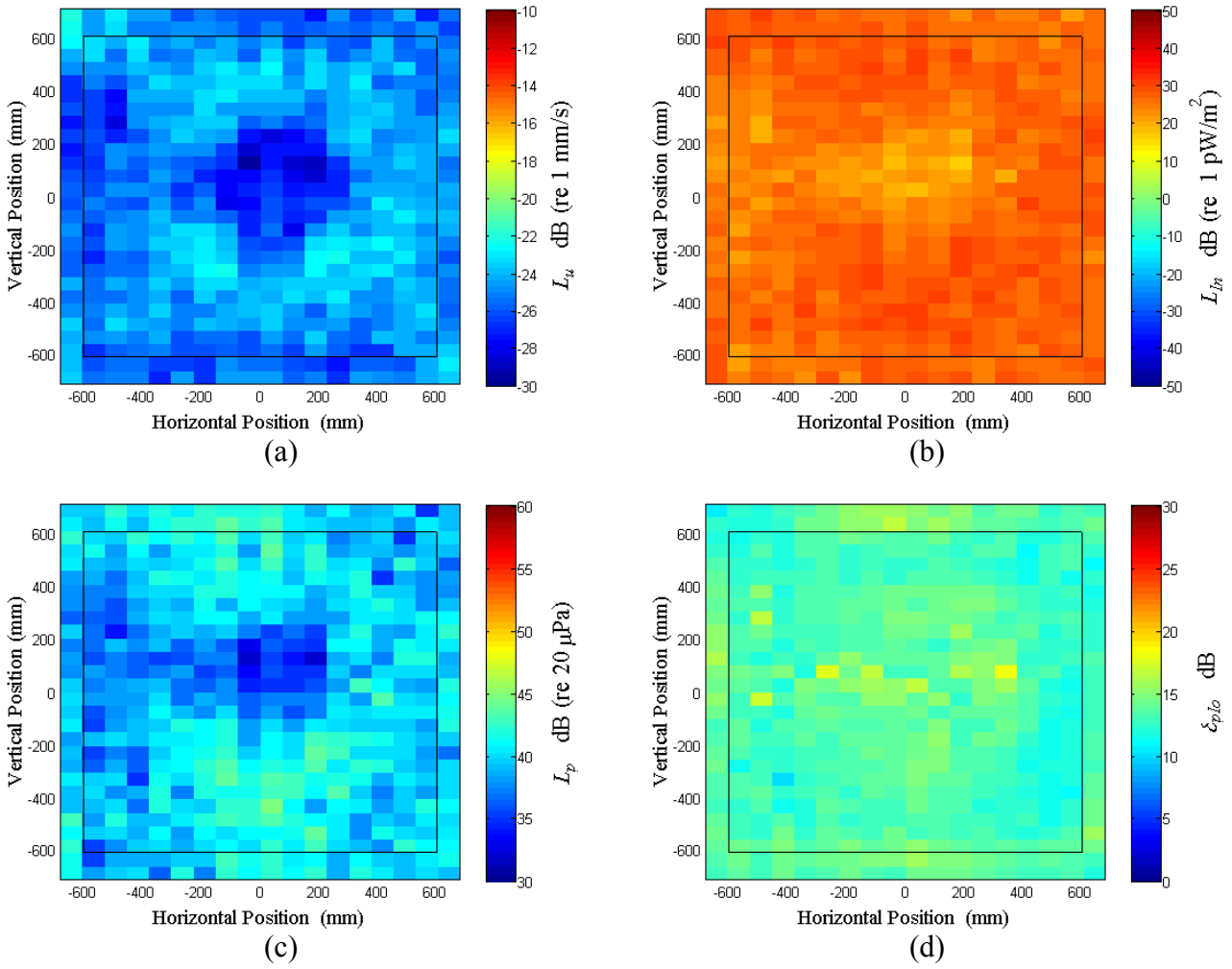

Figure E.46: Surface scan of Window E at 260 Hz (a) particle velocity level, L_u (b) normal signed sound intensity level, L_{In} (c) sound pressure level, L_p (d) pressure-residual intensity index, δ_{pIo}.

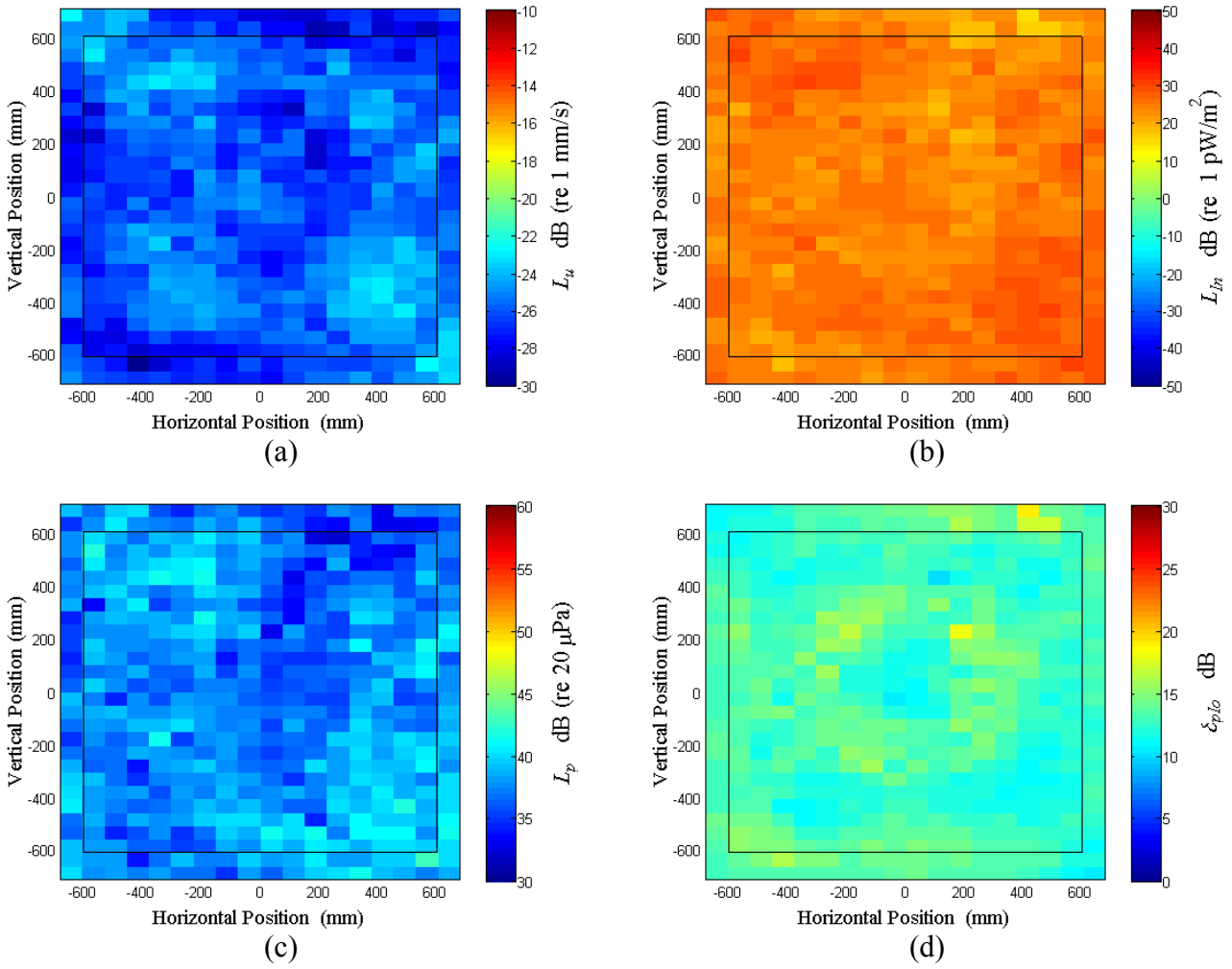

Figure E.47: Surface scan of Window E at 270 Hz (a) particle velocity level, L_u (b) normal signed sound intensity level, L_{In} (c) sound pressure level, L_p (d) pressure-residual intensity index, δ_{pIo}.

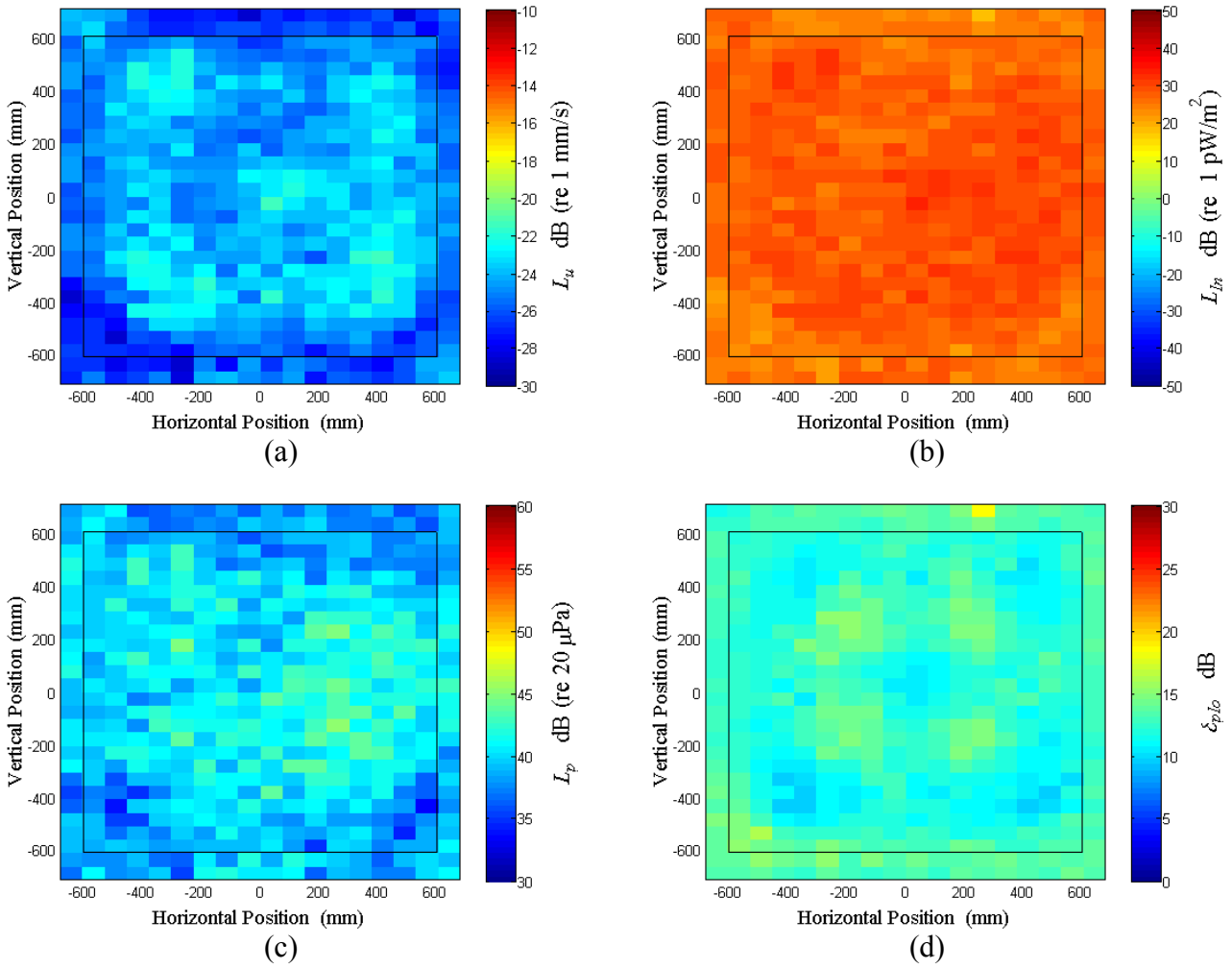

Figure E.48: Surface scan of Window E at 280 Hz (a) particle velocity level, L_u (b) normal signed sound intensity level, L_{In} (c) sound pressure level, L_p (d) pressure-residual intensity index, δ_{pIo}.

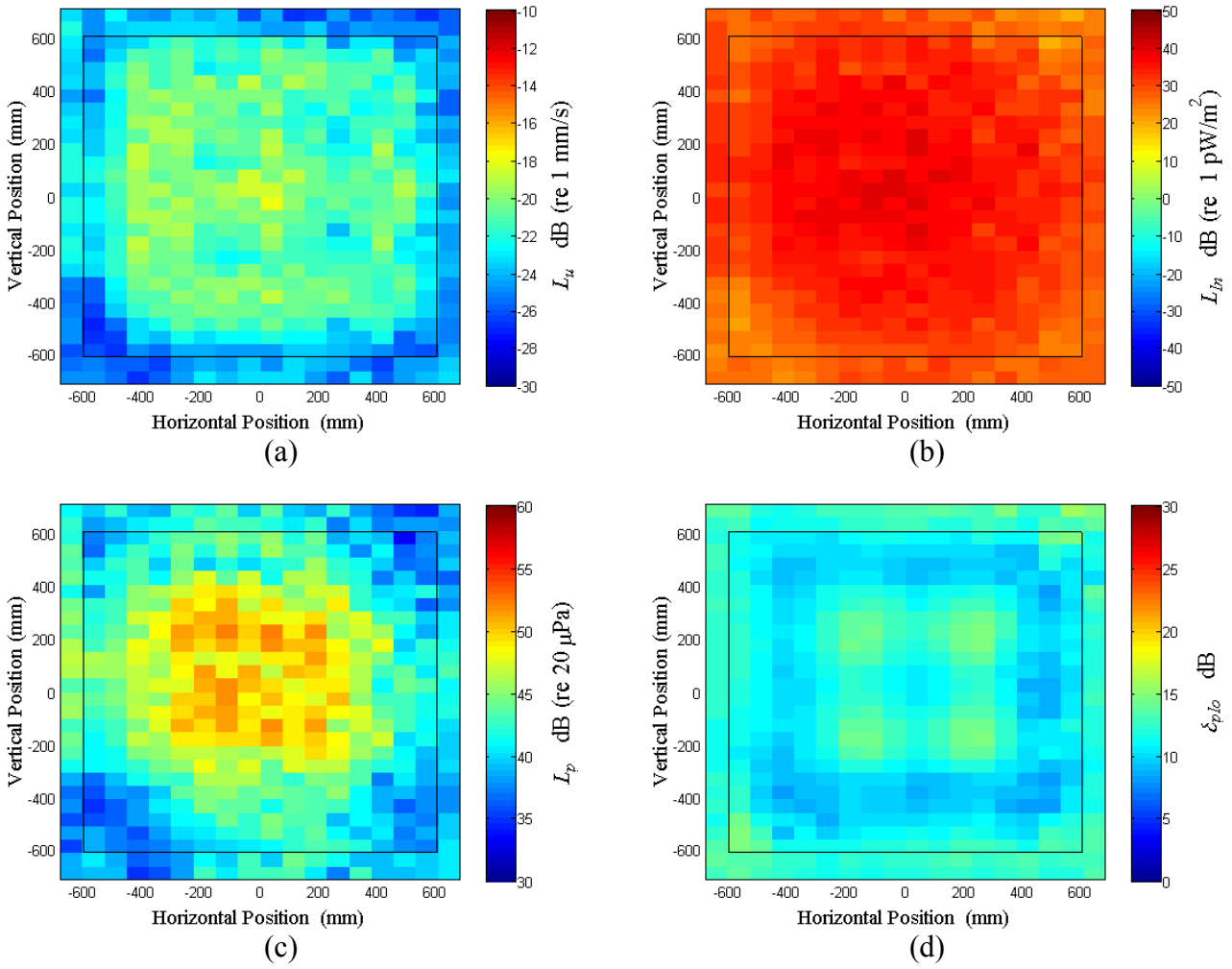

Figure E.49: Surface scan of Window E at 290 Hz (a) particle velocity level, L_u (b) normal signed sound intensity level, L_{In} (c) sound pressure level, L_p (d) pressure-residual intensity index, δ_{pIo}.

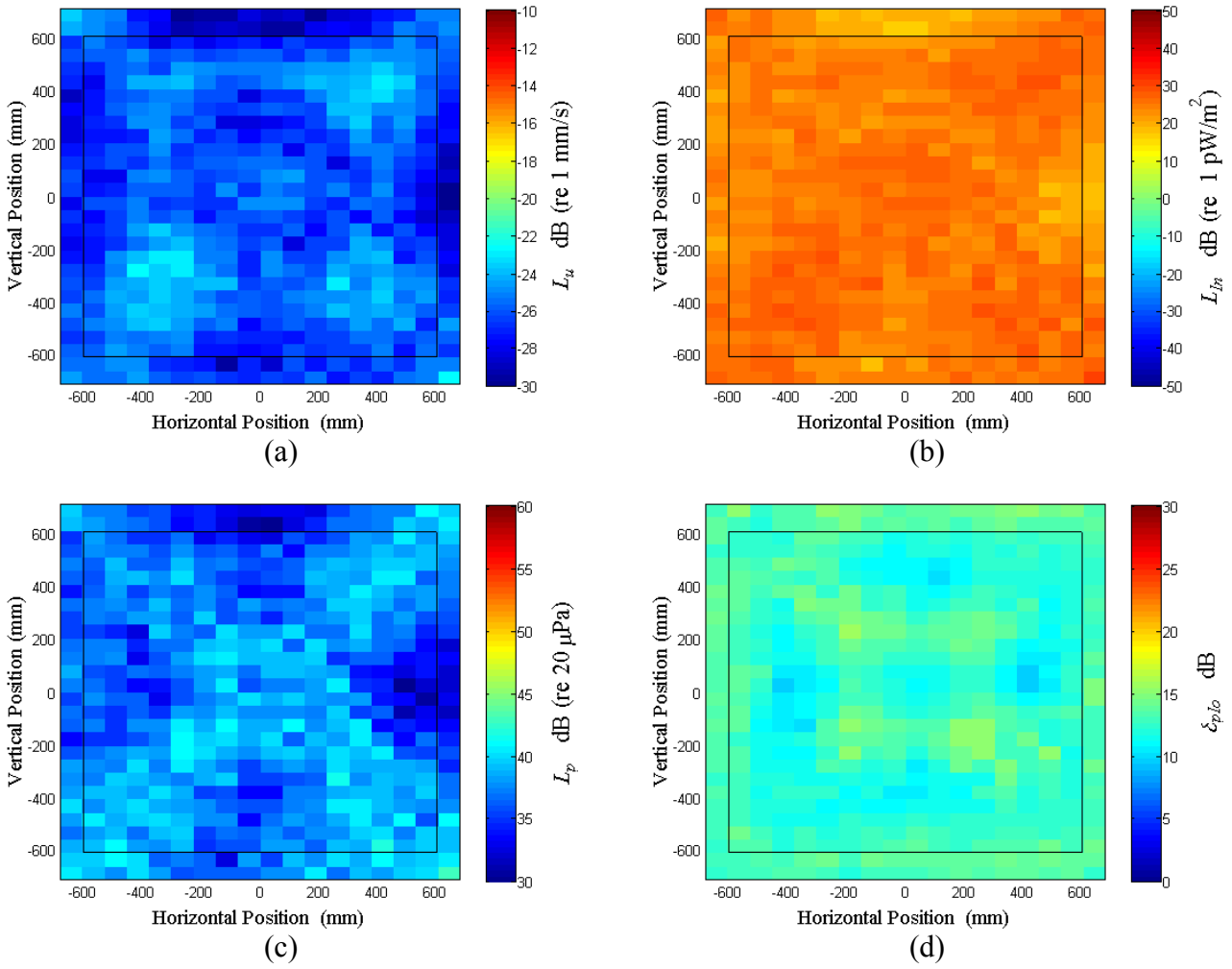

Figure E.50: Surface scan of Window E at 300 Hz (a) particle velocity level, L_u (b) normal signed sound intensity level, L_{In} (c) sound pressure level, L_p (d) pressure-residual intensity index, δ_{pIo}.

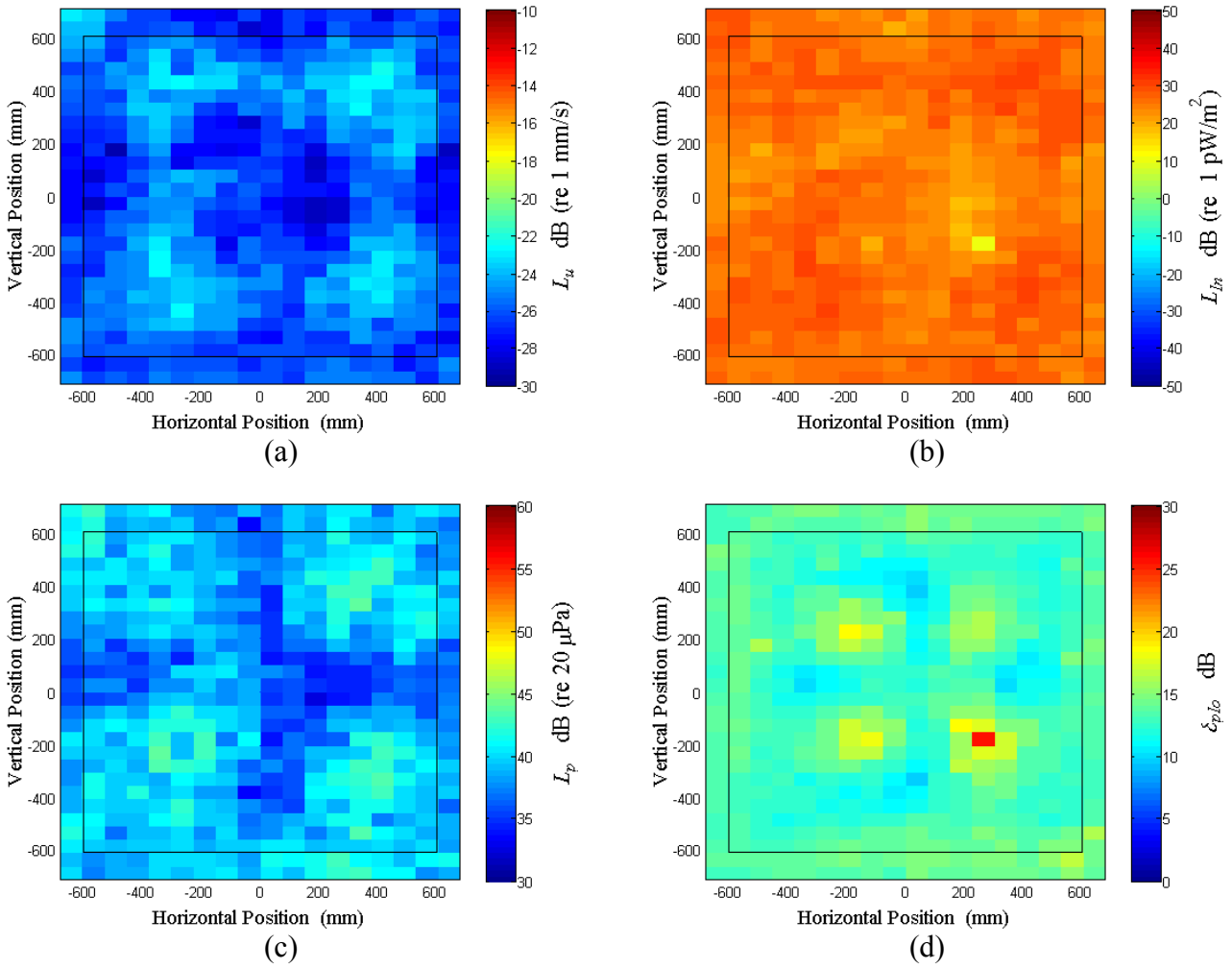

Figure E.51: Surface scan of Window E at 310 Hz (a) particle velocity level, L_u (b) normal signed sound intensity level, L_{In} (c) sound pressure level, L_p (d) pressure-residual intensity index, δ_{pIo}.

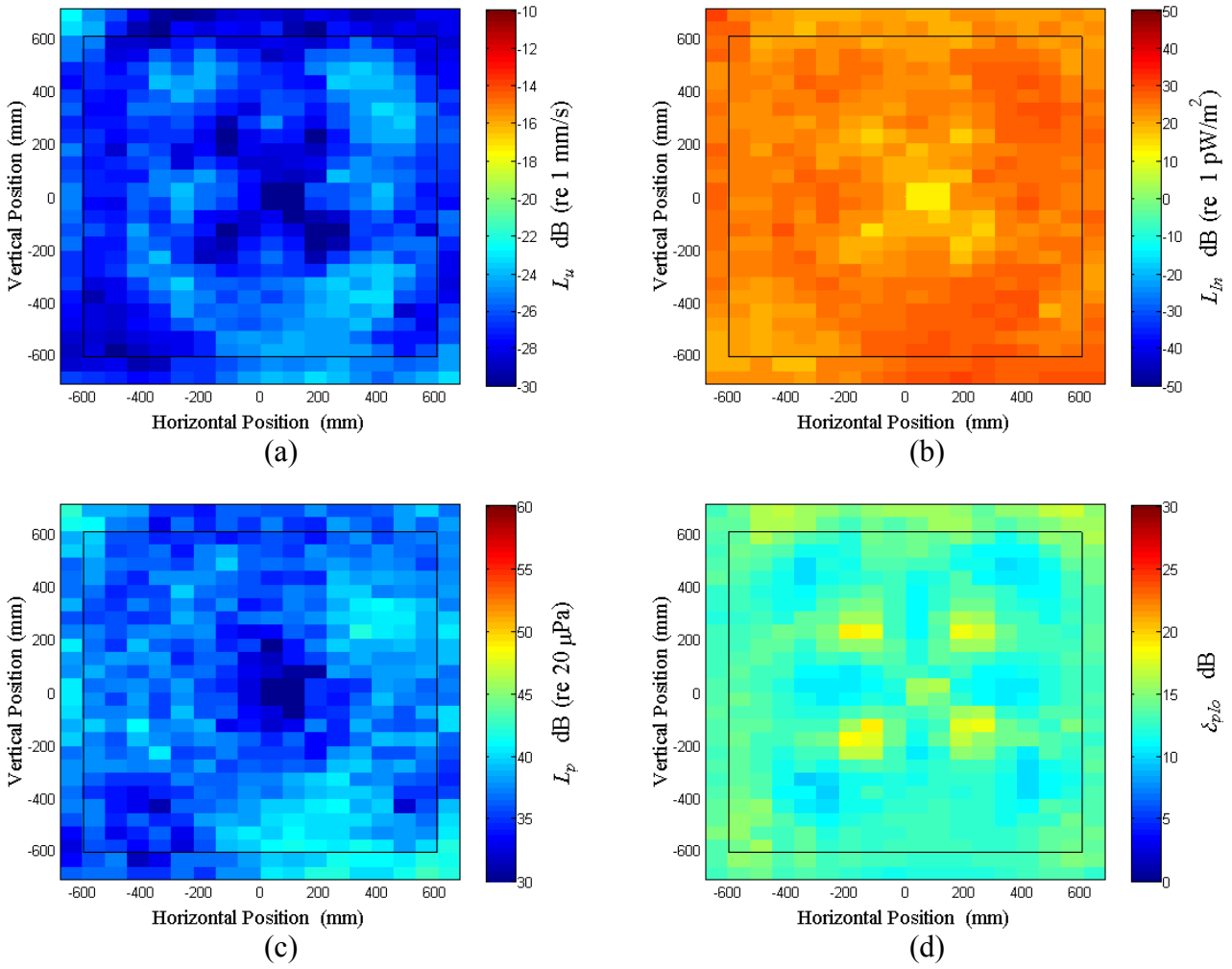

Figure E.52: Surface scan of Window E at 320 Hz (a) particle velocity level, L_u (b) normal signed sound intensity level, L_{In} (c) sound pressure level, L_p (d) pressure-residual intensity index, δ_{pIo}.

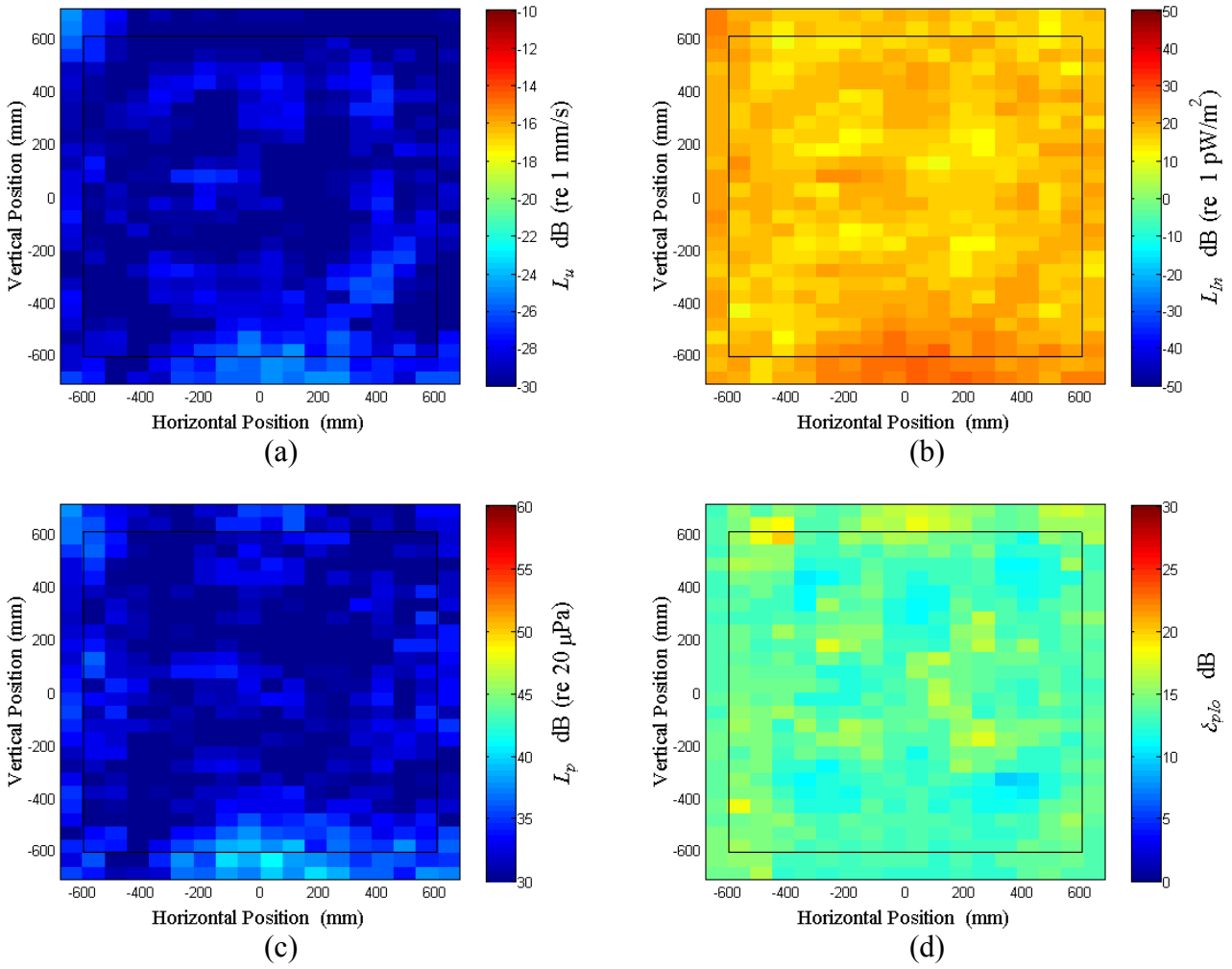

Figure E.53: Surface scan of Window E at 330 Hz (a) particle velocity level, L_u (b) normal signed sound intensity level, L_{In} (c) sound pressure level, L_p (d) pressure-residual intensity index, δ_{pIo}.

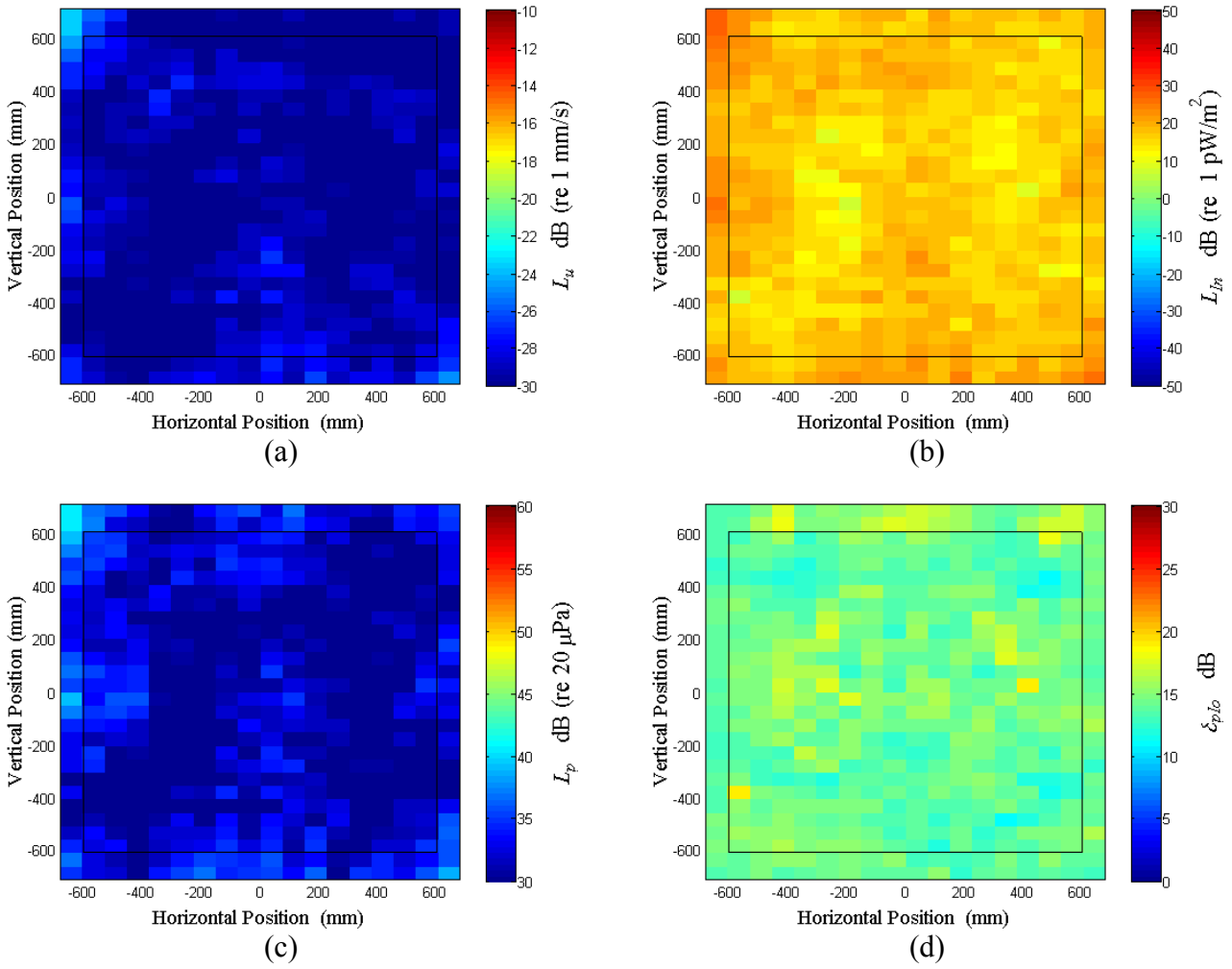

Figure E.54: Surface scan of Window E at 340 Hz (a) particle velocity level, L_u (b) normal signed sound intensity level, L_{In} (c) sound pressure level, L_p (d) pressure-residual intensity index, δ_{pIo}.

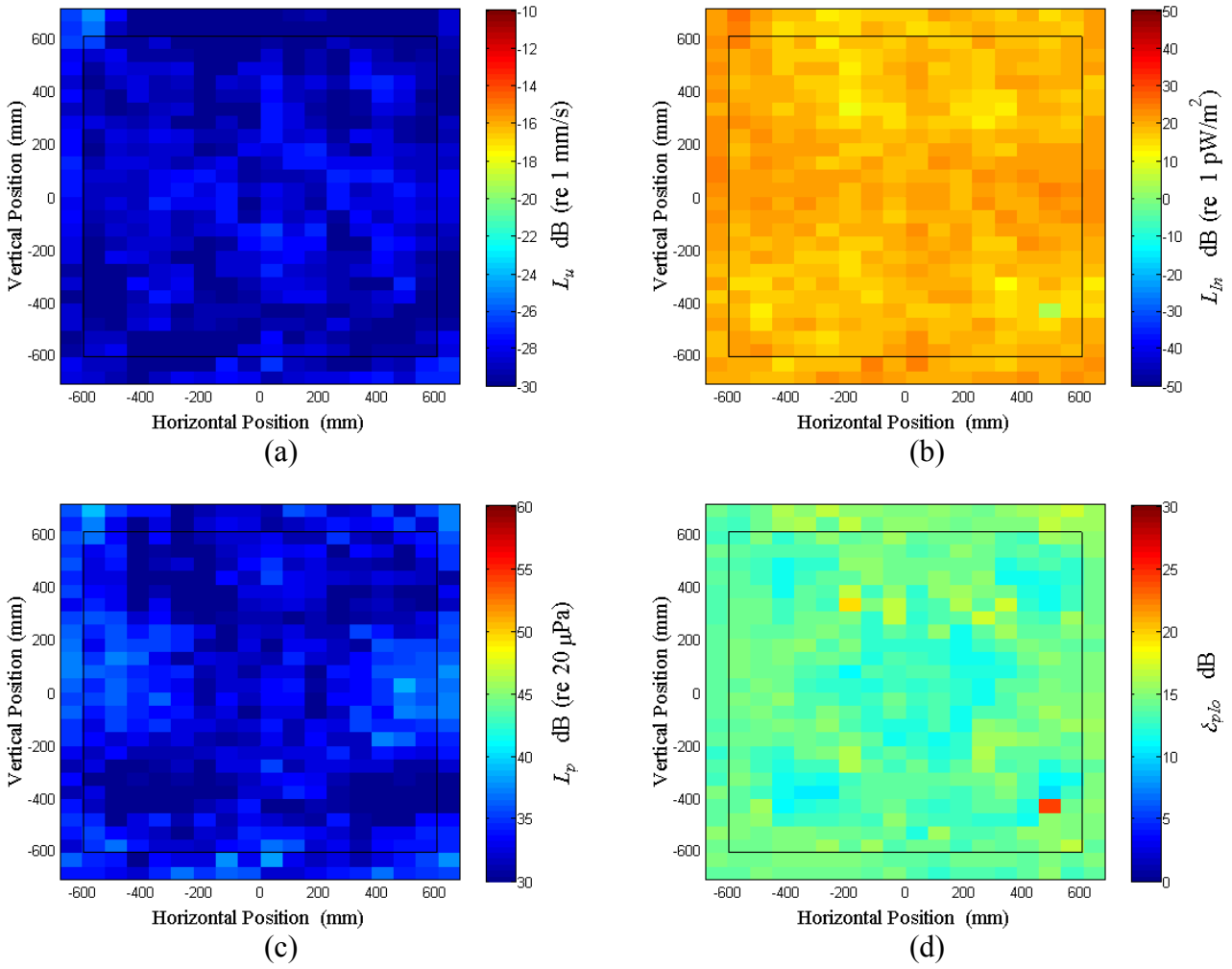

Figure E.55: Surface scan of Window E at 350 Hz (a) particle velocity level, L_u (b) normal signed sound intensity level, L_{In} (c) sound pressure level, L_p (d) pressure-residual intensity index, δ_{pIo}.

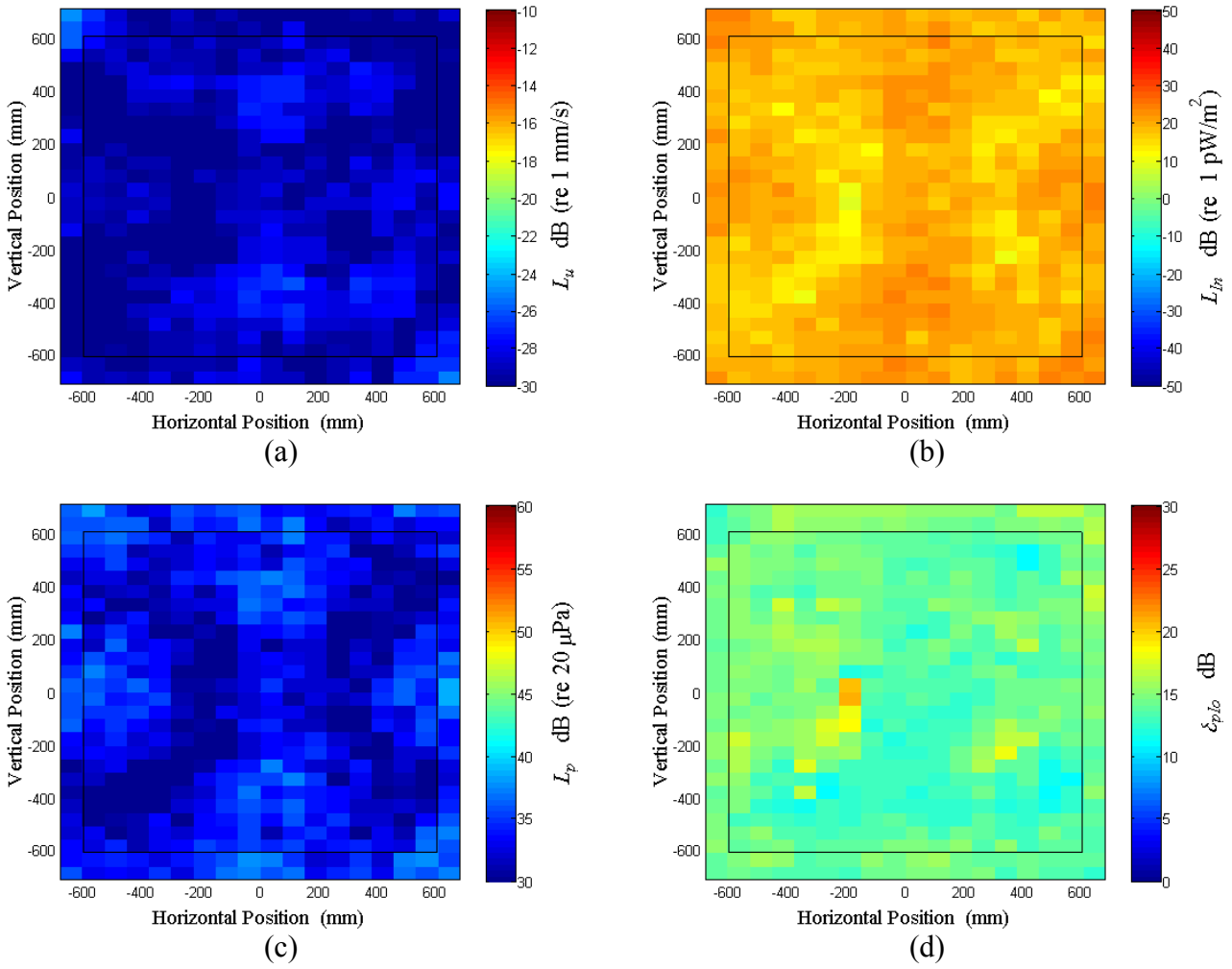

Figure E.56: Surface scan of Window E at 360 Hz (a) particle velocity level, L_u (b) normal signed sound intensity level, L_{In} (c) sound pressure level, L_p (d) pressure-residual intensity index, δ_{pIo}.

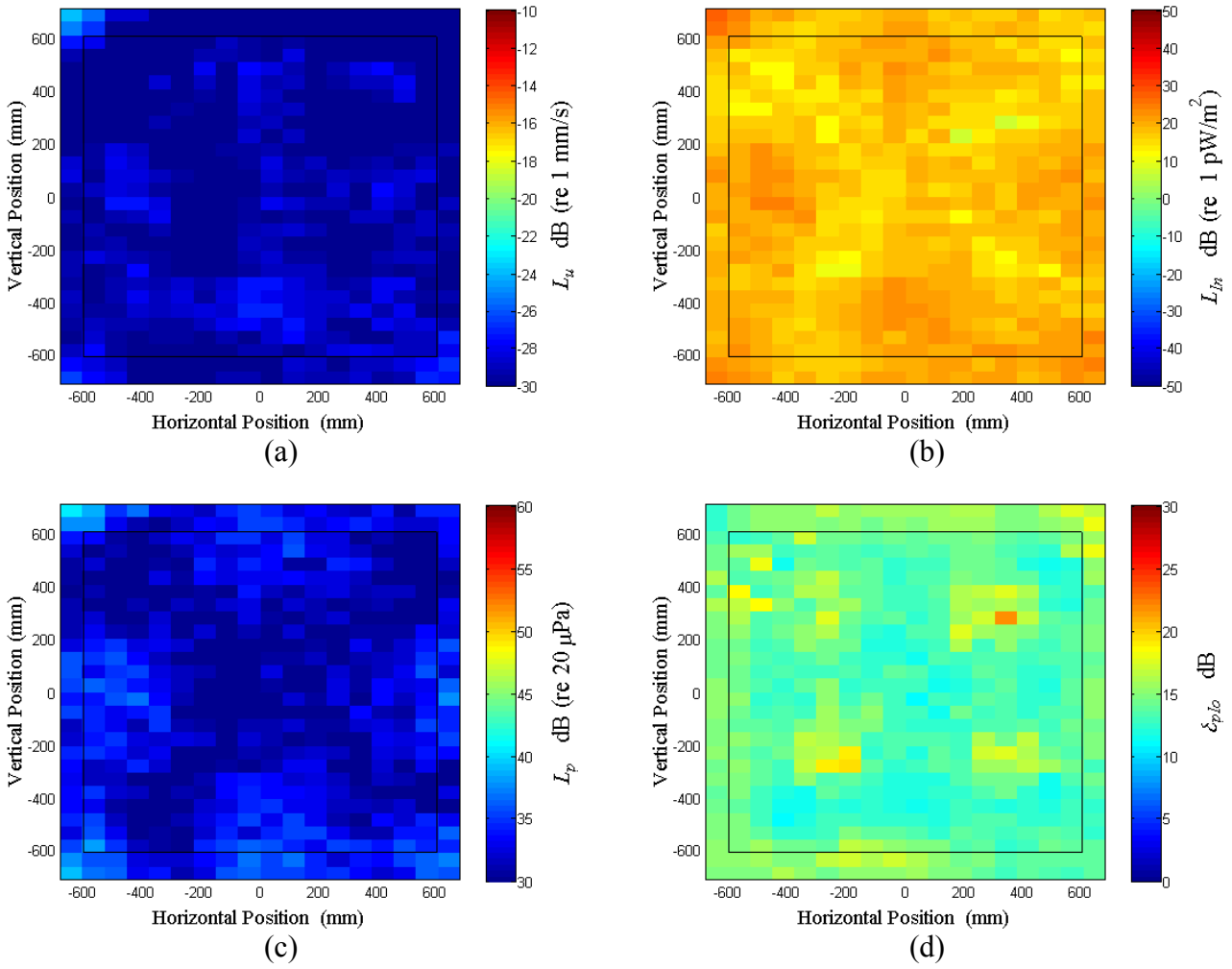

Figure E.57: Surface scan of Window E at 370 Hz (a) particle velocity level, L_u (b) normal signed sound intensity level, L_{In} (c) sound pressure level, L_p (d) pressure-residual intensity index, δ_{pIo}.

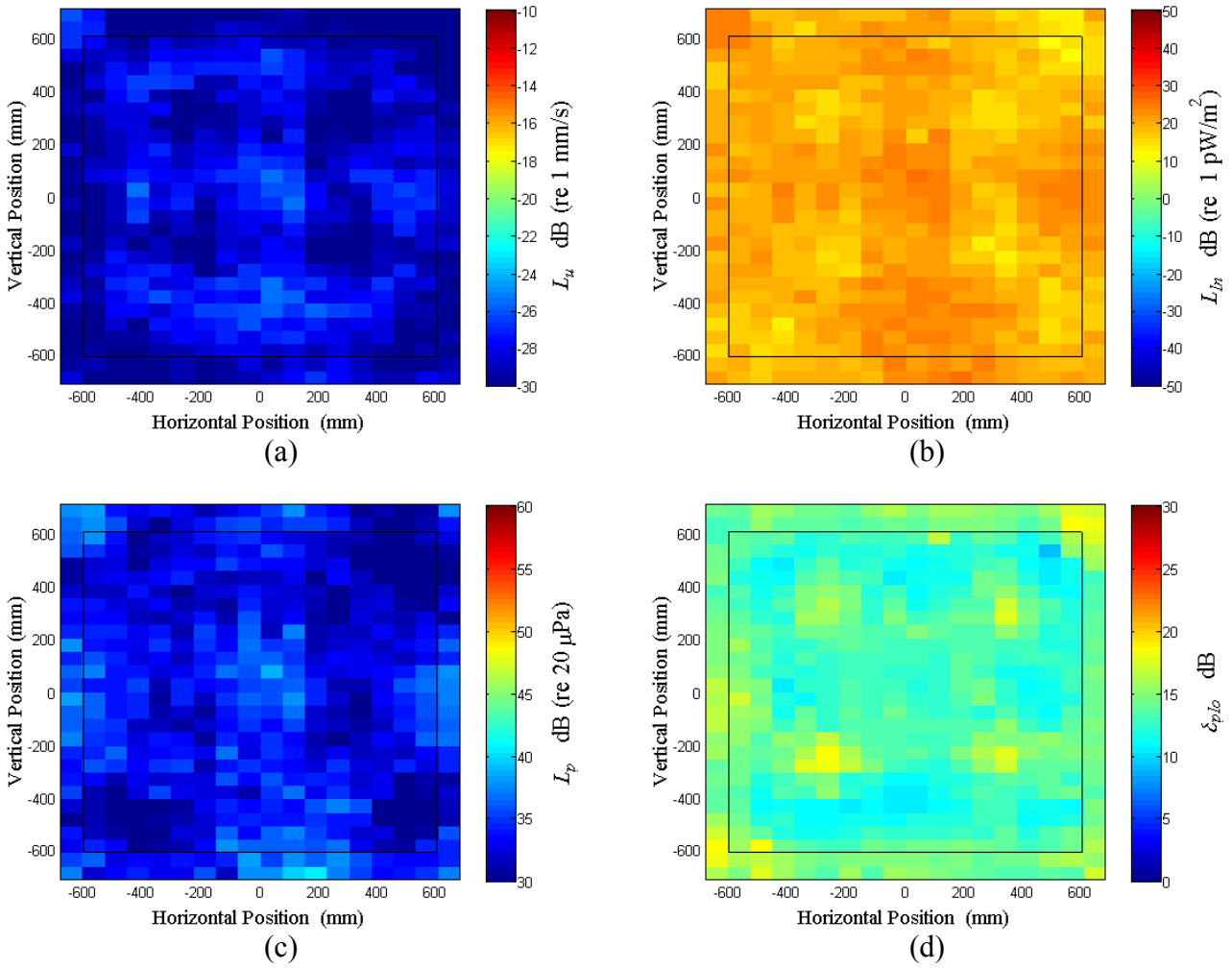

Figure E.58: Surface scan of Window E at 380 Hz (a) particle velocity level, L_u (b) normal signed sound intensity level, L_{In} (c) sound pressure level, L_p (d) pressure-residual intensity index, δ_{pIo}.

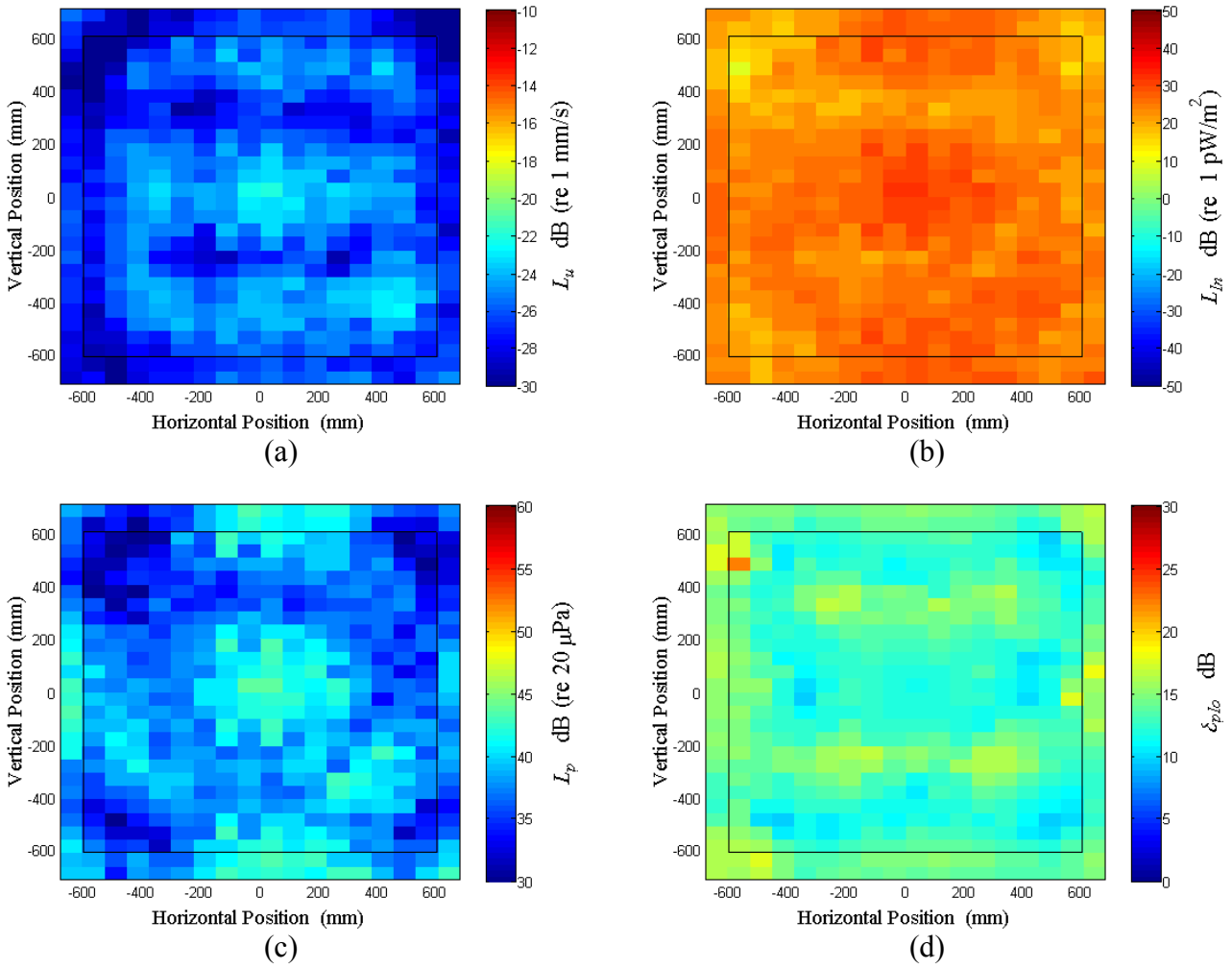

Figure E.59: Surface scan of Window E at 390 Hz (a) particle velocity level, L_u (b) normal signed sound intensity level, L_{In} (c) sound pressure level, L_p (d) pressure-residual intensity index, δ_{pIo}.

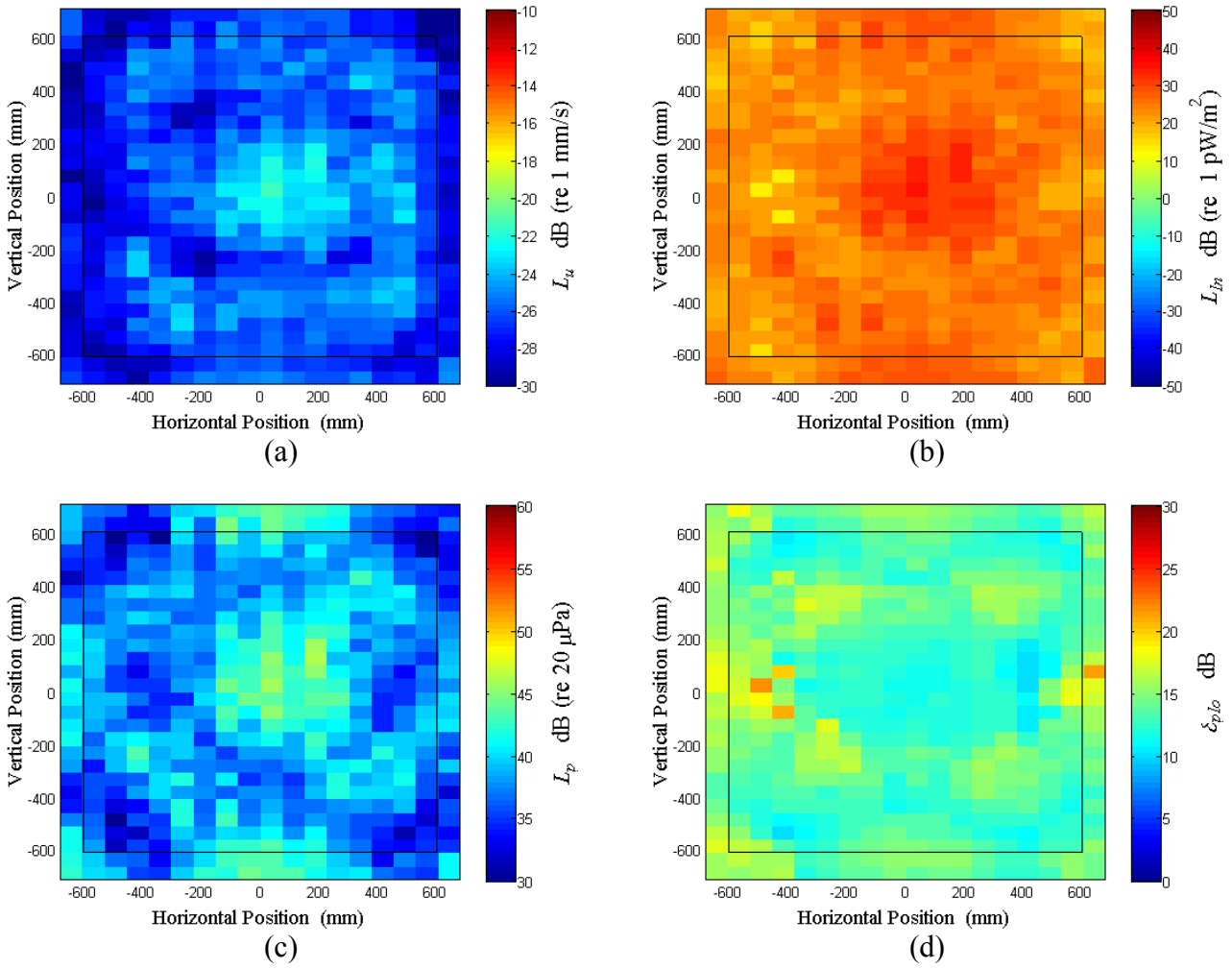

Figure E.60: Surface scan of Window E at 400 Hz (a) particle velocity level, L_u (b) normal signed sound intensity level, L_{In} (c) sound pressure level, L_p (d) pressure-residual intensity index, δ_{pIo}.

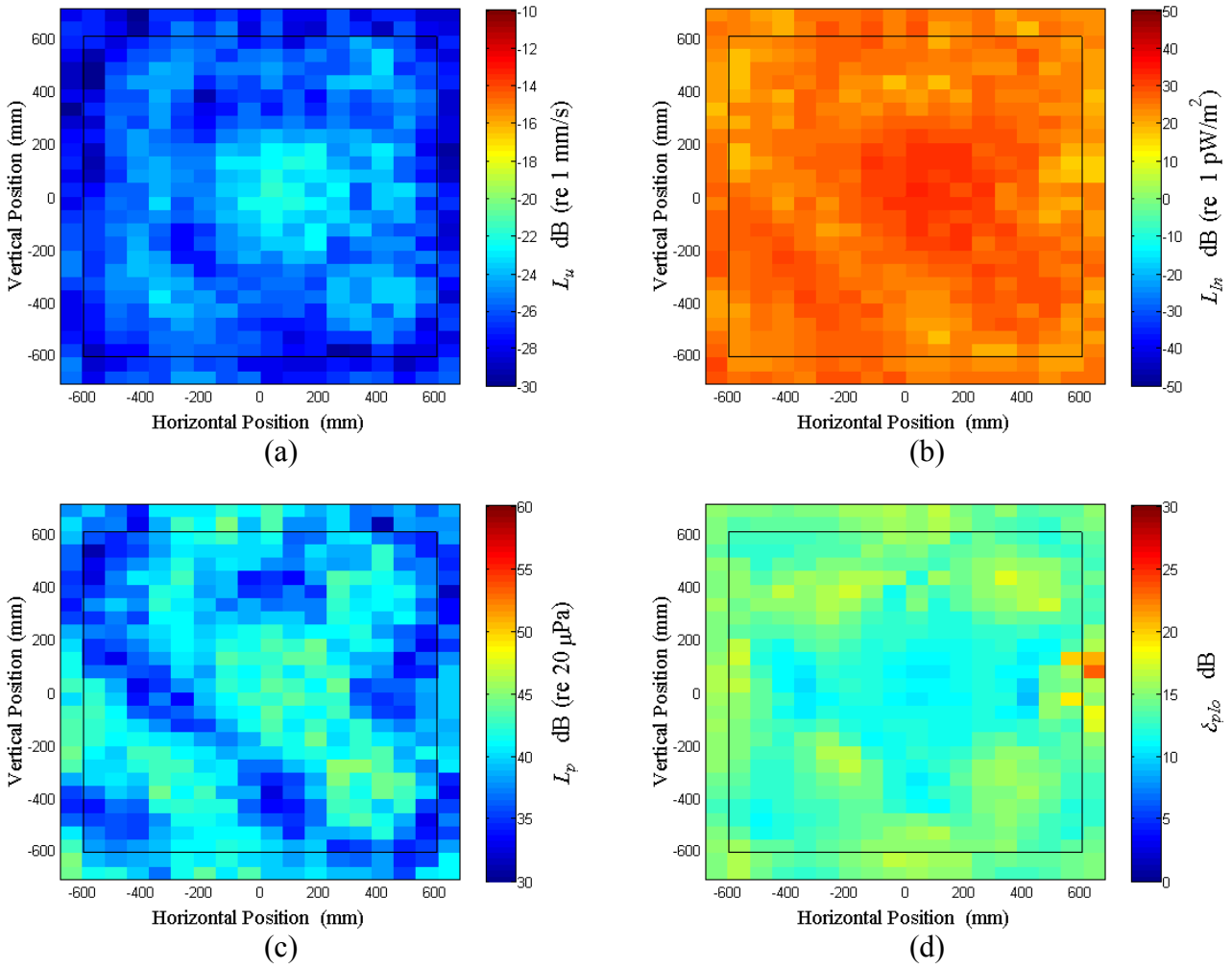

Figure E.61: Surface scan of Window E at 410 Hz (a) particle velocity level, L_u (b) normal signed sound intensity level, L_{In} (c) sound pressure level, L_p (d) pressure-residual intensity index, δ_{pIo}.

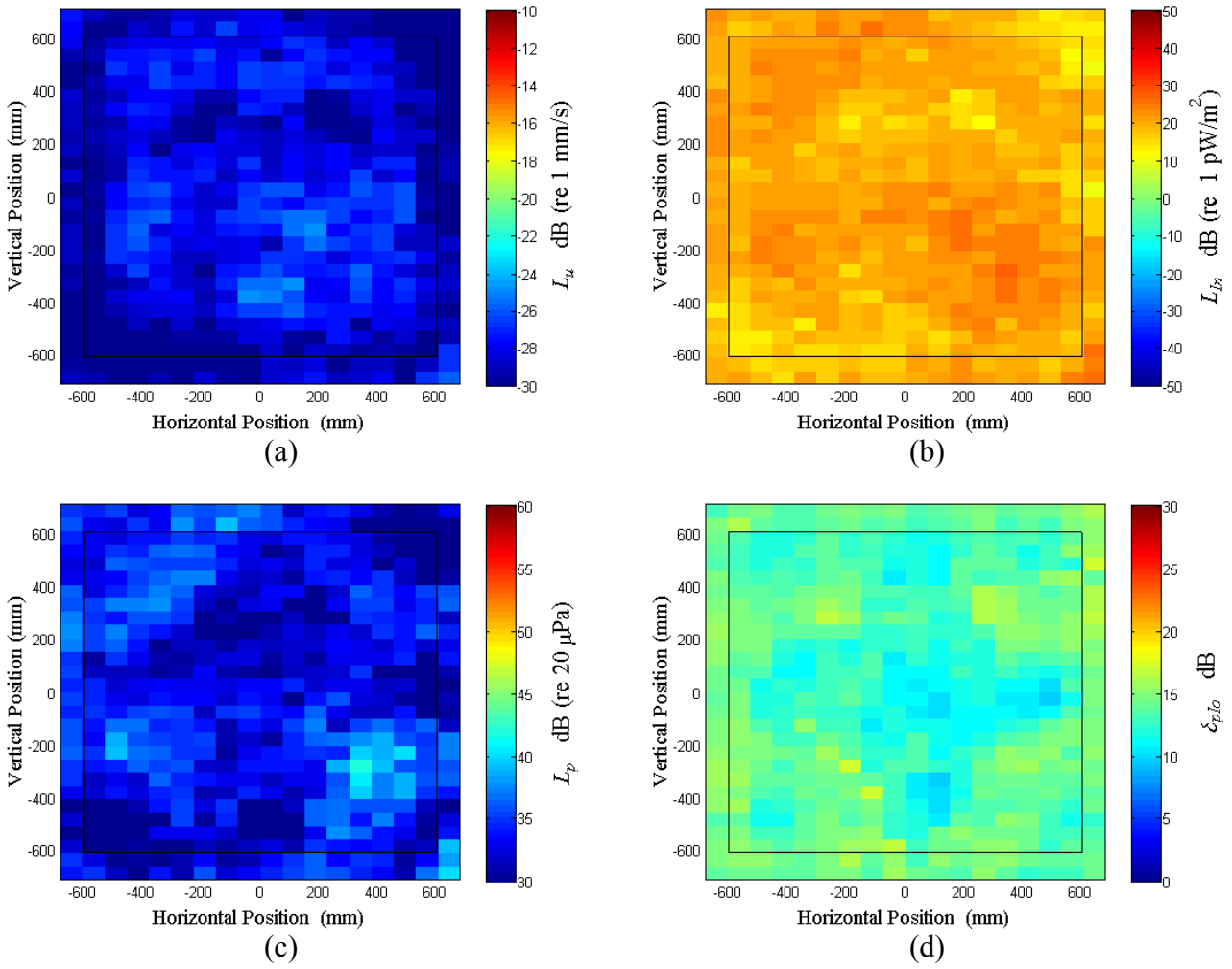

Figure E.62: Surface scan of Window E at 420 Hz (a) particle velocity level, L_u (b) normal signed sound intensity level, L_{In} (c) sound pressure level, L_p (d) pressure-residual intensity index, δ_{pIo}.

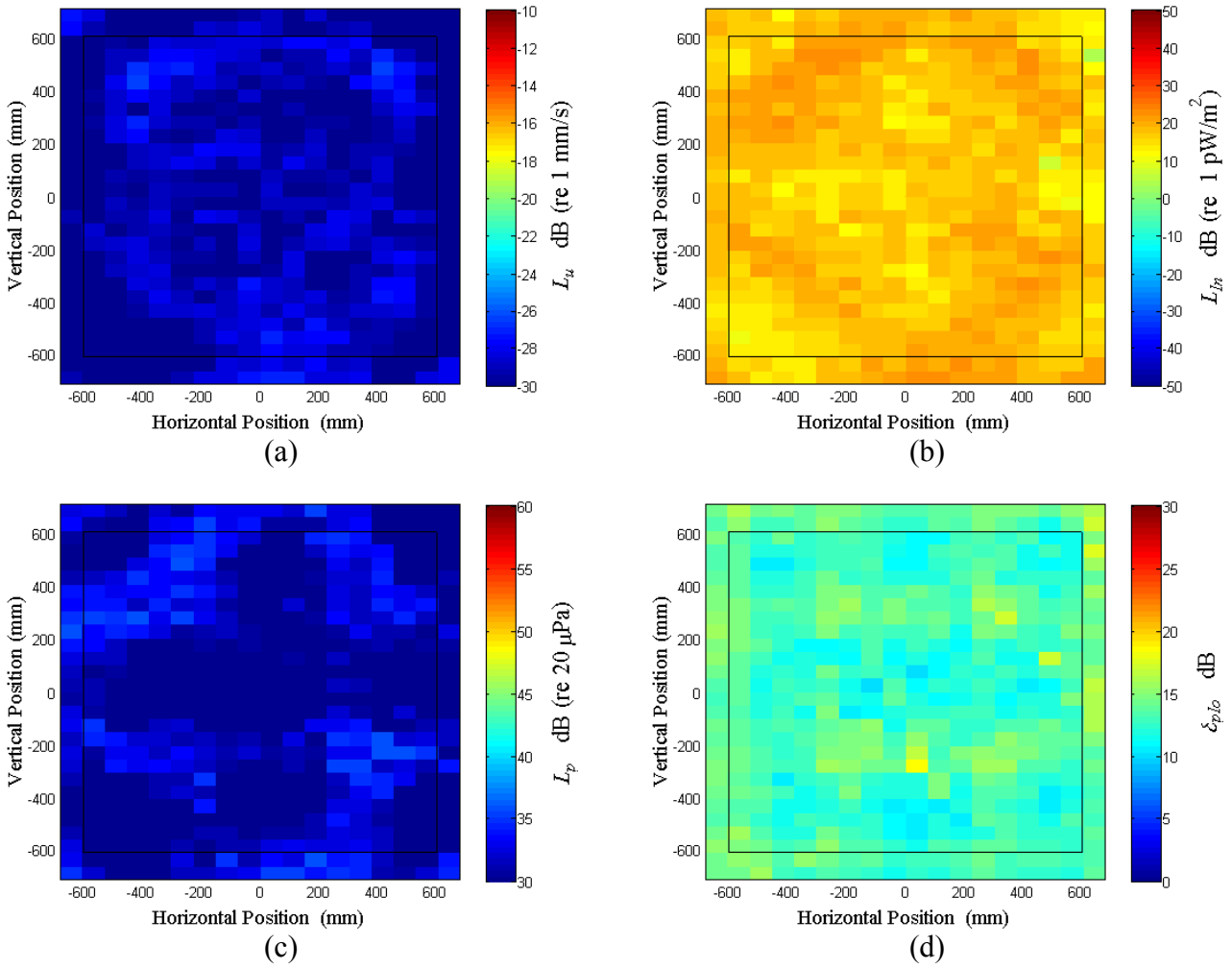

Figure E.63: Surface scan of Window E at 430 Hz (a) particle velocity level, L_u (b) normal signed sound intensity level, L_{In} (c) sound pressure level, L_p (d) pressure-residual intensity index, δ_{pIo}.

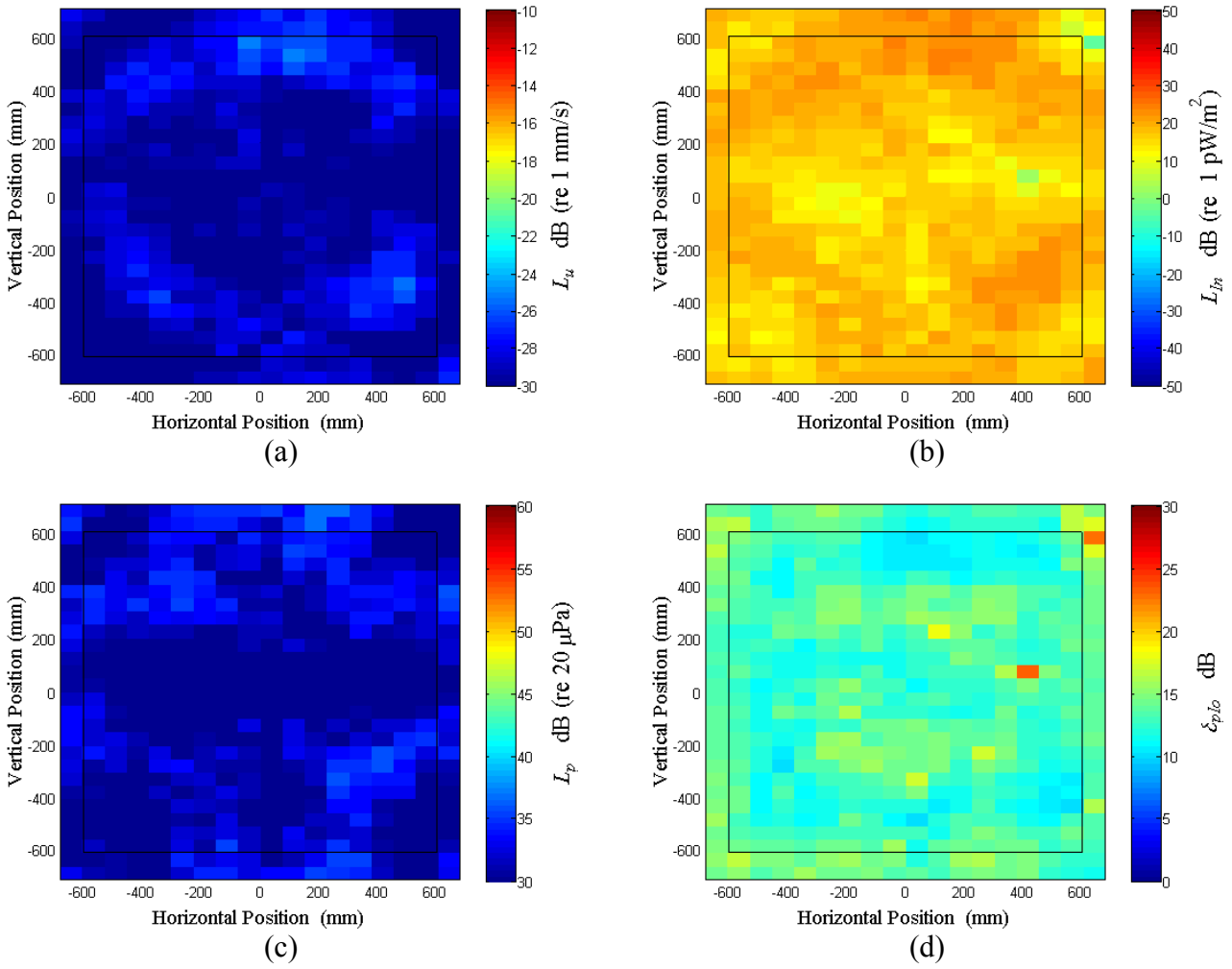

Figure E.64: Surface scan of Window E at 440 Hz (a) particle velocity level, L_u (b) normal signed sound intensity level, L_{In} (c) sound pressure level, L_p (d) pressure-residual intensity index, δ_{pIo}.

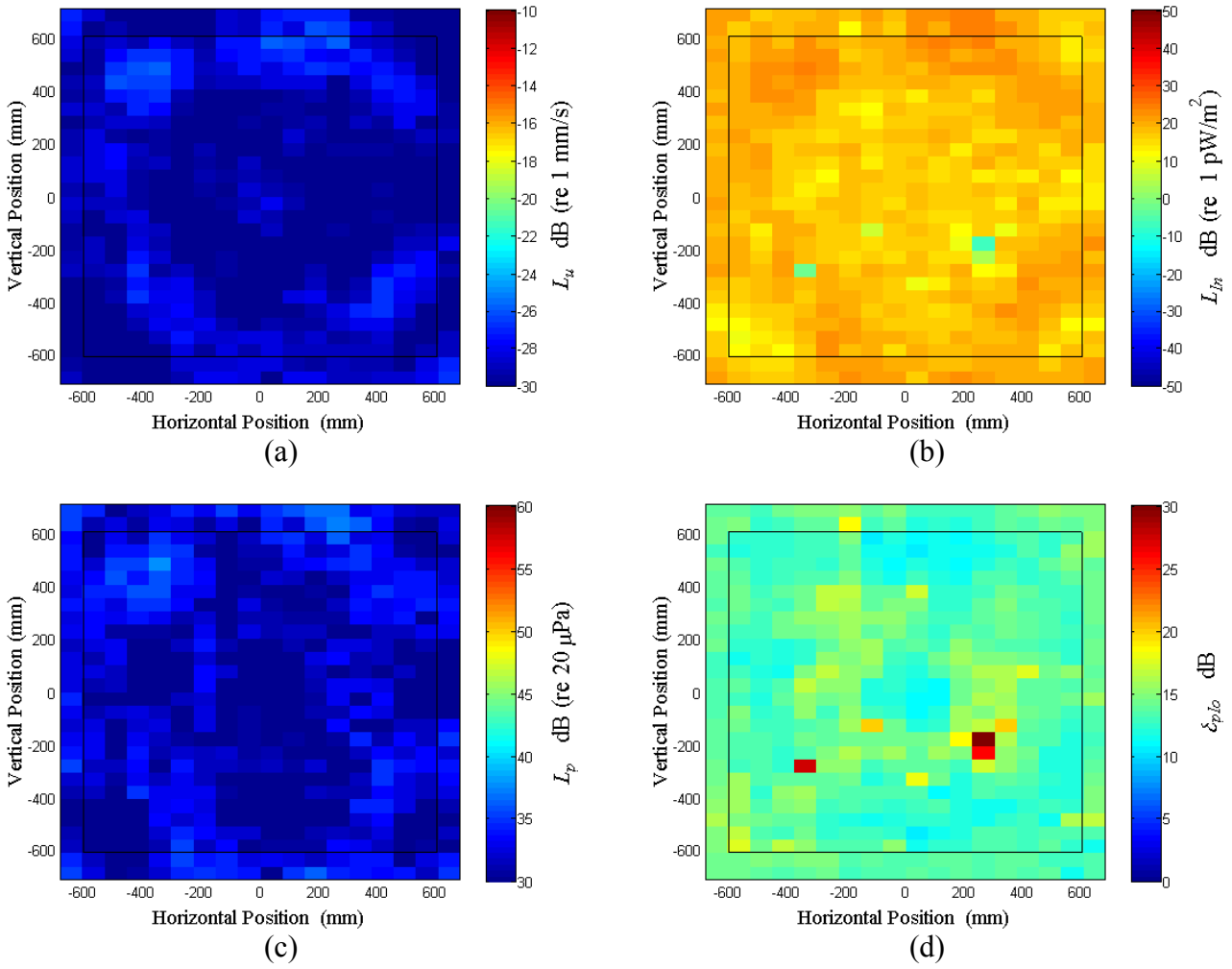

Figure E.65: Surface scan of Window E at 450 Hz (a) particle velocity level, L_u (b) normal signed sound intensity level, L_{In} (c) sound pressure level, L_p (d) pressure-residual intensity index, δ_{pIo}.

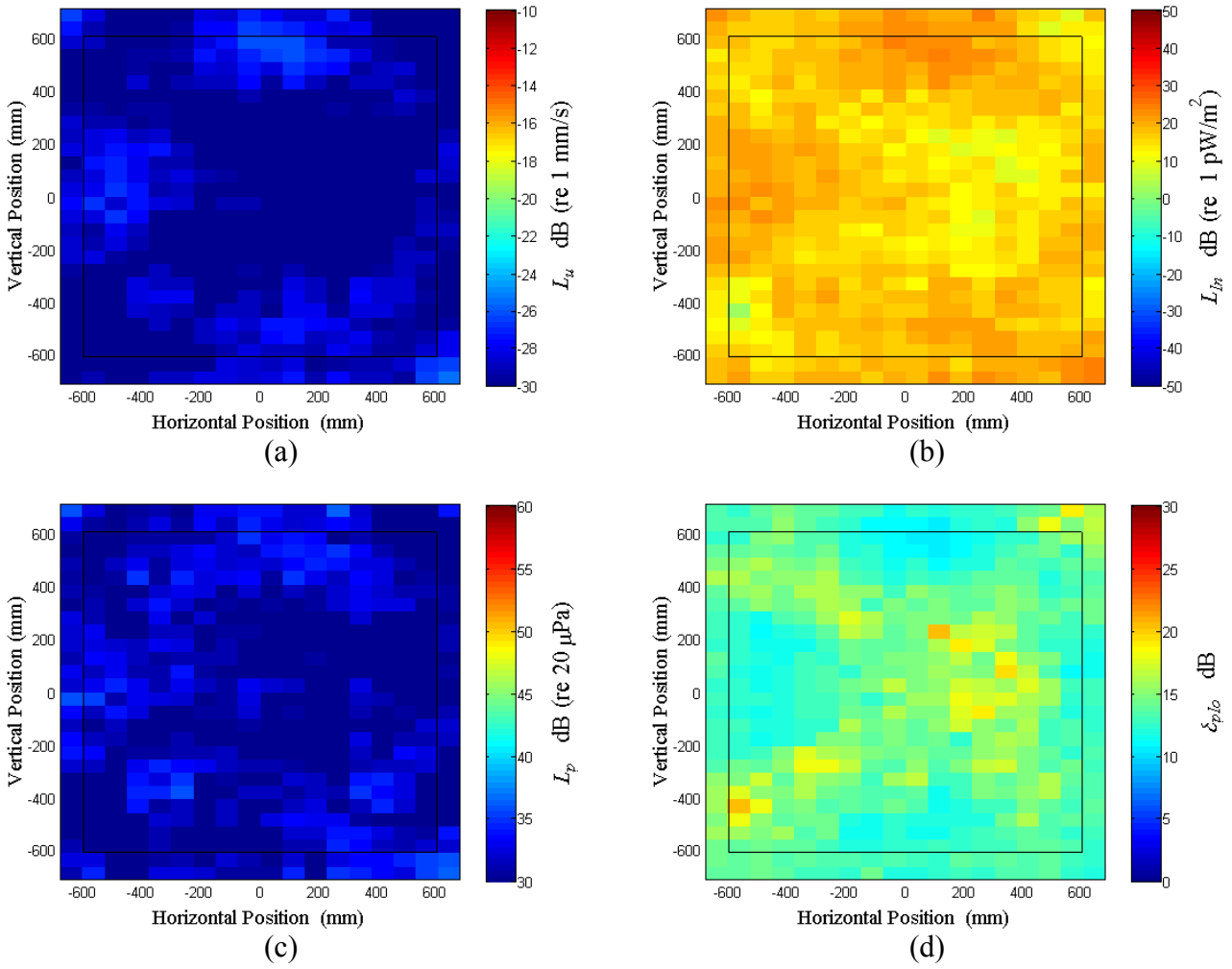

Figure E.66: Surface scan of Window E at 460 Hz (a) particle velocity level, L_u (b) normal signed sound intensity level, L_{In} (c) sound pressure level, L_p (d) pressure-residual intensity index, δ_{pIo}.

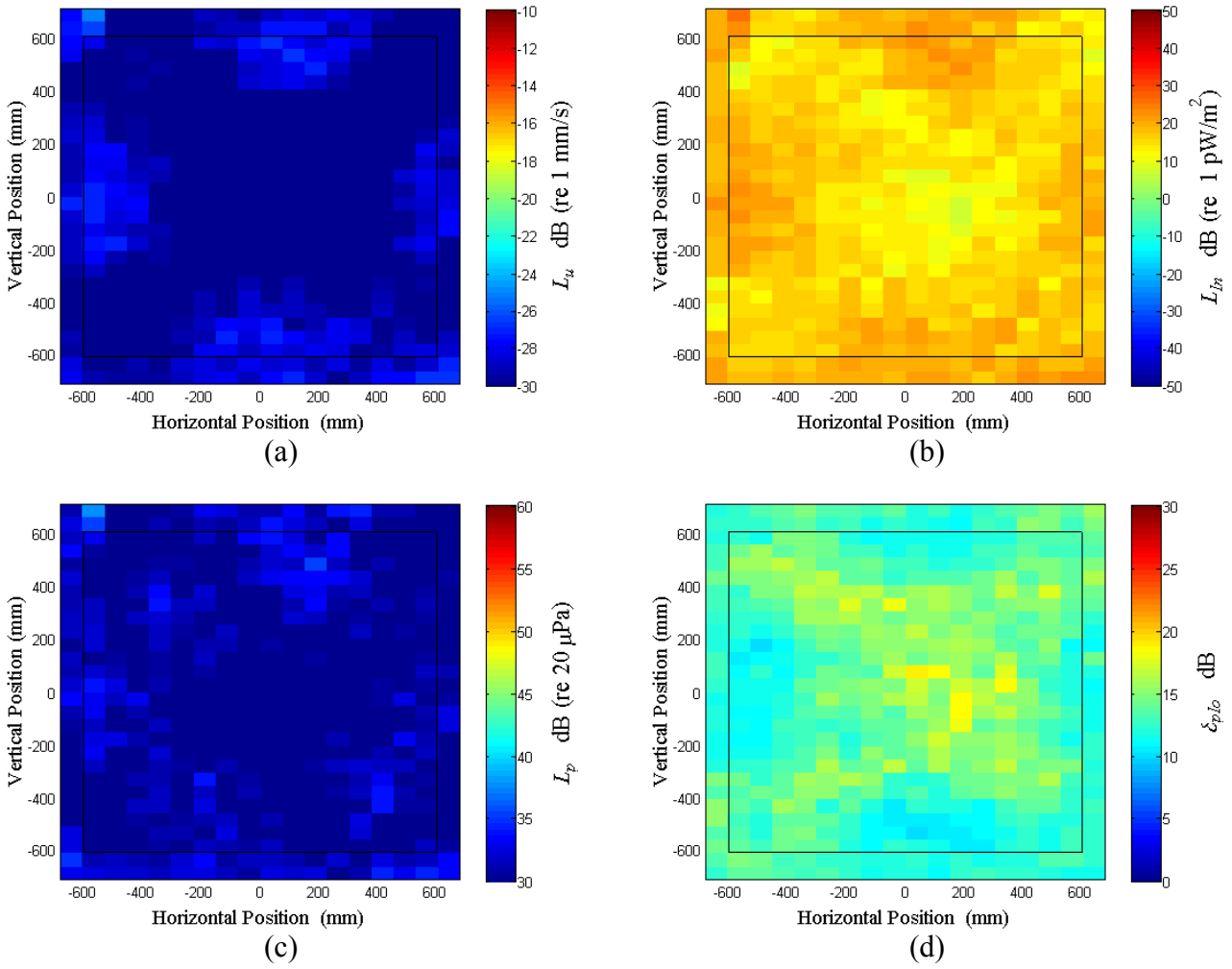

Figure E.67: Surface scan of Window E at 470 Hz (a) particle velocity level, L_u (b) normal signed sound intensity level, L_{In} (c) sound pressure level, L_p (d) pressure-residual intensity index, δ_{pIo}.

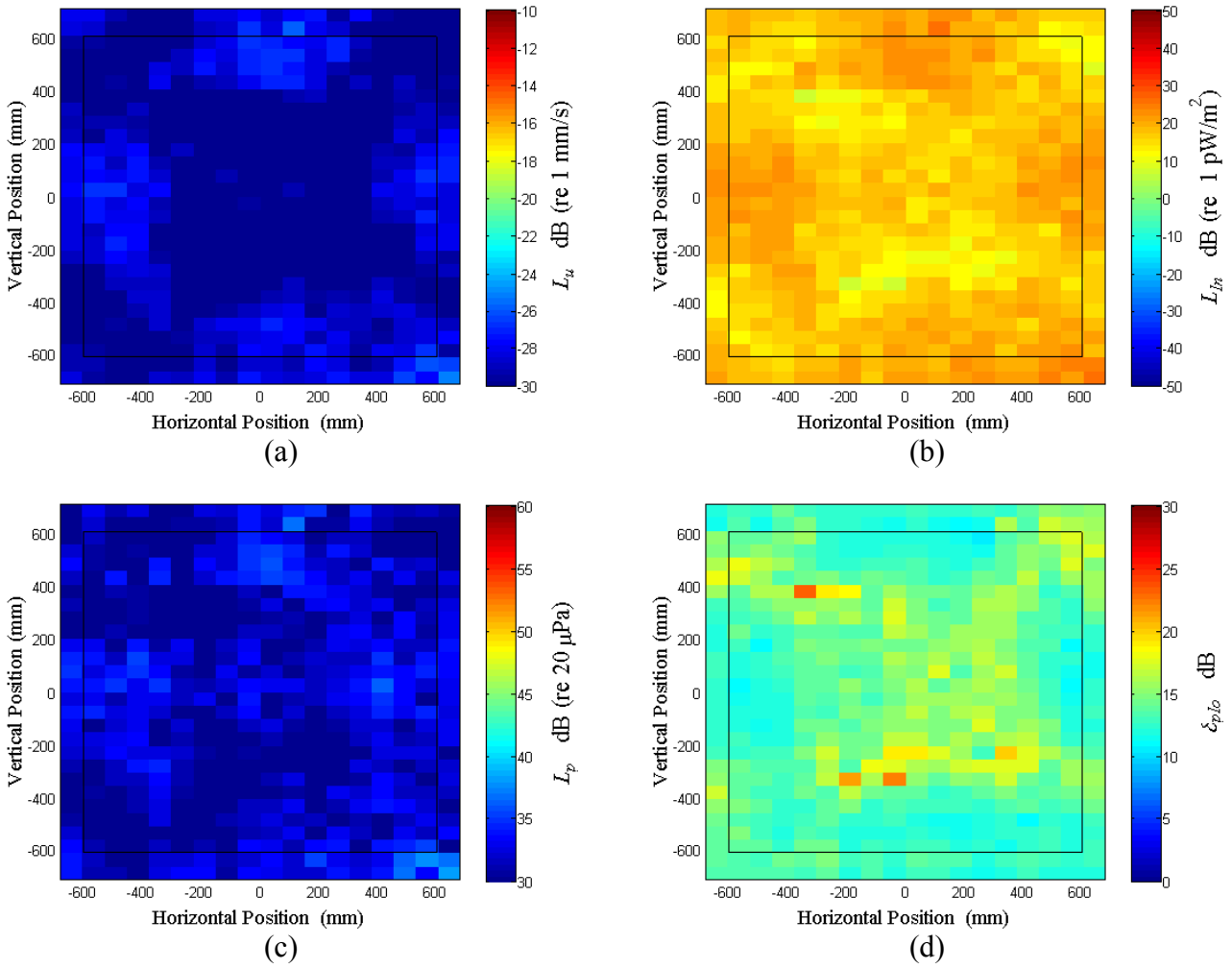

Figure E.68: Surface scan of Window E at 480 Hz (a) particle velocity level, L_u (b) normal signed sound intensity level, L_{In} (c) sound pressure level, L_p (d) pressure-residual intensity index, δ_{pIo}.

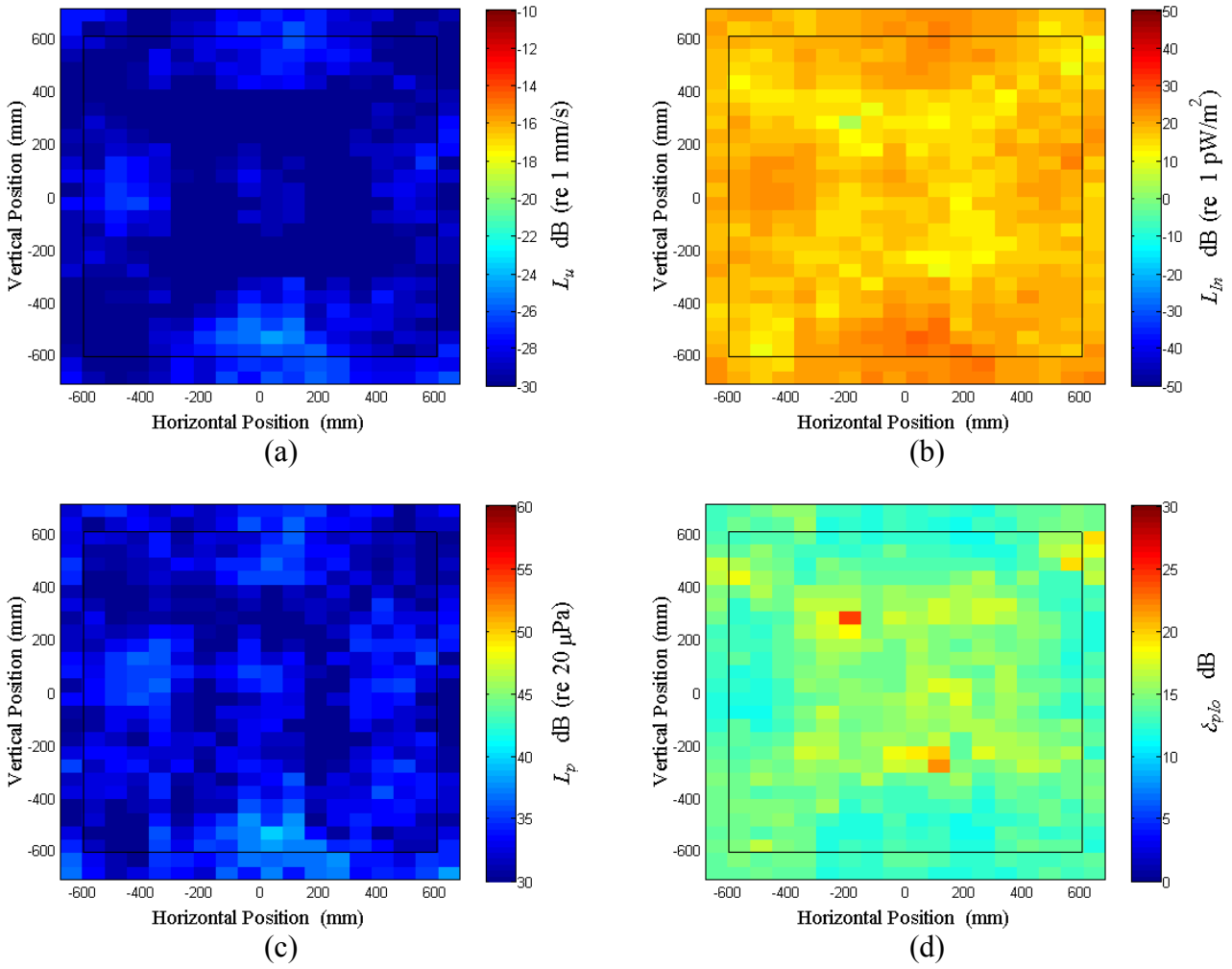

Figure E.69: Surface scan of Window E at 490 Hz (a) particle velocity level, L_u (b) normal signed sound intensity level, L_{In} (c) sound pressure level, L_p (d) pressure-residual intensity index, δ_{pIo}.

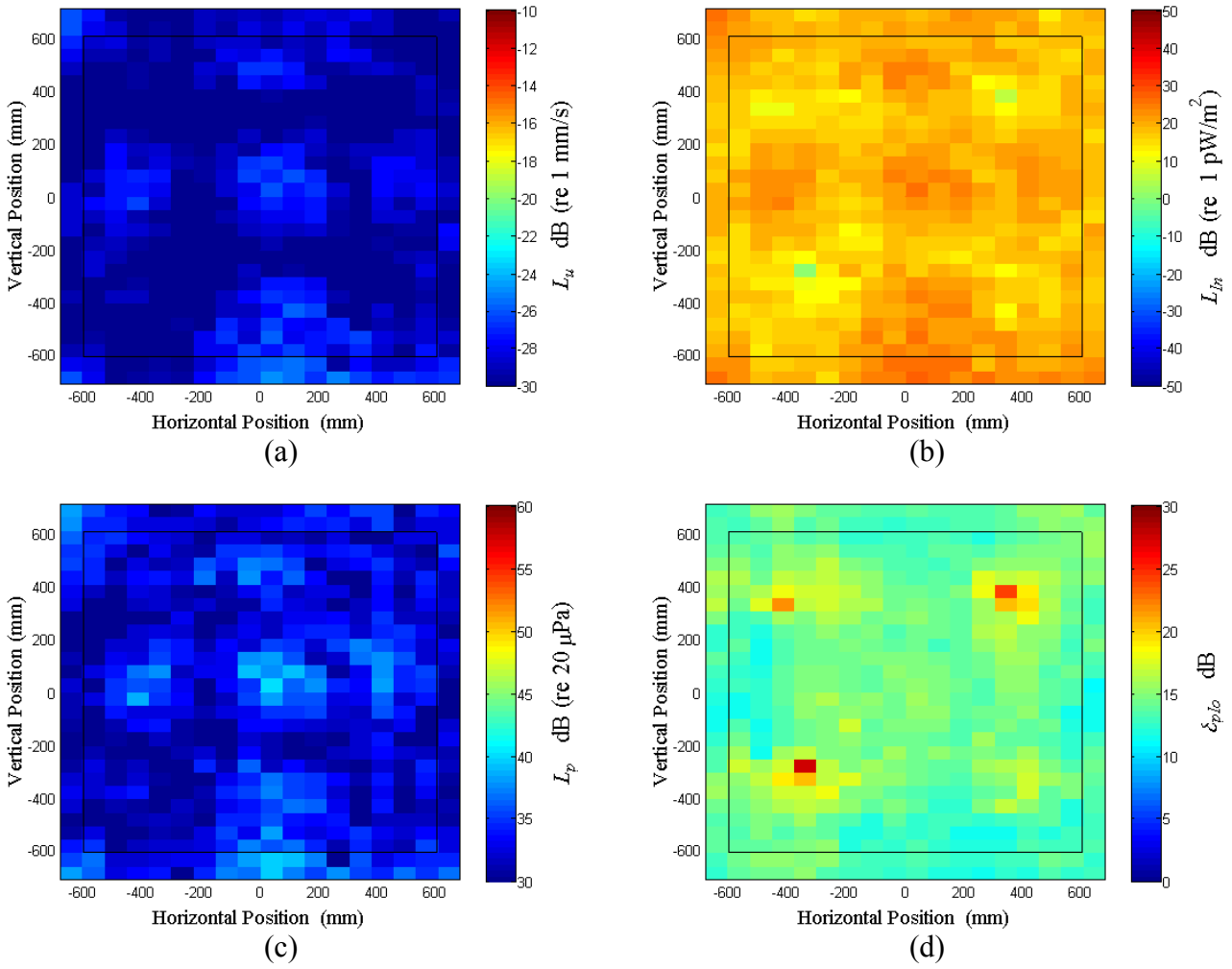

Figure E.70: Surface scan of Window E at 500 Hz (a) particle velocity level, L_u (b) normal signed sound intensity level, L_{In} (c) sound pressure level, L_p (d) pressure-residual intensity index, δ_{pIo}.